CRANFIELD UNIVERSITY

J A MONTGOMERY

SEVERE SLUGGING AND UNSTABLE FLOWS IN AN S-SHAPED RISER

SCHOOL OF ENGINEERING

PhD. THESIS

CRANFIELD UNIVERSITY

SCHOOL OF ENGINEERING

PhD. Thesis

Academic Year 2001-2002

J A MONTGOMERY

Severe Slugging and Unstable Flows in an S-Shaped Riser

Supervisor: Dr H Yeung

February 2002

This thesis is submitted in partial fulfilment of the requirements for the degree of Doctor of Philosophy

Abstract

Severe slugging and unstable flow in an S-Shaped riser has been investigated in three research themes – experiments, criterion modelling and transient code modelling.

A series of experiments were carried out on the Cranfield University Three Phase Facility and Riser Rig using a 10 m high riser over the pressure range 2, 4 and 7 bar(a). The collected information was used to characterise the unstable flows in terms of pressure cycling, riser liquid inventory and fluid production characteristics. From analysis of the flow behaviour, it was found that in terms of slug characteristics, transitional severe slugging and oscillation flows are as potentially problematic as 'classical' severe slugging. This is due to the magnitude of peak flow in excess of the average fluid throughput in the riser and the size of the liquid slugs generated.

A criterion for the occurrence of unstable flows in an S-Shaped riser was developed based upon considerations of bubble penetration at the riser base. This proved to be successful at predicting the experimental results from this work and an independent source.

Comparisons were made between the experimental results and a transient code. The code could predict the occurrence of 'classical' severe slugging however the detailed characteristics of the experiments were not predicted by the code. The results for transitional severe slugging and oscillation flow showed further differences between the code prediction and the experiments. Drawing all simulation results together it was concluded that the prediction of pipeline behaviour and the propagation of flow regimes local to the riser base and in the curved riser pipe were significant sources of error in the simulation.

Acknowledgements

A research thesis is never completed by one person, many people contribute in one way or another over the time, hence, the tribute list below, is not exhaustive and is by no means in order!

Firstly I would like to thank my supervisor, Dr. Hoi Yeung for his guidance and enthusiastic discussions on and around the subject at hand.

Secondly I would like to thank Dr. Wai Lam Loh, Stan Collins and John Knopp for their varied contributions in running and supporting the operation of the Riser Rig at Cranfield. Their invaluable help deciphering the mysteries of data acquisition and electronics was never more than a phone call away and for that I am very grateful.

Thirdly, many thanks to the support staff in the Department at Cranfield, particularly the secretaries – Janet Dare and Millie and the others who have been, gone and arrived recently – Enza, Melanie (B or K) and Sarah. They have all been really helpful, right to the last second of a deadline. Also many thanks Chris Evans, whose inspiration for getting kit together has been availed of on many occasions and whose treatises on fishing will be sorely missed.

There is a group of people without whom none of this could have even been contemplated – my parents and brothers, my girlfriend and friends in Ireland and the UK – all have been a constant source of encouragement and support. Thanks one and all. A big thanks to Sujata who has been a constant source of help, listening, encouragement with an amazing amount of patience.

Finally to Mum and Dad, thanks always for encouraging me to be exactly who I wanted to be.

This work has been undertaken within the Transient Multiphase Flows' Co-ordinated Research Project. The Author wishes to acknowledge the contributions made to this project by the Engineering and Physical Sciences Research Council (EPSRC) and to the following industrial organisations: - ABB; AEA Technology; Amerada Hess; BG International; BP Exploration; CALtec; Chevron; Conoco; Enterprise Oil; Granherne; Exxon Production Research; Institutt for Energiteknikk; Institut Francais du Petrole; Marathon Oil; Mobil North Sea; Norsk Hydro; Scandpower; Texaco Britain; TotalFinaElf. The Author wishes to express his sincere gratitude for this support.

Table of Contents

		Page
Abstract		**ii**
Acknowledgements		**iii**
Table of Contents		**iv**
List of Figures		**viii**
List of Tables		**xiv**
Nomenclature		**xv**
Chapter 1 – Introduction		**1**
1.1	Offshore Marginal Field Development	1
1.2	Multiphase Production Issues	1
1.3	Floating Production in Deepwater Environments	2
1.3.1	Flexible Risers and the Challenges of Deepwater	2
1.3.2	Severe Slugging in Flexible Risers	4
1.4	Research Objectives	6
1.5	Thesis Structure	6
Chapter 2 – Literature Review		**7**
2.1	Severe Slugging in a Pipeline/Riser System	7
2.1.1	Severe Slugging Mechanism	7
2.1.2	Fluid Production Characteristics	11
2.1.3	Transitional Flows	12
2.2	Steady-State Modelling of Flow Stability	13
2.2.1	The Stratified Flow Criterion	14
2.2.2	The Bøe Criterion	15
2.2.3	The Π_{SS} Criterion	16
2.2.4	The Taitel Criterion	17
2.2.5	Fuchs' Pressure Criterion	19
2.3	Prevention and Control of Severe Slugging	20
2.3.1	Topsides Choking	20
2.3.2	Riser Base Gas Injection	21
2.3.3	Other Methods of Severe Slugging Control	22
2.4	Transient Modelling of Severe Slugging	23

2.4.1 Specific Severe Slugging Models 23
2.4.2 Generalised Multiphase Flow Codes 26
2.5 Severe Slugging in Flexible Risers 35
2.5.1 Experimental Investigations 35
2.5.2 Modelling Investigations 42
2.6 Severe Slugging and Terrain Slugging 43
2.7 Outstanding Issues and Research Plan 45
2.7.1 Flow Regimes 45
2.7.2 Steady-State Modelling 46
2.7.3 Transient Code Modelling 46

Chapter 3 – Experimental 47

3.1 Three Phase Facility 47
3.1.1 Fluid Supply Facilities 47
3.1.2 Fluid Receiving Facilities 48
3.1.3 Instrumentation 50
3.2 Flexible Riser Rig 52
3.2.1 Riser Test Section and Topsides Separator 52
3.2.2 Instrumentation 54
3.2.3 Data Acquisition System 55
3.3 Data Processing/Analysis 57
3.3.1 Pressure Characteristics 58
3.3.2 Liquid Holdup Characteristics 63
3.3.3 Inlet Gas Flow Characteristics 63
3.3.4 Inlet Liquid Flow Characteristics 64
3.3.5 Liquid Production Characteristics 64
3.3.6 Gas Production Characteristics 67
3.4 Test Procedure and Experimental Conditions 72
3.4.1 Test Procedure 72
3.4.2 Test Conditions and Programme 73

Chapter 4 – Experimental Results 75

Part 1 – Flow Regime Characteristics 75

4.1 Severe Slugging 1 Characteristics 75
4.2 Transitional Severe Slugging 90
4.2.1 Severe Slugging 2 Characteristics 90
4.2.2 Severe Slugging 3 Characteristics 99
4.3 Oscillation Characteristics 108
4.4 Stable Flow Characteristics 118
4.4.1 Slug Flow Characteristics 118
4.4.2 Bubble Flow Characteristics 121
4.5 Generalised Flow Regime Characteristics 124
4.5.1 Flow Regime Characteristics 124
4.5.2 Production Deviations During Unstable Flows 126

4.6 Pressure Effects of Flow Processes 127
4.6.1 Classical Severe Slugging 127
4.6.2 Oscillation Flow 129

Part 2 – Flow Regime Maps 130

4.7 Flow Regime Behaviour 131
4.8 Comparison with Stability Criteria 134
4.8.1 Criteria for Comparison 134
4.8.2 Comparison Results 136
4.9 Summary 139

Chapter 5 Criterion for Unstable Flow 140

5.1 Basic Formulation of Criterion 140
5.1.1 Existing Criteria 141
5.1.2 Criterion for Large Scale Instabilities 143
5.2 Development of Criterion 144
5.2.1 Model Assumptions 144
5.2.2 Pressure Change in the Pipeline 145
5.2.3 Pressure Change at the Riser Base 147
5.2.4 Final Formulation 148
5.3 Implementation Issues 148
5.3.1 Velocity of Gas Entering the Riser Base 149
5.3.2 Void fraction Behind the Bubble Nose 149
5.3.3 Distribution Parameter and Drift Velocity 150
5.3.4 Effective Height of Liquid in the Riser 151
5.3.5 Calculation of the Criterion 152
5.3.6 Effect of Inclination 154
5.4 Criterion Validation 155
5.4.1 Comparison with Experimental Data 155
5.4.2 Comparison with Tin and Sharshar (1991) Data 158
5.5 Summary 159

Chapter 6 – Transient Code Simulations 161

6.1 Test Series Description 161
6.2 Model Formulation 164
6.2.1 Model Assumptions 164
6.2.2 PVT Description 164
6.2.3 Pipeline Model 165
6.2.4 Boundary Conditions 166
6.2.5 Model Execution 167
6.3 Primary Simulation Results 168
6.3.1 Global Results 168
6.3.2 Detailed Results – Severe Slugging 1 170
6.3.3 Detailed Results – Transitional Severe Slugging 173
6.3.4 Detailed Results – Oscillation Flow 177

6.3.5 Detailed Results – Slug Flow 179
6.4 Numerical Experiments 181
6.4.1 Grid Density 181
6.4.2 Timestep Size 183
6.5 Summary 184

Chapter 7 – Conclusions & Recommendations 187

7.1 Experimental Work 187
7.1.1 Research Summary 187
7.1.2 Conclusions 188
7.2 Unstable Flow Criterion 188
7.2.1 Research Summary 189
7.2.2 Conclusions 189
7.3 Transient Code Modelling 189
7.3.1 Research Summary 190
7.3.2 Conclusions 190
7.4 Recommendations and Suggestions for Further Work 190
7.4.1 Recommendations 191
7.4.2 Suggestions for Further Work 191

References 193

Publications 201

Appendix A – Matlab Scripts

Appendix B – Frictional Loss Calculations

Appendix C – Operating Procedures

Appendix D – Results Tables

Appendix E – Taitel Correlation

Appendix F – Generic Transient Code Model

List of Figures

Figure	Title	Page
1.1	Multiphase Production Issues	2
1.2	Deepwater Environmental Conditions	3
1.3	Riser Shapes	4
1.4	Fluid Production During Severe Slugging	5
2.1	Flow Regime Map for Vertical Riser Severe Slugging	8
2.2	Riser Base Pressure During Severe Slugging	8
2.3	Stages of Severe Slugging	10
2.4	Liquid Production During Severe Slugging	11
2.5	Geometry Used for Pipeline/Riser Models	13
2.6	Taitel and Duckler (1976) Stratified Flow Criterion	15
2.7	Bøe (1981) Criterion	16
2.8	Π_{SS} Criterion	17
2.9	Taitel (1986) Criterion	18
2.10	Generalised Vertical Flow Regime Map	31
2.11	Generalised Horizontal Flow Regime Map	32
2.12	Tin and Sharshar's Experimental Arrangement	36
2.13	Severe Slugging with Intermediate Cycles on the Lower Limb (SS1i)	38
2.14	Oscillation Flow Pressure Cycling Characteristics	39
2.15	Oscillation Flow Pressure Cycling Characteristics	41
2.16	Pressure Cycling and Liquid Production During Terrain Slugging, after DeHenau and Raithby (1995c)	45
3.1	Cranfield University Three Phase Facility P&I Diagram	48
3.2	Three Phase Separator	49
3.3	Three Phase Separator Level Control Schematic	49
3.4	Water Flow Metering Station	51
3.5	Gas Flow Metering Station	51
3.6	Pipeline/Riser P&I Diagram	52
3.7	Riser DAS	56

3.8	Pipeline/Riser Liquid Distribution	59
3.9	Separator Pressure Variation During Severe Slugging 1	60
3.10	Comparison of Riser Base and Riser Pressure Difference Profiles	61
3.11	Outlet Liquid Separator	65
3.12	Comparison Between the Mass Balance Results With and Without Filtering of the Separator Level	66
3.13	Comparison of Inlet and Outlet Liquid Mass Flow for Steady Flow Regimes	67
3.14	Gas Flow Reading From Separator Outlet Meter	69
3.15	First Derivative of Outlet Gas Flow Reading	70
3.16	Second Derivative of the Outlet Gas Flow Reading	70
3.17	Filtered Gas Flow Reading From The Topsides Separator Outlet Meter	71
4.1	Pressure Difference Over Riser During Severe Slugging 1, U_G^S = 0.0985 m/s, U_L^S = 0.2017 m/s	76
4.2	Liquid Distribution in the Riser During Severe Slugging 1	77
4.3	Pressure Difference Over Each Upward Riser Limb During Severe Slugging 1, U_G^S = 0.0985 m/s, U_L^S = 0.2017 m/s	78
4.4	Pressure Difference Over Riser Downcomer During Severe Slugging 1, U_G^S = 0.0985 m/s, U_L^S = 0.2017 m/s	79
4.5	Probability Density Function of Pressure Difference Over Riser During Severe Slugging 1, U_G^S = 0.0985 m/s, U_L^S = 0.2017 m/s	81
4.6	Liquid Holdup Local to Riser Base During Severe Slugging 1, U_G^S = 0.161 m/s, U_L^S = 0.08674m/s	82
4.7	Liquid Production During Severe Slugging 1, U_G^S = 0.0985 m/s, U_L^S = 0.2017 m/s	83
4.8	Liquid Production and Pressure Cycling During Severe Slugging 1, U_G^S = 0.0985 m/s, U_L^S = 0.2017 m/s	83
4.9	Liquid Slug Size During Severe Slugging 1, 2 bar(a) Data	85
4.10	Size of Liquid Production Transient During Severe Slugging 1, 2 bar(a) Data	86
4.11	Liquid Slug Size During Severe Slugging 1, 4 bar(a) Data	87
4.12	Size of Liquid Production Transient During Severe Slugging 1, 4 bar(a) Data	87
4.13	Peak Liquid Production Rate During Severe Slugging 1, 2 bar(a)	88
4.14	Gas Production During Severe Slugging 2, U_G^S = 0.151 m/s, U_L^S = 0.186 m/s	89

4.15	Combined Gas and Liquid Mass Production Characteristics During Severe Slugging 1, $U_G^S = 0.151$ m/s, $U_L^S = 0.186$ m/s	89
4.16	Pressure Difference Over Riser During Severe Slugging 2, $U_G^S = 0.33$ m/s, $U_L^S = 0.5$ m/s	91
4.17	Liquid Distribution in the Riser During Severe Slugging 2	92
4.18	Pressure Difference Over Each Upward Riser Limb During Severe Slugging 2, $U_G^S = 0.33$ m/s, $U_L^S = 0.5$ m/s	93
4.19	Probability Density Function of Pressure Difference Over Riser During Severe Slugging 2, $U_G^S = 0.33$ m/s, $U_L^S = 0.5$ m/s	93
4.20	Liquid Holdup Local to Riser Base During Severe Slugging 2, $U_G^S = 0.343$ m/s, $U_L^S = 0.372$ m/s	94
4.21	Liquid Production During Severe Slugging 2, $U_G^S = 0.209$ m/s, $U_L^S = 0.058$ m/s	95
4.22	Liquid Slug Size During Severe Slugging 2, 2 bar(a)	96
4.23	Peak Liquid Production Rate During Severe Slugging 2, 2 bar(a)	96
4.24	Gas Production During Severe Slugging 2, $U_G^S = 0.209$ m/s, $U_L^S = 0.058$ m/s	98
4.25	Combined Gas and Liquid Production Characteristics During Severe Slugging 2, $U_G^S = 0.209$ m/s, $U_L^S = 0.058$ m/s	98
4.26	Pressure Difference Over Riser During Severe Slugging 3, $U_G^S = 0.672$ m/s, $U_L^S = 0.165$ m/s	99
4.27	Liquid Distribution in the Riser During Severe Slugging 3	100
4.28	Pressure Difference Over Riser During Severe Slugging 3, $U_G^S = 0.672$ m/s, $U_L^S = 0.165$ m/s	101
4.29	Pressure Difference Over Each Upward Riser Limb, $U_G^S = 0.672$ m/s, $U_L^S = 0.165$ m/s	102
4.30	Probability Density Function of Pressure Difference Over Riser During Severe Slugging 3, $U_G^S = 0.672$ m/s, $U_L^S = 0.165$ m/s	103
4.31	Liquid Holdup Local to Riser Base During Severe Slugging 3, $U_G^S = 0.672$ m/s, $U_L^S = 0.165$ m/s	104
4.32	Liquid Production During Severe Slugging 3, $U_G^S = 0.906$ m/s, $U_L^S = 0.213$ m/s	104
4.33	Liquid Slug Size During Severe Slugging 3, 2 bar(a)	105
4.34	Peak Liquid Production Rate During Severe Slugging 3, 2 bar(a)	106
4.35	Gas Production During Severe Slugging 3, $U_G^S = 0.906$ m/s, $U_L^S = 0.213$ m/s	107
4.36	Combined Gas and Liquid Mass Production Characteristics During Severe Slugging 3, $U_G^S = 0.906$ m/s, $U_L^S = 0.213$ m/s	107

4.37	Pressure Difference Over Riser During Oscillation Flow, U_G^S = 0.248 m/s, U_L^S = 0.431 m/s	108
4.38	Pressure Difference Over Each Upward Riser Limb U_G^S = 0.248 m/s, U_L^S = 0.431 m/s	109
4.39	Liquid Distribution in the Riser During Oscillation Flow	110
4.40	Pressure Difference Over Downcomer and Upper Riser Limb, U_G^S = 0.248 m/s, U_L^S = 0.431 m/s	111
4.41	Probability Density Function of Pressure Difference Over Riser During Oscillation Flow, U_G^S = 0.248 m/s, U_L^S = 0.431 m/s	112
4.42	Liquid Holdup Local to Riser Base During Oscillation Flow, U_G^S = 0.248 m/s, U_L^S = 0.431 m/s	112
4.43	Liquid Production During Oscillation Flow, U_G^S = 0.267 m/s, U_L^S = 0.683 m/s	113
4.44	Liquid Production and Pressure Cycling During Oscillation Flow, U_G^S = 0.267 m/s, U_L^S = 0.683 m/s	114
4.45	Liquid Surge Size During Oscillation Flow, 4 bar(a)	115
4.46	Gas Production During Oscillation Flow, U_G^S = 0.267 m/s, U_L^S = 0.683 m/s	116
4.47	Gas Production and Pressure Cycling During Oscillation Flow, U_G^S = 0.267 m/s, U_L^S = 0.683 m/s	117
4.48	Pressure Difference Over Riser During Slug Flow, U_G^S = 0.94 m/s, U_L^S = 0.602 m/s	119
4.49	Probability Density Function of Pressure Difference Over Riser During Slug Flow, U_G^S = 0.94 m/s, U_L^S = 0.602 m/s	119
4.50	Liquid Holdup Local to the Riser Base During Slug Flow, U_G^S = 0.94 m/s, U_L^S = 0.602 m/s	120
4.51	Combined Gas and Liquid Mass Production Characteristics During Slug Flow, U_G^S = 2.718 m/s, U_L^S = 0.608 m/s	121
4.52	Pressure Difference Over Riser During Bubble Flow, U_G^S = 0.075 m/s, U_L^S = 0.941 m/s	122
4.53	Probability Density Function of Pressure Difference Over Riser During Bubble Flow, U_G^S = 0.075 m/s, U_L^S = 0.941 m/s	122
4.54	Liquid Holdup Local to the Riser Base During Bubble Flow, U_G^S = 0.075 m/s, U_L^S = 0.94 m/s	123
4.55	Combined Gas and Liquid Mass Production Characteristics During Bubble Flow, U_G^S = 0.075 m/s, U_L^S = 0.941 m/s	124
4.56	Pressure Difference Over Riser During Severe Slugging, 7 bar(a), U_G^S = 0.055 m/s, U_L^S = 0.085 m/s	128

4.57	Liquid Holdup Local to Riser Base During Severe Slugging 1, 7 bar(a), $U_G^S = 0.055$ m/s, $U_L^S = 0.085$ m/s	128
4.58	Liquid Production During Severe Slugging 1, 7 bar(a), $U_G^S = 0.055$ m/s, $U_L^S = 0.085$ m/s	129
4.59	Pressure Difference Over Lower and Upper Riser Limb, 7 bar(a), $U_G^S = 0.28$ m/s, $U_L^S = 0.466$ m/s	130
4.60	Basic Experimental Flow Regime Map	131
4.61	Flow Regime Map, 2 bar(a)	132
4.62	Flow Regime Map, 4 bar(a)	132
4.63	Flow Regime Map, 7 bar(a)	133
4.64	Flow Regime Map Comparison with Stability Criteria, 2 bar(a)	136
4.65	Flow Regime Map Comparison with Stability Criteria, 4 bar(a)	137
4.66	Flow Regime Map Comparison with Stability Criteria, 7 bar(a)	137
5.1	Vertical Riser Geometry	141
5.2	Geometry at Base of S-Shaped Riser	145
5.3	Unstable Flow Regime Criterion Calculation Algorithm	152
5.4	Sample Plot of the Criterion for Large-Scale Instabilities	153
5.5	Effect of Riser Base Inclination Angle on Criterion Results	154
5.6	Comparison of 2 bar(a) Experimental Data with Stability Criteria	155
5.7	Comparison of 4 bar(a) Experimental Data with Stability Criteria	156
5.8	Comparison of 7 bar(a) Experimental Data with Stability Criteria	157
5.9	Comparison of MPE Data (Tin and Incoll, 1991) with Stability Criteria	159
6.1	Flow Regime Map Denoting the Test Series	162
6.2	Combined Experimental and Simulated Pressure Difference Profiles for Case A, Severe Slugging 1	171
6.3	Combined Experimental and Simulated Liquid Production Profiles for Case A, Severe Slugging 1	172
6.4	Combined Experimental and Simulated Pressure Difference Profiles for Case C, Severe Slugging 2	174
6.5	Simulated Pressure Difference Profile for Case D, Severe Slugging 3	174
6.6	Simulated Riser Base Liquid Holdup Profile for Case C, Severe Slugging 2	175

6.7	Simulated Riser Base Liquid Holdup Profile for Case D, Severe Slugging 3	175
6.8	Experimental Riser Base Liquid Holdup Profile for Case D, Severe Slugging 3	177
6.9	Simulated Pressure Difference Profile Over Each Riser Limb for Case E, Oscillation Flow, Base Simulation	178
6.10	Simulated Pressure Difference Profile Over Downcomer For Case E, Oscillation Flow, Base Simulation	178
6.11	Experimental Pressure Difference Profile Over Downcomer For Case E, Oscillation Flow	179
6.12	Simulated Riser Base Liquid Holdup Profile for Case F, Slug Flow, Base Simulation	180
6.13	Experimental Riser Base Liquid Holdup Profile for Case F, Slug Flow	180
6.14	Simulated Riser Base Liquid Holdup Profile for Case F, Slug Flow, 'x4' Grid Density Simulation	182

List of Tables

Table	Title	Page
3.1	Three Phase Facility Instrumentation	50
3.2	Co-Ordinates of the Pipeline/Riser Test Section	53
3.3	Test Section Instrumentation	54
3.4	Look-Up Table for the DAS	57
3.5	Data Series for Examination	58
3.6	Test Conditions	74
4.1	Generalised Flow Regime Characteristics	126
4.2	Liquid Production Characteristics Summary	126
6.1	Test Series Summary	163
6.2	Pipe Properties	166
6.3	Main Simulation Results	169

Nomenclature

Symbol	Variable	Unit
A	Area	m^2
C_0	Distribution (drift-flux) parameter	
D	Diameter	m
f	Fanning friction factor	
	Function value (Equation 4.3)	
f'	Moody friction factor	
G	Mass Flow	kg/s
g	Acceleration due to gravity	m/s^2
H	Enthalpy	kj/kg
h	Height	m
K	Signal gain	<variable>
L	Length	m
M	Total mass	kg
M_w	Molecular Weight	kg/kmol
N	Velocity number	
P	Pressure	Pa or bar
$P(x)$	Probability of x (Equation 4.1)	
p	Probability density function	
Q	Volume flow	m^3/s or l/s
	Heat flow (Equations 2.37-2.46)	W
R	Ideal gas constant	j/mol K
S	Wetted perimeter	m
	Discrete-time signal (Eq. 3.11, 3.22 & 3.31)	
T	Temperature	K or °C
t	Time	s
U	Velocity	m/s
	Internal Energy (Equation 2.36)	kj/kg
V	Volume	m^3 or l
	Voltage (Eq. 3.1)	V
x	Co-ordinate direction	m

y	Co-ordinate direction	m
Z	Compressibility factor	
z	Co-ordinate direction	m

Greek Symbols

α	Angle of inclination	°
β	Angle of inclination	°
ε	Holdup or phase fraction	
	Absolute pipe roughness (Appendix B)	
ϕ	Correlation variable (Appendix E)	
Γ	Mass source term (PLAC and TACITE Model)	<variable>
φ	Droplet entrainment rate	<variable>
μ	Dynamic viscosity	Ns/m^2
ν	Kinematic viscosity	m^2/s
θ	Angle of inclination	°
ρ	Density	kg/m^3
σ	Surface tension	dyn/cm
τ	Shear force	N/m
ζ	Mass source term (OLGA model)	<variable>

Subscripts

B	Base
Bub	Bubble
D	Downstream
d	Downcomer (Bottom)
FR	Friction
G	Gas
HYD	Hydrostatic
I	Inlet
L	Liquid
l	Lower limb (Top)
$Loss$	Losses (due to acceleration and friction)
M	Mixture
MAX	Maximum

MIN	Minimum
O	Outlet
P	Pipeline
R	Riser
REC	Receiver
REF	Reference Condition
S	Separator
U	Upper limb (Top)

Superscripts

S	Superficial

Chapter 1 – Introduction

This thesis details investigations on flow instabilities leading to severe slugging and oscillation flows in an S-shaped riser. As such this work is broken into three major research themes - experimental investigations, theoretical studies in flow stability and numerical simulations of riser behaviour. This first chapter provides a background to the work and an outline of the overall thesis structure.

1.1 Offshore Marginal Field Development

The current trend in offshore oil and gas production has been summarised by Hunt (1999) as: 'smaller, deeper, further'. This highlights the focus on the development of marginal fields in deeper water, further offshore for the recovery of hydrocarbons. Marginal fields in this sense are those fields where the rate of return on investment is the main feature in deciding the development prospects (Hunt, 1999). As marginal developments move further offshore and into deeper waters, up to 2,500m of water depth, the per-barrel cost of recovering hydrocarbons increases, Hunt (1998). The reduction in field size induces further economic pressures on the development due to the reduced revenue available.

The key in successfully developing these fields has been stated by Hill (1997) as minimising both Capital Expenditure (CAPEX) and Operational Expenditure (OPEX). Multiphase technology is seen as a vital means of exploiting marginal fields, maximising the rate of return and minimising both forms of expenditure (Klemp, 1999). For example, by transporting multiple fluid phases in a single flowline, duplicate pipelines and receiving facilities for separate phases, costing both money and space, are eliminated, reducing CAPEX. Alternatively, subsea separation and re-injection of water and gas save both CAPEX and OPEX, by reducing the size of the fluid transport/handling facilities and the maintenance required for the pipeline operation.

Given the savings that are available for operators using multiphase technology, the market for multiphase technology is an expanding one. McNulty (1995) stated that multiphase technology was expected to be critical in the development of some 130 fields. In the same study, there was an expected 500% increase in investment in multiphase technology by operators in the USA. However the reliability with which multiphase technology can be used is a constant barrier to its application in a field (Hunt, 1998).

1.2 Multiphase Production Issues

There are a number of issues that must be constantly addressed throughout the lifetime of a multiphase asset. As the field matures, the pressure, temperature and chemical characteristics of the well fluids change and water cut increases. All of these will have a significant impact on fluids recovery over the asset life (Fairhurst, 1997). Hill (1997) classifies these issues into three broad categories for multiphase production in pipelines (see Figure 1.1):

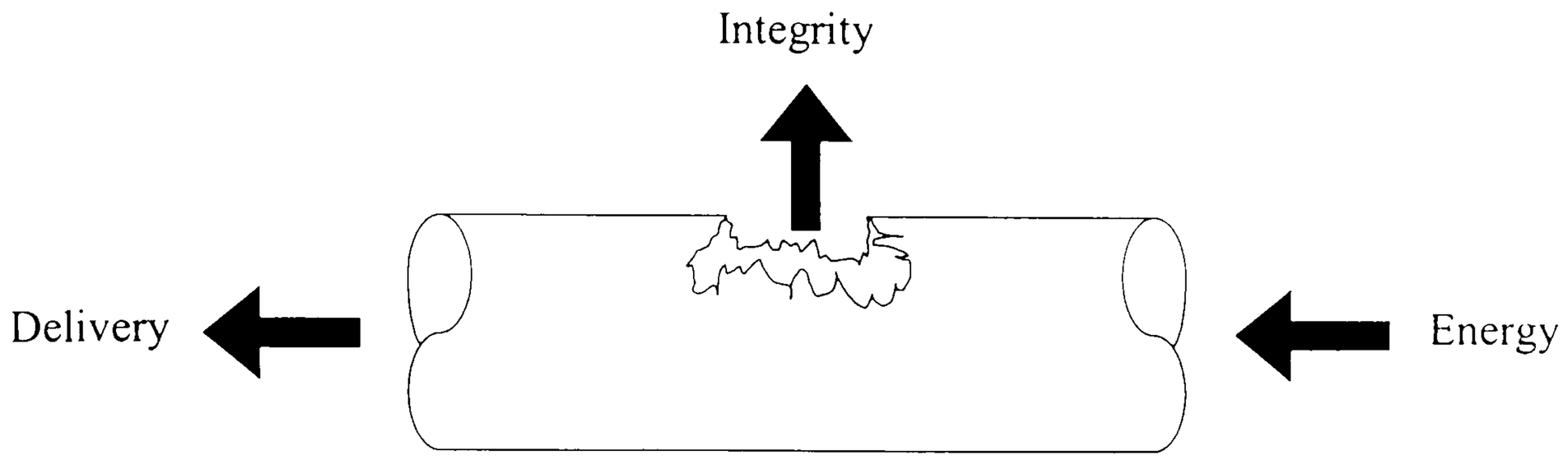

Figure 1.1 – Multiphase Production Issues

1. Energy - ensuring there is enough motive energy to transport the fluids from the reservoir to the receiving facilities. This involves predicting the pressure and temperature behaviour of the well, the loss characteristics along the pipe and any requirement for additional energy, for example through gas-lift.
2. Integrity - maintaining the containment of the fluids and ensuring their passage is not impeded. Mechanical loading during slug flow, corrosion, erosion, sand transport/deposition, wax formation and hydrate formation are all covered by this category.
3. Delivery - design and maintaining of the transport, receiving and handling facilities to ensure a steady delivery of fluids. This also entails the successful management of any potential variations in the gas and/or liquid flows. Steady state and transient modelling both play an important role in predicting the future flow behaviour, necessary for correct operational planning and design. The fiscal metering of fluids also lies in this category - the complex nature of the well fluids require advanced metering methods that can handle multiple fluid types, physical properties and chemical composition.

1.3 Floating Production in Deepwater Environments

Floating production systems allow the use of an asset for the production life of the field and subsequent re-location to another field (Cottrill, 1999). This minimises the pre-production infrastructure investment in a development and allows a more cost-effective use of an asset at a number of locations. Flexible riser technology is an essential component of floating production and can be viewed as 'enabling technology' in this respect. Flexible risers provide the necessary compliance to the vessel motion and can allow for the imprecise stationing of a floating production vessel (Das *et al.* 1999).

1.3.1 Flexible Risers and the Challenges of Deepwater

When seeking to use flexible risers in deep waters, there are a large number of challenges to be overcome (Hill, 1997). Increased depth causes greater hydrostatic

stress on the pipe walls. Water current gradients induce Vortex Induced Vibrations of different intensity along the riser length, increasing torsional loading and risers must be designed on a case-by-case basis. Figure 1.2 shows some of the varying conditions faced when deploying flexible risers in deepwater environments.

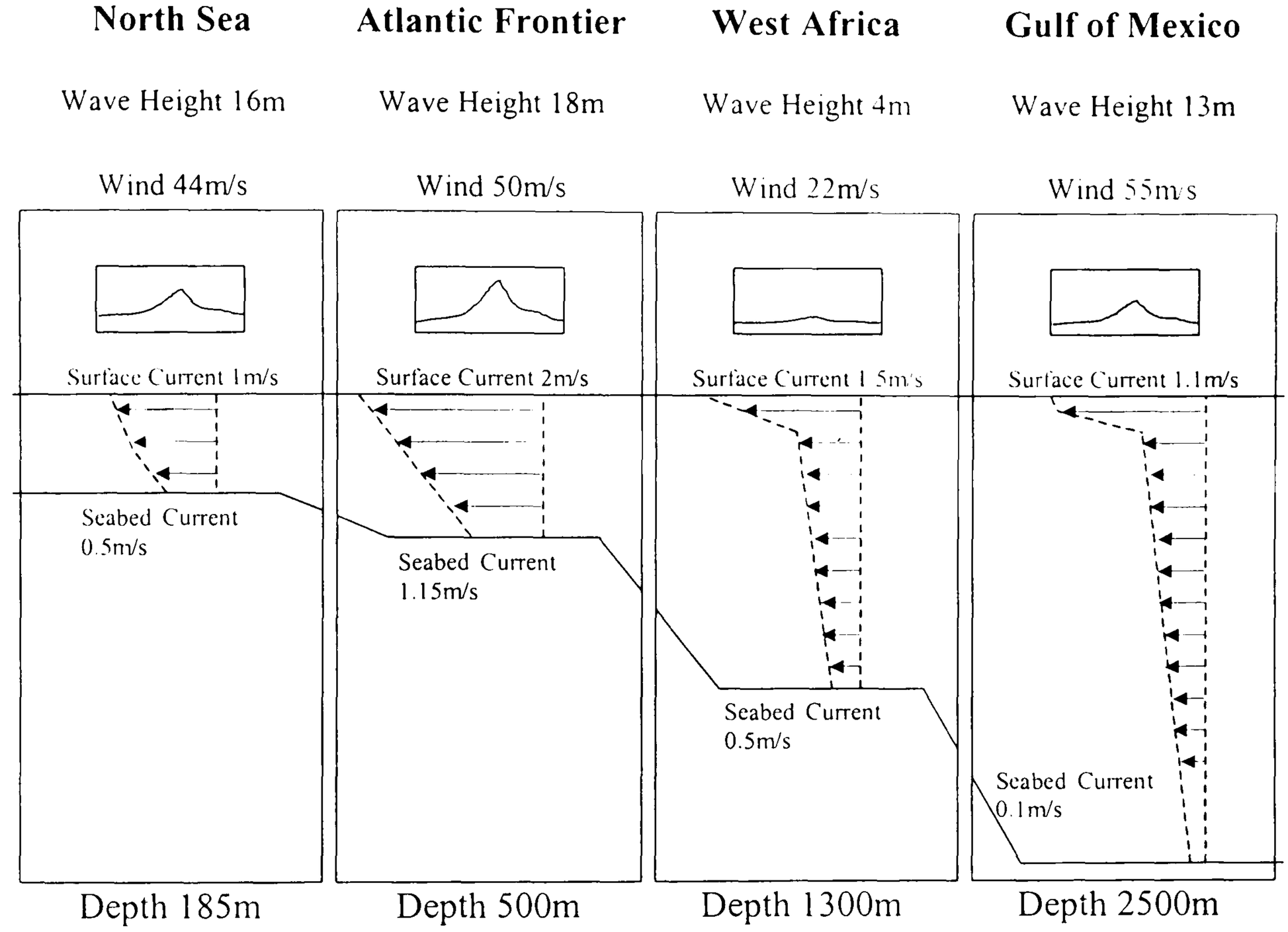

Figure 1.2 – Deepwater Environmental Conditions

The nature of the water current gradients in a particular development, dictates the riser shape, the type and relative positions of any riser limbs. Figure 1.3 shows some of the different flexible riser shapes developed for these environments. Over long riser lengths, temperature changes become larger, affecting the flow characteristics, emulsion formation, the chemical properties and the likelihood of wax/hydrate formation. Sufficient insulation must be added to the riser without compromising the drag and/or the mechanical performance of the riser.

With deeper water comes higher reservoir pressure and temperature and so a riser will have to cope with High Pressure High Temperature (HPHT) related problems: internal mechanical loads, potential creep issues and increased corrosion. The final challenge is predicting the internal hydrodynamic behaviour; this has an impact on the mechanical loads in the riser, the variations in fluid delivery and corrosion/erosion of the internal pipe surface.

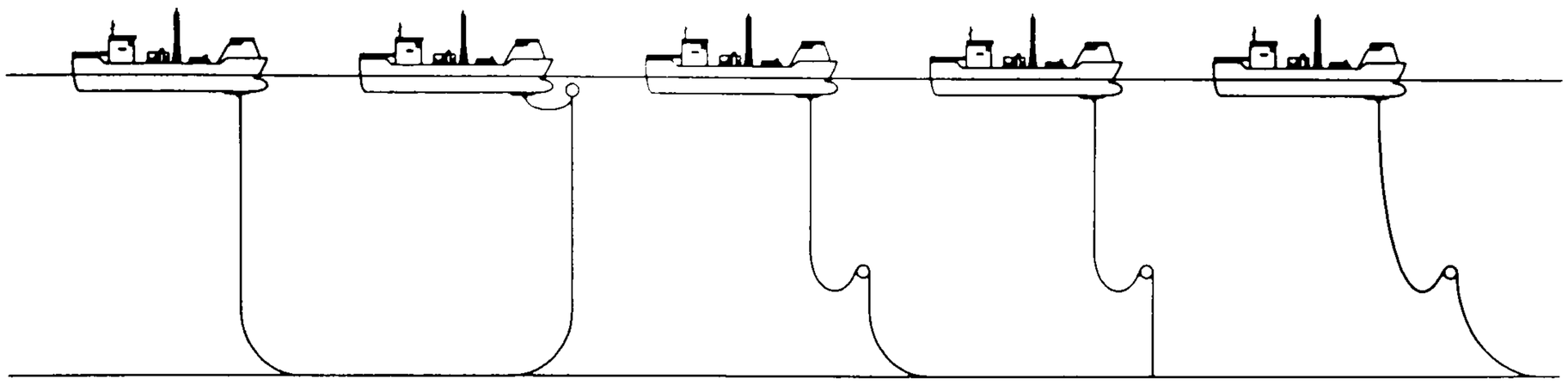

Figure 1.3 – Riser Shapes

Overcoming each of these challenges places an additional cost of development, installation and operation on the asset. Costs for a riser system operating in 350m to 500m of water depth in the North Sea have been quoted at between $20 million to $30 million (Das *et al.*, 1999). The costs for such riser systems are largely dependent on the environmental conditions, water depth, number of risers, duty and vessel motion (Fairhurst and Hassanein, 1997). As production shifts towards more harsh environments in deeper waters, see Figure 1.2, it is predicted that flexible riser systems will become very expensive and the capabilities of flexible pipe technology will begin to approach their limits (Fairhurst and Hassanein, 1997). It is vital to be able to correctly predict the characteristics of flexible risers for effective design of these application-critical components for a given set of operation conditions.

1.3.2 Severe Slugging in Flexible Risers

As stated above, one outstanding challenge in flexible risers is the prediction of the hydrodynamic behaviour of the riser system. The maintenance of steady delivery from the riser outlet and the minimisation of process upsets is one of the key issues of multiphase technology. One particular problem experienced in flexible risers at low-flow conditions is riser-induced severe slugging. This flow regime is particular to flowline-riser combinations and is characterised by: long periods of no fluid production; a period of pure liquid production at a low flow rate; a rapid increase in the liquid production, followed by a large, fast moving liquid mass, containing significant amounts of gas; and finally a period of high gas delivery, completing the cycle. Figure 1.4, after Schmidt *et al.* (1985), shows a hypothetical fluid production cycle from vertical riser during severe slugging.

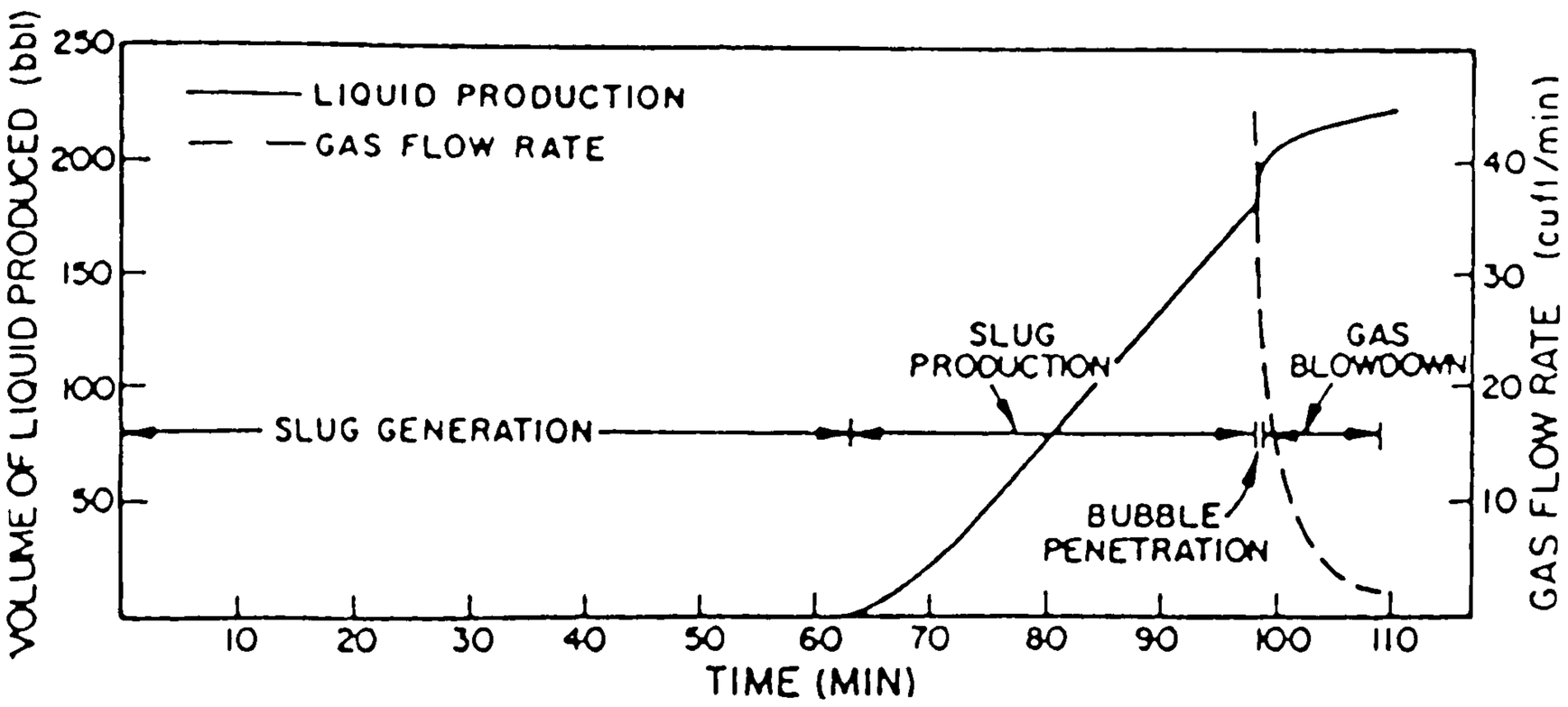

Figure 1.4 – Fluid Production During Severe Slugging
(After Schmidt *et al.*, 1985)

The large-scale movement of liquid and gas through the pipeline-riser poses the following process problems (Shotbot, 1986; Hill and Wood, 1994; Das *et al.* 1999) in terms of the generalised multiphase production issues:

1. Increased backpressure (Energy) - During the severe slugging cycle, the riser fills and empties, associated with this is a fluctuating hydrostatic liquid head. This leads to an increased average backpressure at the wellhead, reducing the overall fluid production. Yocum (1973) reported possible production reductions of 50%. In some cases this may be severe enough to 'kill-off' or stop all production from the well.
2. Increased mechanical wear (Integrity) - Two mechanisms increase the mechanical wear during severe slugging. The first is the fluctuating weight of liquid in the riser as the riser empties and fills, placing loads on the pipework and supports. The second mechanism is a more localised form of loading. As the slugs move around bends or impact on obstructions, momentum change induces additional local loading.
3. Large flow variations (Delivery) - Fluid handling systems must be able to receive and control the fluids as they arrive for processing. During severe slugging, large liquid and gas deliveries can cause high-level alarms, high pressure trips, unnecessary flaring/venting and overloading of the gas compressors. If there is no liquid production, there may be gas carry-under into the liquid handling process and low-level trips. Finally, during the period of no fluid production the gas compressors stall, causing trips in the gas handling process (Fairhurst, 1999).

Given these potential challenges posed by severe slugging in a flowline/riser combination, the characterisation for control or prevention of severe slugging is a highly necessary undertaking.

1.4 Research Objectives

The objectives of this work are quantifying and the understanding of the characteristics of severe slugging from experiments. From this starting point, it is intended to develop a better understanding of the mechanisms and hence the limiting conditions for severe slugging in a flexible riser. Finally, the experiments will provide a series of test conditions for the assessment of the ability of transient multiphase codes to predict severe slugging and other unstable flows in a pipeline riser.

1.5 Thesis Structure

This work has been divided into three primary research strands - experimental, flow stability and transient code investigations - and is broken down as follows:

Chapter 2 details previous investigations of severe slugging, the basic phenomenon of severe slugging, offshore experience and efforts on modelling severe slugging using specific models and generalised transient codes. At the end of this chapter the research objectives will be restated in a more technical manner, based on the literature review.

Chapter 3 details the experimental facilities, techniques and experimental conditions. The results of these experiments are presented in Chapter 4.

Chapter 5 details a model for the occurrence of severe slugging in an s-shaped riser, comparing the results of predictions with experimental results.

Chapter 6 describes the specification of a model for the pipeline/riser system and the comparison of transient simulation results against a series of experimental data points, representing a range of flow regimes.

Finally, Chapter 7 brings this work to a close, discussing the general findings and proposing future avenues for further work.

Chapter 2 – Literature Review

A review of the existing literature on severe slugging is presented in this chapter. The first section deals with the experimental investigations of severe slugging in a vertical riser. The steady-state models that have been developed to predict the occurrence of severe slugging are presented in the second section. The third section presents work carried out on the control of severe slugging. The application of a commercial transient multiphase flow code to predicting the characteristics of severe slugging is presented in the fourth section. Section five presents a more detailed review of work on severe slugging in a flexible riser. Section six addresses the similarities and differences between severe slugging and generalised terrain slugging. Finally, Section seven completes this chapter by identifying outstanding issues and the objectives of the present work.

2.1 Severe Slugging in a Pipeline/Riser System

Initial research on severe slugging focused on determining the mechanism and general characteristics of severe slugging in a pipeline/riser system. Further investigations focused on experimental observations of the effect of severe slugging on fluid production. As with many other multiphase flow regimes, there is a continuous transition from stable flows (such as slug and bubble flow) to severe slugging as gas and liquid superficial velocities change. In an effort to understand the mechanism of severe slugging these transitional flow regimes have been studied.

2.1.1 Severe Slugging Mechanism

Schmidt (1977), as part of the Tulsa University Fluid Flow Projects (TUFFP), first identified severe slugging during experiments on a 50.8mm i.d. pipeline-riser combination, using air and kerosene as test fluids. The system consisted of 30.5m (100') long pipeline, inclined at -2° to the horizontal, and 15.25m (50') high vertical riser. Investigations found that two forms of slug flow occurred in the riser - normal hydrodynamic slugging and severe slugging, also termed terrain-induced slugging (Schmidt *et al.*, 1980, 1981). Hydrodynamic slugging in the riser was due to the propagation of slugs formed in the pipeline, entering the riser base and continuing through the riser (Schmidt *et al.*, 1981). Severe slugging consisted of an entirely different mechanism, based around the formation and spontaneous removal of a large liquid column in the riser.

Severe slugging was characterised by slugs whose lengths were greater than or equal to one riser height (Schmidt *et al.*, 1980) and a maximum hydrostatic pressure at the riser base equivalent to the total height of the riser. This flow regime was found to be characteristic of low inlet gas and liquid flows, as shown on the flow regime map generated from experiments, Figure 2.1 (after Schmidt *et al.*, 1980).

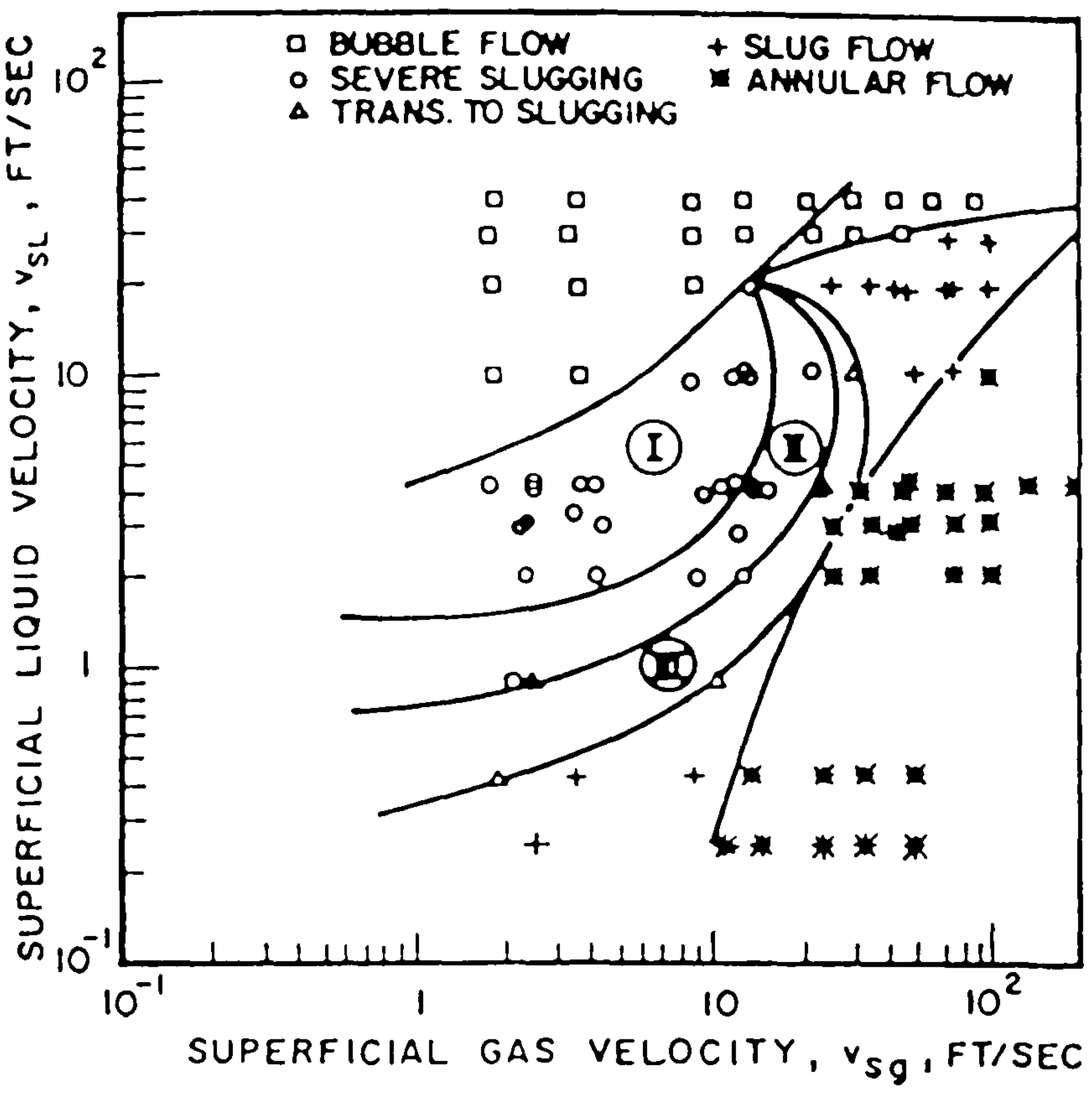

Figure 2.1 – Flow Regime Map for Vertical Riser Severe Slugging
(Schmidt *et al.* 1980)

The riser base pressure trace over time identified the severe slugging process in the riser. From these measurements, the severe slugging cycle was split into the following stages (see Figures 2.2 and 2.3):

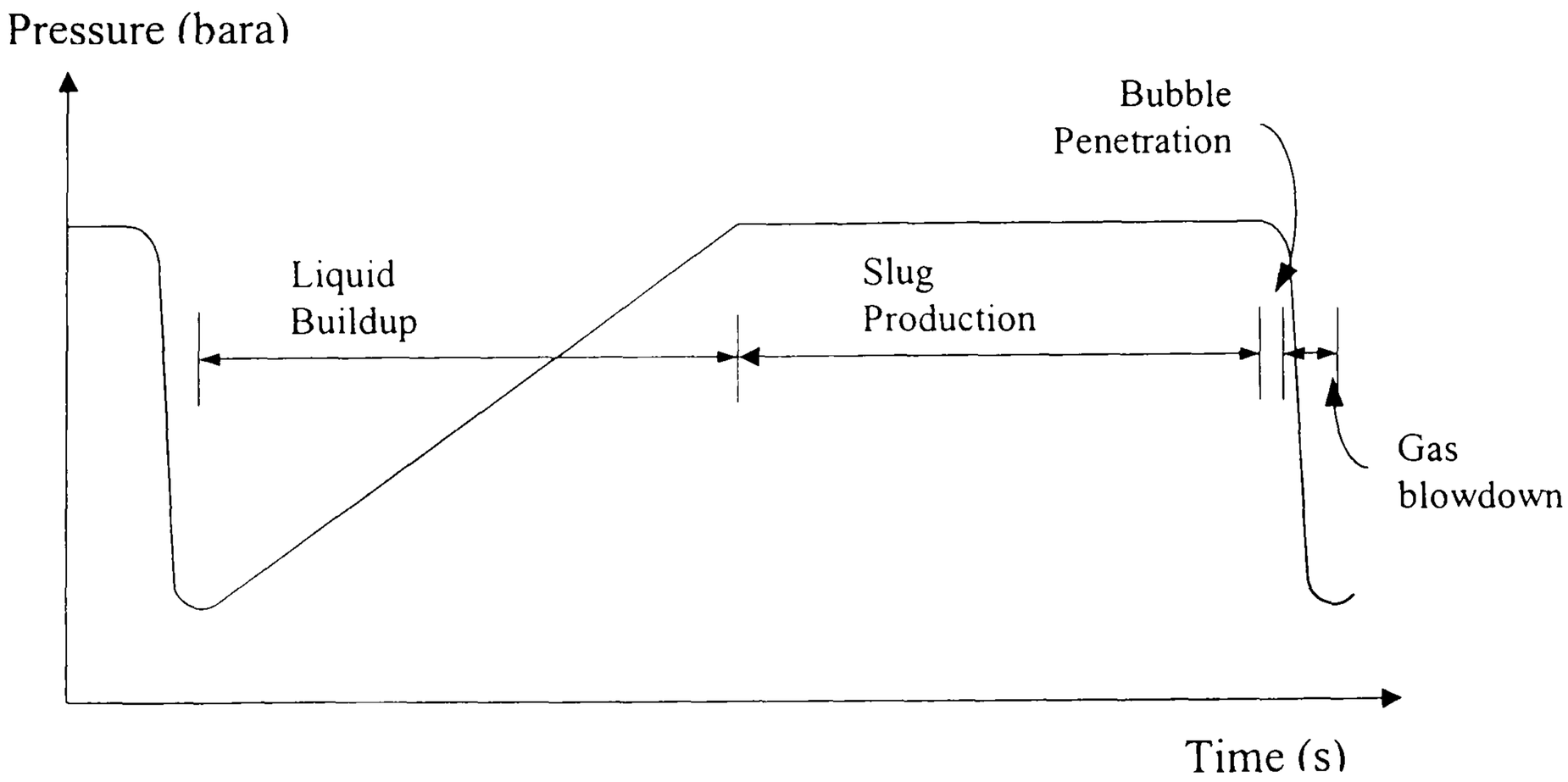

Figure 2.2 – Riser Base Pressure During Severe Slugging

1. Liquid Buildup - at the start of the cycle, liquid accumulation in the riser base blocks the pipe cross-section to gas flow. Initially, the net pressure difference across the accumulated liquid mass is unable to move the liquid from the riser base into the riser and clear the blockage. The stratified flow of liquid from the pipeline continues the accumulation of liquid at the riser base, causing the liquid level in both the pipeline and riser to increase. Gas accumulation acts against the increase in hydrostatic head buildup at the riser base and resists the liquid backing up the pipeline. This causes the preferential accumulation of liquid in the riser, see Figure 2.3 (a). The liquid buildup stage continues until the liquid in the riser reached the top of the riser and the outlet to the separator.
2. Slug Production - once the liquid reaches the top of the riser, the hydrostatic head at the base of the riser stops increasing, Figure 2.2. The gas accumulation in the pipeline continues and starts to move the accumulated liquid in the pipeline into the riser. This pushes the gas-liquid interface towards the riser base, see Figure 2.3 (b). The bulk movement of liquid in the pipeline gives a corresponding flow of liquid out of the riser into the separator, forming the liquid body of the slug. The slug production stage ends once the gas-liquid interface in the pipeline reaches the riser base.
3. Bubble Penetration - as the gas-liquid interface reaches the riser base, the gas continues to push liquid into the riser. Proceeding around the bend at the riser base, the gas-liquid interface forms a bubble front, similar to a large Taylor bubble, Schmidt *et al.* (1980) and Moe *et al.* (1989). The motion of the bubble up the riser, reduces the hydrostatic head at the riser base, accelerating the gas into the riser. Bubble penetration is also the beginning of the production transient (Schmidt *et al.*, 1985). As the bubble moves further into the riser, it forms a continuous gas cap, see Figure 2.3 (c).
4. Gas Blowdown and Liquid Fallback - as the gas-cap goes up the riser, the drop in pressure at the riser base accelerates the gas flow into the riser. Blowdown of the system occurs after the bubble has substantially moved into the riser. Gas blowdown is characterised by the sweep-out of all remaining liquid in the riser by the gas and the subsequent delivery of the accumulated gas from the pipeline, Figure 2.3 (d). As the liquid column in the riser is swept out, a thin liquid film is left on the riser walls, which is depleted by the gas flow over time. When the pipeline pressure reaches the minimum, the gas velocity reduces and the liquid film, present during blowdown begins to fall back towards the riser base (under counter-current annular flow conditions). This liquid fallback accumulates at the riser base and blocks the cross-section to gas flow for the next cycle to begin.

This is the basic process of severe slugging that has been reported by a number of authors in offshore applications, Hill (1987), Barbuto and Caetano (1993), McGuinness and Cooke (1993), Courbot (1996) and Larsen and Hedne (2000).

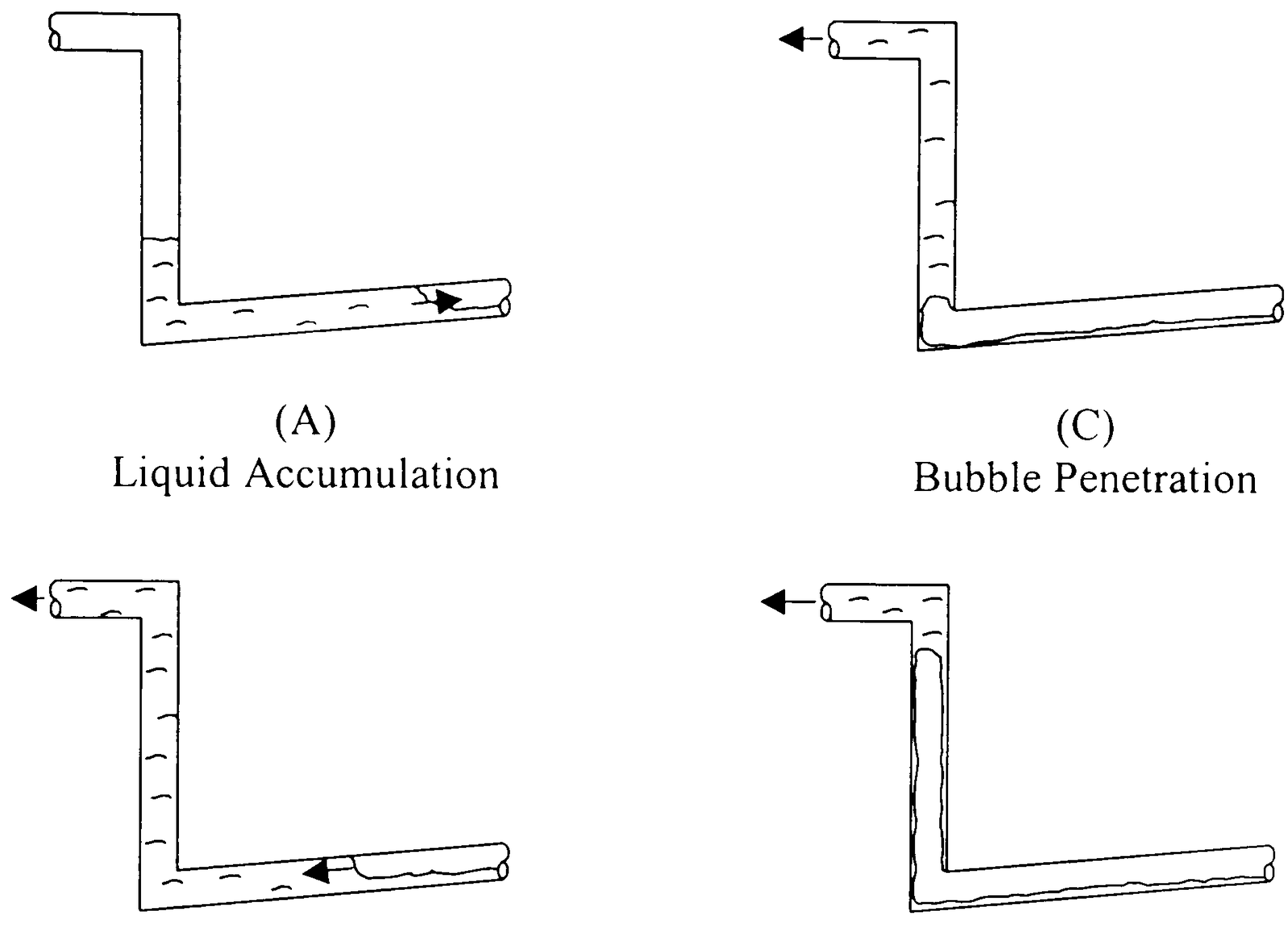

Figure 2.3 – Stages of Severe Slugging

The accumulation of liquid at the riser base is directly attributable to the inclination of the pipeline. A downward-inclined pipeline is a condition for the occurrence of severe slugging, this was confirmed through experiments by Pots *et al.* (1985). In field applications a downward pipe inclination is a consequence of the sub-sea terrain local to the riser base, for this reason severe slugging has been termed 'terrain-induced slugging', Lund (1987) and Fuchs (1987).

'Stalling' Mechanism for Severe Slugging

An alternative mechanism for severe slugging was identified by Linga (1987) in experiments in the SINTEF test facility in Norway. The observed severe slugging was caused by the deceleration of a terrain slug train, formed in the upstream pipeline, as it approached the riser base. Upon arrival at the riser base, the slug train slowed to a halt and gas re-distribution occurred. This formed a single slug at the riser base, starting the slug accumulation in the riser. This gradually built up with the arrival of further slugs until the riser was filled with liquid. As the final slug train approached the riser, the gas trapped between the train and the slug in the riser was compressed, moving the slug tail towards and through the riser base, inducing gas blowdown. The compression of the gas in the pipeline acted as a retarding force on the arriving slug train, beginning the cycle again. This 'stalling' of slugs at the riser base to form a severe slug has been observed in field applications (Fairhurst, 1999), however there have been no further details of this mechanism in the open literature.

2.1.2 Fluid Production Characteristics

As discussed in Chapter 1, a major effect of severe slugging is the variation in fluid delivery. Knowledge of the phase velocities is important in addressing 'Integrity' and 'Delivery' issues as defined previously. In terms of fluid production, there has been little direct measurement of the flow of liquid or gas from the riser outlet. In some part, this is due to the intrinsic difficulty of direct measurement of the multiphase flow, to do so requires either an accurate multiphase meter or an instrumented separator volume to measure the flowrate of each phase. Hill (1987) presented results for the total amount of liquid produced during severe slugging in a 15m high, 50.8 mm i.d. riser, connected to a 50 m pipeline, using air and water. Referring to Figure 2.4 after Hill (1987), during the liquid buildup stage there was no liquid production, reflected by no change in the total volume produced. As the liquid reached the top of the riser, liquid began to flow at a constant rate, giving a steady increase in the mass produced. Bubble penetration started the acceleration of the liquid from the riser outlet, causing an increase in the slope of the produced volume graph. Gas blowdown caused a large increase in the slope of the produced liquid graph, reflecting the jump in produced fluid velocity. A subsequent tail-off occurred as the accumulated liquid in the pipeline and riser was depleted, leading to a flattening of the produced liquid plot. The blowdown period also caused a discontinuity or 'jump' in the produced volume trace.

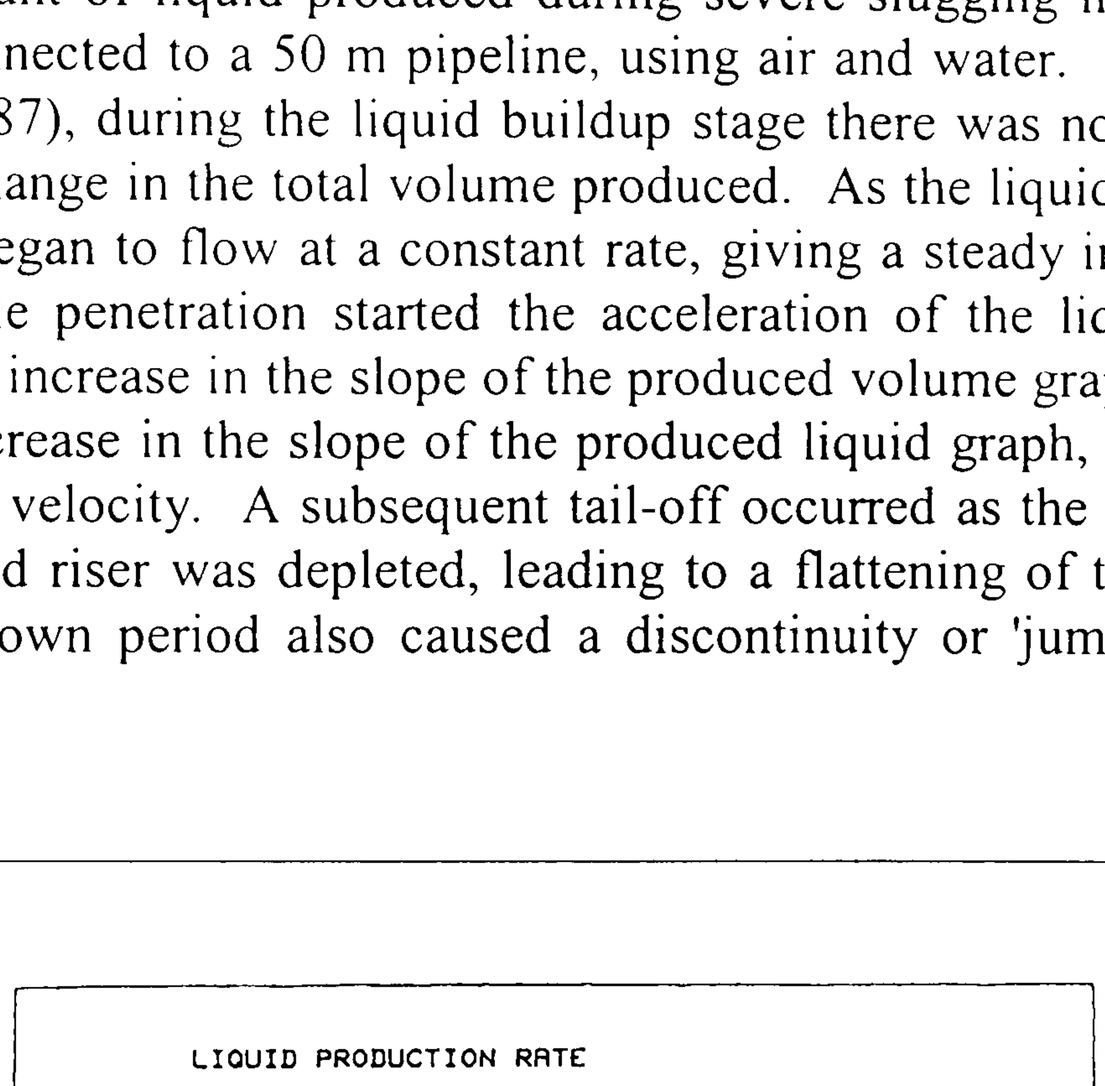

Figure 2.4 – Liquid Production During Severe Slugging
(After Hill, 1987)

The results of Hill (1987) for the liquid volume produced agreed qualitatively with earlier simulation results presented by Schmidt *et al.* (1985), see also Section 2.3. However, there was no direct comparison between the Schmidt *et al.* (1985) model and experimental data. To date, there have been no measurements made of gas production characteristics. The importance of this measurement has been highlighted by the findings of Shotbot (1985) and Fairhurst (1999). They have observed that high rates of gas delivery occurring during severe slugging have the potential to cause process upsets, particularly high pressure and low level trips in topsides separators.

Larsen and Hedne (2000) presented some data for liquid production rate during severe slugging for the Gannet field. This was aimed at validating the transient code PeTra, see Section 2.3. In this case the measured liquid production rate showed a period of no liquid production, followed by an erratic period of liquid flow from the riser outlet, i.e. severe slugging without a period of constant liquid production, transitional severe slugging.

2.1.3 Transitional Flows

Aside from the 'classical' severe slugging mechanism first identified, Schmidt *et al.* (1980) also reported an additional flow regime 'transition to severe slugging' and denoted it Severe Slugging Type II. This was characterised by intermediate penetration of the riser base by gas bubbles. Thus the riser was not completely filled with liquid during the cycle and the maximum hydrostatic head experienced was less than during 'classical' severe slugging (Severe Slugging Type I). Transition to severe slugging was observed at higher gas flows than Severe Slugging Type I. Visually the flow regime resembled normal slug flow, but sections of the riser continuously emptied and filled in an unstable manner.

Linga (1987) classified flow in a pipeline/riser system using three main divisions: continuous flow, transitional flow (with occasional severe slugs) and severe slugging. The severe slugging experienced was further classified as:

- Severe Slugging Type I – blockage at the riser base consists entirely of liquid
  - Type IA – the liquid slug reaches the top of the riser before blowdown
  - Type IB – the liquid slug is blown out prior to filling the entire riser
- Severe Slugging Type II – liquid blockage at the riser base is aerated.

Taitel *et al.* (1990) considered the bubble penetration stage of the severe slugging cycle when classifying severe slugging. Following bubble penetration, three possibilities were observed:

- Cyclic operation of the riser without fallback
- Cyclic operation of the riser with fallback
- Oscillation of the gas flow into the riser base, leading to stable flow

The cyclical operation with fallback included Severe Slugging Type I. These cycles were initiated by the inability of the gas to move liquid accumulated at the riser base due to fallback. Cyclic operation without fallback covered transitional flows where there was continuous movement of fluids through the riser base, cycles were initiated by the interaction of each phase as they moved up through the riser. This corresponds to Severe Slugging Type II above. The last of these corresponds to the actual

transition from cyclic operation to stable flow. Thus according to Taitel *et al.* (1990), the behaviour of the fluids at the riser base dictated the overall riser behaviour.

2.2 Steady-State Modelling of Flow Stability

To date, the modelling of severe slugging has sought to answer two basic questions: 'When will severe slugging occur?' and 'What are the characteristics of the severe slugging?' Experiments described thus far have addressed the second question. In order to answer the first of these questions steady state models are often used. These seek to model a particular process required for severe slugging and hence predict the likelihood of severe slugging; as such these models are termed criteria for severe slugging. Figure 2.5 shows the geometry used for the models presented in this chapter. The results of the criteria form a region of a flow regime map, indicating the region of severe slugging. Figures 2.6-2.9 contain examples of these plots for a model system.

The work by Schmidt *et al.* (1980) formed the basis of much of the early work, they suggested that three conditions were required for severe slugging:

- a downward inclined flowline (later confirmed by Pots *et al.*, 1985)
- stratified flow in the pipeline
- the rate of hydrostatic head accumulation at the riser base being greater than the rate of pipeline gas pressure increase.

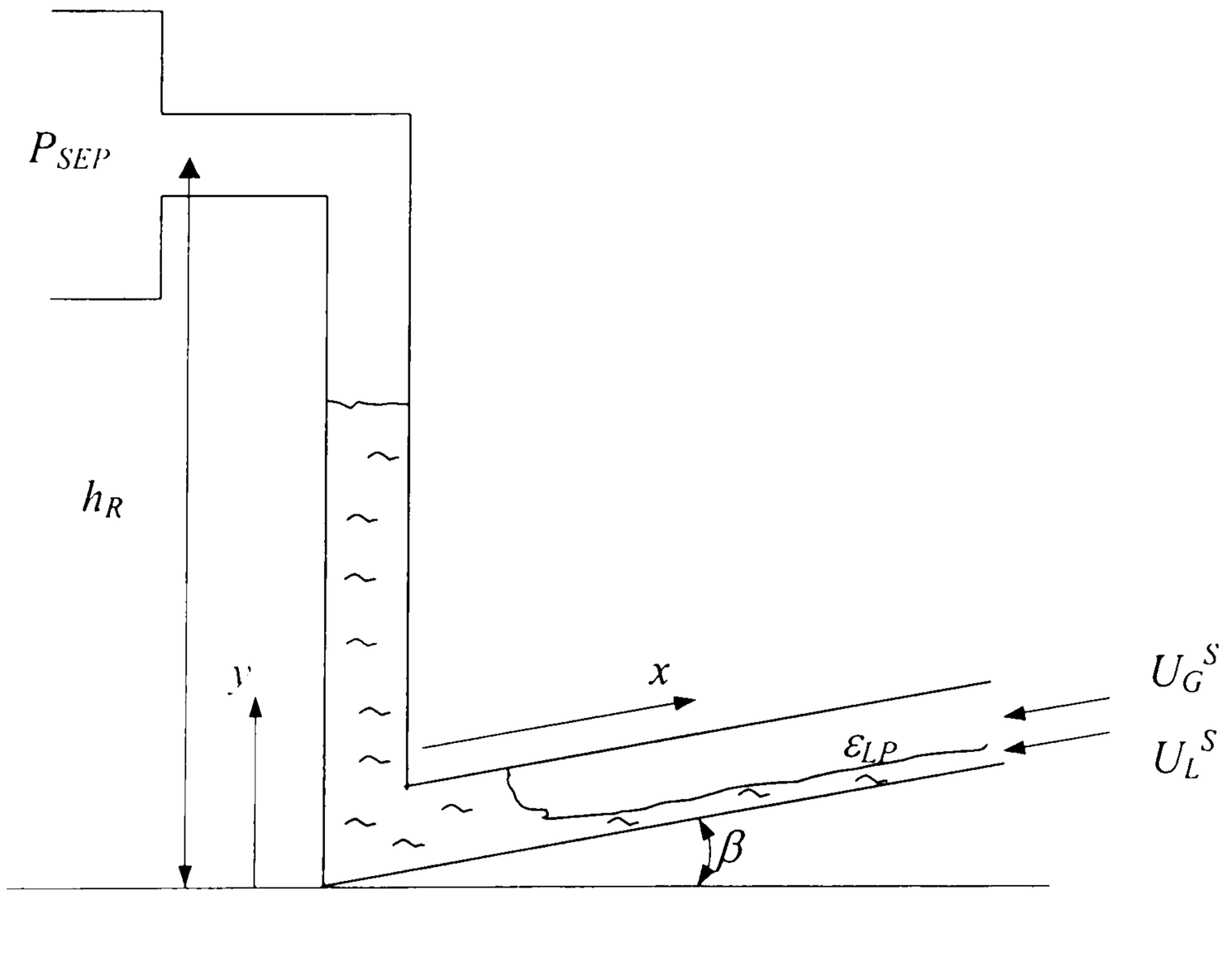

Figure 2.5 – Geometry Used for Pipeline/Riser Models

2.2.1 The Stratified Flow Criterion

Starting with the Schmidt *et al.* (1980) assertion that for severe slugging to occur, stratified flow must be present in the main flowline, previous work by Taitel and Dukler (1976) is employed as the first criterion for severe slugging flows. Taitel and Dukler (1976) developed a criterion for stratified flow in horizontal and near-horizontal pipeline. Though this criterion was not explicitly developed as a severe slugging criterion, it has been used by many authors (Bøe 1981, Pots *et al.* 1985, Taitel 1986 and Barbuto 1993). Using the inviscid Kelvin-Helmholtz theory (Milne-Thompson, 1960), the condition for small wave growth between parallel plates was:

$$U_G^S > \left[\frac{g\left(\rho_L - \rho_G\right)h_G}{\rho_G}\right]^{\frac{1}{2}} \qquad (2.1)$$

where U is velocity, ρ is density and h is height occupied by a given phase between the plates. Note that the subscripts L and G refer to the gas and liquid phases respectively. Below the gas velocity prescribed in Equation (2.1), stratified flow occurs and hence severe slugging is possible in the pipeline/riser. Equation (2.1) was extended to flow in a circular cross-section, taking into account the suppression of the wave formation by gas acceleration over the wave crest. This yields a criterion for stratified flow:

$$U_G^S < C_2\left[\frac{(\rho_L - \rho_G)g\cos\beta\ A_G}{\rho_G\ dA_L/dh_{LP}}\right]^{\frac{1}{2}} \qquad (2.2)$$

where $C_2 \approx A_G/A_L$. A is the flow area, α is the angle of inclination and h is the height of the phase occupying the pipe cross-section. The change in liquid flow area with liquid height dA_L/dh_L is given by Taitel and Dukler (1976) as:

$$\frac{dA_L}{dh_L} = D\sqrt{1-\left(2\frac{h_L}{D}-1\right)^{\frac{1}{2}}} \qquad (2.3)$$

Goldzberg and McKee (1987) considered the formation of slugs in a pipeline dip through the sweep-out of accumulated liquid. The approach centred on a criterion for wave growth to form a slug as gas accelerated over the interface. The analysis of the Bernoulli equation over the surface reduced to Equation (2.2) above. It is worth noting at this time that the applicability of this criterion is somewhat questionable given that Lund (1987) found that pipeline slug flow can also cause severe slugging.

An example plot of this criterion is given in Figure 2.6, the region of stratified flow is the region below the transition line (indicated).

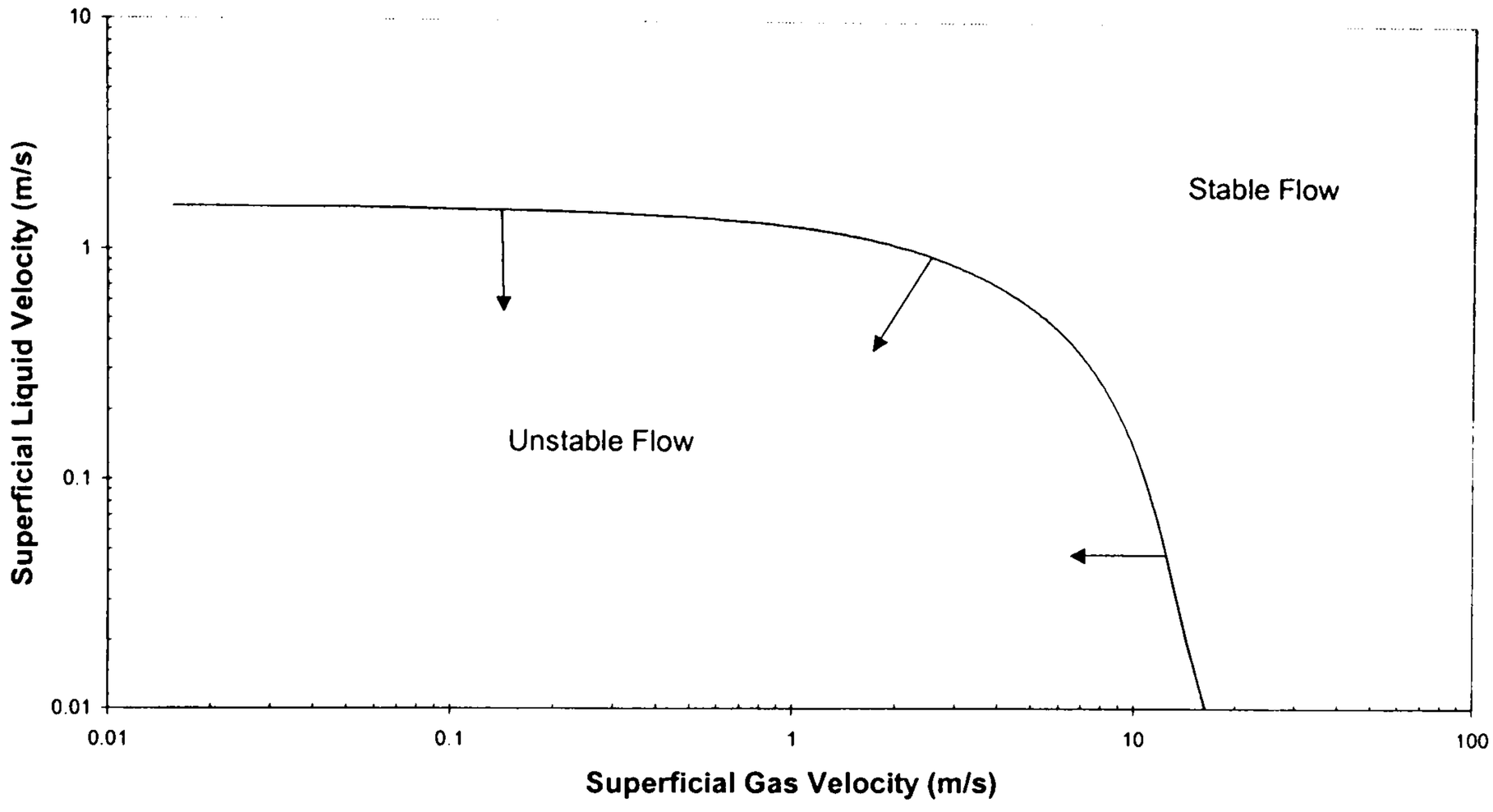

Figure 2.6 – Taitel and Dukler (1976) Stratified Flow Criterion

2.2.2 The Bøe Criterion

Bøe (1981a) developed a criterion for severe slugging based on the assertion of Schmidt *et al.* that the rate of head accumulation at the riser base must be greater than the rate of pipeline gas pressure increase for a severe slug to form. This may be summarised as:

$$\frac{\partial(\Delta P_{HYD})}{\partial t} > \frac{\partial(P_P)}{\partial t} \qquad (2.4)$$

where P is the pressure and t time, the subscripts HYD and P refer to the hydrostatic and pipeline pressures respectively. Based upon constant inlet flowrates, a pressure balance over the riser and the gas mass balance in the pipeline, the criterion, Equation (2.4) was resolved to give:

$$U_L^S \geq \frac{P_P}{\rho_L g(1-\varepsilon_L)L\sin\alpha} U_G^S \qquad (2.5)$$

Note that here that α, the inclination of the riser is included. For a vertical riser sin α = 1. In the initial work by Bøe, the no-slip condition for the pipeline liquid holdup was used:

$$\varepsilon_L = \frac{U_L^S}{U_L^S + U_G^S} \qquad (2.6)$$

This, coupled with Equation (2.5), yielded a straight line, above which severe slugging occurred, see Figure 2.7. Other correlations for the liquid holdup yield an envelope region where severe slugging would take place. The most common correlation employed is that suggested by Taitel (1986), using liquid velocity to calculate first the single phase gas pressure drop, and then relating this to the liquid holdup. Further details of this correlation are presented in Appendix E. Results for the Bøe criterion using this correlation are also presented in Figure 2.7, the arrows showing the region of unstable flow to the left of the transition lines.

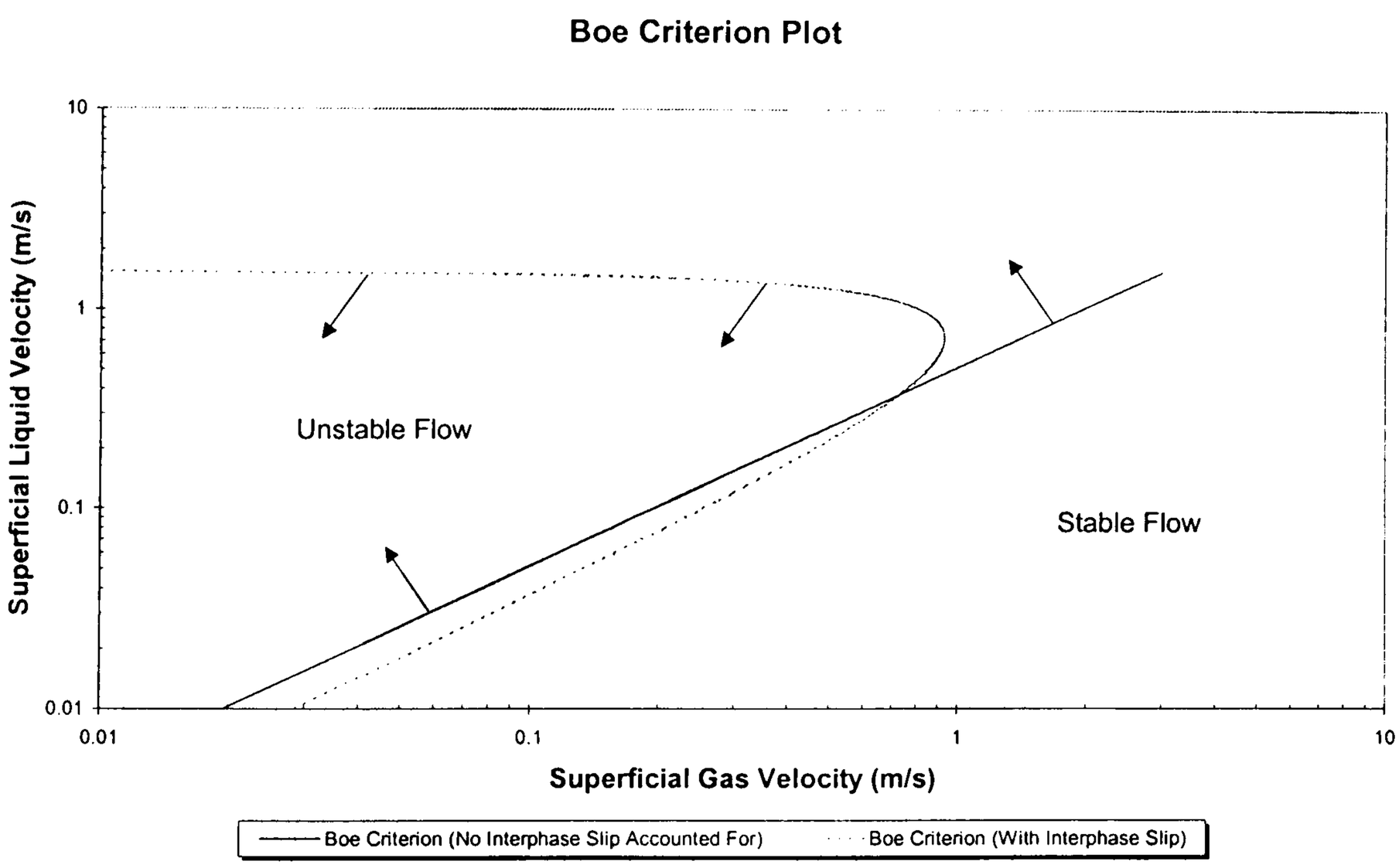

Figure 2.7 – Bøe (1981) Criterion

2.2.3 The Π_{SS} Criterion

Pots *et al.* (1985) again considered the liquid buildup stage of severe slugging and presented a criterion based upon the rate of hydrostatic head buildup in the riser and the accumulation of gas in the pipeline. They assumed that all liquid entering the flowline went into forming the severe slug in the riser. This analysis gave a condition:

$$\Pi_{SS} = \frac{ZRT/M_W}{g\varepsilon_L L}\frac{G_G}{G_L} \qquad (2.7)$$

where severe slugging would occur if and only if $\Pi_{SS} < 1$. In Equation (2.7) Z is the compressibility of the gas, M_w is the molecular weight of the gas and G is the mass flowrate. Pots *et al.* (1985) also used the value of Π_{SS} to denote the 'degree' of severe slugging, i.e. to quantify the severity of the slugging with a lower Π_{SS}, giving more severe (larger) slugs. Equation (2.7) reduces to the Bøe criterion when stated in terms of velocity and pressure, however it is important to note that implicit in Equation 2.6 is the fact that the riser is vertical, i.e. sin α = 1. Figure 2.8 gives sample plots for the Π_{SS} criterion, with ε_L being calculated using the no-slip condition and the Taitel (1986) correlation.

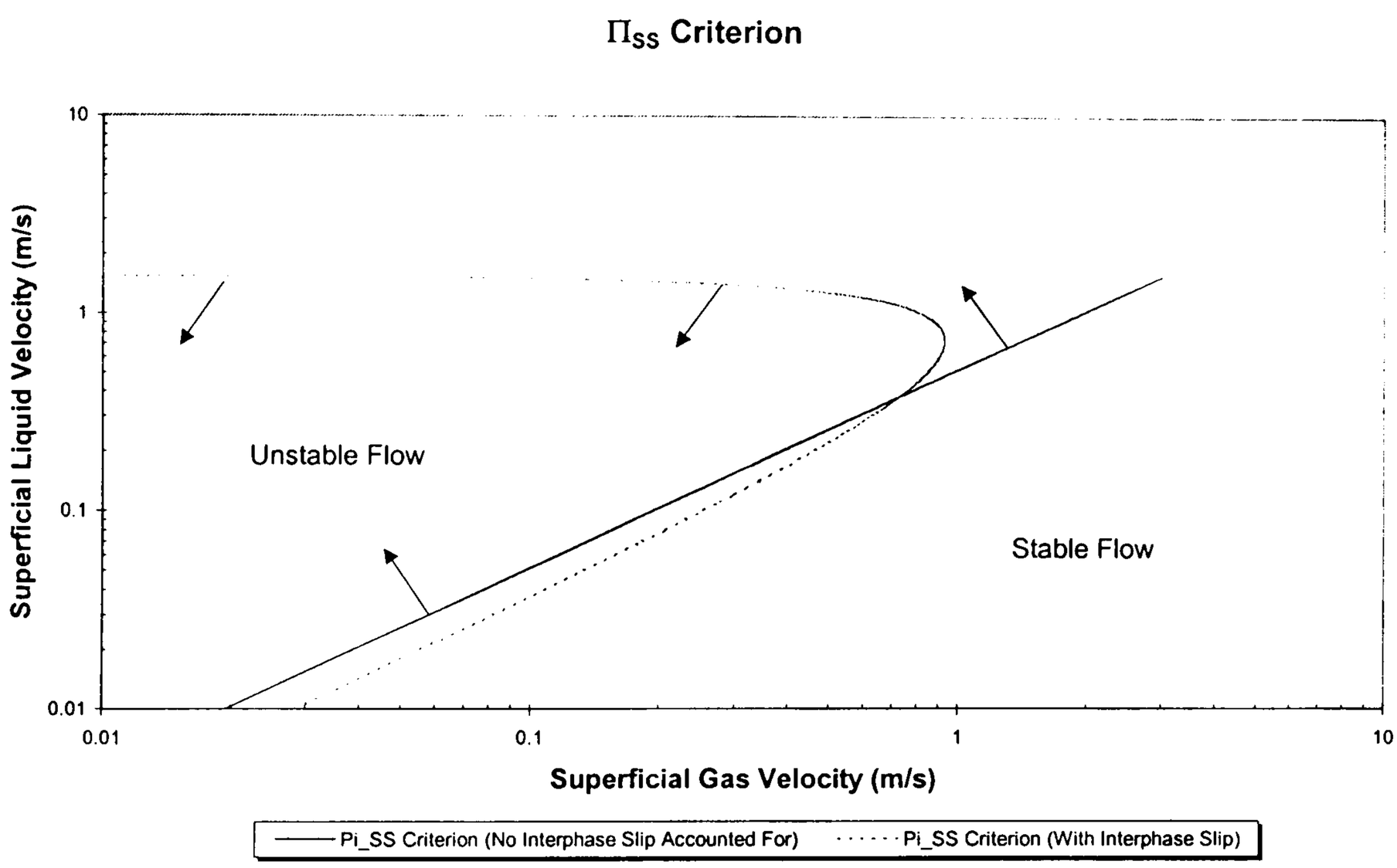

Figure 2.8 – Π_{SS} Criterion

2.2.4 The Taitel Criterion

The Taitel (1986) criterion is based on considerations of the blowdown of the pipeline/riser. The aim of this criterion was to quantify the effect of separator pressure on the likelihood of severe slugging. In the analysis Taitel supposed that in order for blowdown to occur, the liquid column in the riser must be unstable. Such an unstable column was spontaneously blown-out of the riser as soon as Taylor bubbles penetrated the riser base. Taitel showed that the condition for instability was:

$$\frac{\partial(\Delta F)}{\partial y} > 0 \qquad (2.8)$$

For $y = 0$. ΔF is the force difference over the riser as a bubble penetrates the riser base. Note that in the original work, the criterion was for stable flow an hence the inequality was reversed. A force balance over the liquid column was given as:

$$\Delta F = \left[\left(P_S + \rho_L g\, h_R \right) \frac{\varepsilon_{GP} L}{\varepsilon_{GP} L + \varepsilon'_G L} \right] - \left[P_S + \rho_L g \left(h_R - y \right) \right] \qquad (2.9)$$

where ε_G' is the gas holdup immediately behind the penetrating Taylor bubble front. Combining Equations (2.8) and (2.9) gives the final form of the criterion (when referenced to atmospheric conditions):

$$\frac{P_S}{P_0} < \frac{\left(\varepsilon_{GP} / \varepsilon'_G \right) L - h_R}{P_0 / \rho_L g} \qquad (2.10)$$

Examining Equation (2.10), most of the parameters are specified by the pipeline/riser geometry and operating conditions. The remaining variables are the gas holdup in the pipeline and behind the bubble front. Taitel assumed that the gas holdup in the bubble tail is a constant 0.89 for vertical flow. Thus, in order to plot the results on a flow regime map, an expression for the pipeline gas holdup, ε_{GP}, is required. Taitel (1986) provided the correlation for gas holdup as a function of the inlet liquid velocity.

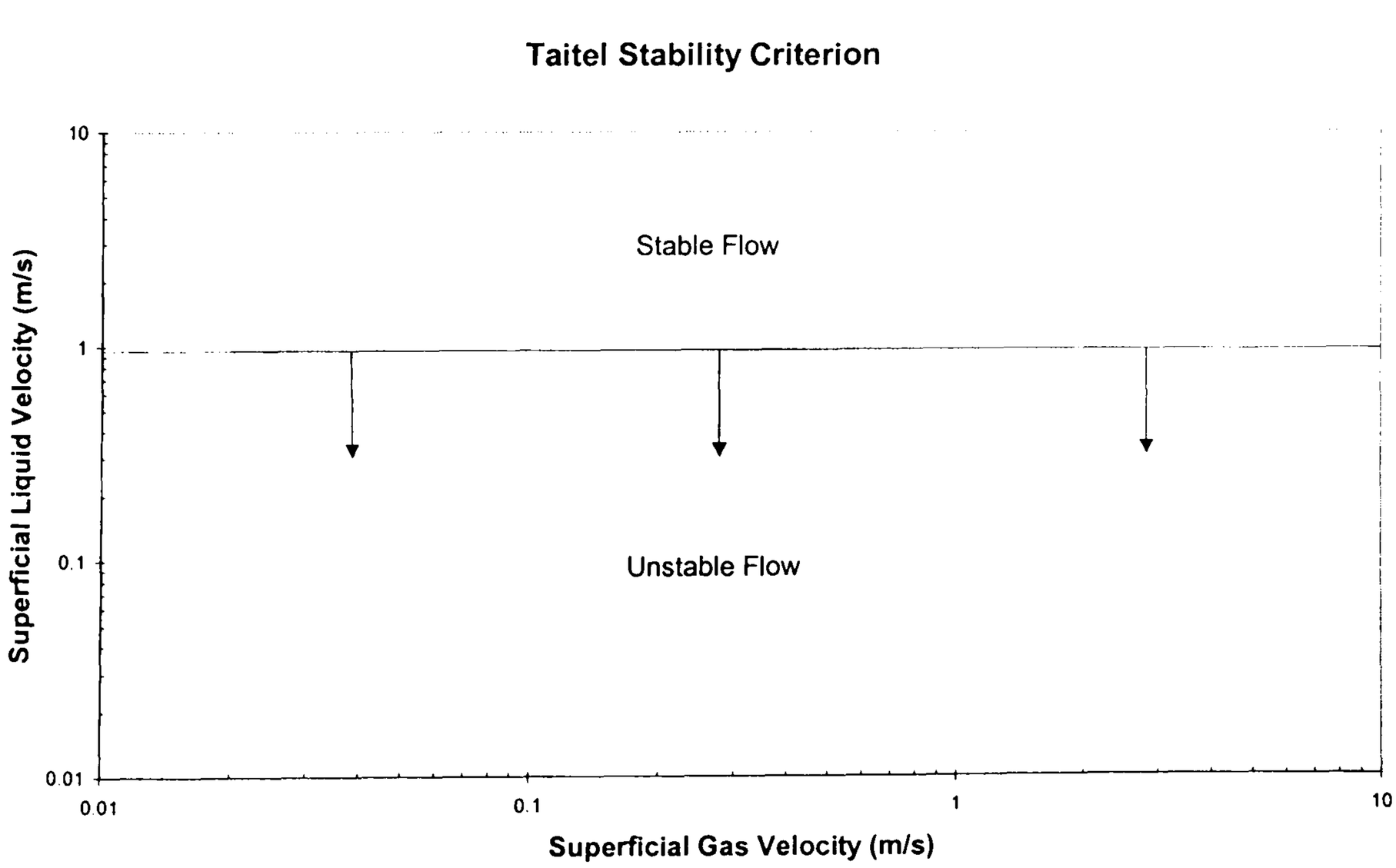

Figure 2.9 – Taitel (1986) Criterion

Using this correlation, the Taitel criterion becomes a function of the liquid velocity only. As only a single value of ε_{GP} is obtained for any given separator pressure, the

Taitel criterion gives a single limiting liquid velocity for severe slugging, see Figure 2.9. Taitel also modified the criterion to account for non-zero gas fraction in the body of the slug, taking this fraction as ε_{SL}, Equation (2.10) became:

$$\frac{P_S}{P_0} < \frac{\varepsilon_{SL}\left[(\varepsilon_G/\varepsilon'_G)L - h_R\right]}{P_0/\rho_L g} \qquad (2.11)$$

In the reported work, Taitel (1986) showed the successful application of the developed criterion to data collected by Schmidt *et al.* (1980).

2.2.5 Fuchs' Pressure Criterion

Fuchs (1987) developed a criterion based upon considerations of the 'release' of a severe slug, equivalent to the blowdown of the riser. The basic form of the criterion for the acceleration of a gas bubble entering the riser base was:

$$\frac{d\left(P_U - P_D\right)}{dt} > \frac{d\left(\Delta P_{HYD}\right)}{dt} \qquad (2.12)$$

In this equation, the subscripts U and D refer to upstream and downstream conditions, at points removed from the riser. In certain cases these can be approximated by the pipeline and separator conditions, see Fuchs (1987). Differentiating the mass balances on the upstream and downstream volumes, V_U and V_D, the left hand side of Equation (2.12) was resolved. Using the Ideal Gas Equation of State (EOS), the pressure change was related to changes in the mass of gas and volume:

$$\frac{dP_U}{dt} = \frac{P_U A}{V_{GU}}\left[\left(U^S_{GP} - U^S_{GR}\right) + \left(U^S_{LP} - U^S_{LR}\right)\right] \qquad (2.13)$$

for the upstream gas and for the downstream gas:

$$\frac{dP_D}{dt} = \frac{P_D A}{V_{GD}}\left[\left(U^S_{GP} - U^S_{GR}\right) + \left(U^S_{LP} - U^S_{LR}\right)\right] \qquad (2.14)$$

The right hand side of Equation (2.12) was evaluated from considerations of the bubble penetration, giving:

$$\frac{d\left(\Delta P_{HYD}\right)}{dt} = -g\sin\alpha\left(\rho_L - \rho_G\right)\left(\varepsilon_L - \varepsilon'_L\right)\frac{dy}{dt} \qquad (2.15)$$

Combining Equations (2.13) to (2.15) and resolving in terms of the gas velocity entering the riser base (Fuchs, 1987) gave the final form of the criterion:

$$\frac{\left(\frac{P_S A}{V_{GU}}\right)+\left(\frac{P_P A}{V_{GD}}\right)}{g\sin\alpha\left(\rho_L-\rho_G\right)} < \frac{\varepsilon_L-\varepsilon_L'}{1-\varepsilon_L'}\,\frac{U_{GB}^S}{\left(U_{GB}^S+U_{LB}^S\right)-\left(U_{GI}^S+U_{LI}^S\right)} \qquad (2.16)$$

In Equation (2.16), the subscripts *GB* and *LB* refer to the gas and liquid entering at the riser base. The left hand side of Equation (2.16) is the characteristic severe slugging parameter for the system. The right hand side relates to the 'stiffness' of the system (Fuchs, 1987) and is an experimentally determined quantity, and as such reduces the applicability of the criterion. The exact values of the riser base velocities U^S_{GR} and U^S_{LR} were considered to be the maximum velocities experienced during the severe slugging process. Fuchs (1987) showed the equivalence of his approach with that of earlier workers, and showed under which assumptions this analysis reduced to those of Bøe (1981) and Taitel (1986).

2.3 Prevention and Control of Severe Slugging

In general, severe slugging mitigation and prevention strategies seek to prevent severe slugging by one of the following methods:

1. prevention of liquid accumulation or fallback at the riser base
2. imposition of stable flow in the riser through the application of backpressure from the separator

This section describes the techniques and results of control strategies applied pipeline/riser systems under severe slugging conditions.

2.3.1 Topsides Choking

Topsides choking was one of the first methods proposed for the control of severe slugging flows, Schmidt *et al.* (1980b). Choking, applied manually using a valve or an actuated valve, induced bubble flow or normal slug flow in the riser by increasing the effective backpressure at the riser outlet. This built upon the earlier work of Yocum (1973) who used a choke to control hydrodynamic slug flow in a vertical riser. Schmidt *et al.* (1985) described the mechanism by which choking controls severe slugging, particularly in the light of flow regime prediction. The increase of backpressure effectively prevents the spontaneous blow out of the liquid column in the riser by increasing the pressure drop through the riser relative to gas velocity. This in effect increases the retarding force acting on a bubble penetrating the riser, preventing it from accelerating to such a velocity as to cause blowdown of the pipeline/riser. In this way, either normal hydrodynamic slugging or bubble flow is induced.

In terms of implementation of this technology, Courbot (1996) reported the successful implementation of a topsides choke, based on feedback control from a measurement of the riser base pressure. Jansen *et al.* (1996) carried out a theoretical and experimental investigation of choking, modifying the Taitel (1986) criterion to account for the additional backpressure of choking. The backpressure upstream of the choke, P_{U}, was given by:

$$P_U = P_S + C\,U_L^{S\,2} \qquad (2.17)$$

where C is an experimentally determined parameter. As the gas bubbles penetrate the riser base, an incremental jump in the pressure upstream of the choke was incorporated into Equation (2.17), giving:

$$P_U - \left(P_S + C\,U_L^{S\,2}\right) = Ky \qquad (2.18)$$

where K is a constant of proportionality. Equation (2.18) was substituted into the pressure balance used in Taitel's (1986) analysis, so that with choking in operation, the criterion for severe slugging became:

$$\frac{P_S + C\,U_L^{S\,2}}{P_0} < \frac{\dfrac{\varepsilon_G L}{\varepsilon_G'}\left(1 - \dfrac{K}{\rho_L g}\right)}{P_0/\rho_L g} \qquad (2.19)$$

Predictions were compared against experimental data collected in a 25.4 mm vertical riser/pipeline rig, with the pipeline inclined at -1° to the horizontal, open to atmosphere. The results obtained compared favourably with the criterion predictions for different choke settings.

2.3.2 Riser Base Gas Injection

Gas lift in wells is a technique that has been employed since the 1950's to improve the well flow by reducing the mixture density, thereby increasing the flow along the production string and reducing backpressure seen by the well. Riser base gas injection is a development of gas lift that was first used to control hydrodynamic slugging in vertical risers (Schmidt *et al.*, 1981). In severe slugging control, gas-lift reduces the local mixture density, promoting upward flow and limiting liquid fallback. In turn this prevents the accumulation of a stagnant mass of liquid at the riser base that leads to severe slug formation.

Hill (1989) first described the application of riser base gas-lift to control severe slugging. Initial experiments in a 50 m long, 15 m high pipeline-riser of 50 mm i.d. at atmospheric pressure provided data on the application of gas-lift to severe slugging. These studies were used to predict the required quantity of gas for the full-scale operation. The gas-lift system was then installed on the offshore platform and proved to be successful in start-up conditions and in re-starting a well that had been 'killed-off' by the backpressure from the riser.

As part of the work described in the previous section on choking, Jansen *et al.* (1996) also investigated riser base gas injection. They extended the Taitel (1986) criterion for severe slugging to include steady-state gas injection into the riser base. This gave the criterion for severe slugging as:

$$\frac{P_S}{P_0} < \frac{(\varepsilon_{GP}/\varepsilon'_G)L - h_R}{P_0/\varepsilon_{GR}\rho_L g} \qquad (2.20)$$

where ε_{GR} is the void fraction in the riser due to the gas-lift, this is calculated using a simple bubble flow model:

$$\varepsilon_{GR} = 1 - \frac{U_{GR}^S}{U_{Bub}} \qquad (2.21)$$

$$U_{Bub} = C_0 U_M + U_D \qquad (2.22)$$

here C_0 is the drift parameter equal to 1.2 and U_D is the bubble drift velocity, $0.35\sqrt{gD}$. A quasi-equilibrium model was also developed to simulate the time-dependent nature of the flow, this model was based on the work by Taitel *et al.* (1990), see Section 2.4. Comparisons of these models were carried out against experimental data from a 25.4 mm i.d., 9.1 m long and 3 m high pipeline/riser rig. Experiments demonstrated the mitigation of severe slugging using gas lift. However it was found that large amounts of gas were required to eliminate pressure cycling altogether. Indeed Jansen *et al.* (1996) found that the flow in the riser must 'approach annular flow before steady riser flow is achieved'. The successful prediction of the severe slugging region and the severe slugging characteristics by the criterion and the quasi-equilibrium model was demonstrated.

2.3.3 Other Methods of Severe Slugging Control

Choking and riser base gas injection are two continuous control methods for severe slugging. However 'continuously acting' control methods may prove to be costly in the medium to long term, increasing CAPEX or OPEX and possibly leading to a reduction in overall production due to increased backpressure. Different methods for preventing severe slugging have focused on the balance between these three concerns.

One basic method of controlling severe slugging as described in the open literature was to prevent the multiphase flow in the pipeline/riser totally. The stabilisation of fluid production to a platform in Malaysia reported by McGuiness and Cooke (1993) serves as an example of this approach. This involved preventing any opportunity for severe slugging in the flowline/riser. Production from a satellite to the main platform was under severe slugging conditions, causing a 20% drop in production and high-liquid level and high-pressure trips in the production separator. The mitigation strategy was to separate the fluids on the satellite platform and export along individual pipelines, hence eliminating the opportunity for severe slugging.

Feedback control methods have been developed for the control of severe slugging to maximise the fluid production while minimising expenditure. Hollenberg *et al.* (1995) detailed an experimental method for severe slugging control that used an estimation of U_M, the mixture velocity, from the riser outlet as the basis for a control scheme. In order to measure the individual phase flowrates from the riser, a small

metering separator was installed immediately upstream of the main separator. The single phase gas and liquid outlet flows from this metering separator were metered, giving U_M. The level in the metering separator was controlled using a simple feedback mechanism to prevent liquid overflow. The U_M measurement was then used in a control loop that acted upon the main separator pressure and level controls, i.e. the outlet gas and liquid flows from the main separator. The entire pipeline/riser and separator system was initially modelled using the TRAFLOW computer code (see Section 2.4.2) to find initial controller settings. Experiments demonstrated the success of this system, presented results showing the stabilising the flow and a backpressure at the base of the riser.

Almeida and Gonçales (1999) used a venturi at the riser base to disturb the flow entering the riser base, the principle of this method of control was to: (a) prevent the accumulation of liquid at the riser base and (b) to disturb the flow regime at the riser base and hence prevent the stratified flow necessary to cause severe slugging. Experiments showed the successful suppression of the pressure cycling using the venturi, the degree of damping increasing with decreasing throat diameter. The use of the venturi increased the average riser base pressure in a manner similar to topsides choking. Comparisons between choking and the venturi confirmed this. Tests were all carried out in a 25 mm pipeline/riser, with a pipeline inclination of -7° to the horizontal. At the time of writing the behaviour of this method of severe slugging control has yet to be tested on a real scale system.

Molyneux *et al.* (2000) developed a feedback control mechanism for preventing severe slugging. This was developed as an alternative to topsides choking, where an 89% reduction in average production was observed when controlling severe slugging using topsides choking. The control system used a measurement of the riser base pressure to detect the formation of a severe slug, this was then used to control the flow of gas from the topsides separator. Once the pressure reached the control setpoint, the gas flow from the separator was increased, reducing the separator pressure and increasing the pressure driving force across the slug. This then moved the short slug from the riser base into the receiving facilities. During experiments it was found that the control action reduced over time as the severe slugging experienced was damped out by the controller. However, once the controller was switched off, severe slugging re-established in the pipeline/riser.

2.4 *Transient Modelling of Severe Slugging*

A number of transient models have been developed to predict severe slugging in a flowline/riser. These models can be broken into two main classes: specific severe slugging models (often quasi-steady state models) and generalised multiphase codes, both are dealt with in this section.

2.4.1 Specific Severe Slugging Models

Schmidt at al. Model for Severe Slug Formation

Schmidt *et al.* (1980) developed the first model of severe slugging, attempting to predict the slug length and the slug buildup time. The model was based upon mass

and pressure balances for the pipeline and riser during the liquid buildup stage. In order to close the model equations, information was required to account for the previous severe slugging cycle. These relations took the form of empirical correlations for the pipeline liquid holdup and liquid fallback post-blowdown. These closure relations were formulated from experimental results on a pipeline/riser system (see Section 2.1.1). Due to the use of empirical correlations, the generality of this model was limited, however good agreement was obtained with the experimental results. Bøe (1981) described this model and presented results for full-scale pipeline/riser systems, showing how increasing pipe length increased the slug lengths and buildup time.

Schmidt et al. Model for Severe Slugging Cycle

Schmidt *et al.* (1985) developed a model of the entire severe slugging cycle using different mass and pressure balance equations for each stage of the cycle. The transitions between each stage in the severe slugging cycle were defined in terms of the position of the gas-liquid interface, Schmidt *et al.* (1985). As in the previous case, in order to close the model the post-blowdown liquid fallback and the pipeline liquid holdup were required. Schmidt *et al.* (1985) treated this information as input parameters to the model. Results of simulations compared favourably against the experimental data of Schmidt *et al.* (1980). Hill (1987) and Mackay (1987) both described the application of this code to modelling severe slugging in the Forties field and the effect of severe slugging on topsides facilities. Pots *et al.* (1985) extended this model to account for pipeline inclinations and showed how increasing the pipeline inclination increased the slug length and buildup times.

Fabre et al. Severe Slugging Model

Fabre *et al.* (1987) recognised that severe slugging was essentially the propagation of large scale instabilities and void fraction waves through a vertical column of liquid. In order to model these phenomena, they developed a model based upon considerations of the unstable flow in the riser. The model used a simplified stratified flow model for the pipeline and partial differential equation (PDE) model in x and t for the riser. The pipeline behaviour was described by:

$$U_{LI}^{S} - U_{LB}^{S} = 0 \qquad (2.23)$$

for the liquid. For the gas phase:

$$\rho_{GP}\left(U_{GI}^{S} - U_{GB}^{S}\right) = \varepsilon_{GP} L \frac{d\rho_{GP}}{dt} \qquad (2.24)$$

In contrast to previous attempts at modelling severe slugging, the same general formulation of equations was used for each stage of the severe slugging cycle in the riser. Thus the riser governing equations were:

$$-\frac{\partial \varepsilon_{GR}}{\partial t} + \frac{\partial U_{LR}^{S}}{\partial x} = 0 \qquad (2.25)$$

for the liquid phase and for the gas:

$$\frac{\partial(\rho_{GR}\varepsilon_{GR})}{\partial t}+\frac{\partial(\rho_{GR}U_{GR}^{S})}{\partial x}=0 \qquad (2.26)$$

The momentum equation reduced to the pressure balance:

$$\rho_{GR}=\rho_{GO}+\frac{\rho_L g}{RT}\left[h_R-x-\int_x^{h_R}\varepsilon_{GR}\,dx\right] \qquad (2.27)$$

The drift flux model (Zuber and Findlay, 1965) was used to close the equations. The final set of PDE's were solved using the method of characteristics. Simulations gave results for void fraction, velocity and pressure profiles during severe slugging. The results of the code were in good agreement with experimental results for the liquid buildup and gas blowdown periods of severe slugging. However, the slug production period was not well predicted by the model. Fabre and co-workers suggested that the model was unable to predict the experimentally-observed void fraction waves propagating along the pipeline during the slug production period due to the simplicity of the pipeline model. The observed void fraction waves corresponded to the gas-liquid interface that backs up the pipeline during the slug formation stage (Sarica and Shoham, 1991).

Moe et al. Model for Severe Slug Propagation

Moe *et al.* (1989) developed a model for the propagation of a severe slug through a pipeline/riser. The model was based upon mass and momentum conservation for a series of moving control volumes. The severe slug was split into a series of these control volumes, one each was assigned to the annular slug tail, the bubble front, the slug body and the slug front. Moe *et al.* (1989) discussed the use of the jump condition for the mass and momentum in the bubble wake, these were used to close the model equations. The formation process of the slug was beyond the scope of this study and so predicting the characteristics of severe slugging was limited to outlet liquid flowrate and slug velocities.

Taitel et al. Model of Severe Slugging

Taitel and co-workers (1990) presented a model that was aimed at predicting both the severe slugging and transitional flows experienced in a vertical riser. The initial condition for the model was the beginning of riser base penetration by gas bubbles where bubbles entered a full column of liquid. These bubbles corresponded to a void fraction wave propagating through the riser, similar to the Fabre *et al.* (1987) model. The mass flow of gas into the riser base was given by:

$$G_{GB}=G_{GI}-\frac{\varepsilon_{GP}LA}{RT}\frac{dP_P}{dt} \qquad (2.28)$$

The propagation of the bubble front through the riser was then calculated based upon the mixture velocity entering the riser base. The model assumed an average gas density through the riser and that the bubbles penetrating were Taylor bubbles,

allowing the correlation for the bubble velocity in Equation (2.22) to be used. This allowed the pressure to be calculated through a pressure balance equation. The model also considered interactions between flow in the riser and the pipeline to allow liquid fallback during severe slugging. The slug front in the riser and the backing up of the liquid in the pipeline were calculated from gas and liquid mass balances over the system as a whole. Results from the model calculations gave three unstable flow regimes in the riser, corresponding to those observed experimentally, see Section 2.1.3. The model was able to reasonably predict the flow regime boundary for unstable flow when compared with experiments, however below the Taitel stability line, predictions for the severe slugging characteristics suffered from inaccuracies as the model equations became ill-posed below this limit and simulations did not converge to a meaningful result.

Sarica and Shoham

Sarica and Shoham (1991) extended the Fabre *et al.* model (1987), including a model for the gas-liquid interaction in the pipeline. As shown in Figure 2.5 Sarcia and Shoham (1991) assumed stratifed gas/liquid flow in the pipeline, with the liquid accumulation at a distance x upstream of the riser base (x being in the positive co-ordinate direction). Mass conservation equations in the pipeline gave:

$$U_{LI}^{S} = U_{LB}^{S} - \varepsilon_{GP} \frac{dx}{dt} \qquad (2.29)$$

for the liquid, and

$$U_{GL}^{S} = \frac{1}{P_P}\left\{U_{GB}^{S} P_B - \varepsilon_{GP} \frac{d\left[(L_P - x)P_P\right]}{dt}\right\} \qquad (2.30)$$

for the gas. The other model equations were identical to those of Fabre *et al.* (1987), Equations (2.20) to (2.24). The model considered pure liquid flow and continuous gas penetration at the riser base, using a different solution procedure for each. However there were few details of when the different flow models were applied, thus it was impossible to gauge their relative contribution to modelling severe slugging. The combination of these two flows allowed successful prediction of unstable flows in the Bøe region. However in the region below the Taitel (1986) line, the model results were only a rough approximation of the experimental results. Sarica and Shoham suggested this was due to dynamic effects such as liquid acceleration and the associated pressure losses that were not included in the momentum equation, Equation (2.27).

2.4.2 Generalised Multiphase Flow Codes

The generalised multiphase flow codes used in the oil and gas industry are characterised by a one-dimensional time-varying fluid model in two or three phases, based on the Navier-Stokes equations, Yeung (1997). The model equations are closed by a series of flow regime dependant relationships or 'closure laws', which aim to reflect three-dimensional effects and source terms. Some examples of these effects

are wall and interfacial friction and the entrainment and deposition of droplets. This section primarily deals with the three main commercial multiphase codes PLAC, OLGA and TACITE. Brief descriptions of other propriety codes will also be given.

OLGA

The first dedicated pipeline multiphase code was the OLGA transient code, developed in 1983 by IFE and SINTEF in Norway (Bendiksen *et al.*, 1991). The OLGA code was based on an extended two-fluid model, details of which are given below. The latest version, OLGA2000, includes a three-phase model, however as there are few published details of this model this discussion will centre on the two-phase formulation.

The basic formulation of the model is a series of mass and momentum conservation equations for each phase and a mixture energy conservation equation. The mass conservation equations are as follows – for the gas:

$$\frac{\partial}{\partial t}(\varepsilon_G \rho_G) + \frac{1}{A_P}\frac{\partial}{\partial x}(A_P \varepsilon_G \rho_G U_G) = \varphi_G + \zeta_G \qquad (2.31)$$

Here φ is the gas mass transfer rate between phases, ζ is the mass source term and the subscript G refers to the gas as usual.

For the liquid, the mass conservation equation is:

$$\frac{\partial}{\partial t}(\varepsilon_L \rho_L) + \frac{1}{A_P}\frac{\partial}{\partial x}(A_P \varepsilon_L \rho_L U_L) = -\varphi_G \frac{\varepsilon_L}{\varepsilon_L + \varepsilon_D} - \varphi_e + \varphi_d + \zeta_L \qquad (2.32)$$

In this equation, φ_e is the entrainment rate of droplets and φ_d is the deposition rate of the droplets; the subscript D refers to the droplet 'phase' and L refers to the liquid phase. The OLGA model treats the droplets in the gas as a separate phase, this means that the droplet mass conservation equation is:

$$\frac{\partial}{\partial t}(\varepsilon_D \rho_L) + \frac{1}{A_P}\frac{\partial}{\partial x}(A_P \varepsilon_D \rho_L U_D) = -\varphi_G \frac{\varepsilon_D}{\varepsilon_L + \varepsilon_D} + \varphi_e - \varphi_d + \zeta_D \qquad (2.33)$$

This additional droplet phase is used to account for additional longitudinal pressure drop in separated flow regimes such as annular and stratified flows. Experiments on the SINTEF experimental loop showed that in vertical annular flow, a two-fluid formulation of OLGA under-predicted *dP/dx* by up to 50%, hence necessitating the separate droplet phase.

When formulating the momentum equations, the gas and liquid droplet phases are combined into a single relation:

$$\frac{\partial}{\partial t}\left(\varepsilon_G \rho_G U_G + \varepsilon_D \rho_D U_D\right) + \frac{1}{A_P}\frac{\partial}{\partial x}\left(A_P \varepsilon_G \rho_G {U_G}^2 + A_D \varepsilon_D \rho_D {U_D}^2\right)$$
$$= -\left(\varepsilon_G + \varepsilon_D\right)\left(\frac{\partial P}{\partial x}\right) + \varphi_G \frac{\varepsilon_L}{\varepsilon_L + \varepsilon_D} U_a + \varphi_e U_i - \varphi_d U_D$$
$$- \lambda_G \frac{1}{2}\rho_G U_G \left|U_G\right| \frac{S_G}{4A_P} - \lambda_i \frac{1}{2}\rho_L U_r \left|U_r\right| \frac{S_i}{4A_P} \qquad (2.34)$$
$$+ \left(\varepsilon_G \rho_G + \varepsilon_D \rho_L\right) g \cos\alpha$$

In Equation (2.34) λ is a friction coefficient and S is the wetted perimeter. The subscript r refers to relative values between the gas and liquid, in this case U_r, the relative velocity is termed the 'slip velocity'. Subscript a refers to the fluid acceleration, in Equation (2.34) this is perpendicular to the flow and is used to account for the momentum source term. The use of a combined momentum equation for the gas and entrained drops eliminates the necessity for modelling the drag force on the liquid particles.

The liquid momentum equation is:

$$\frac{\partial}{\partial t}\left(\varepsilon_L \rho_L U_L\right) + \frac{1}{A_P}\frac{\partial}{\partial x}\left(A_P \varepsilon_L \rho_L {U_L}^2\right) = -\varepsilon_L\left(\frac{\partial P}{\partial x}\right) - \varphi_G \frac{\varepsilon_L}{\varepsilon_L + \varepsilon_D} U_a$$
$$- \varphi_e U_i + \varphi_d U_D - \varepsilon_L\left(\rho_L - \rho_G\right) g\, D \sin\alpha \frac{\partial \varepsilon_L}{\partial x} \qquad (2.35)$$
$$- \lambda_L \frac{1}{2}\rho_L U_L \left|U_L\right| \frac{S_L}{4A_P} + \lambda_i \frac{1}{2}\rho_g U_r \left|U_r\right| \frac{S_i}{4A_P}$$
$$+ \varepsilon_L \rho_L g \cos\alpha$$

Finally, the mixture energy equation is:

$$\frac{\partial}{\partial t}\left[\sum_j m_j \Theta_j\right] + \frac{\partial}{\partial x}\left[\sum_j m_j U_j \Xi_j\right] = H_S + Q_W \qquad (2.36)$$

Where subscript j refers to each phase G, L and D. H is the enthalpy and Q is the heat transfer. In Equation (2.36) H_S is the enthalpy associated with the mass sources. Θ_j and Ξ_j are given by:

$$\Theta_j = E_j + \frac{1}{2}U_j^2 + gh \quad ; \quad \Xi_j = H_j + \frac{1}{2}U_j^2 + gh$$

Where E denotes the internal energy of the fluid phase.

A series of flow regime dependent closure laws are used to solve the model, specifically these relate to the friction factors, the interfacial transfer, the source terms and the relative (slip) velocity. The closure laws are based on two main flow regime classifications, separated flow and distributed flow. In the case of separated flows such as annular and stratified flow, the closure laws are in the form of correlations for each flow-regime dependent parameter. For distributed flows such as bubble and slug, the closure laws are in the form of a 'slip relations', relating the phase velocities to one another. A description of these closure laws is beyond the scope of this work, readers are referred to Bendiksen *et al.* (1991) for additional information. At this point it worth noting that there is little published information on the treatment of source terms in the model, at the time of writing, much of this information is propriety to the code developers.

OLGA employs two numerical schemes to solve the model equations, an implicit scheme for separated and bubbly flows and a Lagrangian tracking scheme for slug flows (Straume *et al.*, 1992). The implicit scheme is used for most normal transient calculations as the phase velocities for typical pipeline flows are typically much less than the propagation of sound in the fluids, a factor of 10^2 or 10^3 smaller. Bendiksen *et al.* (1991) stated that implicit numerical schemes are more efficient and stable for pipeline simulations of slow transients and so are favoured over explicit schemes in these cases due to the improved computational efficiency. Indeed, Bendiksen *et al.* (1991) observed that for the typical slow flows encountered in multiphase systems, explicit schemes require a timestep size 10^3 smaller than implicit schemes.

In the case of the slug flow regime, purely implicit schemes are highly undesirable (Stramue *et al.* 1992). Numerical diffusion inherent in implicit schemes causes a 'smoothing out' of void fraction discontinuities, such as the slug front or tail, leading to inaccurate modelling of the flows. In order to track the propagation of the slugs, a Lagrangian slug-tracking scheme is used by OLGA. The slug-tracking scheme traces the movement of a discontinuity (either a slug front or tail), dividing the cell that this discontinuity occupies into two regions with separate flow regimes and then calculates the flow behaviour based on each flow regime.

PLAC/ProFES

The PLAC code, developed by AEA Technology, is a development of the earlier TRAC (Transient Analysis Code) used for studying rapid transients in nuclear reactors (Black *et al.*, 1990). It exists as one model, denoted ProFES-Transient, within the ProFES (Produced Fluid Engineering Software) environment released by AEAT.

The PLAC model is based upon a six-equation, two-fluid model with a liquid and gas phase equation for the mass and momentum conservation, a gas energy conservation equation and a total energy conservation equation. The mass conservation relationships are:

$$\frac{\partial}{\partial t}(\varepsilon_G \rho_G) + \frac{\partial}{\partial x}(\varepsilon_G \rho_G U_G) = \Gamma \qquad (2.37)$$

for the gas, for the liquid the mass conservation is:

$$\frac{\partial}{\partial t}(\varepsilon_L \rho_L)+\frac{\partial}{\partial x}(\varepsilon_L \rho_L U_L)=-\Gamma \qquad (2.38)$$

In Equations (2.37) and (2.38), the Γ term is the "net volumetric vapour production rate caused by phase change" (AEAT, 2000). As such this is analogous to the mass transfer and source terms used by OLGA.

The momentum conservation equations for the gas and liquid are:

$$\frac{\partial U_G}{\partial t}+U_G\frac{\partial U_G}{\partial x}=-\frac{1}{\rho_G}\frac{\partial P}{\partial x}-\frac{c_i}{\varepsilon_G \rho_G}(U_G-U_L)|U_G-U_L| - \frac{\Gamma^+}{\varepsilon_G \rho_L}(U_G-U_L)-\frac{c_{WG}}{\varepsilon_G \rho_G}U_G|U_G|+g\sin\alpha \qquad (2.39)$$

and

$$\frac{\partial U_L}{\partial t}+U_L\frac{\partial U_L}{\partial x}=-\frac{1}{\rho_L}\frac{\partial P}{\partial x}+\frac{c_i}{\varepsilon_L \rho_G}(U_G-U_L)|U_G-U_L| - \frac{\Gamma^-}{\varepsilon_L \rho_L}(U_G-U_L)-\frac{c_{WL}}{\varepsilon_L \rho_L}U_L|U_L|+g\sin\alpha \qquad (2.40)$$

In Equations (2.39) and (2.40) the c terms are the friction coefficients which are obtained from flow regime dependent relations. PLAC uses a combination of a total energy conservation equation and a gas energy conservation equation. The total energy conservation equation is:

$$\frac{\partial}{\partial t}(\varepsilon_L \rho_L E_L+\varepsilon_G \rho_G E_G)+\frac{\partial}{\partial x}(\varepsilon_L \rho_L E_L U_L+\varepsilon_G \rho_G E_G U_G)= P\frac{\partial}{\partial x}(\varepsilon_L U_L+\varepsilon_G U_G)+Q_{WL}+Q_{WG} \qquad (2.41)$$

While the gas energy conservation equation is:

$$\frac{\partial}{\partial t}(\varepsilon_G \rho_G E_G)+\frac{\partial}{\partial x}(\varepsilon_G \rho_G E_G U_G)=-P\frac{\partial \varepsilon_G}{\partial t}-P\frac{\partial}{\partial x}(\varepsilon_G U_G) + Q_{EG}+Q_{iG}+\Gamma H_G \qquad (2.42)$$

The use of the total energy equation simplifies the numerical implementation of the thermal equilibrium calculation (AEAT, 2000). Only one equation is required for manipulation in the equilibrium calculation, rather than separate gas and liquid relations.

In order to obtain values for the wall and interfacial friction, a set of flow regime dependent closure laws are applied. Flow regime is determined through comparison with pre-determined flow regime maps (see Figures 2.10 and 2.11) one vertical, used for $\alpha > 10°$ and one horizontal for $\alpha < 10°$. Based upon the flow regime classification, the friction factors are calculated. Details of each closure law are beyond the scope of this work and the reader is referred to the PLAC technical manual (AEAT, 2000) for additional information. It is important to note that similar to the case of the OLGA code, there is little detail published regarding the source terms.

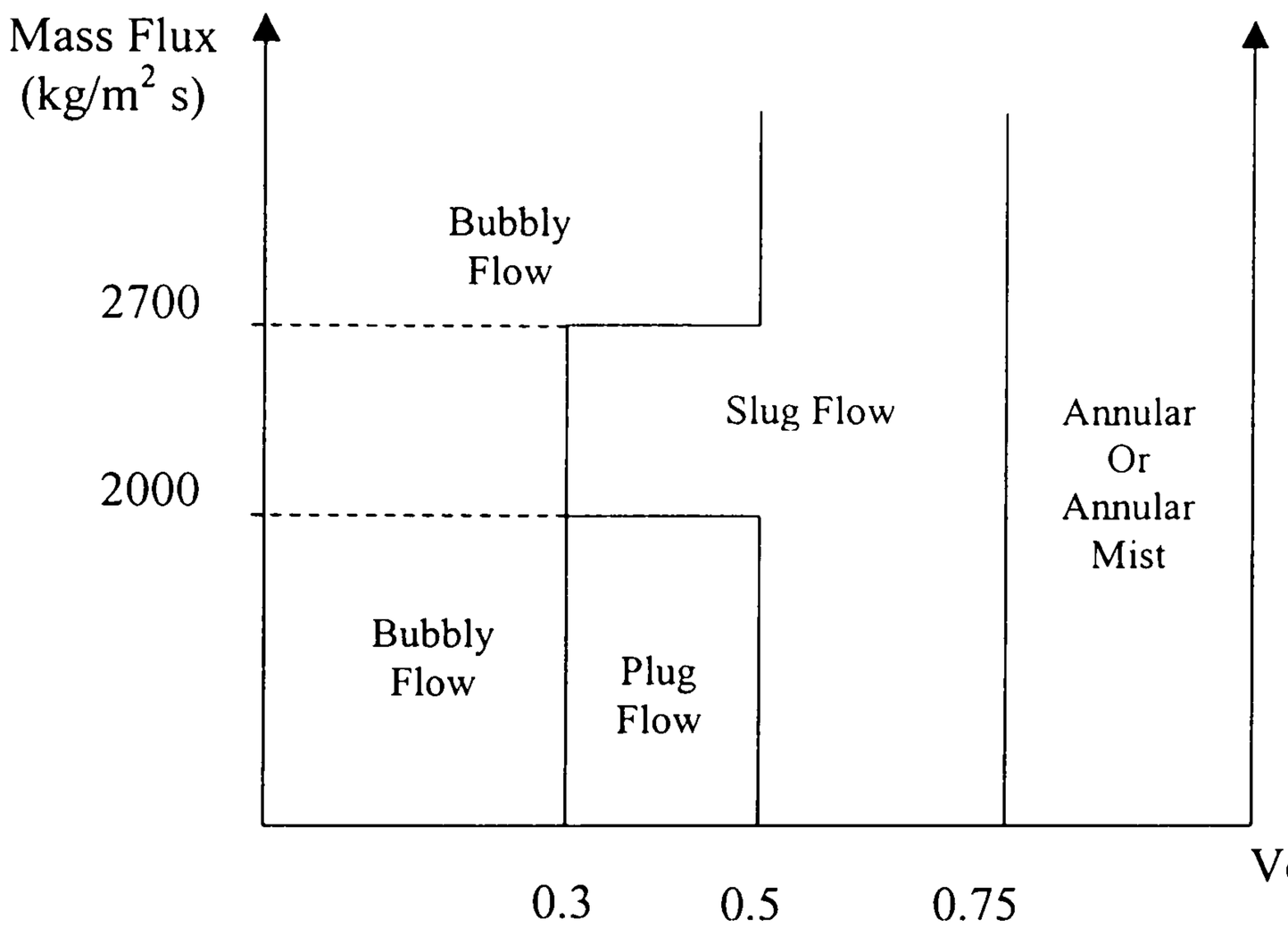

Figure 2.10 – Generalised Vertical Flow Regime Map

The model equations are solved using the SETS (Stability Enhancing Two Step) method, detailed by Lima (1999) and AEAT (2000), this algorithm employs a basic time advancing step and a stabilising step. The basic step using a semi-implicit numerical scheme and provides information on the propagation of the pressure waves through the system.

The implicit elements of the scheme are applied to the convective terms in the mathematical model. This is used to reflect the relatively slow propagation of waves in the system, compared to the speed of sound in the fluids. The stabilising step then gives information on the propagation of density, energy and momentum from cell to cell. The SETS method is employed to allow the scheme to take large time step sizes (characteristic of implicit calculations) and still retain sufficient resolution to capture shocks (characteristic of explicit schemes).

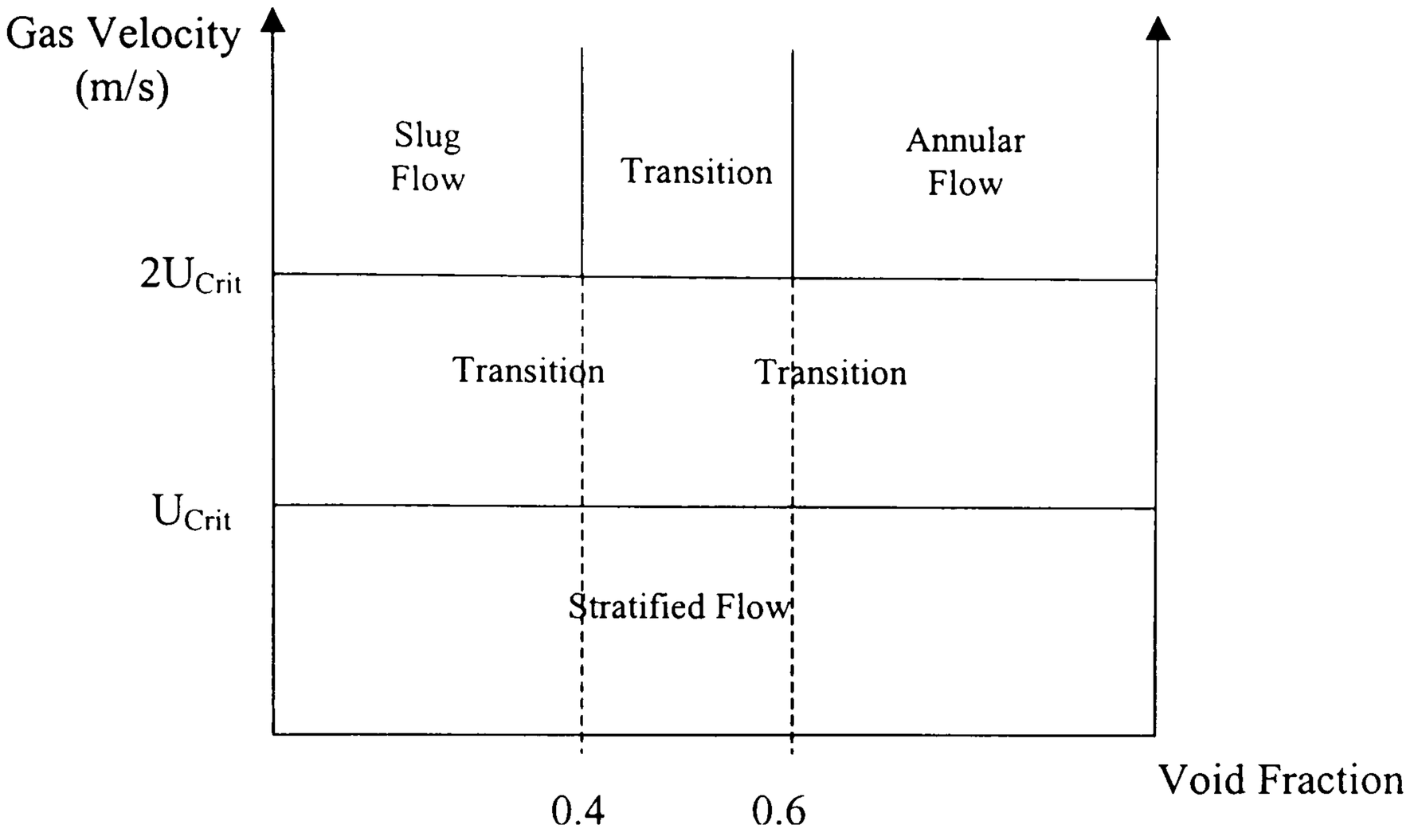

Figure 2.11 – Generalised Horizontal Flow Regime Map

TACITE

TACITE is a transient multiphase code that uses two methods to model the system behaviour (IFP, 2000). The first uses a flow model based upon a four-equation drift-flux model for a two fluid mixture and is discussed below (Pauchon *et al.* 1993, 1994). The second is a compositional model that uses a lumped-parameter approach, distributing the input components into two lumped 'pseudo-fluids'. Physical properties and phase characteristics are then computed for the binary fluid system (Pauchon *et al.*, 1994). The mass conservation equations are resolved for each component and the momentum and energy conservation equations are resolved for each phase (Pauchon *et al.*, 1994). Detailed discussion of this model is beyond the scope of this work, readers are referred to the work of Pauchon *et al.* (1994) for further information.

It is assumed in the TACITE model that all flow regimes are made up of two flow patterns, distributed flow (bubble flow) and separated flow (stratified and annular flows). The degree of phase distribution is reflected in the parameter, β, (Pauchon *et al.* 1993), separated flow this corresponds to $\beta = 1$ while dispersed flow corresponds to $\beta = 0$. In the case of intermittent (slug) flow β lies between 0 and 1. This reflects the regions of bubble flow (the slug body) and separated flow (the stratified film). The variation of β with gas and liquid velocity is found from a pre-determined flow regime map (Pauchon *et al.*, 1994).

For the binary fluid model, there are two mass conservation equations in TACITE, one for the gas:

$$\frac{\partial}{\partial t}(\varepsilon_G \rho_G) + \frac{\partial}{\partial x}(\varepsilon_G \rho_G U_G) = \Gamma \qquad (2.43)$$

and one for the liquid:

$$\frac{\partial}{\partial t}(\varepsilon_L \rho_L) + \frac{\partial}{\partial x}(\varepsilon_L \rho_L U_L) = -\Gamma \qquad (2.44)$$

The remaining conservation equations are mixture relations, for the momentum this is:

$$\begin{aligned} &\frac{\partial}{\partial t}(\varepsilon_G \rho_G U_G + \varepsilon_L \rho_L U_L) + \frac{\partial}{\partial x}\left(\varepsilon_G \rho_G U_G^{\,2} + \varepsilon_L \rho_L U_L^{\,2}\right) = \\ &\qquad -\frac{\partial P}{\partial x} - \frac{\partial M_C}{\partial x} + T_W - (\varepsilon_G \rho_G U_G + \varepsilon_L \rho_L U_L) g \sin\alpha \end{aligned} \qquad (2.45)$$

and for the energy:

$$\begin{aligned} &\frac{\partial}{\partial t}\left[\varepsilon_G \rho_G \left(H_G + \frac{U_G^{\,2}}{2}\right) + \varepsilon_L \rho_L \left(H_L + \frac{U_L^{\,2}}{2}\right) - P + \frac{M_C}{2}\right] \\ &+ \frac{\partial}{\partial x}\left[\varepsilon_G \rho_G U_G \left(H_G + \frac{U_G^{\,2}}{2}\right) + \varepsilon_L \rho_L U_L \left(H_L + \frac{U_L^{\,2}}{2}\right) + E_C\right] = \\ &\qquad Q_W - (\varepsilon_G \rho_G U_G + \varepsilon_L \rho_L U_L) g \sin\alpha \end{aligned} \qquad (2.46)$$

In Equations (2.45) and (2.46) above, T is the total friction force. M_C and E_C are functions of β that account for the non-homogeneous distribution of void fraction and velocities in intermittent flow. In the cases of pure dispersed and homogeneous flow, these terms disappear. Further details of M_C and E_C are beyond the scope of this discussion and readers are referred to the work of Pauchon *et al.* (1994) for more information.

The system of equations is closed using an algebraic slip law, governed by the flow regime. The distribution parameter, β, specifies the closure law for each flow regime. For distributed flows the closure relation is the drift-flux relation. In the case of separated flow the momentum equation is modified, eliminating the pressure gradient term, giving the closure relation. In the case of intermittent flows ($0 < \beta < 1$), an extension of the Nicklin *et al.* (1962) relation and a closure law for the slug void fraction is used to complete the model (Pauchon *et al.* 1993).

The numerical scheme used for TACITE two-fluid calculations is described by (Pauchon *et al.* 1994) as having an explicit time advancing step and a hybrid flux-preserving special discretisation. Faille and Heintze (1999) describe the 'rough finite volume scheme' used for the compositional model. This scheme has a combined explicit/implicit time advancing step, explicit for void fraction waves and implicit for

pressure waves, (Henriot et al, 1997). The scheme also uses a finite volume scheme in space, based upon an approximate Reimann solver. Each of these schemes aims to provide both good front tracking capability for slug modelling and to allow individual component calculations for the modelling of pipeline networks (Pauchon *et al.*, 1994, 1997).

Other Codes

TRAFLOW (Hollenberg *et al.*, 1997) and PETRA (Larsen *et al.*, 1997) are the other transient multiphase flow codes currently in use for oil and gas pipeline modelling. They are propriety in nature, with little information available in the open literature regarding their formulation or models. TRAFLOW is a code developed by Shell for transient simulations and modelling control scenarios (Griffith *et al.*, 1994a and b). It consists of a four-equation model using two mass conservation equations, one each for the liquid and gas phase, one mixture momentum equation and one total energy equation. Flow regime dependent closure relations are used to complete the model and the resulting difference equations are solved using an explicit up-wind Roe-scheme.

PETRA (Larsen *et al.*, 1997) is an extension of the OLGA code and developed by Statoil and the Norwegian Institute for Energy Technology (IFE). PETRA was developed with the specific aim of tracking flow discontinuities, either slugs or pigs, in a multiphase pipeline (Larsen *et al.*, 1997). It employs a three-phase model, with three mass conservation equations, three momentum equations, one pressure equation and one mixture energy equation. Flow regime dependent closure laws for wall friction, interfacial friction and mass transfer between the phases are used to complete the calculation. A major feature of the PETRA model is the dynamic grid structure, where the grid moves with discontinuities in the flow. Thus at each time step, the velocity and position of the grid are updated, giving improved slug tracking capability when compared to a static grid (Larsen *et al.*, 1997). Unfortunately, further details of the time advancing numerical treatment are unavailable in open literature at the time of writing.

Applications of Transient Codes to Severe Slugging in a Vertical Riser

For the most part, published comparisons of code results with severe slugging data are restricted to validation cases carried out by the code developers. Furthermore, few third-party comparisons of codes with experiments available have been presented in the public domain. Thus there is little published information on the flow conditions or the model set-up used for modelling the flow phenomenon.

Some of the first attempts at predicting severe slugging were those carried out as part of the OLGA code development (Bendiksen *et al.* 1991). The code results were compared against the data of Schmidt *et al.* (1980) and results from the SINTEF Two-Phase Flow Laboratory (Linga and Østvang, 1985). Results showed how the numerical scheme employed smoothed out liquid holdup discontinuities during severe slugging. However, the code did predict the pressure cycling characteristic reasonably well. Mazzoni *et al.* (1993) described the prediction of severe slugging in an offshore field using OLGA, results clearly showed the pressure cycling and liquid accumulation process in the riser. Courbot (1996) reported the use of OLGA to

predict the region of potential severe slugging in an offshore pipeline/riser application. Unfortunately in both cases, there was little recorded data reported to compare predictions against, due in some part to the lack of suitable instrumentation.

Philbin (1991) demonstrated the successful prediction of the severe slugging reported by Hill (1987) in a series of laboratory tests using PLAC. The PLAC simulations were reported as being within 99% and 95% of the experimental results in terms of slug volume and cycle time respectively. Results were also presented for simulations on severe slugging in the Tern subsea pipeline/riser system, however there was no comparison of the results with field data. These results remain the only publicly available information on PLAC predictions of severe slugging.

Masella *et al.* (1998) presented results of severe slugging simulations for two different fluid models, the drift flux model used in TACITE and a no pressure wave model, i.e. a model where the pressure term has been eliminated from the . They demonstrated the ability of each model to predict the pressure cycling of severe slugging, however the treatment of the outlet boundary was critical to the simulation using a drift flux model. It was found that a fictitious outlet boundary cell containing pure gas was required before liquid fallback from the top of the riser was correctly predicted. Faille and Heintzé (1999) showed further results of the application of the drift flux model to severe slugging. The results demonstrated how instabilities occurred in the liquid column in the riser. However in both cases, there was no constant production period predicted.

Hollenberg *et al.* (1997) demonstrated the ability of the TRAFLOW code to predict the separator behaviour when controlling severe slugging and showed some preliminary results for the flow of liquid during severe slugging. Larsen and Hedne (2000) presented results for a severe slugging test case in a vertical riser with PETRA. The simulation was carried out both with and without a slug tracking scheme, results showed a longer period of slug production and larger peaks in production when slug tracking was used. Unfortunately, at the time of writing, there are few details on either code.

2.5 Severe Slugging in Flexible Risers

Severe slugging in a flexible riser was first investigated as part of the Multiphase Pipelines and Equipment (MPE) Joint Industrial Project. This section presents the work to date on severe slugging flexible risers in two parts – experimental and modelling investigations

2.5.1 Experimental Investigations

The first reported experimental study of severe slugging in a flexible riser was by Tin (1991) as part of the MPE project. Experiments were conducted in a flexible riser rig to determine the basic severe slugging mechanism and to determine the extent of severe slugging on a flow regime map. The experimental arrangement (Figure 2.12) consisted of a 60 m long pipeline of 50.8 mm (2") nominal bore, inclined at -2° to the horizontal. This was connected to a 33 m high riser that was open to atmosphere at

the outlet. The riser was arranged in one of three configurations – catenary (free-hanging), Lazy S and Steep S. The air and water test fluids were supplied from a centrifugal pump and reciprocating compressor respectively. A buffer vessel was used in the gas supply line to simulate additional pipeline volume. From the riser outlet, fluids were returned to processing facilities using a 152.4 mm (6") vertical downcomer.

Instrumentation consisted of a set of boundary measurements and a set of pipeline/riser measurements. Boundary measurements were made up of inlet gas and liquid flows, liquid holdup measurements and pressure at the riser outlet. An electromagnetic flowmeter was placed at the riser outlet in an attempt to determine the exit flow velocity. The presence of gas bubbles in the liquid stream made measurement of the liquid velocity impossible during the later stages of gas blowdown due to excessive noise induced by gas bubbles present in the slug tail. Measurements along the pipeline and riser consisted of pressure measurements at various points in the system, liquid holdup at the riser base and outlet and a series of slug progression measurements using Light Emitting Diodes (LEDs). Pressure measurements were made at the pipeline inlet, riser base, top and bottom of the S-bend.

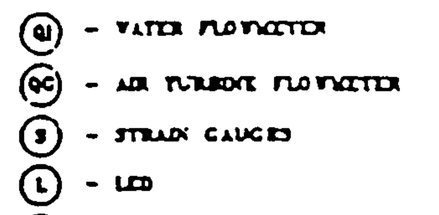

Figure 2.12 – Tin and Sharshar's Experimental Arrangement
(Tin 1991)

Results reported by Tin (1991) consisted mainly of the time-series recordings of the riser base pressure, showing the pressure cycling characteristic during severe slugging. This, coupled with the riser base liquid holdup, was used as the primary method of identifying the flow regime within the riser. However visual observations were also used to give an added degree of discrimination in the results.

Tin (1991) identified the following severe slugging flow regimes for a catenary riser:

1. Severe Slugging 1 (SS1) – Similar to severe slugging in vertical risers (Section 2.1.1), however riser base bubble penetration was in the form of a series of bubbles rather than a single gas cap.
2. Severe Slugging 1a (SS1a) – Similar to SS1, with the difference that gas blowdown was not initiated by the penetration of the first bubble at the riser base but after a number of bubbles.
3. Severe Slugging 2 (SS2) – A transitional severe slugging flow where there was no backup of liquid along the pipeline and bubble penetration occurred before the riser was completely filled with liquid. The riser base pressure remained substantially above the outlet pressure post-blowdown, indicating substantial levels of liquid fallback.
4. Severe Slugging 3 (SS3) – A transitional severe slugging flow, visually similar to normal slug flow, characterised by blowdown of the system, periodically reducing the riser base pressure to near-outlet pressure. The high degree of gas penetration reduced the size of the slug.
5. Oscillation Flow (OSC) – A cyclic flow pattern, similar to severe slugging flows, with a near-sinusoidal riser base pressure variation with time.

For both types of S-shaped risers, Tin (1991) found identical severe slugging flow regimes. These were classified as:

1. Severe Slugging 1p (SS1p) – Severe slugging, similar to SS1 in catenary risers, with gas blowdown initiated by penetration of gas bubbles at the riser base. Trapped gas in the riser downcomer was compressed as the hydrostatic head accumulated in the riser
2. Severe Slugging 1b (SS1b) – Severe slugging, again similar to SS1 in catenary risers, with no liquid backing up the pipeline and hence no steady slug production stage.
3. Severe Slugging 1t (SS1t) – Severe slugging, similar to SS1 in a catenary riser, with the upper limb of the riser being penetrated by gas trapped in the downcomer of the S-bend. This trapped gas penetration initiated gas blowdown. SS1t was experienced at higher liquid flows as compared against SS1p. The trapped gas penetration was attributable to the higher friction of the faster-moving liquid in the downcomer of the S-bend, moving the bubble into the upper riser limb.
4. Severe Slugging 1 with intermediate cycles on the lower limb (SS1i) – In this case the severe slugging cycle was distinguished by a unique liquid buildup mechanism, see Figure 2.13. During gas blowdown, the bulk of liquid in the upward limbs of riser was removed. Post-blowdown the liquid began to accumulate in the lower limb of the riser. However, instead of the liquid filling the lower limb completely and then flowing freely into the upper limb,

the liquid accumulated in the lower limb was periodically moved into the upper limb by the pipeline gas. This process continued until the riser was filled with liquid and a severe slug was formed. The severe slug formed was then blown out into the separator as in standard severe slugging. Tin (1991) suggested that this behaviour was similar to two catenary risers connected in series with the lower catenary operating at a different cycling frequency to the upper.

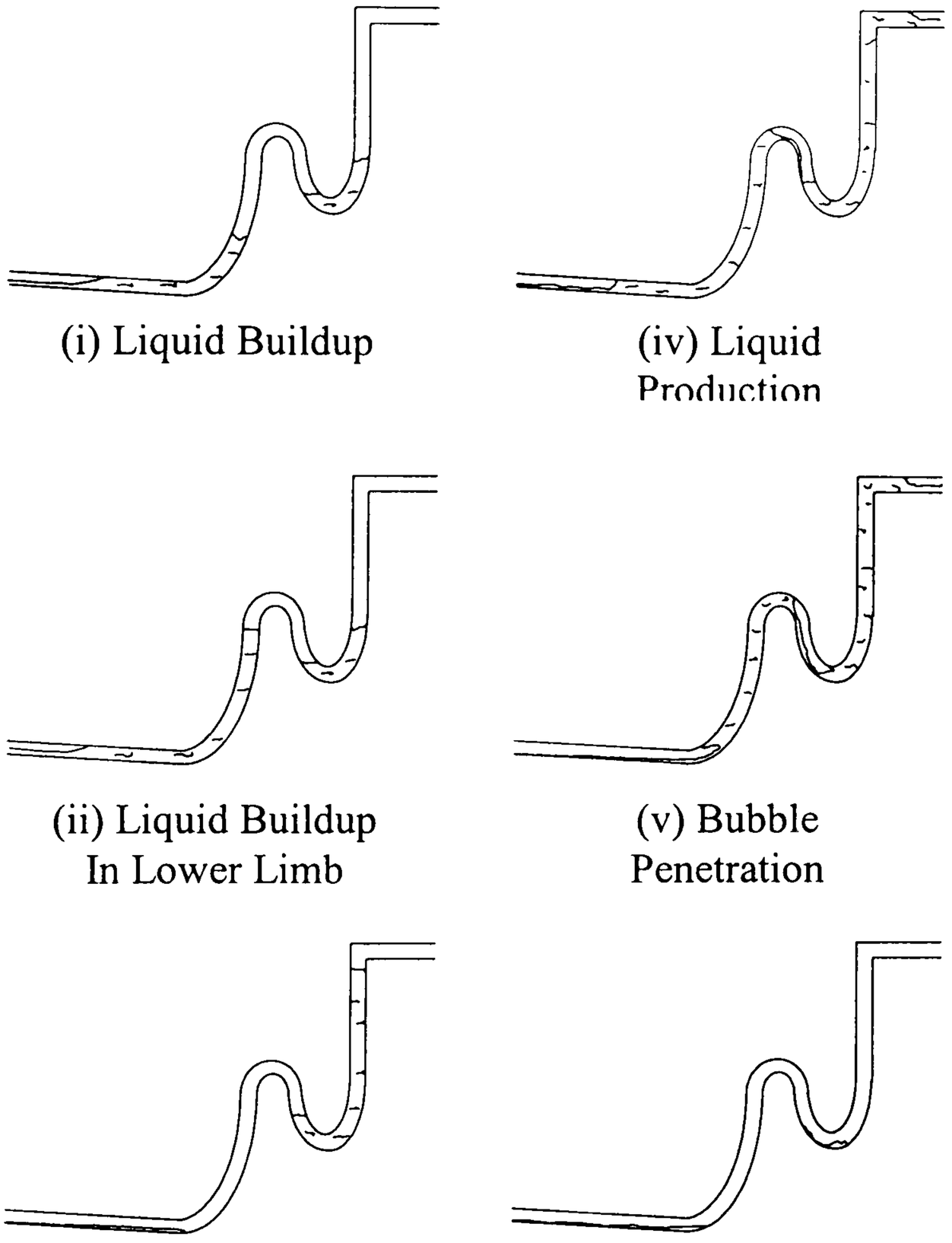

Figure 2.13 – Severe Slugging with Intermediate Cycles on the Lower Limb (SS1i)

5. Severe Slugging 2 (SS2) – A transitional severe slugging flow similar to SS2 in a catenary riser, characterised by no backup of liquid in the pipeline. Substantial quantities of liquid remained at the riser base and in the base of the S-bend post-blowdown.

6. Severe Slugging 3 (SS3) – Again, similar to SS3 in a catenary riser, exhibiting a high degree of riser base gas penetration with the riser being periodically blown down to a near-outlet pressure.
7. Severe Slugging 3 with intermediate cycles on the lower limb (SS3i) – This flow regime was identified by pressure signals from the base of the S-bend. Liquid accumulation was initiated by periodic blowdown of the lower limb, moving liquid into the upper limb. As with SS3, continuous gas penetration of the riser base was evident, reducing the liquid fraction in the slug body.
8. Severe Slugging 4 (SS4) – During SS4 high levels of gas penetrated the riser base and accumulated at the top of the riser S-bend. When the downcomer of the S-bend was filled with gas, penetration of the upper riser limb was initiated and gas blowdown began.
9. Oscillation Flow (OSC) – Oscillation flow was identified by a sinusoidal fluctuation in the riser base pressure reading. Tin (1991) described the signal as being made up of two parts, see Figure 2.14, a high-frequency fluctuation associated with the change in the upper limb holdup and a low-frequency 'trend' that may be associated with changes in the outlet pressure. Tin and Sharshar (1990) reported siphoning of the liquid in the 100 mm return line, this was thought to cause pressure fluctuations at the riser outlet in the order of 0.1-0.2 bar. Unfortunately this was not measured and the effect cannot be confirmed. Tin and Sharshar noted that oscillation flow is an example of each limb of the riser acting independent of the other, however no description of explanation of the reason for this was presented.

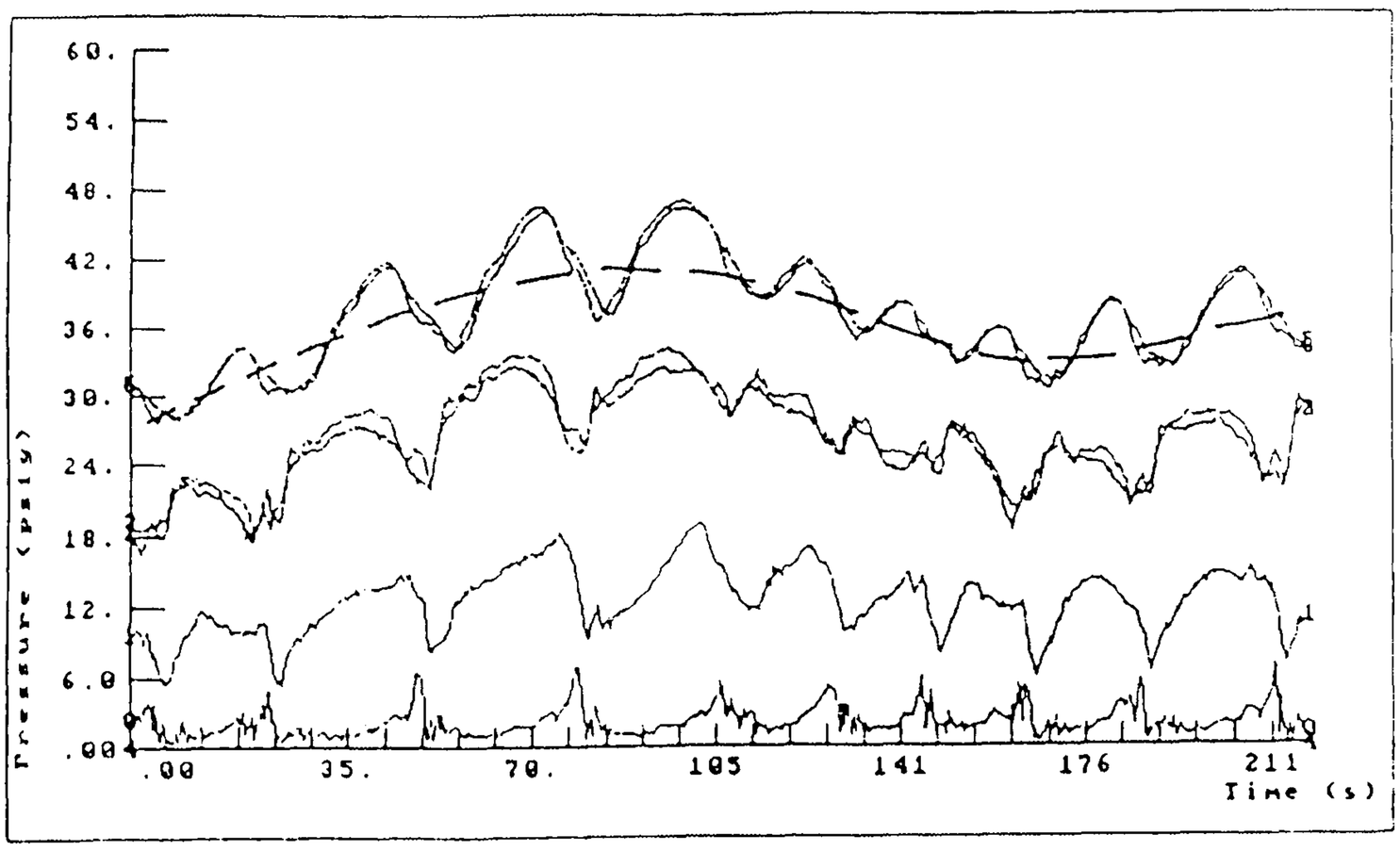

Figure 2.14 – Oscillation Flow Pressure Cycling Characteristics
(After Tin and Sharshar, 1991)

Tin and Sharshar (1991b) presented a series of flow regime maps, showing the limits of the severe slugging and unstable flow regions, Figures 2.15 (a)-(c). These showed that for the geometries studied, the region of severe slugging and unstable flows was the same for all three risers.

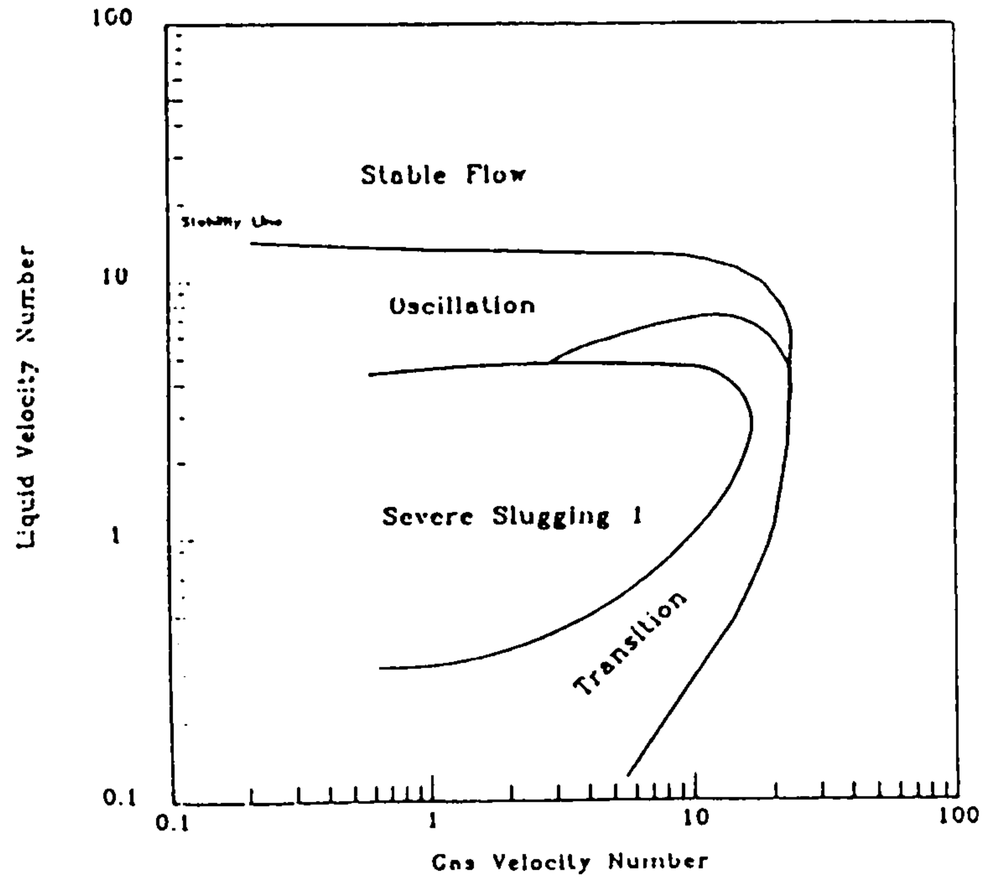

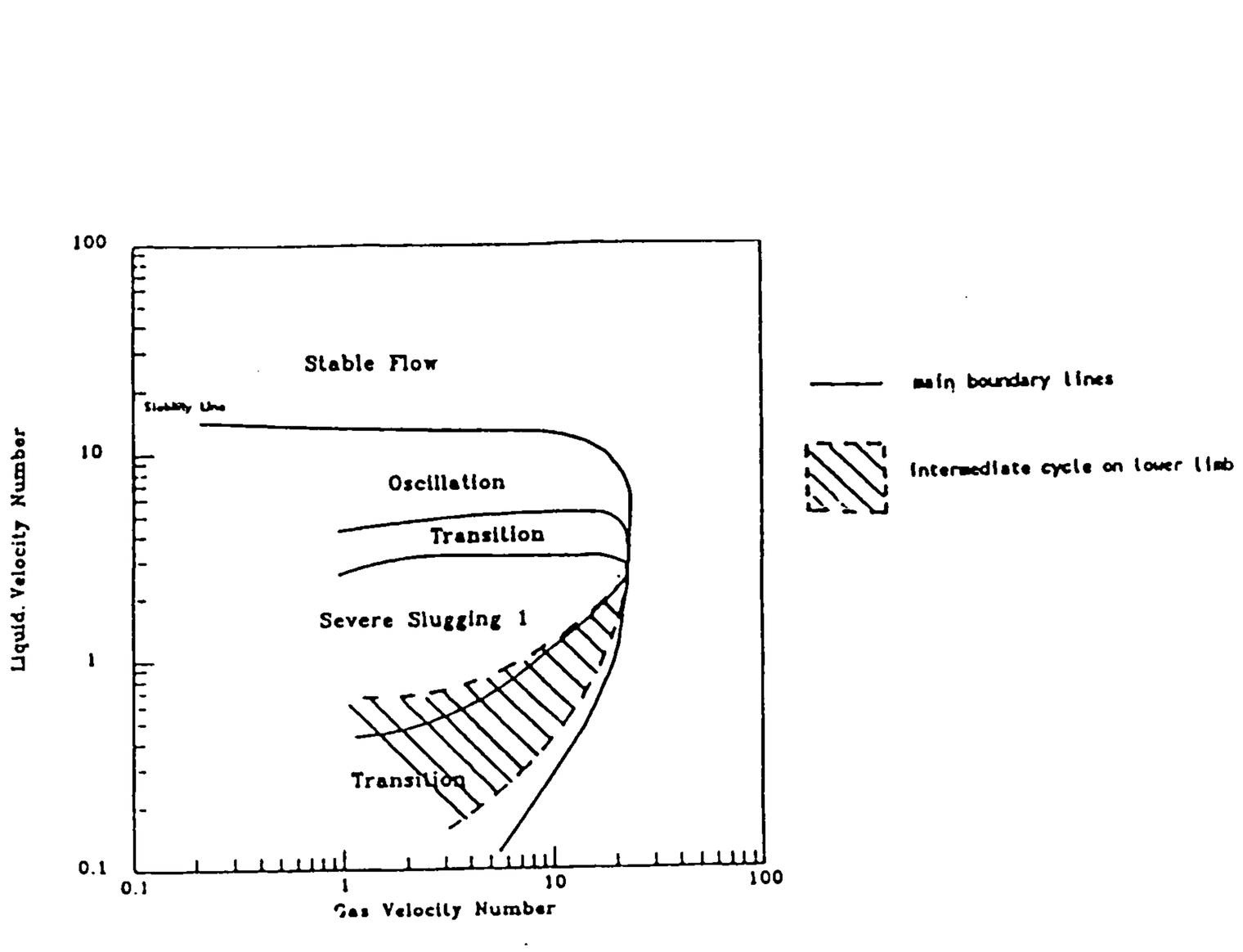

Figure 2.15 – Experimental Flow Regime Maps, Tin (1991)

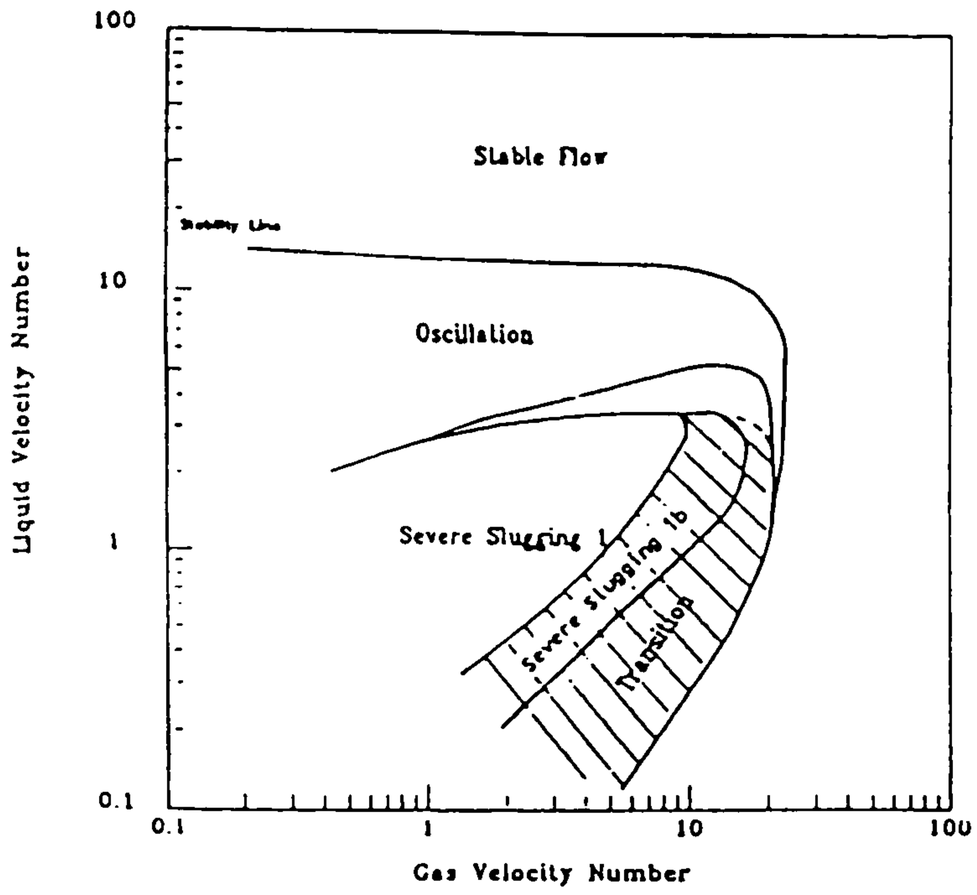

Figure 2.15 – Experimental Flow Regime Maps, Tin (1991)

Unfortunately the experimental data-points were omitted from these maps, meaning the relative differentiation between each flow regime region cannot be determined and the transition lines as presented are arbitrary. Other results of this work were published by Tin and Sharshar (1993), comparing results from a severe slugging model against experimental data, see Section 2.5.2.

Das *et al.* (1999a, b) reported the results of experimental investigations into severe slugging in a caternary riser. These detail investigations into the effect of compressible gas volume on severe slugging in a 10 m high catenary riser. The compressible volume was intended to simulate the gas volume in a long pipeline, this was achieved by placing an air receiver in the gas supply line. Results indicated that increasing gas volume increased the limiting gas velocities for severe slugging and increased the cycle time and slug length as a function of gas velocity. This was attributed to reducing the rate of gas pressure accumulation in the pipeline, thereby allowing a longer time liquid slug accumulation.

Nydal *et al.* (2001) reported the results of severe slugging experiments in a 7 m high, 50 mm (2" n.b.) i.d. S-shaped riser. Instrumentation consisted of a series of impedance probes and pressure transducers located in the upward limbs of the riser. A buffer volume was inserted in the pipeline, making the effective pipeline volume equivalent 167 m. Results presented included a series of flow regime maps and time series of the impedance probe and pressure measurements. Flow regimes were classified into three regimes – Terrain Slugging Types I and II and stable flows. The terrain slugging definitions were consistent with the definitions of Lund (1987):

- Terrain Slugging I – Where there is significant backup of liquid into the pipeline during slug buildup and there is a substantial period where no gas penetrates the liquid at the riser base. This corresponds to Severe Slugging 1 and 2 as defined by Tin (1991)

- Terrain Slugging II – Where there is continuous gas penetration at the riser base, however fluctuations in the rate of gas penetration are caused by the varying liquid holdup in the riser. This corresponds to Severe Slugging 3, 4 and Oscillation flow as defined by Tin (1991)

Liquid holdup measurements along the riser showed the bubble penetration taking the form of a series of bubbles rather than a single gas-cap. Experimental results of the pressure cycle variation with superficial gas and liquid velocity were compared against a computer model developed, see below.

2.5.2 Modelling Investigations

Steady-State Modelling

As part of the Managed Programme on Transient Multiphase Flows (Hewitt, 1996), Yeung (1997) compared the experimental results of Tin and Sharshar to the stability criteria of Bøe, Taitel and the Π_{SS} slugging criterion. The experimental results showed some deviation from the model predictions, particularly at low liquid and high gas flow velocity numbers. Yeung (1997) suggested that these inaccuracies were due to the models being unable to represent the behaviour in and around the riser base during the bubble penetration stage of severe slugging.

Specific Severe Slugging Models – Tin and Sharshar (1993)

Tin and Sharshar (1993) presented a model of the severe slugging process based on mass and pressure balances during the liquid buildup, slug production and bubble penetration stages of severe slugging. The model equations relied on experimental correlations to close the equations enabling the calculation of the total mass flow of liquid and gas through the riser. Frictional losses were calculated using the Moody correlation (Perry and Green, 1984) for the periods of single-phase flow during the cycle and the Beggs and Brill (1973) correlation for the two-phase flow periods. The model was used to predict the time of each severe slugging stage, the liquid velocity and slug length during severe slugging. Results presented some success in predicting the cycle characteristics for a catenary riser. However the model was not as successful at predicting S-shaped riser behaviour, under-predicting cycle times, slug lengths[†] and over-predicting the peak liquid production velocity. The reduced performance of the model was attributed to inadequate modelling of the downcomer of the S-bend.

Specific Severe Slugging Models – Nydal et al. (2001)

Nydal *et al.* (2001) presented the results of a computational model used for predicting severe slugging in an S-shaped riser. This model is a development of an earlier slug flow model, developed by Nydal and Banjeree (1996) to study terrain slugging. The model uses a Langrangian approach, using mass and momentum balances over a unit slug and the interspersing bubble to model the slugging characteristics. Appropriate correlations for the liquid front and bubble velocities close the model. In the case of slug flows, the formation of a slug is dependent on the accumulation of a predetermined critical mass of liquid. Once this is formed, a slug unit is inserted into

---

[†] Experimental slug lengths were calculated as the product of the average inlet flow times the cycle time, divided by the pipe cross-sectional area, see Tin and Sharshar (1991a)

the pipeline and the growth or propagation of the slug is modelled from there on. For severe slugging, the formation of the slug is based upon the flow of liquid into the riser base from the upstream and downstream directions, once a sufficient volume of liquid, equivalent to a volume length of 5-10 diameters, has entered the riser base, an equivalent slug is placed into the riser base.

In the published work, the ability of the code to predict the pressure cycling behaviour during severe slugging was demonstrated. The code was also able to predict the effect of increasing superficial gas velocity for a constant liquid velocity on the pressure characteristics. However the code was unable to replicate the behaviour for the effect of liquid velocity variations for a constant inlet gas velocity. Further computations centred on the initiation of slug flow in the pipeline and confirmed both experimentally and computationally that the onset of hydrodynamic slug flow stabilised flow in the riser.

Transient Code Predictions of Severe Slugging

To date only limited studies of severe slugging in flexible risers using transient codes have been carried out (SCANDPOWER, 1997 and AEAT, 1997), however little information on these comparisons is available in the open literature. The only published comparison was carried out by Kashou (1996), using data generated from the MPE project as validation data for the OLGA code. Two riser configurations were simulated – catenary and lazy-S – and a total of thirteen tests were carried out – seven for the catenary riser, six for the lazy-S. All simulations were carried out with the outlet pressure boundary specified at atmospheric pressure. In general, simulations showed a degree of success in predicting the overall flow regime in the pipeline/riser, however upon examination, details of the severe slugging characteristics were not correctly predicted by the code. OLGA experienced difficulty in predicting the slug production period, particularly at higher gas velocities. This would have a knock-on effect on the outlet liquid production velocity and the peak slug velocity during blowdown. Unfortunately these characteristics were not used in the comparisons. Furthermore, the pressure drop during slug production and the pressure post-blowdown were over-estimated, indicating errors in predicting the fallback and frictional pressure drop.

2.6 Severe Slugging and Terrain Slugging

When first discovered, severe slugging in a vertical riser was termed 'terrain slugging' (Schmidt *et al.* 1980a), indeed many workers have used the term to describe severe slugging in the past. Terrain slugging is also applied to stable slugs that are formed within a pipeline dip along the pipeline; though severe slugging is similar to this it remains a subset of a larger class of flow behaviour. During terrain slugging liquid accumulates in a pipeline dip, either through liquid fallback from the uphill section and inflow of liquid from the downhill section (Taitel *et al.*, 1990) or the stalling of a slug train (Lund, 1987). The formation of the slug is through one of two processes – liquid (slug) accumulation and blowout or wave formation. The first process is the same as during severe slugging where the slug is formed by liquid accumulation in the pipeline dip, blocking the cross-section. High pressure gas upstream of the slug builds up, leading to the blowout of the slug, this is described by Zeng *et al.* (1994).

The second mechanism is the destabilisation of the stratified gas-liquid interface in the dip due to gas acceleration over the accumulated mass of liquid in a pipeline dip. This forms a wave that bridges the pipe, forming a slug, Goldzberg and McKee (1985). Examining the mechanisms involved in terrain slugging, severe slugging is a subset of terrain slugging in that only the first slug formation mechanism occurs and the location of slug formation is restricted to the riser base. The slug is made up of the accumulated liquid column in the uphill section (the riser). In this respect it is important to note that the slug is fundamentally different to the second form of terrain slug and other hydrodynamic slug, these are formed through instabilities in the gas-liquid interface.

For the remainder of this work, the term 'severe slugging' refers to riser-induced terrain slugging and the term 'terrain slugging' refers to generalised terrain slugging in a long pipeline. Though an attempt to distinguish severe slugging as a subset of terrain slugging, this does not seek to exclude research results on terrain slugging from being applied to severe slugging. A number of investigations have been made of terrain slugging (Zeng *et al.* 1994, Hill *et al.* 1996, Yuan *et al.*, 1999) however for the most part these works centre on the propagation of terrain slugs through long pipelines and so are beyond the scope of this work.

Wood (1991) studied the accumulation of liquid in a pipeline dip and the formation of slugs through a 'liquid pickup' process. Experiments consisted of filling a pipeline dip with a known volume of liquid and examining how varying gas flows formed a slug by lifting the liquid into the uphill pipe section. Experiments showed that the liquid would behave in one of six ways – the liquid will remain in the dip; ripples appear over the liquid surface; the liquid is totally removed; a slug is initially formed and then collapses at some point further upstream; a slug is formed or finally, wavy stratified flow occurs. Experiments also gave the frequency of slugs formed against the liquid accumulation volume and gas velocity. Wood (1991) formulated a model to predict the characteristics of the slug formation based upon an analysis of one-dimensional steady-state flow. Results were presented for the critical gas velocity for slug formation, the maximum possible liquid accumulation and the slug formation frequency. The model performed well in the first two cases, however the formation frequency were underpredicted by the model which was unable to take account of the unstable nature of the flow downstream of the dip.

DeHenau and Raithby (1995c) demonstrated the application of a transient two-fluid model (DeHenau and Raithby, 1995a and b) to terrain slugging. The results of the model were compared against experimental data from a dip-slugging rig. The model compared well against measurements of upstream pressure and outlet liquid flow during terrain slugging. However upon examination of the experimental rig and pressure characteristic of the experiments it becomes evident that the flow regime is very similar to severe slugging in that the dip forms a shallow pipeline/riser arrangement. Thus the qualitative results may be applied to severe slugging. Referring to Figure 2.16 after DeHenau and Raithby (1995c) the liquid outflow characteristic shows a period of no production, during which the liquid slug is being formed, as reflected on the pressure trace; a period of steady liquid production, where the slug tail is moving towards the base of the pipeline dip, akin to slug production is

severe slugging; and a final transient as the liquid is spontaneously blown out of the system. This behaviour is very similar to the severe slugging process as described by Hill (1987), however no such time-varying measurement of the flow has been made for severe slugging.

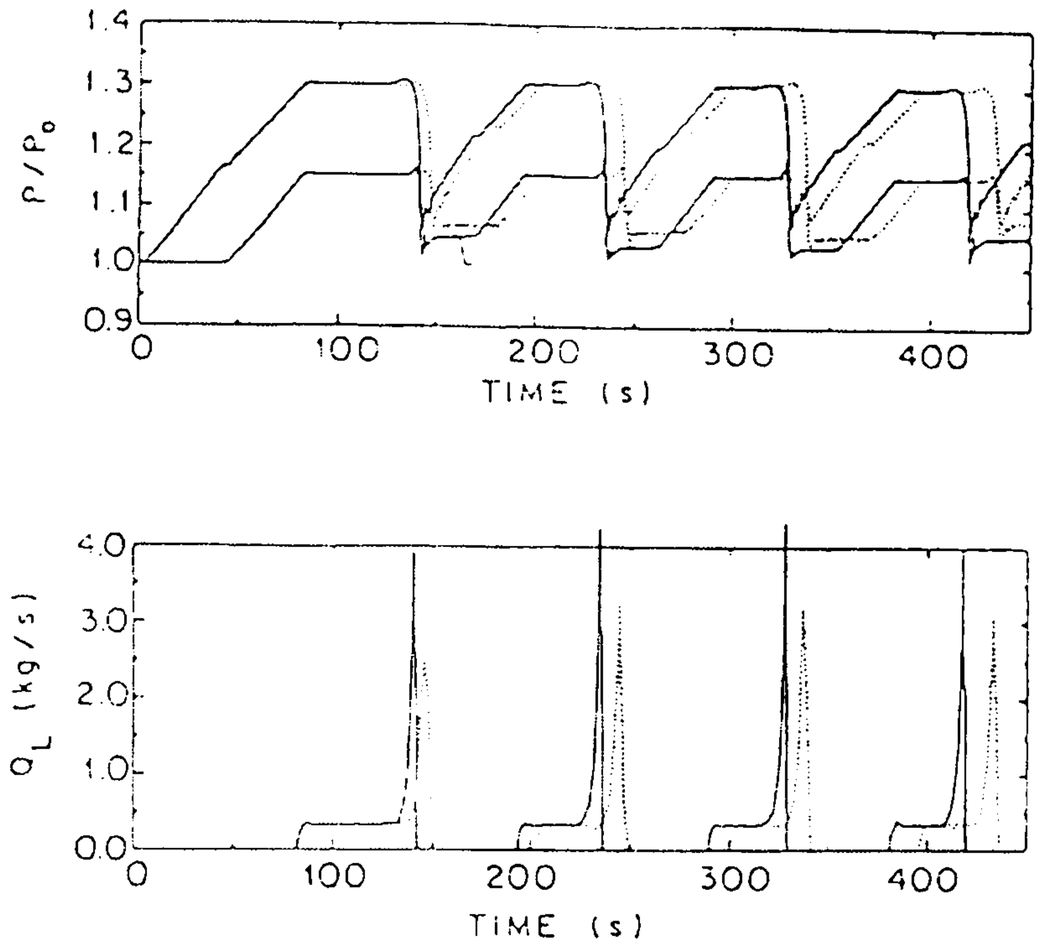

Figure 2.16 – Pressure Cycling and Liquid Production During Terrain Slugging, after DeHenau and Raithby (1995c)

2.7 Outstanding Issues and Research Plan

Reviewing the work to date on severe slugging, there are a number of outstanding issues that remain to be resolved. These have been gathered together in this section to formulate the research plan detailed below.

2.7.1 Flow Regimes

Severe slugging in a flexible riser has only been characterised in terms of pressure fluctuations at the riser base and in the upper limb, Tin and Sharshar (1991, 1993). Fluid production characteristics are necessary to estimate the relative deviation of peak flows from average flow during severe slugging and to obtain accurate measurement of slug size and peak slug velocity.

The relative severity of transitional severe slugging has not been clearly identified by previous investigations. If the size of slugs is comparable to the size of the riser, Transitional Severe Slugging (SST) may pose as many challenges for oil and gas production as 'classical' Severe Slugging 1 (SS1). Additional experiments are required to characterise SST.

The effect of outlet pressure on the severe slugging process has not been quantified - increasing the backpressure at the riser outlet via a choke has been used in the past to mitigate severe slugging. To date, no systematic investigation of how pressure effects the characteristics of severe slugging in a flexible riser has been carried out.

As shown by previous workers, severe slugging in a catenary riser behaves similarly to that in a vertical riser. S-shaped risers still pose significant challenges in terms of hydrodynamic characterisation, particularly in terms of the interactions between pressure cycling in each limb such as during oscillation flows. Hence the characterisation and flow pattern studies outlined above should be carried out in an S-shaped riser.

2.7.2 Steady-State Modelling

Though the flow regime maps generated by experiments are plotted using dimensionless parameters, removing fluid properties dependence, they are still dependent on the flowline/riser topography as identified by Yeung (1997). In order to provide meaningful results for flow regime behaviour in a flexible riser, experimental results must also be compared against steady state models that are capable of incorporating topographical effects.

2.7.3 Transient Code Modelling

Previous comparisons between experiments and code predictions have only focused on the overall flow regime, cycle times and slug lengths as a means of assessing the code results. Comparisons are also required on more detailed characteristics of the fluid production such as peak production rate, the steady production rate and the pressure cycling characteristics in each limb of the riser.

Transient code comparisons are also required to gauge the ability of the codes to predict the overall flow regime behaviour of the riser, including Transitional Severe Slugging and stable flows. This would provide an assessment of how successful transient codes are as predictive tools for the whole range of conditions in a flexible riser. Tests against transitional flows would also highlight the mechanisms that cause the transition between flow regimes and assess the ability of the codes to predict these mechanisms during severe slugging.

Chapter 3 – Experimental

This chapter describes the experimental facilities used in this work, the data analysis carried out and the test conditions. The experimental facilities consisted of a series of fluid supply/processing facilities, the Cranfield University Three Phase Facility, and a test section, the Cranfield University Riser Rig. The description in this Chapter covers the Three Phase Facility and Riser Rig separately. Readers are referred to the work of Das (2002) for additional information on the operation of the Cranfield University Three Phase Facility and Riser Rig.

3.1 Three Phase Facility

The Cranfield University Three Phase Facility, Figure 3.1, is a multiphase storage, supply, receiving and treatment facility designed to process continuous flows of oil, water and air to and from a test loop. The facility operates over a range of test pressures, with a maximum operating pressure of 25 bar(g). The test fluids for the Three Phase Facility are lubricating oil (BP 7269), water (doped with biocide) and air. This section describes the Three Phase Facility in three parts – the Fluid Supply Facilities, the Fluid Receiving Facilities and Instrumentation.

3.1.1 Fluid Supply Facilities

Liquid Supply

Oil and water are stored in two main tanks T101 and T102, of 8 m^3 and 10 m^3 capacity respectively. The liquids are pumped to the test section using two positive displacement pumps, P101 and P102. The oil pump (P101) is a Mono pump with a maximum capacity of 30 m^3/hr and a maximum discharge pressure of 6 bar(g). The water pump (P102) is a Worthington Simpson D-Line positive displacement pump, which has a maximum capacity of 35 m^3/hr and a maximum discharge pressure 6 bar(g). The liquid flow from each pump is controlled by means of a by-pass line with the fluid from each pump outlet being recycled back to the inlet via valves V103 and V107. From each pump, the liquids pass to an individual metering station, see Section 3.1.3. Following this the combined liquids pass along the liquid export line to the centrifugal booster pump, P103, a Worthington Simpson centrifugal pump. This pump has a maximum capacity of 45 m^3/hr and is used for experiments at pressures above 6 bar(g). For flows greater than 14 m^3/hr, the P101 and/or P102 are operated in series with P103 to avoid cavitation. From P103, the liquids proceed to the mixing point where they are combined with the gas flow and pass to the Test Section.

Gas Supply

Gas is supplied from C101, a water-cooled Atlas Copco DR 4 two-stage reciprocating compressor. This compressor has a maximum supply capacity of 600 m^3/hr Free Air Delivery (FAD) and a maximum discharge pressure of 18 bar(g). From the compressor outlet, the gas is passed to a 2.54 m^3 receiver, T103. As the compressor cycles through loading and unloading, pulsations are induced in the gas supply, these must be damped before the gas reaches the test section to prevent the pulsations influencing the flow regime in the pipeline/riser.

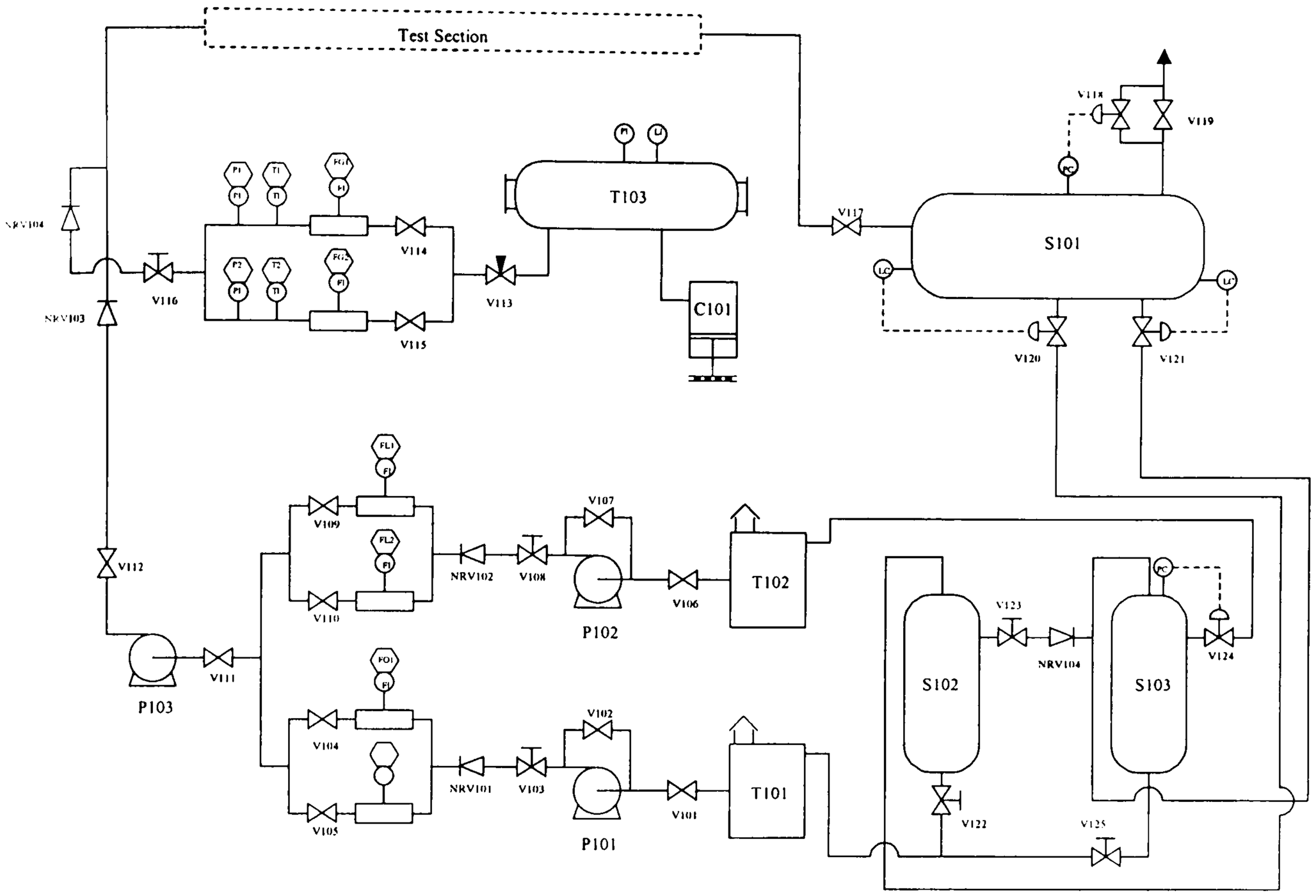

Figure 3.1 – Cranfield University Three Phase Facility P&I Diagram

The arrangement of the receiver before the test section stabilises the gas supply from the compressor. From the receiver, air flow goes to the gas metering station, see Section 3.1.3, via a needle valve, V113. This valve chokes the flow to the metering station, maintaining a constant mass flow for a given receiver pressure, and further acts to stabilise the flow entering the Test Section. From the gas metering station, the gas passes to the mixing point, is combined with the liquid flow and enters the Test Section.

When a buffer vessel volume is required to simulate larger compressible volumes upstream of the test section, the air receiver is reconnected after the gas flow metering station. In this configuration, the gas from the compressor passes firstly to the needle valve, then the metering station and finally to the buffer volume.

3.1.2 Fluid Receiving Facilities

Upon returning from the Test Section, the fluids pass to the receiving facilities. The oil/water/air mixture enters S101, the main three-phase separator, Figure 3.2. This separator is designed to remove the air from the process and carry out the bulk separation of the oil and water.

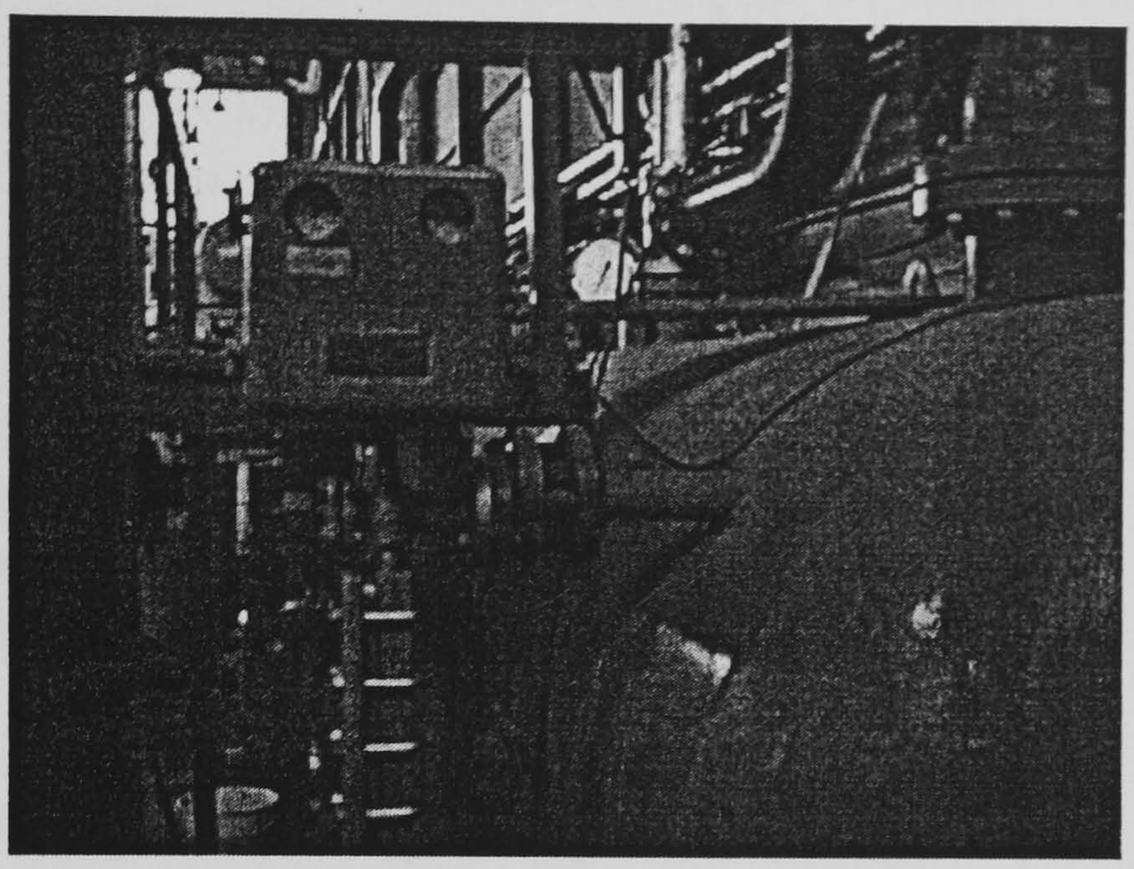

Figure 3.2 – Three Phase Separator

Air is immediately separated from the process stream and filtered before being released to atmosphere. Pressure is regulated in the separator by a Masoneilan 2700 pressure controller and a Masoneilan Series 35002 Camflex valve. This combination acts on the outlet air flow to maintain the set point pressure and in effect controls the pressure in the Three Phase Facility and Test Section as a whole.

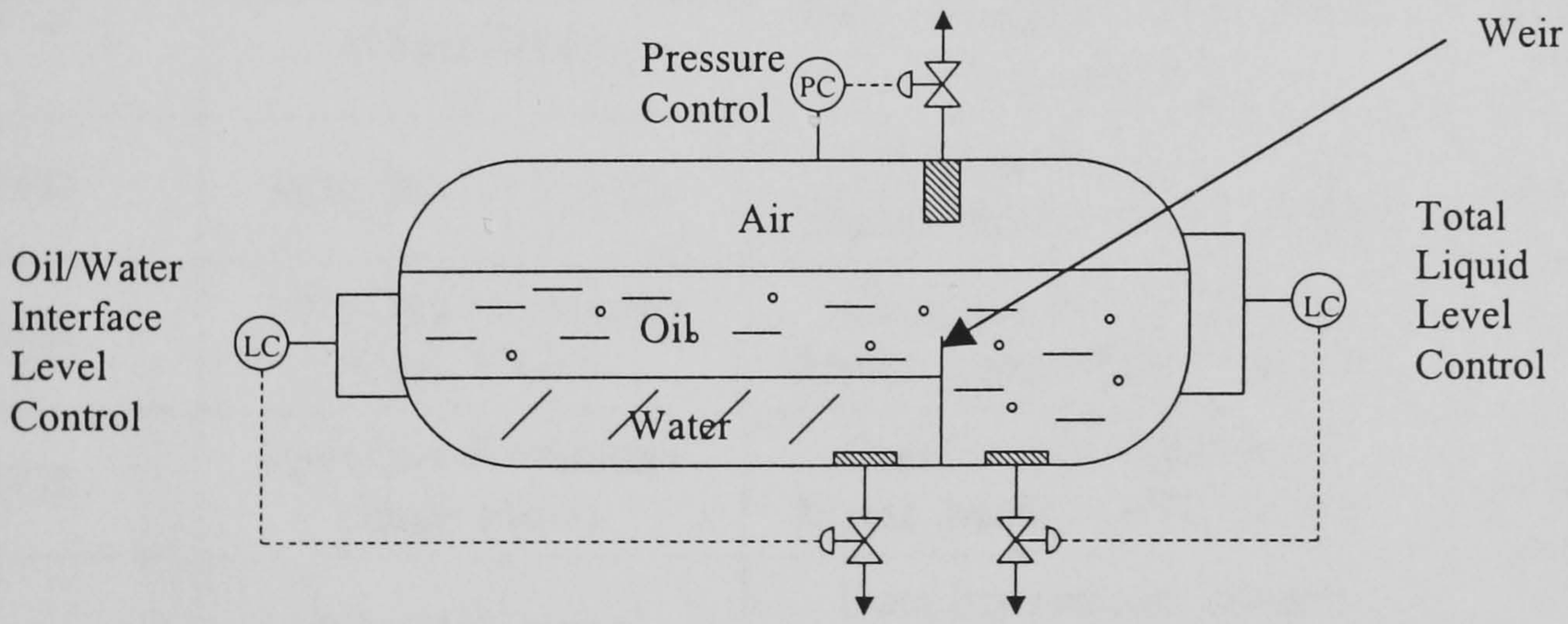

Figure 3.3 – Three Phase Separator Level Control Schematic

Bulk liquid separation is controlled by a pair of level controllers, both Masoneilan 12000 level controllers. The first controller regulates the height of the oil/water interface before the separator weir, see Figure 3.3, and the second maintains the total liquid level in the separator by controlling the oil level after the weir. Each controller uses a Masoneilan Series 35002 Camflex actuated valve to regulate the flow of water and oil from the separator.

The liquids exiting the separator then pass to the liquid coalescers S102 and S103 for fine fluids separation. Water and oil enter the top of the water (S102) and oil (S103) coalescers respectively. The level in the oil coalescer is controlled via a Masoneilan 2700 pressure controller – Camflex valve combination. This acts on the measurement of pressure in the coalescer and regulates the oil outlet flow, returning oil to the oil storage tank. The recycling of oil from the water coalescer to the oil coalescer is a continuous operation, not automatically controlled, but regulated through a gate valve. Similarly, return of water from the water coalescer and the oil coalescer to the water tank is regulated through gate valves but not automatically controlled. In order for the fluid processing system to operate, a minimum pressure of 0.5 bar(g) is required in the Three Phase Separator. This pressure is required to provide motive force for the fluids to pass through the coalescers and to the respective storage tanks.

3.1.3 Instrumentation

The instrumentation for the Three Phase Facility consists of the fluid metering stations, the details of which are provided in Table 3.1.

Sensor Designation	Sensor Description	Sensor Details	Range
FL1	Inlet Liquid Flowmeter (Low Flow)	Khrone Altoflux Electromagnetic Flowmeter, Model K180AS	0.4-6 m^3/hr
FL2	Inlet Liquid Flowmeter (High Flow)	Khrone Altoflux Electromagnetic Flowmeter, Model K280AS	3-45 m^3/hr
FO1	Inlet Oil Flowmeter	Quadrina Q-Flo Turbine Meter, Model QLG/25B/EP1	6-60 m^3/hr
FG1	Inlet Gas Flowmeter (Low Flow)	Quadrina Q-Flo Turbine Meter, Model QFG/13B/EP1	1-8 m^3/hr
FG2	Inlet Gas Flowmeter (High Flow)	Quadrina Q-Flo Turbine Meter, Model QFG/25B/EP1	6-60 m^3/hr
P1	FG1 Reference Pressure Sensor	Data Instruments Model, Model SA200 Pressure Transducer	0-200 psi(g)
P2	FG2 Reference Pressure Sensor	Data Instruments Model SA200 Pressure Transducer	0-200 psi(g)
T1	FG1 Reference Temperature Sensor	In-House Type 'T' Thermocouple	0-100 °C
T2	FG2 Reference Temperature Sensor	In House Type 'T` Thermocouple	0-100 °C

Table 3.1 – Three Phase Facility Instrumentation

The liquid instrumentation consists of two separate metering stations, one each for the oil and water. The oil flow is metered using a Quadrina liquid turbine flowmeter, designation QLG/25B/EP1, with a range of 6-60 m^3/hr. Water flow is metered using a pair of Krohne Altoflux Series electromagnetic flowmeters, see Figure 3.4. The first, a K180 AS model, has a range 0.4-6.0 m^3/hr and the second, a K280 AS model, has a range 3-45 m^3/hr.

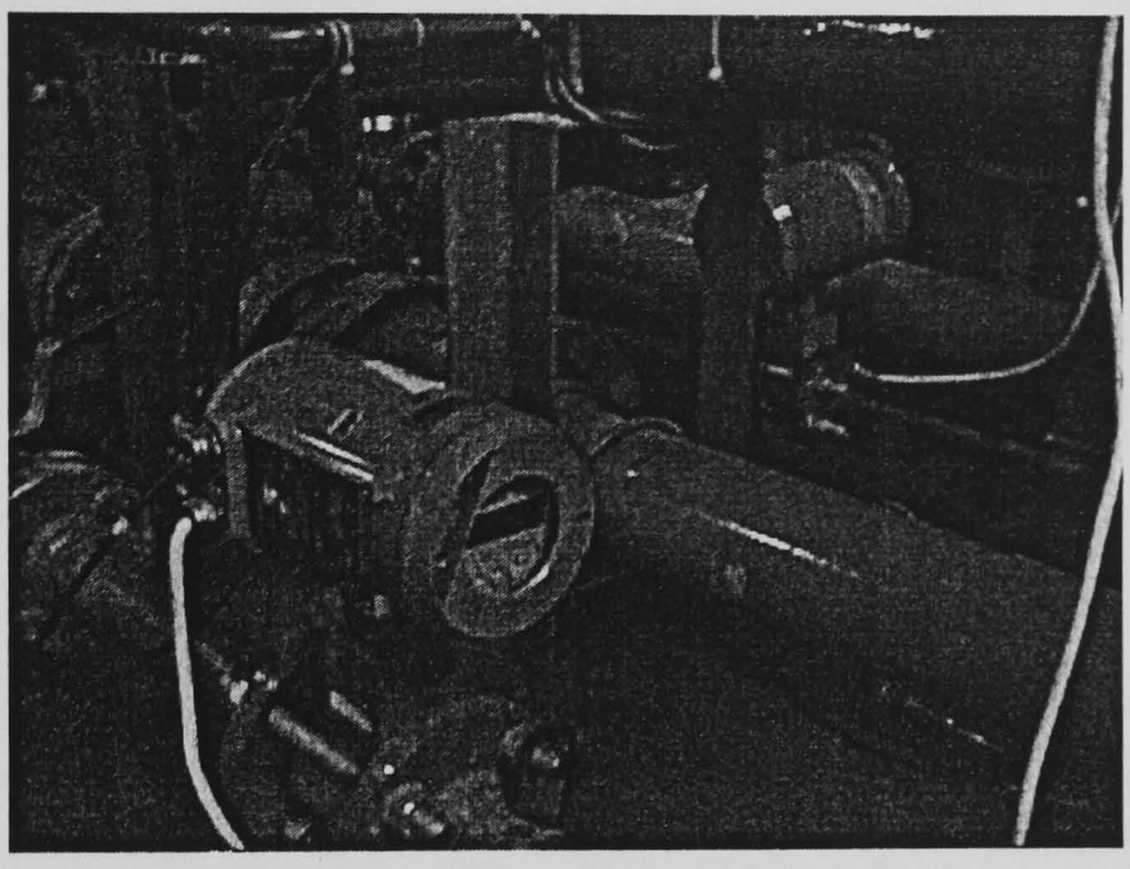

Figure 3.4 – Water Flow Metering Station

Gas flow is metered using a pair of Quadrina gas turbine flowmeters, see Figure 3.5, the first, designation QFG/13B/EP1, has a range of 1-8 m^3/hr and the second, designation QFG/25B/EP1 has a range of 6-60 m^3/hr.

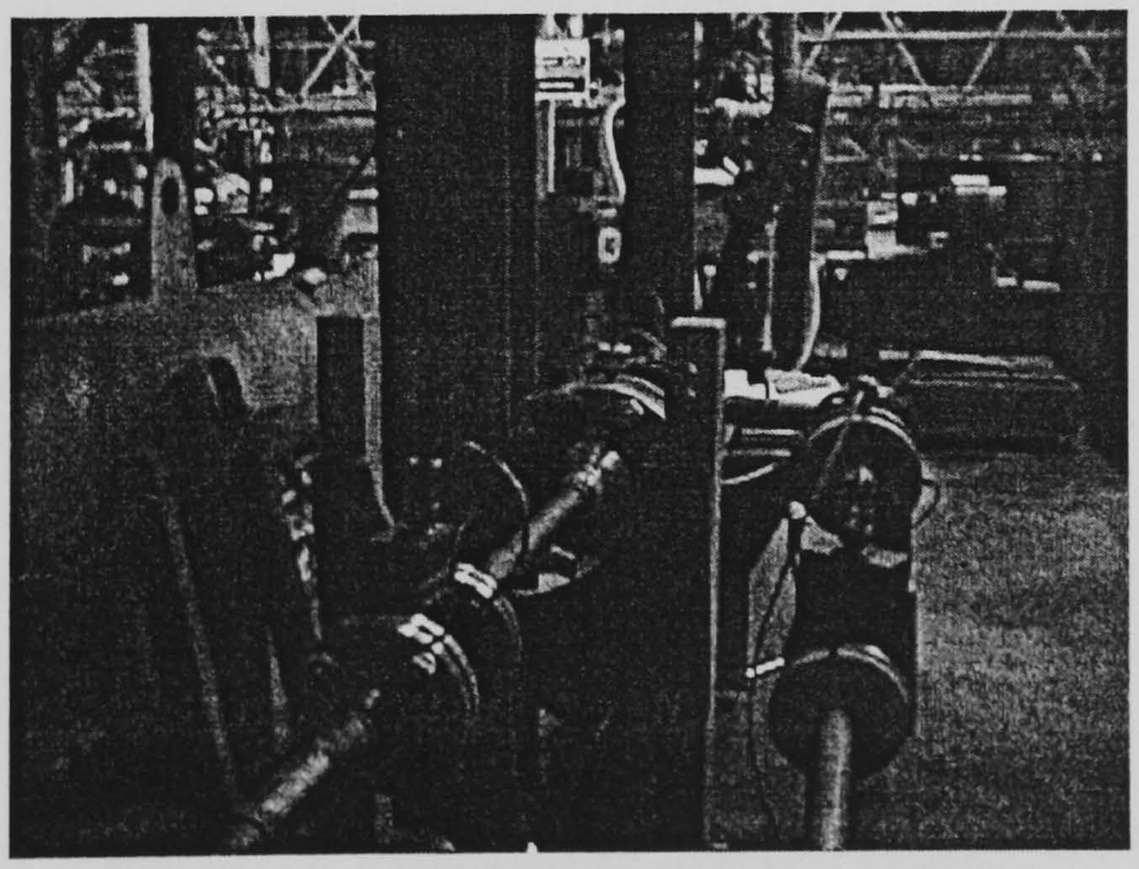

Figure 3.5 – Gas Flow Metering Station

At the gas metering point temperature and pressure are measured to give the mass flow of the gas entering the test section, see Section 3.3.3 below. All data from the Three Phase Facility instrumentation is recorded by the Data Acquisition System for the Flexible Riser Rig, see Section 3.2.3.

3.2 Flexible Riser Rig

The Flexible Riser Rig used in this work consisted of a pipeline and riser test section with the flow exiting the riser into a top separator, Figure 3.6. This section describes in detail the pipeline/riser rig, covering the test section, the instrumentation and the Data Acquisition System. As stated in Section 2.7, the greatest challenge in terms of the current understanding of severe slugging remains to be the behaviour of S-shaped riser systems under severe slugging conditions. Hence, the rig used in these experiments was of a lazy-S configuration.

3.2.1 Riser Test Section and Topsides Separator

The pipeline/riser, Figure 3.6, was made up of flanged 50 mm (2") nominal bore carbon steel sections, rated to ANSI Schedule 40. The carbon steel flanges were welding-neck flanges and were rated to BS 1540 Class 300. The pipeline had a total length of 57.4 m and was inclined at -2° to the horizontal. The pipeline length was such to allow the stabilisation of the pipeline flow regime before entry into the riser base and to provide sufficient gas compressible volume for severe slugging to occur (Caltec, 1999). The riser was in a Lazy-S configuration, with a total height of 9.98 m and a total length of 18 m. Table 3.2 gives the x-y coordinates describing the riser profile.

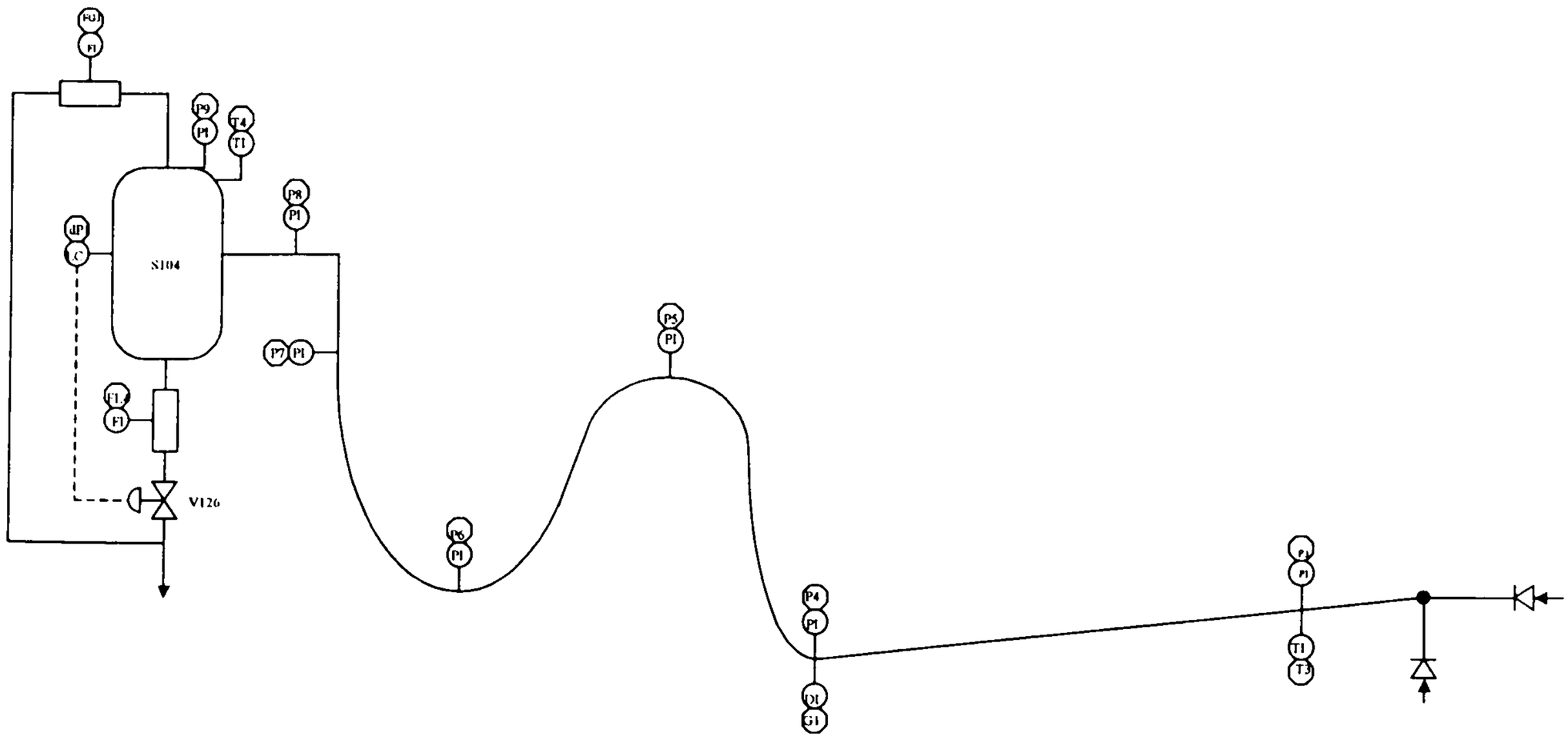

Figure 3.6 – Pipeline/Riser P&I Diagram

At the top of the riser, the fluids proceeded around a 90° bend and through a 3 m section of horizontal pipe, finally entering the top separator, S104. This separator simulated the first stage of an offshore topsides facility and was used in the mass balance calculation to determine the outlet flowrates of each phase. The separator was a cylindrical separator with semi-ellipsoidal ends, in a vertical orientation with air and water exiting from the top and bottom of the separator respectively. The internal diameter of the separator was 0.5 m and the main volume had a height of 0.5 m, the dished ends had a height of 0.0762 m. The liquid level in the separator was controlled using a Control and Readout 452+ PID level controller. The control loop used a measurement of the differential pressure over the separator height to infer the liquid level and manipulated the outlet liquid flow via a Masonelian Series 35002 Camflex actuated valve. Fluids exiting the separator were recombined post-metering (see Section 3.2.2) for return to the Three Phase Facility.

X Co-Ordinate (m)	Y Co-Ordinate (m)
-57.4	2
0	0[1]
0.831	0.223
1.494	0.961
2.032	2.059
2.198	2.889
2.315	3.933
2.369	4.435
2.441	4.778
2.524	4.873
2.663	4.945
2.814	4.954
2.949	4.907
3.075	4.788
3.117	4.700
3.151	4.520
3.186	4.295
3.218	4.089
3.259	3.837
3.382	3.472
3.948	2.829
4.238	2.679
4.621	2.624
5.032	2.730
5.426	3.047
6.025	3.756
6.412	4.394
6.659	4.944
6.884	5.680
7.006	6.498
7.020	7.835
7.020	9.258
7.020	9.982
10.020	9.982

Table 3.2 – Co-Ordinates of the Pipeline/Riser Test Section

[1] The (0, 0) co-ordinate is the riser base

3.2.2 Instrumentation

The instrumentation along the Test Section and Separator, see Figure 3.6, consisted of 13 analogue measurements, summarised in Table 3.3 below. For the Test Section, pressure and temperature were measured at the inlet so that phase velocities were referenced to pipe conditions in flow pattern studies.

Sensor Designation	Sensor Description	Sensor Details	Range
P3	Inlet Pressure	Data Instruments Model SA300	0-19.5 bar(g)
P4	Riser Base Pressure	Data Instruments Model SA300	0-19.5 bar(g)
P5	Pressure at Top of S-bend	Data Instruments Model SA300	0-19.5 bar(g)
P6	Pressure at Base of S-bend	Data Instruments Model SA300	0-19.5 bar(g)
P7	In-Line Pressure in Upper Limb	Data Instruments Model SA300	0-19.5 bar(g)
P8	Pressure in Outlet Line	Data Instruments Model SA200	0-13 bar(g)
P9	Separator Pressure	Data Instruments Model SA200	0-13 bar(g)
G1	Riser Base Density	ICI Tracerco Gamma Ray Densitometer	0-1000 kg/m^3
T3	Inlet Temperature	In-House Type 'T' Thermocouple	0-100 °C
T4	Separator Temperature	In-House Type 'T' Thermocouple	0-100 °C
dP1	Separator Liquid Level	IDP10-I Intelligent d/p cell transmitter	0-+4.905 kPa
FL4	Separator Outlet Liquid Flowrate	ABB MagMaster Electromagnetic Flowmeter	0-21.6 m^3/hr
FG3	Separator Outlet Gas Flowrate	Quadrina Q-Flo Turbine Meter, Model QFG/25B/EP1	6-60 m^3/hr

Table 3.3 – Test Section Instrumentation

Pressure was measured at the riser base to allow flow regime identification, after Schmidt et al. (1981) and Tin and Sharshar (1991). Pressure measurements were also made in the pipeline; at the top and bottom of the riser S-bend and entering and exiting the 90° bend. The pressure measurements were used to determine the liquid inventory in each limb of the riser and the riser as a whole (see Section 3.3). The liquid density was measured local to the riser base using an ICI Tracerco single beam gamma ray densitometer, the system was made up of a PRI 116 Detector and PRI 121 Control Unit. This system gave the density, which was then converted to liquid holdup (see Section 3.3.2). The location of the gamma densitometer was slightly upstream, 100 mm, of the minimum point of the riser base dip. This was due to installation restrictions with the gamma source. Hence this measurement is not the riser base liquid holdup but the holdup local to the riser base. As such this measurement was used primarily for flow regime identification purposes and not for extracting exact information on the liquid holdup, except under exceptional circumstances that will be dealt with in the appropriate section.

The outlet separator was instrumented with a pressure transducer, thermocouple and a differential pressure transducer giving the liquid level. The pressure, temperature and level were used in the separator mass balances to obtain the mass of the fluids in the separator at a given time instant. The separator pressure measurement was also used to obtain a measure of the overall pressure of the system, a set condition for the tests. The flowrates of the gas and liquid exiting the separator were measured by a Quadrina QFG/25B/EP1 turbine flowmeter and an ABB Magmaster electromagnetic flowmeter; these had a range 6-60 m^3/hr and 0.36-36 m^3/hr respectively. The electromagnetic flowmeter was located upstream of the control valve V126 to keep the meter volume filled with liquid at all times. The presence of gas in this volume, either from the meter draining or bubbles in the liquid flow, would have caused erroneous liquid flow signals.

3.2.3 Data Acquisition System

Data from the Three Phase Facility metering stations, the Test Section and Separator instrumentation was acquired by a dedicated PC-based Data Acquisition System (DAS), see Figure 3.7. The DAS hardware consisted of a Signal Conditioning Extensions for Instrumentation (SCXI) unit supplied by National Instruments and a series of custom-built signal conditioning units (Caltec, 1999). The signal conditioning units provided the input signals to the transducers/instruments, where required, and processed the returning signals which were then passed to the SCXI unit. This system was made up of an SCXI 1000 housing unit, an SCXI 1100 32 channel multiplexer and an SCXI 1200 parallel port multiplexer. Data was collected over a set of 21 channels, with a range of 0 to 5 V d.c. The incoming data was received by the 32 channel multiplexer and converted to an appropriate digital signal, this was then transferred to the PC via the parallel port multiplexer.

The maximum potential sampling frequency of the hardware was 25 kS/s over all channels, this gave a potential sample frequency of 1.19 kS/s per channel when 21 channels were in use. However, due to limitations in the gamma ray densitometer, the

recording frequency was set at 10 S/s, the maximum output frequency of the gamma ray densitometer.

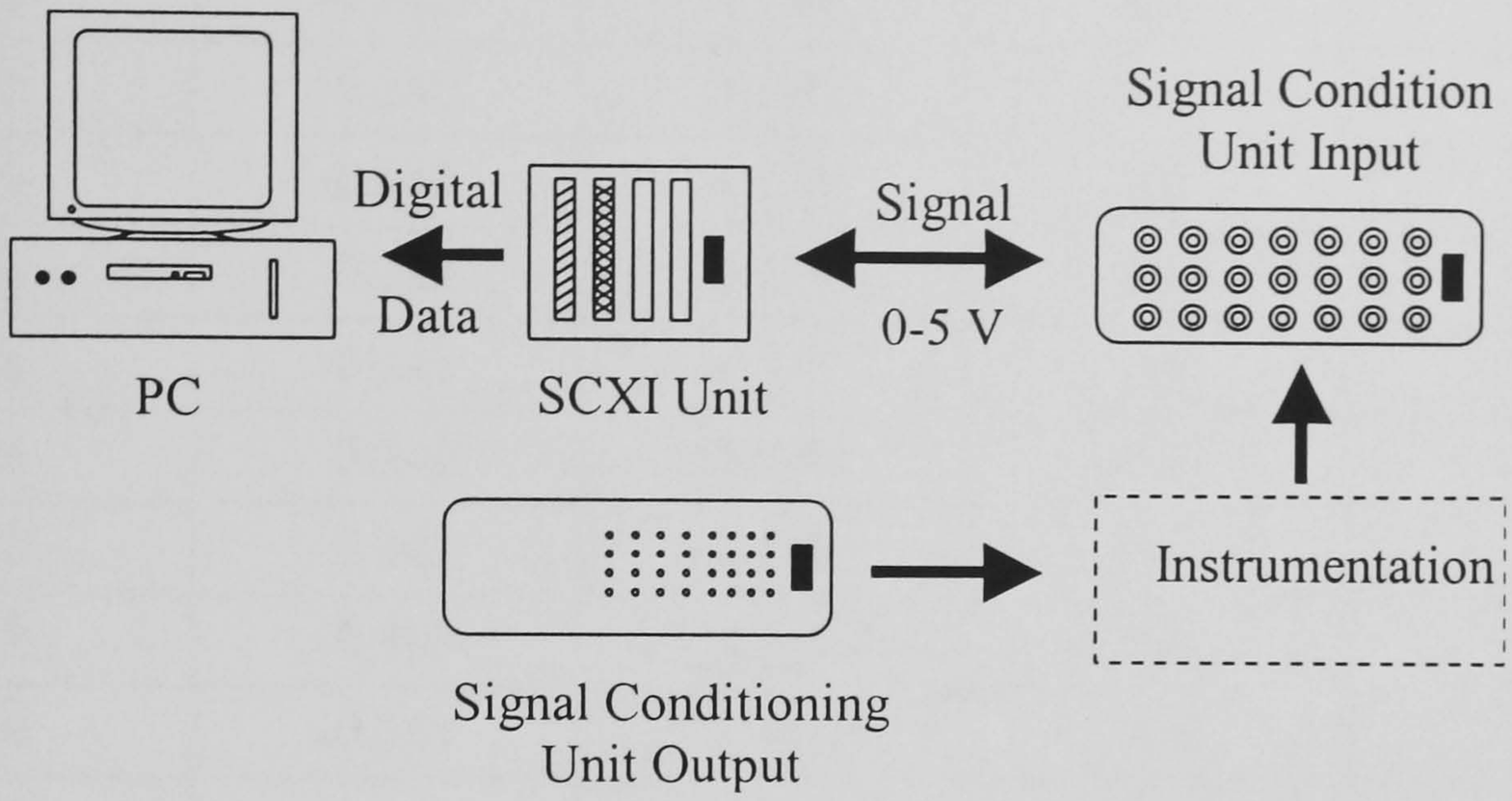

Figure 3.7 – Riser DAS

Data from the SCXI units was sent to a dedicated PC, this computer was a Pentium 166 MHz computer with 48 Mb of RAM, running the Windows 3.11 operating system. A runtime version of a LabView 'Virtual Instrument' was used to gather data in real time from the DAS hardware and display the results to the computer screen for control purposes.

The DAS software took information on the raw voltage information entering the computer from the DAS hardware and converted this information to engineering units for the corresponding instruments. In order to do this, the following equation was used:

$$EU = K(V - V_0) \qquad (3.1)$$

In Equation (3.1), EU is the required engineering unit (the measured variable), K the gain and V is the voltage signal. V_0 is the voltage at the zero signal reading, i.e. where the measured variable is zero, this is commonly referred to as the 'zero' or 'offset'. The required gains and zeros for each channel were held in a look-up table and text file that was accessed by the DAS software during execution. This table is replicated below in Table 3.4.

The data produced from the DAS was written to an ASCII text file. This file contained a variable length header describing the test and conditions and the data, recorded in tab-delimited form, at the same frequency as the DAS sampling rate, in this case 10 Hz. Data processing was then carried out at a later stage and is described in the next section.

Signal	Zero	Gain	Units	Channel
P1	-0.242	4.124	bar	1
P2	-0.242	4.124	bar	2
P3	-0.242	4.124	bar	3
P4	-0.242	4.124	bar	4
P5	-0.242	4.138	bar	5
P6	-0.242	4.138	bar	6
P7	-0.242	4.138	bar	7
P8	-0.363	2.757	bar	8
P9	-0.364	2.751	bar	9
T1	0	20	°C	10
T2	0	20	°C	11
T3	0	20	°C	12
T4	0	20	°C	13
G1	0	220	kg/m^3	14
FG1	0	0.448	l/s	15
FG2	0	1[2]	l/s	16
FG3	0	3.316	l/s	17
DP1[3]	0	20	%	18
FL1	0	2.507	l/s	19
FL2	0	7.85	l/s	20
FL4	1	2	l/s	21

Table 3.4 – Look-Up Table for the DAS

3.3 Data Processing/Analysis

In the past, the measurements of the riser base pressure and liquid holdup have been the preliminary methods of identifying flow regime in a pipeline/riser. This practice has been continued in the present work. However, in order to gain further information on the characteristics and mechanisms of severe slugging, additional measurements were made of the pressure cycling in each riser limb and the fluid production characteristics. Additional data processing was carried out on the inlet flow

[2] A polynomial calibration was used, hence the raw voltage signal was acquired by the DAS
[3] This was the level measurement signal with a scale of 0 to 5 V corresponding to 0 to 100% level

characteristics to provide data for flow pattern map studies and code comparisons. The data series extracted during data processing are summarised in Table 3.5 below. A custom-written Matlab script file DATAPROCLG.M was used to extract this information and is provided in Appendix A.

Signal	Description	Units
P_{RB}	Riser Base Pressure	bar(a)
P_S	Separator Pressure	bar(a)
ΔP_R	Pressure Difference Over Riser	bar(a)
ΔP_L	Pressure Difference Over Lower Limb	bar(a)
ΔP_D	Pressure Difference Over Downcomer	bar(a)
ΔP_U	Pressure Difference Over Upper Limb	bar(a)
ε_{LB}	Riser Base Liquid Holdup	
G_{GI}	Inlet Gas Mass Flow	kg/s
U_{GI}^{S}	Inlet Gas Superficial Liquid Velocity	m/s
G_{LI}	Inlet Liquid Mass Flow	kg/s
U_{LI}^{S}	Inlet Liquid Superficial Liquid Velocity	m/s
G_{LO}	Outlet Liquid Mass Flow	kg/s
U_{LO}^{S}	Outlet Liquid Superficial Velocity	m/s
G_{GO}	Outlet Gas Mass Flow	kg/s
U_{GO}^{S}	Outlet Gas Superficial Liquid Velocity	m/s

Table 3.5 – Data Series for Examination

3.3.1 Pressure Characteristics

Pressure Difference

As stated above and in accordance with previous investigations, the riser base pressure characteristic was retained as a primary means of flow regime identification. However in the case of the Riser Rig, the basic pressure balance equation must be examined.

The riser base pressure is given by (see Figure 3.8):

$$P_B = P_D + \rho_L g h' + \Delta P_{Loss} \qquad (3.2)$$

Where h' is the effective height of liquid in the riser and ΔP_{Loss} is the pressure losses in the system (due to acceleration and friction losses), other symbols have their usual meaning.

In the case of all previous experiments, the downstream pressure P_D was atmospheric pressure and essentially constant. Furthermore the riser was in a vertical orientation and this meant that the measurement of pressure at the riser base was only a function of the height of liquid in the riser and the loss terms. Hence the effective height of liquid was the true height of liquid in the riser, h_R. Assuming the loss terms are relatively small compared to the hydrostatic term, the riser base pressure measurement gave the hydrostatic head within the riser during severe slugging and the total liquid inventory in the riser. Previous workers then identified and characterised severe slugging according to the hydrostatic head variation in the riser.

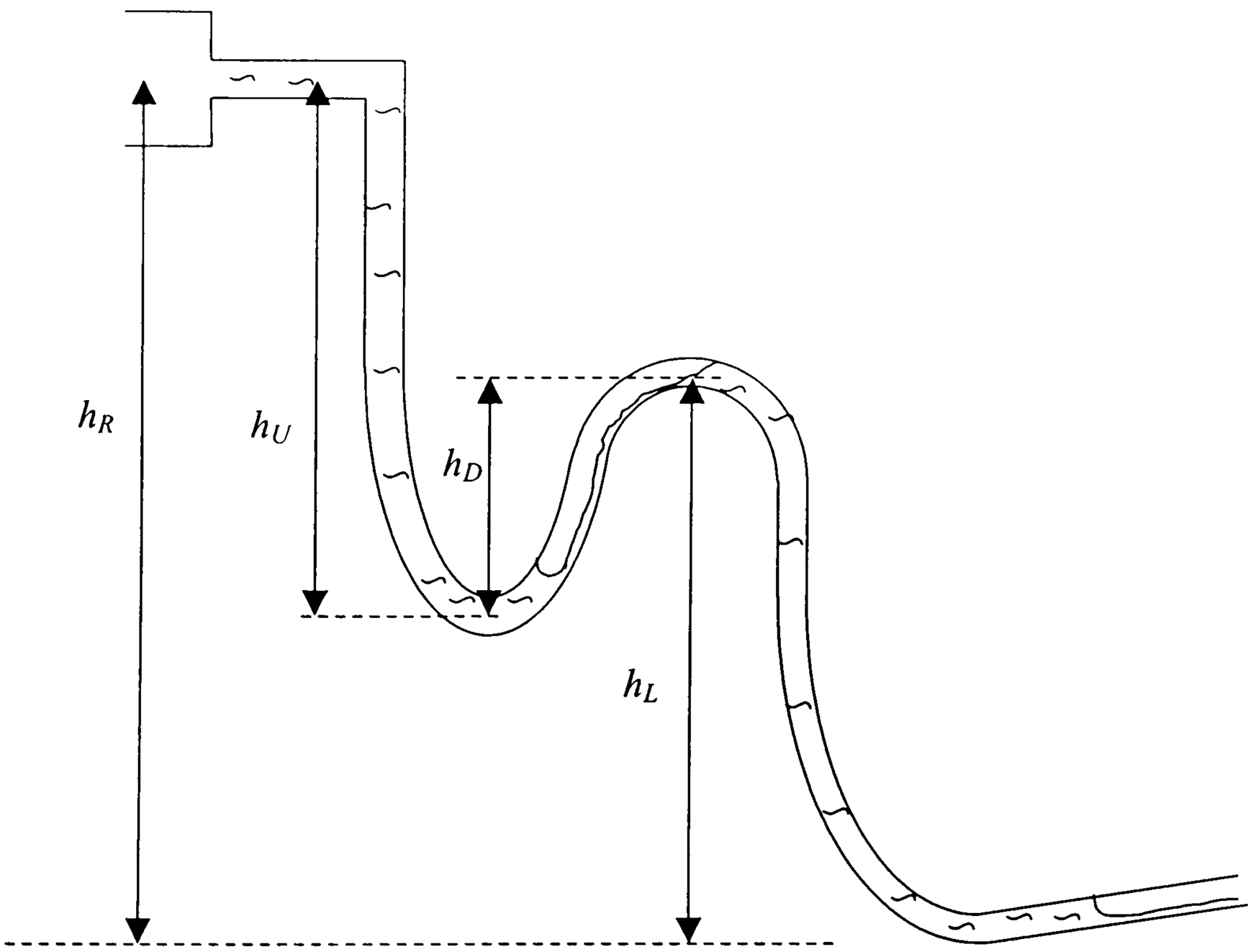

Figure 3.8 – Pipeline/Riser Liquid Distribution

In the case of the Riser Rig used in this work, the downstream pressure was the separator pressure, P_S. Though the system pressure was controlled ultimately in the Three Phase Facility, there was the potential for variation in the top separator pressure. Variations occurred during the bubble penetration and gas blowdown stages of severe slugging. These variations were caused by a combination of the rapid deliveries of liquid and gas individually during the severe slugging process and the dynamic response of the liquid level control in the top separator and the pressure

control in the three phase separator. Figure 3.9 shows a typical variation of the separator pressure during severe slugging 1, in this case the variation is ~0.1 bar, 5% of the average separator pressure.

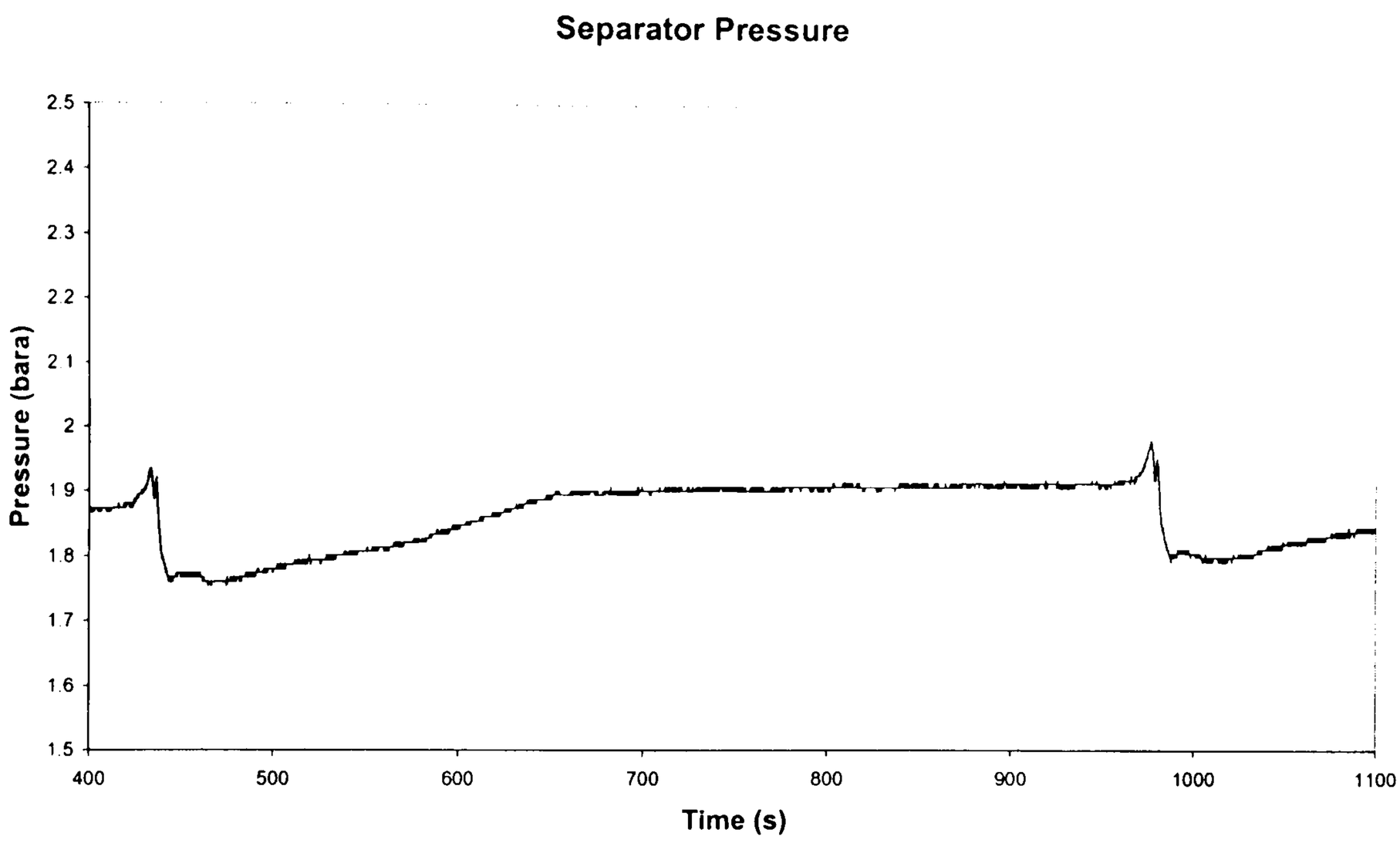

Figure 3.9 – Separator Pressure Variation
During Severe Slugging 1

In order to extract the variation in 'effective' hydrostatic head from the riser base pressure signal, the time-varying separator pressure was subtracted from the riser base pressure at each timestep. This gave the pressure difference over the riser against time, ΔP_R:

$$\Delta P_R = P_B - P_S = \rho_L g h' + \Delta P_{Loss} \approx \rho_L g h' \qquad (3.3)$$

As noted above, this examination of the pressure difference over the riser relies on the pressure losses due to friction and acceleration being small compared to the hydrostatic pressure. Single phase flow experiments, conducted during commissioning, showed that for single phase liquid flow, the pressure drop was of the order of 0.02 bar at a water flowrate of 0.6 m/s, see Appendix B, hence ΔP_{Loss} was small when compared to the effective hydrostatic pressure in the riser.

Figures 3.10 shows the contrast between the riser base pressure profile and pressure difference over the riser profile during severe slugging. Referring to the figures, the time at which slug formation stops is clearly identifiable from the pressure difference trace, Point A.

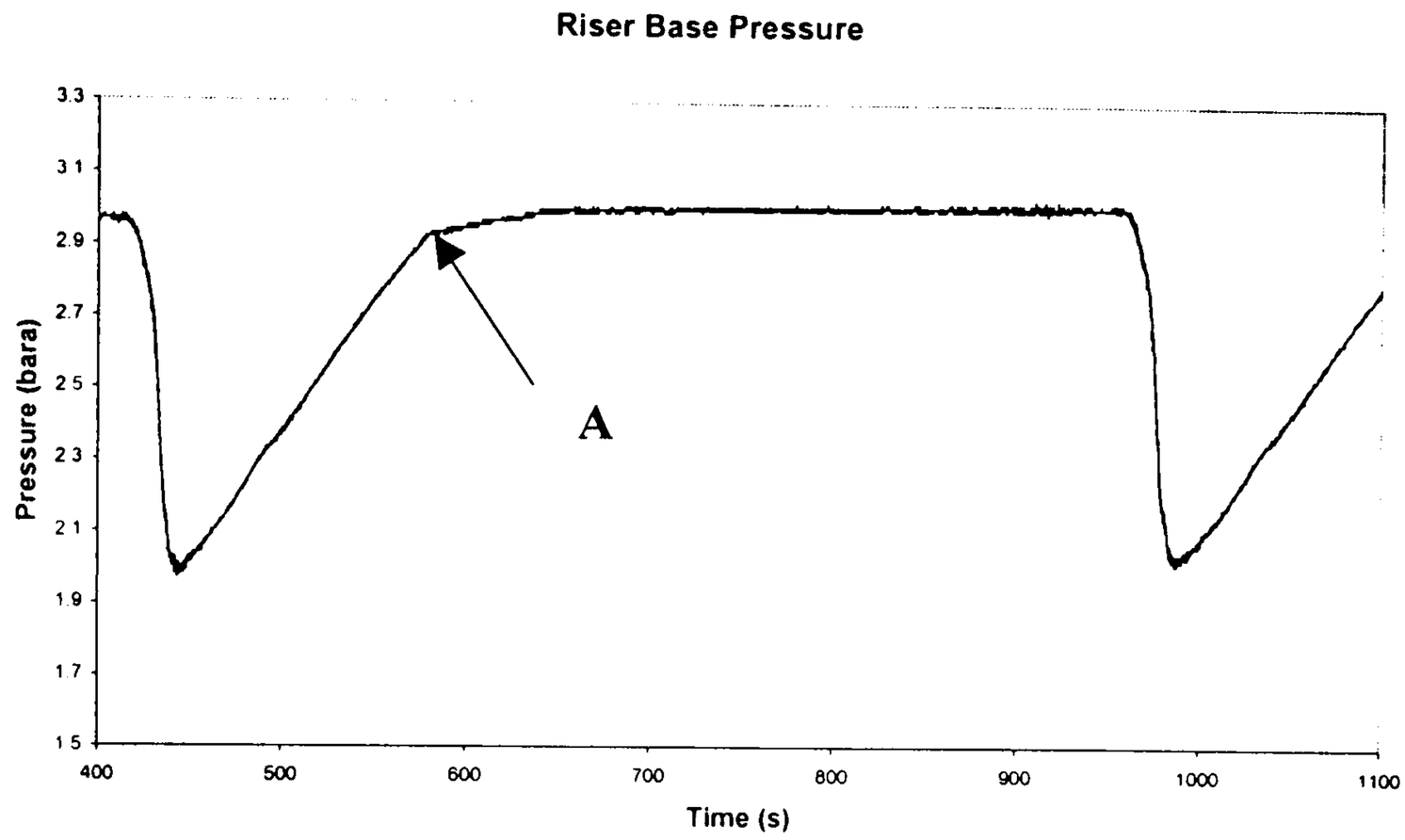

(a) Riser Base Pressure Profile

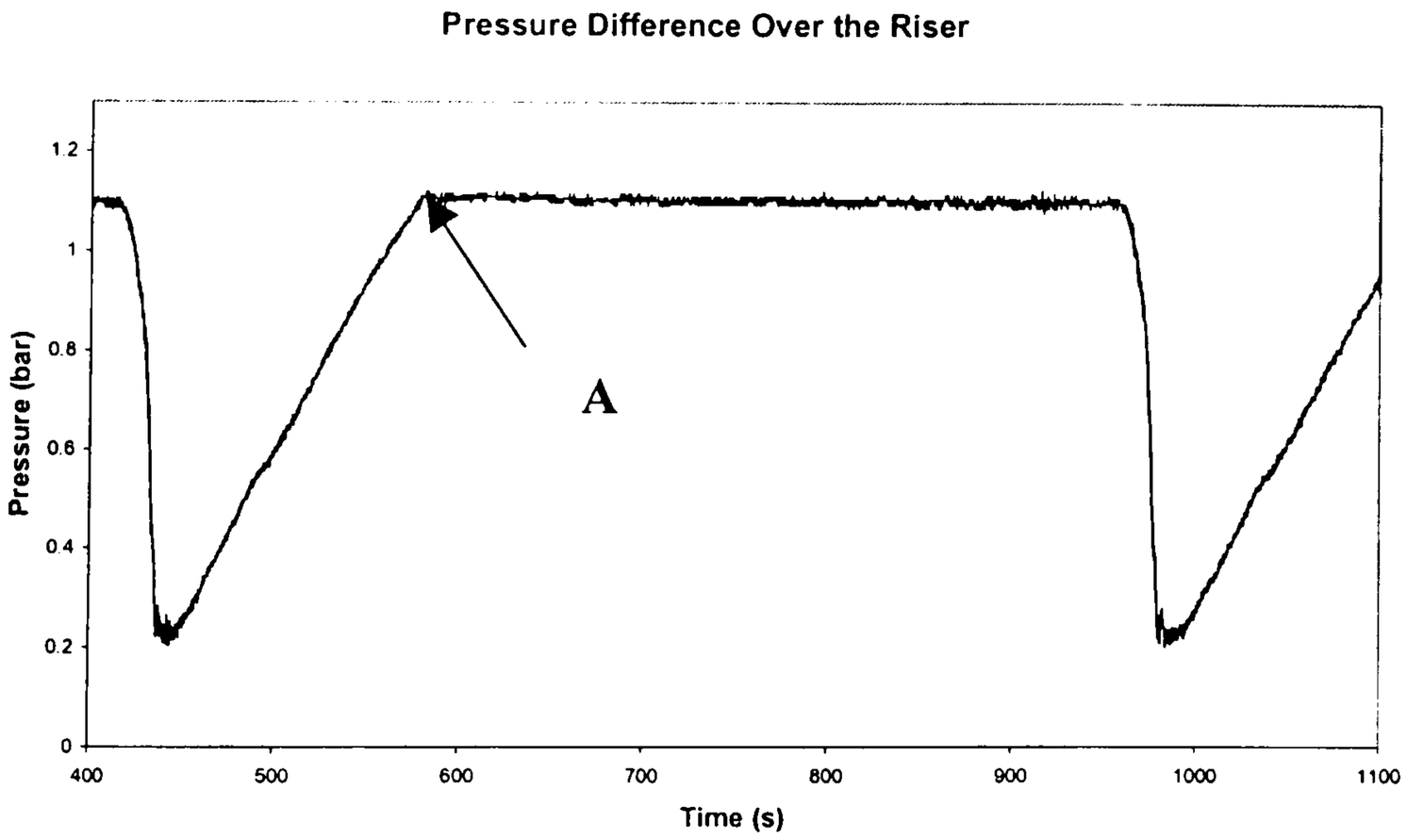

(b) Pressure Difference Over Riser Profile

Figure 3.10 – Comparison of Riser Base and Riser Pressure Difference Profiles

Recalling the severe slugging mechanism, Section 2.1.1, slug formation is complete once the slug front has reached the top of the riser and the hydrostatic pressure has stopped increasing. In the case of the riser base pressure trace, the pressure continues to increase beyond Point A, making identification of this point more difficult. The additional distinction between the stages of severe slugging when using the pressure difference over the riser highlights the various stages during severe slugging. Thus the pressure difference over the riser is used as a primary method of characterising the flow regime in the pipeline/riser.

In a manner similar to the above approach, signals for the pressure difference over the lower limb of the riser, the downcomer of the S-bend and the upper limb were extracted from the raw data. These can be summarised below (assuming pressure losses are small):

$$\Delta P_l = P_{RB} - P_l = \rho_L g h_l \qquad (3.4)$$

$$\Delta P_d = P_d - P_l = \rho_L g h_d \qquad (3.5)$$

$$\Delta P_u = P_u - P_d = \rho_L g h_u \qquad (3.6)$$

Where the subscripts *d*, *l* and *u* correspond to the downcomer, lower and upper limbs respectively.

Effective Height of Liquid in the Riser – Pressure Recovery

As stated above, in Equation (3.2), h' was the effective height of the riser, giving the effective hydrostatic pressure difference over the riser. This term was used as the pressure difference over the riser but was not equal to the hydrostatic head of liquid in the riser. Examining the pressure balance equation for the entire riser and neglecting the pressure losses gives:

$$P_B = P_S + \Delta P_u - \Delta P_d + \Delta P_l \qquad (3.7)$$

Substituting the appropriate terms from Equations (3.3) - (3.7) gives the expression for the pressure difference over the riser:

$$\Delta P_R = \rho_L g h' = \rho_L g h_u - \rho_L g h_d + \rho_L g h_l = \rho_L g\left(h_u + h_l - h_d\right) \qquad (3.8)$$

This gives the expression for the effective height of liquid in the riser as:

$$h' = h_u + h_l - h_d \qquad (3.9)$$

Thus, depending on the height of liquid in the downcomer, the effective height of the liquid column in the riser could be greater than the actual height of liquid of the riser, or an equivalent vertical riser. In terms of the Riser Rig in this work, the maximum pressure difference over the riser was 1.195 bar and the minimum pressure difference was 0.972 bar. Examining Figure 3.10 (b) the maximum pressure difference experienced was 1.131 bar, showing that the downcomer was substantially empty. This behaviour has been described as a 'lack of pressure recovery' in the S-bend (Fairhurst, 1999), with the analogy being made to pressure recovery in downward inclined pipelines as described by Barratt *et al.* (1999).

3.3.2 Liquid Holdup Characteristics

As stated previously, liquid holdup was used primarily as a means of flow regime identification. The instantaneous liquid holdup local to the riser base was obtained from the time-varying density measurement according to the following relation:

$$\varepsilon_{L,i} = \frac{\rho_i}{\rho_L} \qquad (3.10)$$

However gamma ray instrumentation is susceptible to a substantial degree of noise. This is associated with the random nature of the signal, particularly the emission of gamma particles from the source. Gamma ray densitometry readings are highly sensitive to the number of counts arriving at the source over a given sampling period. With the emission of gamma particles being a statistical process, fluctuations in the rate of release of gamma particles causes erroneous density measurements, effectively noise on the true reading. In order to compensate for these fluctuations, a central moving average filter was used to smooth the data. This was implemented using the following equation:

$$\hat{S}_n = \frac{1}{2k+1}\sum_{i=n-k}^{i=n+k} S_i \qquad (3.11)$$

With k = 5, this gave a 1 second moving average for data recorded at 10 Hz. This filter was found to be sufficient for smoothing liquid holdup data without losing significant detail of the flow structure (Montgomery and Yeung, 2000).

3.3.3 Inlet Gas Flow Characteristics

Inlet gas flow characteristics were determined from the gas flow measurement and the Equation of State for the gas. The basic equation for the mass flowrate being:

$$G_{GI} = \rho_{GI} Q_{GI} = (\rho_G Q_G)_{REF} \qquad (3.12)$$

Where the symbols have their usual meaning and the subscript *REF* denotes the reference condition, in this case the condition at the metering point. Equation (3.12) assumes there is no accumulation of gas within the system between the metering station and the entrance to the Test Section. Using the Ideal Equation of State for the gas below 10 bar(a):

$$\frac{P}{\rho} = \frac{RT}{M_w} \qquad (3.13)$$

This gives the density of the gas:

$$\rho = \frac{M_w}{R}\frac{P}{T} \qquad (3.14)$$

Substituting the expression for the density into Equation (3.12), gives the mass flow of gas entering the system:

$$G_{GI} = \left(\frac{M_W}{R}\right)\left(\frac{P_{REF}}{T_{REF}}\right)Q_{G,REF} \qquad (3.15)$$

And the flowrate of gas into the Test Section:

$$Q_{GI} = \left(\frac{P_{REF}}{P_I}\right)\left(\frac{T_I}{T_{REF}}\right)Q_{G,REF} \qquad (3.16)$$

The value for the superficial velocity of the gas entering the Test Section is:

$$U_{GI}^{S} = \left(\frac{P_{REF}}{P_I}\right)\left(\frac{T_I}{T_{REF}}\right)\frac{Q_{G,REF}}{A_P} \qquad (3.17)$$

3.3.4 Inlet Liquid Flow Characteristics

In a similar manner to the gas flow characteristic, the liquid flow and velocity entering the Test Section are obtained from the flowrate measured at the metering station, Q_{REF}. Given that there is only liquid in the liquid supply line of the Three Phase Facility:

$$G_{LI} = \rho_L Q_{LI} = \rho_L Q_{L,REF} \qquad (3.18)$$

As the liquid density is constant, the liquid flow entering the Test Section is equal to the measured flow, and the superficial liquid velocity entering the Test Section is:

$$U_{LI}^{S} = \frac{Q_{L,REF}}{A_P} \qquad (3.19)$$

The inlet flow characteristics were checked against the liquid production characteristics to verify the accuracy of the measurements, see below.

3.3.5 Liquid Production Characteristics

In order to determine the outlet flow of gas and liquid from the riser, a pair of mass balances on the gas and liquid in the top separator were carried out. This section details the liquid mass balance on the separator, illustrated in Figure 3.11. It is important to note the nomenclature used in the mass balances, in particular the subscripts *I* and *O* (corresponding to the inlet and outlet conditions) refer to the fluid entering and exiting the separator, not the Test Section.

The basic balance equation for the liquid mass balance on the separator is:

$$G_{LI} - G_{LO} = \frac{dM_{LS}}{dt} \qquad (3.20)$$

Assuming the liquid is incompressible and recalling that the desired quantity is the liquid flow entering the separator, this yields:

$$G_{LI} = \rho_L Q_{LO} + \frac{d}{dt}(\rho_L V_{LS}) = \rho_L Q_{LO} + \rho_L A_S \frac{dh_{LS}}{dt} \qquad (3.21)$$

During experiments the outlet flow from the separator, Q_{LO}, was measured by FL4 and the level by dP1 (see Section 3.2.2). Thus the liquid mass flow into the separator can be found from Equation (3.21) and the experimental measurements.

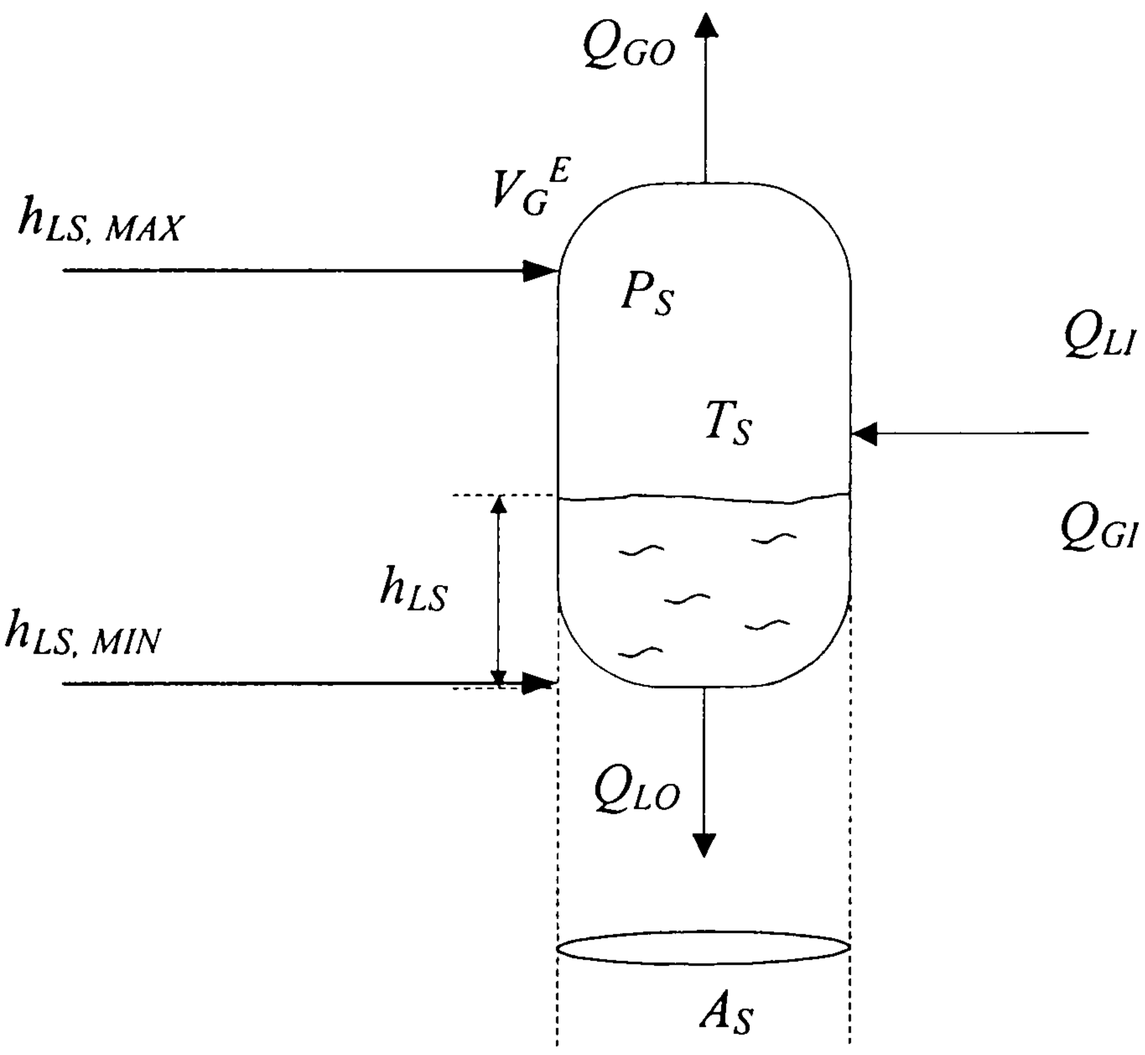

Figure 3.11 – Outlet Liquid Separator

Implementation Issues

The rate of change in liquid height in the separator was obtained by numerical differentiation of the level measurement. However, noise present in experimental data for differentiation caused large fluctuations in the differentiated signal and smoothing of the original data was required (Perry and Green, 1984). The effect of noise in the level signal on the numerical differentiation was reduced using a filter on the level signal and a three-point differentiation formula. The filter was a centred moving average filter with a 1 s window, as described in Section 3.3.2. The three-point differentiation formula is:

$$\left.\frac{dS}{dx}\right|_{x=x_n} = \frac{S(x_{n+1}) - S(x_{n-1})}{2\Delta x} \qquad (3.22)$$

Thus the rate of change of liquid height in the separator is:

$$\left.\frac{dh_{LS}}{dt}\right|_{t=t_n} = \frac{h_{LS}(t_{n+1}) - h_{LS}(t_{n-1})}{2\Delta t} \qquad (3.23)$$

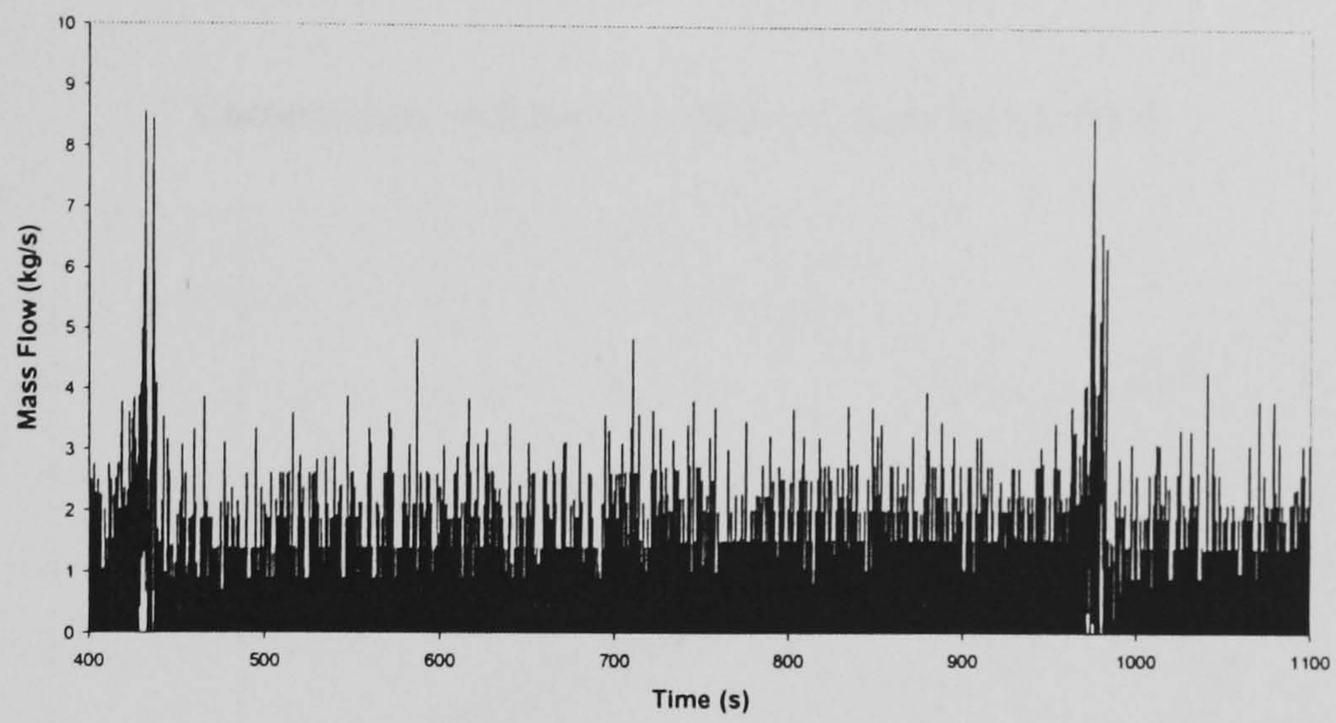

(a) Unfiltered

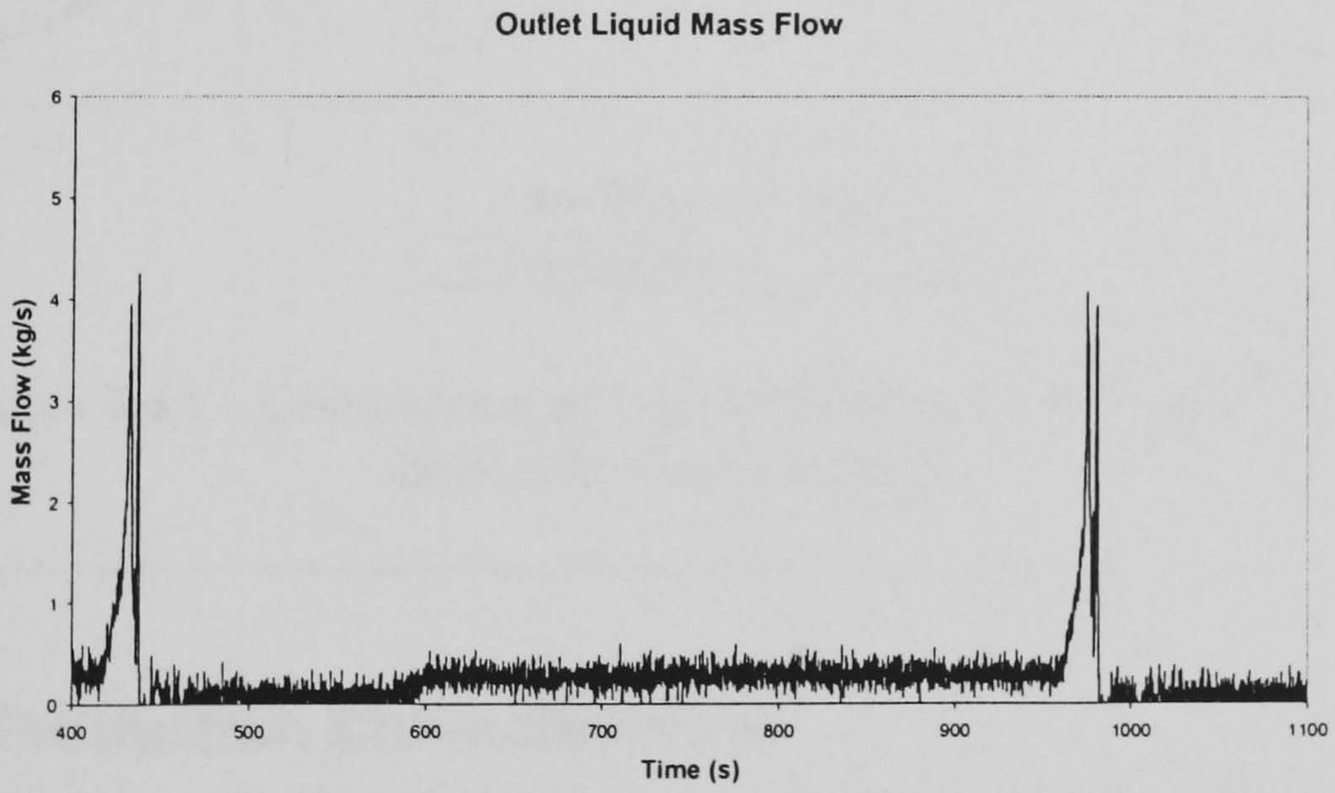

(b) Filtered

Figure 3.12 – Comparison Between the Mass Balance Results With and Without Filtering of the Separator Level

Figure 3.12 shows the significant effect of smoothing on the liquid mass balance calculation. The first profile is the mass flow calculated without any filtering and using a first-order Taylor differentiation formula. The second profile was calculated using the noise compensation procedure described. The results for this calculation are substantially less noisy and give sufficient experimental information to describe the liquid production behaviour at the separator inlet.

This is confirmed by comparing the average flow through the Test Section with the inlet flow. Figure 3.13 shows the comparisons carried out for steady flows. This confirms that the average measured outlet flow is consistent with the average measured inlet flow to within 5% of the reading in 94% of the cases presented below, with an uncertainty of 0.42%. During the experimental programme any errors found with the inlet flow measurement could be identified and compensated for using the liquid mass balance reading.

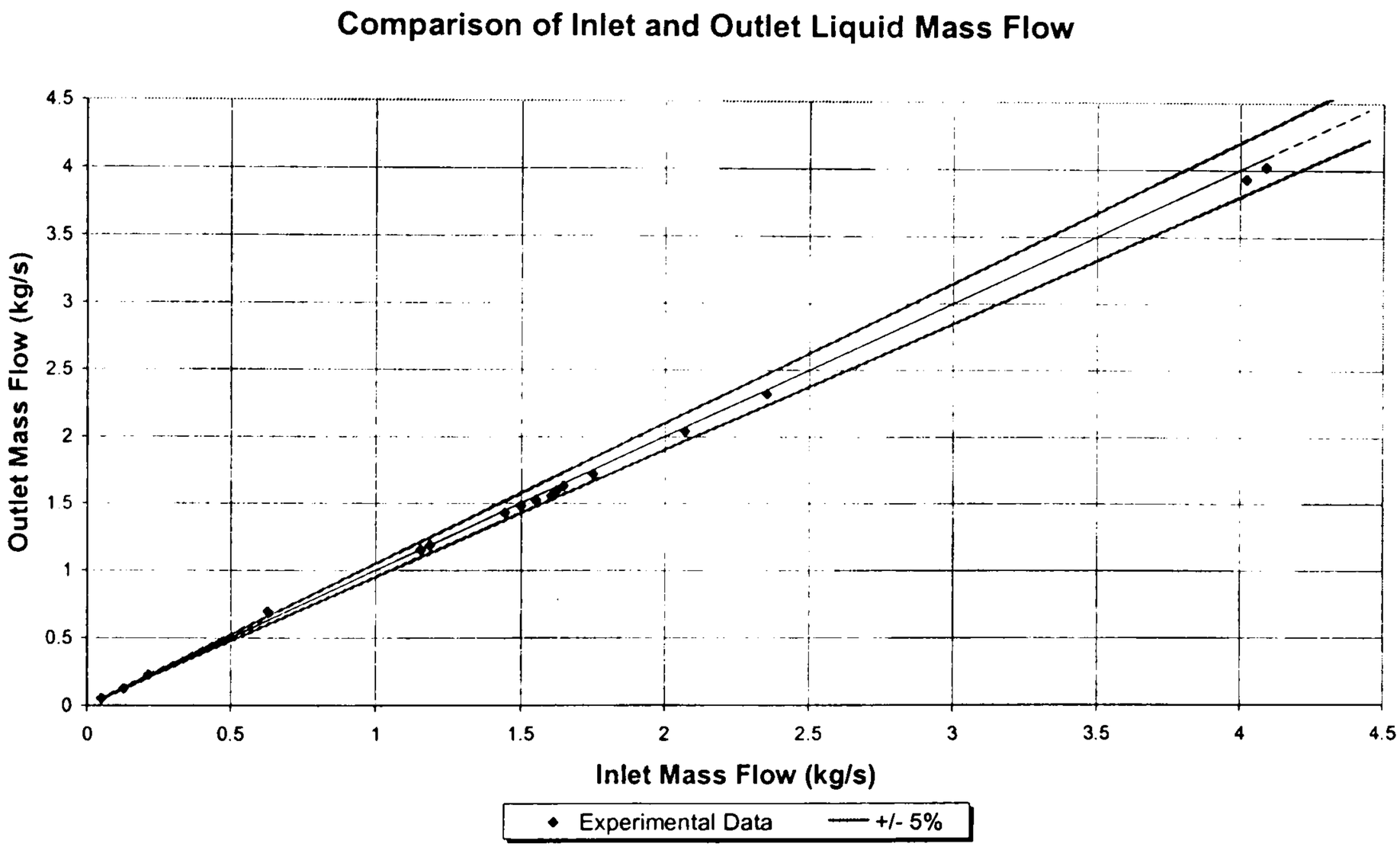

Figure 3.13 – Comparison of Inlet and Outlet Liquid Mass Flow for Steady Flow Regimes

3.3.6 Gas Production Characteristics

In a similar manner to the determination of the liquid mass flow, the outlet gas mass flow from the riser used the equation:

$$G_{GI} - G_{GO} = \frac{dM_G}{dt} \qquad (3.24)$$

As before, it is important to note that the subscripts *I* and *O* refer to the inlet and outlet of the separator. As in the case of the liquid mass balance, each term of this equation was resolved into measured variables at the topsides separator. However in the case of gas, pressure and temperature effects in the separator are important. The mass flow of gas from the separator is given by:

$$G_{GO} = \rho_G Q_{GO} \qquad (3.25)$$

Using the ideal gas Equation Of State for gases at pressure less than 10 bar(a) (Perry, 1984), this becomes:

$$\frac{P}{\rho} = \frac{RT}{M_W} \qquad (3.26)$$

Assuming that the temperature and pressure of the exit gas stream were at the separator conditions, this gives the mass flow exiting the separator as:

$$G_{GO} = \left(\frac{M_W P_S}{RT_S}\right) Q_{GO} \qquad (3.27)$$

The outlet gas flowrate Q_{GO} was measured by FG3 and the temperature and pressure in the separator were measured by T4 and P9 respectively (Section 3.2.2).

The mass of gas in the separator was calculated from the equation of state:

$$PV = nRT = \frac{M}{M_W} RT \qquad (3.28)$$

Rearranging gave the mass of gas in the separator as:

$$M_{GS} = \frac{M_W P_S V_{GS}}{RT_S} \qquad (3.29)$$

Where V_{GS} was the volume of the gas space in the separator. This was found from the level measurement and also included the vapour space above the level measurement points in the separator, this region is constantly filled with gas, hence:

$$V_{GS} = A_S\left(h_{LS,MAX} - h_{LS}\right) + V_G^E \qquad (3.30)$$

Where V^E_G is the excess volume of gas in the region above the level measurement.

When calculating the gradient term, dM_{GS}/dt, the mass in the separator was calculated at each time step and the resulting data series was used for differentiation. This was done to prevent separate differentiation terms for the effect of pressure, temperature and level changes on the mass of gas. A three-point differentiation equation was used to calculate dM_{GS}/dt. In order to reduce noise effects on the differentiation, a centred moving average filter with a 1 second window was applied to the gas mass time series.

Implementation Issues
Examining Figure 3.14, the measurement of gas flow from the separator was susceptible to large peaks that appear to occur at random in the signal.

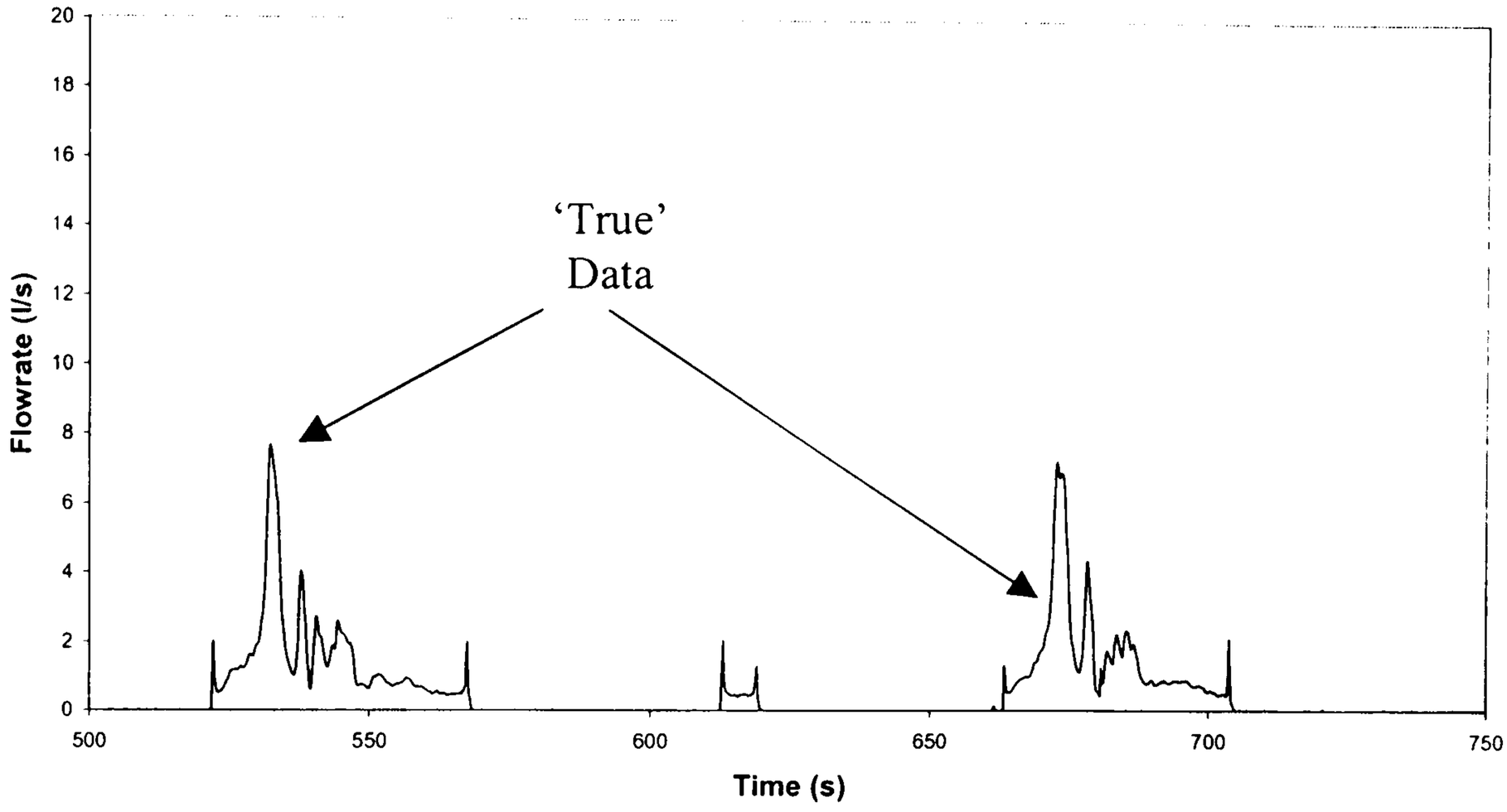

Figure 3.14 – Gas Flow Reading From Separator Outlet Meter

This was associated with flowrates below the range of the flowmeter, in these cases, the impeller of the turbine flowmeter was not turning sufficiently fast to give a continuous signal to the electromagnetic pickup, causing it to give an erroneous maximum flow signal in the DAS as the impeller begins to accelerate from a static position. However the 'true' data can be visually identified, with peak flows of some 8 l/s (indicated). Due to this behaviour, confidence in the exact value of the gas mass balance was reduce, hence, the results of these calculations were only used in a qualitative manner. Further processing of this data is intended to facilitate interpretation of the gas production characteristic

In order to eliminate these impulse-type peaks in the data, a moving average filter was applied. The filter window was applied local to the erroneous data to prevent excessive smoothing of the true peaks in the data. In order to select the points at which to apply the moving average filter, the raw gas flow signal was processed to give the first and the second derivative of the flow against time. The discontinuities in the registered flow to the maximum flow would have large, near infinite, increase in the derivative values. For each calculation, a three-point differentiation formula was used. An example plot is given in Figure 3.15, plotting the raw data and the first derivative. The peaks in the gradient trace are clearly evident in this plot, however they coincide with the erroneous data and the 'true' experimental peaks.

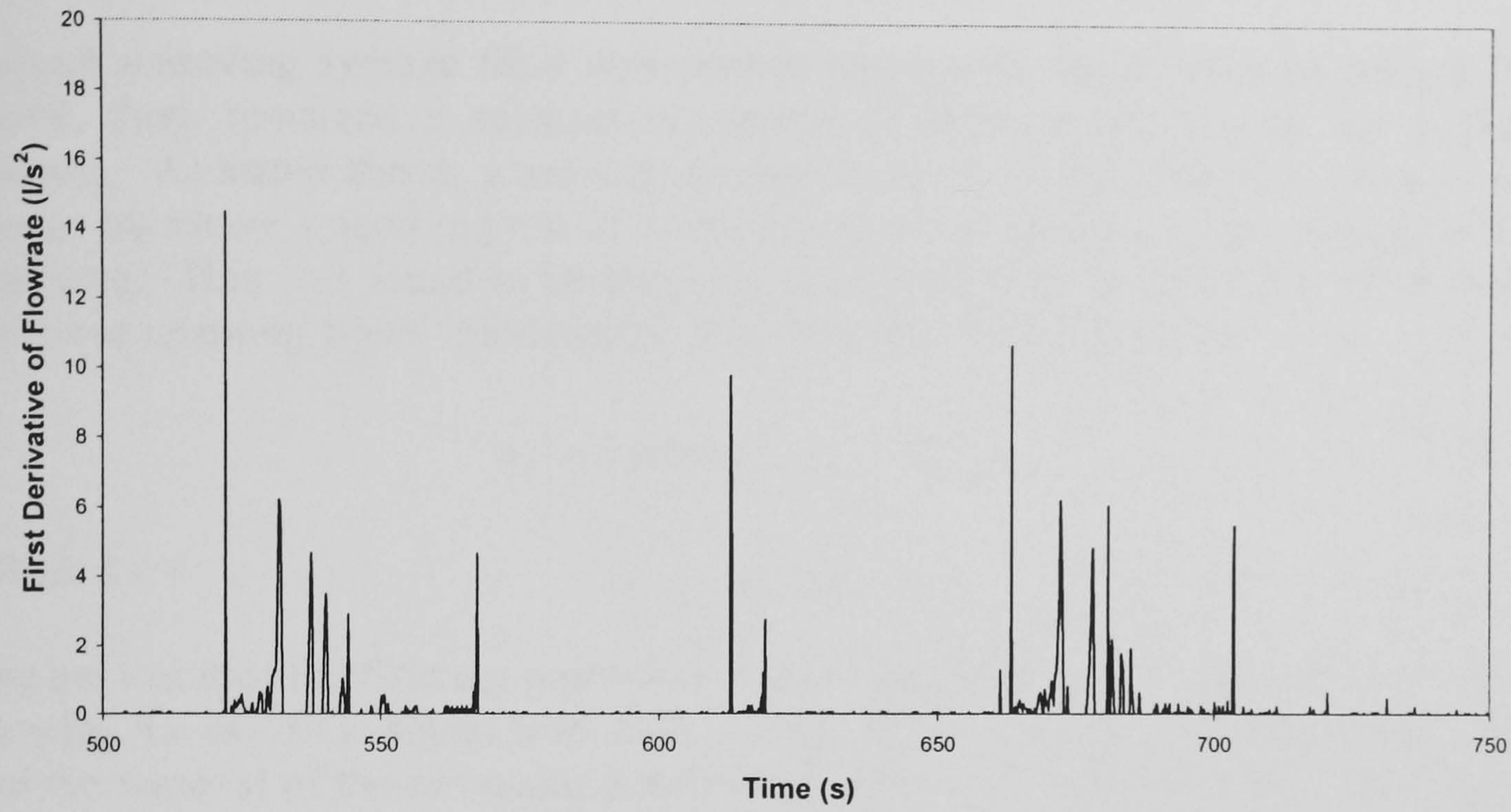

Figure 3.15 – First Derivative of Outlet Gas Flow Reading

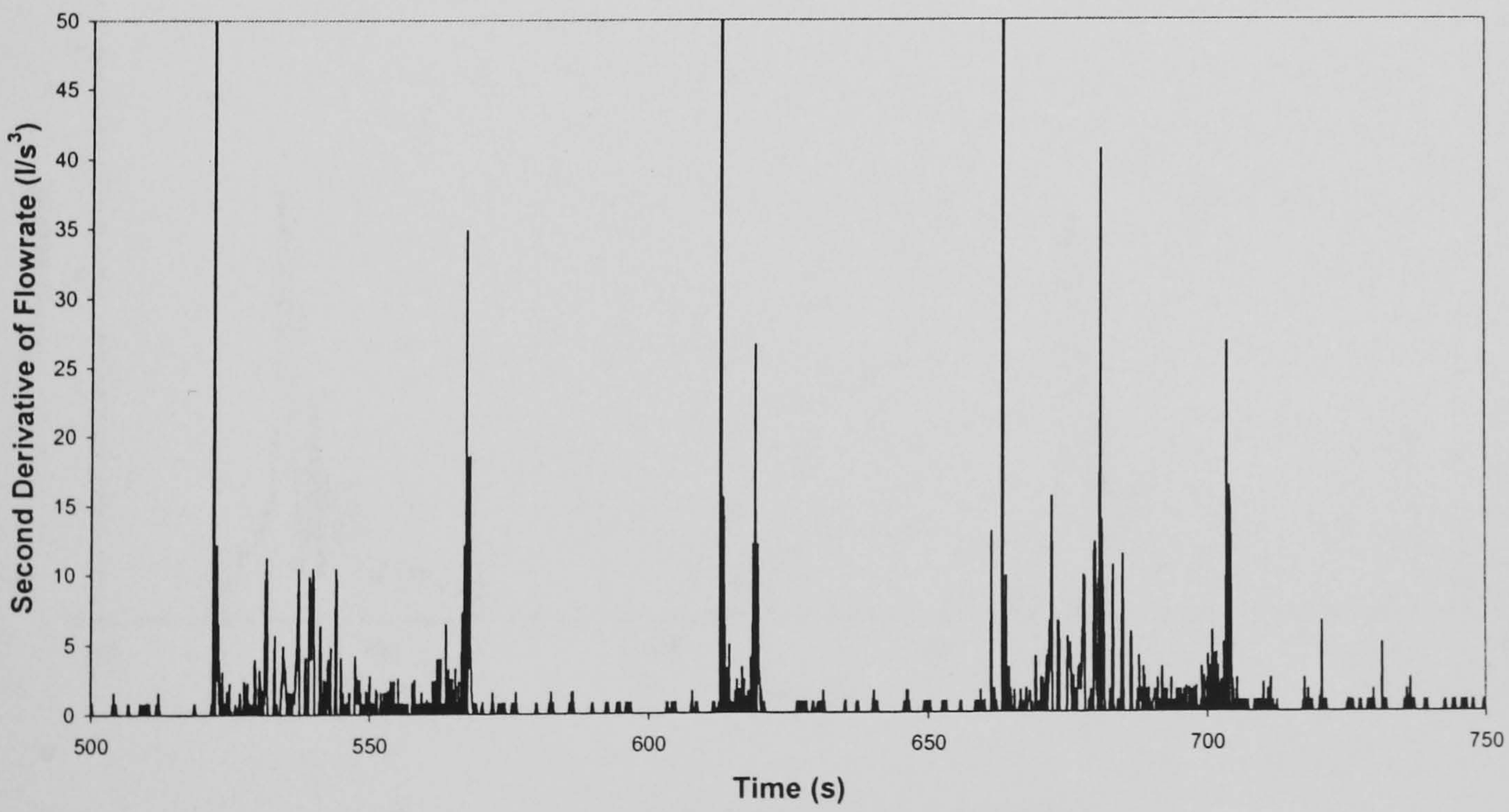

Figure 3.16 – Second Derivative of the Outlet Gas Flow Reading

Examining Figure 3.16, showing the double derivative, the erroneous data is clearly identified, not just by the presence of peaks in the double derivative, but also the

magnitude of the peaks, erroneous data points have a second derivative greater than 15 l/s^3. In this way the points where the moving average filter was applied were selected.

Though a moving average filter was used to remove the large peaks in the gas flow signal, there remained a substantial amount of noise in the signal that required filtering. As stated above, a moving average filter for all the data series would have caused excessive smoothing out of empirical peaks in the data. Thus, a median filter was used. This was found to be the most successful filter in removing the recorded noise but retaining signal information. This was implemented using:

$$\hat{S}_n = median(S_{n-k}, \ldots, S_{n+k}) \qquad (3.31)$$

Where $k = 4$

The net result of the filtering process is summarised by Figures 3.14 and Figure 3.17, showing the raw flow signal from FG3 and the filtered signal. The reduction in noise and the removal of the erroneous peaks is evident in the second figure. This method of data filtering was then applied to all gas flow information and allowed the successful calculation of the gas mass flow into the separator.

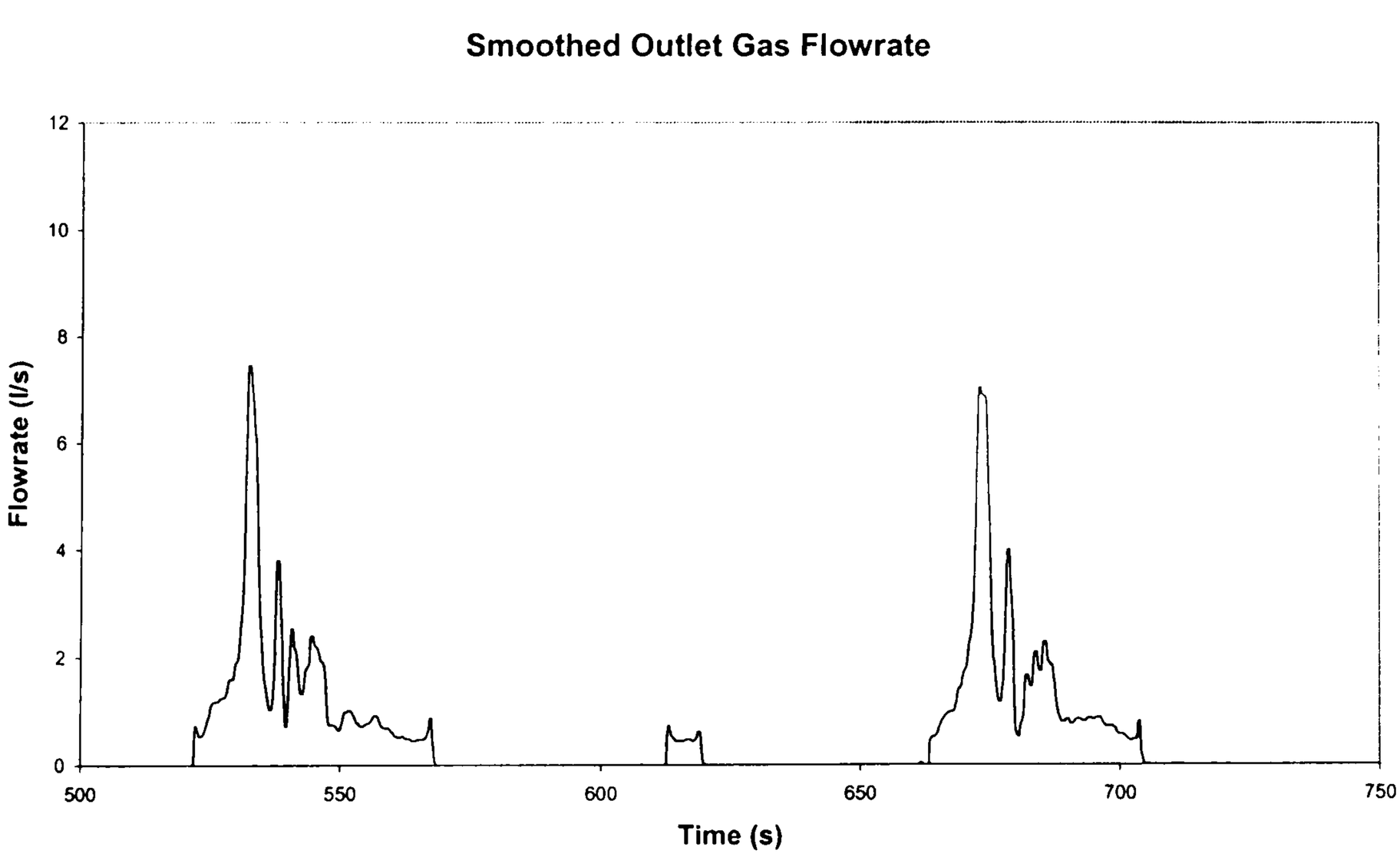

Figure 3.17 – Filtered Gas Flow Reading
From The Topsides Separator Outlet Meter

3.4 Test Procedure and Experimental Conditions

This section describes the test procedure and the test conditions for the experiments carried out in this work. Details of the exact operation procedures for the Three Phase Facility are available in Appendix C. The test conditions selected are presented along with the limiting conditions that the facilities can provide.

3.4.1 Test Procedure

The Riser Rig operations consist of a set of basic startup, operation and shutdown procedures. These focus on the control mechanisms for the Three Phase Facility and the top separator.

Startup

1. All manually operated gas flow control valves to and from the test section are closed, including air receiver outlet and three-phase separator gas outlet valve.
2. Electrical control switches for the top separator level turned on, 5 minutes allowed for the control unit to activate. DAS system turned on, see below.
3. Works air compressor started and air lines to pneumatic controls filled, time allowed for all valves to be actuated to 'closed' position. When the system is shut down all pneumatic valves fail to the fully 'open' position.
4. Air compressor started according to manual instructions, Das (2001) and Caltec (1999).
5. Air receiver filled to main supply pressure this is maintained throughout the testing to maintain a constant mass flow into the Test Section, see below for details.
6. Gas flow control valve opened and three-phase separator brought to test pressure.
7. Gas flow reduced and the three-phase separator pressure controller adjusted for the test gas flow. The setting is adjusted to a gas flow rate close to the expected conditions to minimise the effect of the slow response action of the separator pressure controller.
8. Gas flow stopped, pressure maintained at setpoint for 10 minutes. This step is a test of the controller performance.

DAS Setup

1. Turn on SCXI hardware, this must be operation before the PC to ensure detection and fault-free communication between hardware.
2. Turn on DAS PC, boot up DAS software, checking communication to the SCXI unit.
3. Check DAS calibrations, particularly check the flowmeter settings appropriate to the test flows

Test Setup

1. Liquid flow adjusted to desired setpoint using by pass valve on the water supply pump. This flow allowed to stabilise prior to introduction of the gas.
2. Once riser is filled with liquid, gas flow started, flow regulated through needle valve. Again allowed to stabilise for 10 minutes.

3. Once regular behaviour established, either severe slugging or stable flow, the flowrates are re-examined to observe any drift in the median flow to the test section. If substantial variation has occurred, steps 1 and/or 2 are repeated as necessary.
4. Once flowrates are within desired tolerance, flow behaviour allowed to stabilise over a period of 20 minutes to establish regularity in the flow regime
5. Data recorded for 25 minutes or as required (10 minutes for stable flows)
6. Allow test to continue for 5 minutes after recording stops to ensure that a stable operating condition was achieved.
7. Repeat step 1 for next test condition

Shutdown

1. Liquid flow stopped by opening of the re-circulation valve and pump shut down
2. Gas flow increased to sweep out liquid remaining in the pipeline, at the riser base and the bottom of the S-bend
3. Three phase separator vent opened, venting gas to atmosphere
4. Gas supply compressor stopped and the gas receiver is blown down
5. DAS system and top separator control unit turned off
6. Works air supply turned off and manual flow control valves opened

As stated above, the pressure in the air receiver, T103, must be set to a level appropriate to the test conditions. Furthermore, choked flow was imposed through the needle valve, to keep the mass flow entering the system constant during the tests, irrespective of the downstream pressure. This was to prevent the fluctuations in the pressure at the Test Section inlet during severe slugging from effecting the inlet gas flow. In order to maintain choked flow, the pressure ratio between the pressure in the receiver and the metering station was maintained at double the maximum downstream pressure. Note however that the pressure at the gas metering station is equal to the maximum system pressure during a test, this is equal to the separator pressure plus the maximum pressure difference over the riser, 1.2 bar. Thus the desired pressure in the receiver (in bar(a)) was calculated according to the following rule:

$$P_{REC} = 2(P_S + 1.2) \qquad (3.32)$$

Where the subscript *REC* refers to the receiver.

3.4.2 Test Conditions and Programme

The test series conducted in this work was based upon two considerations – firstly the required operating parameters of the system and secondly the maximum pressure for unstable flows. Previous tests carried out during commissioning of the Three Phase Facility showed that if the operating pressure was above 15 bar(g), the operation of the three phase separator level controller valve and subsequent level change could induce large fluctuations in the top separator pressure. This was due to the large flow induced through the control valve by the high pressure in the separator. These fluctuations were large enough to induce blowdown in the Test Section even when stable flow was normally present. In order to restrict these fluctuations, a separator

pressure of 6 bar(g) was set as the maximum operating pressure. Also previous experiments using the riser facility determined that the maximum system pressure where severe slugging was observed was 7.0 bar(a). Coupled with the requirement for at least 0.5 bar(g) in the separator for the recycling of fluids, the range of operation in terms of pressure was 1-6 bar(g), corresponding to test pressures of 2-7 bar(a).

The fluid delivery facilities and metering stations also placed a restriction on the flow conditions that could be used in the experiments. These were a range of 0.1-5 l/s for the liquid and 0.1-7 l/s for the gas. For the liquid this range was determined by the minimum flow that could be accurately measured by FL1 and the the maximum delivery of the pump against a head of 7 bar(a). For the gas, the range of flows was set by the minimum flow that could be accurately measured by FG1 and the requirement to keep the receiver above P_{REC}. So in summary the envelope of test conditions was as follows, Table 3.6:

Variable	Minimum	Maximum
Pressure (bara)	2	7
Liquid Flow (l/s)	0.1	5
Gas Flow (l/s)	0.1	7

Table 3.6 – Test Conditions

In terms of the Test Programme, a total of 140 tests were carried out over three pressures – 2, 4 and 7 bar(a). The experiments were split as follows: 2 bar(a) – 55 Tests; 4 bar(a) – 45 Tests; 7 bar(a) – 40 Tests.

Chapter 4 – Experimental Results

This chapter presents the results of the experiments carried out as part of this work, it seeks to address the issues outlined in Section 2.7.1 and 2.7.2. The results are presented in two main parts. The first part summarises the characteristics of flow regimes experienced in the pipeline/riser in terms of time-varying behaviour of pressure cycling and fluid production. The second part deals with the flow regime distribution as a function of gas and liquid velocity and examines the effect of system pressure on flow stability. It also examines the experimental results in comparison with existing steady-state criteria for unstable flows and severe slugging.

Part 1 – Flow Regime Characteristics

This first part of the chapter details the characteristics of the flow regimes experienced during the experimental programme of this work. It describes the flow regimes in terms of the overall riser pressure cycling behaviour, the pressure cycling behaviour in each limb, liquid holdup characteristics and the fluid production characteristics. At the end of Part 1 there is a table summarising the characteristics of each flow regime.

4.1 Severe Slugging 1 Characteristics

Pressure Cycling Characteristics

The general severe slugging 1 (SS1) pressure cycling characteristic in terms of riser pressure difference is presented in Figures 4.1 and 4.2 below. It is broken into four basic periods:

1. Liquid Buildup – This is the time period during which the liquid slug accumulates within the system. The riser base cross-section has been blocked to the passage of gas due to liquid fallback (Figure 4.1 Point A, Figure 4.2 (a)) and the pressure difference across the liquid mass is insufficient to move the slug into the riser proper. Inflowing liquid from the pipeline continues to accumulate at the riser base, increasing the overall slug size, backing up in the pipeline and accumulating in the riser. The accumulation of gas in the system continues and gives a preferential accumulation of liquid in the riser, increasing the height of liquid in the riser, the pressure difference over the riser and the pressure at the riser base. Examining the profile in detail there is a small discontinuity in the rate of pressure increase (Point E), this is the point at which the liquid reaches the top of the downcomer and begins to pour into the upper limb, further details of this will be presented below.
2. Slug Production – Once the riser is filled with liquid (Figure 4.1 Point B, Figure 4.2 (b)), the gas accumulation continues and begins to move the liquid in the pipeline into the riser, pushing the gas/liquid interface in the pipeline towards the riser base. This causes a corresponding flow of liquid through the riser, out of the system and into the separator. During this liquid production period, the pressure difference over the riser is at its maximum value. As the riser is completely filled during the period, there is a minimal variation in the

pressure difference over the system and the liquid flow out remains reasonably constant.

3. Bubble Penetration – As the gas/liquid interface reaches the riser base, the gas continues to push through into the riser proper (Figure 4.1 Point C, Figure 4.2 (c)). Moving around the shallow bend at the riser base, the gas forms a series of bubbles that accelerate along the riser as described by Tin (1991). These bubbles displace further liquid from the riser, expanding and reducing the pressure difference over the riser.
4. Gas Blowdown and Liquid Fallback – The drop in pressure difference over the riser during bubble penetration reduces the riser base pressure, inducing acceleration of the pipeline gas into the riser. This in turn increases the rate of change in pressure difference, effectively feeding back into the gas inflow process. In this way, there is a spontaneous sweep-out of the liquid slug and depressurisation or gas blowdown of the pipeline. This blowdown is characterised by a large liquid delivery, followed by a rapid gas delivery, carrying remaining liquid in an annular-flow type of behaviour (Figure 4.1 Point D, Figure 4.2 (d)). Towards the end of the gas blowdown period, the gas flow into the separator decreases. The reduction in momentum transfer is insufficient to support the upward motion of the liquid on the riser walls, which begins to fall, under gravity and in counter-current conditions, into the riser base. The liquid accumulates, blocking the riser base to the passage of gas and initiating the formation of the next slug (Point A*)

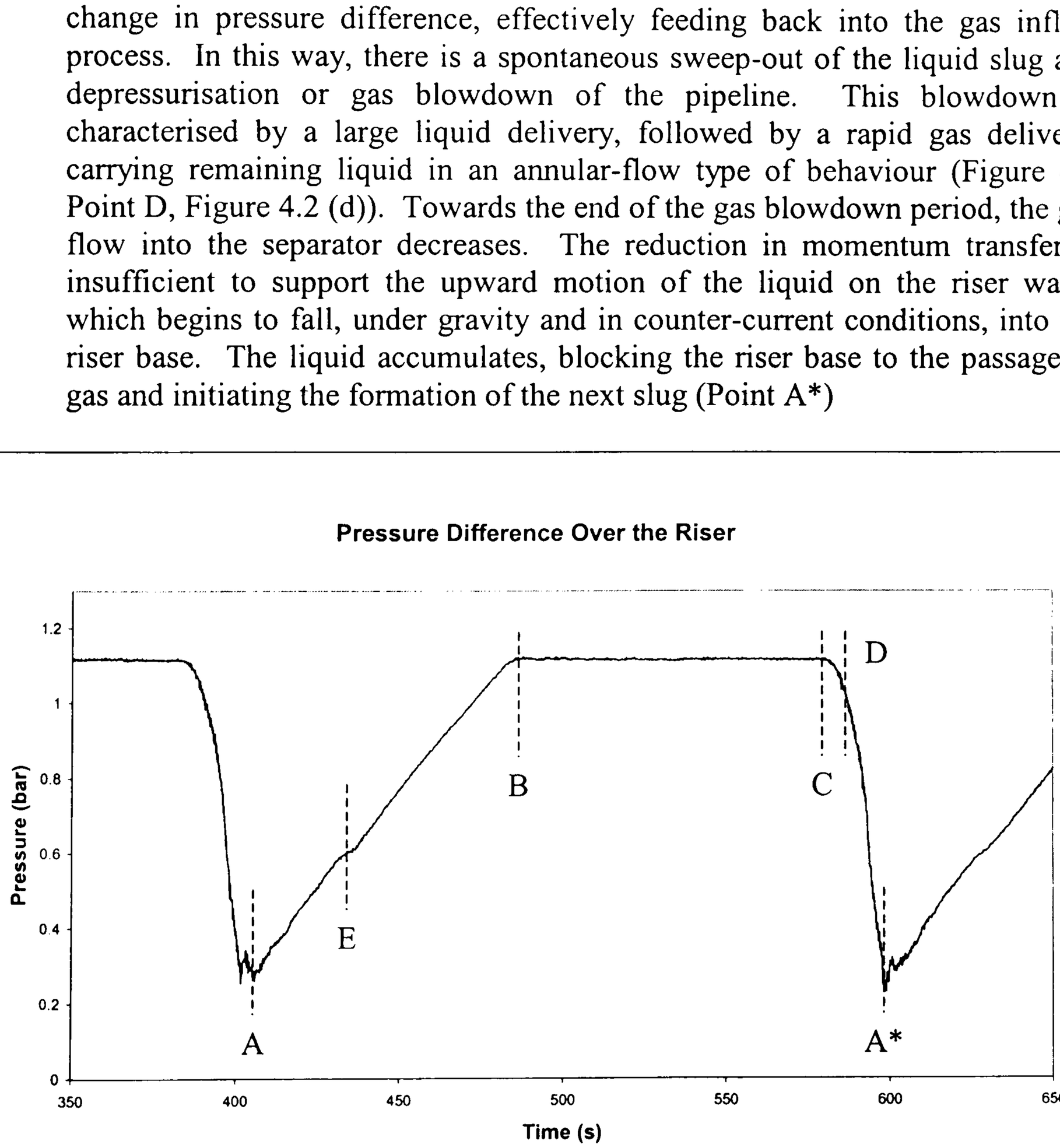

Figure 4.1 – Pressure Difference Over Riser During Severe Slugging 1, $U_G^S = 0.0985$ m/s, $U_L^S = 0.2017$ m/s

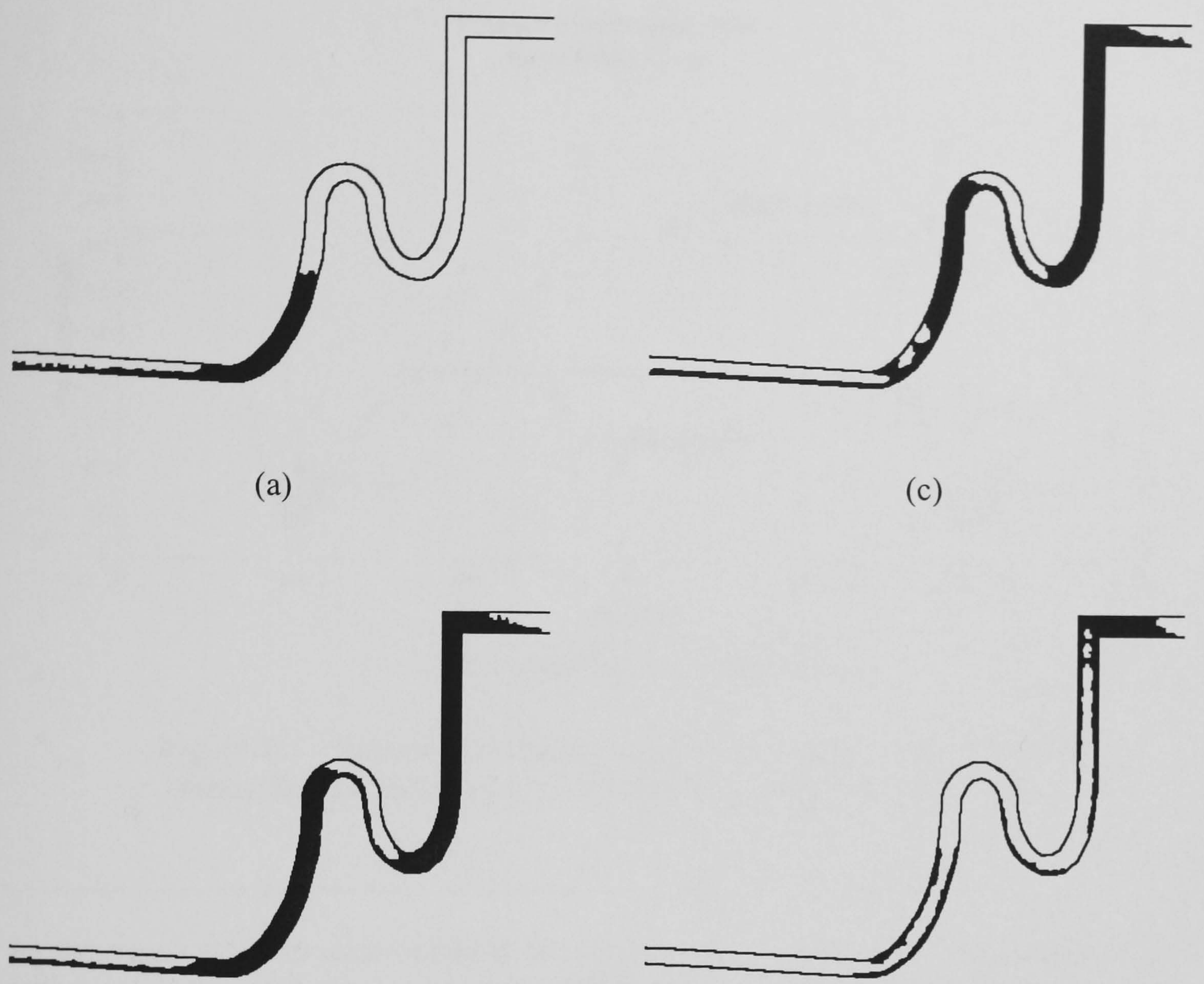

Figure 4.2 – Liquid Distribution in the Riser
During Severe Slugging 1

The basic mechanism of severe slugging is better understood when the pressure difference over each limb is examined, Figure 4.3 below. At the start of the severe slugging cycle, each limb is at the minimum liquid content. In the case of the lower limb, it is almost empty, while in the upper limb there is some 1 m of liquid. This would be attributable to liquid fallback from both the upper limb and the downcomer. Though the lower limb seems empty of liquid, the liquid height required to block the passage of gas is small, of the order of diameters (0.005 bar $\approx$ 50 mm liquid head). Hence the value of 0.04 bar for the pressure difference easily accounts for the liquid blocking the base of the riser.

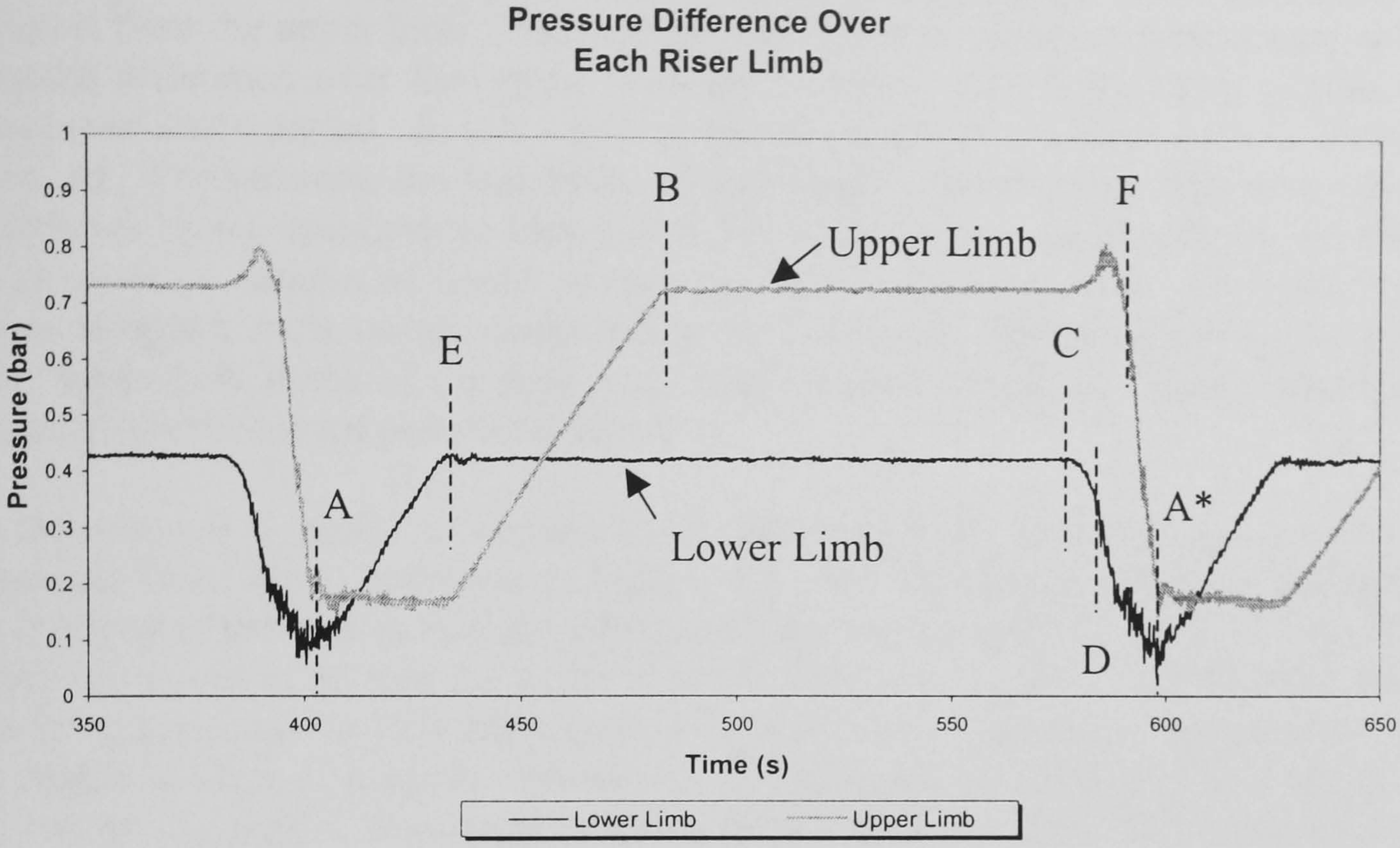

Figure 4.3 – Pressure Difference Over Each Upward Riser Limb During Severe Slugging 1, $U_G{}^S = 0.0985$ m/s, $U_L{}^S = 0.2017$ m/s

As the liquid starts to accumulate in the lower limb (Point A onwards), the pressure difference in the lower limb increases steadily while the upper limb remains constant. Once the liquid has reached the top of the lower limb (Point E), the liquid begins to pour over the top of the S-bend and into the base of the bend, being carried through to the upper limb. At this time, the pressure difference over the upper limb begins to increase. From this point on, the pressure difference in the lower limb does not change until bubble penetration. The liquid continues to accumulate in the upper riser limb until both upward limbs of the riser are filled (Point B). Once each upward limb of the riser is full, slug production begins and the pressure difference over each limb is constant as the liquid is moved from the pipeline into the riser and liquid in the riser is moved into the separator. This continues until bubbles begin to penetrate the lower limb (Point C).

As the bubbles begin to penetrate the riser base, the pressure difference in the lower limb starts to decrease, reflecting the reduction in total liquid inventory in the lower limb. The reduction in total pressure at the riser base during bubble penetration accelerates the movement of gas into the riser proper, inducing the blowdown of the system (Point D). This initiates the bulk removal of liquid from each limb of the riser, starting with the lower limb. At the start of the blowdown, the upper limb is full of liquid, reflected in the 0.74 bar pressure difference. As the liquid in the lower limb is removed rapidly, a corresponding acceleration takes place of the liquid in the upper. This causes a jump in the frictional pressure drop in the single phase liquid flow in the upper limb and hence an increase in the pressure difference over the upper limb (Point

C-D). Once approximately 50% of all liquid has been removed from the lower limb, gas penetration of the upper limb (Point F) begins, leading rapidly to the bulk removal of liquid from the upper limb. The bubble penetration of the upper limb occurs as the pressure difference over the upper limb drops below that experienced during the liquid production period. In this way, the blowdown of each upward limb of the riser is linked. Furthermore, the instability of the liquid column in the riser as a whole, manifested by the spontaneous blowout of the liquid during gas blowdown, is reliant on an unstable column of liquid in each upward limb of the riser. The end of the severe slugging cycle occurs at the point of minimum pressure difference over the riser, when both limbs of the riser have reached their minimum liquid content and consequently the lowest pressure difference.

At this point it is useful to observe other features of the severe slugging cycle as presented thus far. Examining Figure 4.1, the maximum pressure difference experienced in the riser is during liquid production and is equal to 1.1 bar. Returning to the discussion in Section 3.3.1, the pressure difference experienced reflects the fact that the downcomer is 20% filled during the severe slugging cycle, hence there is a noticeable amount of pressure recovery in the downcomer. This is characteristic of the severe slugging 1 flow regime and was identified by Tin (1991) however the reasons for this were unexplained. Confirmation of this behaviour is found in Figure 4.4 below showing the pressure difference over the downcomer.

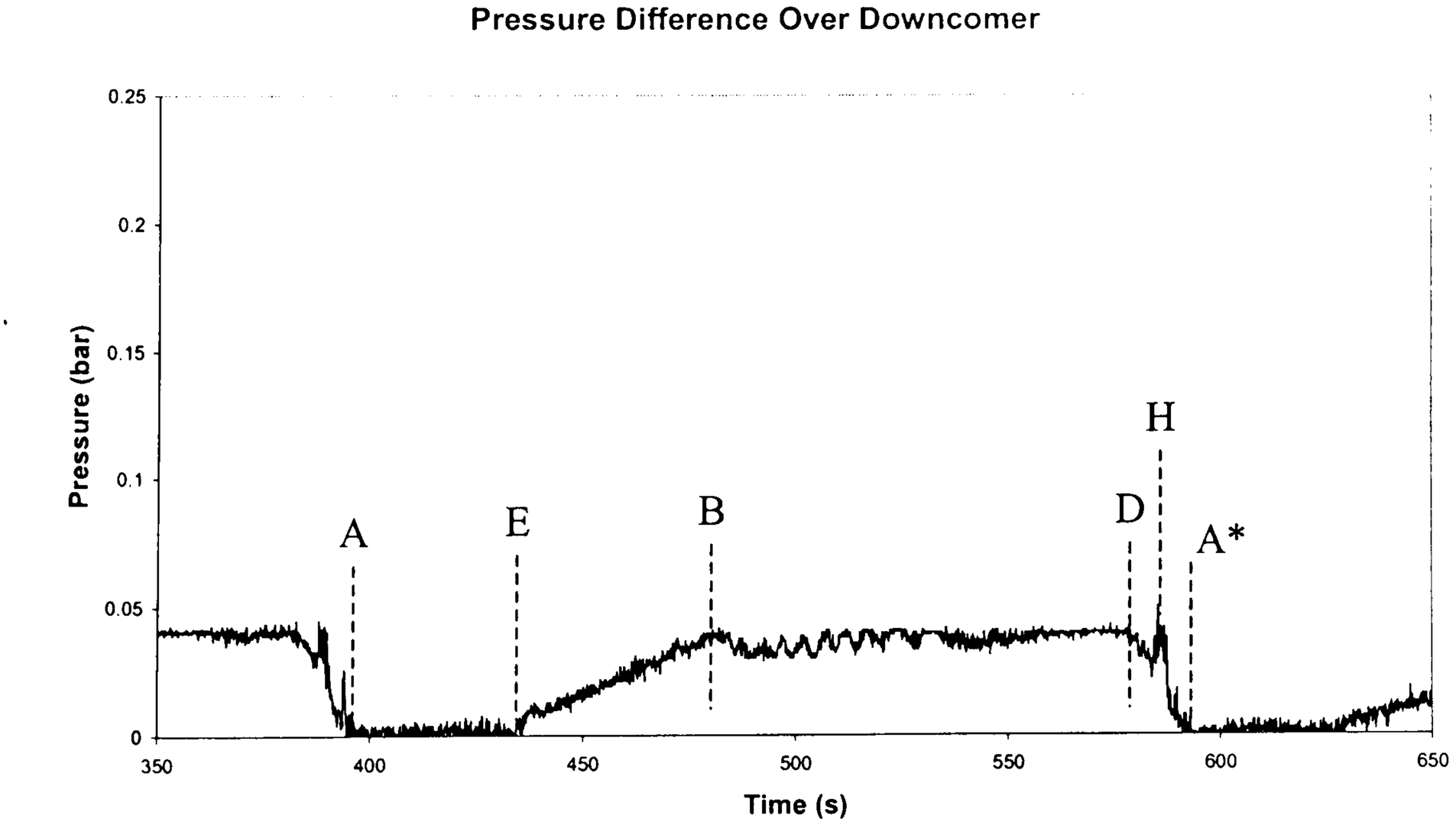

Figure 4.4 – Pressure Difference Over Riser Downcomer During Severe Slugging 1, $U_G^S = 0.0985$ m/s, $U_L^S = 0.2017$ m/s

Post-blowdown and during the initial stages of liquid buildup, the downcomer of the riser is empty, reflected by the zero pressure difference. Once the liquid has reached

the top of the lower limb (Point E previously), the liquid starts to pour over and the accumulates in the downcomer, giving an accompanying increase in pressure difference. The accumulation continues until the maximum pressure difference is reached, in this case a value of approximately 0.04 bar. When the downcomer is completely filled with liquid, the pressure difference is 0.22 bar, hence in this case the downcomer is approximately 20% filled with liquid. As the liquid fills up the lower and upper limbs of the riser, the gas compresses. This compression of the trapped gas resists the further accumulation of liquid in the downcomer over the rest of the cycle. During liquid production (Point B) the pressure difference remains relatively constant until the blowdown of the gas begins. As the liquid is swept from the lower limb, the surge of liquid moves the trapped gas and liquid in the downcomer toward the riser base, reducing momentarily the pressure difference in the downcomer. The liquid from the lower limb then arrives, increasing the pressure difference once again as accumulation occurs before finally being swept out prior to the bubble penetration of the upper limb (Point G). As the liquid arriving from the lower limb contains a proportion of bubbles, the pressure difference over the downcomer does not indicate a pure liquid column at any stage of the blowdown.

Finally, it is useful to examine the distribution of pressure signals measured, to do this the probability density function of the pressure difference signal is used. The probability density function *p(x)* is defined by:

$$P(x_1 < X < x_2) = \int_{x_1}^{x_2} p(x)\,dx \qquad (4.1)$$

Where $P(x_1 < X < x_2)$ is the probability that some value of a variable X lies between x_1 and x_2. In this case, the variable X is the riser base pressure, a measured quantity. This probability density function is calculated using standard techniques described by Walpole and Myers (1989) and Perry and Green (1984). A Matlab script file, riser_pdf.m, was used to implement this and is provided in Appendix A where additional information on the calculation procedure is also provided.

Examining the probability density function for the pressure difference over the riser during severe slugging 1, Figure 4.5, a distinctive profile is observed. There is a broad spread of pressure differences experienced in the riser and a single characteristic pressure that predominates in terms of occurrence (Point I). This pressure corresponds to the pressure experienced during liquid production and reflects the fact that for the majority of the severe slugging cycle the pressure difference is equal to this value. That the pressure corresponds to the pressure difference during production this can be said to be the 'most likely maximum pressure difference experienced in the riser'. For severe slugging 1 this is always greater than or equal to the hydrostatic head for a riser full of liquid. The spread of the peak around this pressure is characteristically very narrow as during severe slugging 1 the pressure difference during production is steady and highly repeatable from cycle to cycle.

The other pressure values correspond to the intermediate values of pressure that occur during the liquid buildup and gas blowdown periods. These all occur in relatively

equal degrees and hence have broadly similar pdf values, however there are two points of note (Points J and K) where the pdf value is higher. The first, K, is the 'most likely minimum pressure difference' and corresponds to the minimum pressure difference experienced during severe slugging 1, i.e. post-blowdown. This is a repeatable value and hence gives rise to the slightly higher pdf value. The second point of interest K corresponds to the pressure difference at which liquid arrives at the top of the lower limb. This pressure difference is again highly repeatable from cycle to cycle and again gives a slightly higher pdf value.

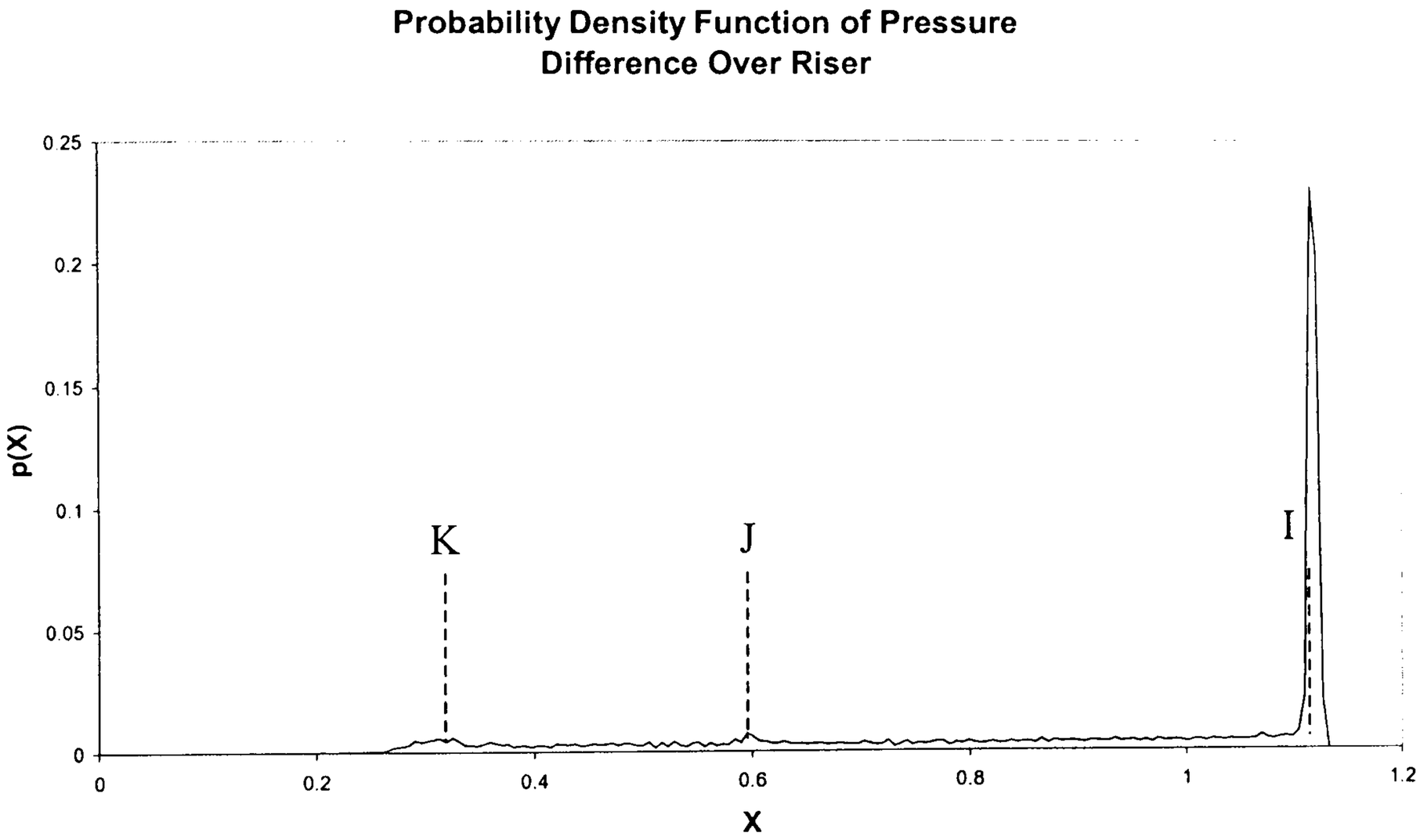

Figure 4.5 – Probability Density Function of Pressure Difference Over Riser During Severe Slugging 1, $U_G^S = 0.0985$ m/s, $U_L^S = 0.2017$ m/s

Liquid Holdup Characteristics

As stated previously, the liquid holdup local to the riser base was used to identify the flow regime. Figure 4.6 shows the variation in liquid holdup local to the riser base during severe slugging 1.

As can be seen, post-blowdown the liquid holdup local to the riser base is at the minimum value. Once liquid fallback occurs the liquid accumulates in the pipeline, blocking the cross-section to the passage of gas and giving a unity liquid holdup reading. The riser base is blocked to the passage of gas until the gas/liquid interface in the pipeline moves into the riser base (Point C) and initiates bubble penetration. Finally, during blowdown, the liquid in the pipeline is swept out into the riser, returning the liquid holdup to the minimum value.

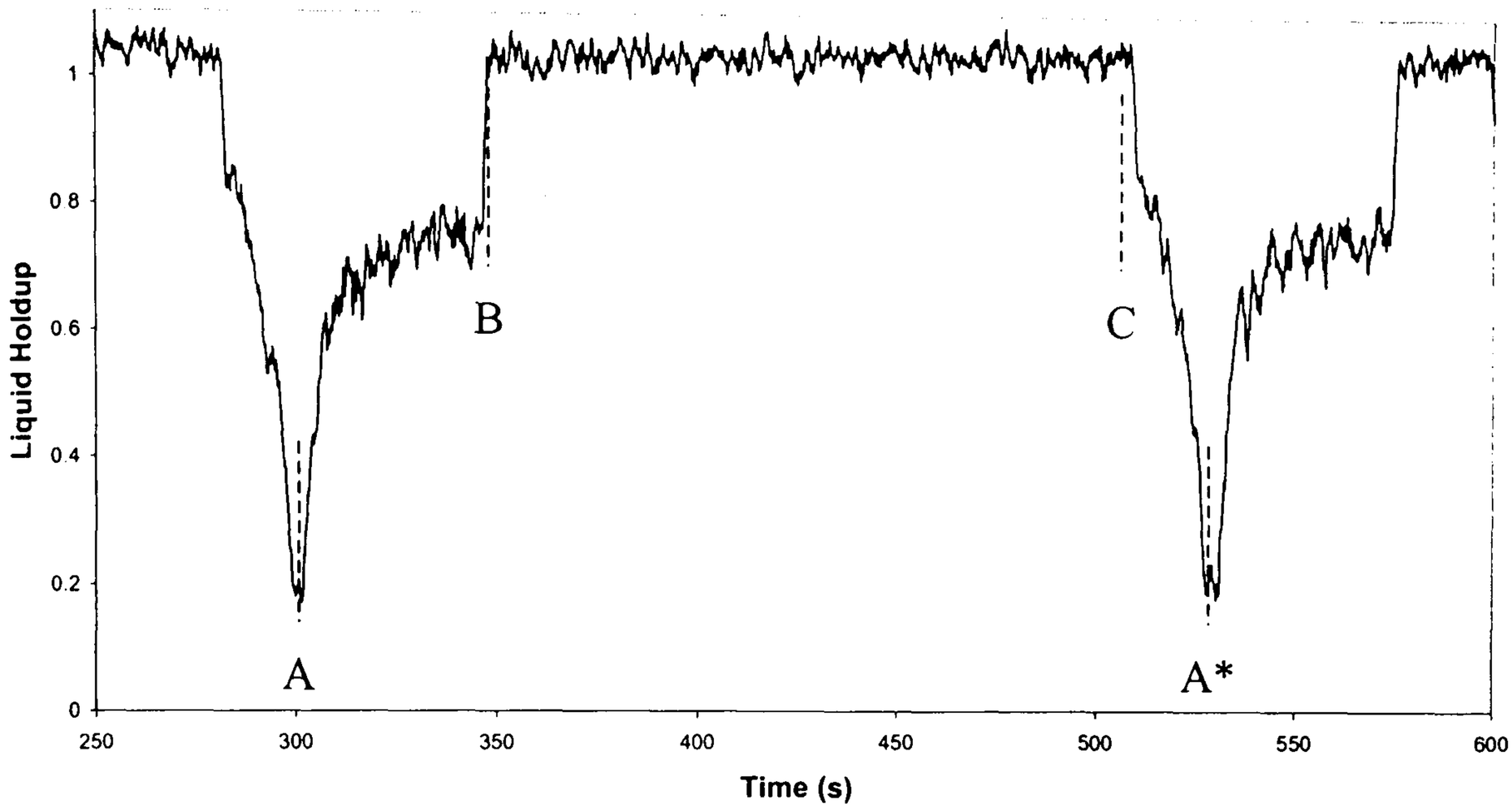

Figure 4.6 – Liquid Holdup Local to Riser Base During Severe Slugging 1, $U_G^S = 0.161$ m/s, $U_L^S = 0.08674$m/s

Fluid Production Characteristics

A typical example of liquid mass production during severe slugging, obtained from the separator mass balance, is shown in Figure 4.7 below.

It is characterised by three main periods, the period of no production, the period of constant liquid production and the production transient. Each of these periods is directly related to the pressure cycle for severe slugging as described above. Figure 4.8 shows an overlay of the pressure cycling characteristic with the liquid production characteristic. The production periods are related as follows to the pressure cycling:

- No Production ⇔ Liquid Buildup
- Constant Production ⇔ Slug Production
- Production Transient ⇔ Bubble Penetration and Gas Blowdown

During the no production period, the liquid is accumulating in the upward limbs of the riser and has not yet reached the outlet to flow into the separator. Once the liquid has reached the top of the riser, liquid production begins (Point B). The gas entering the pipeline pushes the gas/liquid interface towards the riser base, moving the liquid in the pipeline into the riser and causing a corresponding flow of liquid from the riser outlet.

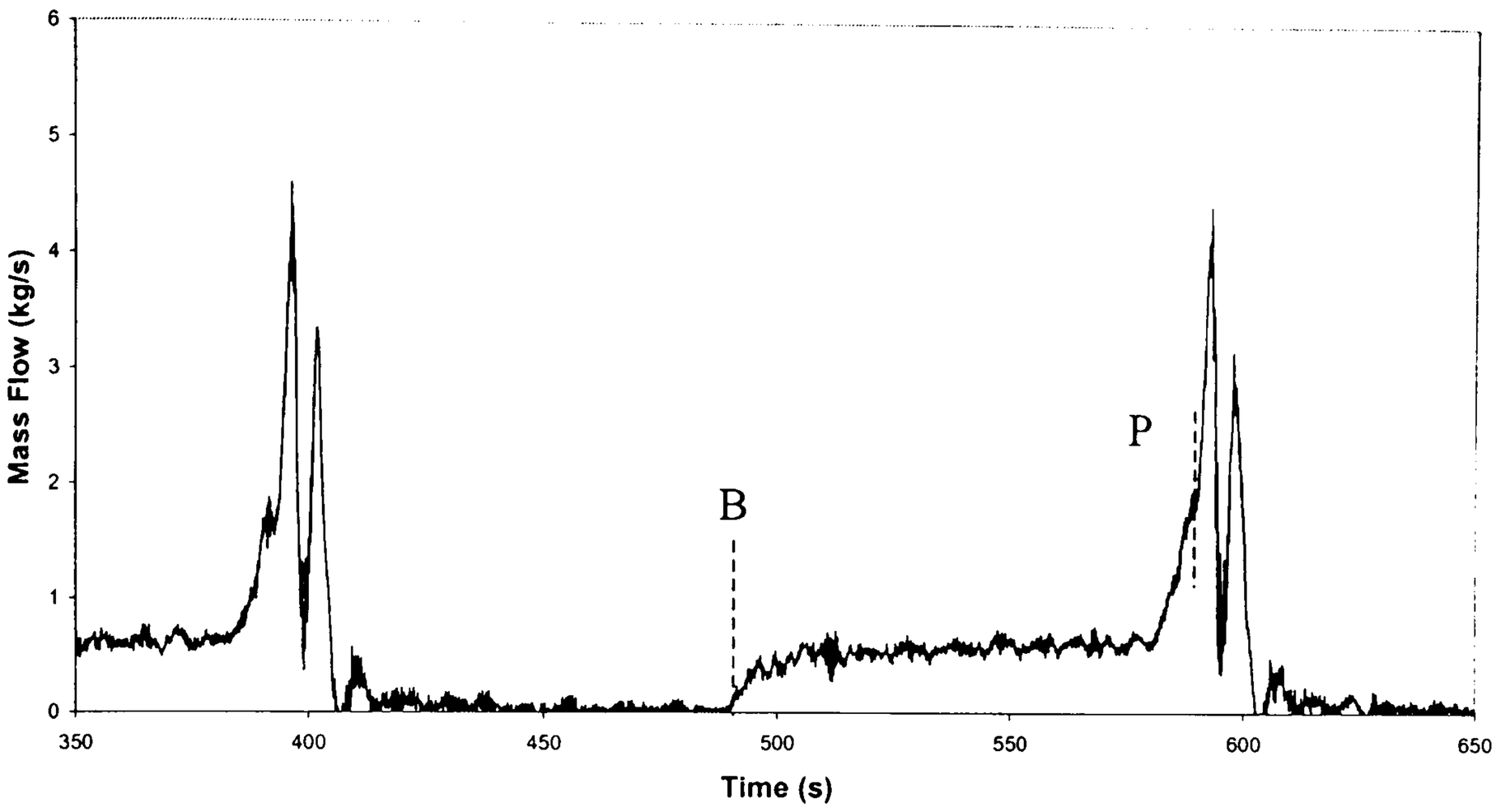

Figure 4.7 – Liquid Production During Severe Slugging 1,
$U_G^S = 0.0985$ m/s, $U_L^S = 0.2017$ m/s

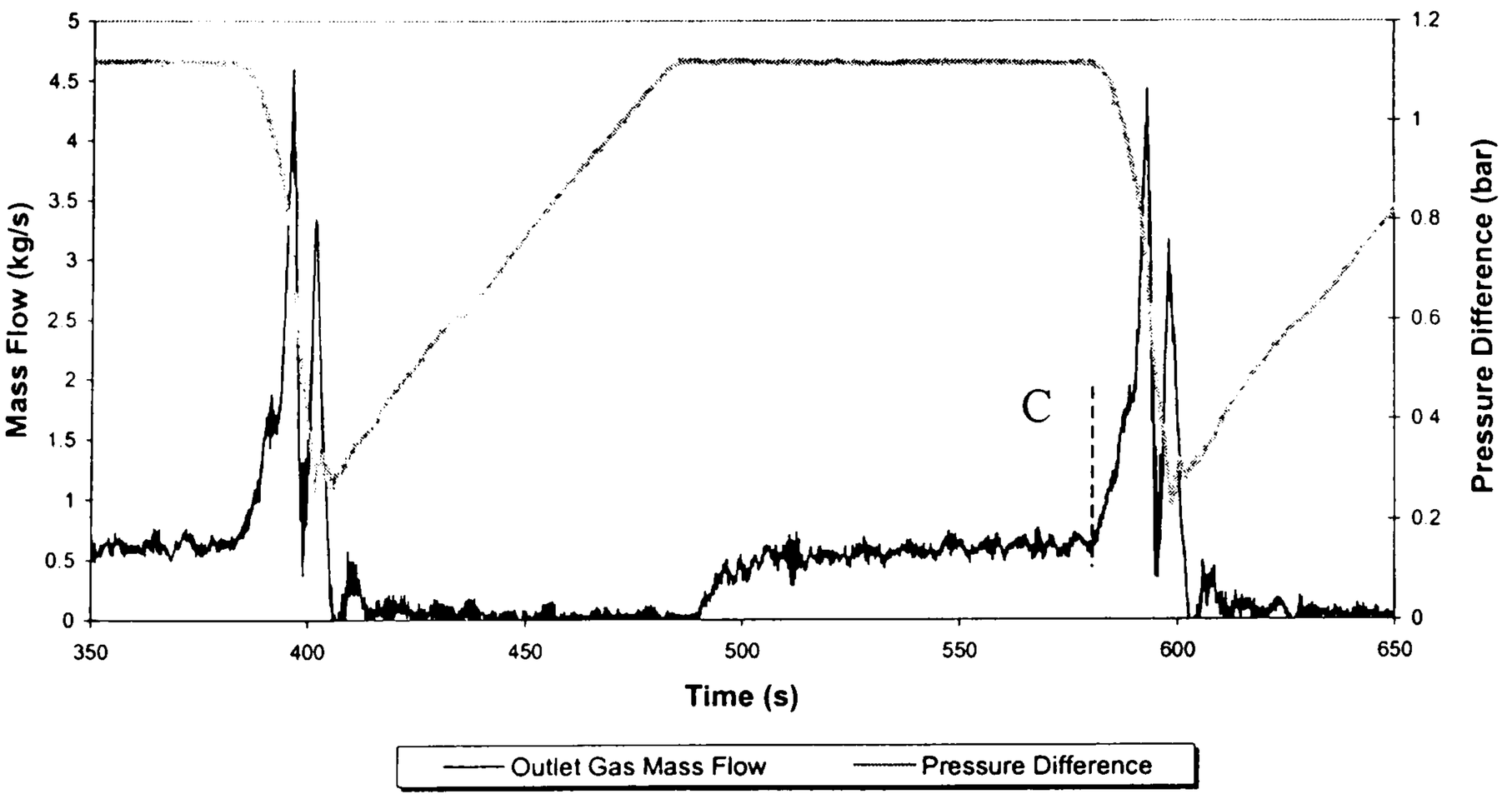

Figure 4.8 – Liquid Production and Pressure Cycling During
Severe Slugging 1, $U_G^S = 0.0985$ m/s, $U_L^S = 0.2017$ m/s

As the constant production period continues, the rate of liquid flow out of the riser increases marginally, most likely due to the acceleration of the gas/liquid interface as it reaches the riser base. A suggestion for this is that as the slug moves from the pipeline into the riser, there is less surface contact between the slug and the wall, hence the frictional pressure drop over the slug is reduced, allowing a higher slug velocity. However this phenomenon has not been confirmed through the experiments and would require further investigation beyond the scope of this work.

The liquid production transient begins as the first bubbles begin to penetrate the riser base, see Figure 4.8 (Point C). Rapidly and in-line with the pressure characteristic of the riser limbs, the liquid production accelerates to give the production transient response that contains two characteristic 'spikes'. These correspond to the arrival of liquid from the upper and lower limbs of the riser respectively. During the production of the first spike, gas begins to enter the upper limb causing a change in the fluid production rate (Point I). This is identified by comparison of the liquid production profile with the pressure difference profiles for each riser limb.

As stated in Chapter 1, a major concern with regard to severe slugging in a riser system is the fluctuations in the fluid delivery, involving both the rate and the total size of the fluctuations. In this respect, the liquid total slug size and the rate of fluid delivery are now examined. As the *volume* is the parameter of concern for slugcatcher design and operation, the analysis of the production is in terms of slug volume and volumetric production rate.

The total liquid slug size for a severe slug is obtained from the liquid production profile using the following relation:

$$V_{SL} = \frac{M_{SL}}{\rho_L} = \frac{1}{\rho_L}\int_{t_1}^{t_2} G_{LO}(t)\,dt \qquad (4.2)$$

Where G_{LO} is the outlet liquid mass flow from the riser or the liquid mass production rate. The integration method used for the calculation is an extended version of Simpson's Rule for non-overlapping intervals as described by Press *et al.* (1992):

$$\int_{x_1}^{x_n} f(x)\,dx = h\left[\frac{1}{3}f_1 + \frac{4}{3}f_2 + \frac{2}{3}f_3 + \frac{4}{3}f_4 + \cdots + \frac{2}{3}f_{N-2} + \frac{4}{3}f_{N-1} + \frac{1}{3}f_N\right] \qquad (4.3)$$

Where N, the number of intervals is an uneven integer. The integration above is implemented using the Matlab script rinteg.m. Details of which are provided in Appendix A. The limits for the integration for the total slug size are the start and end times of the severe slugging production cycle.

Examining Figure 4.9, showing the slug size during severe slugging for the 2 bar(a) tests, there is a broad spread of slug sizes, ranging from 138.74 l to 48.53 l.

Characteristically of severe slugging, the standard deviation of the slug sizes from the mean for any given test condition is small, less than 1.8 l (3% of the mean slug size for the test) for each case. However the variation in slug sizes from an overall average is much higher, with a standard deviation of some 16.1 l (24.4% of the average over all severe slugging 1 tests). Appendix D presents a summary table of the test data collected. At this point, it is useful to compare slug sizes to the volume of the riser, in this way some relative estimate of the 'severity' of the observed slugging. The total riser length to the top bend is 17.8 m, giving a volume of 38.5 l. Comparing this to the severe slug sizes, all of the type 1 severe slugs are greater than this volume, a further characteristic of severe slugging 1.

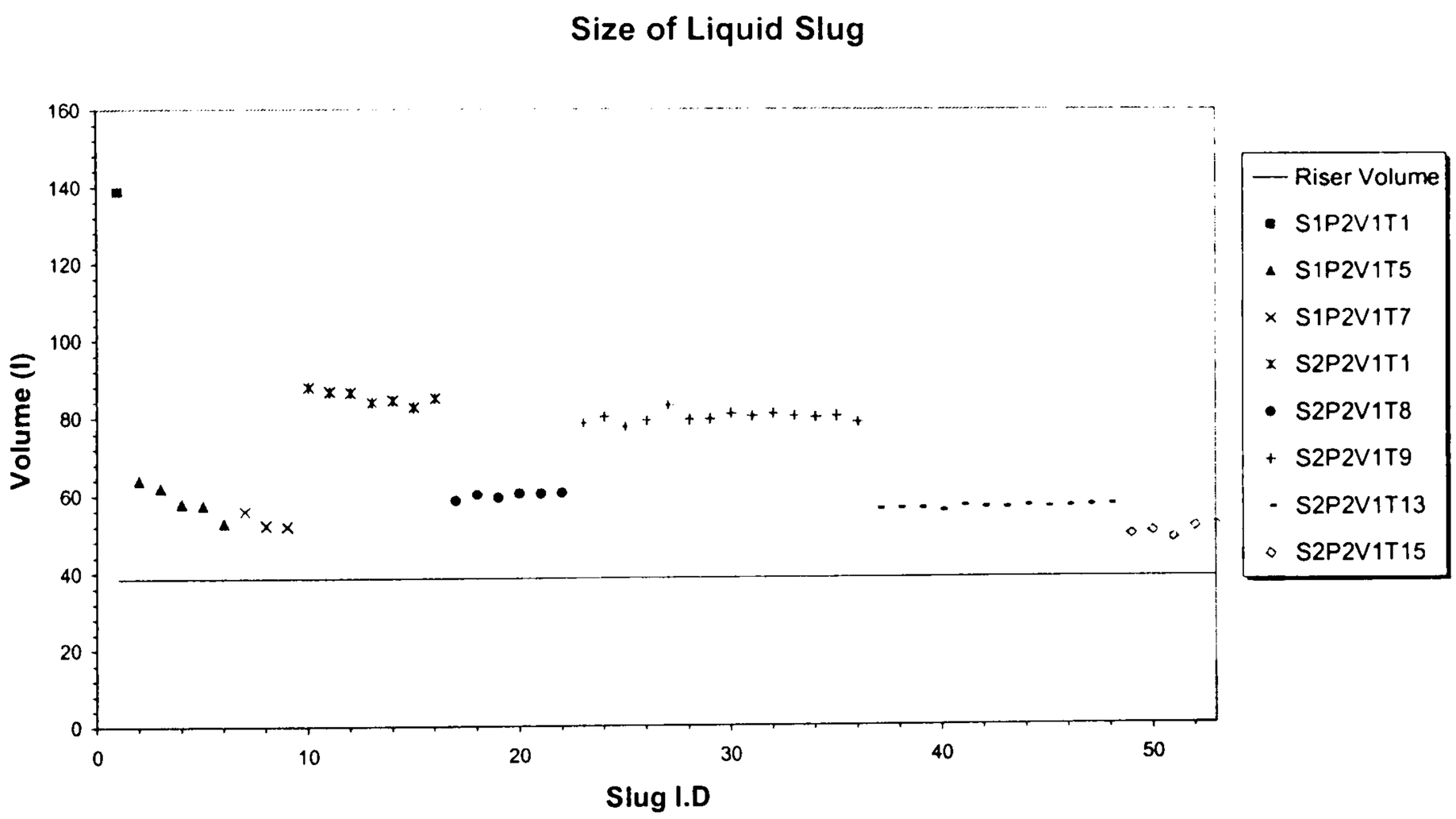

Figure 4.9 – Liquid Slug Size
During Severe Slugging 1, 2 bar(a) Data

In the above figure, the I.D. Number refers to the individual slug identification and the legend corresponds to the experimental test codes in Appendix D.

The relative contribution of each stage of the liquid production to the severe slug size is another point of interest. In terms of slugcatcher design, an area of concern is the maximum surge size over and above the constant throughput the catcher will be designed for. In terms of severe slugging, hypothetically a slugcatcher may be able to handle the liquid flow during the constant production period of severe slugging as this may be close to the designed-for average flow. However, the arrival of the production transient may cause level alarms and pressure surges. In this way, the liquid slug size may become less important and the size of the liquid transient becomes the area of most concern.

To show the relative size of the production transient during severe slugging 1 to the overall slug size and the riser volume Figure 4.10 is used. Examining the figure, it is evident that the volume of liquid produced during the transient is close to the volume of the riser. The average transient size of the test data is 37.2 l (96.65% of the riser volume) with a standard deviation of 3.34 l (8.9% of the mean size over all severe slugging 1 cases).

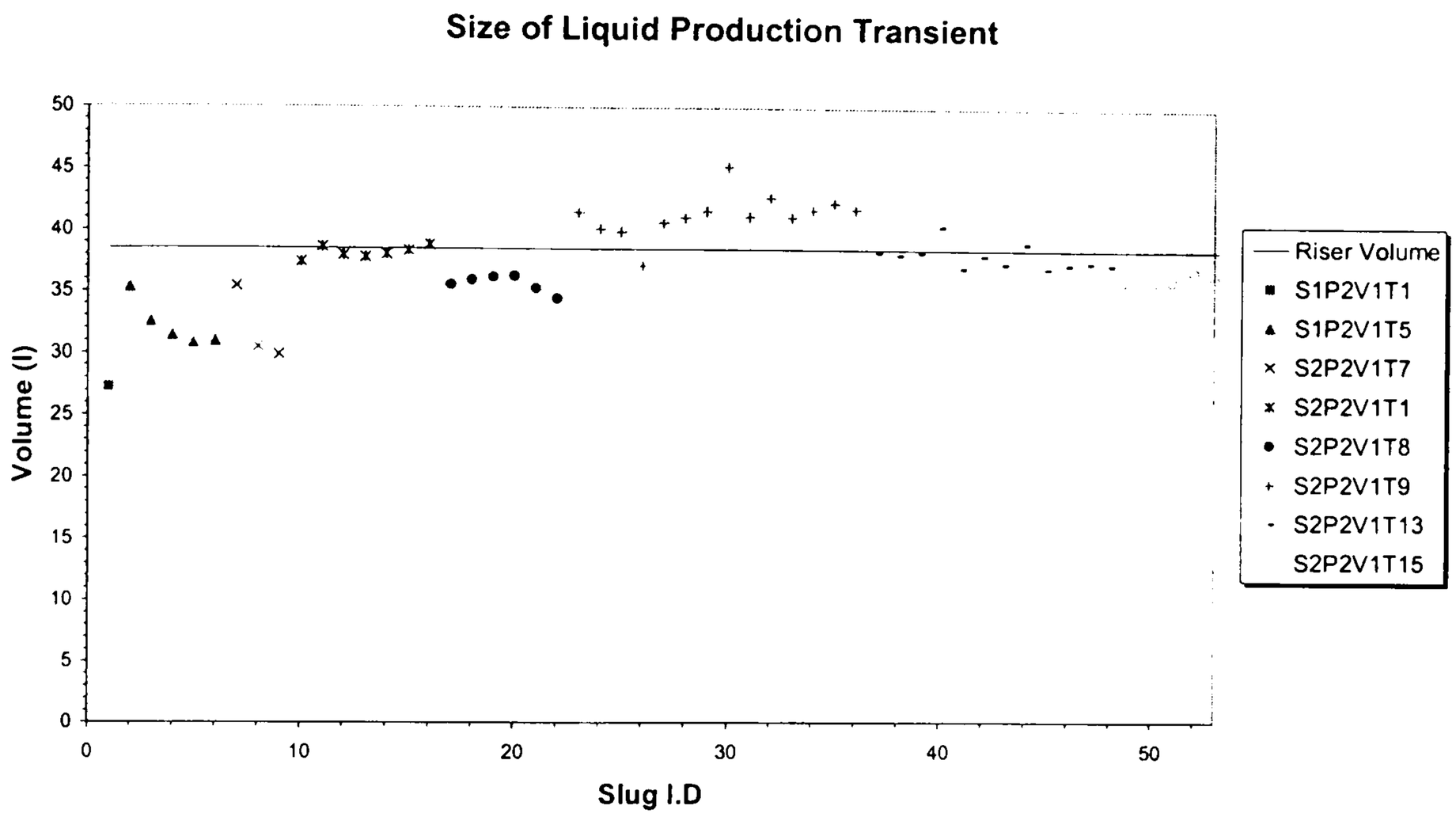

Figure 4.10 – Size of Liquid Production Transient
During Severe Slugging 1, 2 bar(a) Data

Thus, it is reasonable to state that for these cases, the size of the liquid transient is approximately equal to the riser volume. Furthermore it may be asserted that 99% of the transient sizes will be between 45.82 l and 28.63 l (118% and 74% of the riser volume respectively) for these conditions. Comparing these results with the variations in total slug volume, it can be asserted that the main difference in terms of slug size is the amount of constant production present during the severe slugging period.

Similar observations may be made for the 4 bar(a) test cases, Figures 4.11 and 4.12. In these cases, the variation on the results is higher, the average transient size is 33.8 l and the standard deviation is 3.3 l (9.9% of the mean for all tests). This increase in the standard deviation may be attributable to the number of samples taken, with 38 samples as opposed to 52 in the previous case. Again however, when compared to the variation in slug size of 11.2 l (19% of the average size for all cases), it shows how the majority of the slug size variation is effectively attributable to the differences in the amount of constant production during severe slugging.

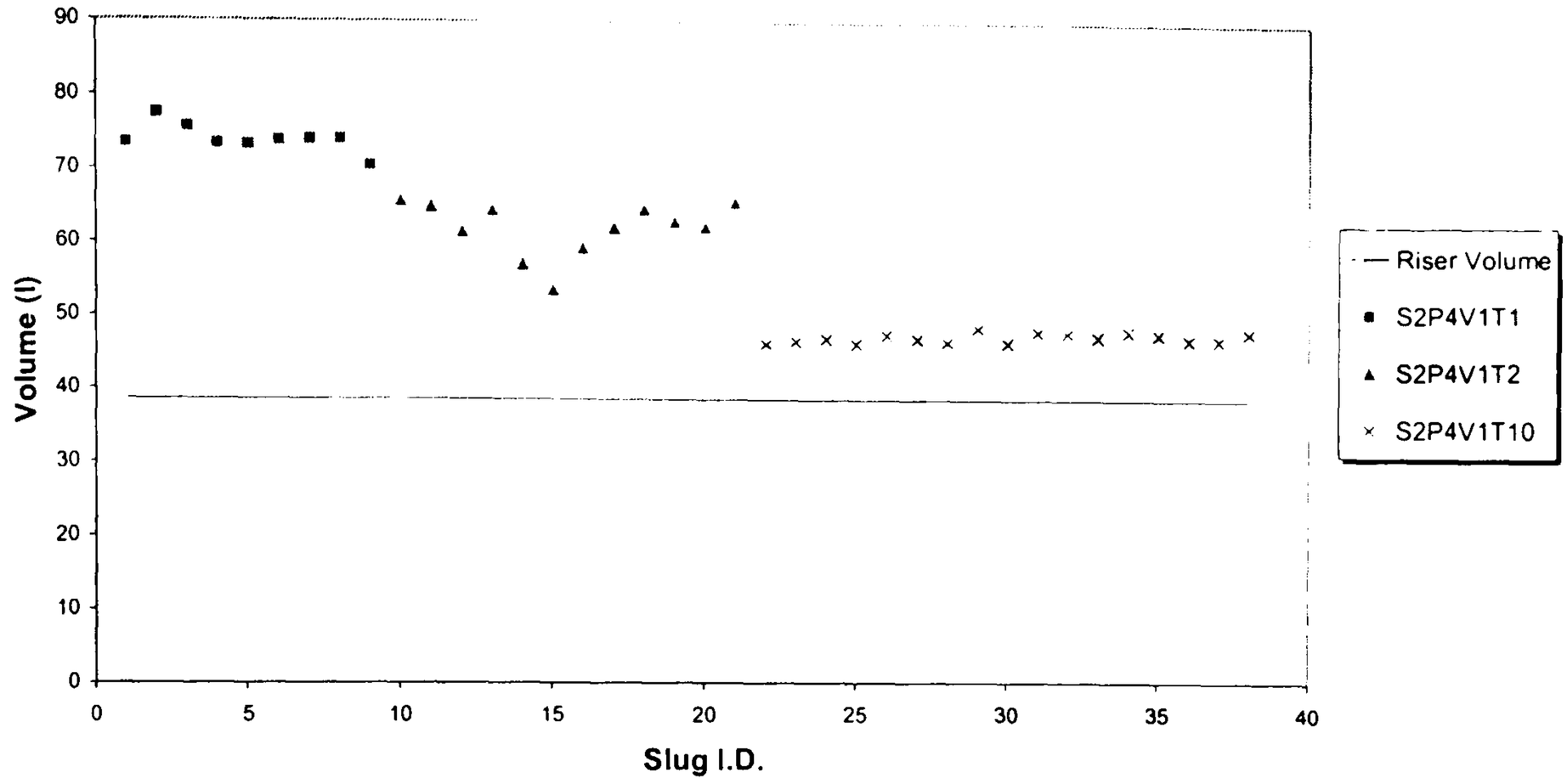

Figure 4.11 – Liquid Slug Volume
During Severe Slugging 1, 4 bar(a) Data

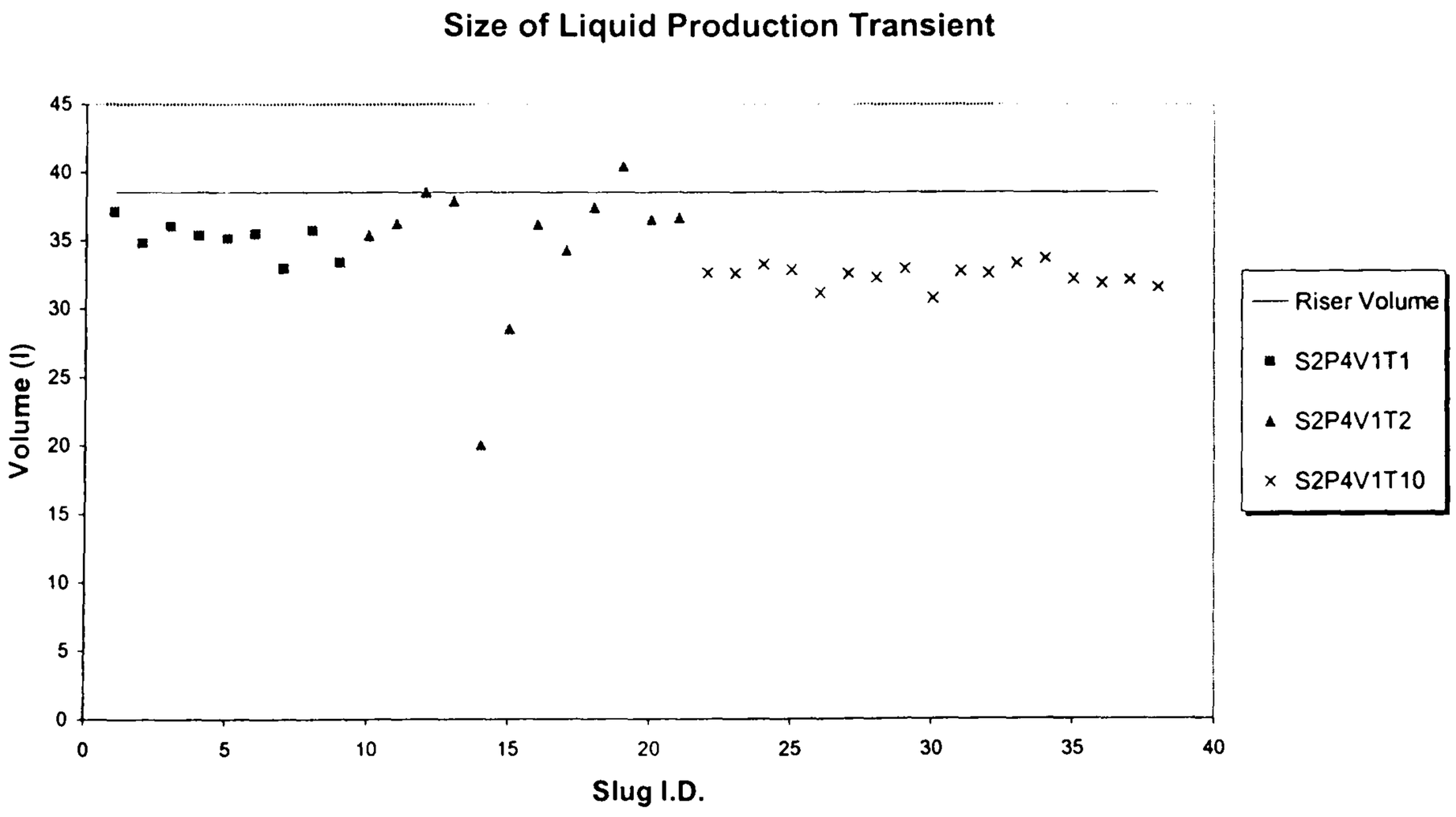

Figure 4.12 – Volume of Liquid During Production Transient
For Severe Slugging 1, 4 bar(a) Data

Furthermore, the data shows that the liquid production transient during severe slugging is approximately equal to the volume of the riser, being within ±15% of the riser volume.

The next area of interest is the peak production during severe slugging and the relative size of this in comparison to the average production rate during the cycle as a whole. Figure 4.13 shows the peak flows experienced during severe slugging in the pipeline/riser. During severe slugging 1 the average peak production is 3.95 l/s, however there is significant variation in the results between tests, reflected in the standard deviation of 0.68 l/s (17% of the average peak flow). Thus the limits of the peak flow are between 5.72 l/s and 2.19 l/s to a 99% level of confidence. Note that though there was a significant variation in peak flow over tests as a whole, within tests the standard deviation was much lower, some 0.21 l/s (6% of the average for a given test). When comparing the peak flow with the average flow over the entire test period, a per-test basis is used to compare flows, before averaging over all tests. This showed that during severe slugging, the peak flow was an average of 1045% greater than the average liquid flow through the system over each test.

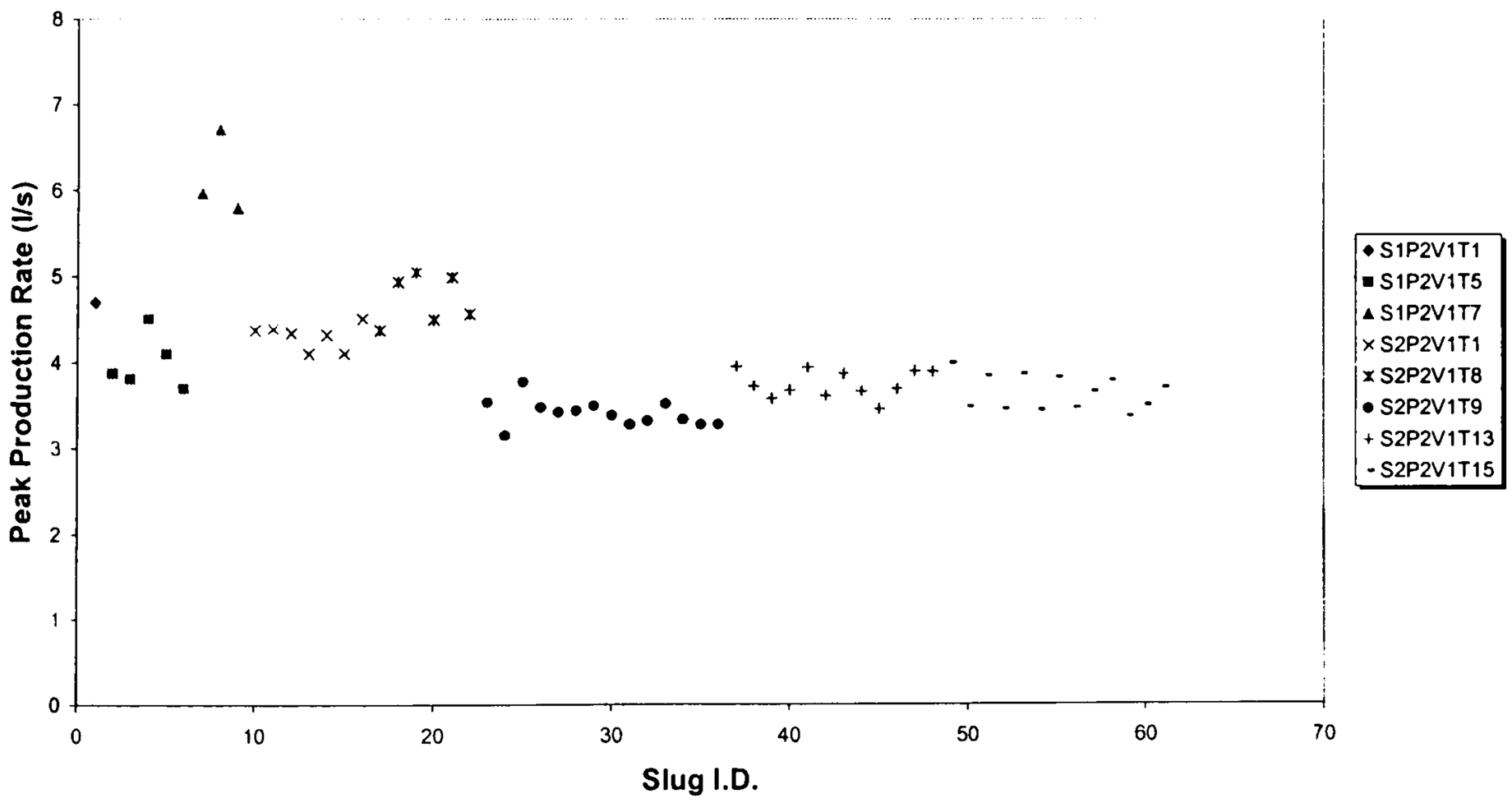

Figure 4.13 – Peak Liquid Production Rate During Severe Slugging 1, 2 bar(a)

In terms of gas production, a typical result is shown in Figure 4.14. The gas production cycle is made up of two parts, the period of no gas production and the gas production transient. The period of no gas production occurs during the liquid buildup, slug production and bubble penetration parts of the severe slugging cycle.

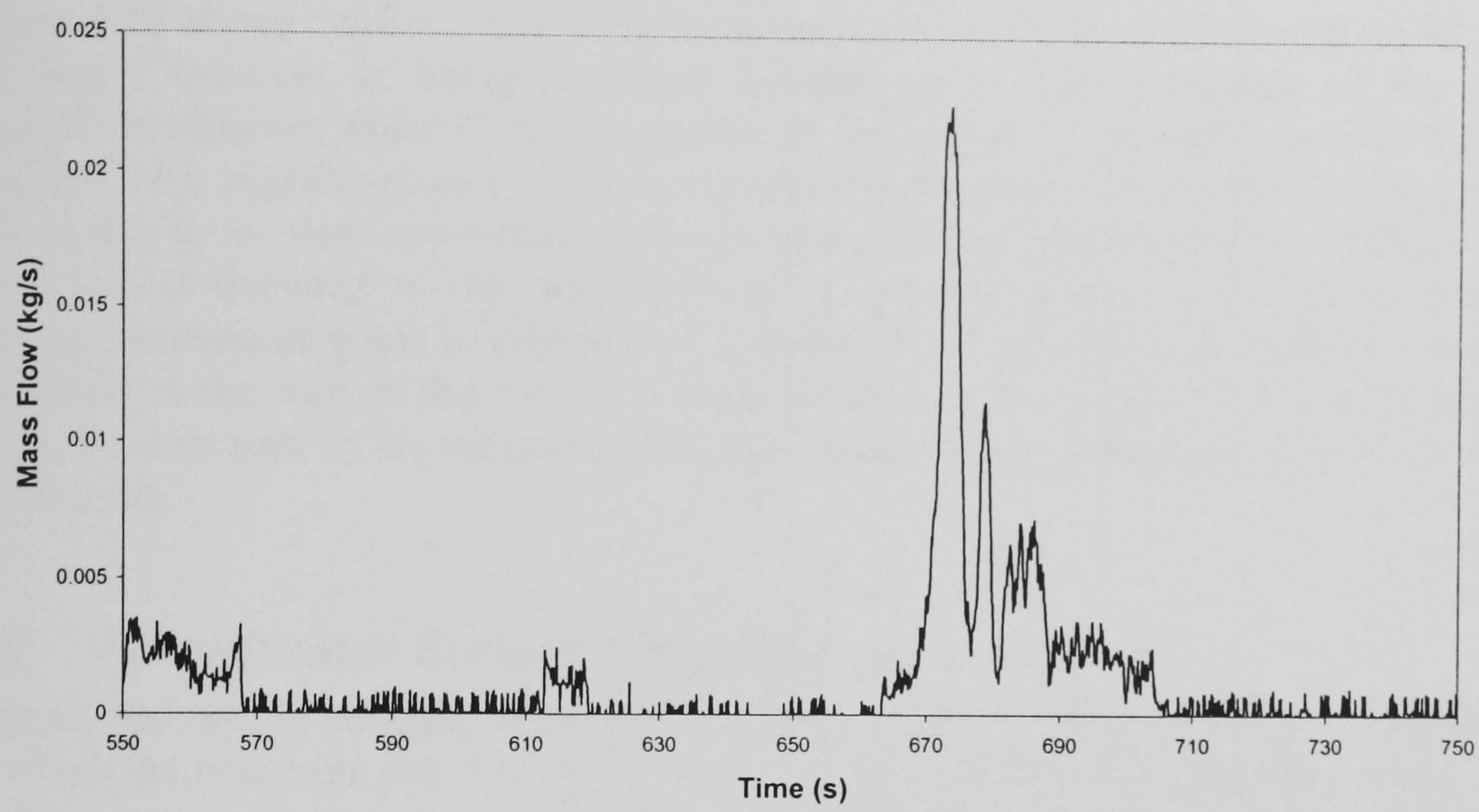

Figure 4.14 – Gas Production During Severe Slugging 1,
$U_G^S = 0.151$ m/s, $U_L^S = 0.186$ m/s

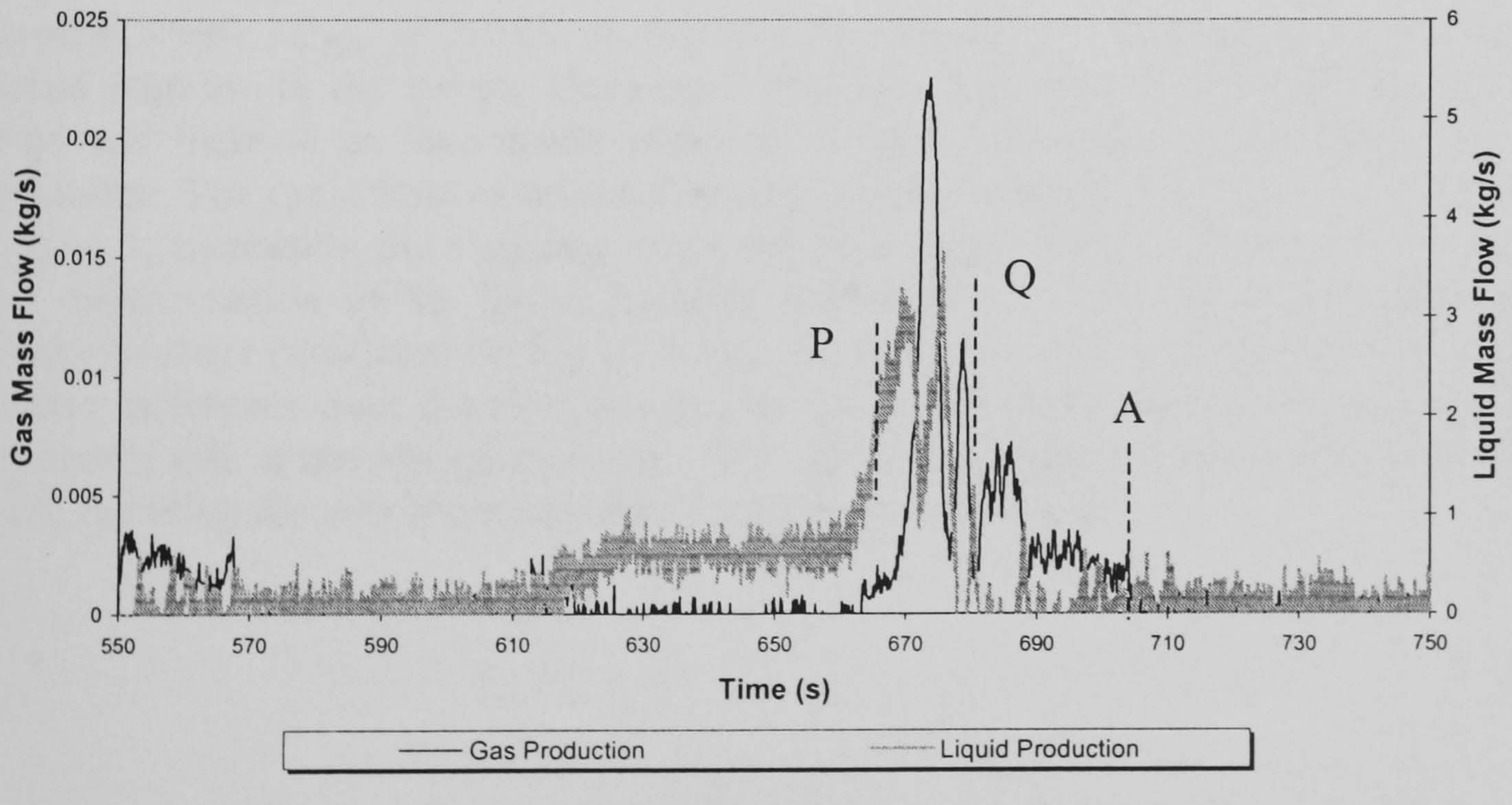

Figure 4.15 – Combined Gas and Liquid Mass Production Characteristics
During Severe Slugging 1, $U_G^S = 0.151$ m/s, $U_L^S = 0.186$ m/s

Furthermore, for a substantial portion of the gas blowdown stage of the cycle there is no gas production, as the tail of the severe slug has not reached the outlet of the riser.

Figure 4.15 above confirms this behaviour, as shown there is a period of time where the liquid transient is being produced without gas. The beginning of the gas production (denoted Point P) commences with the arrival of the highly aerated liquid slug tail of a significant size. This is caused by the series of bubbles entering the severe slug in the riser immediately prior to blowdown as observed by Tin (1991). As the liquid is depleted in the pipeline/riser, the rate of liquid production tails off, leaving the remaining gas to vent to the separator (Point Q). At some stage (Point A), the liquid at the wall of the riser falls back under counter-current flow conditions to block the riser base to the passage of gas, cutting off the remaining gas flow at the end of the cycle.

4.2 Transitional Severe Slugging

Transitional severe slugging is generally characterised by pressure cycling behaviour in which the riser base pressure is often less than that of classical severe slugging 1. It is then supposed that the liquid slugs do not completely fill the riser prior to blowdown and hence are significantly smaller than the riser volume. The data presented here divides transitional severe slugging into two classifications – severe slugging 2 and severe slugging 3. 'Transitional' in this sense relates to flow regime behaviour between 'classical' severe slugging and stable flow.

4.2.1 Severe Slugging 2 Characteristics

Pressure Cycling Characteristics

A typical severe slugging 2 cycle as depicted in Figures 4.16[1] and Figure 4.17 show a marked contrast to the severe slugging 1 cycle in that there is no slug production period and there is an incomplete removal of liquid from the riser during the gas blowdown. The cycle time of severe slugging 2 flows is also lower than that of severe slugging 1, increasing the slugging frequency (see Appendix D). There is however a clear differentiation of the liquid buildup, bubble penetration and an extended gas blowdown stage (indicated on Figure 4.16). In this particular instance the maximum pressure difference over the riser is equal to that experienced during severe slugging 1, however this is not always the case. The upper limb may not completely fill with liquid, reducing the maximum pressure difference experienced.

[1] Note the labelling of stages during pressure cycling applies to the individual sections

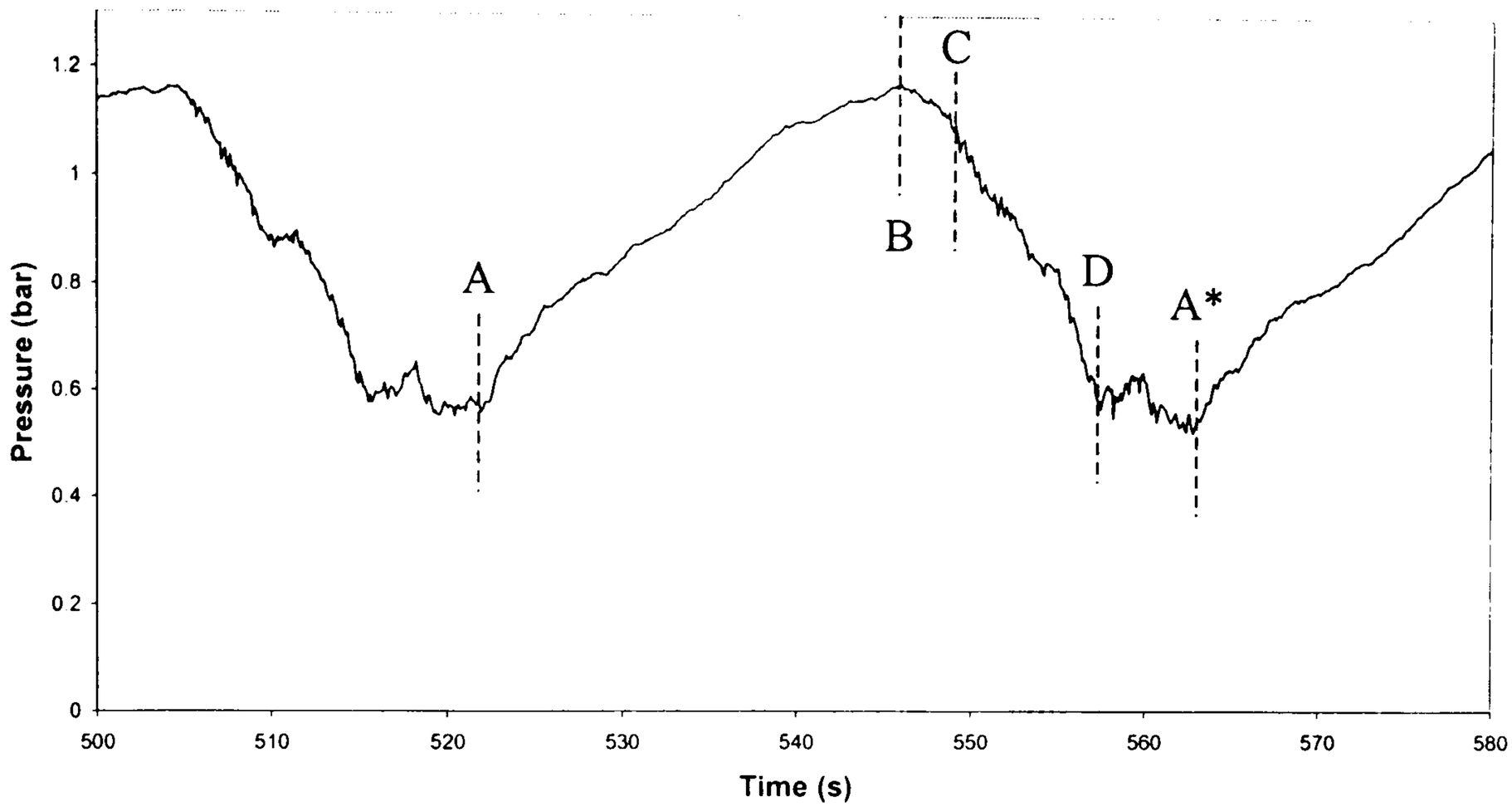

Figure 4.16 – Pressure Difference Over Riser During Severe Slugging 2, $U_G^S = 0.33$ m/s, $U_L^S = 0.5$ m/s

The lack of a slug production stage during the cycle indicates that no liquid is backed up the pipeline when the severe slug is fully formed, i.e. at the point of maximum pressure difference. There is substantially more liquid remaining in the system post-blowdown than during severe slugging 1. This manifests in the higher pressure difference over the riser at the end of the cycle. Comparing the case presented with the severe slugging in Figure 4.1, the pressure difference of 0.52 bar far greater than the 0.351 experienced in the severe slugging 1 case.

The pressure cycling characteristics in each upward limb are shown in Figure 4.18 below. Here it is evident that during severe slugging 2 the lower limb of the riser is filled completely, as evidenced by the pressure difference of 0.42 bar in the lower limb. Once the lower limb is filled (Point E), the upper is filled, to a maximum pressure difference of 0.74 bar, representing a full upper limb of liquid. As soon as the upper limb of the riser is filled, bubble penetration at the riser base begins (Point B and (b) in Figure 4.17). This rapidly increases the pressure difference in the upper limb (Point F). As in the case of severe slugging 1, gas blowdown (Point C) begins after bubble penetration with the sweep out of liquid from the lower limb preceding the sweep out of liquid from the upper limb. Additionally, sweep out of the liquid in the upper limb occurs when the lower limb liquid quantity drops to or below 50% (equivalent to 0.2 bar pressure difference). Thus, in a similar way to severe slugging 1, severe slugging 2 relies on there being an unstable column of liquid in both upward limbs of the riser.

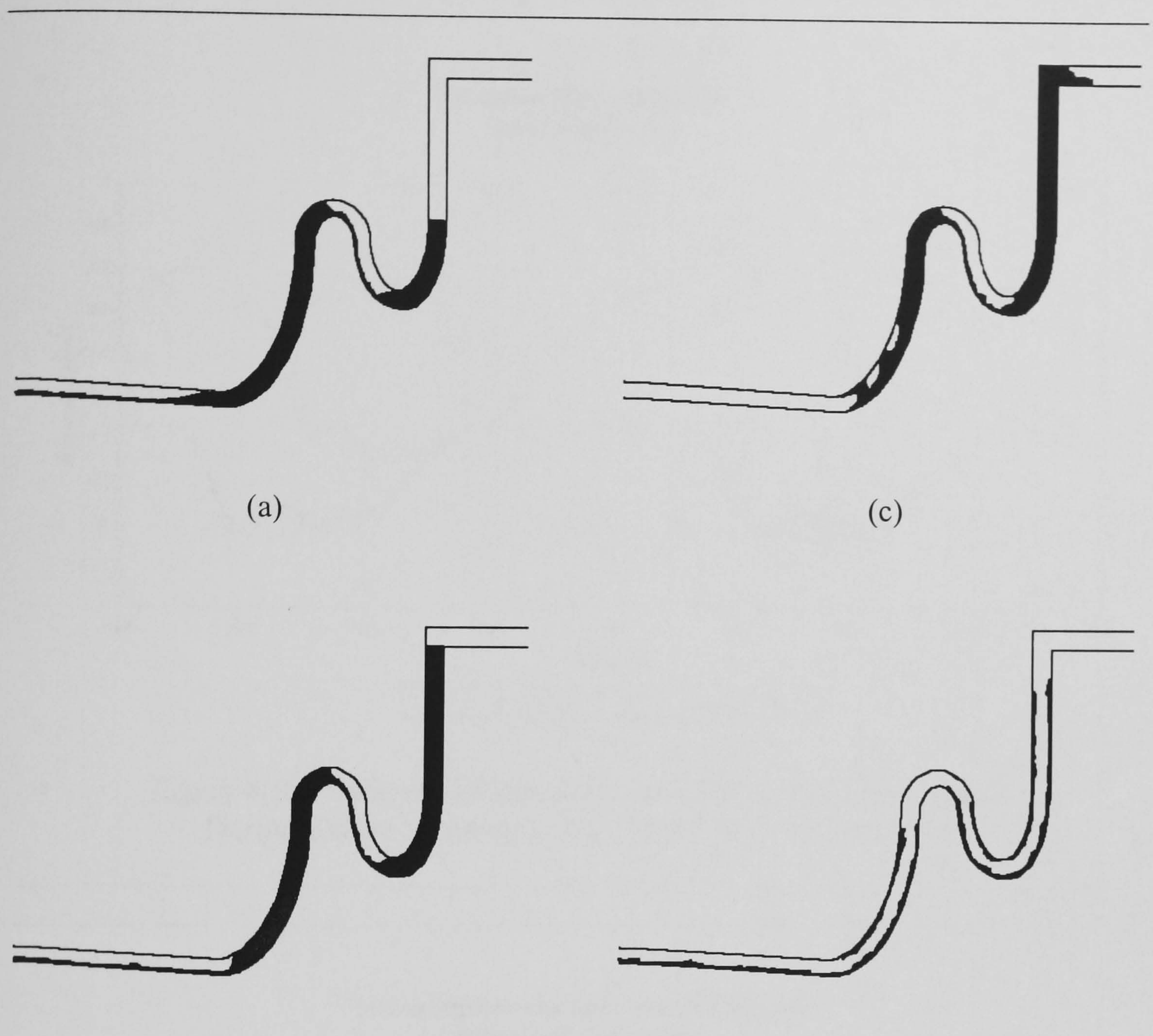

Figure 4.17 – Liquid Distribution in the Riser
During Severe Slugging 2

The probability density function of the pressure difference signal is given in Figure 4.19. During severe slugging 2 there is a much more even distribution of pressure difference over the cycle, reflected in the spread of experienced pressure difference values and pdf values. Though there is a higher pdf value for the peak pressure difference, the magnitude of this peak, 0.021 for severe slugging 2, is much less than the severe slugging 1 case where the peak value is 0.23.

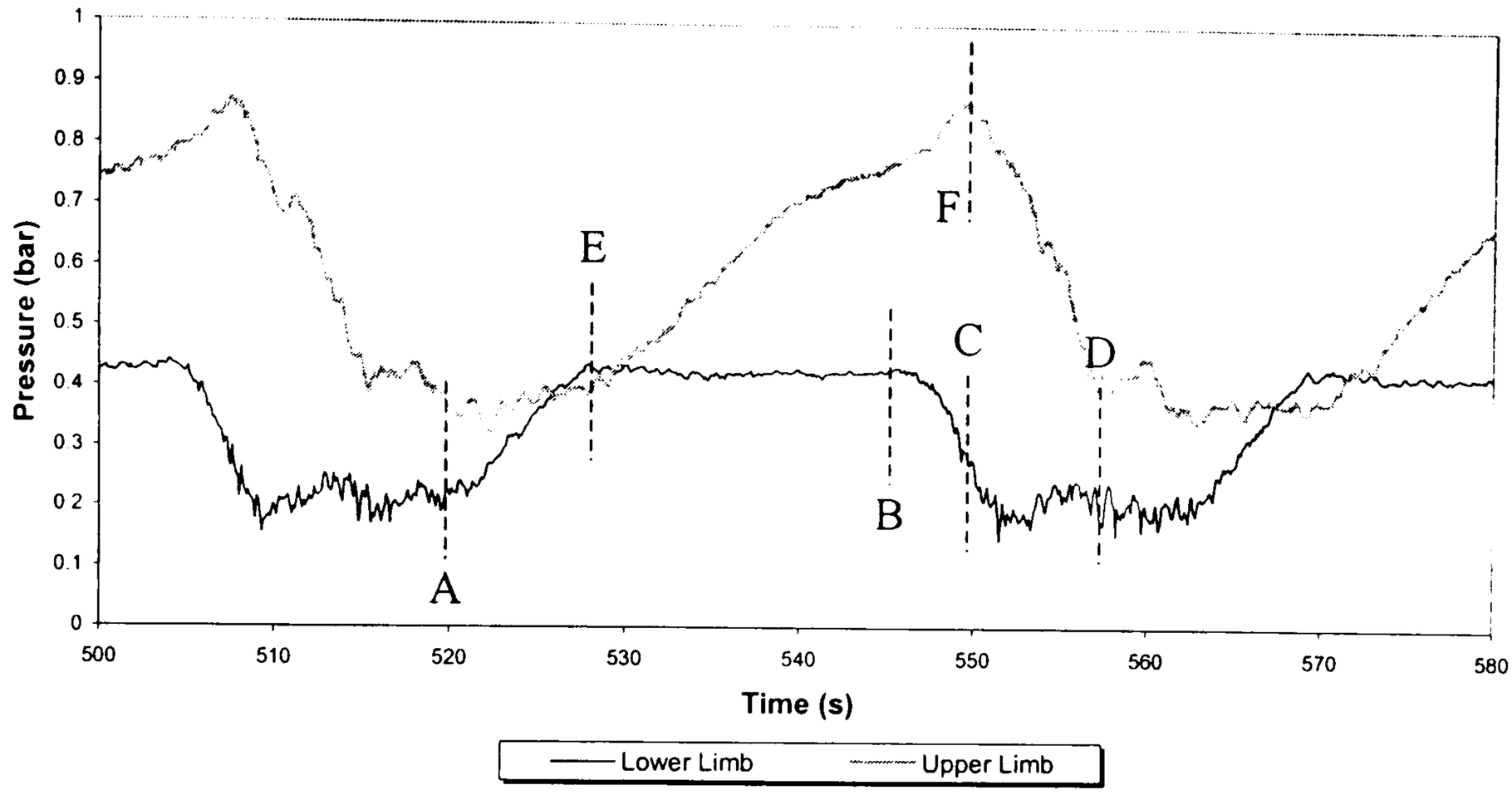

Figure 4.18 – Pressure Difference Over Each Upward Riser Limb During Severe Slugging 2, $U_G^S = 0.33$ m/s, $U_L^S = 0.5$ m/s

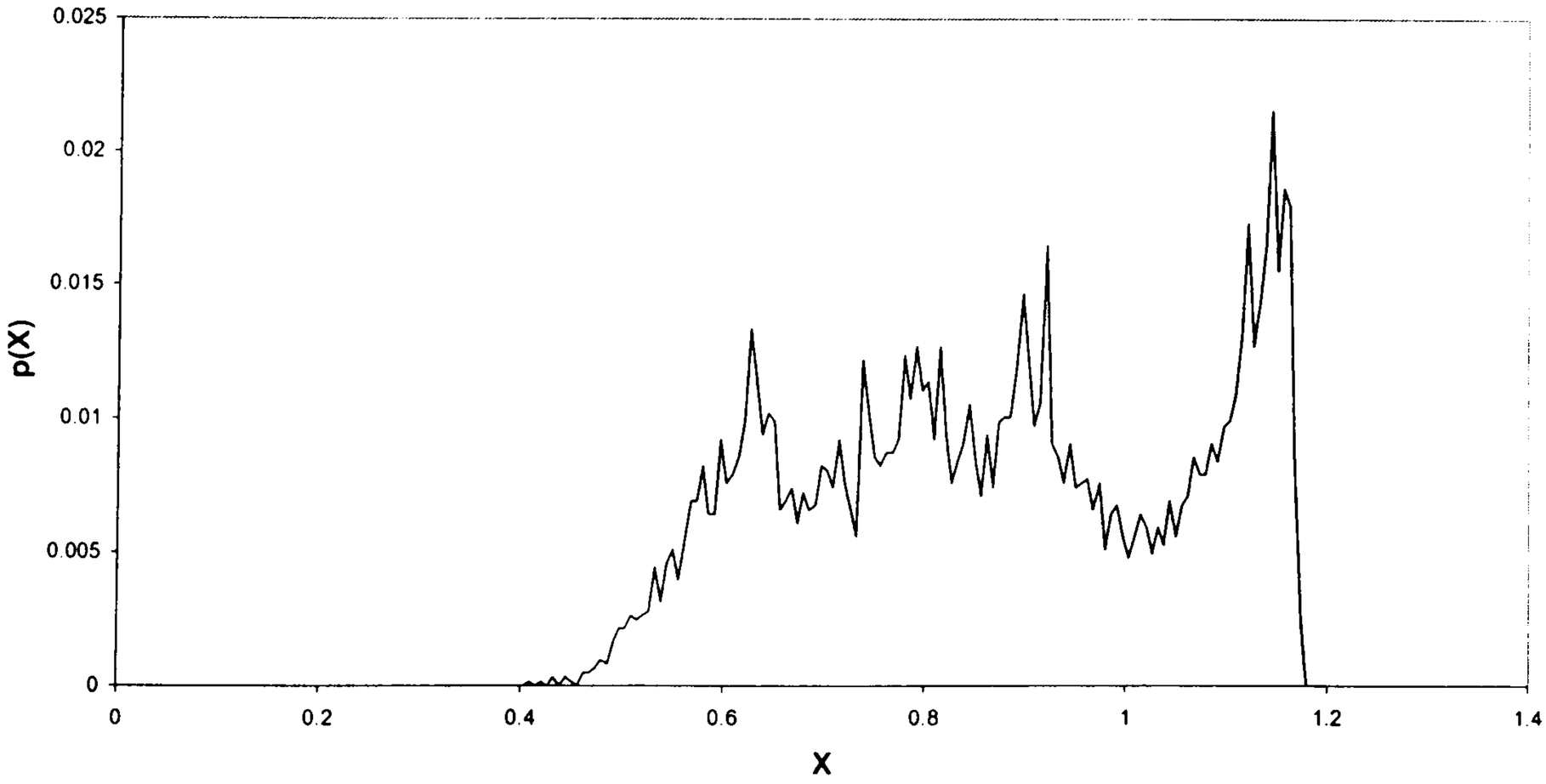

Figure 4.19 - Probability Density Function of Pressure Difference Over Riser During Severe Slugging 2, $U_G^S = 0.33$ m/s, $U_L^S = 0.5$ m/s

Moreover, the deviation of this peak from the other data is much less. There is a maximum deviation of 0.021 from the average of 0.008 in the severe slugging 2 case, rather than a maximum deviation of 0.23 from an average of 0.006 during severe slugging 1. This reflects the more even distribution of the pressure difference signal, though still with a propensity towards a particular maximum value of pressure difference and a relatively high degree of noise. Finally, the more narrow range of pressure values experienced during severe slugging 2 is reflected in the limits of pressure difference (X values) for which there is a meaningful pdf value.

Liquid Holdup Characteristics

The liquid holdup local to the riser base is presented in Figure 4.20 below. As stated previously, both upward limbs of the riser contained columns of pure liquid immediately prior to the blowdown. For this to occur, there must be no gas penetration at the riser base during the liquid buildup stage. Figure 4.20 confirms this behaviour, showing a unity liquid holdup local to the riser base during the cycle (Points A to B).

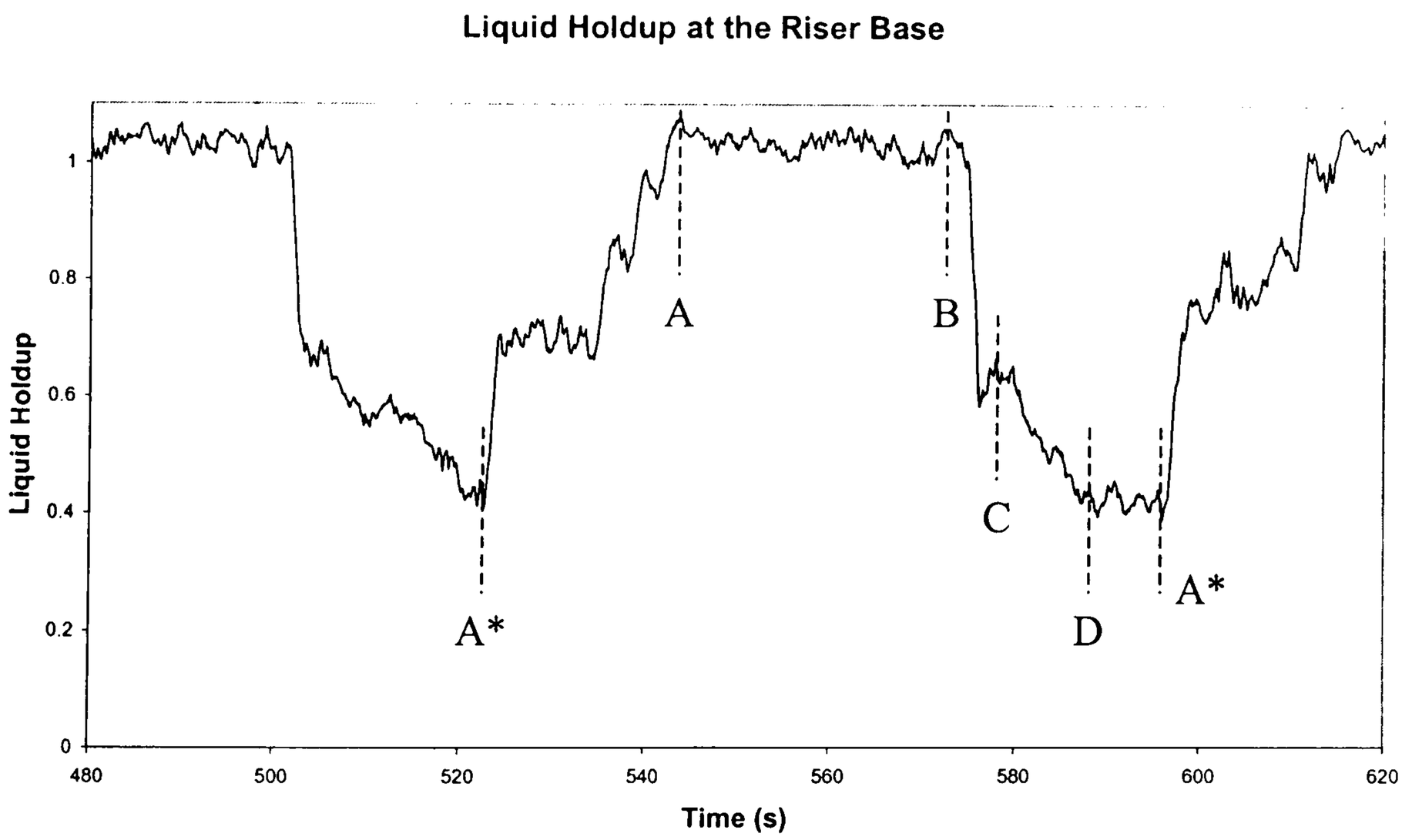

Figure 4.20 – Liquid Holdup Local to Riser Base During Severe Slugging 2, U_G^S = 0.343 m/s, U_L^S = 0.372 m/s

Fluid Production Characteristics

As stated previously, there is no constant production period during severe slugging 2, hence all fluid production in this flow regime is of a purely transient nature. Figure 4.21 shows an example of the liquid production profile during severe slugging 2.

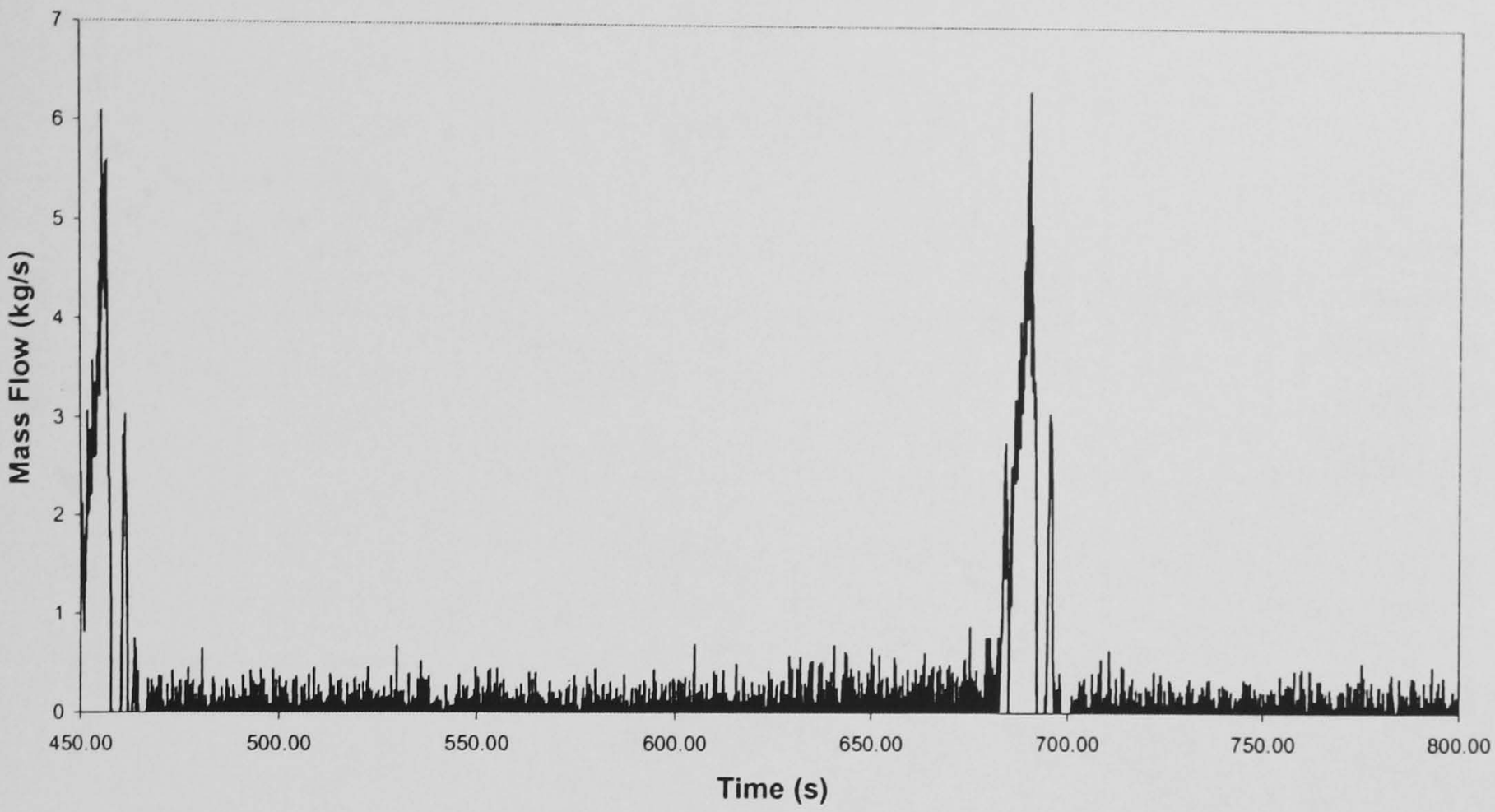

Figure 4.21 – Liquid Production During Severe Slugging 2,
$U_G^S = 0.209$ m/s, $U_L^S = 0.058$ m/s

As can be seen, the liquid production is in the form of a single liquid transient that occurs during the gas blowdown period of the severe slugging. Characteristically, the production consists of a single large production spike, immediately followed by a highly fluctuating tail-off in production. This is caused by the high degree of aeration in the slug tail and is confirmed below in the discussion of the gas production.

The liquid slug size during severe slugging 2, shown in Figure 4.22, exhibits a high degree of variation, with slug sizes ranging from 61.5 l to 19 l approximately for the data analysed. Indeed, though the average slug size is 47.45 l (123% of the riser volume), the standard deviation is 8.92 l (18.8% of the average), reflecting the high deviation of values. This means that 99% of the slug sizes will lie between 70.46 l and 24.5 l (182% and 63.5% of the riser volume). The distribution of slug sizes is caused by the different distributions of liquid present in the riser immediately prior to gas blowdown. The larger slug sizes, greater than or equal to the riser volume, are associated with the slugs that completely occupy both upward limbs of the riser prior to blowdown. The smaller slugs are those where the slug tail reaches the base of the riser before the upper limb is completely filled with liquid. The size of such slugs is less than the riser volume.

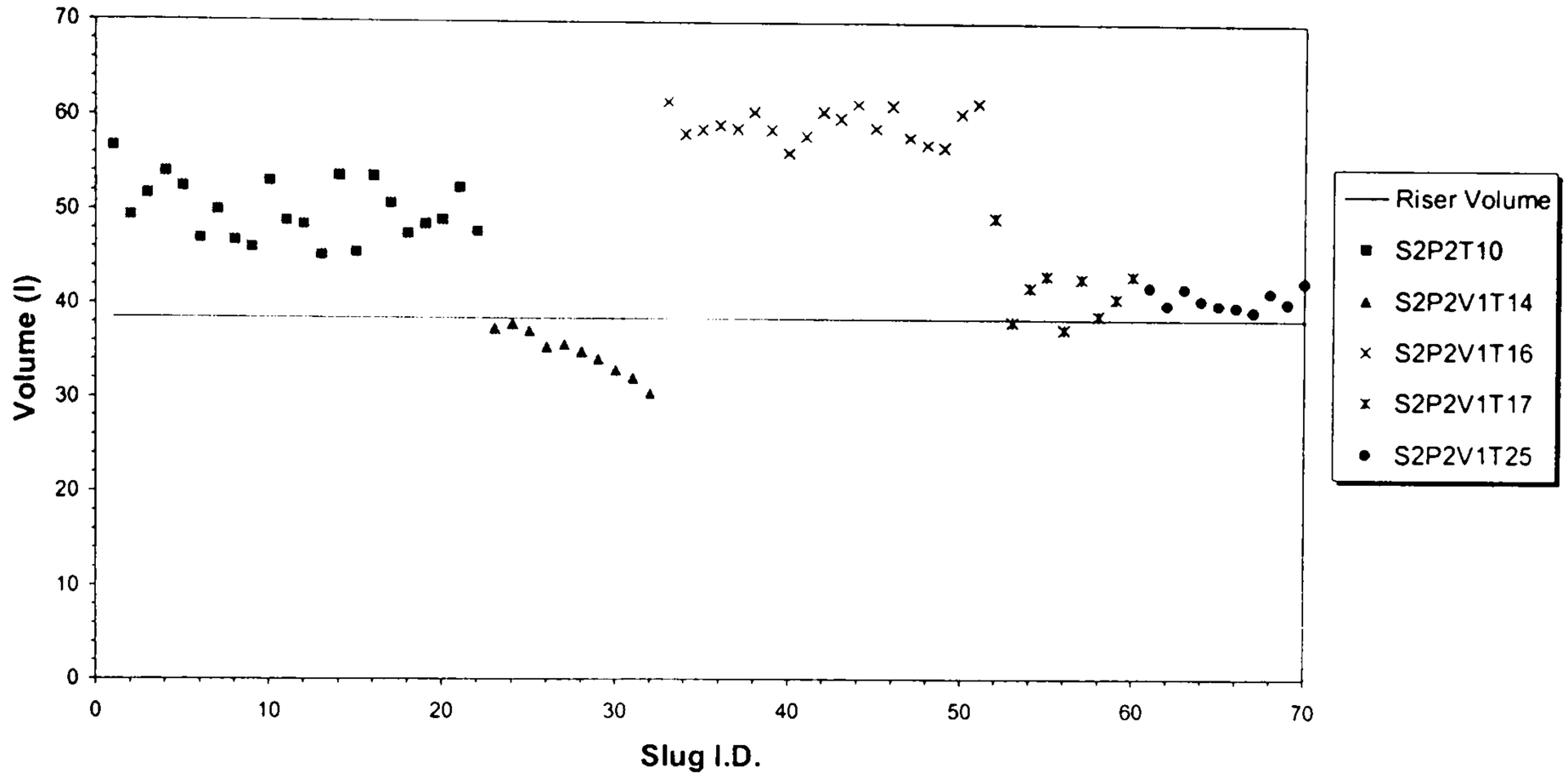

Figure 4.22 – Liquid Slug Size
During Severe Slugging 2, 2 bar(a)

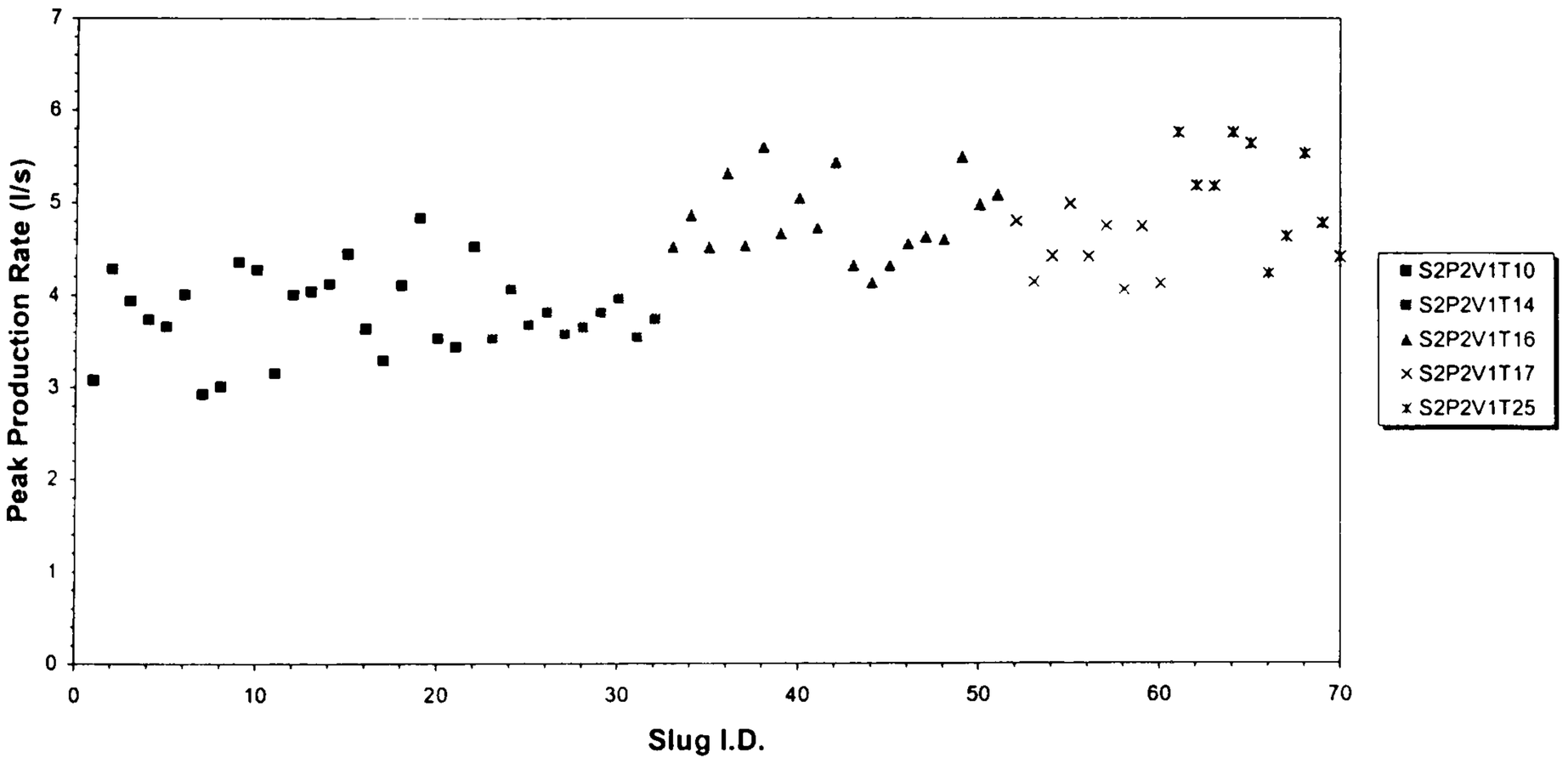

Figure 4.23 – Peak Liquid Production Rate
During Severe Slugging 2, 2 bar(a)

Peak flows during severe slugging 2 are shown in Figure 4.23 above. In these cases, the average peak liquid flow is 4.42 l/s with a standard deviation of 0.76 l/s (17% of the global average). Thus 99% of the peak flow values will be within the range 8.44 l/s and 2.5 l/s. Comparing this to the case of severe slugging 1, the peak flows are significantly higher and exhibit a similar degree of variation. It is worth noting however that the standard deviation within a test is of a similar magnitude to the global standard deviation – 0.54 l/s (11% of the average). Comparing the peak flow during a test to the average flow during that test, it is found that the peak flow, on average is 645% greater than the average flow.

As identified previously, the production transient may be the most problematic part of the production cycle of severe slugging, hence as severe slugging 2 has production transients of similar size to those encountered during severe slugging 1, severe slugging 2 can be said to be as problematic as severe slugging 1. This is due in part to their potential size – 123% of the riser volume as opposed to 96.65% for severe slugging 1 – and potential peak flow – 8.44 l/s as opposed to 5.72 l/s.

A typical gas production characteristic for severe slugging 2 is shown below in Figure 4.24. The gas production is in the form of a gas production transient followed by a period of constant gas production. The gas production transient in this case has two peaks. Combining the liquid and gas production profiles in Figure 4.25 shows how the gas production transient occurs during the liquid production transient. This is the cause of the fluctuations in the liquid production as a bubbly liquid mixture enters the separator. As the proportion of gas within the liquid slug increases, fluctuations in the liquid production rate become more prominent before finally the main bulk of the gas production begins. The high degree of gas during the liquid production stage shows that though there is no riser base gas penetration during the liquid accumulation period, there is a substantial bubble penetration period before gas blowdown. This bubble penetration gives a long, highly aerated slug tail. Once the main portion of liquid has been removed, the gas production transient occurs, followed by the period of constant gas production. Towards the end of this period of gas production, there is an interaction between the gas flowing into the riser and the liquid falling back under counter-current conditions. As the liquid falls back, the gas production continues for a certain period, the exact length determined by the test conditions. This interaction creates a bubbly mixture at the riser base that is readily identified by the pressure difference trace (Points D–A*, Figure 4.16).

In the case presented in Figure 4.16 there is a period of pressure difference at the riser base that is greater then the expected minimum. During this period there is no liquid head accumulation due to inflowing liquid. The bubbles passing through the already-accumulated liquid cause fluctuations in the pressure difference signal, akin to the case of bubble flow, see Section 4.4 below.

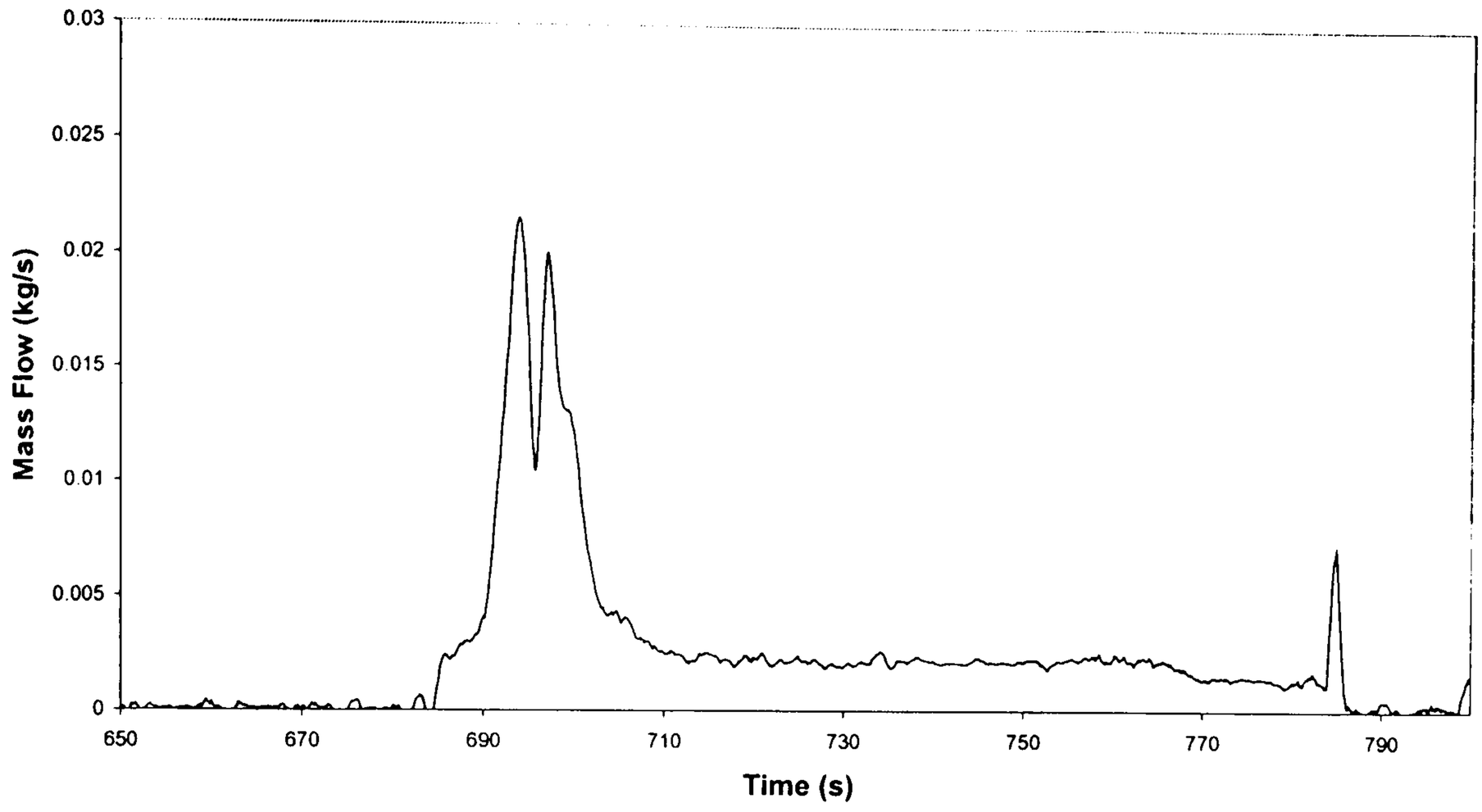

Figure 4.24 – Gas Production During Severe Slugging 2,
$U_G^S = 0.209$ m/s, $U_L^S = 0.058$ m/s

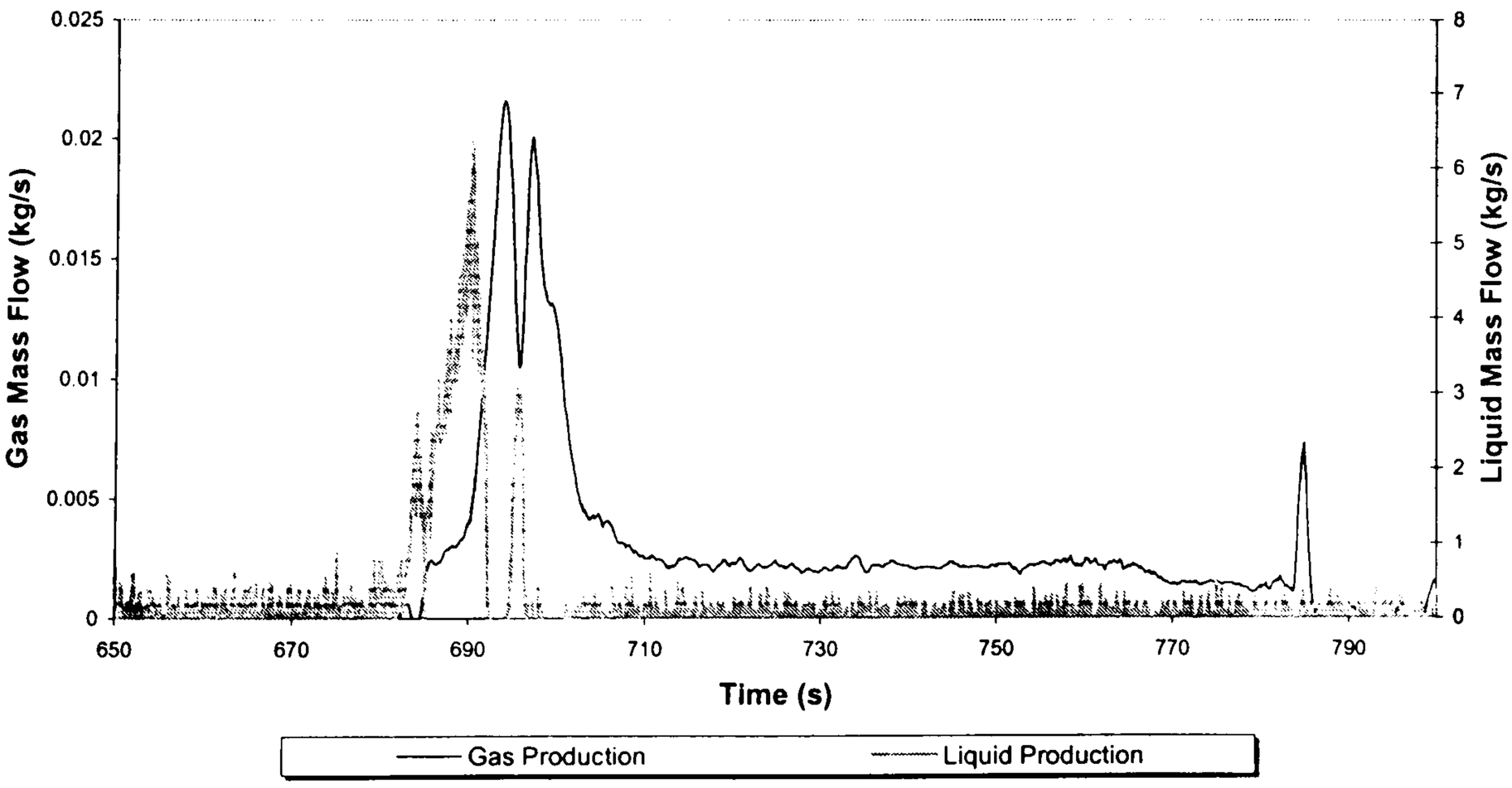

Figure 4.25 - Combined Gas and Liquid Production Characteristics
During Severe Slugging 2, $U_G^S = 0.209$ m/s, $U_L^S = 0.058$ m/s

There are some severe slugging 2 cases where during the constant gas production period there is liquid head accumulation at the riser base due to inflowing liquid from the pipeline. The rate of pressure difference increase is substantially lower than that during the main part of slug accumulation and, similar to the case described above, there are fluctuations in the pressure difference profile analogous to the case of bubble flow.

4.2.2 Severe Slugging 3 Characteristics

Pressure Cycling Characteristics

Severe slugging 3, as presented in Figures 4.26 and 4.27 below, consists of three main stages – liquid buildup, bubble penetration and an extended gas blowdown stage. Also included is a period of gas production, similar to, but longer than, the case of severe slugging 2. Furthermore, as in severe slugging 2, there is a substantial amount of liquid remaining in the riser post-blowdown. As in all transitional severe slugging, the cycle time is relatively shorter than during severe slugging 1, hence giving higher slugging frequencies (see Appendix D).

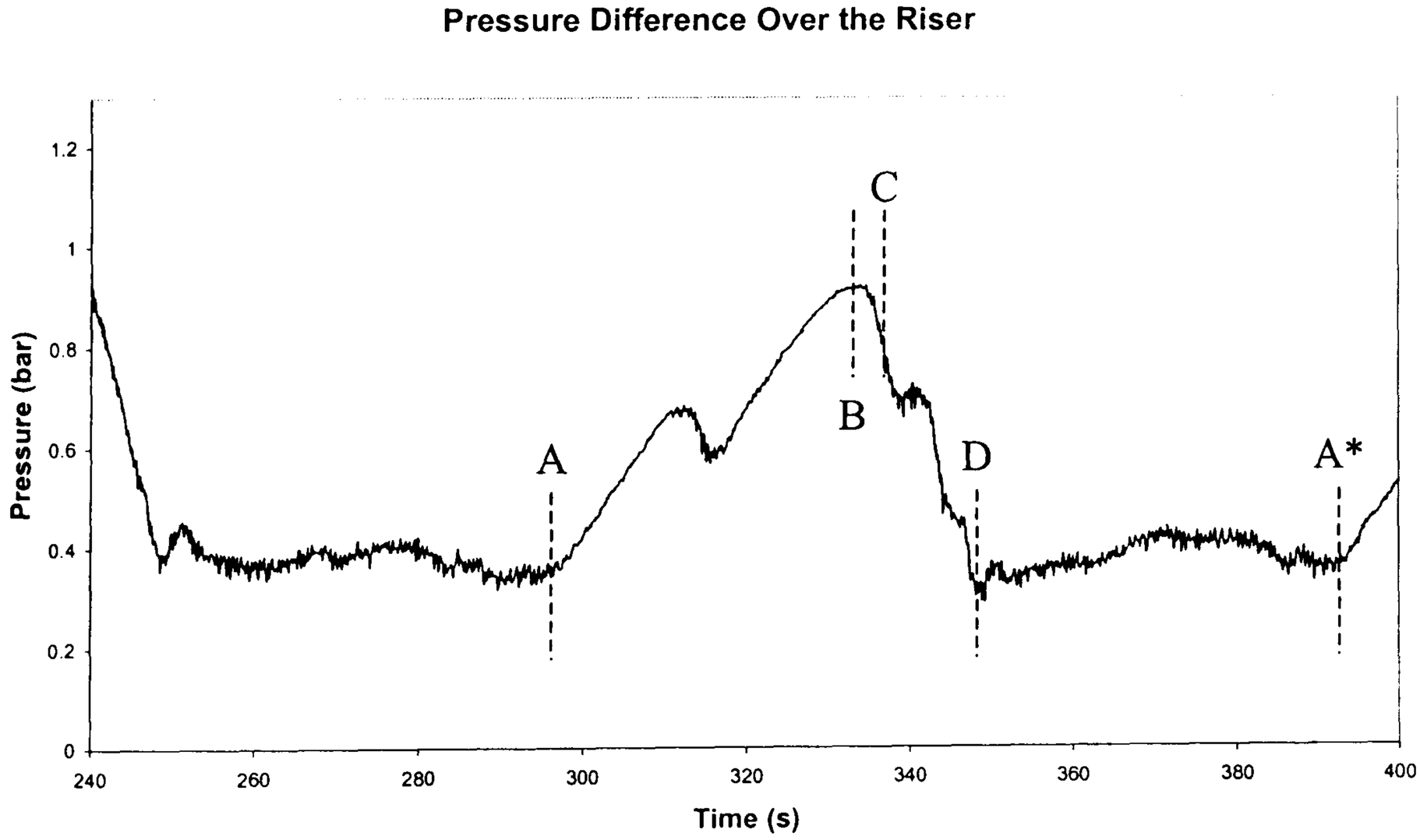

Figure 4.26 - Pressure Difference Over Riser During Severe Slugging 3, $U_G^S = 0.672$ m/s, $U_L^S = 0.165$ m/s

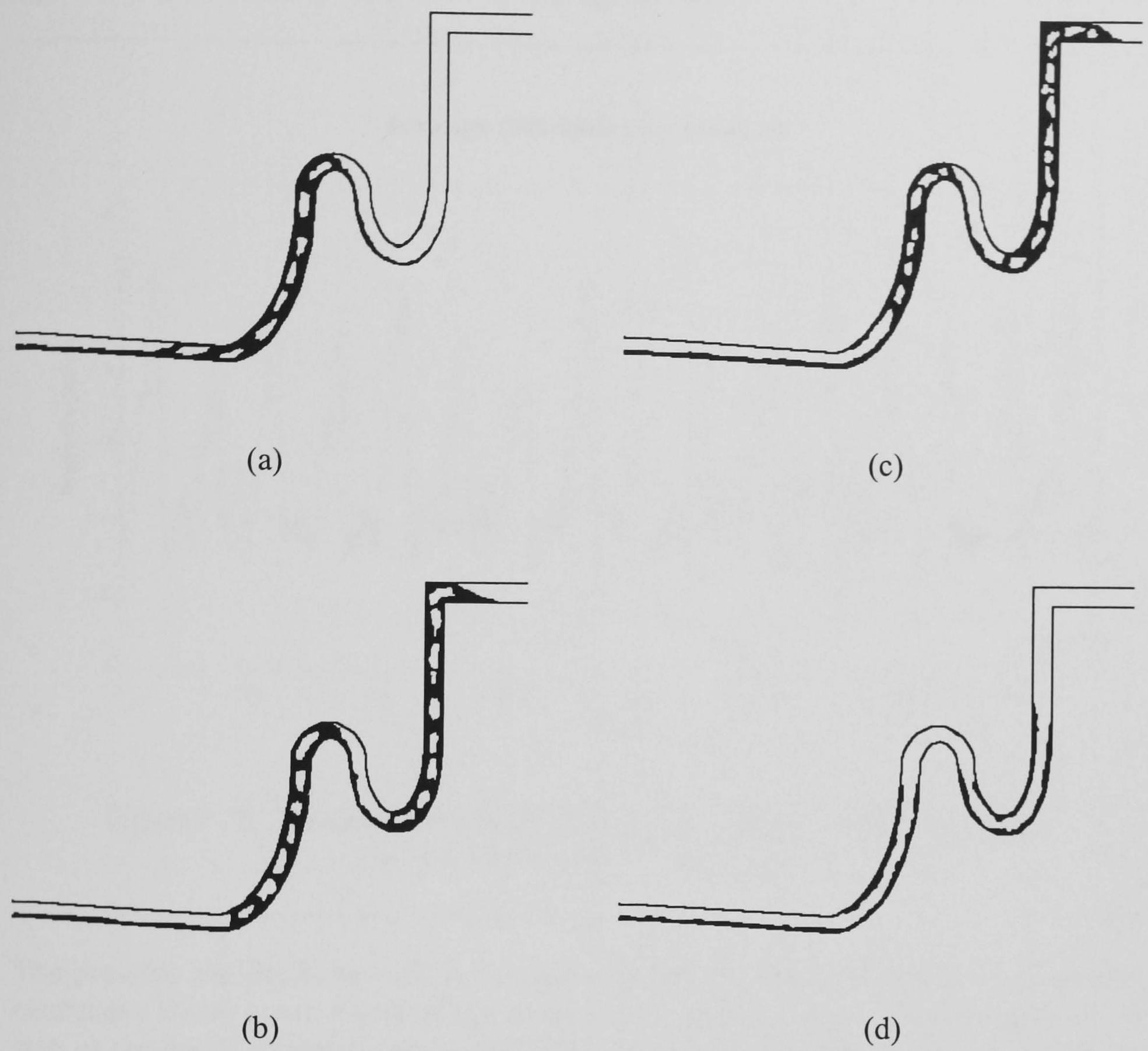

Figure 4.27 – Liquid Distribution in the Riser
During Severe Slugging 3

The characteristic difference between severe slugging 3 and other severe slugging flows is the degree of gas penetration throughout the cycle. During severe slugging 2, there are significant periods of no gas penetration or production, particularly during the liquid buildup stage when no gas enters the riser base. In the case of severe slugging 3, the slug is being continuously penetrated by gas, this leads to a highly aerated slug in the riser. In comparison, during severe slugging 2, there is pure liquid in each upward limb of the riser during slug formation. The net effect of this continuous gas penetration is the maximum pressure difference over the riser during the slugging cycle is less than the maximum possible during severe slugging 1. As Taitel *et al.* (1990) observed, during transitional severe slugging flows, the penetration of gas at the riser base is unstable, hence the quantity of gas entering the

slug is varying continuously. This is indeed reflected in the variation in the maximum pressure experienced from cycle to cycle, Figure 4.28.

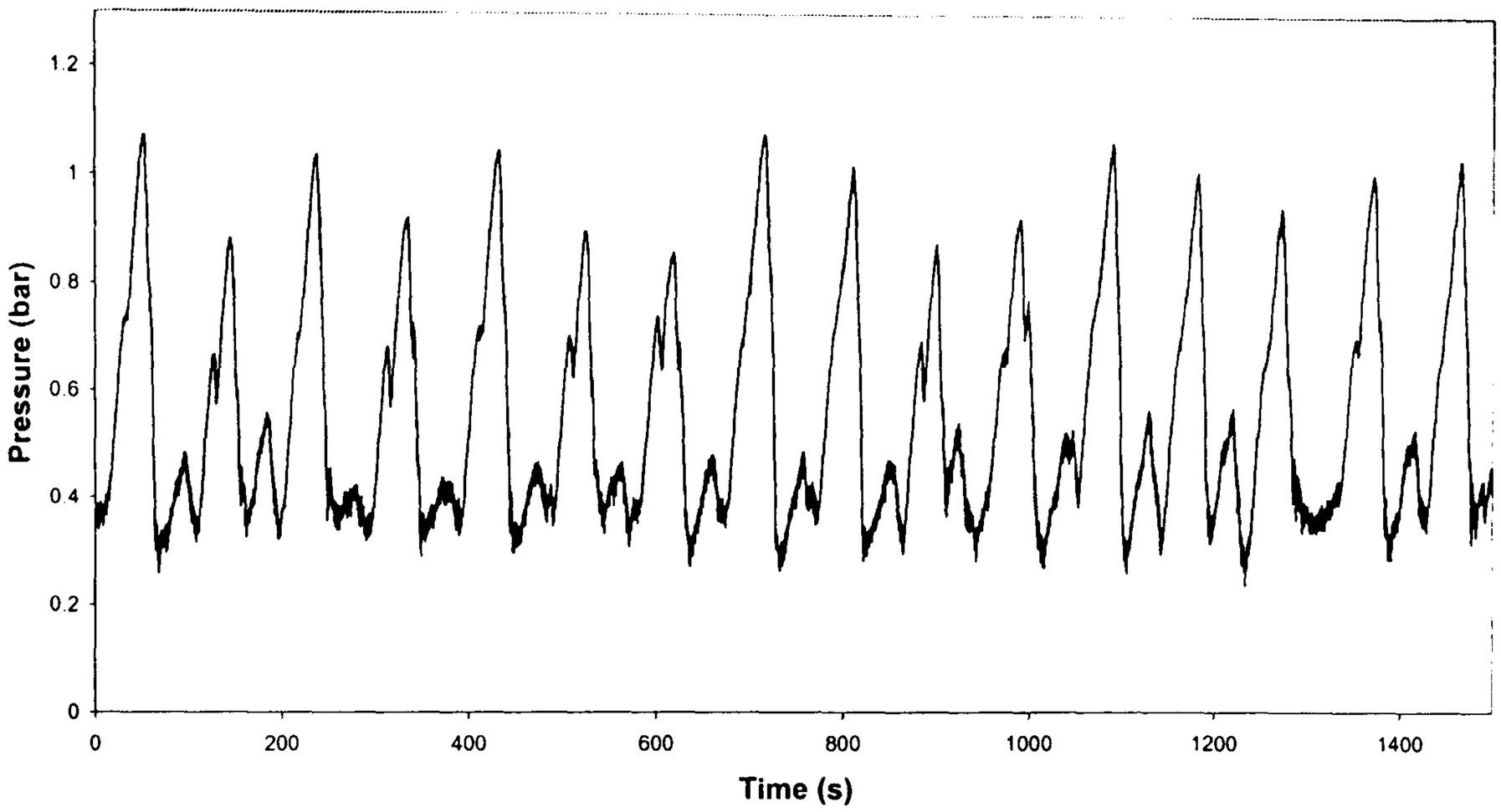

Figure 4.28 – Pressure Difference Over Riser During Severe Slugging 3, $U_G^S = 0.672$ m/s, $U_L^S = 0.165$ m/s

The pressure cycling behaviour in the upward limbs of the riser, Figure 4.29 on the next page, shows more detail of the severe slugging 3 process. Beginning from the start of the liquid accumulation period (Point A), the slug begins to form in the lower limb of the riser. This continues, filling approximately 90% of the lower limb. As the liquid reaches the top of the lower limb (Point E) the liquid is swept into the upper limb, reflected in the jump in the pressure difference in the upper limb. Following this first blow-out[2] of the lower limb, the liquid begins to form a second time. As the lower limb fills with liquid, the gas in the downcomer section is compressed and moves into the upper limb (Point F), reducing the liquid head and hence the pressure difference, preventing the upper limb being filled with liquid. As the lower limb again reaches near-maximum pressure difference, the liquid is blown out and into the upper limb of the riser (Point B), again increasing the liquid content in the upper limb. After this second blow-out, gas penetration of the riser base continues, eventually leading to penetration of the liquid in the upper limb and removal of the liquid in the upper limb, giving the final blowdown of the gas.

[2] Note that this nomenclature is used to distinguish this process from the gas blowdown later.

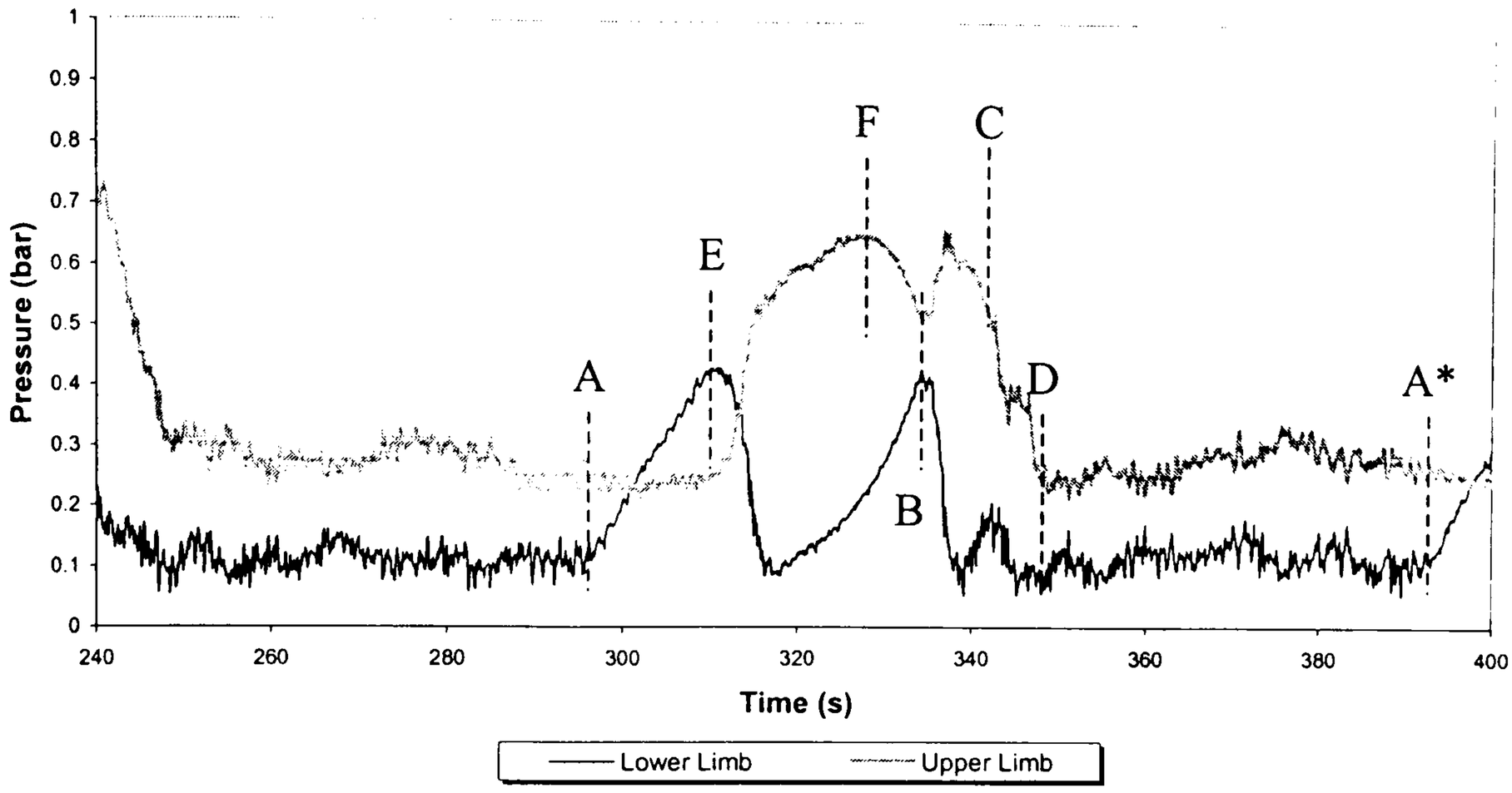

Figure 4.29 – Pressure Difference Over Each Upward Riser Limb
$U_G{}^S = 0.672$ m/s, $U_L{}^S = 0.165$ m/s

Though the liquid column in the lower limb is unstable, with pressure cycling occurring, the liquid in the upper limb remains stable and is not swept out until it has been penetrated by a substantial quantity of gas from the pipeline. This is indicated by the slow rate of drop in pressure difference in the upper limb after the liquid has been swept out of the lower limb. That is, there is a significant time delay, after the beginning of bubble penetration of upper limb by pipeline gas, before the upper limb liquid is swept out. This period is indicated by the time period B–C. However, though there are indications that there is some independence in the behaviour of each limb, the fact that the liquid in the upper limb is eventually swept out indicates that there is unstable flow in both limbs of the riser at some point in the severe slugging cycle.

The pdf of the pressure signal, shown in Figure 4.30, shows a reverse characteristic to the severe slugging 1 and 2 pdf profiles. In this case there is a peak in the probability corresponding to the minimum pressure difference. This reflects the greater occurrence of low-pressure values, corresponding to the gas production period. The relatively large width of this peak, compared to severe slugging 1, indicates the degree of variation of these values.

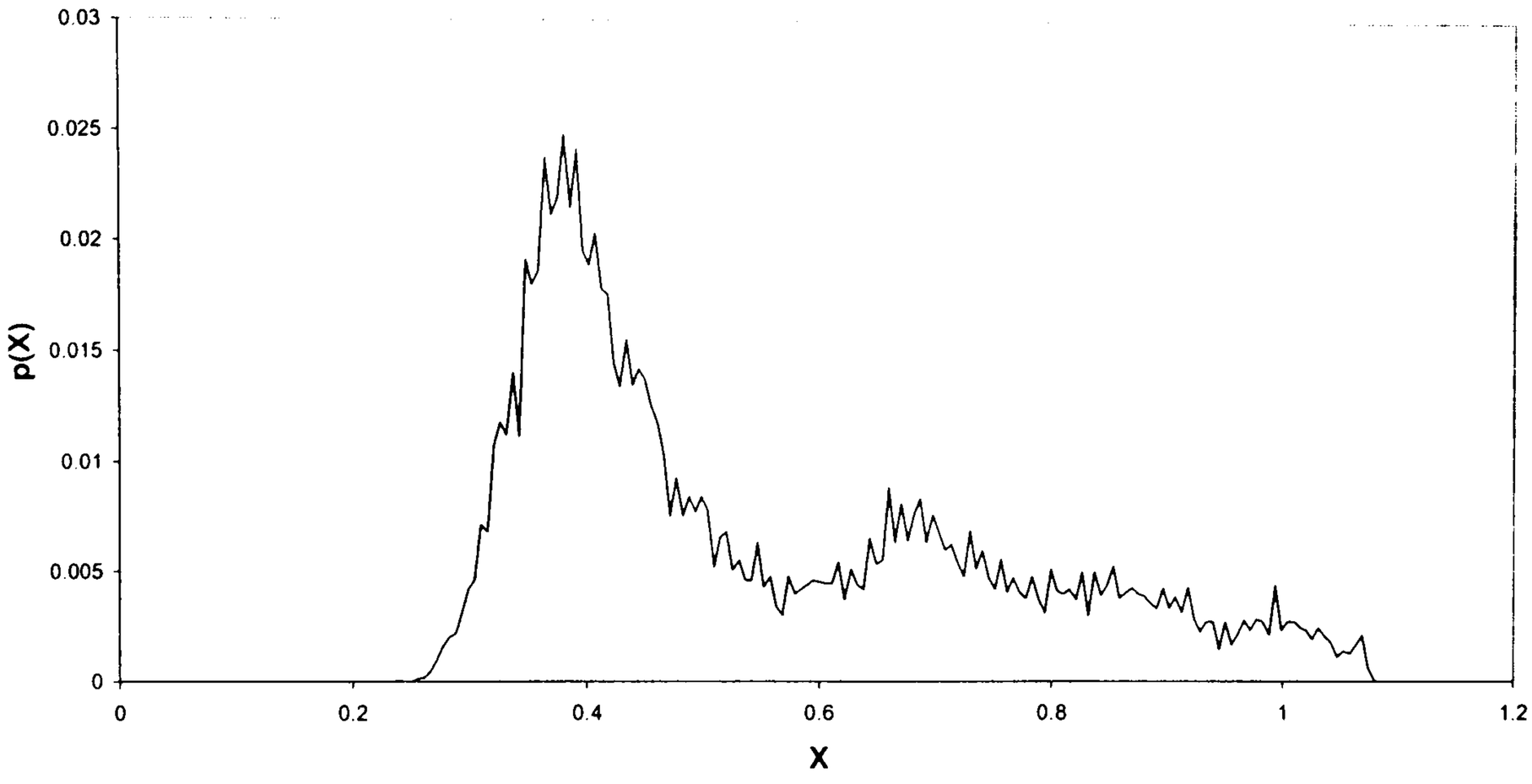

Figure 4.30 – Probability Density Function of Pressure Difference Over Riser During Severe Slugging 3, $U_G{}^S = 0.672$ m/s, $U_L{}^S = 0.165$ m/s

Comparing the peak value of the pdf to the average indicates that as for severe slugging 2 there is a smaller deviation in the peak pdf value from the average pdf value for the cycle compared to severe slugging 1 – a deviation of 0.0248 from an average of 0.0064. This reflects a narrower spread of pressure difference values during severe slugging 3. However, the propensity to a lower pressure value is greater than the case of the most likely pressure during severe slugging 2, whose peak pdf value is 0.021.

Liquid Holdup Characteristics

The liquid holdup characteristic for severe slugging 3 is shown in Figure 4.31 below. The bubble penetration at the riser base during the severe slugging cycle is confirmed by a liquid holdup value of less than unity during the majority of the cycle. The only times where there is pure liquid local to the riser base are when the liquid is being swept from the lower limb into the upper limb of the riser. This sweep-out process is accompanied by the movement of liquid from the pipeline into the riser, increasing the liquid holdup measurement momentarily.

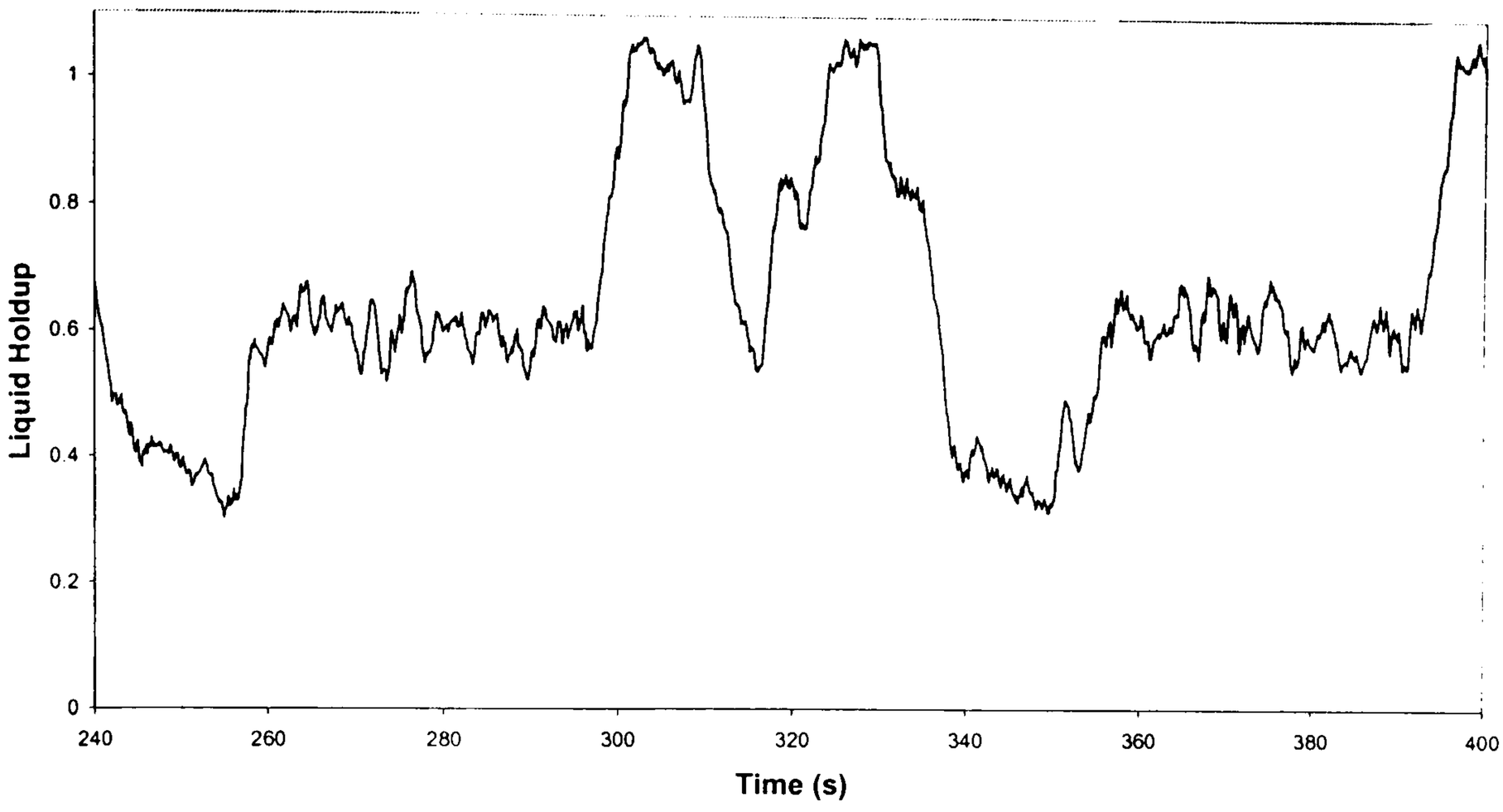

Figure 2.31 - Liquid Holdup Local to Riser Base During Severe Slugging 3, $U_G^S = 0.672$ m/s, $U_L^S = 0.165$ m/s

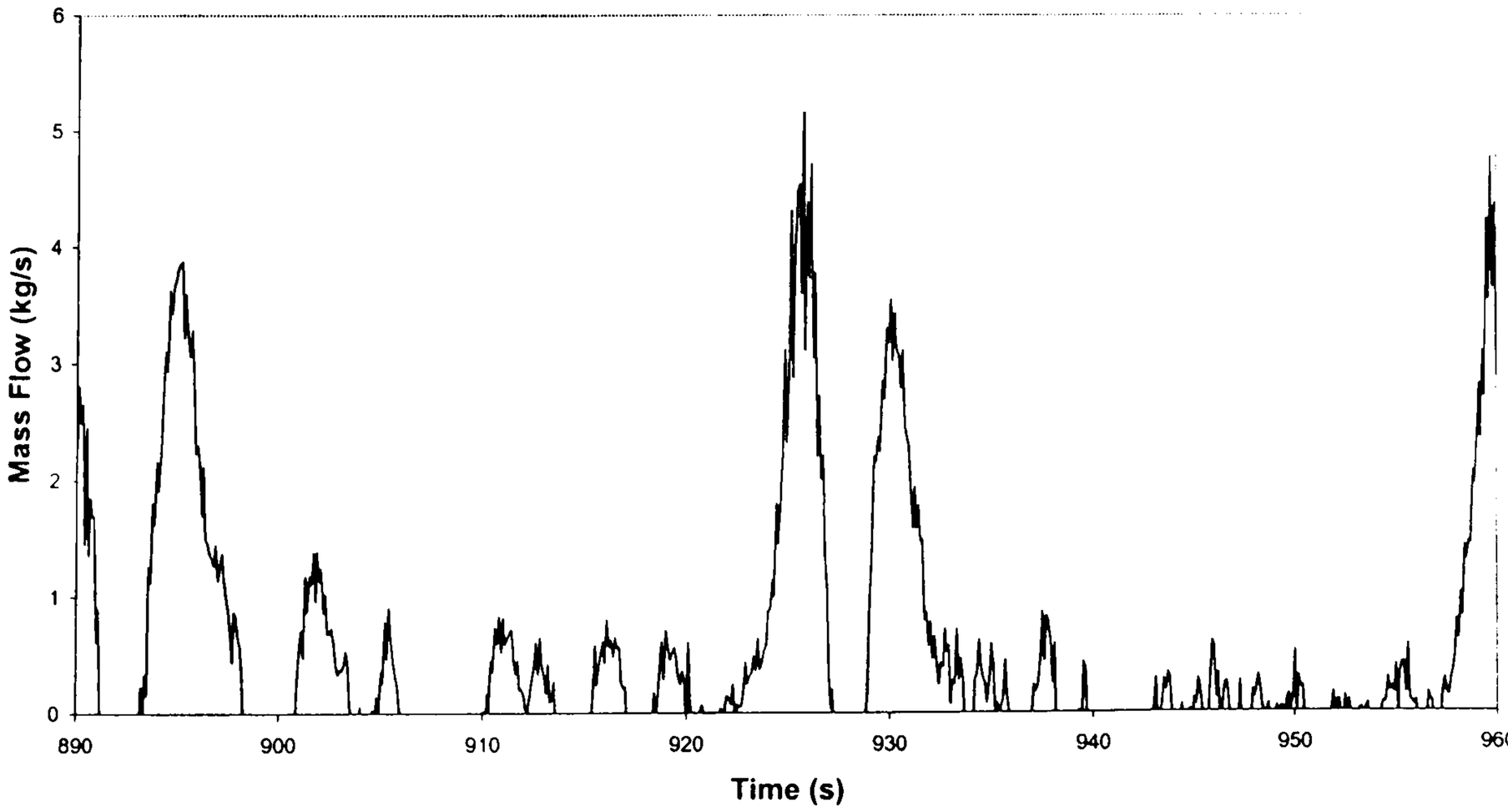

Figure 4.32 - Liquid Production During Severe Slugging 3, $U_G^S = 0.906$ m/s, $U_L^S = 0.213$ m/s

Fluid Production Characteristics

The liquid production profile in Figure 4.32 above shows the purely transient nature of the liquid production during severe slugging 3. In the case of severe slugging 2, a period of highly-fluctuating liquid production was observed, this was caused by the highly aerated slug tail arriving at the riser outlet. During severe slugging 3, the slug was continuously penetrated by gas from the pipeline, meaning that the entire liquid slug is aerated. Thus the entire liquid production exhibits such fluctuations.

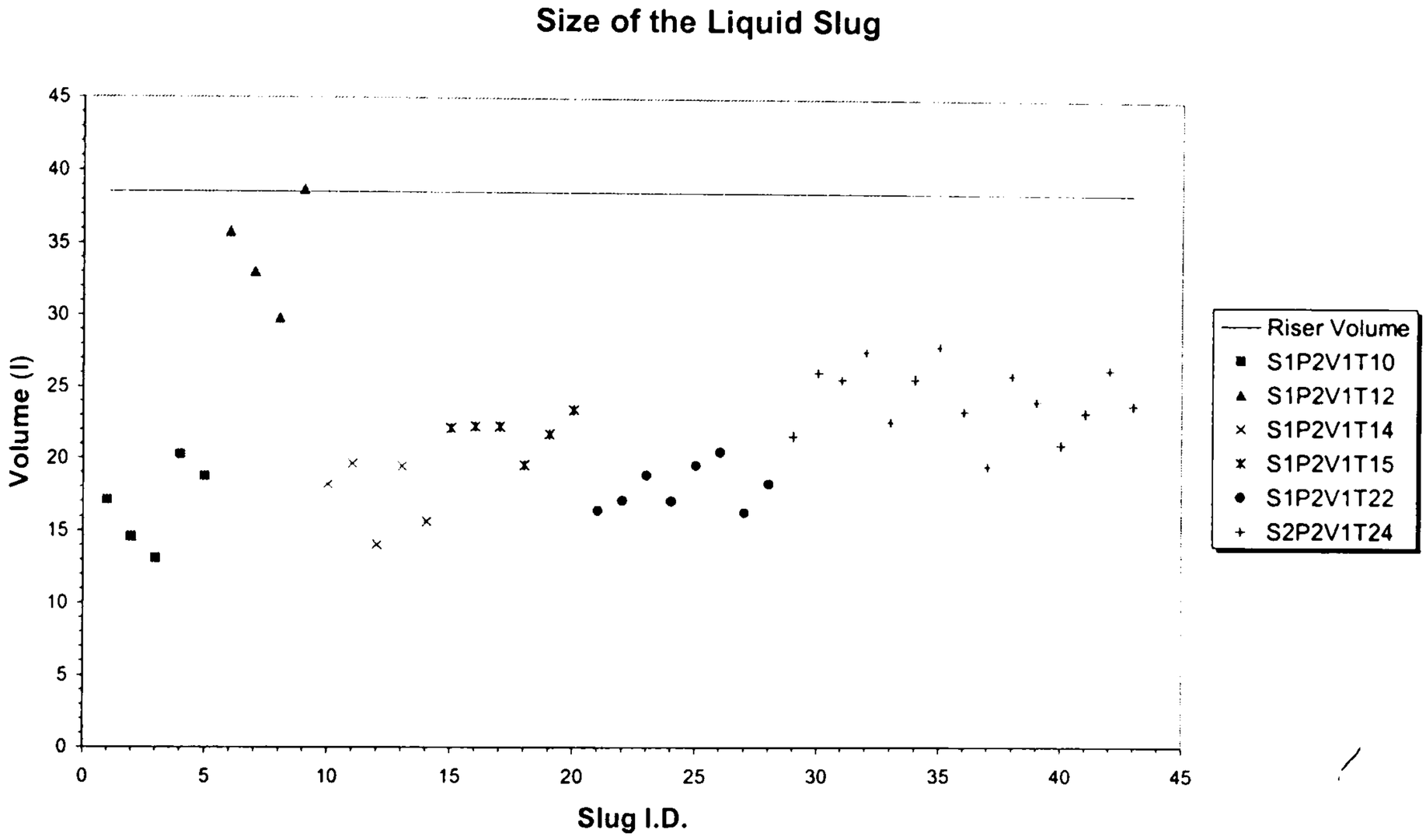

Figure 4.33 – Liquid Slug Size
During Severe Slugging 3, 2 bar(a)

Examining Figure 4.33, the slug sizes for severe slugging 3 are significantly smaller than the riser volume, with an average of 22.05 l (58% of the riser volume). Furthermore, there is a lower relative variation in the slug sizes when compared to severe slugging 2. The standard deviation of severe slugging 3 sizes is 5.47 l (24.8% of the average), smaller than the case of severe slugging 2 whose variation is 12.75 l (29.4% of the average). Thus 99% of slugs during severe slugging 3 are expected to lie between 36.16 l and 7.85 l (20.6% and 93.9% of the riser volume), indeed it may be stated that a slug size less than the riser volume is a characteristic of severe slugging 3. Such a low slug size is again directly attributable to the degree of gas penetration in the riser during the slug cycle as a whole.

The peak flow during severe slugging 3 (Figure 4.34) exhibits a similar scale and degree of variation to severe slugging 2. The average peak production rate is 4.42 l/s and the standard deviation is 0.88 l/s (20% of the average), this compares to values of 4.73 l/s and 0.67 l/s for the case of severe slugging 2. The similarity in the results for the these values could be explained by the fact that during the final stages of the

severe slugging cycle where these peak flows occur, the observed slugs are similar in nature – during the blowdown there are high levels of gas in the slug tail, rapidly accelerating the liquid flow from the riser. Comparing the peak flow experienced to the average flow, the peak flow is 1285% greater than the average. This is much higher than the 645% increase during severe slugging 2 and is on a similar scale to the 1045% experienced during severe slugging 1. In terms of the potential peak flow experienced during severe slugging 3, the upper limit of the flow is 6.68 l/s (to a confidence of 99%). In comparison, the upper limits for severe slugging 1 and 2 are 5.72 l/s and 8.157 l/s respectively.

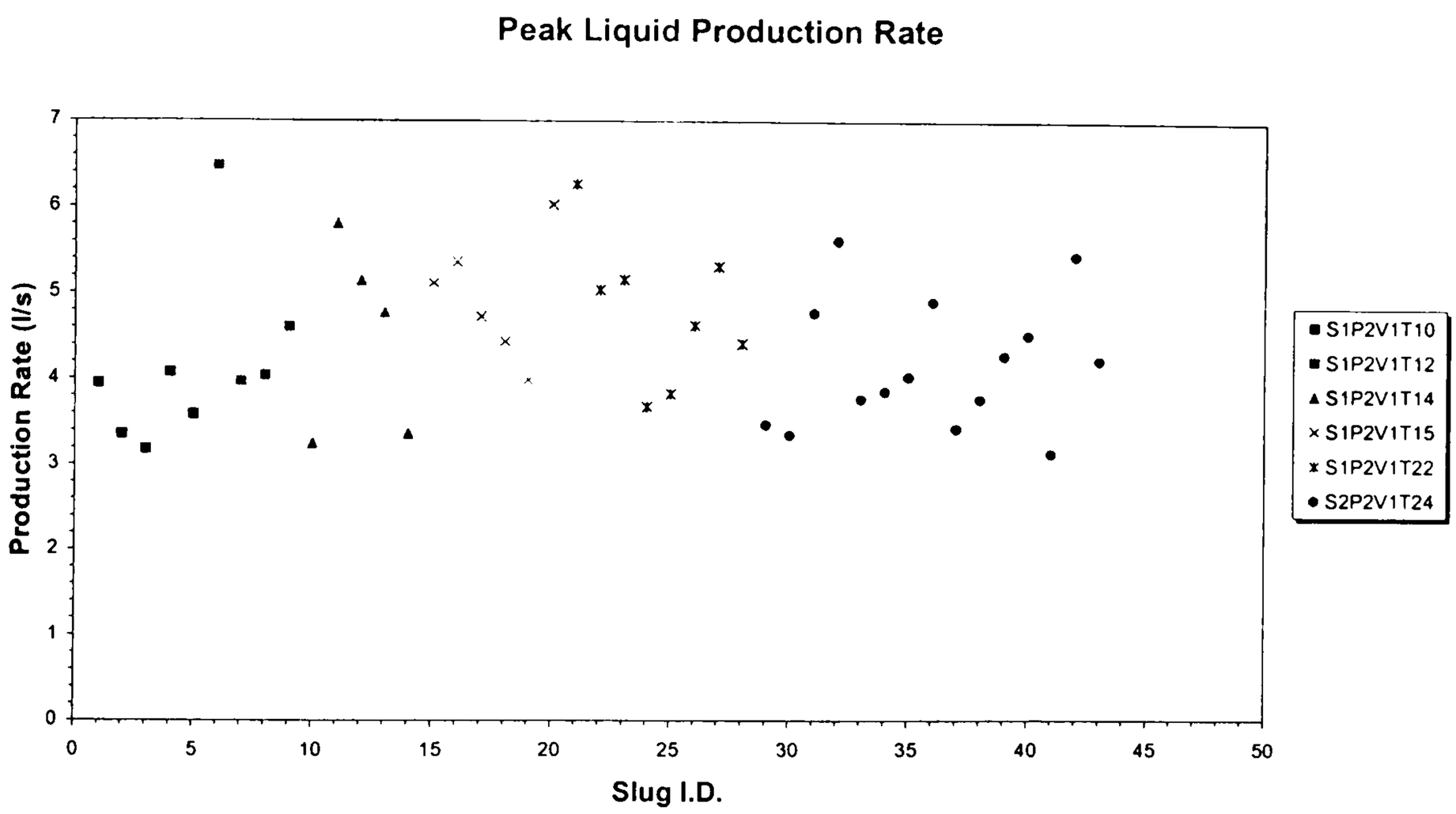

Figure 4.34 – Peak Liquid Production Rate
During Severe Slugging 3, 2 bar(a)

Summarising the above, severe slugging 3 is, in comparison to severe slugging types 1 and 2, less problematic in terms of the maximum potential production transient expected. The maximum potential production transient is 58% of the riser volume for severe slugging 3 as opposed to 96.7% and 112% for severe slugging 1 and 2 respectively. However, in terms of the increase in the flow from the riser, severe slugging 3 is more problematic than either severe slugging 2, or severe slugging 1.

Gas production during severe slugging 3 is continuous, in keeping with the fact that the slug is continuously being penetrated by gas from the pipeline. With respect to the minimum gas production rate, severe slugging 3 is less problematic than severe slugging 2 or 3 as there is a continuous throughput of gas. Other forms of severe slugging have considerable period of zero gas production, such a zero-flow period would cause large problems for compression trains in oil and gas receiving facilities.

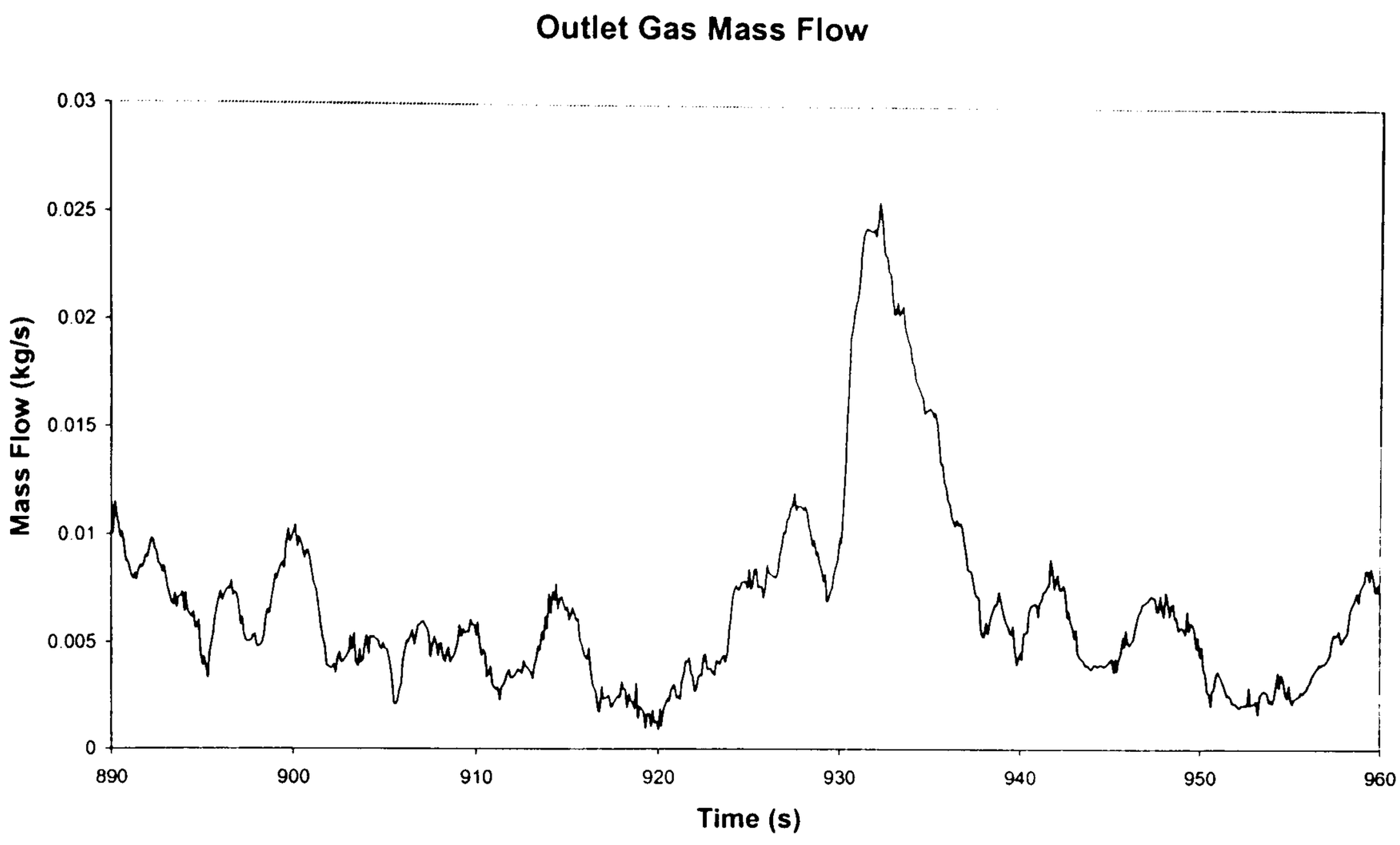

Figure 4.35 – Gas Production During Severe Slugging 3,
U_G^S = 0.906 m/s, U_L^S = 0.213 m/s

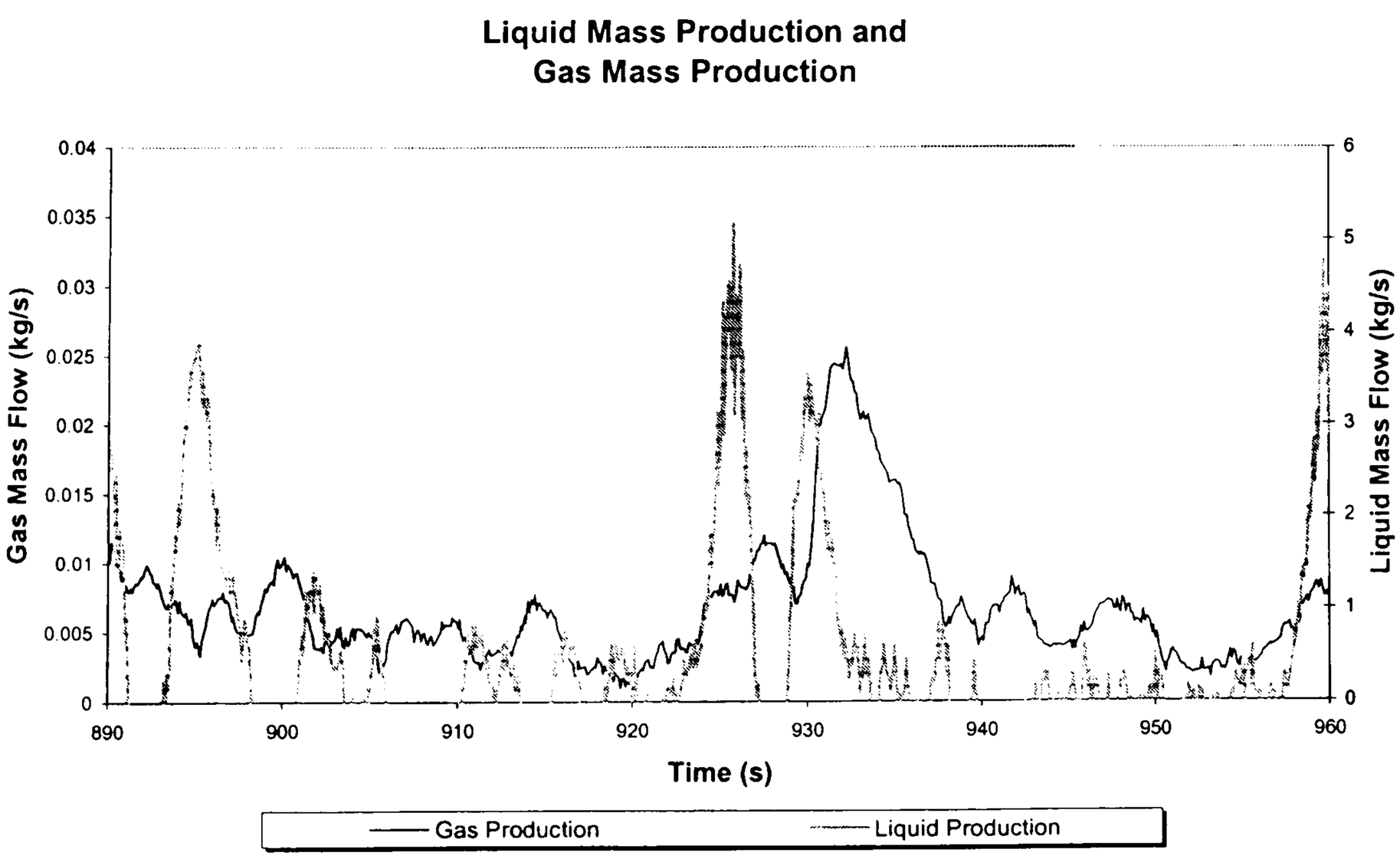

Figure 4.36 - Combined Gas and Liquid Mass Production Characteristics
During Severe Slugging 3, U_G^S = 0.906 m/s, U_L^S = 0.213 m/s

Though there is continuous gas penetration at the riser base, there remains a peak in the gas production rate during the severe slugging process. This peak coincides with the blowdown of the pipeline gas and follows immediately after the sweep-out of the liquid in the upward limbs of the riser. The gas production evident during the liquid production periods also reflects the aerated nature of the liquid slugs during severe slugging 2.

4.3 Oscillation Characteristics

Oscillation flow is a transitional flow regime between severe slugging and stable flows. Though a transitional behaviour, oscillation flow is capable of being sustained indefinitely in the pipeline/riser given appropriate flow conditions and separator pressure.

Pressure Cycling Characteristics

The pressure difference over the riser during oscillation flow is presented in Figure 4.37. The pressure variation in this case is of a sinusoidal type, regularly varying between 0.97 and 0.62 bar. This means that the riser is not completely filled with liquid during the observed pressure cycling and at the end of each cycle there is a substantial quantity of liquid remaining in the riser. The pressure cycling is of a noticeable shorter cycle time than the severe slugging discussed thus far, in this example the cycle time is 18 s as compared to severe slugging cycle times of 195 s.

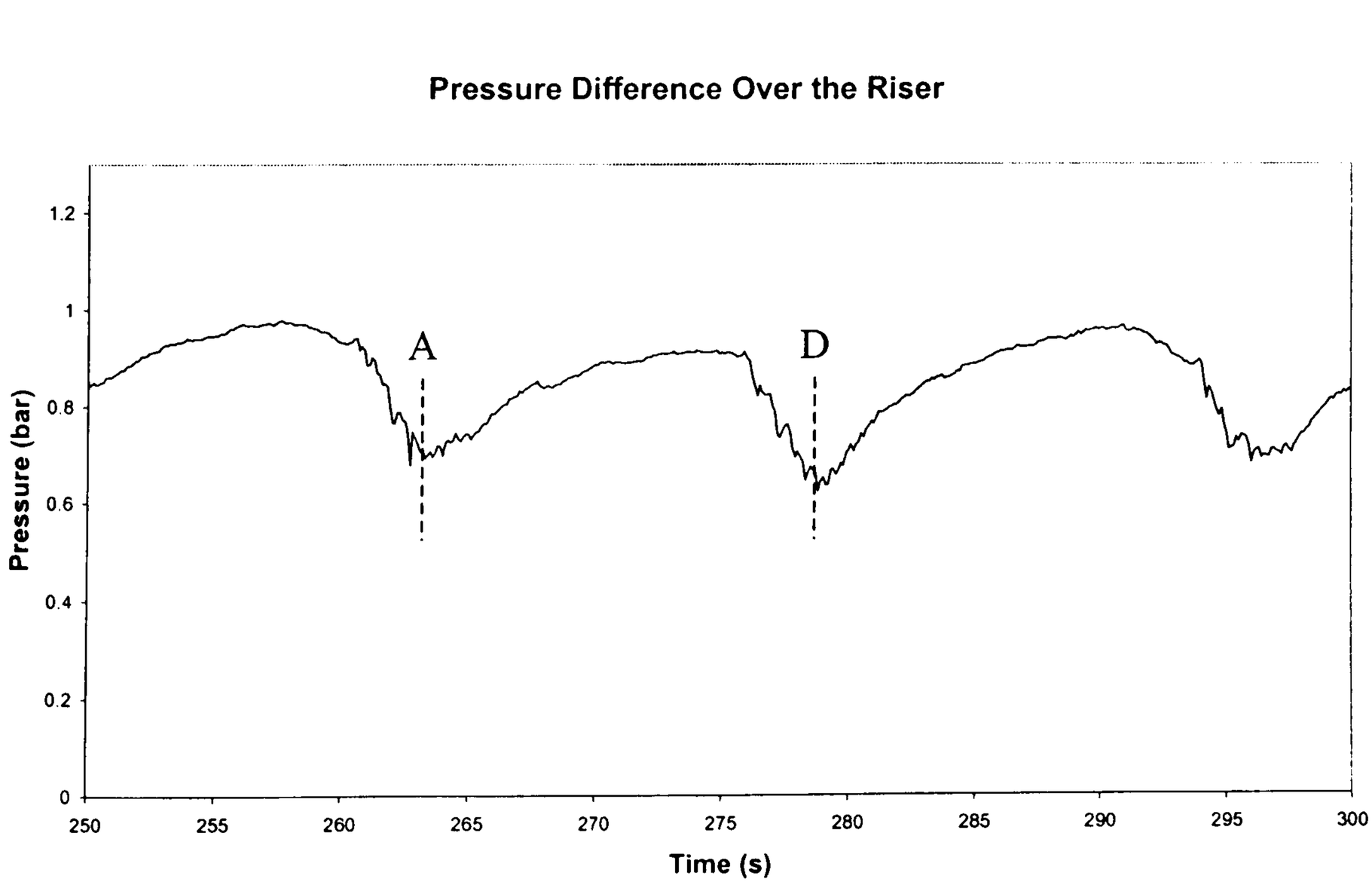

Figure 4.37 – Pressure Difference Over Riser During Oscillation Flow, $U_G^S = 0.248$ m/s, $U_L^S = 0.431$ m/s

Examining the pressure difference in the upward limbs of the riser, Figure 4.38, highlights the mechanisms occurring during oscillation flows. Pressure cycling occurs in both the lower and upper limbs of the riser, though there is a marked difference between the behaviour in each. The lower limb undergoes cyclical filling and emptying, giving a pressure cycling characteristic that varies cyclically between approximately 0.1 and 0.5 bar. The upper limb also undergoes a degree of pressure cycling, however the change in liquid inventory is small giving a variation in pressure difference of approximately 0.2 bar. Indeed, though the lower limb is subject to unstable conditions with the formation and sweep-out of a column of liquid, the upper limb is under stable conditions with no bulk removal of the liquid. Hence, in terms of the stability of the liquid column in each riser limb, the upper limb is independent of the lower limb.

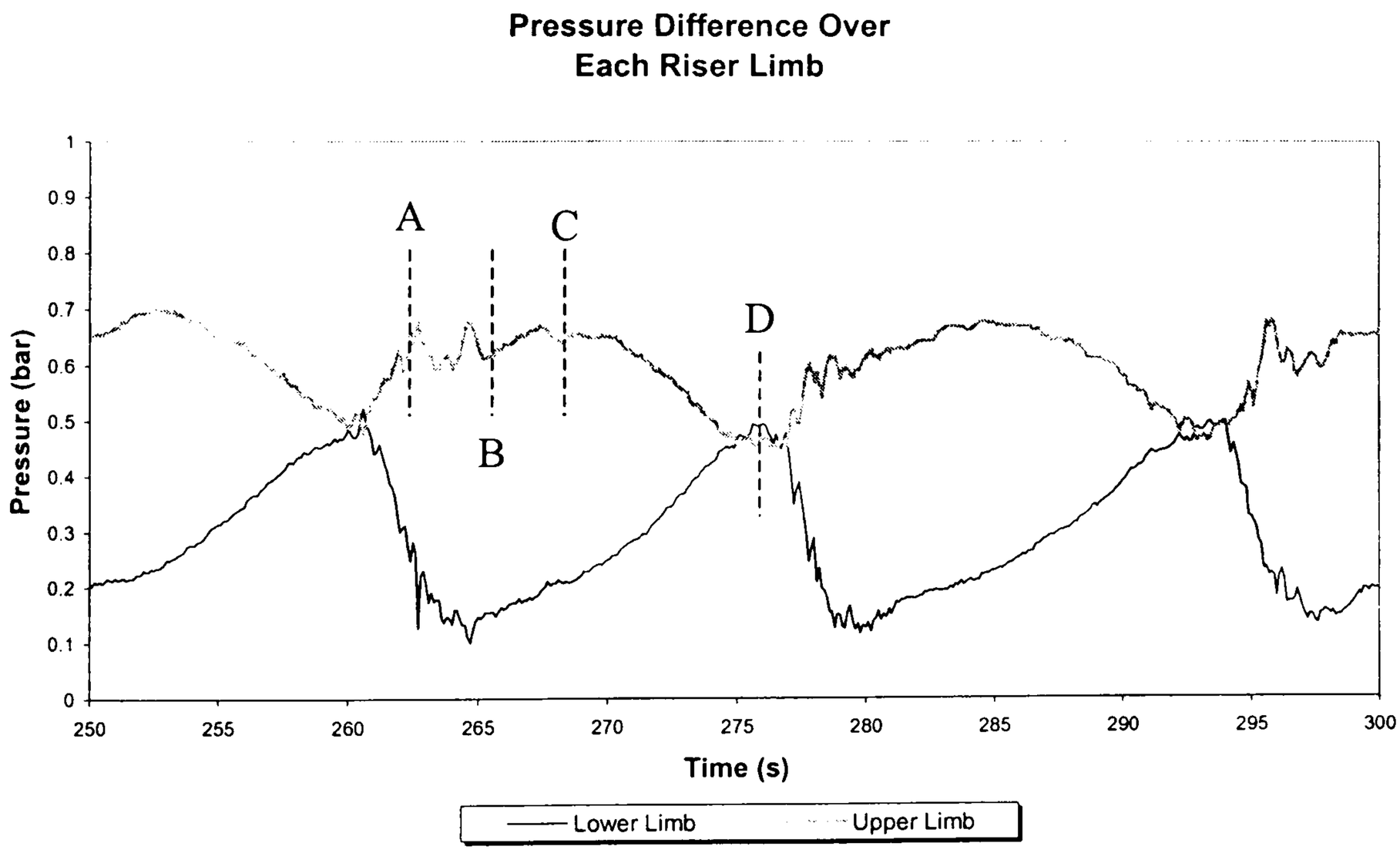

Figure 4.38 – Pressure Difference Over Each Upward Riser Limb
$U_G{}^S = 0.248$ m/s, $U_L{}^S = 0.431$ m/s

The reason for this behaviour is due to the interaction between the upper and lower riser limbs and trapped gas in the downcomer. At the start of an oscillation cycle, the lower limb is at the minimum liquid content, the upper limb is being penetrated by gas bubbles and in the downcomer, there is a significant quantity of liquid, Figure 4.38 Point A and Figure 4.39 (a). As the cycle continues, the liquid level starts to increase in the lower limb, compressing the gas trapped in the S-bend and moving the liquid from the downcomer into the upper limb. Furthermore, the gas bubbles present at the start of the cycle migrate out of the riser. These two processes cause the overall liquid content in the upper limb, thereby increasing the pressure difference in the upper limb to the maximum value, Figure 4.38 Point B, Figure 4.39 (b).

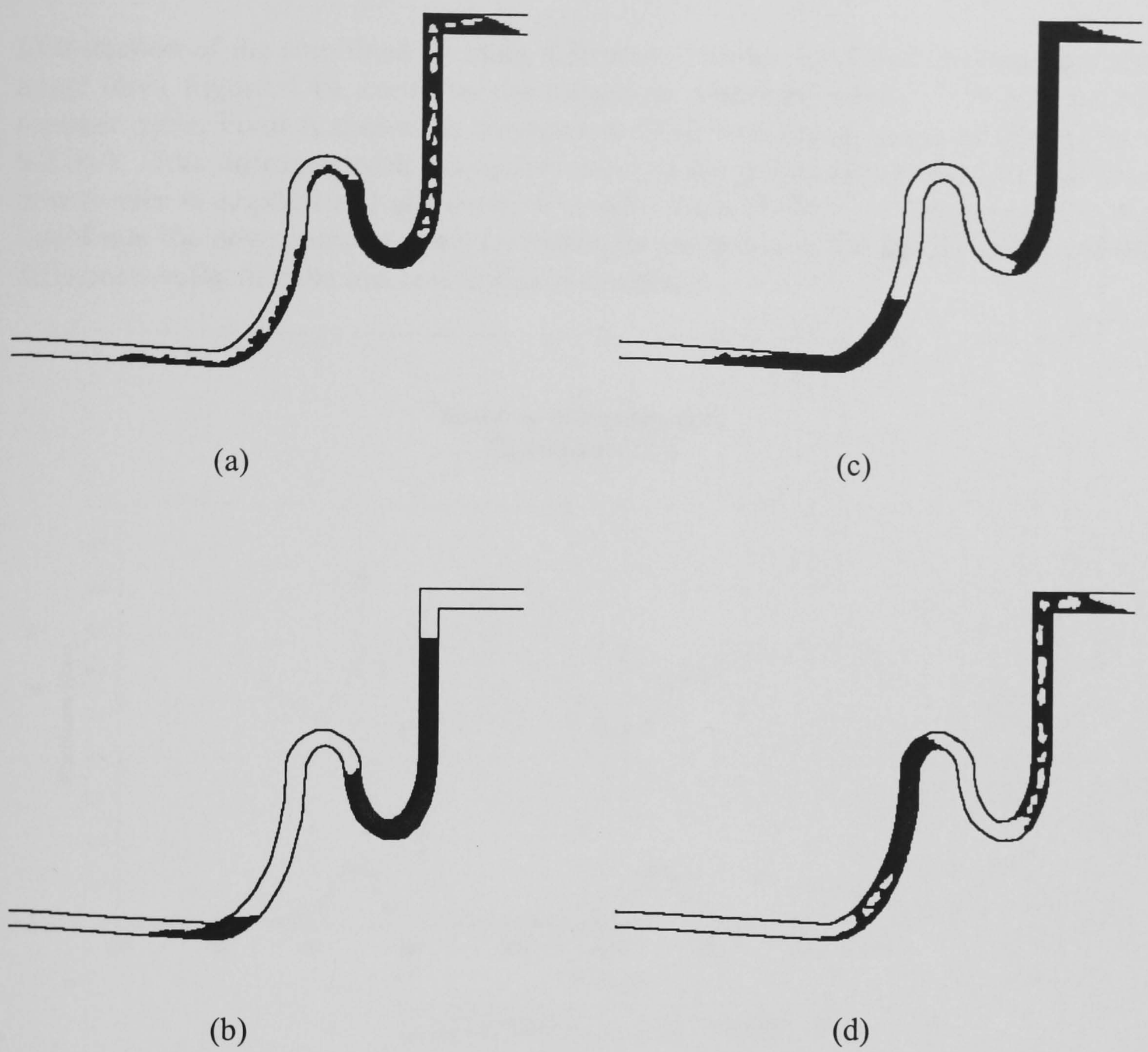

Figure 4.39 – Liquid Distribution in the Riser
During Oscillation Flow

As the liquid continues to accumulate in the lower limb, all the liquid is moved from the downcomer into the upper limb and bubbles begin to penetrate the upper limb. This reduces the liquid inventory in the upper limb as the liquid is displaced from the riser and the gas bubbles expand. The liquid buildup in the lower limb and bubble penetration of the upper limb continue until the lower limb is filled with liquid. At this point a large proportion of the trapped gas has moved from the S-bend into the upper limb and the upper limb inventory is at a minimum, Point C Figure 4.38 and Figure 4.39(c). Immediately afterwards, the lower limb of the riser is blown out, Point D Figure 4.38, Figure 4.39(c), shunting the liquid from the lower limb into the S-bend and into the upper limb of the riser. Gas trapped between the liquid in the upper limb and the lower limb is also moved into the upper riser limb. This combined movement of fluids into the S-bend and upper limb causes an increase in upper limb liquid content and hence pressure difference and also causes the formation of bubbles

in the upper limb, confirmed by the lower-than-maximum pressure difference value. The movement of fluids into the upper riser limb ends the oscillation cycle.

Examination of the combined pressure difference profiles for the downcomer and the upper limb, Figure 4.40, confirms the behaviour described above. The start of the pressure cycle, Point A shows the downcomer filled with liquid (pressure difference ~ 0.2 bar). This decreases with the compression of the gas in the downcomer until the downcomer is emptied and gas enters the upper limb, Point C. The shunting of the liquid into the downcomer gives a corresponding increase in the downcomer pressure difference, reflecting the increase in liquid inventory.

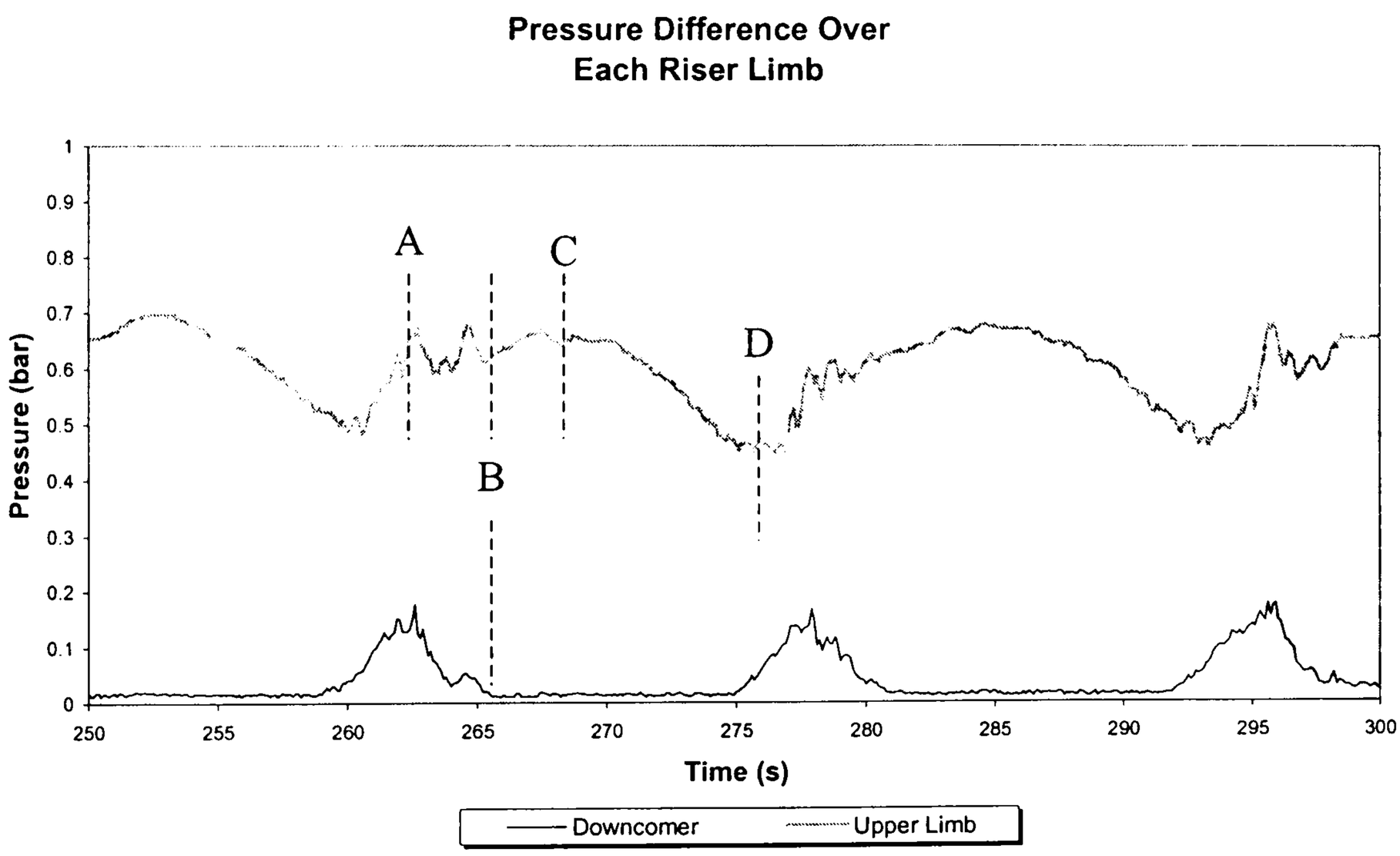

Figure 4.40 – Pressure Difference Over Downcomer and Upper Riser Limb, $U_G^S = 0.248$ m/s, $U_L^S = 0.431$ m/s

As shown above, the pressure difference during oscillation flow varies between a narrow range of values, to the upper limit of the allowable pressure difference range. The probability density function characteristic of the pressure difference signal, Figure 4.41, reflects this behaviour, with higher pdf values over a narrow band of X-values that correspond to the pressure differences experienced during experiments. The deviation of the pdf value reaches a peak 0.03074 from an average 0.01136, indicating a more probable pressure difference during oscillation. Examining the value of pressure difference corresponding to this highest pdf value during oscillation flow, 0.935 bar, the pdf value indicates that there is a propensity towards a higher pressure difference during oscillation flow. This behaviour is similar to the severe slugging 2 case presented previously, though the pressure difference corresponding to the maximum pdf value was greater.

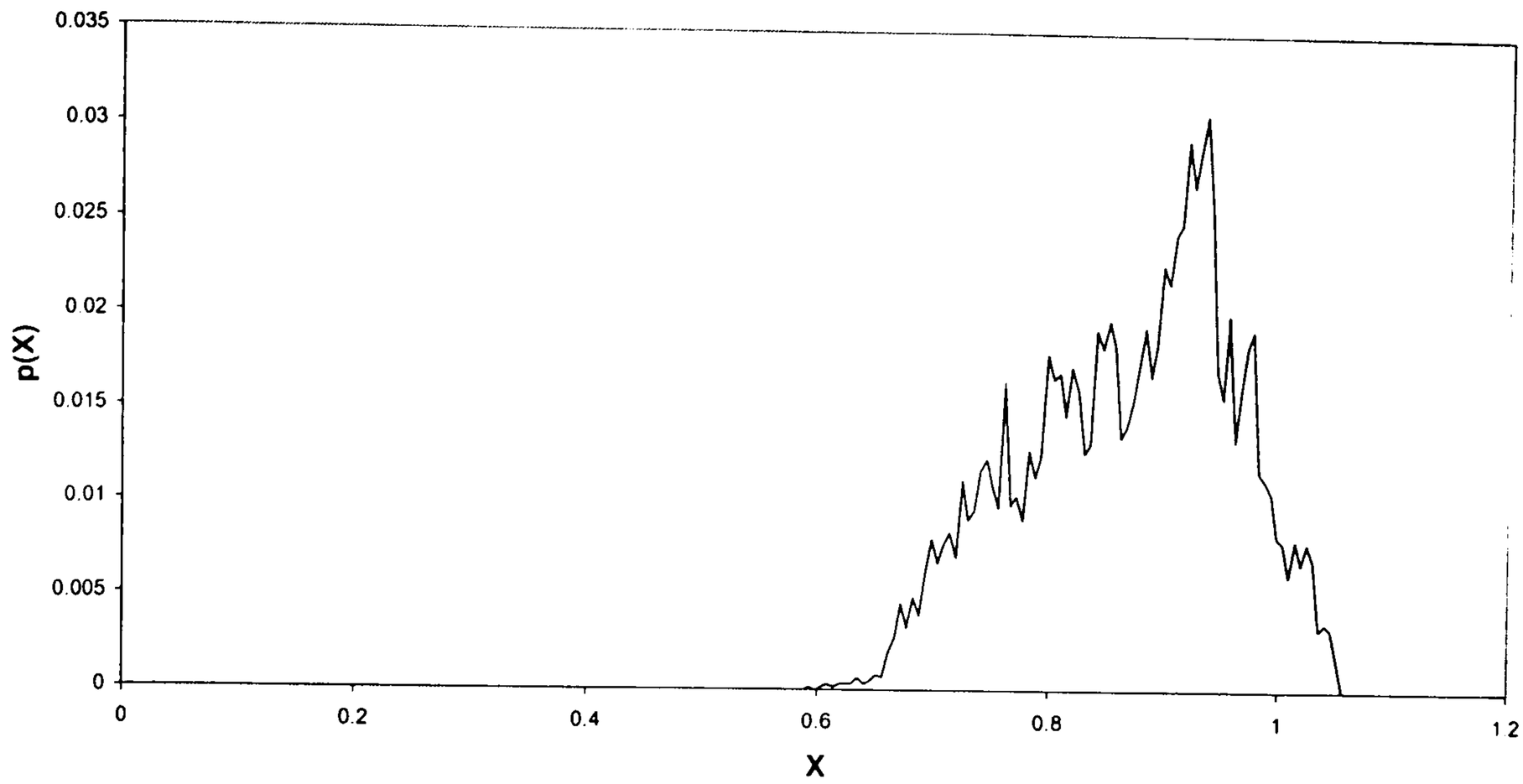

Figure 4.41 – Probability Density Function of Pressure Difference Over Riser During Oscillation Flow, $U_G^S = 0.248$ m/s, $U_L^S = 0.431$ m/s

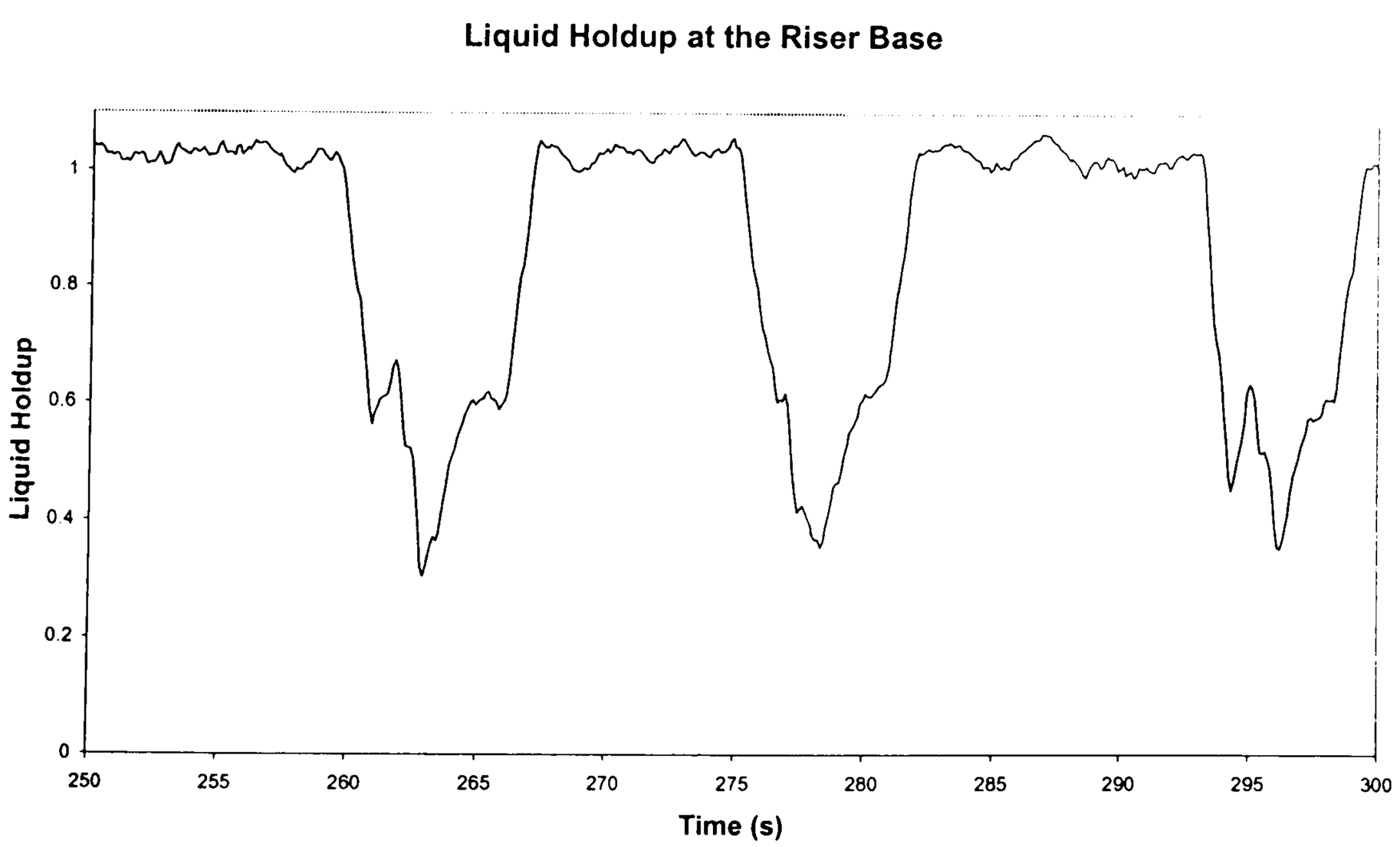

Figure 4.42 - Liquid Holdup Local to Riser Base During Oscillation Flow, $U_G^S = 0.248$ m/s, $U_L^S = 0.431$ m/s

Liquid Holdup Characteristics

The liquid holdup local to the riser base during oscillation flow is qualitatively similar to the case of severe slugging 1, in that there is a distinct period of no bubble penetration at the riser base, followed by a period where the liquid is swept out of the base region and into the riser proper. In the case of severe slugging 1, this corresponds to the overall pressure cycling behaviour, for oscillation flow, this corresponds to the emptying and filling of the lower limb of the riser.

Comparison of Figures 4.42 and 4.38 confirms this. Point A at the start of the cycle corresponds to the beginning of the period of liquid accumulation in the lower limb, from this time until Point D there is pure liquid at the riser base. At Point D the sweep-out of liquid from the lower limb begins, this is caused by the penetration of gas from the pipeline into the riser base and hence there is a non-unity liquid holdup local to the riser base after this time.

Fluid Production Characteristics

The production of fluids during oscillation flows is complex and dominated by the emptying and filling process in each riser limb during the cycle. During oscillation flow, there are two periods of liquid production in each oscillation cycle. Gas production takes place almost continuously during the cycle, though there are peaks in gas production that coincide with the bulk removal of gas from the pipeline/riser.

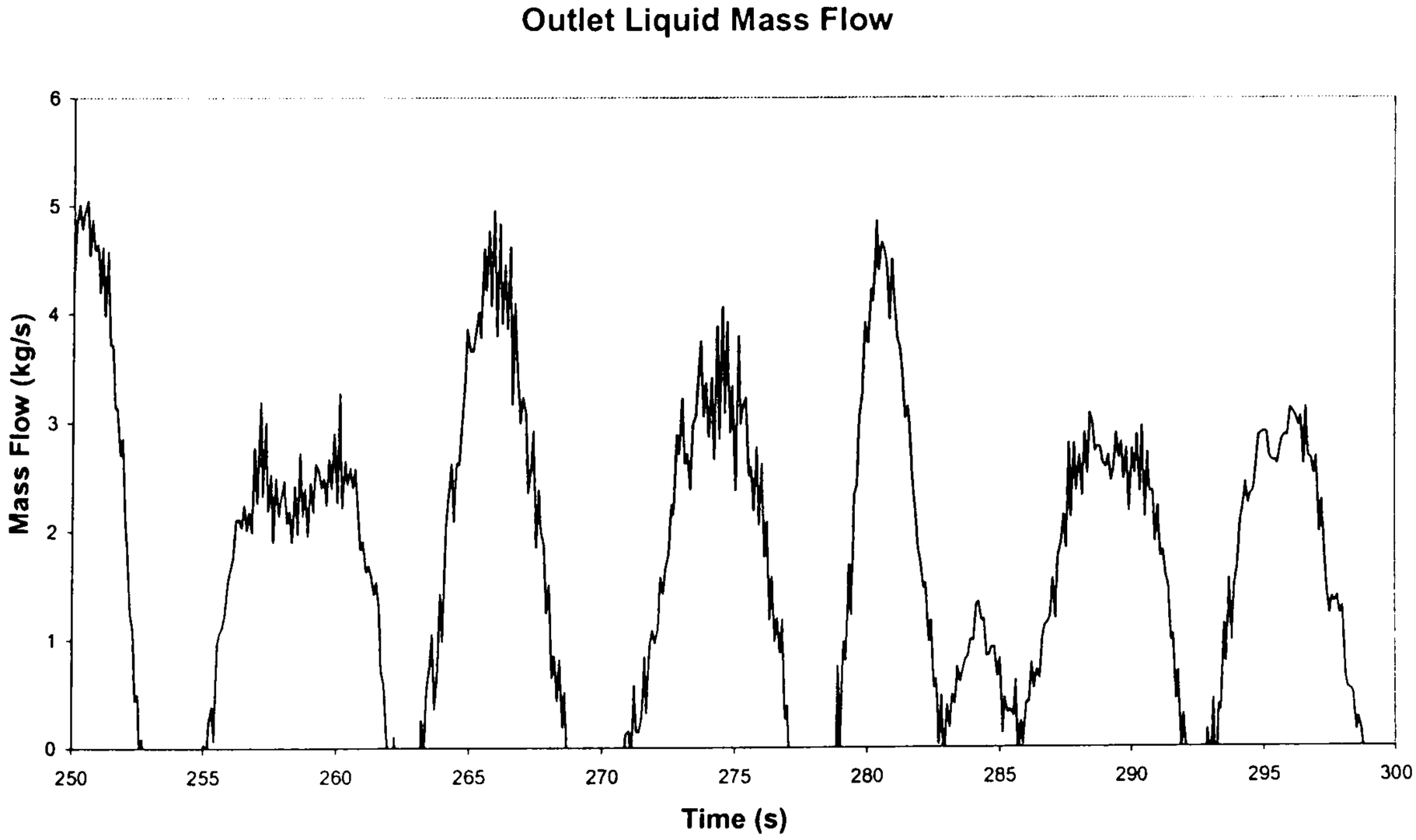

Figure 4.43– Liquid Production During Oscillation Flow,
$U_G^S = 0.267$ m/s, $U_L^S = 0.683$ m/s

An example of the liquid production during oscillation flow is shown in Figure 4.43, this shows the cyclical production being made up of two peaks, one of longer duration and the other of higher maximum flow. Combining the liquid production with the pressure difference profile in each limb of the riser, Figure 4.44(a) and (b), the relation of these two parts (Part I and Part II) to the oscillation cycle can be observed.

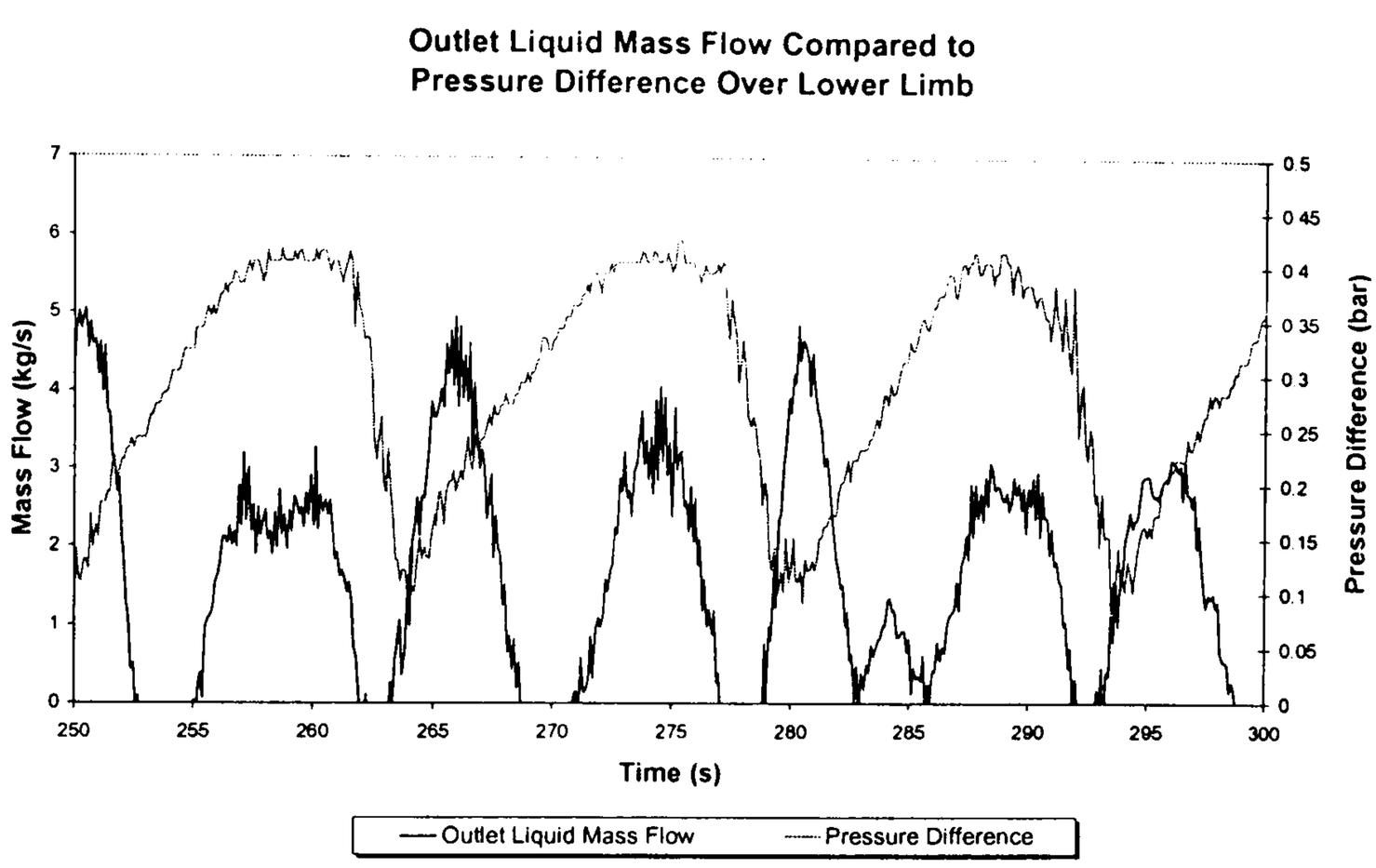

(a) Liquid Production and Pressure Difference Over Lower Limb

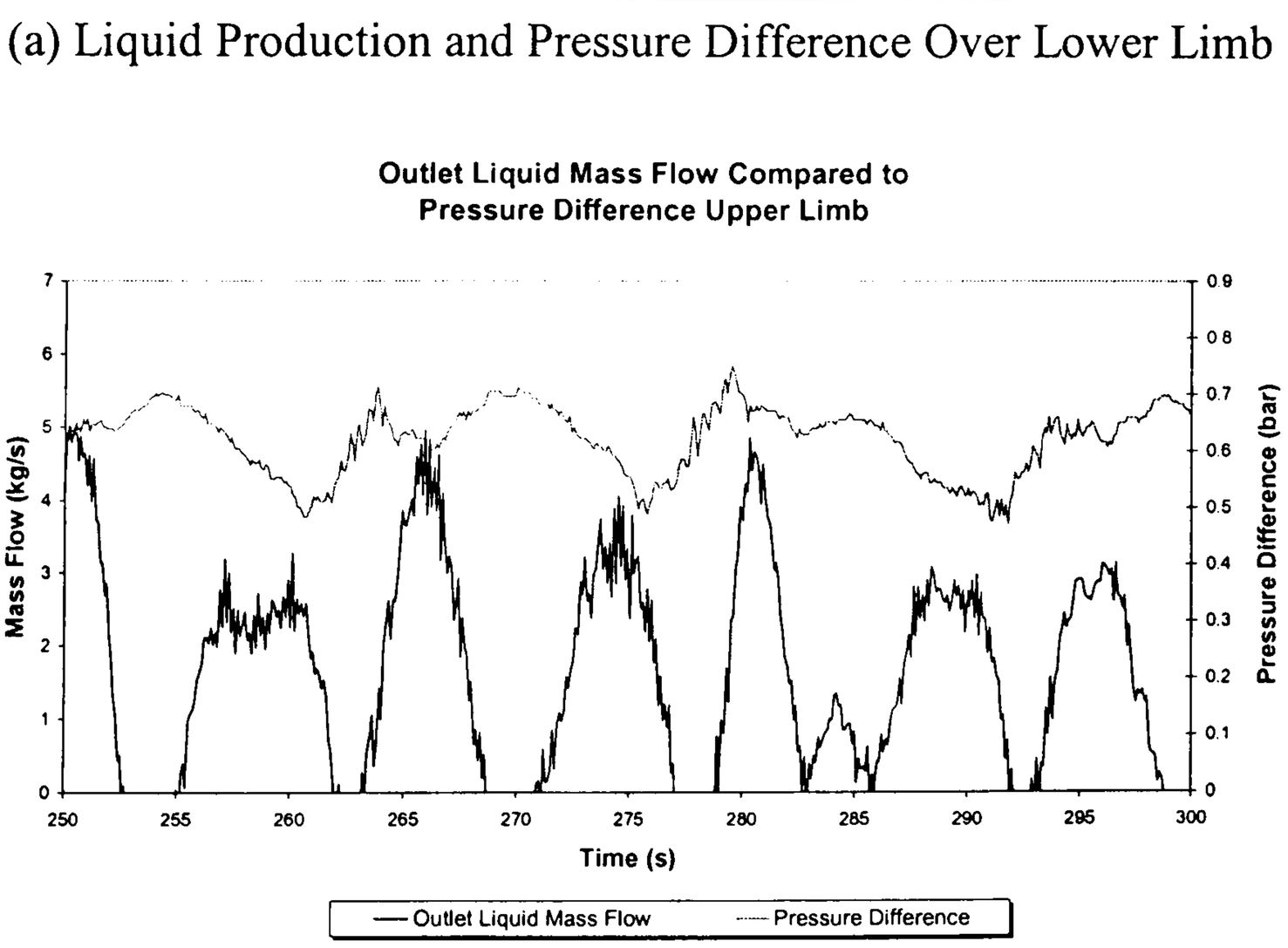

(b) Liquid Production and Pressure Difference Over Upper Limb

Figure 4.44 – Liquid Production and Pressure Cycling
During Oscillation Flow, $U_G^S = 0.267$ m/s, $U_L^S = 0.683$ m/s

The first part of the liquid production cycle (Part I) occurs during the early stages of the oscillation cycle. This surge is associated with the sweep-out of liquid from the lower limb of the riser, Figure 4.44(a). As the liquid is swept out of the lower limb

from the previous cycle, it moves into the downcomer and then the upper limb. Upon arrival it displaces a similar amount of liquid, giving a surge of liquid from the riser outlet. The second element (Part II) of the liquid production cycle is associated with the penetration of the upper limb of the riser by the gas in the downcomer, Figure 4.44 (b). As liquid accumulates in the lower limb, the gas pressure increases in the downcomer and has the net effect of moving the liquid in the downcomer into the upper limb. The gas-liquid interface in the downcomer then moves towards the bottom of the S-bend until the upper limb is filled with liquid and is at the maximum pressure difference. At this point bubble penetration from the gas trapped in the downcomer begins. The bubbles expand as they progress out of the riser, reducing the volume of liquid contained within the upper limb and give the second part of the liquid production.

When examining the effect of oscillation on the fluid production from a flexible riser, the total size of the liquid surge, including both parts, is calculated. Figure 4.45 shows the variation in oscillation surge size. Due to lack of data for the 2 bar(a) test condition, the presented data is for the 4 bar(a) tests.

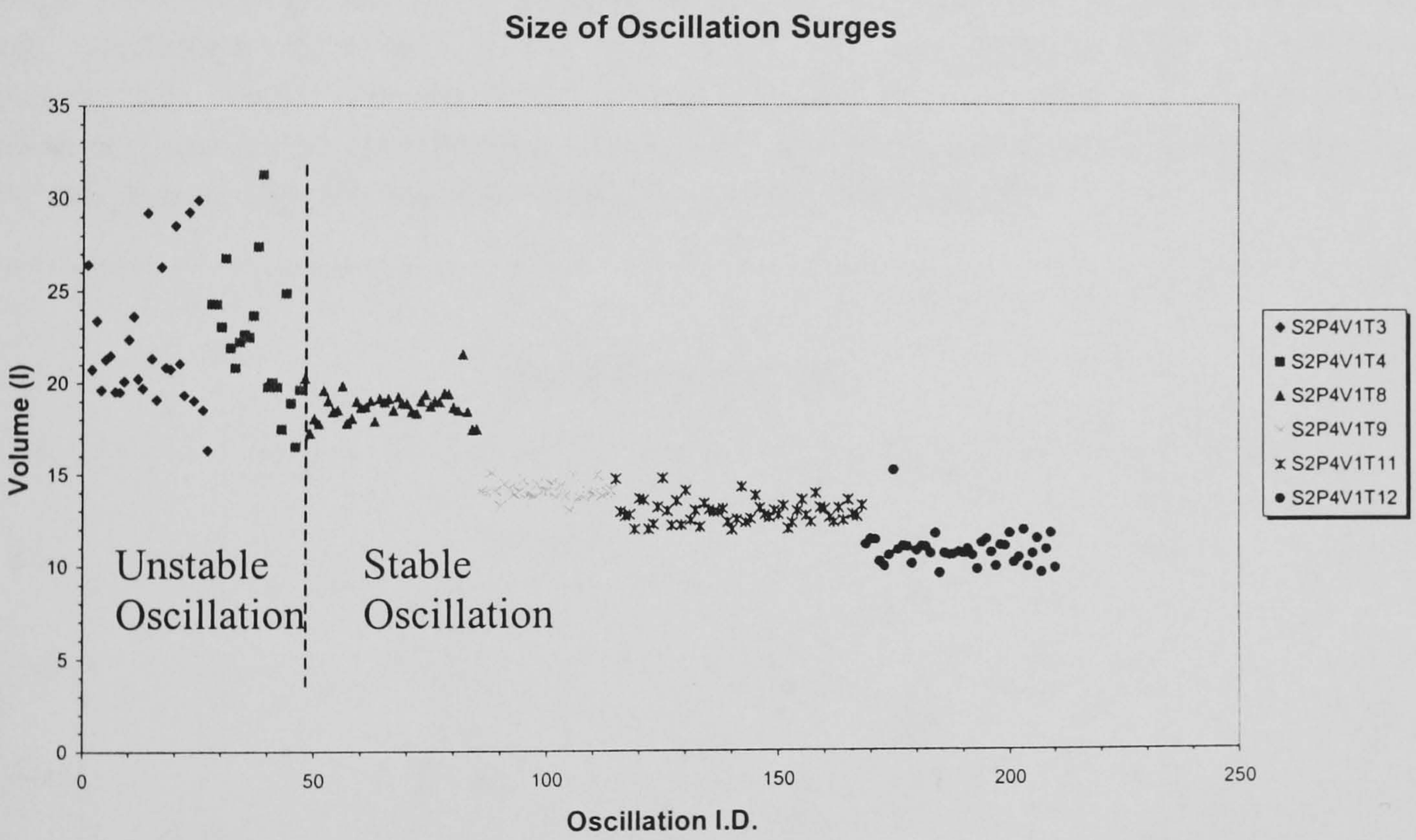

Figure 4.45 – Liquid Surge Size
During Oscillation Flow, 4 bar(a)

From the data presented, there are two distinct types of oscillation surge sizes, synonymous with two types of oscillation flow – unstable oscillations and stable oscillations. Unstable oscillations are characterised by a large distribution of oscillation surge sizes, of comparable size to severe slugging 3 slug sizes. In the cases presented, the first group of oscillations highlighted are unstable oscillation, whose average surge is 22.2 l with a standard deviation of 3.1 l, 16% of the average for all

unstable oscillations. This means that 99% of unstable oscillations as experienced lie between 31.49 l and 12.97 l, some 82% and 33% of the riser volume. The second group, stable oscillation flows, show a markedly narrower spread of surge sizes, with standard deviations in surge sizes between 0.45 l and 0.9 l. This value is less than one third that of the unstable flow cases. The average surge size during stable oscillations varies substantially from test to test, in the cases presented, the variation is from 18 l to 10 l, 48% and 10.7% of the riser volume. Comparing these values to the size of production transients during transitional severe slugging, it is clear that oscillation surge sizes are comparable to those experienced during severe slugging. In this respect, oscillation flows may have liquid surges that are as problematic as severe slugging flows due to their size.

In terms of peak liquid production, the deviation of the peak liquid delivery during oscillation flow is much less than during severe slugging and many transition severe slugging flows. For the two types of oscillation flow, the average peak flows are 1.99 l/s and 2.44 l/s for unstable and stable oscillation flows respectively. The variation in the peak flows is of a similar scale for each type of oscillation, approximately 0.16 l/s and 0.28 l/s, 8% and 11% of the peak flow values, both of which are less than the variation in the peak flow for severe slugging flows. Comparing these values to the average flow through the riser oscillation flows, the peak flow during unstable and stable oscillation flow are 174% and 302% of the average flow respectively. Gathering this result with the others, it may be said that in terms of flow deviations, oscillation flow is less problematic than severe slugging with more regular peaks, of a lower magnitude that deviate less from the average throughput.

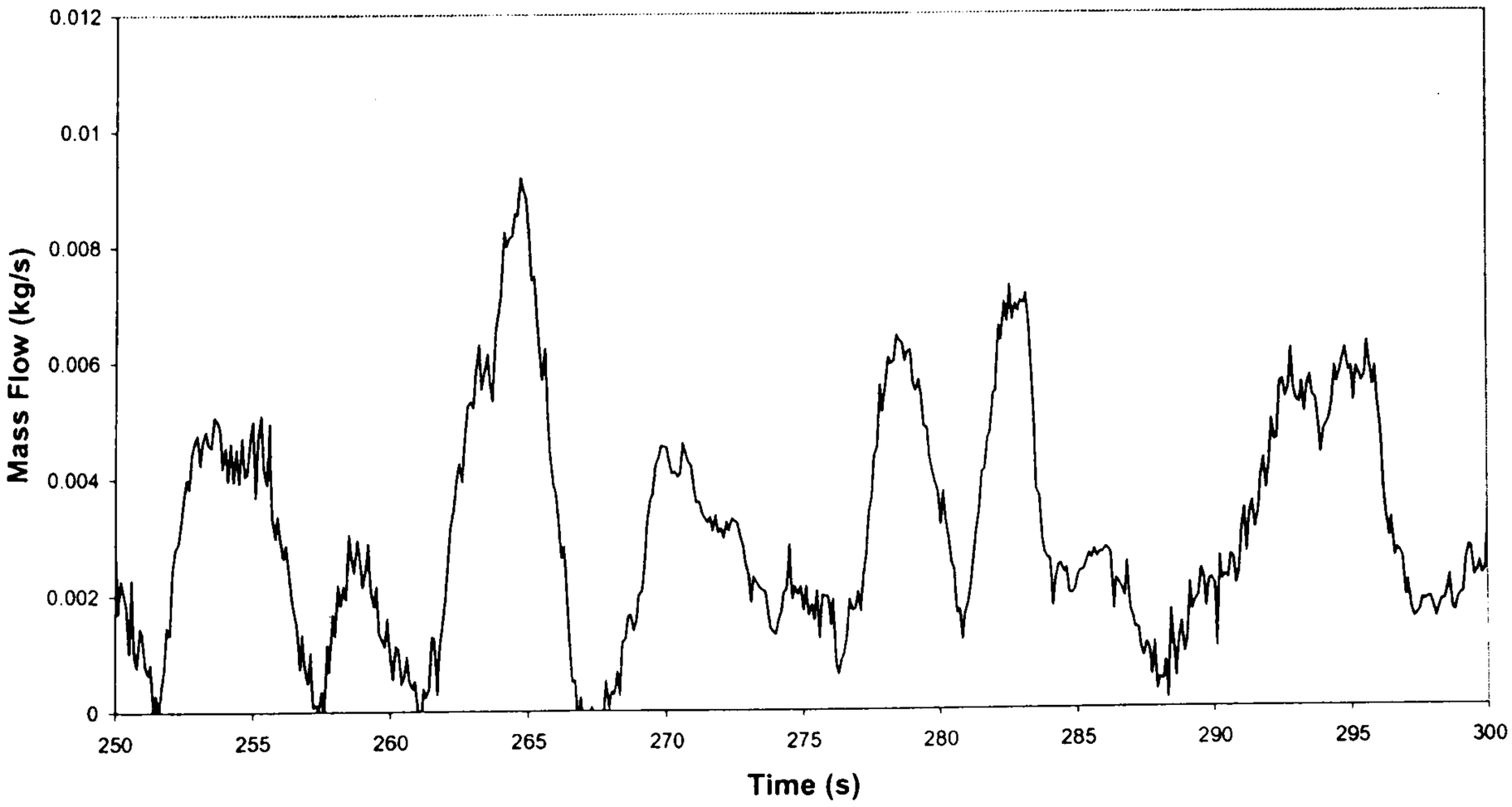

Figure 4.46 – Gas Production During Oscillation Flow,
$U_G{}^S = 0.267$ m/s, $U_L{}^S = 0.683$ m/s

In terms of gas production during oscillation flows, a similar two-peaked delivery cycle is observed as shown in Figure 4.46. As in the case of liquid production, the first peak in gas production occurs towards the beginning of the oscillation cycle, the second peak occurs towards the end of the cycle. As each of these peaks relates again to the pressure cycling in the riser, the combination of the pressure cycling and gas production as used previously is presented in Figures 4.47 (a) and (b).

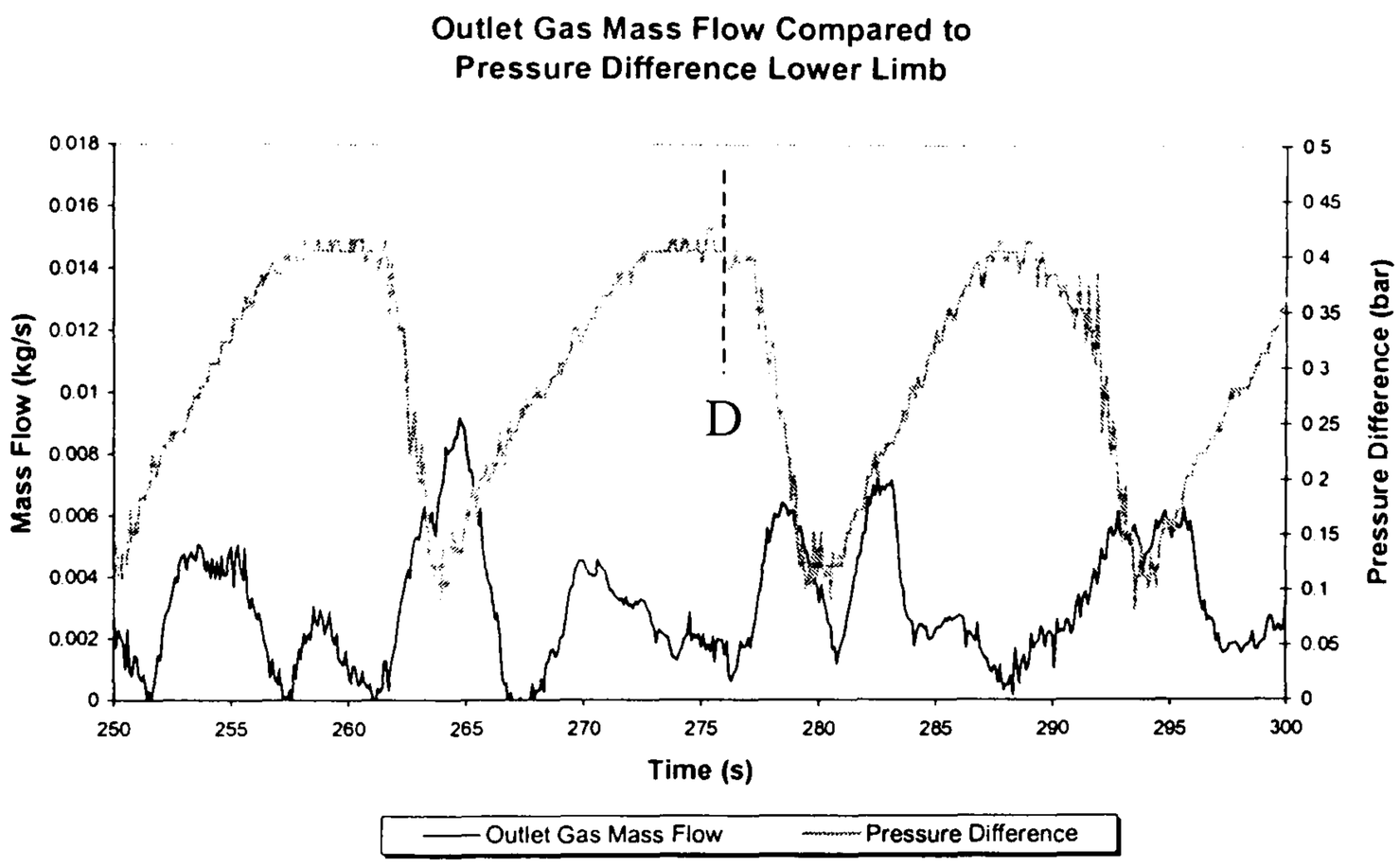

(a) Gas Production and Pressure Difference Over Lower Limb

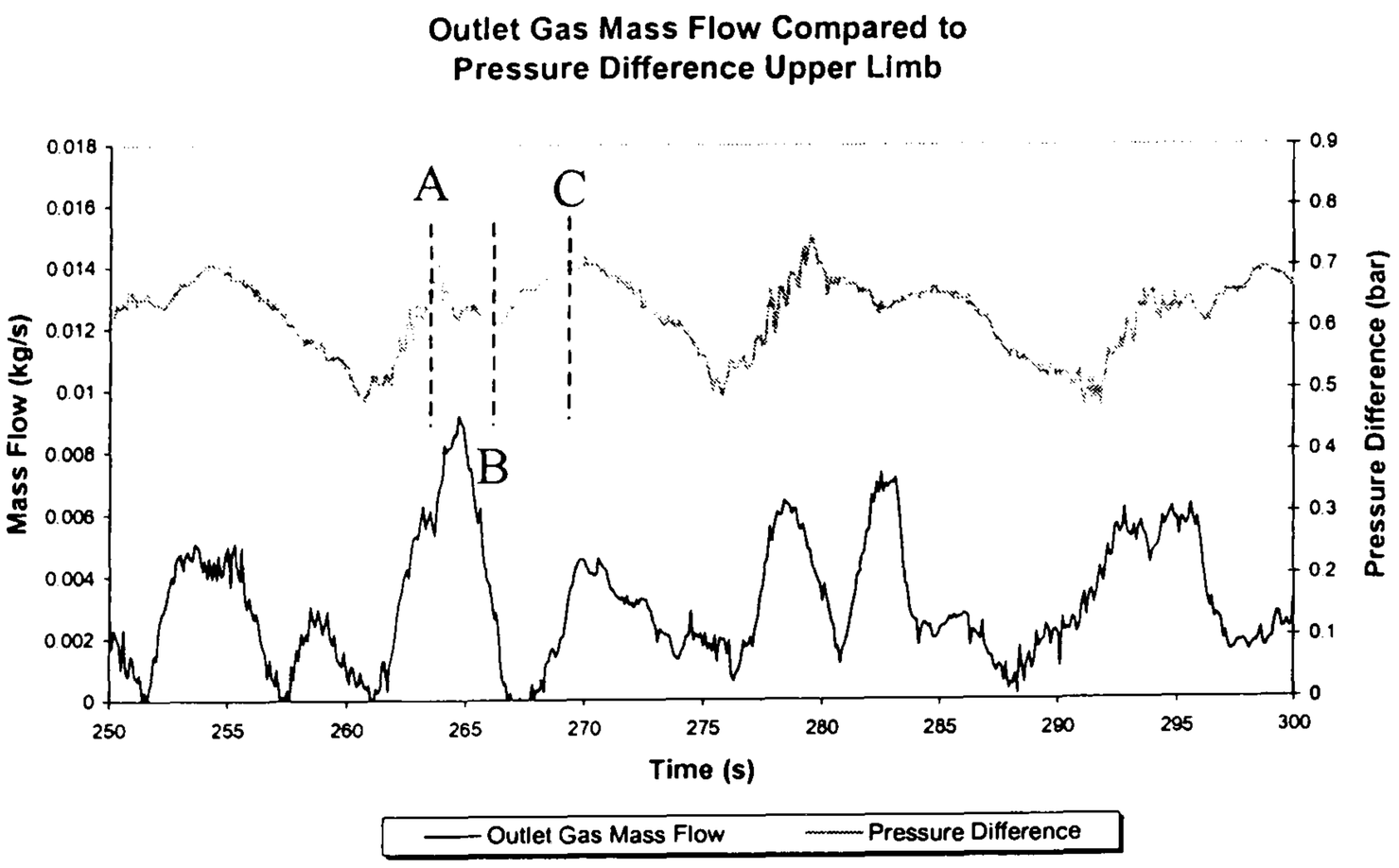

(b) Gas Production and Pressure Difference Over Upper Limb

Figure 4.47 – Gas Production and Pressure Cycling
During Oscillation Flow, $U_G^S = 0.267$ m/s, $U_L^S = 0.683$ m/s

This shows how the first gas production peak occurs during the initial buildup in the lower limb. The first gas production peak is due to the gas bubbles moving through the upper limb of the riser, arriving in the separator. These bubbles were moved into the upper limb during the blowout of the lower limb of the riser during the previous cycle. As these bubbles move out of the limb, this production surge falls off, Point B.

The second surge in gas production begins when the upper limb of the riser begins to be penetrated by gas from the downcomer, Point C. As described above, once the bubbles present at the start of the cycle move out of the riser, the liquid head increases until the liquid accumulation of the liquid in the lower limb forces gas trapped in the downcomer into the upper limb. This gas progresses through the upper limb and gives the second production peak, occurring at Point D.

4.4 Stable Flow Characteristics

Though stable flows are not part of the main focus of this work, their identification is important for the prediction of the flow regime behaviour in the pipeline/riser. There are predominantly two types of stable flow experienced in the system – slug flow and bubble flow. The characteristics of each of these are presented below.

4.4.1 Slug Flow Characteristics

Slug flow is a well-recognised flow regime consisting of a bubbly mass of liquid interspersed by a long bubble/film region. In the pipeline/riser, slug flow is characterised by two means, the first is the pressure difference over the riser and the second is the liquid holdup local to the riser base.

Pressure Cycling Characteristics

During slug flow, the liquid inventory in the riser fluctuates constantly as each slug enters and leaves the system. The frequency of the pressure difference fluctuation is dependent on the frequency at which slugs enter/leave the riser and the magnitude of the fluctuation is dependent on the size of the slugs. A typical example of the pressure difference during slug flow is given in Figure 4.48. This pressure difference profile is characteristic of slug flow, fluctuating rapidly with an overall pressure difference change of approximately 0.6 bar. Given that the riser is not incompletely filled with liquid, the maximum pressure difference during slug flow will be less than that experienced during severe slugging 1.

The probability density function of the pressure difference fluctuations in Figure 4.49 shows the characteristic profile for slug flows. As can be seen, the distribution for the pdf is centred around a value of approximately 0.75, with a skewed tail off to the maximum and minimum values of pressure difference. Compared with the unstable flows presented thus far, the tail-off of the pdf is more even, i.e. lacking discontinuities, reflecting a more even spread of data.

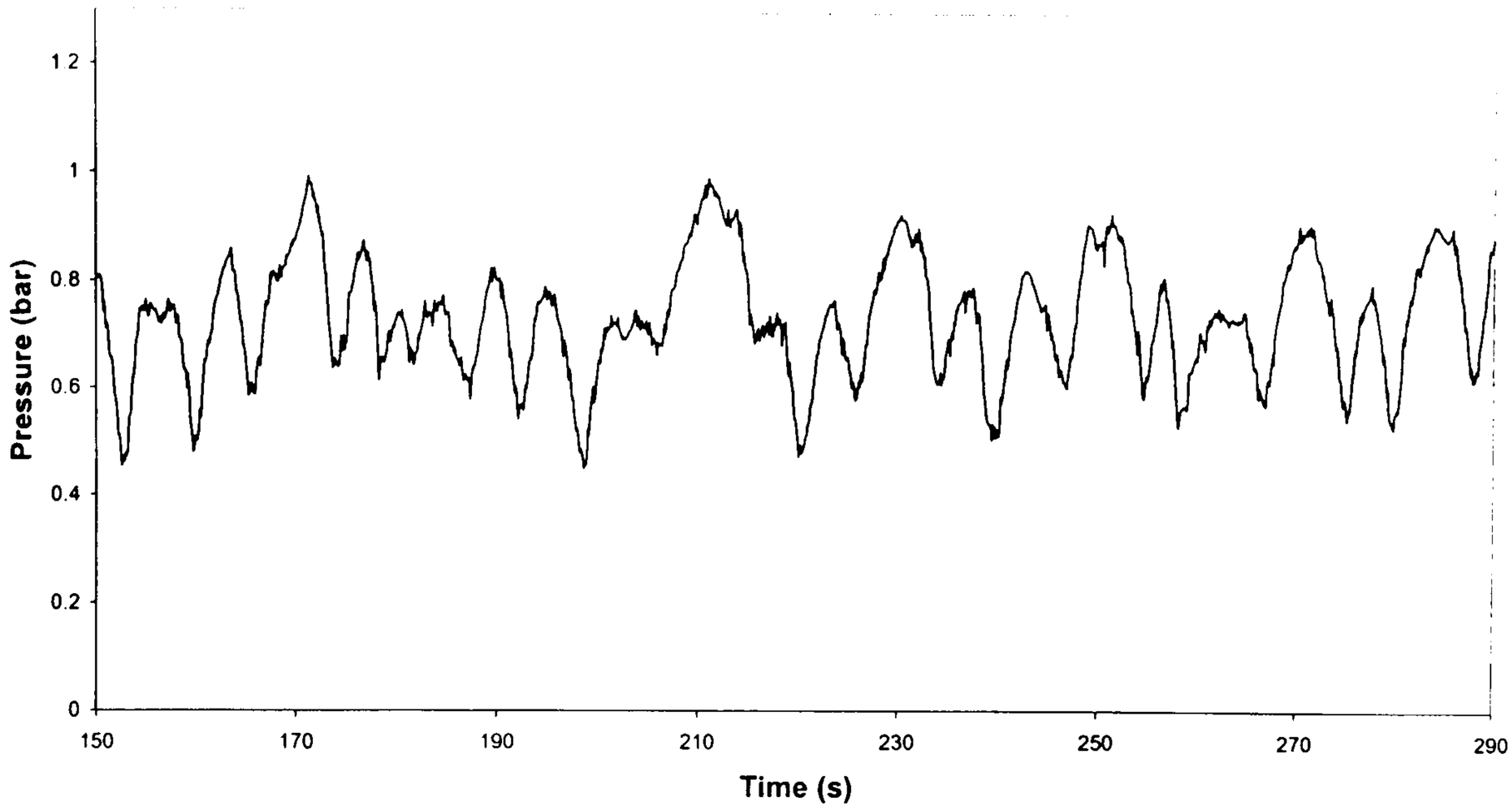

Figure 4.48 – Pressure Difference Over Riser During Slug Flow, $U_G^S = 0.94$ m/s, $U_L^S = 0.602$ m/s

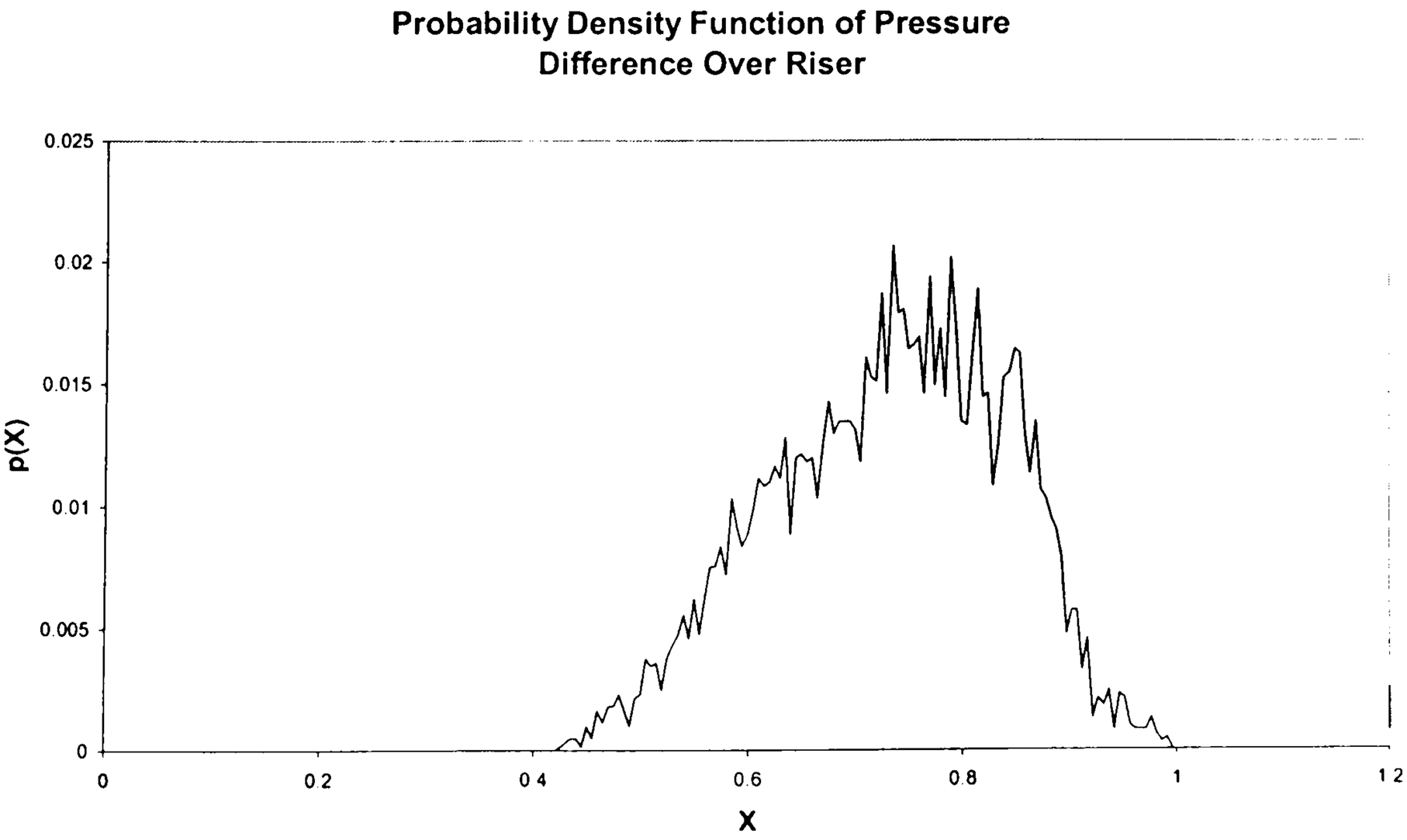

Figure 4.49 – Probability Density Function of Pressure Difference Over Riser During Slug Flow, $U_G^S = 0.94$ m/s, $U_L^S = 0.602$ m/s

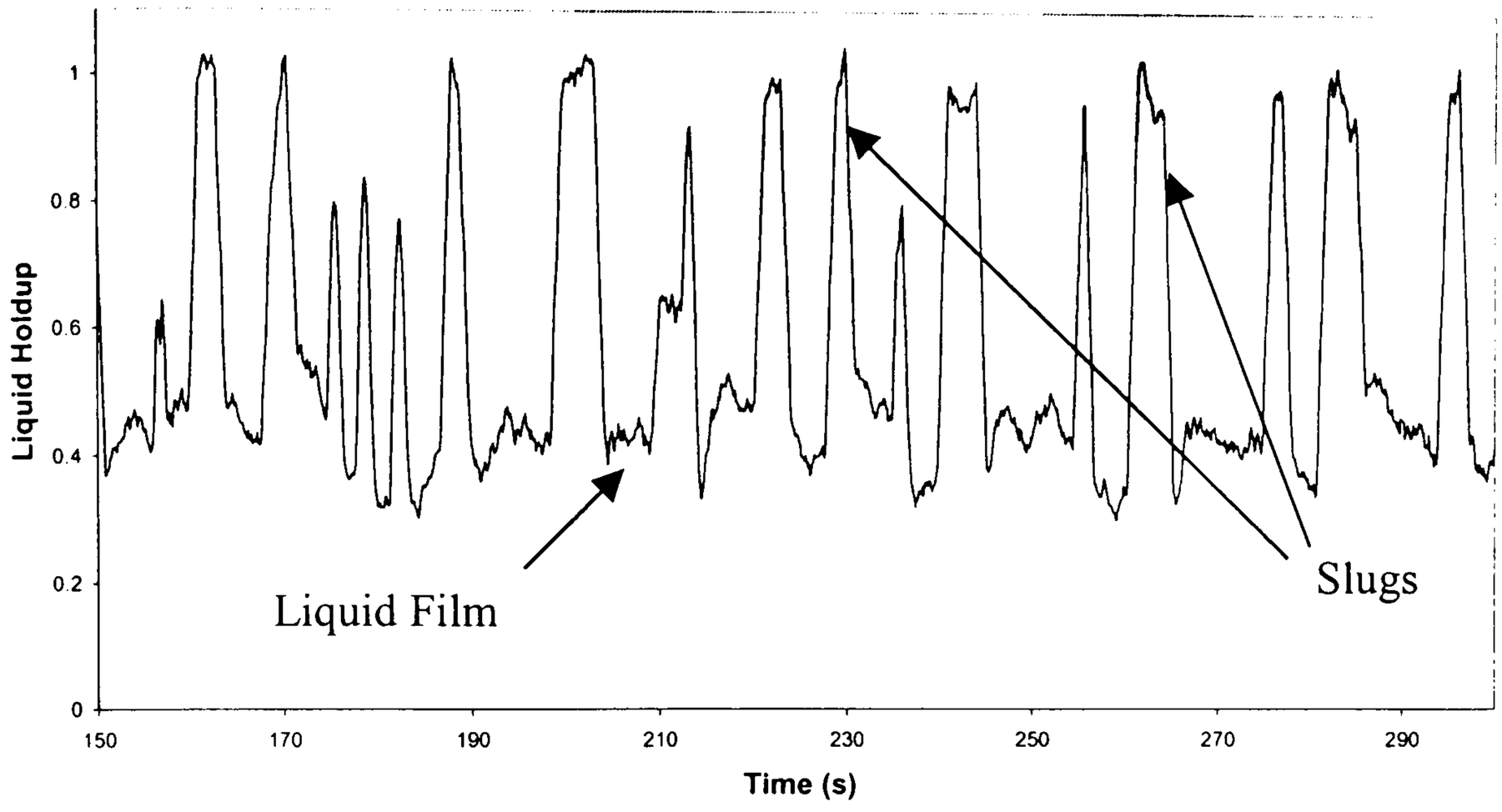

Figure 4.50 – Liquid Holdup Local to the Riser Base During Slug Flow, $U_G{}^S = 0.94$ m/s, $U_L{}^S = 0.602$ m/s

Liquid Holdup Characteristics

The liquid holdup local to the riser base gives a very clear indication of the slug flow regime; a sample liquid holdup profile is presented in Figure 4.50 above. This shows the time-wise progression of the bubbly liquid slugs followed by the bubble/film region. As the liquid slugs contain gas, the liquid holdup is less than unity. The liquid holdup in the bubble/film region is much less than the slug holdup, however the exact value is dependent on a number of factors and is beyond the scope of this work.

Fluid Production Characteristics

As slug flow is made up of a bubbly liquid mass and a long bubble/film region, there is continuous delivery of fluids during slug flow. However, there are surges in production of each phase, particularly associated with the arrival of the slug body or the gas bubble. Figure 4.51 illustrates this, with the coupling of the gas and liquid production profiles for slug flow. The peaks in liquid production – the arrival of liquid slug body – are interspersed by similar peaks in the gas production – the arrival of the gas bubble. Close examination of the production profile shows that the peaks in the phase flowrates are not coincident with one another, i.e. a peak in liquid production does not overlap with a peak in gas production. This behaviour is a consequence of the structure of the slugs.

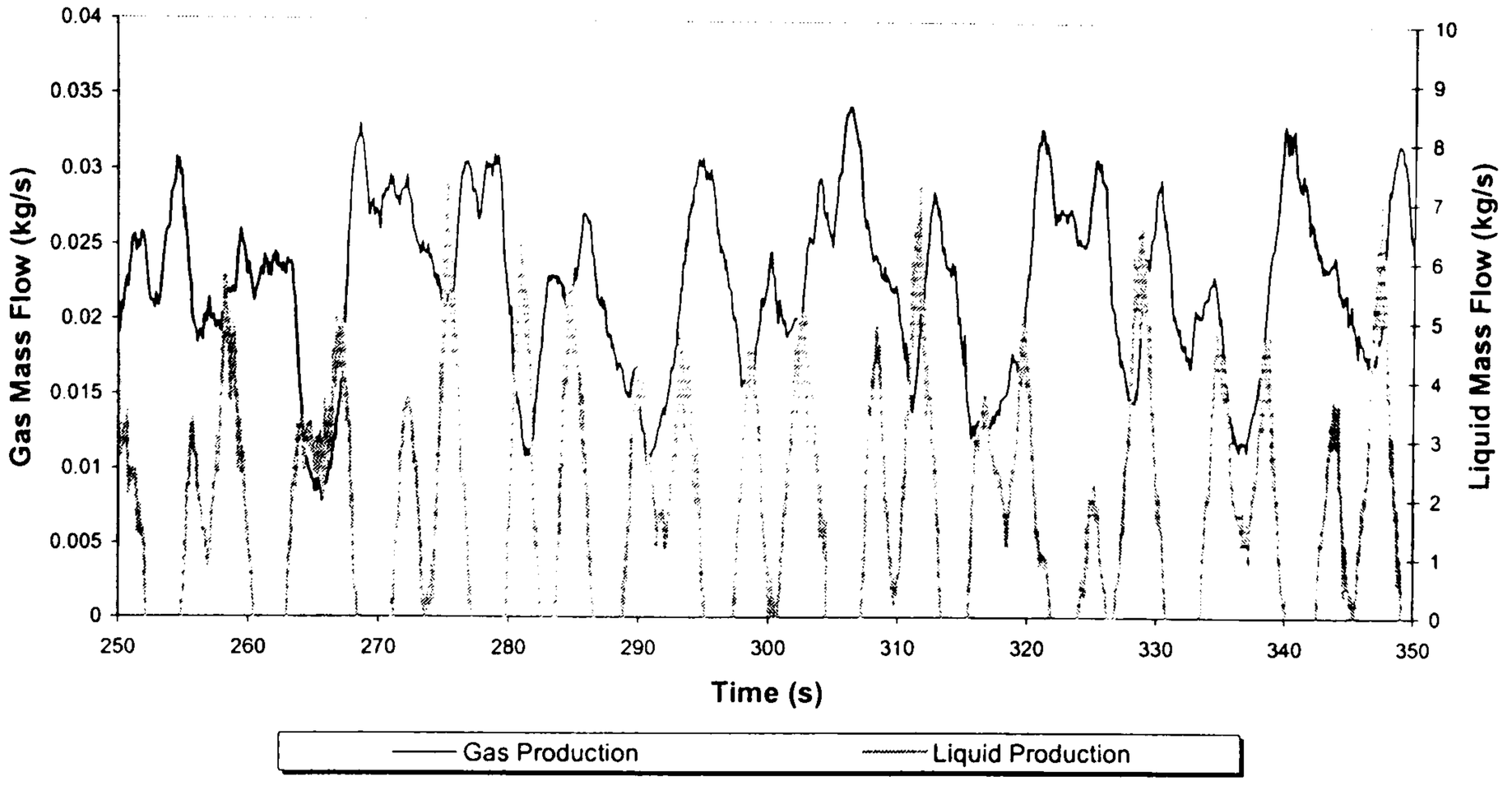

Figure 4.51 – Combined Gas and Liquid Mass Production Characteristics During Slug Flow, $U_G^S = 2.718$ m/s, $U_L^S = 0.608$ m/s

4.4.2 Bubble Flow Characteristics

Bubble flow is again a well-recognised flow regime, with a highly regular behaviour. Conceptually bubble flow is basically a continuous flow of liquid interspersed by regular bubbles propagating through the riser, expanding as they rise.

Pressure Cycling Characteristics

As the gas and liquid flow through the riser is continuous and without large deviations, the pressure difference profile over the riser during bubble flow is highly regular. Figure 4.52 shows a typical example of this. The main point of note in this figure is the high average pressure difference over the riser; indicating a high inventory of liquid in the riser. This agrees with the notional structure of bubble flow – a continuum of liquid with gas bubbles flowing through. It is supposed that the regular oscillations are due to the change in liquid inventory, and hence hydrostatic head, in the riser as bubbles move into and out of the riser. However, detailed measurements of the liquid holdup at the riser outlet would be required to confirm this behaviour.

The relatively high pressure difference over the riser during bubble flow and the low degree of variation in the pressure difference is reflected in the probability density function of the pressure difference, Figure 4.53.

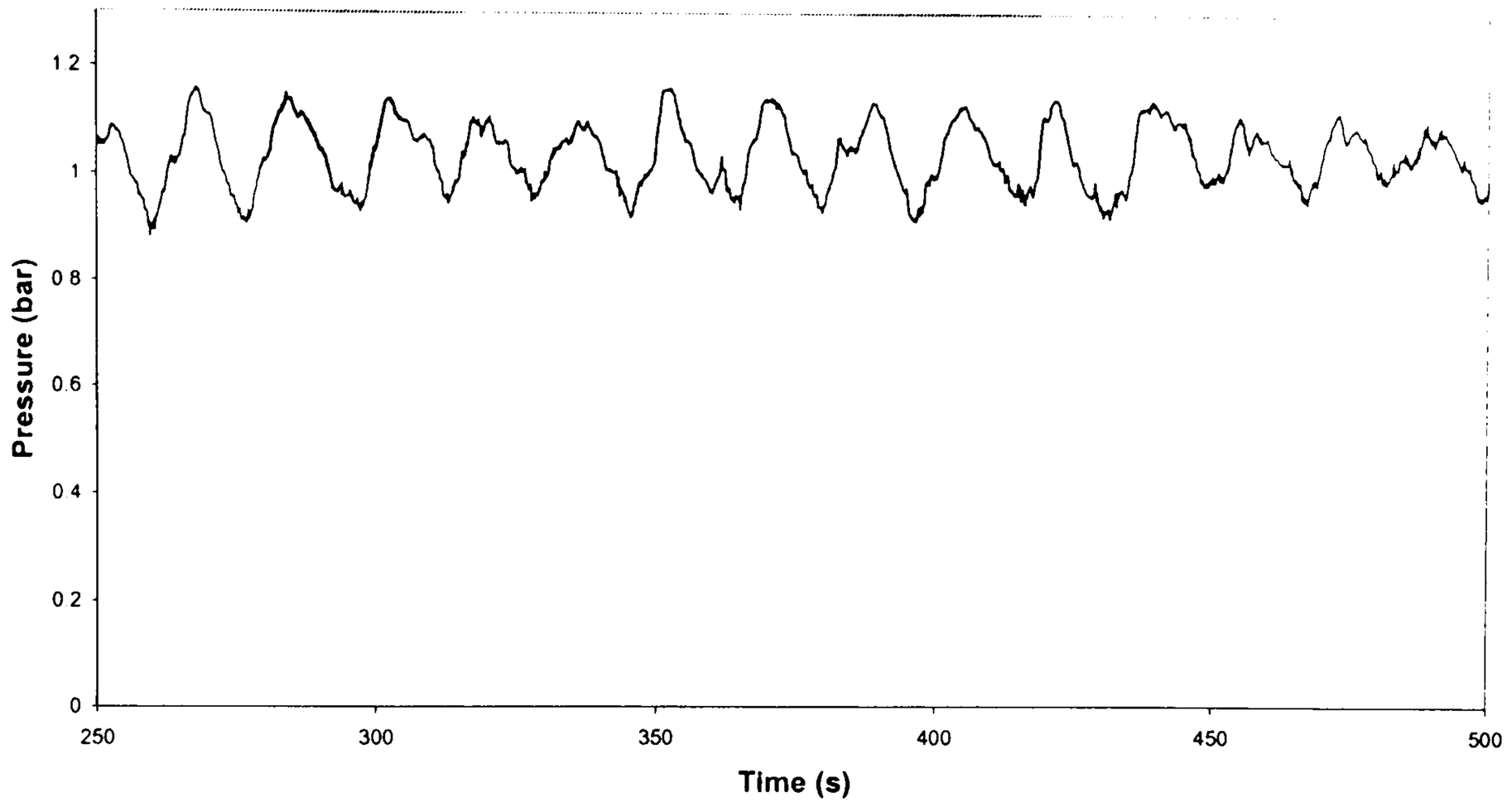

Figure 4.52 – Pressure Difference Over Riser During Bubble Flow, $U_G{}^S = 0.075$ m/s, $U_L{}^S = 0.941$ m/s

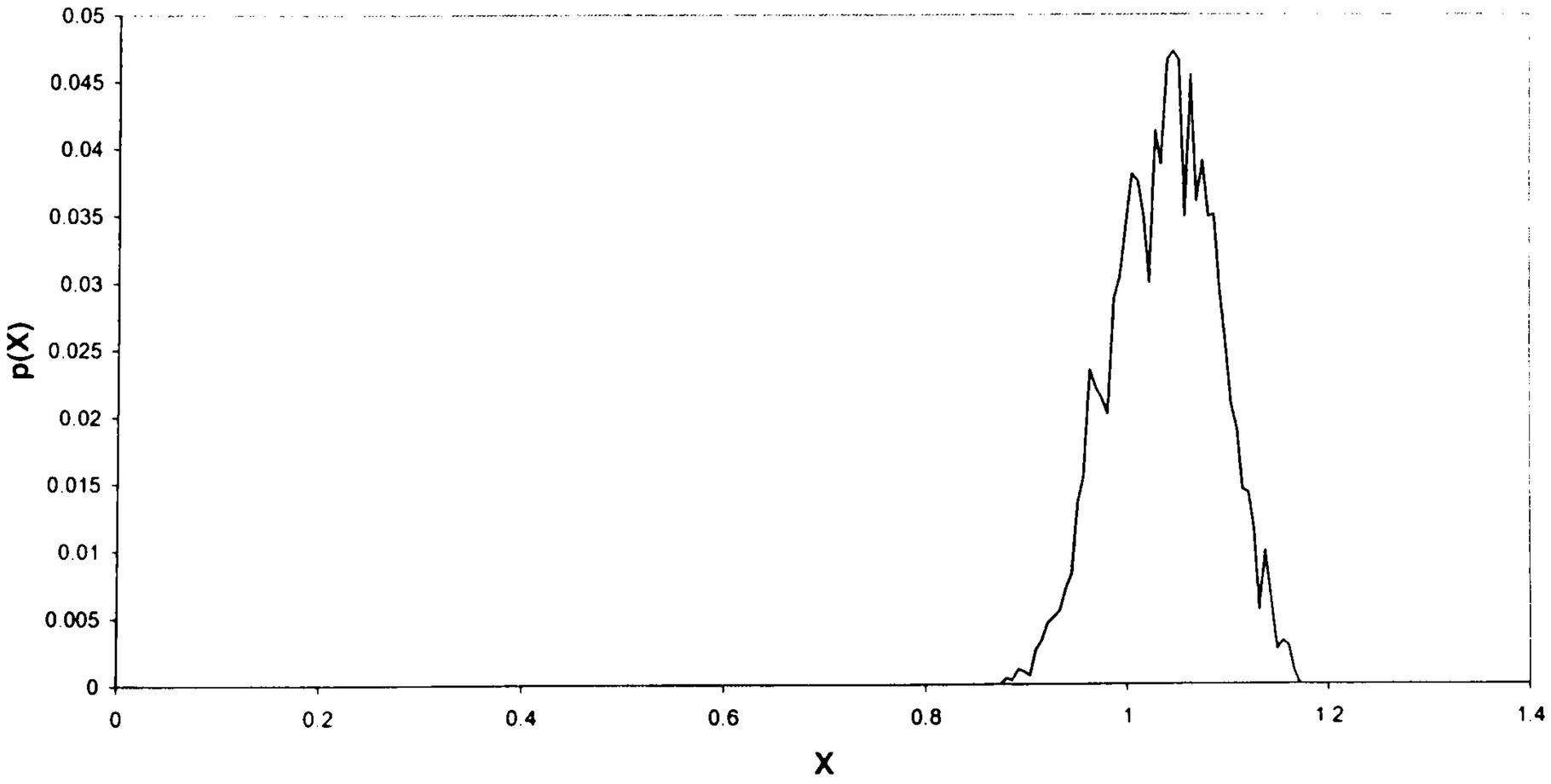

Figure 4.53 – Probability Density Function of Pressure Difference Over Riser During Bubble Flow, $U_G{}^S = 0.075$ m/s, $U_L{}^S = 0.941$ m/s

The low distribution of probabilities shows that there is a narrow spread of pressure difference values during the experiments, significantly less than other flow regimes. Another feature of the probability density function distribution is the peak value of the distribution. This corresponds to the most occurring value of pressure difference in the data. As can be seen from the figure, this peak corresponds to a value of 1.04 bar, greater than the hydrostatic head of a completely liquid-filled riser, this confirms the presence of gas to a significant degree in the downcomer, increasing the maximum potential pressure difference in the riser. Indeed examination of the downcomer data gives an average pressure difference of 0.11 bar, 50% of the maximum pressure difference of 0.22 bar.

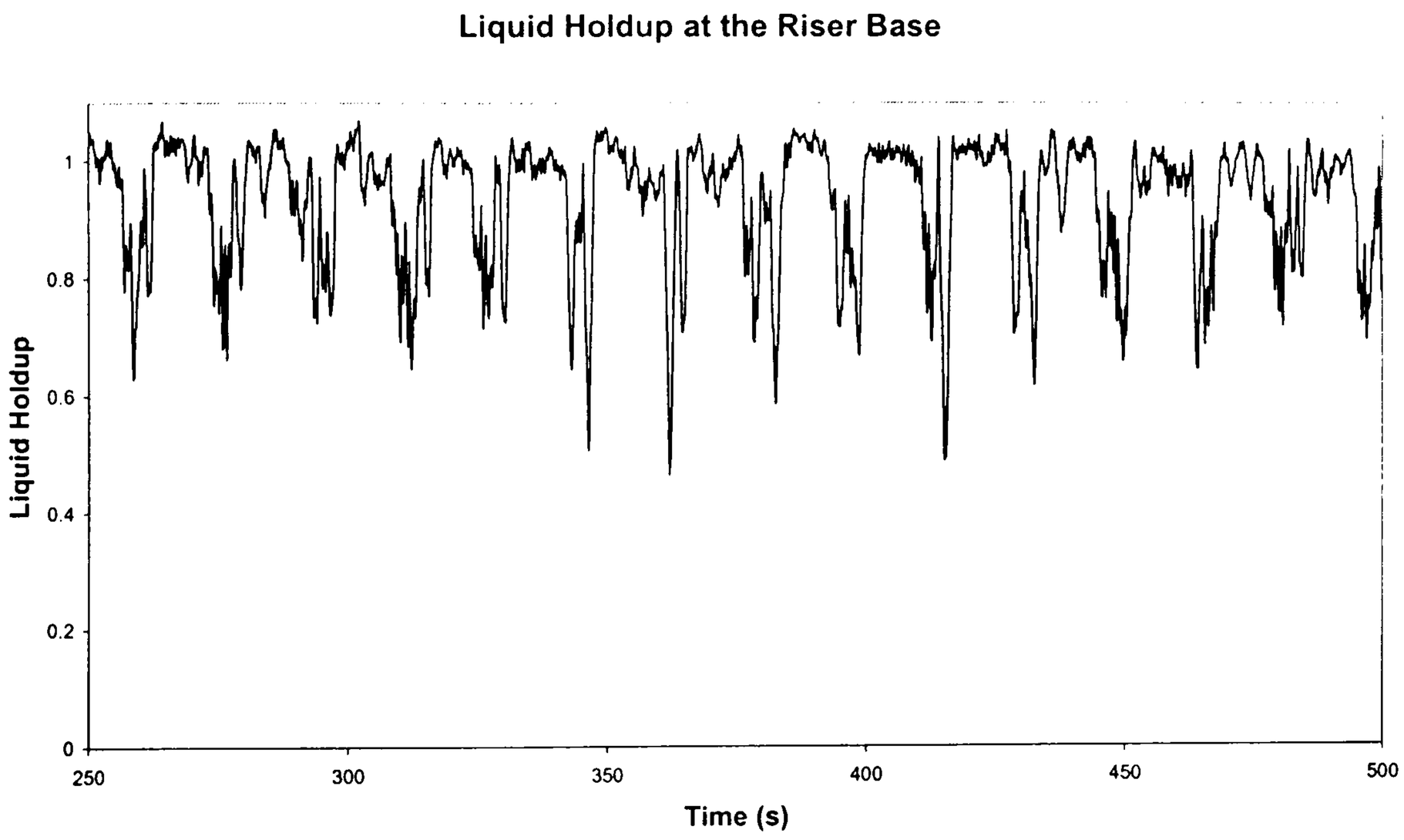

Figure 4.54 – Liquid Holdup Local to the Riser Base During Bubble Flow, $U_G^S = 0.075$ m/s, $U_L^S = 0.94$ m/s

Liquid Holdup Characteristics

As stated above, the idealised structure of bubble flow is a continuous flow of liquid interspersed by bubbles. Liquid holdup measurements local to the riser base confirm this, Figure 4.54 above, with a high average liquid holdup and occasional reductions as the bubbles pass the base, entering the riser.

Fluid Production Characteristics

Fluids production during bubble flow, Figure 4.55, is characterised by a continuous flow of liquid interspersed by the arrival of occasional bubbles. This gives a highly variable gas flow, with significant periods of no gas production.

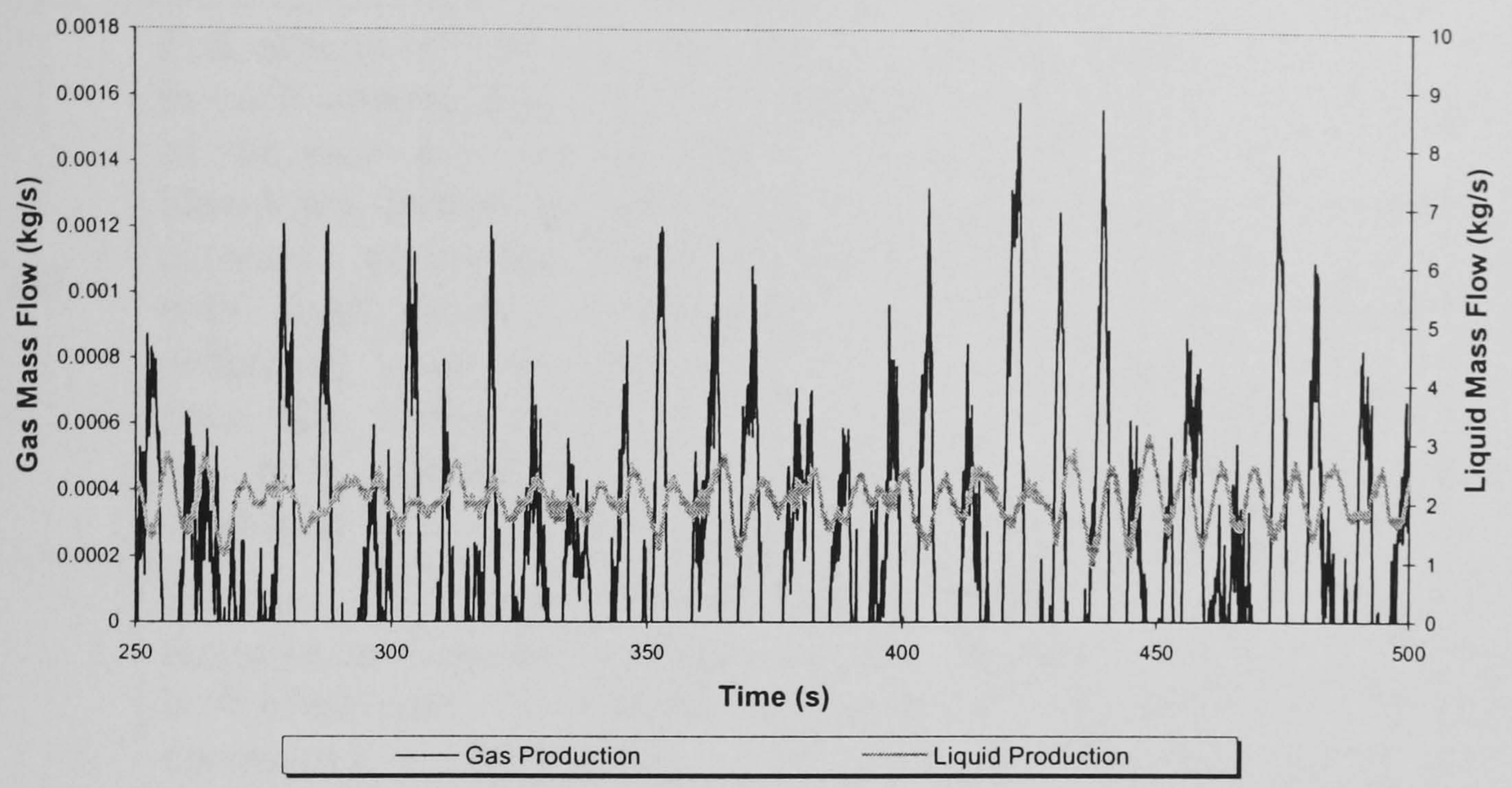

Figure 4.55 – Combined Gas and Liquid Mass Production Characteristics During Bubble Flow, $U_G^S = 0.075$ m/s, $U_L^S = 0.941$ m/s

4.5 Generalised Flow Regime Characteristics

At this point it is useful to draw together all of the characteristics of the observed flow regimes. In this way a systematic method for identification of the different types of flow is possible. Furthermore, the deviations in fluid production during unstable flows are presented, this highlights the relative challenges posed by each regime.

4.5.1 Flow Regime Characteristics

The basic flow regime characteristics are based upon considerations of the liquid inventory in the riser, pressure difference over the riser and fluid production. The classification of the flow regimes are presented in a tabular form. In order to classify a flow regime, these characteristics are used. A test case can be classified to a particular flow regime when it exhibits all three characteristics for a particular flow regime.

Flow Regime	Pressure Cycling Characteristics	Liquid Holdup Characteristics	Fluid Production Characteristics
SS1	Full column of liquid in each upward limb of the riser prior to blowdown. Period of constant production with const pressure difference over the riser. Gas blowdown to near separator conditions.	Long period during liquid buildup and constant production with pure liquid at the riser base, hence no gas penetration at the riser base.	Period of no fluid production, followed by period of const liquid production & production transient. The const production makes up largest part of liquid slug size. Transient is approximately equal to the riser volume.
SS2	Buildup of pure liquid in each upward limb of the riser. Not necessarily complete filling of upward limb of the riser. No period of const. production/pressure.	Period during liquid buildup where pure liquid local to the riser base, hence no gas penetrates the riser base Gas penetration during blowdown and continues for a substantial period of time afterwards.	No period of constant production. Single liquid production transient and that can be greater than the riser volume. Period of no gas production during the liquid buildup. During the final stages of liquid production when a gas production transient arrives followed by a period of constant gas production.
SS3	The liquid buildup in each riser limb, continuously penetrated by gas from the pipeline. Pressure difference peak less than that during SS1.	Continuous gas penetration at the riser base meaning a less-than unity liquid holdup throughout the cycle.	Continuous production of gas with periodic transients of liquid flow, corresponding to the blowout of the liquid column in the riser.
Osc	Periodic oscillation in pressure difference over riser, less than 60% in magnitude compared to severe slugging.	Period of no gas penetration during the liquid buildup in lower limb, hence for approx 50% of the cycle, pure liquid at the riser base.	Characteristic dual surge in terms of gas and liquid delivery.

Slug Flow	Irregular variations in pressure difference, of high frequency and rel. low magnitude, 30% of the maximum potential pressure difference	Hydrodynamic slugs are identifiable from liquid holdup profile at the riser base.	Const. liquid production with gas surges at the arrival of the gas bubble. The peaks in gas and liquid production are not coincident with one another
Bubble Flow	Stable pressure diff. in the riser with small variations	Periodic gas bubbles identifiable in the continuous liquid flow at the riser base	Continuous production of liquid with occasional peaks in gas flow corresponding to the arrival of gas bubbles

Table 4.1 – Generalised Flow Regime Characteristics

4.5.2 Production Deviations During Unstable Flows

In the previous sections, the variations in flow from the pipeline/riser system during unstable flow have been presented. Here these will be gathered together to give an overall comparison between severe slugging 1, transitional severe slugging and oscillation flow. The characteristics for examination are the transient size as a proportion of the riser volume, average slug size, average peak production rate and the deviation of the peak flow from the average outlet liquid flow. These results are for the data analysed in the preceding chapters and do not relate to all data. However it must be noted that as these values are averaged, the truest description of the results lies in the individual sections relating to each flow regime. The analysis below seeks to bring all the previous discussion together in a summary.

	Flow Regime			
	SS1	**SS2**	**SS3**	**Oscillation**
Slug Size (l)	65.8	47.47	22.1	15.79
Transient Size (l)	37.23	47.47	22.1	15.79
Proportion of Riser Volume (%)	96.7	123	57	41
Peak Production (l/s)	3.95	4.42	4.41	2.34
Deviation From Average Flow (%)	1045	646	1285	238

Table 4.2 – Liquid Production Characteristics Summary

Using the results presented in this table, the following summary of liquid production during unstable flows may be made:

1. In terms of slug size, severe slugging 1 is the most problematic flow regime, with the largest slug sizes, followed by severe slugging 2, severe slugging 3 and Oscillation flow.
2. If the production transient is of concern in terms of design or operation, transitional severe slugging (SS2 and SS3) must be considered as the transients occurring during these flow regimes are of a similar scale to those experienced during severe slugging 1.
3. The peak flow experienced during all forms of severe slugging is of the same scale, an order of magnitude greater than the average flow through the system. Thus if the peak flow is of concern, transitional severe slugging is as problematic as 'classical' severe slugging.
4. In terms of surge size, though oscillation surges are less than the average production transients experienced during severe slugging, the surges during oscillation remain a significant proportion of the riser volume. Hence oscillation flow should be considered when examining the effects of unstable flows in design or operation studies.

4.6 Pressure Effects of Flow Processes

As stated in Chapter 3, experiments were carried out at different separator pressures to examine the effect of pressure on unstable flows. This section details these effects, on severe slugging 1 and oscillation flow, observed at 7 bar(a) separator pressure.

4.6.1 Classical Severe Slugging

Figure 4.56 shows the pressure difference over the riser during severe slugging 1 at 7 bar(a). It can be seen that there are small scale fluctuations in the pressure difference during the slug production stage, starting small and gradually increasing.

The source of these fluctuations is determined from the liquid holdup local to the riser base profile, Figure 4.57, is examined. This profile shows a non-unity liquid holdup at the riser base and suggests that small bubbles are entering the riser during the liquid buildup and slug production periods and progressing through the riser. At low pressures, these bubbles would initiate gas blowdown, however due to the reduced expansion of the bubbles, the liquid column in the upward limbs of the riser remain stable for a long period of time. In considering the expansion of the bubbles, for the low pressure experiments, the volume of the bubbles increases by a factor of 3.2/2, or 1.6, going from a pressure of 3.2 bar(a) at the riser base to 2 bar(a) in the separator assuming isothermal expansion. In the case of the 7 bara(a) experiments, the expansion factor is 8.2/7 or 1.17.

The presence of these bubbles indicates that there are potentially two behaviours occurring. Firstly there is a substantial carry-under of gas bubbles during liquid production and secondly that there is a reduced amount of liquid backup along the pipeline during liquid buildup in the riser. The carry-under of bubbles would mean that liquid entering the liquid backed up along the pipeline drags bubbles into the liquid slug body, moving them towards the riser base.

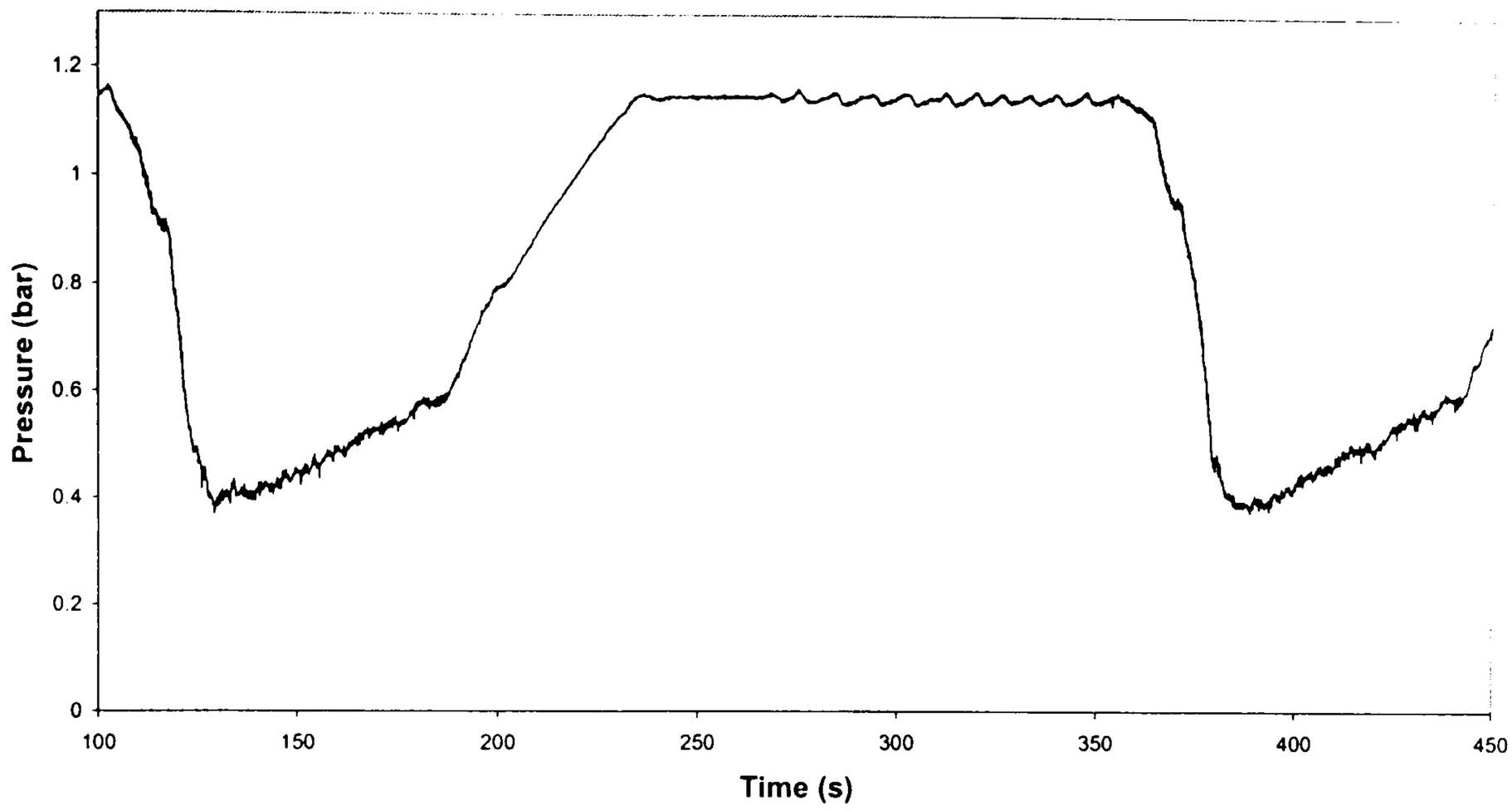

Figure 4.56 – Pressure Difference Over Riser During Severe Slugging, 7 bar(a), U_G^S = 0.055 m/s, U_L^S = 0.085 m/s

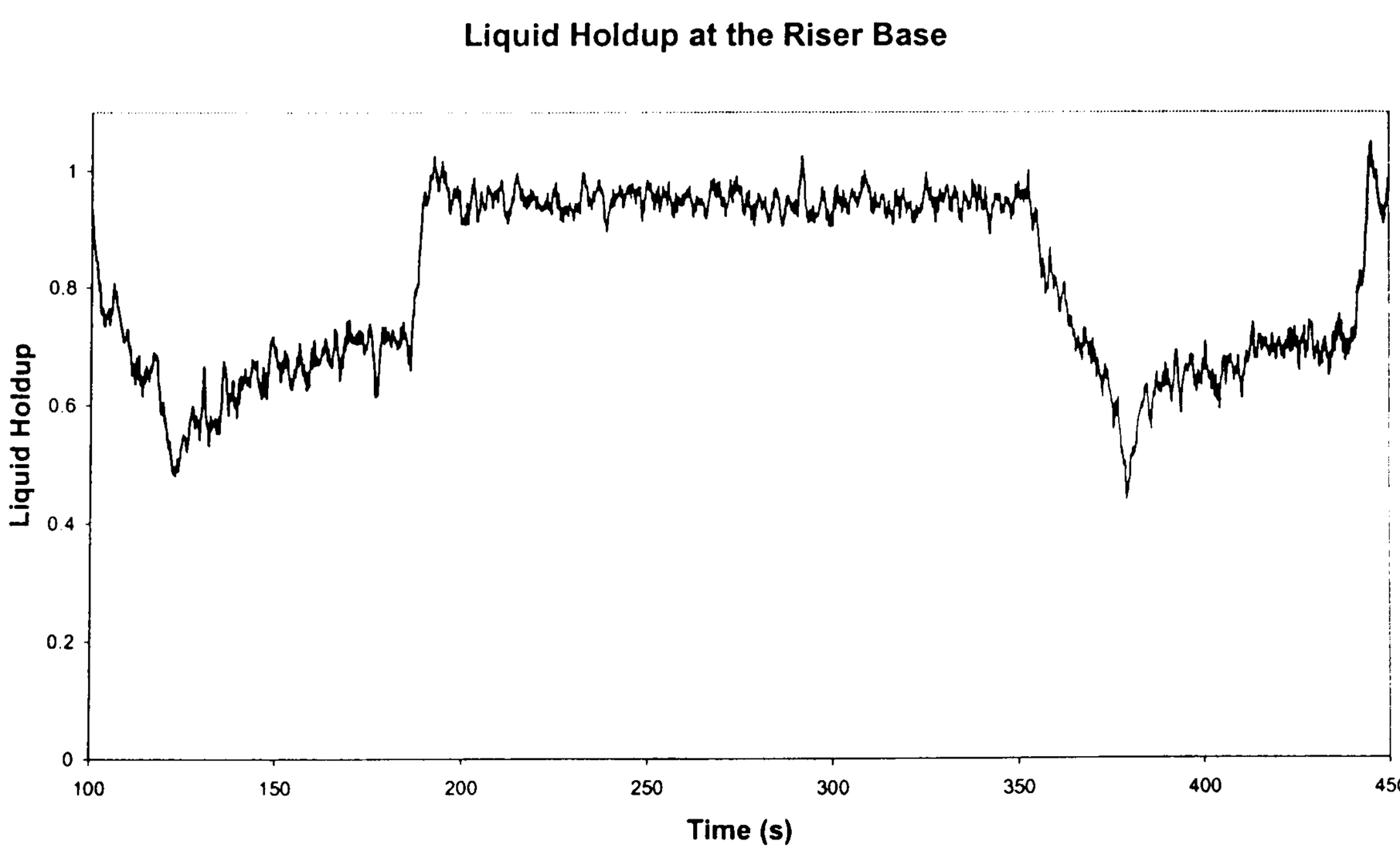

Figure 4.57 – Liquid Holdup Local to Riser Base During Severe Slugging 1, 7 bar(a), U_G^S = 0.055 m/s, U_L^S = 0.085 m/s

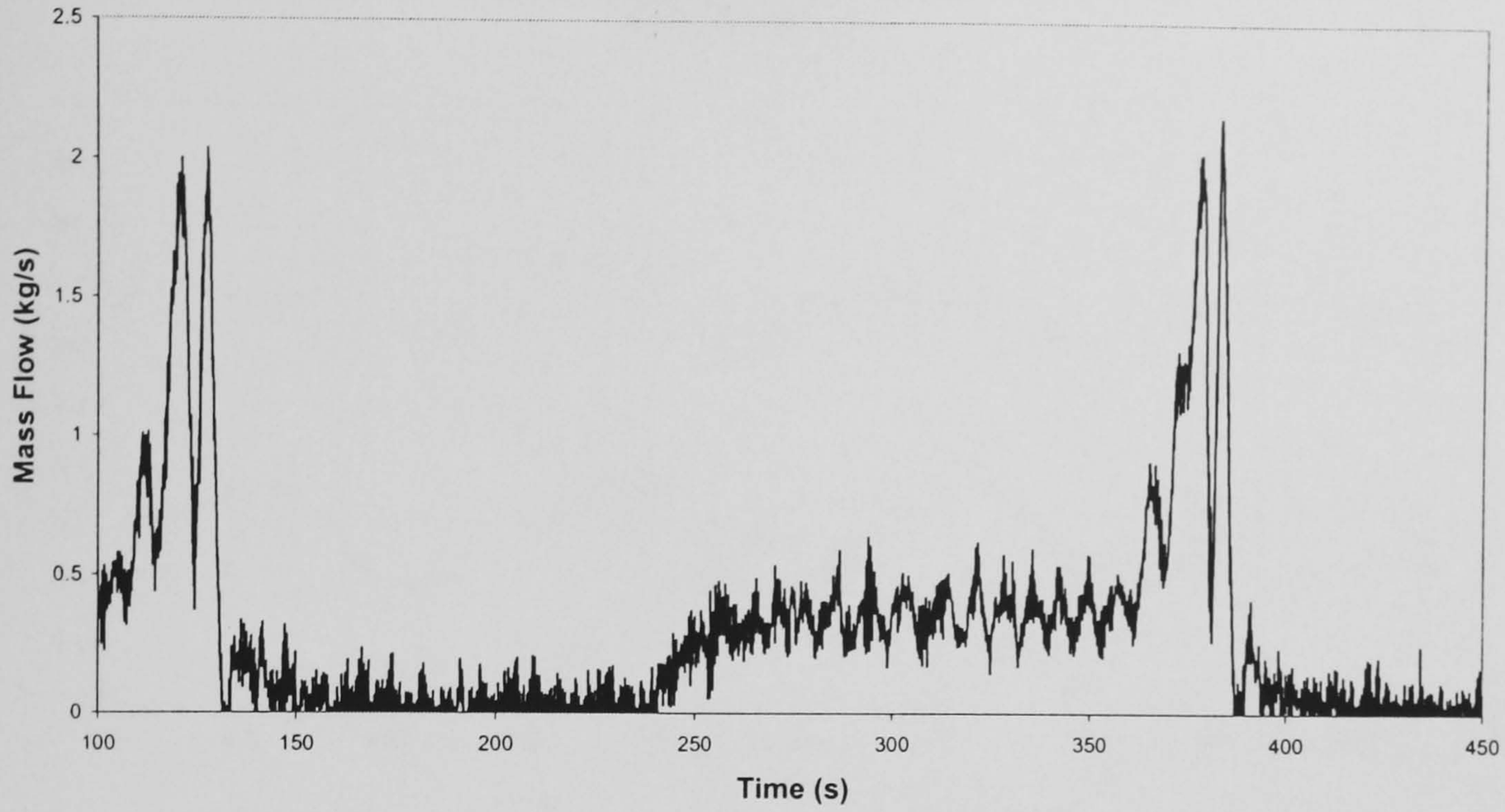

Figure 4.58 – Liquid Production During Severe Slugging 1, 7 bar(a), $U_G^S = 0.055$ m/s, $U_L^S = 0.085$ m/s

The buoyancy force acts against the motion of the bubbles towards the riser base, slowing the bubbles down as they progress along the pipe. Providing the distance from the bubble formation point to the riser base is short, the bubbles would retain a net positive velocity at the riser base and hence would enter the riser proper. Hence, bubbles entering the riser base during production indicates a short backup of liquid along the pipeline. Note however, this postulated behaviour would need confirmation through additional instrumentation along the pipeline. Though it is suggested here that there is a lack of liquid backup along the pipeline during the slug cycle, this flow regime remains classified as severe slugging 1. As there is an identifiable period of liquid production, see Figure 4.58 above, the liquid production characteristic is similar to 'classical' severe slugging 1. This period of liquid production is not constant however as there are fluctuations in the liquid production rate due to the bubbles' expansion. Hence this flow regime is classified as severe slugging 1* a variation of 'classical' severe slugging in this sense but substantially retaining the characteristics of severe slugging 1.

4.6.2 Oscillation Flow

The effect of pressure on oscillation flow is best identified through examination of the pressure difference over each riser limb, Figure 4.59 below. The pressure cycling in the upper limb in this example is approximately 0.1 bar, whereas the lower limb is 50% emptied during the liquid blow-out. In contrast to the low-pressure case, Figure 4.40, the pressure cycling in each limb is in phase with one another, i.e. the minima in the pressure difference are coincident for each riser limb.

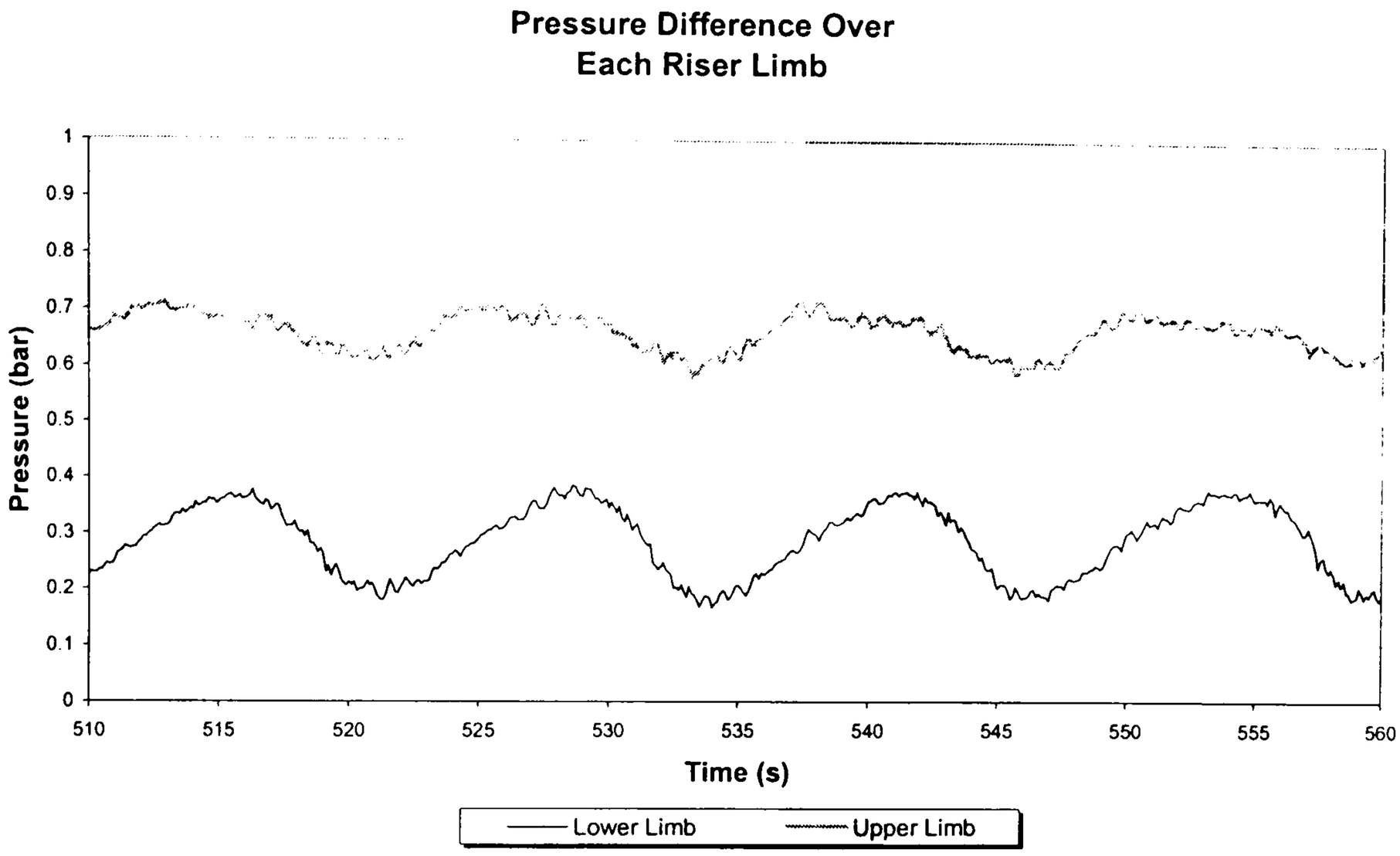

Figure 4.59 – Pressure Difference Over Lower and Upper Riser Limb, 7 bar(a), $U_G^S = 0.28$ m/s, $U_L^S = 0.466$ m/s

This can be attributed to the higher quantity of liquid in the downcomer and the reduced effect of the trapped gas bubbles in the downcomer. The smaller trapped bubble means a smaller period of bubble flow in the upper riser limb, thus the time period over which bubble penetration in the upper limb occurs is the same as the liquid buildup in the lower limb. Added to this, the shunt of liquid from the lower to upper limb reduces the net quantity of liquid in the riser, reducing the pressure difference. These two behaviours couple together to mean that the pressure cycling in each riser limb is synchronized. However there is still no bulk removal of liquid in the upper limb and no blowdown of the system, as the upper limb of the riser remains under stable conditions.

Part 2 – Flow Regime Maps

This second part of the chapter deals with the distributions of the flow regimes with superficial gas and liquid velocity and addresses the stability of the flow regimes as pressure in the separator changes. This analysis is carried out by the use of flow regime maps for the different test conditions and will complete topic 2.7.1 in the research plan. The experimental results are also compared against the criteria for the occurrence of severe slugging that are available in the existing literature. This will address the research plan topic in Section 2.7.2. At this point it is worth noting that the flow velocities in the flow regime map are at the pipeline conditions as described in Chapter 3.

4.7 Flow Regime Behaviour

The basic flow regime map, Figure 4.60, is divided into three parts – an outer stable region, the pressure cycling region and the innermost severe slugging 1 region.

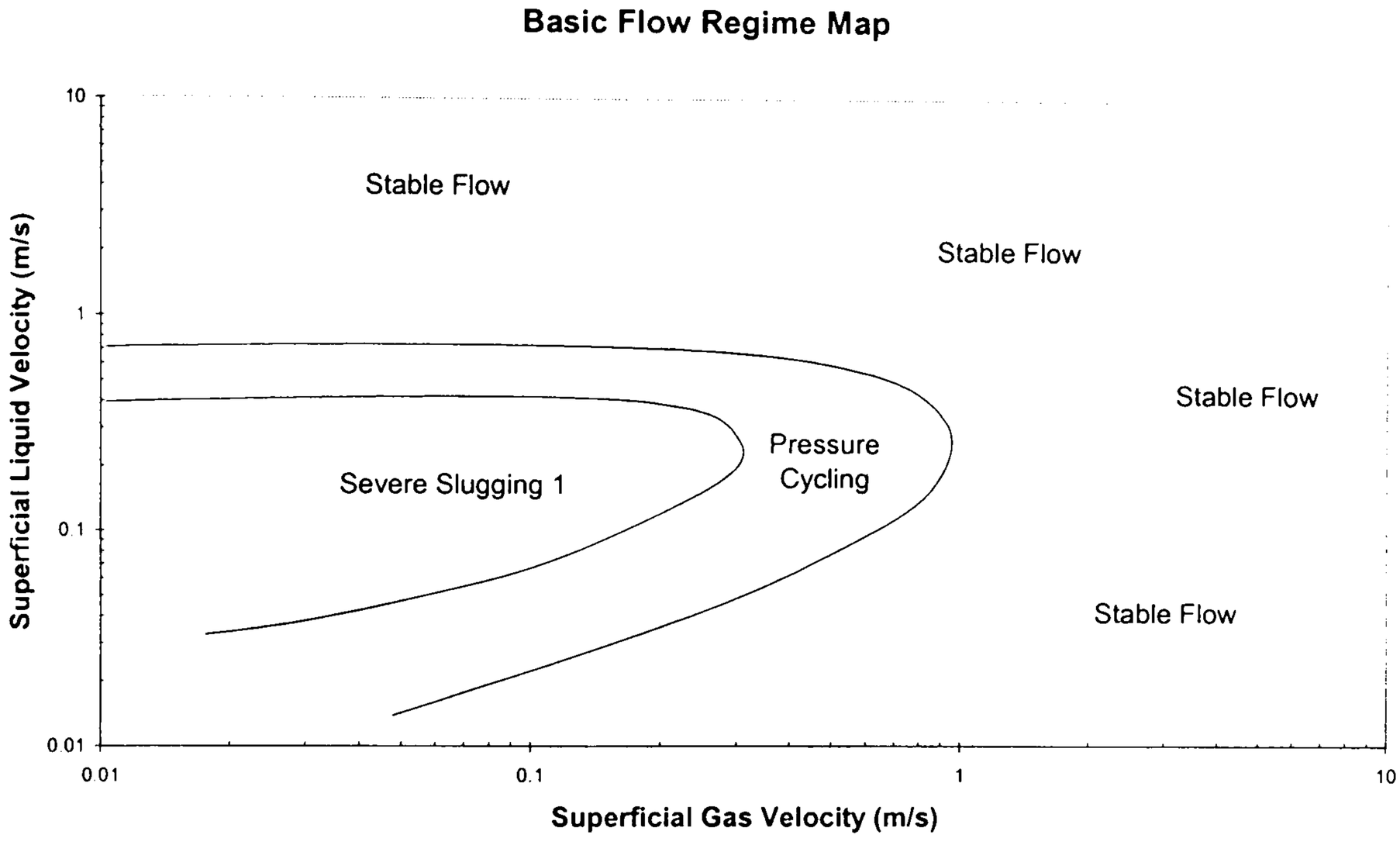

Figure 4.60 – Basic Experimental Flow Regime Map

The stable flow region contains all stable flow regime behaviours, namely bubble flow, slug flow and annular flow, if any. The pressure cycling region contains all transitional severe slugging and oscillation flows while the severe slugging 1 region contains all severe slugging 1. For the S-shaped riser tests in this work, the flow regime behaviour in the riser is summarised in Figures 4.61 to 4.63. As these are experimental flow regime maps, the regions that the maps are divided into are indicative of the results and are not definitive demarcation lines. Furthermore, as with any flow regime map, the transition lines do not indicate a sharp transition from one flow regime to another and transition flow regimes, for example 'transition to oscillation' and 'transition to slug' reflect this behaviour.

Examining the flow regime maps, shows the effect of pressure on the boundaries of the pressure cycling and severe slugging 1 regions. Firstly, as the pressure increases from 2 bar(a) to 4 bar(a), the severe slugging 1 region reduces. Secondly, as pressure increases, the limits of the pressure cycling region are moved to lower gas and liquid velocities, albeit to a lesser extent than the severe slugging 1 region case. Thirdly, at 7 bar(a), the severe slugging 1 region re-establishes itself, though in the form of severe slugging 1* as described above. The effect of separator pressure on the severe slugging 1 is twofold, it reduces the maximum superficial gas and liquid velocities at which severe slugging 1 is experienced. In effect, this is a shift of the severe slugging 1 region to lower values of U^S_G and U^S_L.

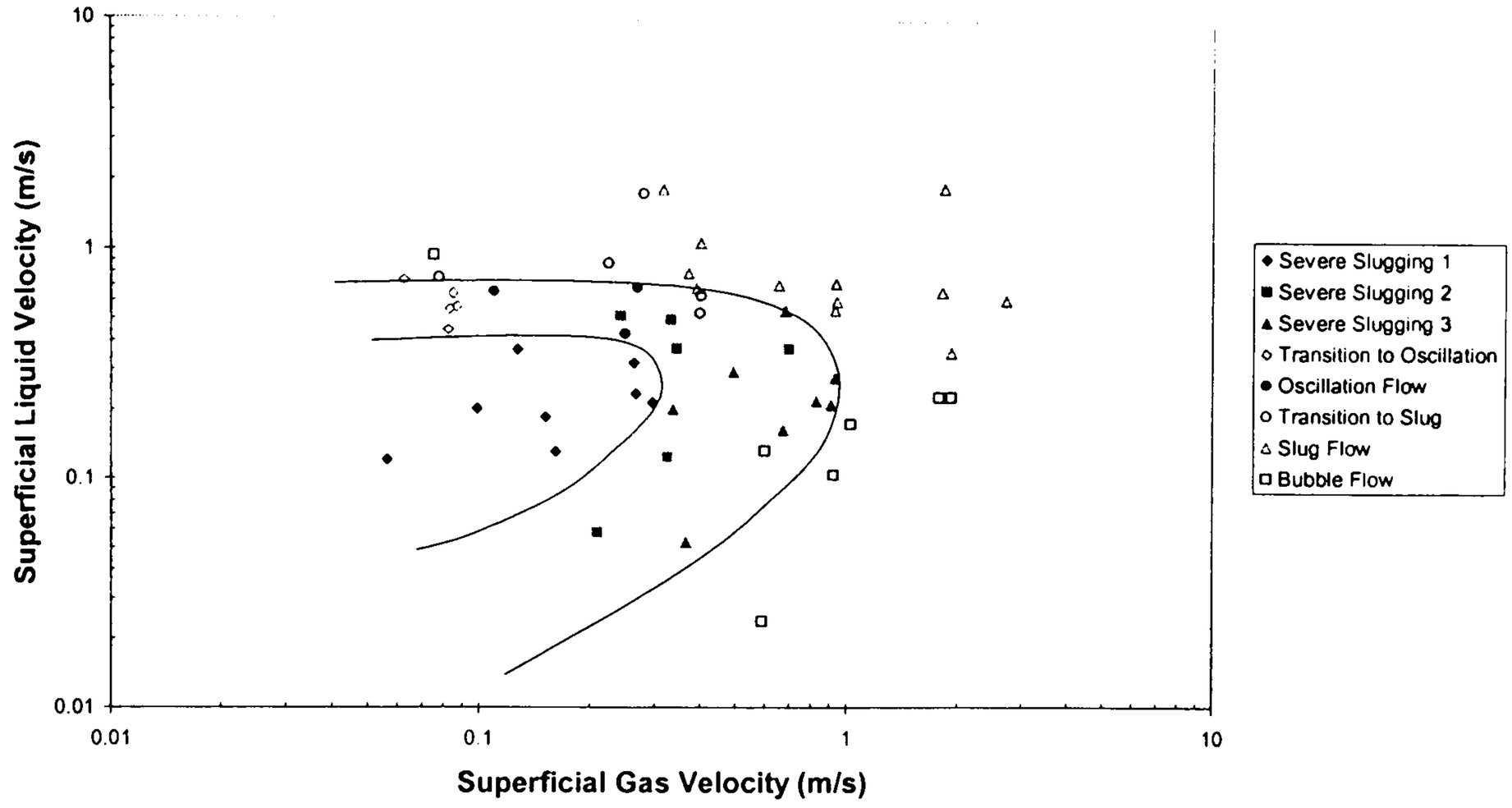

Figure 4.61 – Flow Regime Map, 2 bar(a)

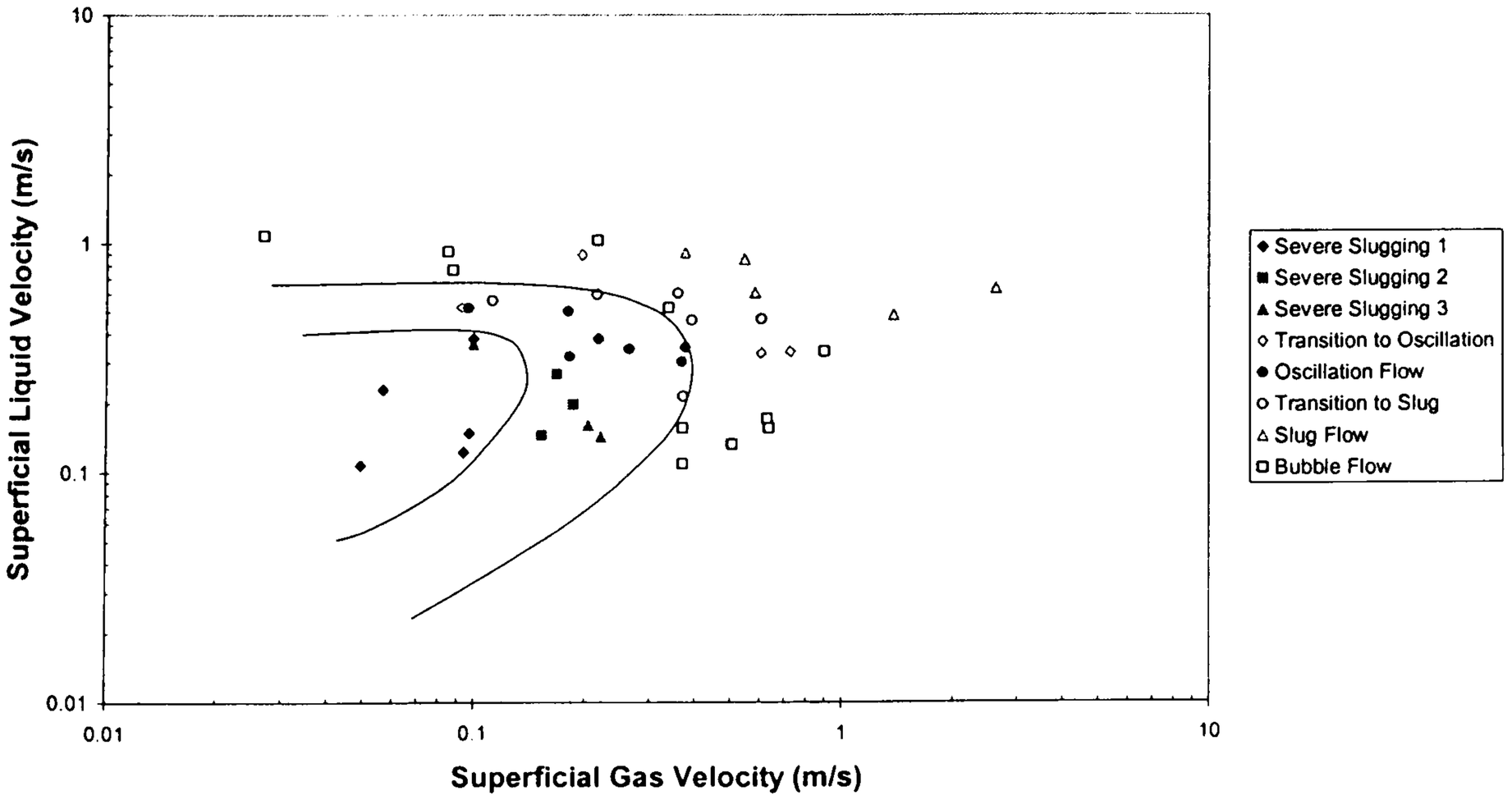

Figure 4.62 – Flow Regime Map, 4 bar(a)

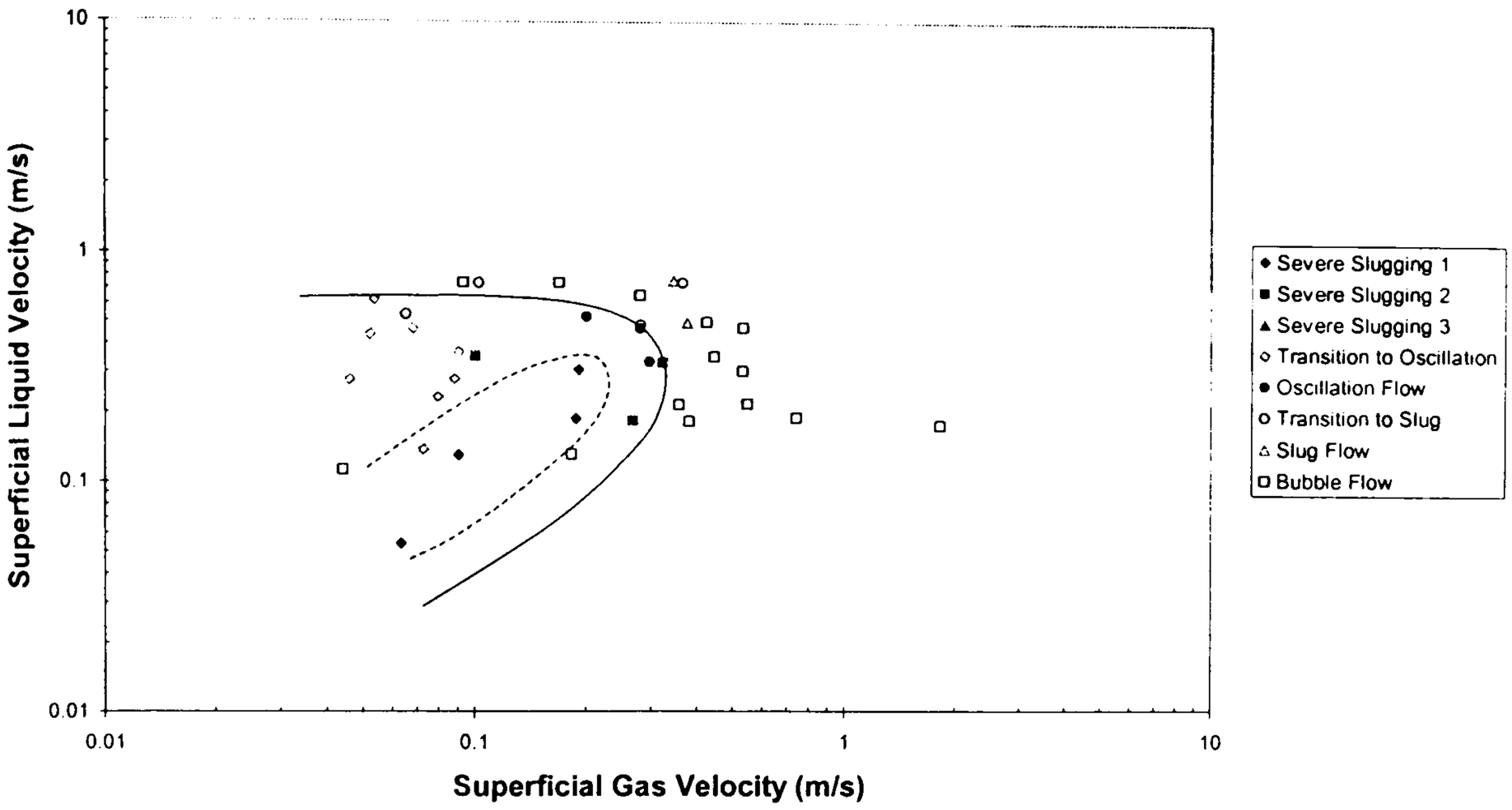

Figure 4.63 – Flow Regime Map, 7 bar(a)

As stated previously, the effect of pressure is more pronounced on one velocity boundary, namely the superficial gas velocity boundary. This means that the application of pressure appears to shift the severe slugging 1 region towards the left hand region of the flow regime map.

There are two factors that can cause this change in the severe slugging 1 boundary:

a) The amount of lift work the gas does during blowdown. 'Classical' severe slugging 1 requires the gas to lift out a large mass of gas and the potential lift energy for this process is related to the expansion of the gas. An increase in the system pressure, reduces the expansion ratio of the gas from 1.6 for 2 bar(a) operation to 1.17 for 7 bar(a) operation and hence reduces the lift energy. This process has been suggested by Montgomery and Yeung (2002).
b) The effect of gas compression on the flow regime. Classical severe slugging also requires liquid backup along the pipeline in order for the severe slug to form. For this to occur, the gas in the pipeline must be able to substantially compress. As the pressure increases, the resistance to compression increases and so pipeline liquid backup is more difficult, reducing the slug size.

Thus, through both mechanisms, the application of higher separator pressure can inhibit severe slugging 1 – the blowdown mechanism is damped down and there is a lack of liquid backup in the pipeline leading to shorter slug lengths, with the net effect being the reduction in the severe slugging 1 region.

The effect of pressure on the pressure cycling region boundary is far less pronounced, with only a marginal shift in terms of the superficial liquid boundary and a reduced shift in terms of the superficial gas velocity limits. Other unstable flows, namely

transitional severe slugging and oscillation flow, do not have liquid backing up the pipeline and so do not rely on the compressibility of the pipeline gas as much as severe slugging 1. These flows are however sensitive to bubble penetration at the riser base, increased bubble penetration can induce stable flows and separator pressure effects flow regime behaviour. Without pipeline gas packing, this bubble penetration is made easier. Hence, as pressure increases, the region of unstable flow is reduced, however the rate of change is substantially less than severe slugging 1. This behaviour is observed in all three flow regime maps, with a shift in the boundary to lower gas superficial velocity as separator pressure increases.

Though it has been stated above that the application of pressure causes the damping out of 'classical' severe slugging 1, in the 7 bar(a) tests carried out, severe slugging 1* was observed. This flow regime is not only stable but exists at superficial gas and liquid velocities of a similar order of magnitude to those severe slugging 1 tests points experienced at 2 bar(a). There are two main reasons why this is the case:

a) As in the case of transitional severe slugging and oscillation flow, severe slugging 1* does not have any backup of liquid along the pipeline. Thus a lack of pipeline liquid accumulation, caused by a lack of gas compressibility, will not effect the severe slugging 1* regime.
b) Bubble penetration occurs throughout the process, reducing the rate of gas pressure buildup in the pipeline. In this way, though the pipeline gas is less compressible than the 2 bar(a) case and hence more likely to sweep out the accumulated liquid, the removal of gas from the pipeline reduces this tendency and hence promotes slug buildup and formation of the severe slug.

Thus severe slugging occurs at elevated separator pressure, though in the severe slugging 1* form, a different flow regime to 'classical' severe slugging, with a different degree of sensitivity to changes in the separator pressure. For this reason, the boundary for this severe slugging is denoted in a broken line, to reflect the difference in flow regime.

4.8 Comparison with Stability Criteria

As part of Section 2.7.2, it was suggested that data collected should be compared against existing criteria for severe slugging and unstable flows. This would give an indication of where further developments/investigations are required to improve existing techniques. The discussion below details the results of this comparison and suggests further avenues of investigation.

4.8.1 Criteria for Comparison

The criteria in common use for the prediction of the occurrence of severe slugging are: the Taitel and Duckler Stratified-Wavy Transition Criterion (1976); the Bøe Criterion (1981); the Π_{SS} Criterion and the Taitel Stability Criterion (1986). The main details of these criteria are given in Section 2.2, however for clarity, only the final equations of each are presented below.

Taitel and Duckler Stratified Flow Criterion

This is a general criterion for the occurrence of stratified flow in horizontal or near-horizontal pipelines. The criterion is based upon considerations of wave growth in a stratified flow and gives the maximum allowable superficial gas velocity for stratified flow. The criterion is summarised by:

$$U_G^S < C_2\left[\frac{(\rho_L - \rho_G)g\cos\beta\ A_G}{\rho_G\, dA_L/dh_{LP}}\right] \qquad (4.4)$$

Where the symbols have their usual meaning as defined in Section 2.2.1. The parameter $C_2 \approx A_G/A_L$ and the change in liquid flow area with liquid height, dA_L/dh_L is given by:

$$\frac{dA_L}{dh_L} = D\sqrt{1-\left(2\frac{h_L}{D}-1\right)^{\frac{1}{2}}} \qquad (4.5)$$

This criterion is used for severe slugging prediction based upon the assertion of Schmidt et al. (1980) that a requirement of 'classical' severe slugging was the occurrence of stratified flow in the pipeline.

Bøe Criterion

The Bøe criterion (1981) is based upon considerations of the formation process for a severe slug. It gives the minimum required liquid velocity such that the accumulation of hydrostatic head in the riser is greater than the pressure increase due to gas compression. This is seen as the criterion for the formation of a severe slug and is given by:

$$U_L^S \geq \frac{P_P}{\rho_L g(1-\varepsilon_L)L\sin\alpha}U_G^S \qquad (4.6)$$

Π_{SS} *Criterion*

This criterion, developed by Pots et al. (1985), also considered the formation of a severe slug in terms of hydrostatic head accumulation and the pipeline gas pressure buildup. The analysis leads to the criterion:

$$\Pi_{SS} = \frac{ZRT/M_W}{g\varepsilon_L L}\frac{G_G}{G_L} \qquad (4.7)$$

Taitel Criterion

The Taitel criterion (1986) aims to predict the damping down of severe slugging by the application of separator pressure. It is centred upon an analysis of the propagation of a bubble penetrating the riser base, causing the liquid column in the riser to become unstable and precipitating blowdown of the pipeline/riser. The criterion is given in terms of the pipeline gas holdup and the pressure in the separator:

$$\frac{P_S}{P_0} < \frac{(\varepsilon_{GP}/\varepsilon'_G)L - h_R}{P_0/\rho_L g} \qquad (4.8)$$

Accepting that the pipeline liquid holdup is a function of the superficial liquid velocity and can be derived from the gas fraction, the criterion gives a limiting liquid velocity for severe slugging.

4.8.2 Comparison Results

The flow regime boundaries as described by the criteria above have been calculated for the Cranfield University pipeline/riser system and the results in the form of a series of flow regime maps in Figures 4.64-4.66.

For the 2 bar(a) case, it can be seen that both the Stratified Transition Criterion and the Taitel Stability Criterion both cover the entire region of severe slugging and unstable flows. In the case of the Stratified Transition Criterion, the upper liquid velocity limit overestimates the transition to stable flows by a factor of approximately two. The corresponding upper limit for the Taitel Stability Criterion almost exactly coincides with the uppermost oscillation test point. In terms of the upper gas velocity limit, the Stratified Transition Criterion substantially overestimates the limit of unstable by more than a factor of thirty. The Taitel Stability Criterion on the other hand is unable to predict such a limit and hence is not applicable in this respect.

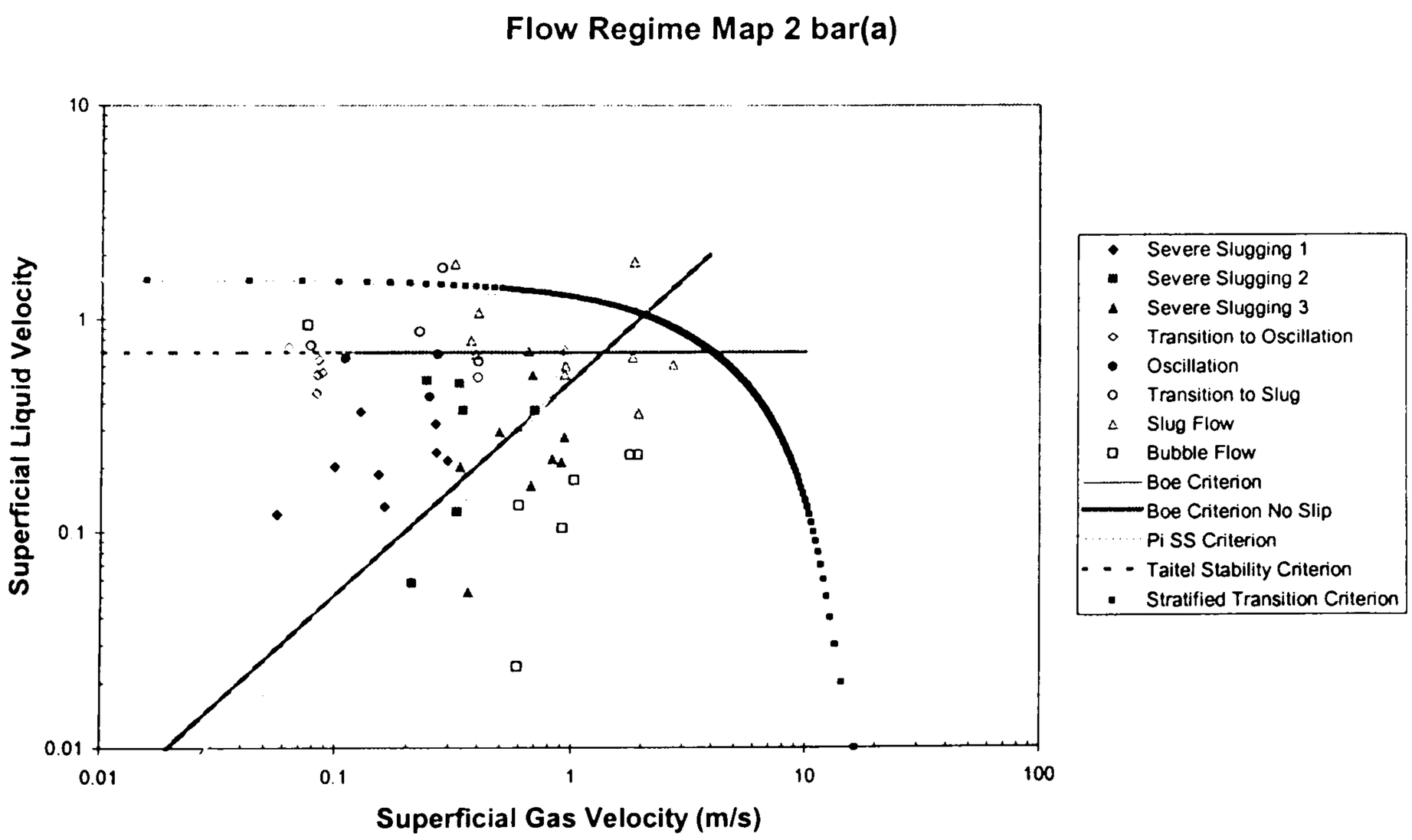

Figure 4.64 – Flow Regime Map Comparison with Stability Criteria, 2 bar(a)

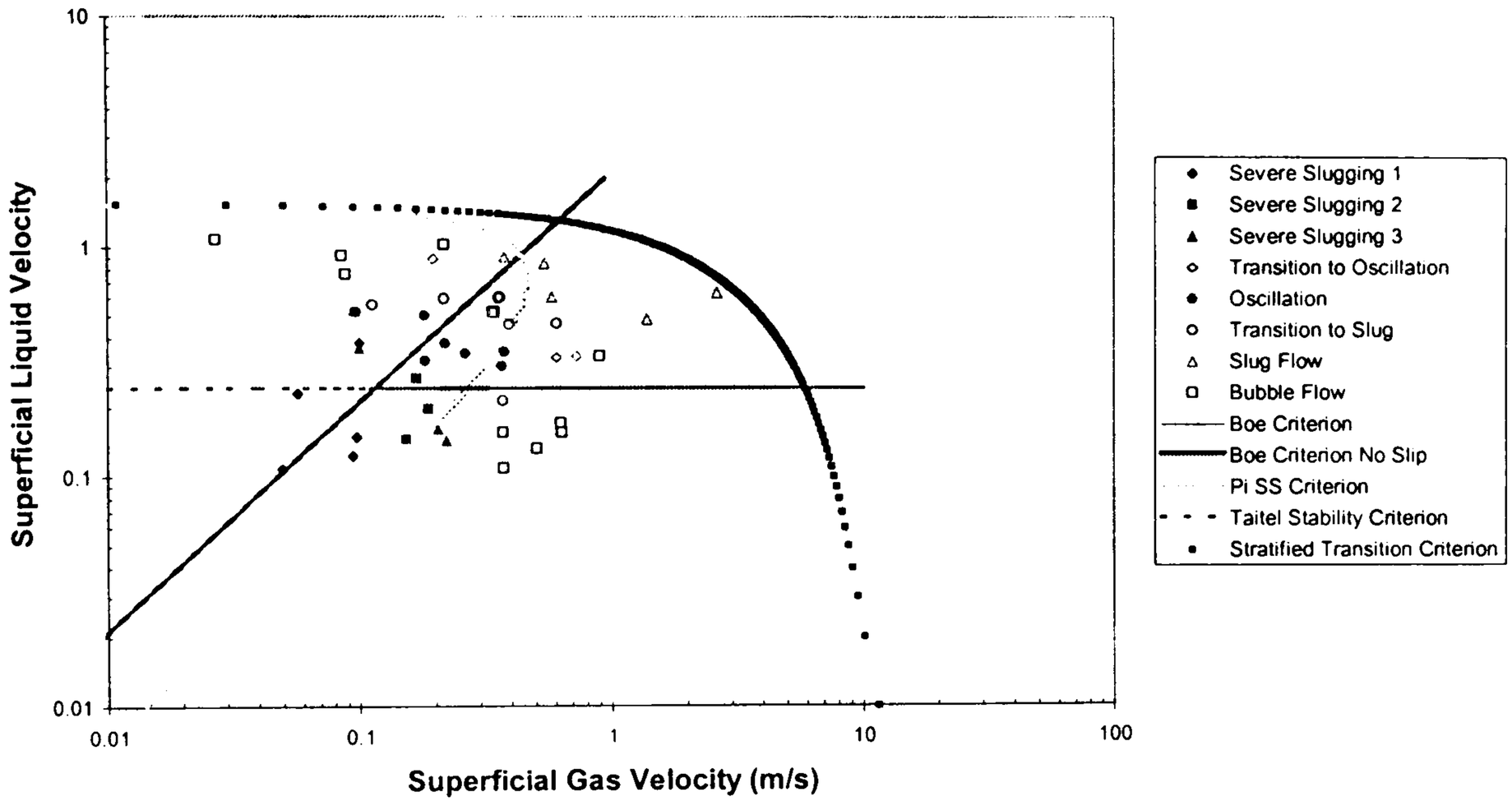

Figure 4.65 – Flow Regime Map Comparison with Stability Criteria, 4 bar(a)

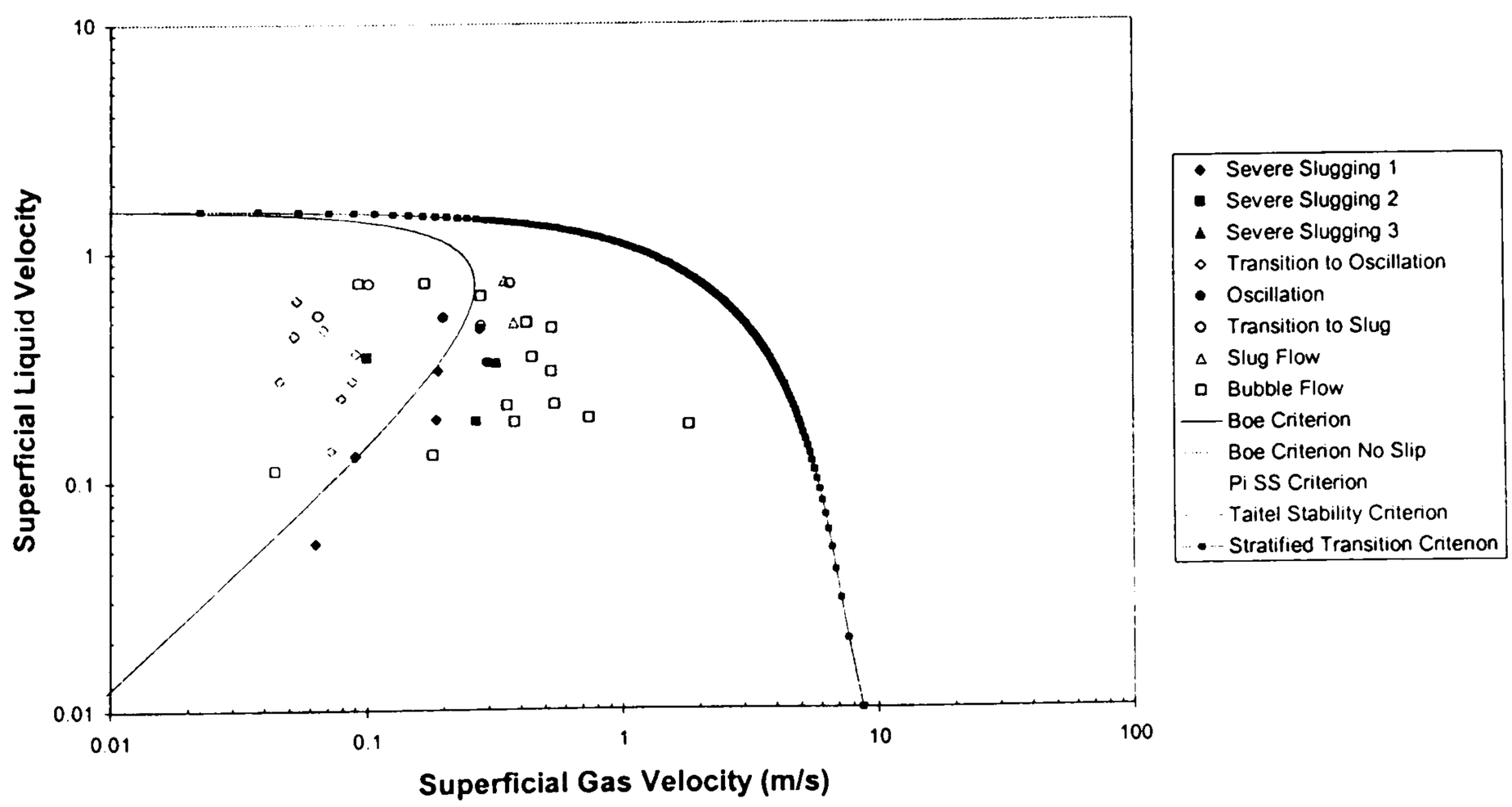

Figure 4.66 – Flow Regime Map Comparison with Stability Criteria, 7 bar(a)

The Bøe and Π_{SS} Criteria, which are coincident, have a limited ability to predict the region of severe slugging and unstable flows. In both cases the criteria both encompass the severe slugging 1 region but miss 50% of the transitional severe slugging cases. In terms of the limits of severe slugging, the Bøe and Π_{SS} Criteria with a non-zero slip both exhibit similar performance to the Stratified Transition Criterion for the liquid velocity limit. It is the upper gas velocity limit that poses the challenges to these criteria, both fail to predict the observed transitional severe slugging at low-liquid/high-gas velocities. The same is true for the no-slip variation of the criteria. This behaviour suggests that gas pressure accumulation is not correctly considered in the formulation of these criteria.

As separator pressure increases from 2 bar(a) to 4 bar(a) and 7 bar(a), the overall performance of the criteria reduces. As pressure increases, the performance of the Stratified Transition Criterion remains largely unchanged, still overestimating the upper liquid velocity limit by a factor of two and the upper gas velocity limit by over an order of magnitude. The Taitel Stability Criterion drops to lower liquid velocities as pressure increases, failing to predict the limiting liquid velocity of oscillation flow and some of the transitional severe slugging cases. At 7 bar(a), the criterion is moved to such low liquid velocities that it does not appear on the flow regime map and hence does not predict the upper liquid boundary of any of the experienced unstable flows.

The Bøe and Π_{SS} Criteria show a variation in performance, particularly going from 2 bar(a) to 4 bar(a). As pressure increases, the gas velocity boundary in both criteria is reduced, effectively shifting the transition line of the criteria to the left of the graph. In terms of the performance of the criteria, the performance numerically improves for the transitional severe slugging data, with more data lying inside the region of the criteria, 66% as opposed to 50% in the previous case. However in terms of oscillation flow, more test cases appear outside the boundary than the 2 bar(a) cases. Upon closer examination of the 2 bar(a) experimental data, the region where the criteria fail to predict the presence of transitional severe slugging is the low-liquid/high-gas velocity region. In terms of actual experimental data in the 4 bar(a) case, there are only limited data in this region, thus the evidence is inconclusive in terms of performance improvement. Indeed, it is suggested that the numerical improvement in the performance of the criterion is due to lack of data in the region of interest in the flow regime map, rather than any actual improvement in the criteria. At 7 bar(a) separator pressure, the Bøe and Π_{SS} No-Slip criteria have moved from the map entirely, not predicting any of the unstable flow. The remaining region predicted by the non-zero slip criteria only encompasses 25% of the severe slugging 1 cases and 50% of the other unstable flow cases occurring. This is particularly true in the low-liquid/high-gas region of the flow regime map.

Thus in summary, the existing flow regime criteria flow regime that are commonly used for predicting the occurrence of severe slugging have been shown to have mixed ability to predict the unstable flow occurring in the flowline riser. Though in come cases, the severe slugging 1 region is predicted, the unstable flow region is not. Considering the first part of this chapter, which has highlighted the importance of

taking into account the transition severe slugging and oscillation flows, this means that the predictions of these existing criteria are subject to question.

The only caveat to the above statement is the Stratified Transition Criterion that has been shown to bound the region of severe slugging and unstable flow in all cases. There is however a degree of overestimation which must be taken into consideration when using this criterion.

4.9 Summary

In this chapter two major avenues of experimental investigations were undertaken, the first examined the characteristics of severe slugging and unstable flows in general. The second examined the occurrence of the flow regimes in terms of inlet flow conditions.

Unstable flows in the pipeline/riser were classified into four broad classes: severe slugging 1, severe slugging 2, severe slugging 3, oscillation flow and stable flow. Severe slugging 1 corresponded to the notional form of 'classical' severe slugging, while severe slugging 2 and 3 were transitional forms of severe slugging. Oscillation was found to be a form of unstable flow where the instability in the lower limb of the riser dominated the pressure cycling as a whole. Through examination of the liquid production characteristics, it was shown that in terms of both design and operation, all forms of unstable flow must be considered with respect to slug/surge volume and deviations from average outlet flow.

When examining the flow regime maps, it was found that the application of increased separator pressure caused a general damping down of the 'classical' severe slugging 1 flow. However at 7 bar(a), the appearance of a similar flow regime severe slugging 1* meant that unstable flow persisted in the system. It was also found that other transitional severe slugging and oscillation flows were not as sensitive as severe slugging 1 to the changes in separator pressure. Comparing the results obtained from experiments to existing criteria for the occurrence of severe slugging, marginal agreement was achieved, particularly as separator pressure increased. An area of particular concern is the fact that the criteria are unable to predict the occurrence of transitional severe slugging and oscillation flows. Though they are not intended for this purpose, the prediction of the flow regimes is important given the results presented in the first part of the chapter.

For this reason, the prediction of the occurrence of severe slugging and unstable flows becomes the focus of the next chapter, where an effort is made to develop a criterion.

Chapter 5 Criterion for Unstable Flow

A first step to predict the likelihood of severe slugging in a pipeline/riser system is the use of steady-state stability criteria, these give the general region of severe slugging on a flow regime map for use in preliminary design calculations. As demonstrated in Chapter 4, the existing severe slugging stability criteria, namely the Bøe (1981) Criterion, the Taitel (1986) Stability Criterion and the Π_{SS} (1985) Criterion, did not correctly predict the region of severe slugging 1 in the Cranfield University S-shaped Riser. This was particularly true as the system pressure increased with some of the criteria failing to predict any of the unstable flows present at 7 bar(a) separator pressures. The only criterion that successfully predicted the occurrence of the unstable flow in the riser was the Taitel and Dukler (1976) Stratified Flow Criterion, though it substantially over-predicts the potential region of severe slugging, particularly at low superficial liquid velocities, see Section 4.8.2. However the Taitel and Dukler Criterion is insufficient in itself for predicting severe slugging as it is a criterion for the occurrence of stratified flow, which though a necessary condition for severe slugging as defined by Schmidt et al. (1985), is not the only criterion for unstable flows.

Of further concern, the existing stability criteria were unsuccessful in predicting the region of transitional severe slugging and oscillation flows, again particularly as the system pressure increased. It was shown in Chapter 4 that 'classical' severe slugging 1 (SS1) is not the only flow regime of concern in terms of fluid production. Both forms of transitional severe slugging (SST), severe slugging 2 (SS2) and severe slugging 3 (SS3), can cause production transients of a similar magnitude to severe slugging 1. Similarly oscillation flow has been shown to be of concern in terms of fluid production, with production transients producing liquid volumes approximately 40% of the riser volume. Hence a workable stability criterion should have the ability to predict the entire region of unstable flows.

Thus a new criterion is required to allow prediction of the region of unstable flow. The development of this criterion is presented in this Chapter. The first section deals with the basic formulation of the criterion, i.e. the condition for unstable flow relating this to other previous works. The second section of the chapter presents the detailed development of the model equations and addresses any implementation issues associated with this. Finally the third section covers the comparison of the criterion against the experimental data presented in Chapter 4 and independent data collected by Tin and Incoll (1991), provided through the Managed Programme of Transient Multiphase Flow (TMF, 1996).

5.1 Basic Formulation of Criterion

The basic formulation of the severe slugging criterion is based upon the penetration of bubbles into the riser base by gas from the pipeline and the change in pressure therein.

5.1.1 Existing Criteria

Before the condition for severe slugging is presented, it is beneficial to examine the work of previous authors, namely Taitel (1986) and Fuchs (1989), regarding the movement of bubbles into a riser.

Taitel (1986) Stability Criterion

For the vertical riser depicted in Figure 5.1, Taitel (1986) stated that for severe slugging to occur in a riser, the slug tail must spontaneously accelerate from the riser base and accelerate through the length of the riser. This is summarised by the following relation:

$$\frac{d(\Delta F)}{dy} > 0 \quad \text{for} \quad y = 0 \qquad (5.1)$$

Note: In the original work by Taitel the criterion was for stable flow, hence the inequality is reversed.

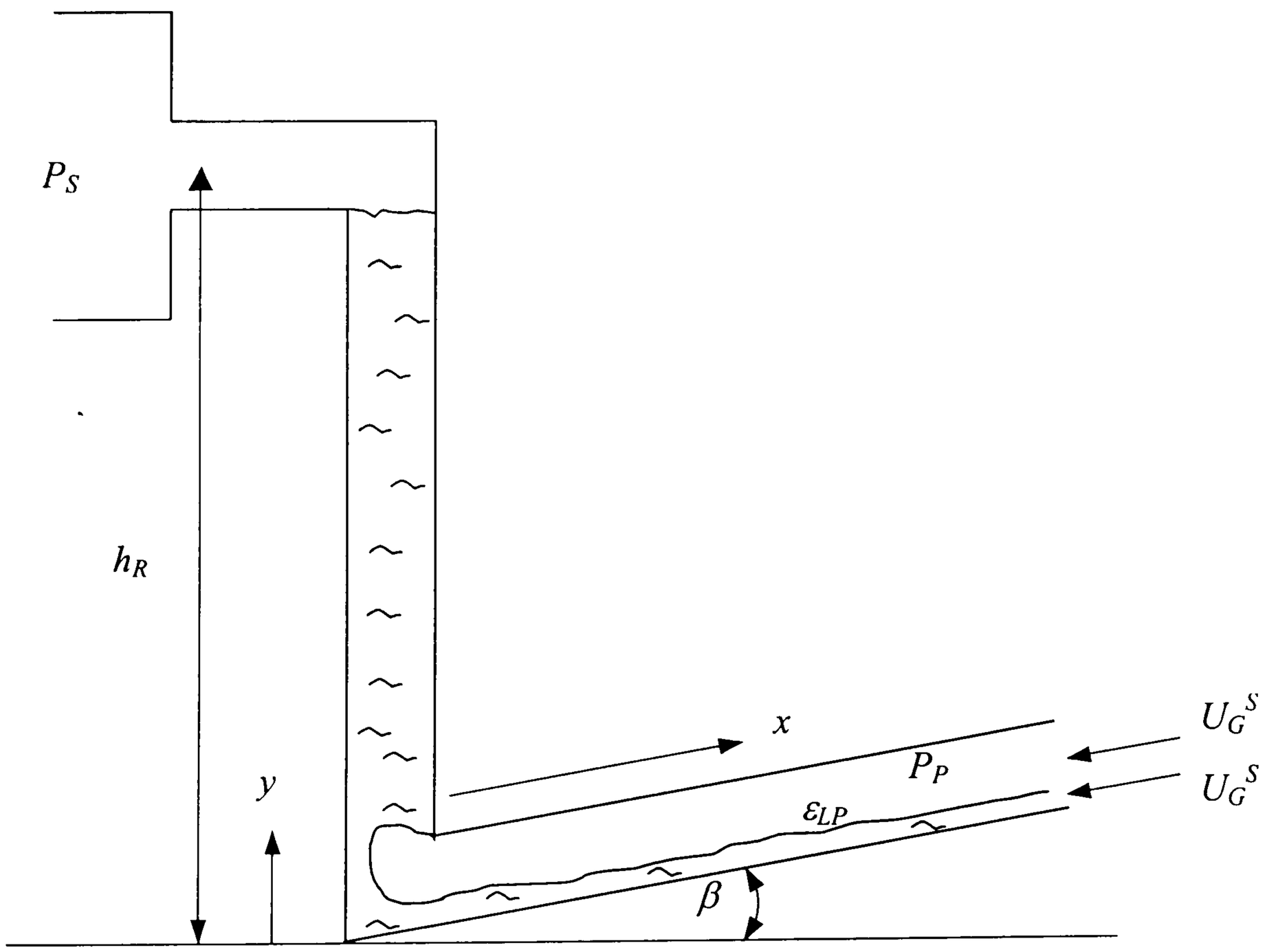

Figure 5.1 – Vertical Riser Geometry

As described in Section 2.2.4, ΔF is the force difference acting across the bubble nose in the first moments of bubble penetration and y is the vertical distance from the base of the riser. Separating the force components, Equation (5.1) effectively becomes:

$$\frac{d(P_P - P_B)}{dy} > 0 \qquad (5.2)$$

Extracting the bubble front velocity:

$$\frac{d(P_P - P_B)}{dy} = \frac{dt}{dy}\frac{d(P_P - P_B)}{dt} = \frac{1}{U_B}\frac{d(P_P - P_B)}{dt} \qquad (5.3)$$

As the bubble is moving up through the riser, the bubble front velocity is positive and greater than zero, thus the criterion becomes:

$$\frac{d(P_P - P_B)}{dt} > 0 \qquad (5.4)$$

This inequality can then be rearranged to give the final form of the condition for severe slugging:

$$\frac{dP_P}{dt} > \frac{dP_B}{dt} \qquad (5.5)$$

Fuchs (1987) Criterion for Slug Release

Fuchs (1987) stated that during the release of a severe slug, the tail of the severe slug accelerated through the riser. This release is the moment in time where the slug tail moves from the pipeline into the riser proper leading to gas blowdown. Starting from the basic pressure balance over the pipeline/riser system:

$$P_P - P_S = \Delta P_{FR} + \Delta P_{ACC} + \Delta P_{HYD} \qquad (5.6)$$

Where the subscripts *F*, *ACC* and *HYD* correspond to friction acceleration and hydrostatic components in the riser, respectively. Differentiation of Equation (5.6) gives:

$$\frac{d(P_P - P_S)}{dt} = \frac{d(\Delta P_{FR})}{dt} + \frac{d(\Delta P_{ACC})}{dt} + \frac{d(\Delta P_{HYD})}{dt} \qquad (5.7)$$

Fuchs (1987) asserts that as the slug accelerates through the riser:

$$\frac{d(\Delta P_{FR})}{dt} > 0 \qquad (5.8)$$

and

$$\frac{d(\Delta P_{ACC})}{dt} > 0 \qquad (5.9)$$

This then gives Fuchs' condition for the 'release' of a severe slug, i.e. the initiation of bubble penetration:

$$\frac{d\left(P_P - P_S\right)}{dt} > \frac{d\left(\Delta P_{HYD}\right)}{dt} \qquad (5.10)$$

Splitting the left hand side of Equation (5.10) gives:

$$\frac{dP_P}{dt} > \frac{d\left(P_S + \Delta P_{HYD}\right)}{dt} \qquad (5.11)$$

At the start of the bubble penetration stage, the right hand side of Equation (5.11) corresponds to the riser base pressure, thus the criterion for slug 'release' is:

$$\frac{dP_P}{dt} > \frac{dP_B}{dt} \qquad (5.12)$$

Equations (5.5) and (5.12) show the equivalence of the two approaches. However when examining severe slugging in a pipeline/riser system, the acceleration of bubbles at the riser base is not unique to severe slugging. Indeed, during hydrodynamic slug and bubble flow, gas bubbles accelerate during the first instants of bubble penetration to their steady velocity further up the riser. It is true however that during severe slugging the bubbles continue to accelerate continuously through the riser length. Unfortunately, the analyses presented thus far, only address the behaviour at the riser base.

There is a period that is unique to severe slugging and other unstable flows in a pipeline/riser – the formation of the liquid column. This is the phenomenon that the criterion for large-scale instabilities will seek to address.

5.1.2 Criterion for Large Scale Instabilities

As mentioned above, the formation of a liquid column in the riser is unique to severe slugging and other unstable flows. During severe slugging 1 this corresponds to the formation of the severe slug in the riser; during transitional severe slugging this corresponds to the formation of a short slug in the riser and during oscillation flow this corresponds to the accumulation of liquid in the lower limb of the riser, with the upper limb remaining predominantly full of liquid.

In the cases of severe slugging 1, severe slugging 2 and oscillation flow it has been shown through experiments, Sections 4.1 – 4.3, that no bubble penetration at the riser base occurs during the formation of the unstable columns. For severe slugging 3, there is substantial riser base gas penetration during the formation of the slug. At this point it is useful to introduce the concept of the *'critical bubble'*. This is the bubble that initiates the blowdown of the pipeline gas, either to the separator pressure (in the

case of severe slugging 1 and severe slugging 3) or to an intermediate pressure (as in the case of severe slugging 2 and oscillation flow).

Relating the characteristics of unstable flow in the pipeline/riser to the bubble behaviour at the riser base, the limiting condition for unstable flows is the lack of penetration of the riser base by the pipeline gas during liquid accumulation in the lower limb of the riser. In this case no bubble or slug tail can accelerate into the riser base, the condition for which is given in the previous section. Thus by reversing the inequality, the condition for no bubbles penetrating the riser base is:

$$\frac{dP_P}{dt} \leq \frac{dP_B}{dt} \qquad (5.13)$$

This is the inequality that will form the basis of the criterion for large-scale instabilities.

At this point, it is useful to examine the approaches of Bøe (1981) and Pots et al. (1985). In each case, the accumulation of a liquid slug was stated as the condition for severe slugging and the criteria is summarised in Equation (5.13). However both Bøe (1981) and Pots and co-workers (1985) examined the accumulation of liquid head in the riser and the gas pressure during slug build-up. However, as shown in Section 4.8.2, the transition lines generated from these criteria are unable to cover the range of unstable flows experienced.

5.2 Development of Criterion

The approach of this criterion is to assume the effect of a gas bubble penetrating the riser base and the effect of this on the riser base pressure and the pipeline gas pressure. Figure 5.2 shows the geometry under consideration in this case.

5.2.1 Model Assumptions

The following assumptions are made in the analysis:

1. Pressure at the riser base and in the pipeline is equal to the inlet pressure
2. Inlet superficial gas and liquid flows are constant
3. The gas pressure in the separator is constant
4. Liquid fraction in the pipeline is constant
5. The bubble entering the riser base is a Taylor bubble, Tin and Sharshar (1991)
6. The volume of the gas bubble nose entering the riser base is negligible compared to the gas volume in the pipeline, hence the volume of gas in the pipeline is constant
7. Frictional and acceleration pressure drop in the riser are negligible compared to the hydrostatic pressure drop, given the low velocities in the pipeline and riser
8. The gas phase acts as an ideal gas
9. The entire system is isothermal

10. The geometry of the pipeline/riser base is symmetrical about the minimum point, i.e. $\theta = \beta$.

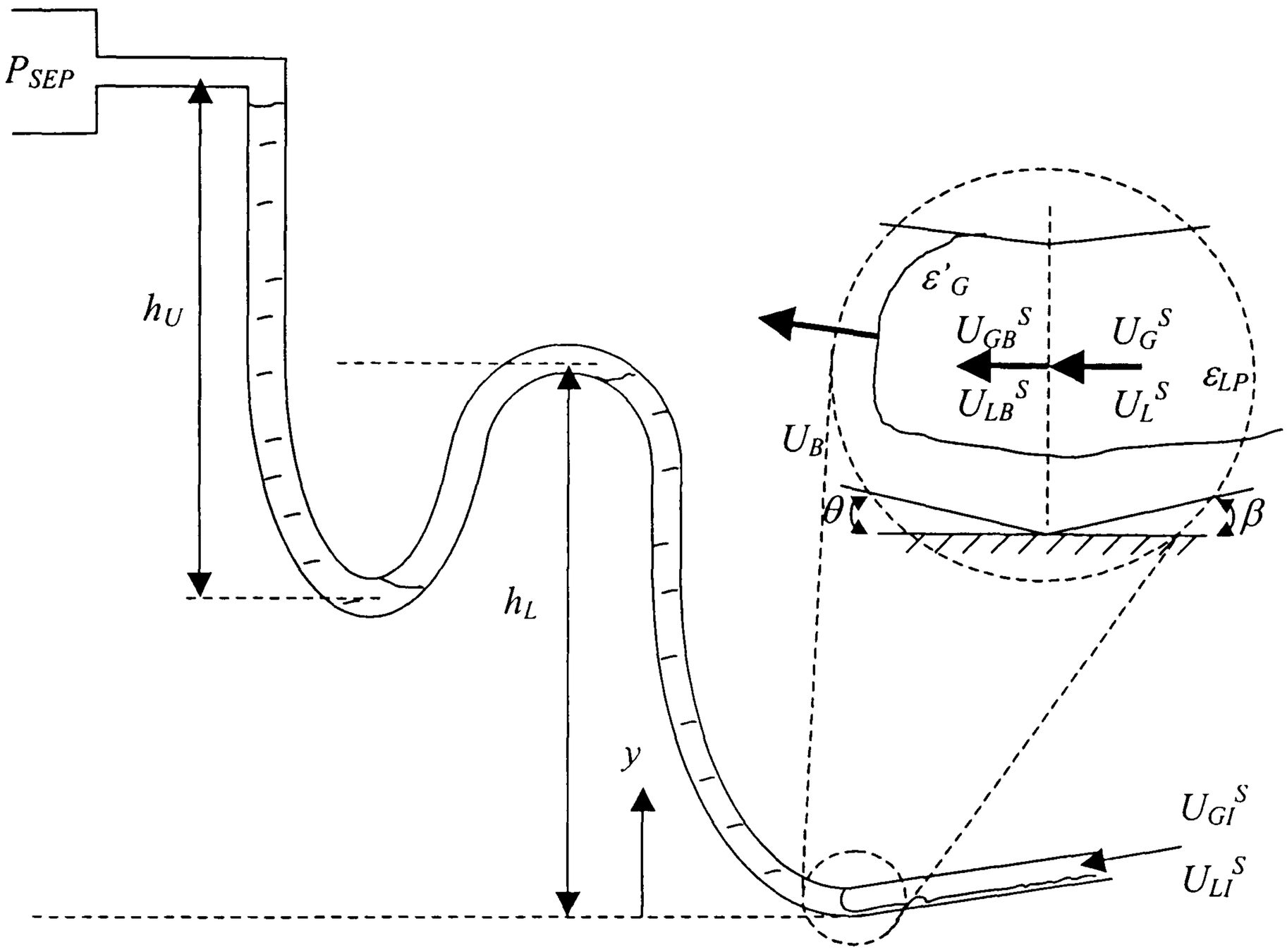

Figure 5.2 – Geometry at Base of S-Shaped Riser

5.2.2 Pressure Change in the Pipeline

The pressure change in the pipeline gas is obtained from a mass balance on the gas, where the basic balance equation is:

$$\text{IN} - \text{OUT} = \text{ACCUMULATION} \qquad (5.14)$$

Substituting the relevant terms into Equation (5.14):

$$\rho_G A_P U_{GI}^S - \rho_G A_P U_{GB}^S = \frac{dM_{GP}}{dt} \qquad (5.15)$$

In order to resolve the mass of gas in the pipeline, the Equation of State for the gas is used, giving:

$$PV = nRT = \frac{M}{M_W} RT \Rightarrow M = M_W \frac{PV}{RT}$$

Thus the rate of change of gas mass is:

$$\frac{dM}{dt} = \frac{M_W}{RT}\left[V\frac{dP}{dt} + P\frac{dV}{dt}\right]$$

$$= \frac{M_W V}{RT}\frac{dP}{dt} + \frac{M_W P}{RT}\frac{dV}{dt}$$

$$= \frac{M}{P}\frac{dP}{dt} + \frac{M}{V}\frac{dV}{dt}$$

In the pipeline/riser system, this gives:

$$\frac{1}{M_{GP}}\frac{dM_{GP}}{dt} = \frac{1}{P_P}\frac{dP_P}{dt} + \frac{1}{V_{GP}}\frac{dV_{GP}}{dt} \qquad (5.16)$$

Using the simple relations:

$$M_{GP} = \rho_G V_{GP} \qquad (5.17)$$

and

$$V_{GP} = \varepsilon_G A_P L_P \qquad (5.18)$$

Equation (5.16) becomes:

$$\frac{dM_{GP}}{dt} = \frac{\rho_G V_{GP}}{P_P}\frac{dP_P}{dt} + \rho_G\frac{dV_{GP}}{dt} \qquad (5.19)$$

Recalling Assumption 3, the change in the gas volume is zero, hence Equation (5.19) becomes:

$$\frac{dM_{GP}}{dt} = \frac{\rho_G \varepsilon_{GP} A_P L}{P_P}\frac{dP_P}{dt} \qquad (5.20)$$

Substituting this into Equation (5.15) gives:

$$\rho_G A_P U_{GI}^S - \rho_G A_P U_{GB}^S = \frac{\rho_G \varepsilon_{GP} A_P L_P}{P_P}\frac{dP_P}{dt} \qquad (5.21)$$

Rearranging this yields the right hand side of Equation (5.13):

$$\frac{dP_P}{dt} = \frac{P_P}{\varepsilon_{GP} L_P}\left(U_{GI}^S - U_{GB}^S\right) \qquad (5.22)$$

5.2.3 Pressure Change at the Riser Base

The pressure change at the riser base is calculated using a pressure balance over the riser as a whole, where the basic balance equation is:

$$P_B = P_S + \Delta P_F + \Delta P_{ACC} + \Delta P_{HYD} \qquad (5.23)$$

Neglecting frictional and acceleration pressure drop, the balance equation reduces to:

$$P_B = P_S + \Delta P_{HYD} \qquad (5.24)$$

When the bubble front has penetrated a small distance y up the riser, the balance equation becomes:

$$P_B = P_S + \rho_L g\left(h_R' - y\right) + \rho_L g\left(1 - \varepsilon_G'\right)y + \rho_G g \varepsilon_G' y \qquad (5.25)$$

The effective height of liquid in the riser is used in Equation (5.25) to yield the correct hydrostatic head. A discussion of the effective riser height for hydrostatic head calculations is presented in a Section 5.3.4. It is assumed that the gas density at the riser base is the same as in the pipeline, following directly from Assumption 1. The last two terms in Equation (5.25) account for the hydrostatic head in the film behind the bubble front, with ε'_G being the void fraction behind the bubble nose.

Differentiating Equation (5.25) with respect to time, recognising that the effective height of liquid in the riser, h_R', is a constant, gives:

$$\frac{dP_B}{dt} = -\rho_L g \frac{dy}{dt} - \rho_L g \varepsilon_G' \frac{dy}{dt} + \rho_g g \varepsilon_G' \frac{dy}{dt} + \rho_L g \frac{dy}{dt} \qquad (5.26)$$

Which can be simplified to:

$$\frac{dP_B}{dt} = -g\left(\rho_L - \rho_G\right)\left(\varepsilon_G' \frac{dy}{dt}\right) \qquad (5.27)$$

When y is small the bubble rise velocity dy/dt may be approximated by:

$$\frac{dy}{dt} = U_B \sin\theta \qquad (5.28)$$

where θ is the angle of inclination, in this case at the riser base. Using the Zuber and Finlay (1965) relation for a Taylor bubble:

$$U_B = \frac{U_G^S}{\varepsilon_G} \qquad (5.29)$$

and assuming that for a small y, $dU_G^S/dt = 0$ with $\varepsilon_G = \varepsilon'_G$ and $U_G^S = U_{GB}^S$, gives the final form for the pressure change at the riser base:

$$\frac{dP_B}{dt} = -g \sin\theta (\rho_L - \rho_G) U_{GB}^S \qquad (5.30)$$

5.2.4 Final Formulation

Combining Equations (5.13), (5.22) and (5.30):

$$\frac{P_P}{\varepsilon_{LP} L_P} \left(U_{GI}^S - U_{GB}^S \right) \leq -g \sin\theta (\rho_L - \rho_G) U_{GB}^S \qquad (5.31)$$

Which then gives the final form of the criterion:

$$U_{GI}^S \leq \left[1 - \frac{g \varepsilon_{LP} L_P \sin\theta (\rho_L - \rho_G)}{P_P} \right] U_{GB}^S \qquad (5.32)$$

This can be stated in terms of the separator pressure and the effective height of liquid in the riser:

$$U_{GI}^S \leq \left[1 - \frac{g \varepsilon_{LP} L_P \sin\theta (\rho_L - \rho_G)}{\left(P_S + \rho_L g h_R' \right)} \right] U_{GB}^S \qquad (5.33)$$

Thus the criterion states that in order to prevent a bubble penetrating the riser base, the inlet gas velocity U_{GI}^S must be lower than some critical gas velocity. Thus the critical velocity depends on the ratio of the hydrostatic head in the pipeline and riser.

5.3 Implementation Issues

Examining Equations (5.32) and (5.33), there are two variables to be determined before calculating the maximum allowable inlet gas velocity for unstable flows. These are the gas velocity entering the riser base, U_{GB}^S and the pipeline liquid holdup, ε_{LP}. The pipeline liquid holdup is calculated using the method of Taitel (1986), detailed in Appendix E. The calculation of the gas velocity entering the riser base and associated issues is discussed in the following sections.

5.3.1 Velocity of Gas Entering the Riser Base

The calculation of the velocity of gas entering the riser base is based upon the assumption that the bubble penetrating the riser base is a Taylor bubble. The drift-flux relation for such bubbles is:

$$U_B = C_0 U_M + U_D \qquad (5.34)$$

Where C_0 is the drift flux or distribution parameter (both terms are used), U_M is the mixture velocity and U_D is the drift velocity. Using the Zuber and Finlay (1965) relation for Taylor bubbles, Equation (5.29), Equation (5.34) becomes:

$$\frac{U_{GB}^S}{\varepsilon_G'} = C_0\left(U_{GB}^S + U_{LB}^S\right) + U_D \qquad (5.35)$$

Assumption 4 states that there is no liquid fraction change along the pipeline, hence the superficial liquid velocity entering the riser base is the same as the superficial liquid velocity at the inlet. Thus the superficial velocity of gas entering the riser base is obtained from:

$$U_{GB}^S = \left(C_0 U_{LI}^S + U_D\right)\left(\frac{\varepsilon_G'}{1-\varepsilon_G' C_0}\right) \qquad (5.36)$$

Thus, the superficial velocity of gas entering the riser base can be obtained from the inlet liquid velocity providing the void fraction behind the bubble nose, the distribution parameter and drift velocity are known. Both of these are discussed in the following sections.

5.3.2 Void fraction Behind the Bubble Nose

At this point one final assumption is made in this analysis – that the liquid fraction behind the bubble nose would be greater than or equal to the pipeline liquid fraction, i.e.:

$$\varepsilon_L' \geq \varepsilon_{LP} \qquad (5.37)$$

Or in terms of the void fraction:

$$\varepsilon_G' \leq \varepsilon_{GP} \qquad (5.38)$$

Thus, the upper bound on the value of void fraction behind the bubble nose is the pipeline void fraction. The equilibrium void fraction behind a Taylor bubble is dependent on both the fluid properties and the angle of inclination and the fluid velocities. In the case of vertical liquid slug flow Taitel (1986) developed a simple slug flow model based on the Fernandes et al. (1983) model. This model calculated the liquid fraction behind a Taylor bubble as a function of the gas and liquid

superficial velocities. Taitel (1986) found that for the air-water system in vertical flows, the liquid fraction was a constant 0.11 over a range of superficial gas and liquid velocities from 0.01 to 10 m/s. In the case of inclined slug flow, Taitel and Barnea (1990) analysed an evolving stratified liquid film behind a bubble nose to obtain the liquid height, the liquid fraction and then the void fraction. In this analysis, such a detailed model is not used. Instead a direct correlation developed by Carew et al. (1995) is employed. Carew and co-workers examined the effect of rheology on the riser velocity of a Taylor bubble in slug flows. As part of this work they developed a correlation for the gas fraction behind a Taylor bubble:

$$\varepsilon_{G,TB} = 0.59 + 0.3031\left(\frac{\theta}{90}\right)^{0.2308} \qquad (5.39)$$

This relation is valid for an Eötvös Number greater than 60, *E*ö > 60, where:

$$E\ddot{o} = \frac{\rho_L g D_P^2}{\sigma} \qquad (5.40)$$

The correlation was developed from data for bubble rise velocities from Zukoski (1966) and Carew et al. (1995) and it was shown that the Reynolds number had little effect on the relation. Examining Equation (5.39), in the case of vertical air-water flows, the limiting value of ε_G is 0.8931, corresponding closely to the value quoted by Taitel (1986).

Equation (5.39) is combined with the condition expressed in Equation (5.38) to give the following value for the void fraction behind the bubble nose as it enters the riser base:

$$\varepsilon'_G = \min\left(\varepsilon_{GP}, \varepsilon_{G,TB}\right) \qquad (5.41)$$

5.3.3 Distribution Parameter and Drift Velocity

The distribution parameter, C_0, and the drift velocity, U_D, are both functions of pipe inclination and the flow velocities. This section addresses the calculation of each of these parameters.

Distribution Parameter

Examining Equation (5.36), there are only meaningful results for:

$$\varepsilon'_G < \frac{1}{C_0} \qquad (5.42)$$

which, assuming the vertical flow value of 1.2 for C_0, gives a limiting value of ε'_G of 0.833. However, Fabre et al. (1987) state that this value corresponds roughly to the upper limit of the Taylor bubble region.

In the riser bend, the angle of inclination is tangential to the profile of the riser. At the minimum point of the riser, the tangent to the riser is horizontal, giving an angle 0°. Hence a more appropriate value for the distribution parameter in near-horizontal flows is required.

Bendiksen (1984) gives a generalised formula for the calculation of the distribution parameter based on experimental data for inclinations from -30° to 90°. For upward inclined pipes, Bendiksen (1984) recommends:

$$C_0(\theta) = C_0^H + \left(C_0^V - C_0^H\right)\sin^2\theta \qquad (5.43)$$

For $Fr_C < 3.5$. $C_0{}^H$ and $C_0{}^V$ are the horizontal and vertical values of the distribution parameter respectively, with values of 1.05 and 1.2 respectively. If $Fr_C > 3.5$, then:

$$C_0 \approx 1.2 \qquad (5.44)$$

The critical Froude number is calculated based upon the superficial liquid velocity:

$$Fr_C = \frac{U_L^S}{\sqrt{gD_P}} \qquad (5.45)$$

Drift Velocity

In the same work as before, Bendiksen (1984) gives a calculation procedure for the drift velocity in an inclined pipe:

$$U_D = U_D^H \cos\theta + U_D^V \sin\theta \qquad (5.46)$$

Where $U_D{}^H$ and $U_D{}^V$ are the horizontal and vertical drift velocities calculated using:

$$U_D^H = 0.54\sqrt{gD_P} \qquad (5.47)$$

and

$$U_D^V = 0.35\sqrt{gD_P} \qquad (5.48)$$

5.3.4 Effective Height of Liquid in the Riser

The calculation of the effective height of liquid in the riser is affected by three major considerations – the first being the flow regime under consideration; the second, the stage during that flow regime which is of interest and finally, the distribution of liquid during the stage. When considering all unstable flow behaviours presented thus far, the critical time where there the critical bubble does not penetrate the riser base is during the slug formation period (the surge formation period of oscillation). Furthermore, the time when the bubble penetration is most likely to occur is when there is the least amount of liquid in the riser, resisting the passage of gas. This

occurs immediately post-blowdown, when the riser is only beginning to fill with liquid. Hence in terms of predicting the region of unstable flows, an effective height of liquid in the riser of 0 m is used.

5.3.5 Calculation of the Criterion

The criterion for unstable flows in a pipeline/riser is calculated according to the following algorithm presented in Figure 5.3. Appendix A details the MATLAB script, slug_stability.m used to implement the equations.

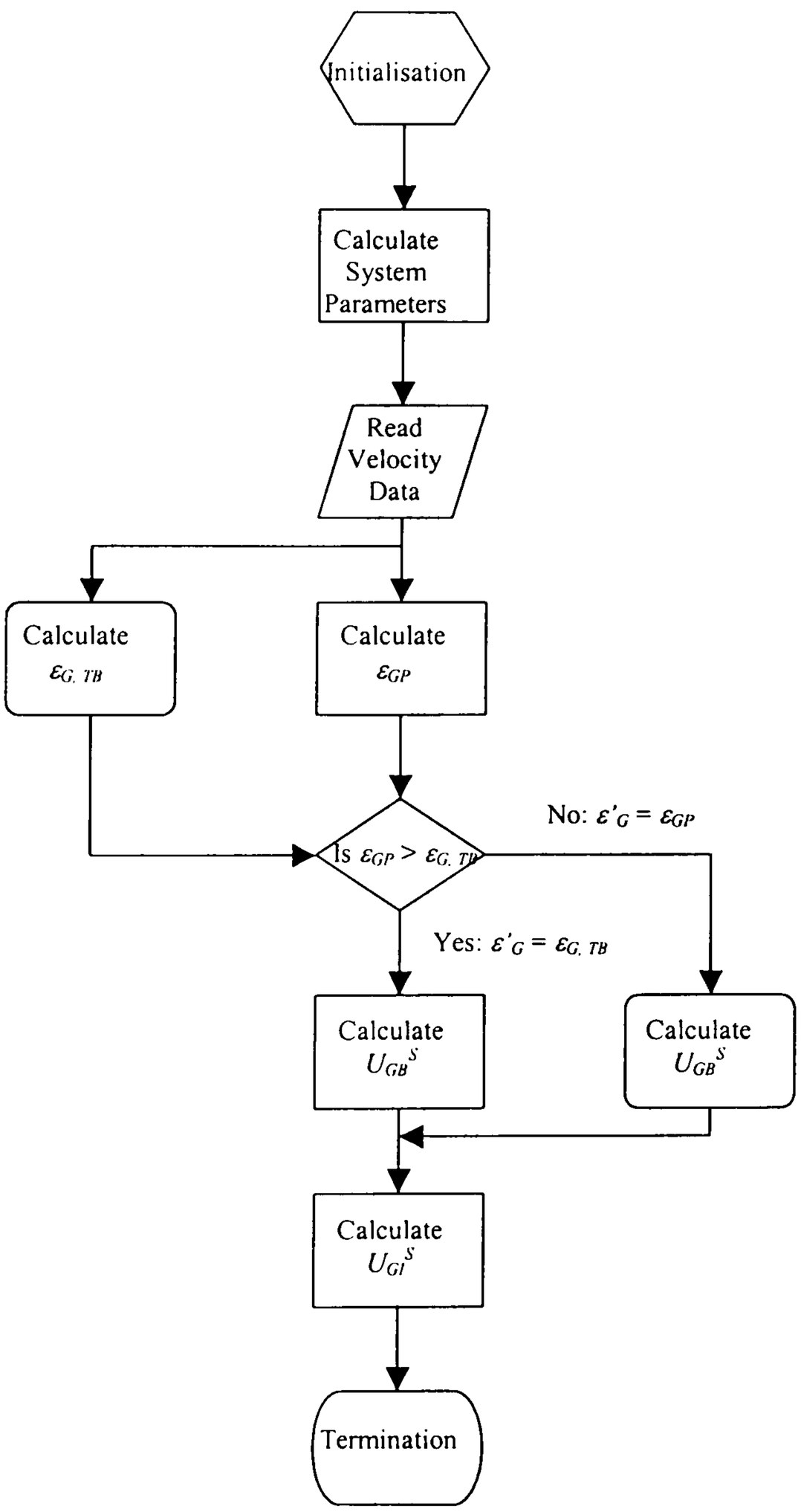

Figure 5.3 – Unstable Flow Regime Criterion Calculation Algorithm

Following Initialisation, the system parameters are found. These are - gas density from the Equation of State; the Taylor bubble film gas fraction via Equation (5.41) and the riser base pressure from a simple hydrostatic pressure balance. An inlet liquid velocity is assumed and the pipeline liquid holdup is calculated after the Taitel (1986) method detailed in Appendix E.

Based upon this value, the void fraction behind the bubble front is selected using the condition in Equation (5.41). The gas velocity entering the riser base can be calculated using Equation (5.36). Once this is found, it a simple matter of calculating the maximum inlet gas flow allowed for unstable flows to take place, using Equation (5.32) or (5.33). Through the use of the Taitel (1986) single-phase/stratified flow calculation method, the effect of the superficial liquid velocity in the pipeline is incorporated into the criterion.

A sample plot of the criterion output is given in Figure 5.4 for a 50 mm i.d., 10 m high riser with a 60 m pipeline inclined at -2° to the horizontal. This shows the region of unstable flows as predicted by the criterion against superficial gas and liquid velocities. The first edge of the envelope, indicated by the lighter line, is where the void fraction behind the penetrating bubble nose is equal to the pipeline void fraction. This section of the envelope gives the upper liquid velocity limit for unstable flows for a given superficial gas velocity. The second part of the envelope is where the void fraction is a constant, determined by the Carew et al. (1995) correlation. This section of the envelope gives the upper gas velocity limit for unstable flows for a given superficial liquid velocity.

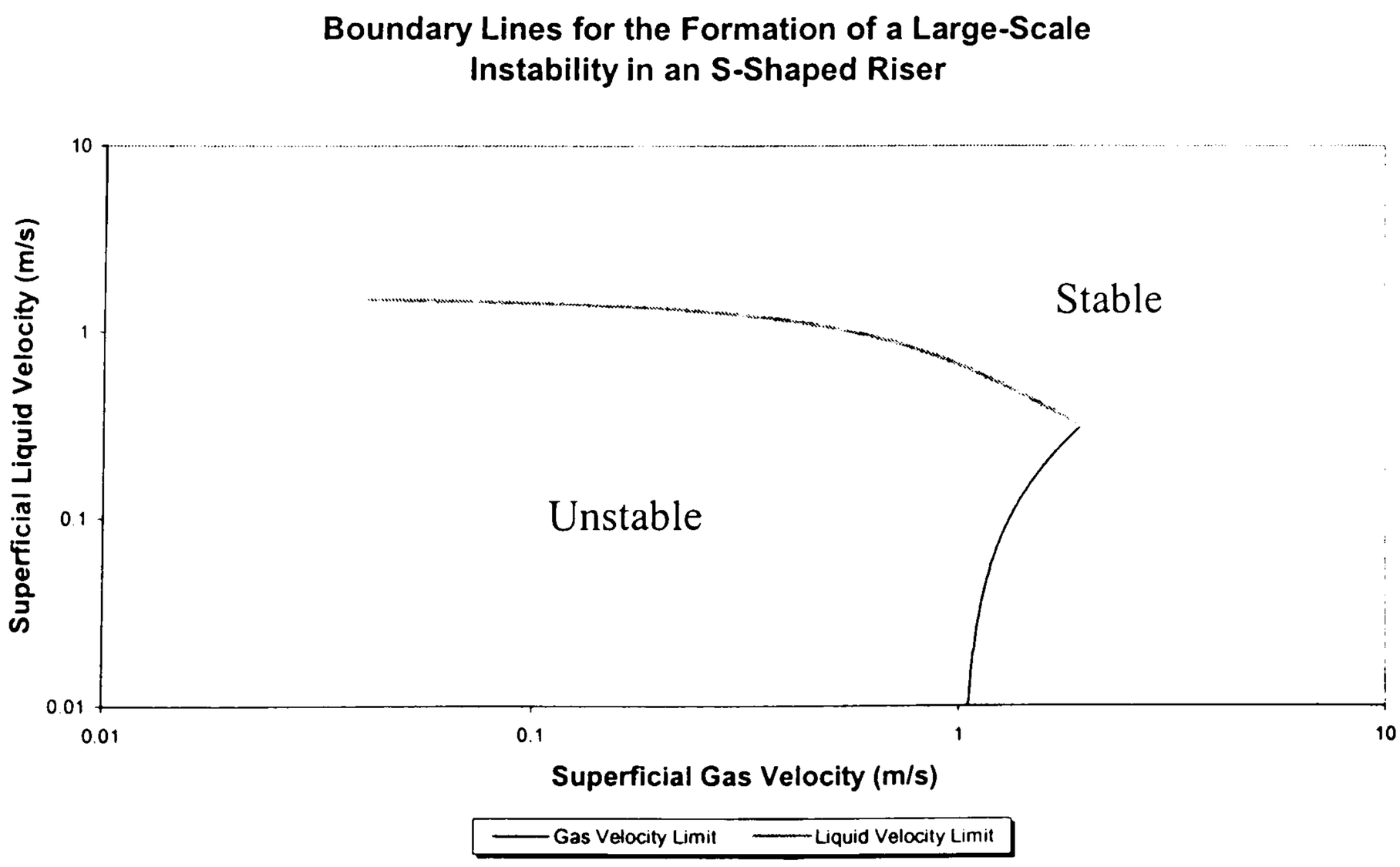

Figure 5.4 – Sample Plot of the Criterion for Large-Scale Instabilities

5.3.6 Effect of Inclination

Equation (5.32) indicates that the criterion is sensitive to inclination, directly through calculation of the criterion, Equation (5.32), and the calculation of the gas fraction behind the nose of the penetrating Taylor bubble. Previously, it has been assumed that the riser base is symmetrical for the purposes of determining θ, the angle at the riser base. In order to assess the effect of inclination, calculations have been carried out over the range 2° to 10°. The low values selected reflect the fact that the angle of inclination is tangential to the riser geometry at the riser base, which is near-horizontal. The results of these calculations are summarised in Figure 5.5

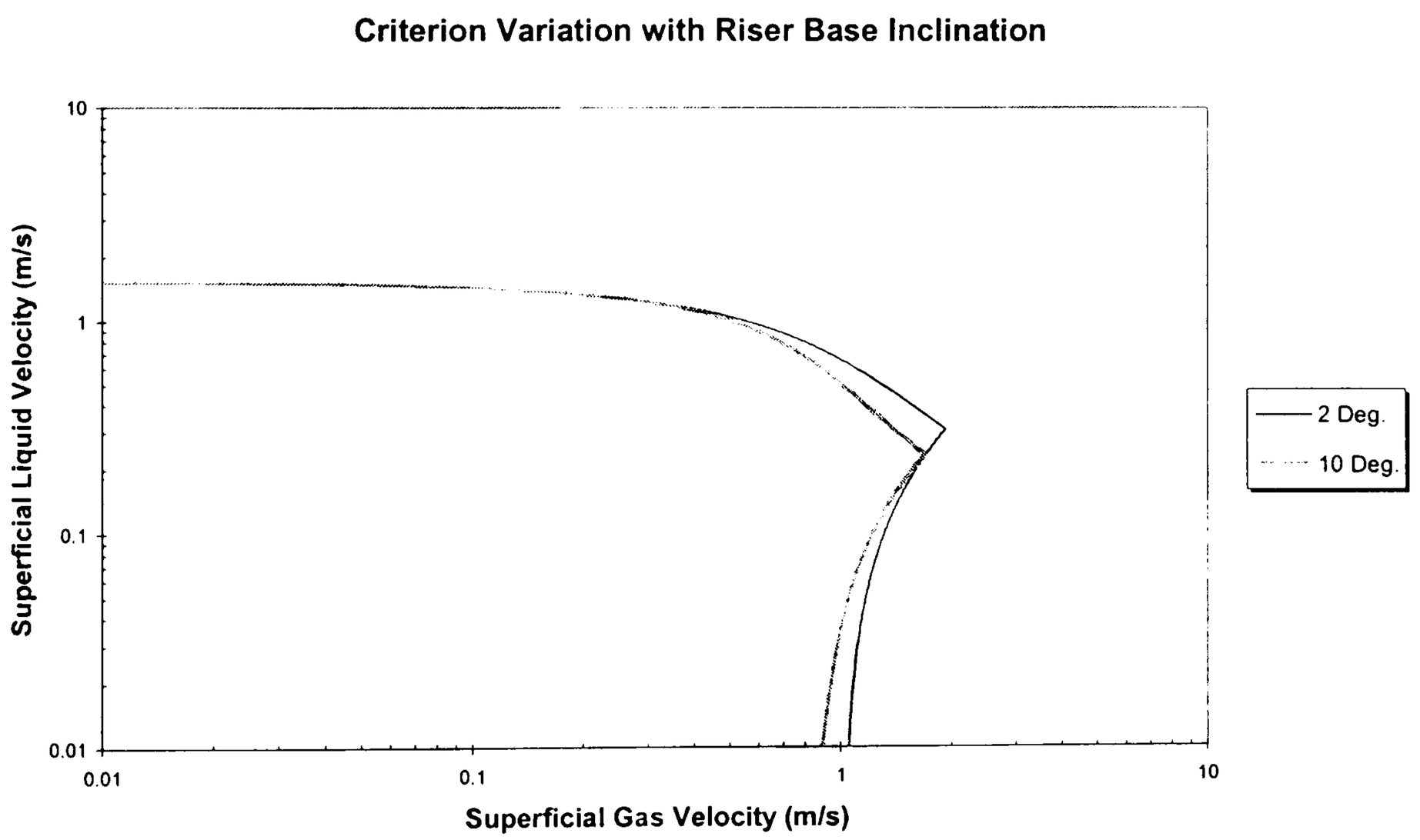

Figure 5.5 – Effect of Riser Base Inclination Angle on Criterion Results

The change in the inclination shrinks the total region of unstable flows as predicted by the criterion, reflecting a reduction in the likelihood of unstable flows as the angle of inclination increases (as predicted by the criterion). With the change in inclination from 2° to 10°, there is no change in the maximum liquid velocity at which unstable flows occur. However, there is a 12% reduction in the maximum gas velocity at which unstable flow over the same range of inclination changes. In terms of the limiting gas velocity for unstable flows at low liquid velocity (<0.1 m/s), the maximum gas velocity for unstable flows changes from 1.05 m/s to 0.894 m/s, a reduction of 15%. These reductions, at the extremes of the unstable flow envelope demonstrate the relative insensitivity of the results to variations in the angle at the riser base.

5.4 Criterion Validation

In order to test and validate the applicability of the criterion, the experimental flow regime maps presented in Section 4.7 are compared against the predicted stable/unstable transition boundaries generated by the criterion. Another set of data, generated by Tin and Incoll (1991) was made available for the present work as an independent set of data for comparison with the criterion.

5.4.1 Comparison with Experimental Data

The experimental flow regime maps developed from the experiments reported in Chapter 4 are compared against the criterion. The characteristics of the flowline/riser used in these comparisons are the same as listed in Section 3.2. The criteria of Taitel and Dukler (1976), Bøe (1981), Taitel (1985) and Pots et al. (1985) are also included in the flow regime maps for comparison with the unstable flow boundary. The results of the criteria calculations are presented in Figures 5.6 – 5.8, this covers the 2, 4 and 7 bar(a) test conditions.

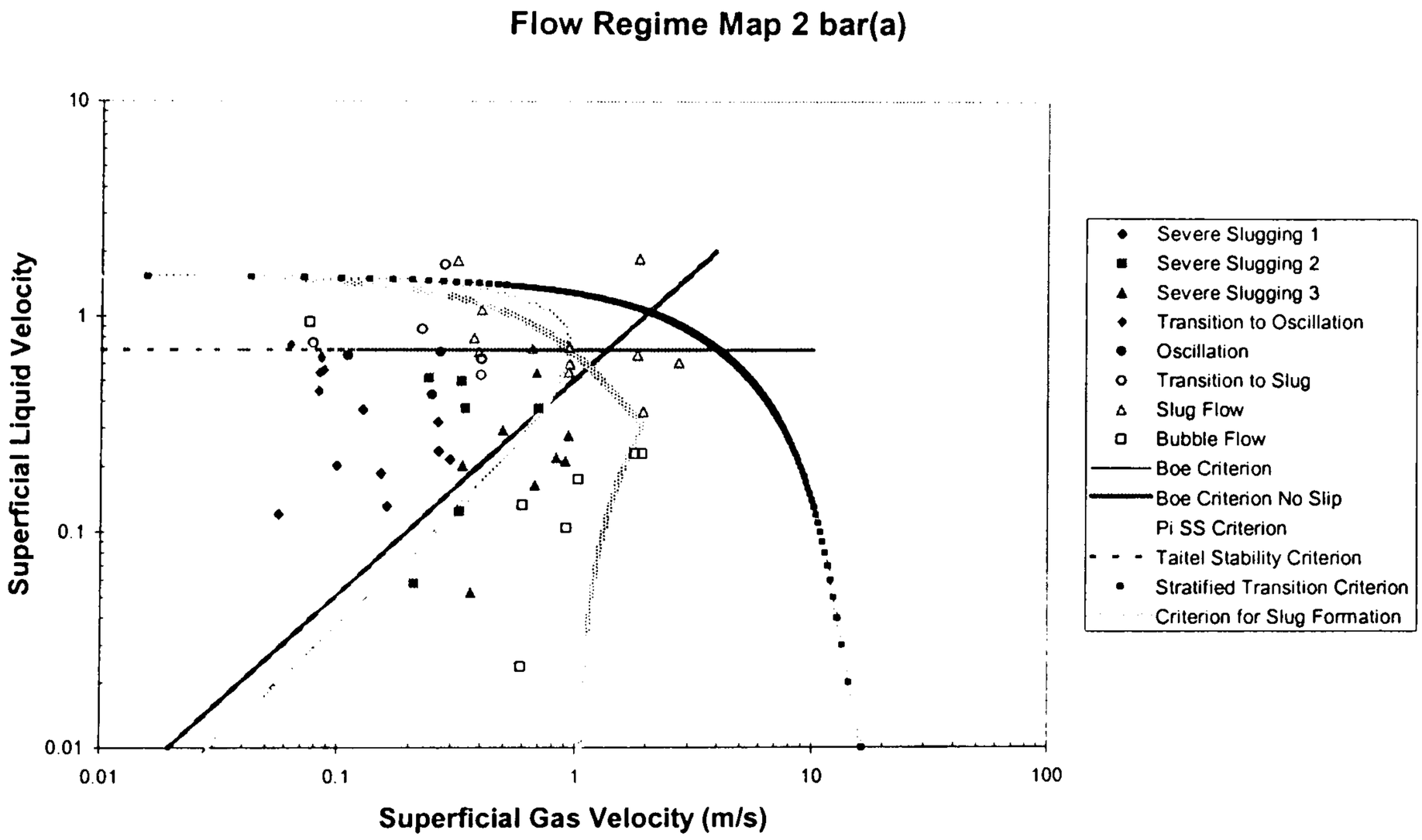

Figure 5.6 – Comparison of 2 bar(a) Experimental Data with Stability Criteria

The existing criteria demonstrate moderate success in predicting the region of unstable flows at the 2 bar(a) condition. The Taitel and Dukler (1976) flow regime boundary encompasses all unstable flow points on the map. However in terms of predicting their limits, substantially over-estimates the limiting gas velocity for unstable flows. All severe slugging 1 data points lie within the Bøe region boundary. The performance of the Bøe criterion with respect to transitional severe slugging and oscillation flows is poorer, with 50% of the transitional severe slugging lying outside

the subtended region. The Taitel transition line provides a good upper bound in terms of liquid velocity for unstable flow. The Pots et al. (1985) model performs very similarly to the Bøe criterion and gives identical results when the inter-phase slip is accounted for. When the no-slip condition is used, the performance of the Pots and Bøe criteria is reduced further, missing additional transitional severe slugging points from within the boundary.

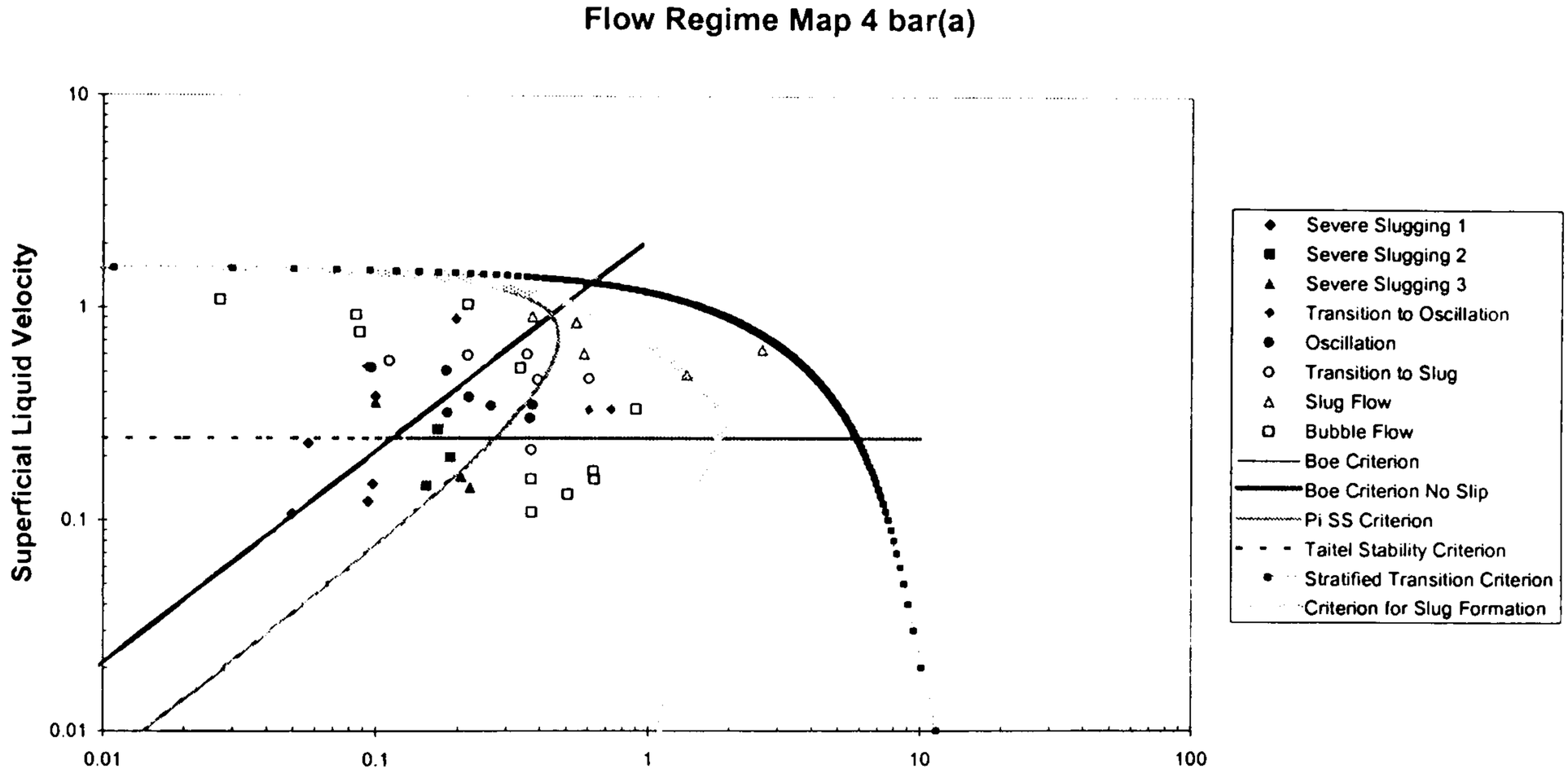

Figure 5.7 – Comparison of 4 bar(a) Experimental Data with Stability Criteria

The criterion for the development of large scale instabilities developed in this work predicts the entire region of unstable flows well in this case. There is a degree of over-prediction in terms of the maximum limits of unstable flows at the low-liquid/high-gas velocities. However in comparison to the other successful criterion at low liquid velocity, the Taitel and Dukler criterion, the unstable flow criterion prediction is an order of magnitude closer to the correct value compared to the previous prediction. At very low gas velocities, the unstable flow criterion approaches the same limit as the Taitel and Dukler and Bøe criteria asymptotically, reflecting all three criteria's use of the same correlation for the pipeline liquid holdup.

As pressure increases, the performance of the Bøe, Taitel and Pots et al. criteria degrade, with each missing more unstable flows from within their boundaries. At 4 bara, the Bøe criterion begins to miss out oscillation flow points and additional transitional severe slugging data from the predicted severe slugging region. While at 7 bara none of the observed severe slugging is within the Bøe region. At 4 bara, the Taitel criterion misses all oscillation flows, 50% of the transitional severe slugging flows and a severe slugging 1 case. At 7 bara, the transition line disappears from the flow regime map entirely, predicting no unstable flows. As before, the Pots et al. criterion behaves as the Bøe criterion when slip is used. When the no-slip condition is

used, the Pots et al. boundary does not encompass 66% of the observed unstable flows and at 7 bara, the criterion boundary is no longer on the flow regime map, missing all unstable flows. As found in Section 4.8, the Tatiel and Dukler stratified flow criterion is relatively immune to changes in pressure, and so the performance of this prediction method is largely unchanged, continuing to significantly over-predict the limiting gas velocity for unstable flows.

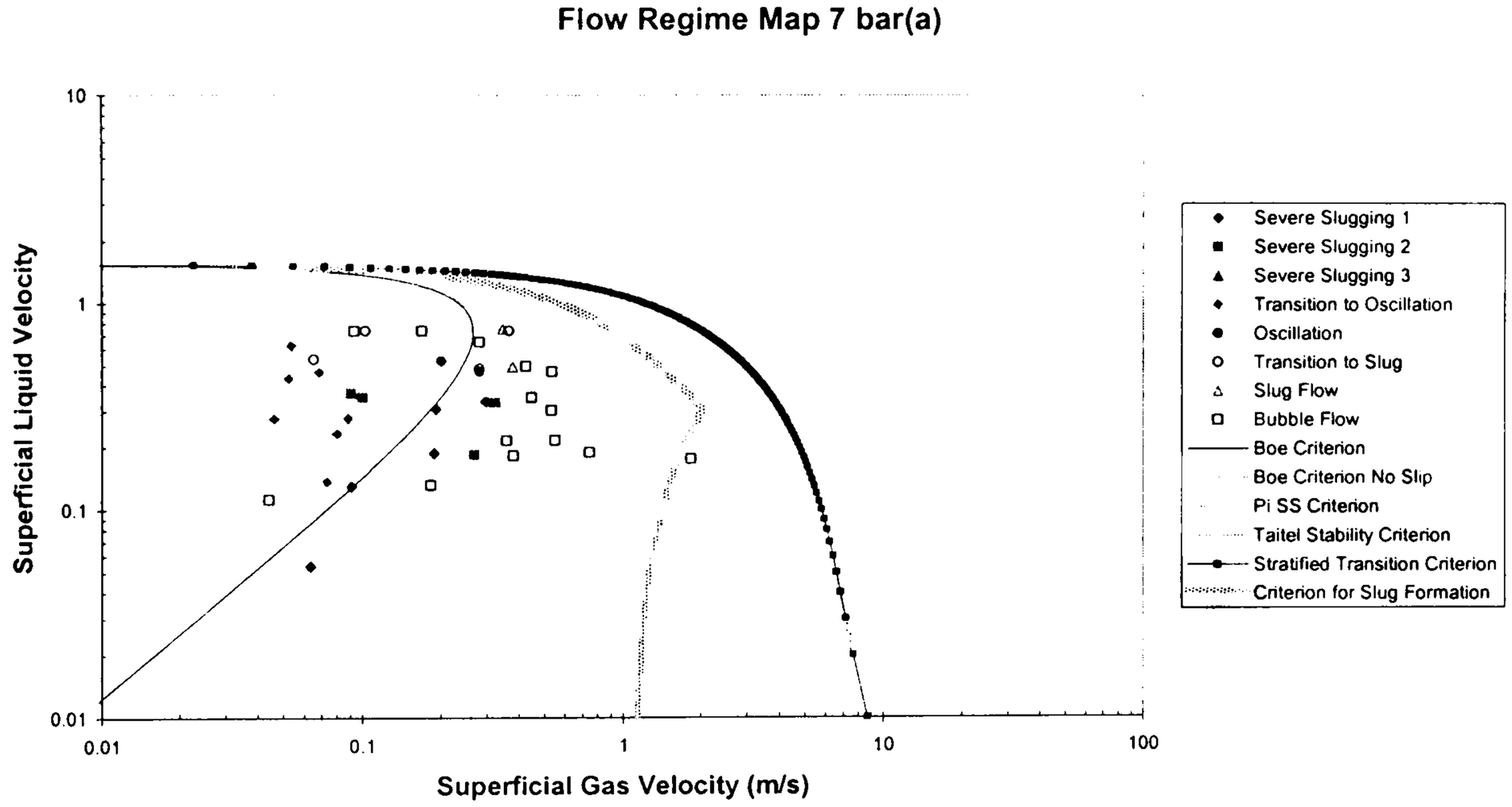

Figure 5.8 – Comparison of 7 bar(a) Experimental Data with Stability Criteria

The unstable flow criterion again shows the ability to predict the entire region of unstable flow with a reduced degree of over-prediction when compared to the existing criteria. As pressure increases, the criterion is more robust, the predicted unstable flow region continuing to cover all experimental unstable flow points. Looking at the results in detail, it can be seen that the flow region increases slightly with pressure, this is because the increased separator pressure effects the denominator in Eq. (5.33), increasing the factor for the critical velocity, increasing the maximum allowable gas velocity for unstable flows.

As is noted in Section 4.7, the reduction in the severe slugging region is attributed to the imposition of stable flows in upward inclined limbs of the riser as pressure increases. In other words, for stable flows to occur, both the upper and lower limbs of the riser must be in stable flow conditions. The criterion for unstable flows is unable to account for these flow regimes as in these cases:

$$\frac{dP_P}{dt} = \frac{dP_B}{dt} = 0 \qquad (5.49)$$

The prediction of such stable flows in the upward limb should be done using an appropriate condition for stable flow such as the universal flow regime map of Barnea (1991). Coupling such criteria with the unstable flow criterion would give an improved means of predicting the severe slugging region.

5.4.2 Comparison with Tin and Incoll (1991) Data

Data presented by Tin and Incoll (1991) was made available through the Managed Programme on Transient Multiphase Flows (TMF, 1997). Yeung (1997) previously compared the flow regime map generated for a Lazy-S riser against the predictions of existing criteria, this data is now compared against the unstable flow criterion. The data used in this comparison are detailed in Appendix D

The riser used in the experiments was a 33 m high, 50 mm nominal bore riser, discharging to atmospheric pressure. The data collected by Tin and Incoll (1991) and presented by Yeung (1997) consisted of flow regime maps using the gas and liquid velocity numbers as co-ordinates. These are given by:

$$N_G = U_{GI}^S \left(\frac{\rho_L}{g\sigma_L} \right)^{\frac{1}{4}} \qquad (5.50)$$

and

$$N_L = U_{LI}^S \left(\frac{\rho_L}{g\sigma_L} \right)^{\frac{1}{4}} \qquad (5.51)$$

where the symbols have their usual meanings. Additionally, the gas velocity was corrected to the atmospheric conditions, rather than the in-situ conditions used in this work. The conversion of the gas to in-situ conditions was carried out using an average between the maximum (54 psig) and minimum (3 psig) inlet pressures.

The data set generated gave the flow regime map shown in Figure 5.9. Comparing the existing stability criteria with the data of Tin and Incoll (1991), the Taitel and Dukler stratified flow criterion again over-predicts the region of unstable flow, by an order of magnitude. The Taitel criterion predicts the limit of severe slugging 1 with some success, though missing two severe slugging 1 cases. However, the Taitel criterion is unable to predict the limit of transitional severe slugging and oscillation flow regions, missing all cases of oscillation from within the predicted region of unstable flows. The Bøe and Pots et al criteria (with slip included) both predict the region of severe slugging 1 reasonably well, but at low liquid velocities, they under-predict the transitional severe slugging region. When a no-slip condition is used for the Bøe criterion, the entire region of unstable flows is within the region predicted by the criteria. Though this is encouraging, the fact that no upper liquid velocity limit is available when using the no-slip formulation of the criteria reduces the practical use of the criterion.

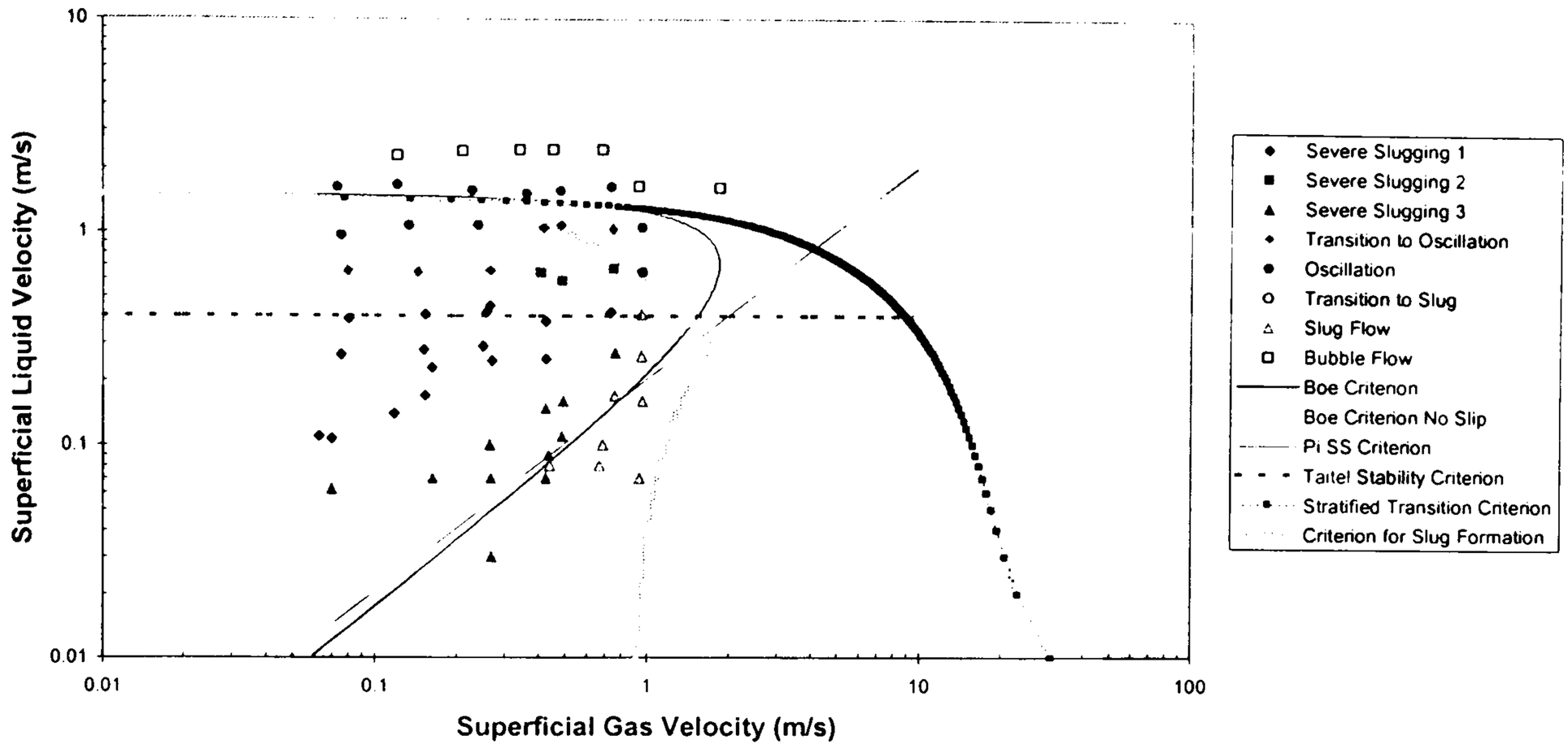

Figure 5.9 – Comparison of MPE Data (Tin and Incoll, 1991) with Stability Criteria

The criterion for large-scale instabilities on the other hand covers the majority of the unstable flow region, including many oscillation flows. All severe slugging 1 and transitional severe slugging test points are within the boundary predicted by the criterion. As before, there is a degree of over-prediction in the limit of unstable flow at low liquid flow rates. However, the results are an improvement on the existing steady-state models that have been applied to the Lazy-S riser. At high liquid flowrates, the criterion fails to encompass all oscillation flows within the predicted unstable flow region. This may be due to the liquid holdup criterion, discussed below, or the classification of the unstable flows as carried out by Tin and Incoll (1991).

Finally, as noted when examining the performance of the criteria – there are a number of oscillation cases that do not lie within any of the flow regime boundaries predicted by the criteria. It is particularly noteworthy that these tests lie above the maximum limit of superficial liquid velocity for all criteria based upon the Taitel (1986) correlation for the pipeline liquid holdup. This may thus suggest that the use of this correlation should be reviewed, and a suitable gas-liquid correlation be used. However this would require an iterative algorithm for the criteria calculations.

5.5 Summary

Based upon further investigations of flow behaviour and the performance of existing criteria for severe slugging, a criterion for the formation of a large-scale instability was developed. The criterion was based upon the premise that for such an instability to form, it was required that there was no gas penetration at the riser base prior to the filling of the upward limbs of the riser. This would allow buildup of liquid in the lower limb of the riser, to be blown out by the pipeline gas during the cycle. This

criterion also corresponds to the behaviour during liquid buildup as part of severe slugging 1 and 2.

The criterion was developed through examination of the bubble propagation into the riser base during the initial stages of bubble penetration and was tested against test data collected as part of this work.

The results showed the region delineated by the criterion successfully encompassed the entire region of unstable flow in terms of superficial gas and liquid velocity. This performance was exhibited over the full range of test pressures. When compared to existing criteria, the criterion developed showed improved performance in terms of the limiting conditions for unstable flows. Furthermore, the criterion also demonstrated successfully the ability to predict the region of unstable flows for a set of independent data.

Though successful in this case, the generality of this criterion remains to be confirmed, particularly in different riser geometries, thus supplementary experiments are required. Additionally, though the criterion does not allow prediction of stable flows, hence the prediction of bubble, slug and annular flow should also be incorporated into the criterion.

Chapter 6 – Transient Code Simulations

This Chapter details the simulation of a representative group of experimental results obtained during the experimental campaign described in Chapter 4. The motive for this work is to identify areas that pose substantial difficulty to the codes and to identify potential methodologies for the simulation of severe slugging in an S-shaped riser. The description below is broken into four broad sections: the first section covers the selected test cases; the second, the model formulation, the third section covers the simulation results and finally the fourth details some numerical experiments undertaken.

The three major commercial codes – PLAC, OLGA and TACITE, were used in this study. Sufficient information applicable to all the three codes is included in describing the model formulation. The multi-fluid models in the codes have been presented in Section 2.4.2. More detailed information can be obtained from the references included in the Section. OLGA has a Langrangian slug tracking scheme, this was not used in the study. It is impractical to present all the simulation results in this thesis. For the reasons of consistency and clarity, the output results of OLGA were used to illustrate a particular point in the discussion where appropriate.

The characteristics of interest in this investigation are the flow regime, the pressure cycling and the fluid production from the pipeline/riser and the ability of the code to predict these for the entire range of flow regimes encountered. In the test of the simulation performance, the question of how well the simulation performed as compared to the experimental measurement is addressed. To obtain a quantifiable means of assessing this performance, the code was said to give a reasonable prediction of the measured quantity if the result lay within the 99% confidence limits for the measurement. This means that the code prediction would be within the band of values that would cover 99% of the experimental results for the particular quantity of interest. These values are contained in Table 6.1.

6.1 Test Series Description

The test data were processed to give the flow regime pressure cycling characteristics and liquid production characteristics as shown. As stated in Section 4.5, the identifying characteristics for each flow regime are:

- Severe Slugging 1 – Both upward riser limbs full of liquid prior to bubble penetration and blowdown with an effective hydrostatic head over the riser greater than or equal to the riser height. Identifiable period of slug production. Pipeline gas blown down to near-separator pressure. Period of no-fluid production. Steady period of liquid production followed by a production transient and finally a gas production transient.
- Severe Slugging 2 – Both upward limbs containing pure liquid column prior to bubble penetration and blowdown. No bubble penctration at the riser base during the liquid buildup stage. Substantial amount of liquid remaining post-blowdown. Period of no-fluid production followed by a liquid production

transient and a gas production transient. Following this, a period of steady gas production.

- Severe Slugging 3 – Continuous gas penetration through the columns of liquid in each riser limb prior to blowdown. Effective hydrostatic head over the riser significantly less than the riser height. Continuous gas production from the riser with occasional slugs of liquid that have a high gas content.
- Oscillation Flow – Stable upper riser limb, with occasional surges of liquid as the lower limb liquid is blown out. There is no total liquid removal from the upper limb of the riser, however liquid from the lower limb is similar to severe slugging with most liquid removed. The pressure cycling behaviour is symmetrical about the point of highest pressure difference over the riser. Fluid production consists of surges of liquid interspersed by the delivery of high gas content surges.

These characteristics are used as the primary means of assessing code predictions of the flow regime in the riser, other parameters for examination are:

- Pressure Cycling – Both the cycle time and the individual times of each stage
- Slug Size – The size of the overall slug and the relative contributions of the liquid production transient and the steady production period.
- Peak Flow – The peak flow of liquid from the riser, also compared against the average flow over the entire simulation period.

The Test Series used in the modelling is summarised in Table 6.1 below. The Series consisted of six Test Cases, labelled A to F, that included two severe slugging 1 cases and one case each of severe slugging 2, severe slugging 3, oscillation flow and slug flow. The test condition was the 2 bara separator pressure as discussed in Section 3.7. The simulation series is summarised in a flow regime map, Figure 6.1 below, where the circles indicate the test cases.

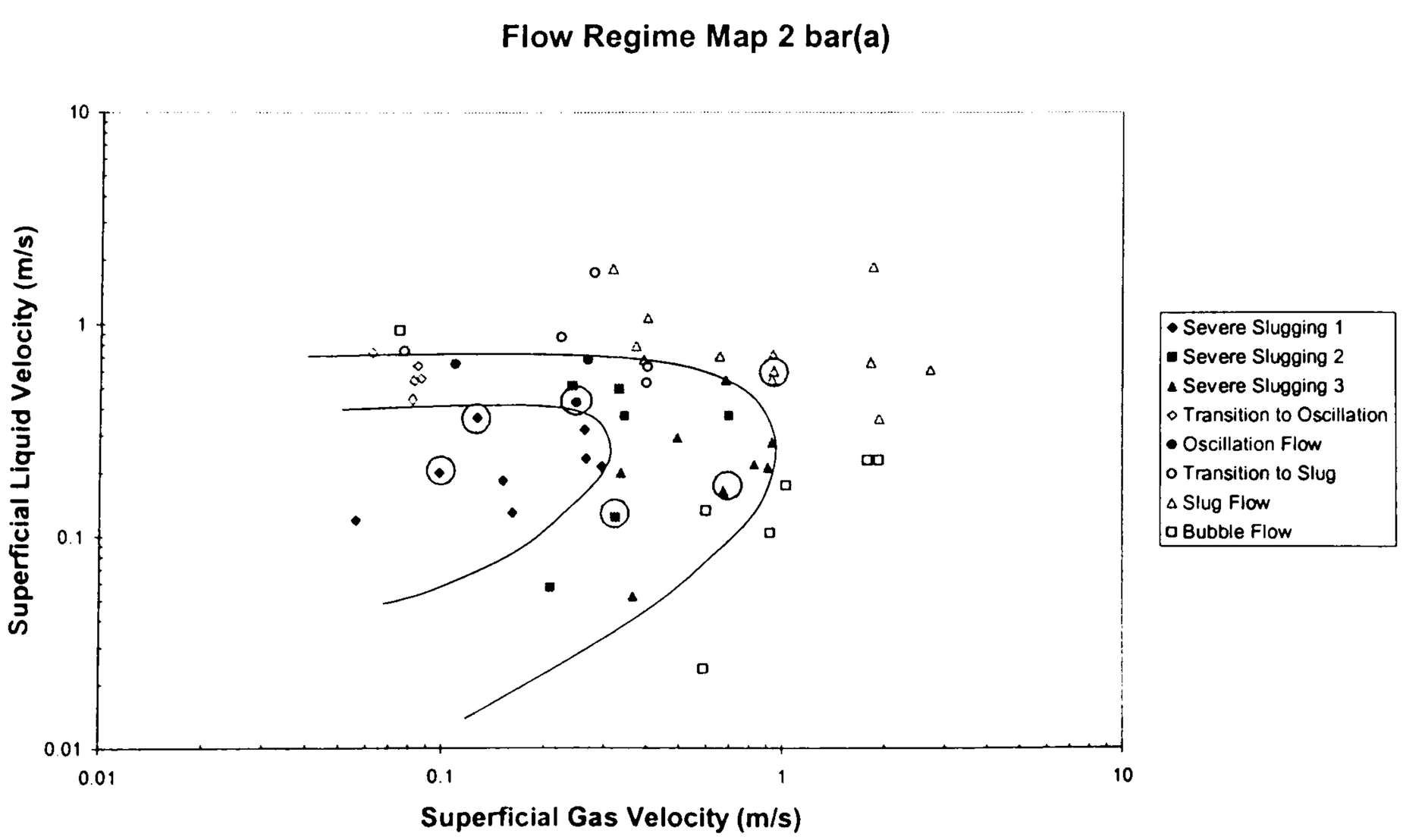

Figure 6.1 – Flow Regime Map Denoting the Test Series

Parameters (As Defined in Chapter 4)	Case A		Case B		Case C		Case D		Case E		Case F	
Flow Regime	SS1		SS2		SS2		SS3		OSC		SLUG	
Superficial Gas Velocity (m/s)	0.99		0.127		0.324		0.672		0.248		0.94	
Superficial Liquid Velocity (m/s)	0.2		0.37		0.124		0.165		0.431		0.38	
Cycle Time (s)	195.9		105		135.6		93.9		16.3		7	
99% Confidence Limits	184.2	207.5	99.2	110.7	119.7	151.4	77.6	110.2	13.7	21.2		
Buildup Time (s)	88		46.1		114		78.9					
99% Confidence Limits	76.6	99.4	42.6	49.5	104.5	123.5	68.5	89.2				
Production Time (s)	91.2		43.3									
99% Confidence Limits	84.9	97.5	39.7	46.9								
Bubble Penetration Time (s)	3.9		2.1		2.3							
Blowdown Time (s)	12.8		13.5		19.3		15					
Size of Constant Production Period (l)	47.14		38.5									
99% Confidence Limits	41.9	52.4	33.7	43.3								
Size of Production Transient (l)	38.15		41.29		34.8		24.3		16.25			
99% Confidence Limits	36.9	39.4	36.8	45.8								
Slug Size (l)	85.29		79.79		34.8		24.3		16.25			
99% Confidence Limits	90	80.6	76.4	83.2	28.6	41.1	18.1	30.5				
Production Rate Const. Period (l/s)	0.53		0.88									
99% Confidence Limits	0.57	0.48	0.84	0.93								
Peak Production Rate (l/s)	4.31		3.4		3.74		4.17		2.459			
99% Confidence Limits	4.69	3.92	3	3.79	3.29	4.19	2.22	6.1				

Table 6.1 – Test Series Summary

6.2 Model Formulation

The model used in this work consists of three major parts – a PVT description of the fluids of concern, a pipeline model and the specification of the boundary conditions. As this is a transient simulation, there are also considerations of initial conditions in the system and the integration/execution of the code. Before any of the above are presented however, the assumptions used in the model formulation are detailed.

A plain-text version of the model used in the simulations is attached in Appendix F. This provides a summary of the details presented here and can be used with any transient multiphase codes to simulate the pipeline/riser system as described.

6.2.1 Model Assumptions

Below, the basic assumptions in the model formulation are presented. The implications for each of these for the model components are discussed in the relevant sections.

1. The test fluids are air and water with standard properties
2. The fluids coexist in a two-phase mixture, i.e. any three-phase options were turned off
3. The overall system pressure is low <10 barg and the gas acts as an ideal gas
4. The heat transfer into and out of the system is small and is ignored
5. The temperature changes associated with pressure change are small
6. The temperature and pressure are low, hence no mass transfer occurs
7. The wall material is carbon steel with standard properties
8. The boundary conditions for the simulation are inlet flows an outlet pressure
9. The inlet flows and outlet pressure are constant and equal to the average measured values for each taken from the test data point
10. The inlet flow specifications are single phase gas and liquid

6.2.2 PVT Description

The PVT behaviour of the system is a look-up table of pre-calculated values for the thermodynamic variables used by the code. The exact thermodynamic variables used in each code are specific and beyond the scope of this description. In the case of OLGA, the PVT behaviour is calculated from a model consisting of a list of fluids, their fraction in the mixture and the temperature and pressure range expected in the system. This section will detail the selection of each of the above.

Component Selection and Fraction Specification

As stated above, the fluids consisted of air and water. These were simulated using a mixture of nitrogen gas and water. Where appropriate, a two-phase mixture option was selected – PVT packages are designed for two-phase oil/natural gas computations and the inclusion of water in the PVT specification causes a three-phase option to be automatically used. For all of the simulations, a Peng-Robinson calculation was used for the calculations of PVT behaviour. This is a common PVT calculation methodology used by many codes.

Though mass transfer is assumed not to occur between the phases, phase change may not be suppressed during computations in OLGA. This may allow flashing to occur within the system, particularly during the blowdown of the gas. Numerical artefacts such as over-estimated pressure changes during blowdown are an issue with predictor-corrector numerical methods, particularly when the timestep size is large. Unrealistic pressure values can then cause local flashing of the fluids, causing discontinuities in velocity and phase fraction. Though in many circumstances, this will merely prevent code execution due to PVT table errors, see timestep specification below, successful executions with inaccurate results may also occur. To prevent this, a saturated air-water mixture is used to prevent phase change. In these simulations an air-water mixture of 1:1000 in mass terms is used in the PVT file specification.

Temperature and Pressure Range

As stated above, the pressure and temperature range of the simulation is used as input to the PVT calculations. This range must not only cover the range of expected conditions within the pipeline/riser but also all conditions that the numerical scheme may encounter. This becomes important in prediction steps of the calculations, particularly if the prediction step gives a pressure or temperature value outside the range of the PVT table. Once the values are beyond the range of the PVT table, the thermodynamic properties cannot be associated with the calculation, causing a PVT table error, halting code execution. In order to prevent such table errors, a combination of timestep size (to prevent over-estimation of temperature and pressure) and PVT table limits are used. In this simulation PVT table limits of 0.5 to 10 bara (pressure) and 5 to 50° C (temperature) are used.

6.2.3 Pipeline Model

The pipeline model consists of a pipe model and a geometry model. Again the aim of this description is to provide generic information that can be used to formulate a simulation using any code.

Pipe Model

As described in Chapter 3, the pipe is made of 50 mm (2") nominal bore Schedule 40 carbon steel pipe. Thus for the simulation the following properties were used:

Property	Value	Unit
Density	7850	kg/m^3
Heat Capacity	500	J/kg C
Thermal Conductivity	50	W/m K
Internal Diameter	52.5018	mm
Thickness	10	mm
Roughness	0.1	mm

Table 6.2 – Pipe Properties

The roughness of the pipe wall was estimated from experiments conducted by Montgomery (2000, 2001), see Appendix B.

Geometry Model

The geometry model used to describe the pipeline/riser, Table 6.3, was taken from the tabulated x-y values for the riser profile, Table 3.2. The pipeline was modelled as a single pipe with an inclination of –2° to the horizontal and a length of 57.4 m. This eliminated the inflection point present in the actual pipe that would be impossible for the code to model. As there was some 35 m for the flow regime in the pipe to stabilise before entering the riser base, this was regarded as a modest simplification. Given that the input data was in the form of x-y co-ordinates, the entrance position of the pipeline was estimated, setting the base of the riser as the origin of the grid (0, 0) and using geometrical considerations, knowing that the angle of inclination was –2° to the horizontal and the overall construction length of the pipeline was 60 m.

The entire simulation length also included the 3 m horizontal section of pipe at the top of the riser, entering the separator. Earlier simulations using a variety of codes (Montgomery, 1998 and Nydal et al. 2000) have confirmed that without such a section, simulation results will give unphysical flows exiting the riser, particularly excess liquid fall-back into the riser post-blowdown.

The x-y points in Table 3.2 form a series of pipe sections of short length. These are again divided up into individual computational cells. The structure of the grid is specified such that at least two cells are in each pipe section and that the ratio of cell length from section to section is approximately two. This is in accordance with recommendations from the code developers (AEAT 2000, Decarre 2000 and Xu, 2001).

6.2.4 Boundary Conditions

Boundary conditions for the simulation consisted of an inlet and outlet boundary corresponding to the pipeline/riser inlet and outlet to the separator. Each is described below.

Inlet Boundary
The inlet boundary was specified as a flow boundary with the gas and liquid entering the first computation cell of the pipeline. The flow was modelled as two sources, one of pure gas, one of pure liquid with the same temperature. The flows were calculated from the experimental measurements of the flow into the Test Section and local temperature/pressure at the entrance to the Test Section as described in Section 3.1. These values were averaged over the test period and were assumed to be constant over the duration of the simulation.

Outlet Boundary
The outlet boundary was simulated as a constant pressure boundary with a pressure equal to the average separator pressure as measured by experiments. This is a simplification as in reality there is a variation of ±5% in the outlet separator pressure. Again this was assumed to be constant over the simulation. Temperature was also set at the average experimental value. The final parameter to be set at the outlet boundary is the gas fraction. This determines the liquid fraction gradient at the final cell boundary for the simulation and must be carefully set to prevent unphysical backflow of liquid, high backpressure or gas siphoning (Scandpower, 2002). The ideal value for this parameter in OLGA is the equilibrium gas fraction of the exiting mixture.

6.2.5 Model Execution

Model execution entails setting the time-related variables, specifically the initial conditions, the integration parameters and the output.

Initial Conditions
The requirements for initial conditions varies from code to code, furthermore, the results may or may not depend directly on the initial conditions. In the case of the OLGA model, the initial temperature equal to the separator temperature was used. Where possible these values may be omitted.

Runtime
In terms of the simulation, when beginning with all the initial conditions listed above, a significant period of time must be allowed for the simulation to reach a 'regular' state. This is the state at which the flow regime is established and the pressure cycling is consistent from cycle to cycle. Thus the simulation time was set to 1500 s initially, if additional time was required, a restart simulation was carried out until a regular behaviour was established.

Timestep Size
All codes have input parameters for the initial, maximum and minimum timestep sizes for a computation. In industrial use, simulations may be run to simulate hours or days of operation and hence a degree of flexibility is required. Each code uses an algorithm for setting the timestep size within the limits specified, selecting the maximum allowable to achieve a desired level of accuracy. Details of these algorithms are proprietary to the developers of the codes and so further discussion of

this aspect of the codes is not presented here. It is important however to select the limits of the timestep size carefully. In these simulations the timestep size was set to an initial value of 10^{-2} s with a maximum limit of 1 s and a minimum limit of 10^{-3} s. The initial value was set to assure convergence of the simulation in the initial stages of computation. The maximum limit was set to prevent the PVT table errors, while the minimum step size was set to ensure practical simulation times.

Output Options

The output from the code consists of data for the pressure, gas and liquid superficial velocities, liquid fraction and flow regime at the inlet to the pipeline/riser, the riser base, the top and bottom of the S-bend and the riser outlet. These allowed calculation of the pressure differences over the riser, the liquid holdup local to the riser base and the outlet mass flowrates for comparison with the experimental results. The frequency at which this data was outputted was 1 Hz, equal to the maximum timestep size and at least more than twice the frequency of the fastest transient expected in the system (to prevent aliasing-type problems).

6.3 Primary Simulation Results

The primary results for the simulations consist of the results from the simulations using the parameters described above. The results of the simulations are given in Table 6.3 below and in Appendix D with further detail.

6.3.1 Global Results

As shown in Table 6.3, the OLGA code is moderately successful in predicting the flow regime in the pipeline/riser. Of the 'classical' severe slugging test cases (Cases A and B), the code successfully predicts severe slugging 1 in both cases. In terms of transitional severe slugging, the code predicts severe slugging 3 in both Cases C and D where severe slugging 2 and severe slugging 3 were observed respectively. For the oscillation flow case, Case E, the code predicts a severe slugging 2. Finally, for Case F, the code predicts bubble flow.

In terms of the severe slugging pressure cycling characteristics, the code globally under-predicts the cycle time. In the cases of severe slugging, the code prediction is 82% and 92 % of the experimentally observed cycle time for Cases A and B respectively. For the transitional severe slugging cases the code prediction shows the most deviation from the experimental results, with cycles 71% of the experimental result for Case C and 45% for Case D. For Case E, the predicted cycling was 337% of the experimental value, reflecting the different flow regime predicted by the code. In the case of slug flow (Case F) there is no bulk variation in the liquid inventory of the kind observed in the previous cases, leading to large-scale pressure cycling. However there are smaller scale fluctuations in the pressure difference over the riser, in the order of 0.2 bar, coinciding with the progression of slugs through the system. In the prediction, there is a flat pressure difference profile for the length of the simulation due to bubble flow predicted by the model.

	Case A		Case B		Case C		Case D		Case E		Case F	
Characteristic	**Sim.**	**%[1]**	**Sim.**	**%**	**Sim.**	**%**	**Sim.**	**%**	**Sim.**	**%**	**Sim.**	**%**
Flow Regime	SS1		SS1		SS3[2]		SS3		SS2		Bubble	
Cycle Time (s)	160.6	82	96.8	92	96.9	71	42.3	45	54.7	337		
Buildup Time (s)	94.1	107	48.3	105	88	77	32.4	41				
Production Time (s)	54.3	60	37.1	86								
Bubble Pen. Time (s)	3.9	102	2.6	122								
Blowdown Time (s)	12.8	65	8.8	65	8.9	46	9.9	66				
Constant Production Size (l)	36.19	77	37.87	98								
Transient Size (l)	34.36	90	37.77	91	25.94	64	15.1	62	51.03	314		
Slug Size (l)	70.55	83	75.64	95	25.94	64	15.1	62	51.03	314		
Constant Prodn Rate (l/s)	0.69	131	1.11	126								
Production Peak (l/s)	5.743	133	4.687	138	6.373	121	3.6	87	5.952	242		

Table 6.3 – Main Simulation Results

[1] The % of the experimentally observed value
[2] During SS3, there is continuous gas penetration, hence no bubble penetration time

In terms of fluid production, the trend associated with the pressure cycling is reflected in the liquid production characteristics. Shorter cycle times in general leading to higher instantaneous outlet liquid flow and smaller slug sizes than observed during experiments. Similarly, longer cycle times are associated with larger slugs. Reviewing the simulation results for Case A the slug size was 83% of the experimentally determined size, while the predicted peak flow is 133% of the experimental measurement. However in Case B, where the predicted pressure cycling characteristic is much closer to the experimental measurement, the same characteristics differ some 98% and 138% for slug size and peak flow respectively. For transitional severe slugging, the predicted slug size and peak flows differ more significantly from the experimental results, reflecting the agreement between the predicted and experimental pressure cycling characteristic. For Case C, the predicted slug size and peak flow are 64% and 121% of the experimental values and for Case D, the slug size and peak flow were 62% and 87% of the experimental results. This could be due to the differences in the overall flow regime, i.e. the code predicting a completely different flow regime to that observed experimentally. Similarly to case above, the code prediction of slug size and peak flow for Case E, the oscillation flow case, were vastly different from the experimental results with a slug size and production peak of 314% and 252% respectively.

6.3.2 Detailed Results – Severe Slugging 1

In order to determine the reasons for the differences between the code and the experimental results, a more detailed examination of the results is required. As stated above, the duration of the severe slugging 1 cycles, as obtained from the simulations were less than the experimental results. In each case the predicted liquid buildup and slug production times were different to those observed – the liquid slug buildup period was longer and the slug production case was shorter than experimental values. This difference is reproduced in Figure 6.2, showing a comparison between the experimental results and the code prediction.

For Case A, the liquid buildup period from the code was 94.1 s compared to an experimental value of 88 s, a difference of +6.1 s. Furthermore, the code-predicted slug production period was 54.3 s compared to 91.2 s for the experiments, a difference of –36.9. For Case B, the differences were +2.1 s and –6.2 s on computational values of 48.3 s and 37.1 s with experimental values of 46.1 s and 43.3 s for the liquid buildup and slug production respectively.

In both Cases A and B, the length of the slug buildup period is within the 99% confidence limits for the experimental result. This indicates that the prediction of the observed behaviour is acceptable being within the limits that cover 99% of experimentally observed liquid buildup times for this particular test condition. The predicted values for the slug production are outside a similar band for the experimental results, indicating that the slug production times are not acceptable predictions. Thus for each case, the main source of error between the simulations and the experimental results in terms of the cycle time is the slug production stage of the severe slugging.

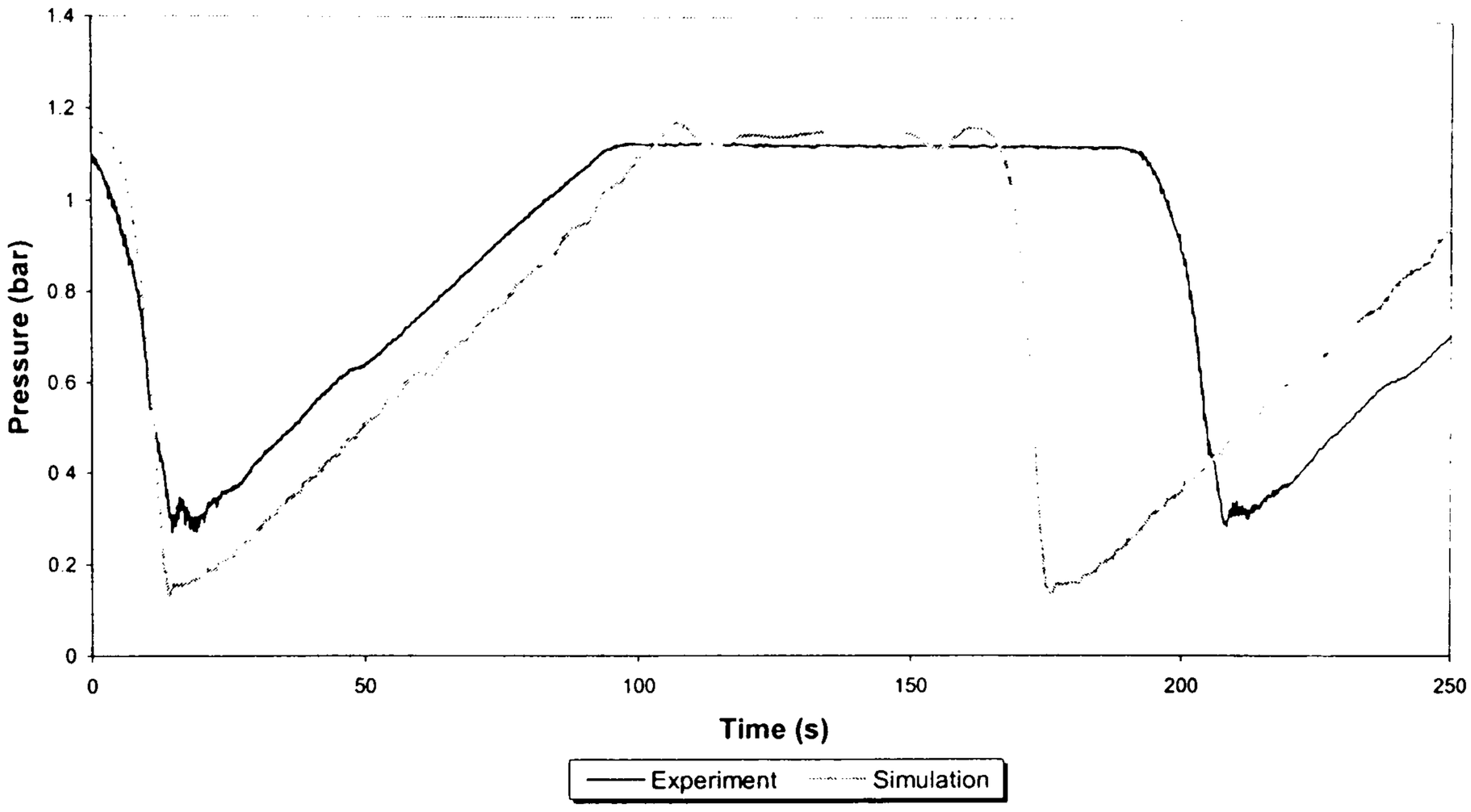

Figure 6.2 – Combined Experimental and Simulated Pressure Difference Profiles for Case A, Severe Slugging 1

Examining the results for the constant production period and the production transient, the prediction of the pipeline behaviour is highlighted as a potential source of the errors in the code results. The quantity of liquid in the constant production period reflects the amount of liquid accumulated in the pipeline and the rate of flow during the constant production period relates the rate at which the liquid is moved from the pipeline into the riser. In each severe slugging 1 case, the amount of liquid in the constant production period is less than that measured – 77% in Case A – and the rate of production during the constant production period is larger than the measured rate – 131%, also in Case A. These results indicate that the observed accumulation of liquid in the pipeline is not correctly reflected in the code prediction. The mechanism that resists the liquid accumulation in the pipeline during slug buildup and then pushes the slug out of the riser during production is the gas accumulation in the pipeline. An influx of additional (less-compressible) gas during the slug production period would act in a piston-type manner, displacing a similar volume of liquid into the riser rather than compressing into a smaller volume (the actual process). Such behaviour would cause both of the symptoms observed above in the model results. Furthermore, the incorrect prediction of the pipeline liquid holdup also affects the pipeline gas behaviour. Thus, the evidence presented above indicates that the anomalies between the experimental results and the prediction in terms of slug cycle time and the constant production period may be due to inaccurate prediction of the pipeline liquid holdup and gas compression behaviour during severe slugging.

When predicting the size of the liquid production transient, the code performance was marginal. The code gave a reasonable prediction for the production transient size for

Case B, whereas the prediction for Case A was unacceptable based upon the statistical considerations of the experimental quantity. However, the code prediction remained within ±10% of the average experimental value in each case and the size of the liquid production transient was less than the maximum potential amount of liquid in the riser (38.521 l). Thus the overall code performance in predicting the size of the production transient remains debatable. It is suggested that further tests, with a greater range of severe slugging 1 test cases, are required to fully assess the code performance in terms of the simulation results as compared to the experimental spread of results.

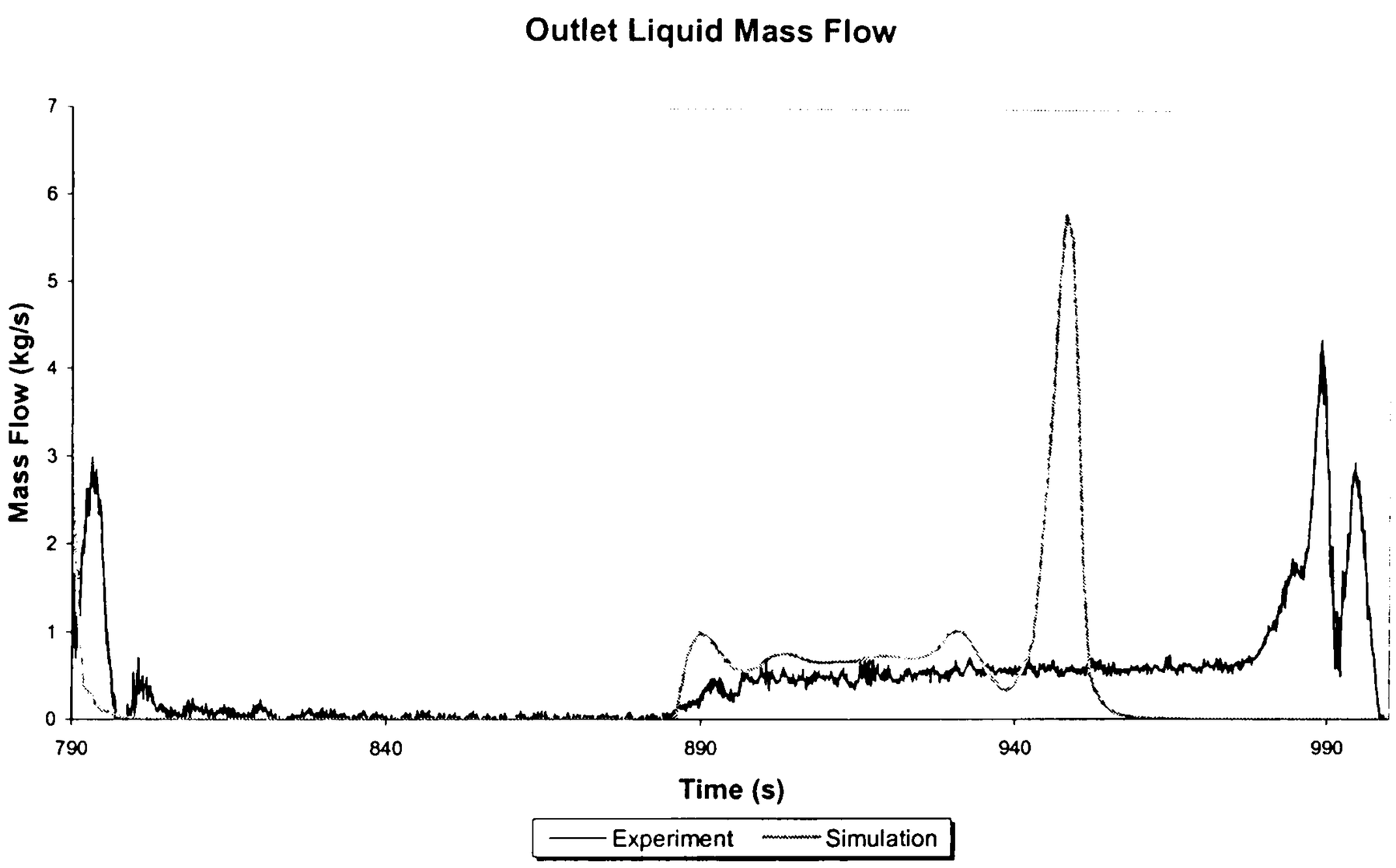

Figure 6.3 – Combined Experimental and Simulated Liquid Production Profiles for Case A, Severe Slugging 1

It was also found that the simulations over-predict the peak liquid production rate during severe slugging 1. Examining the blowdown time for the predicted severe slugging cycles, both simulation cases are 65% shorter than the experimental observation. This result reflects the faster rate of pressure difference drop over the riser which is directly related to the rate of change of the height liquid in the upward limbs of the riser (and thus the rate of liquid production). Hence, the code predicts too high a rate change in the gas-liquid interface position in the riser. Since the gas liquid-interface in the severe slug tail in a flexible riser is in the form of a Taylor bubble (Tin, 1991 and Tin and Sarshar1993) it may be suggested that the prediction of the behaviour of this bubble is a potential source of error. The model could be predicting too high a rate of bubble propagation through the riser. This propagation velocity could be a function of the bubble flow model used and the rate at which gas infiltrates the riser base as for example in the Taylor bubble case (see Chapter 5). Furthermore, the bubble is propagating through a curved pipe, the flexible riser, which is not reflected in the bubble propagation models used by any transient multiphase

code (Montgomery and Yeung, 2000b). Hence the bubble propagation model and the gas behaviour are two potential sources of error in the production transient prediction and go some way to explaining the differences between code predictions and experimental observations. Alternatively, the code may not be predicting the frictional losses in the pipe correctly during bubble penetration.

Examining the predicted liquid production profile during severe slugging 1, Figure 6.3, there is a marked difference between the predicted and experimental liquid production. In the code case, there is a single peak during the liquid transient, whereas there is a characteristic dual peak in the experimental case. Such a lack of a second peak would be due to incorrect prediction of the filling of the downcomer during the slugging cycle. This lack of second peak may also have an effect on the peak liquid production rate and the size of the liquid transient.

6.3.3 Detailed Results – Transitional Severe Slugging

This section deals with the details of the transitional severe slugging cases studied – Cases C and D. Though these are different transitional severe slugging cases, the code has predicted the same overall flow regime. Furthermore, there are some similarities in the variation between the predicted and experimental results for both cases. Thus, the description that follows will focus on the similarities in the cases before turning to case-specific issues.

In both cases of transitional severe slugging, the code predicted severe slugging 3, i.e. transitional severe slugging characterised by continuous penetration at the riser base. In fact for both the simulations, severe slugging 3 with intermittent cycles in the lower limb is observed. For Case C this is markedly different from the observed severe slugging 2, see Figure 6.4. In Case D the predicted severe slugging 3 was not wholly stable, exhibiting a variation from cycle-to-cycle in terms of cycle time and the pressure difference over the riser, see Figure 6.5. Furthermore, a high degree of gas penetration at the riser base is observed, Figures 6.6 and 6.7 below, with the riser base holdup substantially less than unity.

Examining the times for each stage of the severe slugging, it is clear that differences in liquid buildup time between the simulations and the experiments account for the main deviations. For Case C, the predicted pressure cycling time of 96.9 s was 71% of the experimental case, substantially outside the 99% limits of the experimental average of 135.6 s. With continuous gas penetration at the riser base, there is no observed period of bubble penetration in the code results. Examining the liquid buildup and gas blowdown times, both of the predicted values of 88 s and 8.9 s were 77% and 46% of the experimentally observed values – 114 s and 19.3 s respectively. Similar results are found for Case D, with predicted buildup and blowdown times 41% and 66% of the experimental values – 79 s and 15 s.

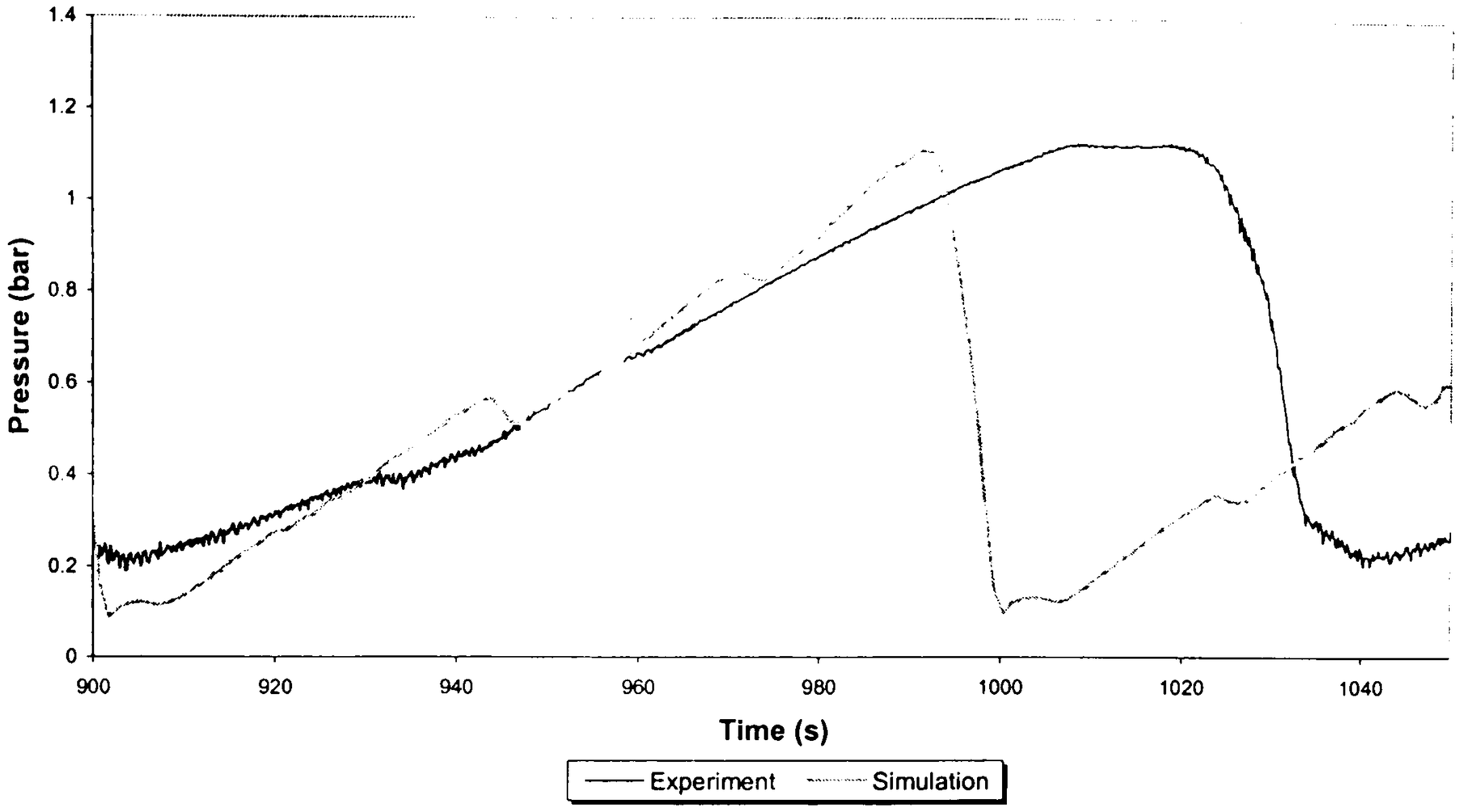

Figure 6.4 – Combined Experimental and Simulated Pressure Difference Profiles for Case C, Severe Slugging 2

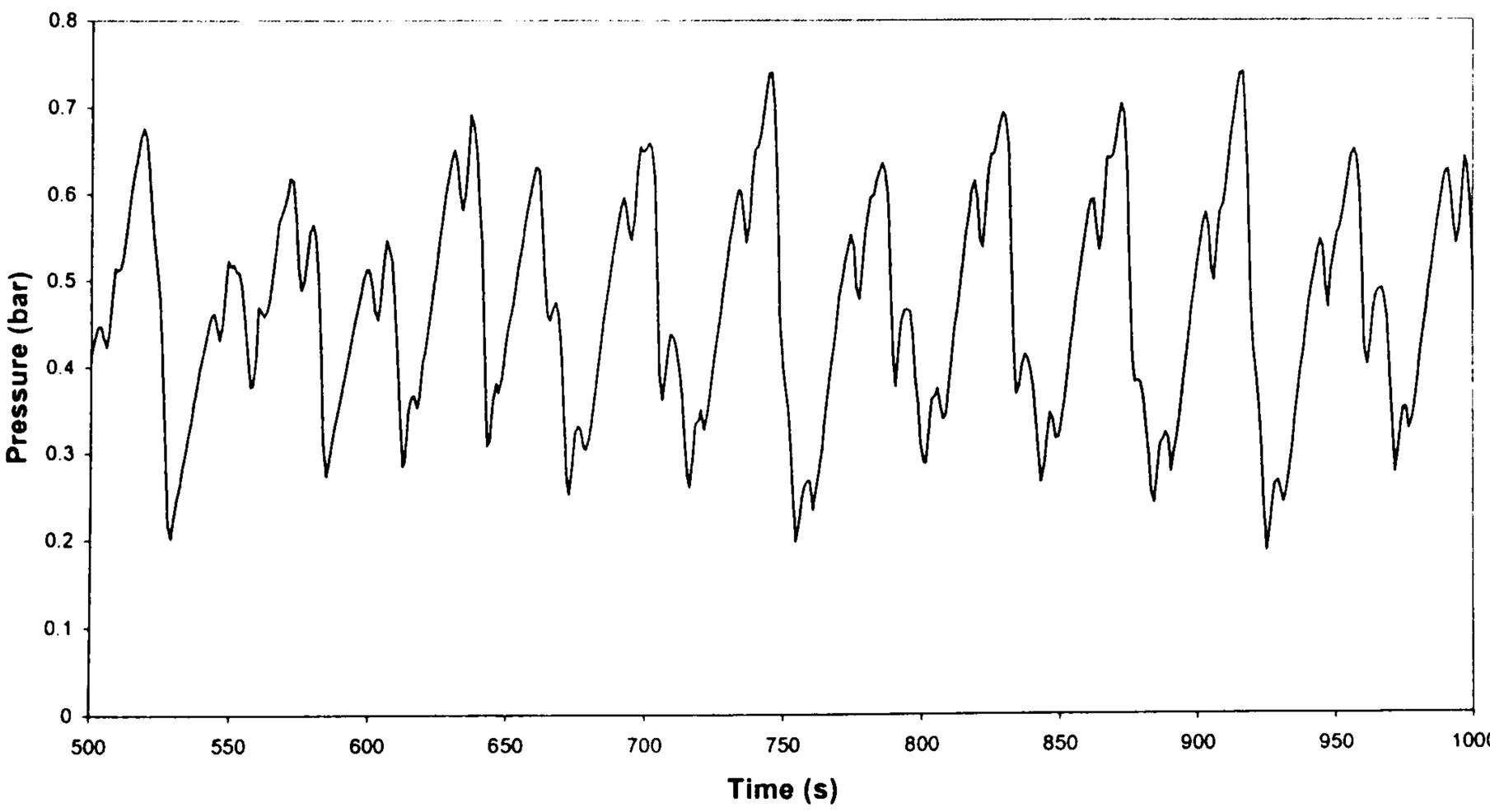

Figure 6.5 – Simulated Pressure Difference Profile for Case D, Severe Slugging 3

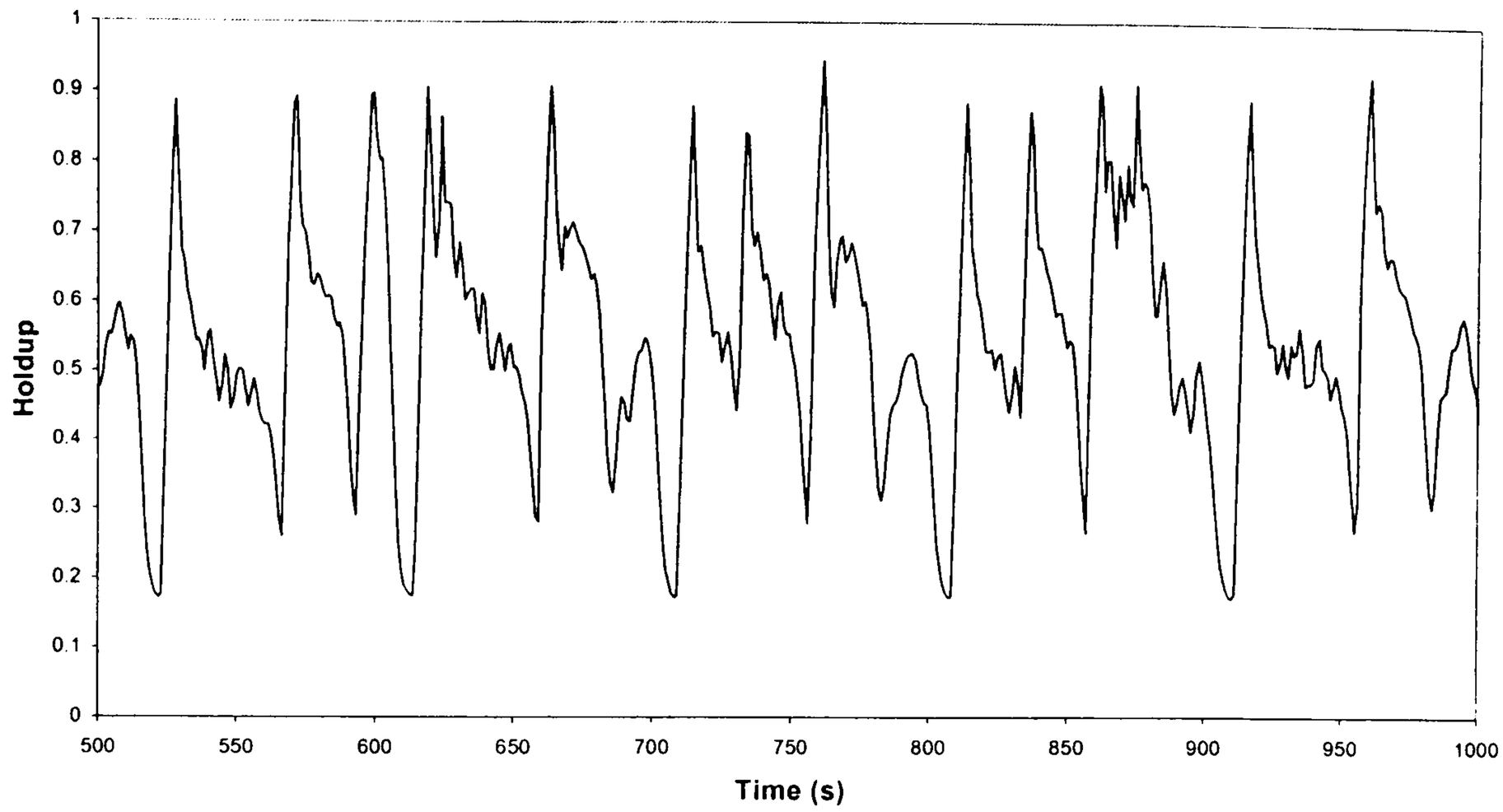

Figure 6.6 – Simulated Riser Base Liquid Holdup Profile for Case C, Severe Slugging 2

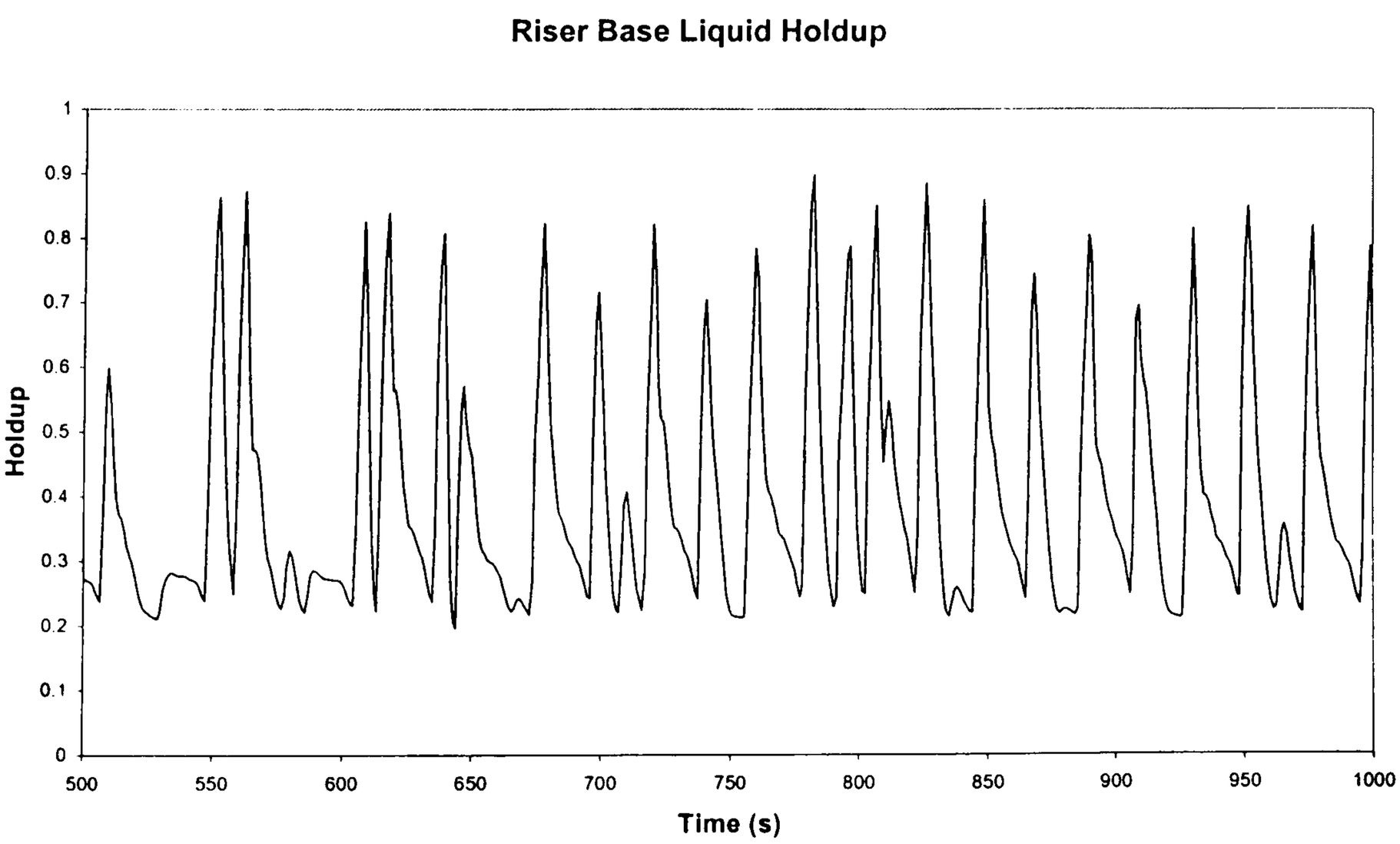

Figure 6.7 – Simulated Riser Base Liquid Holdup Profile for Case D, Severe Slugging 3

Severe slugging 2

Returning to the discussion above on the severe slugging 1 case, incorrect prediction of the pipeline behaviour is again suggested to be the cause behind the incorrect flow regime prediction of the code. The continuous gas penetration at the riser base, Figure 6.6, characteristic of the severe slugging 2, indicates that there is a lack of gas compression in the pipeline which prevents the pure liquid formation in the riser. The gas penetration is also indicative of the lack of gas accumulation within the pipeline. As suggested before in the case of severe slugging 1, this then may suggest that the code is not predicting the pipeline behaviour of the system accurately either in terms of gas behaviour or gas/liquid interface position.

The liquid production results also reflected the difference between the results. The predicted liquid slug size was 25.9 l, 67% of the experimental value of 40.4 kg, reflecting the high gas holdup in the liquid slug present during the predicted severe slugging 3. The presence of gas in the riser during the liquid buildup reduces the volume of the riser that could be occupied by liquid prior to blowdown and hence the liquid transient size.

Finally, the peak rate of liquid production from the riser was substantially over-predicted by the code. During experiments a maximum liquid flow of 3.737 l/s was observed, while the code predicted a peak flow of 6.373 l/s, 171% of the experiments. However the liquid exiting from the riser is a bubbly mixture in both the simulation and experiments. This might indicate that the relative velocity of the gas and liquid in the riser, i.e. the slip between the phases, is not correctly modelled in the curved riser geometry and that frictional losses for the bubbly mixture are not accurately predicted.

Severe Slugging 3

The severe slugging 3 predicted by the model for Case D is unstable, with variations occurring from cycle-to-cycle as evidenced in Figure 6.5. The variation in the pressure cycling is most likely caused by the degree of gas penetration at the riser base causing instability in the liquid in the riser or some numerical artefact. This is supposed given that the simulation has constant boundary conditions, hence there are no sudden pressure or void fraction waves caused by a variation in the boundary conditions. This is confirmed by comparing the predicted riser base holdup Figure 6.7 with the experimental result, Figure 6.8. There is a much lower predicted liquid holdup, evidence of an increased rate of gas penetration. By comparing this variation in the pressure cycling compared to the regular behaviour experienced in the experiments, the simulation may be judged to be predicting too much gas penetration at the riser base and an increased degree of instability in the liquid column in the riser. Hence, as before, the prediction of the pipeline gas is an area of concern in this case. Examining the slug size, the average slug size from the predicted outflow is 15.2 l, 62% of the experimental value. Again, this may be attributable to the gas penetration at the riser base. The added gas throughput in the riser during the simulation gives a liquid content less than that experienced experimentally, hence reducing the slug volume.

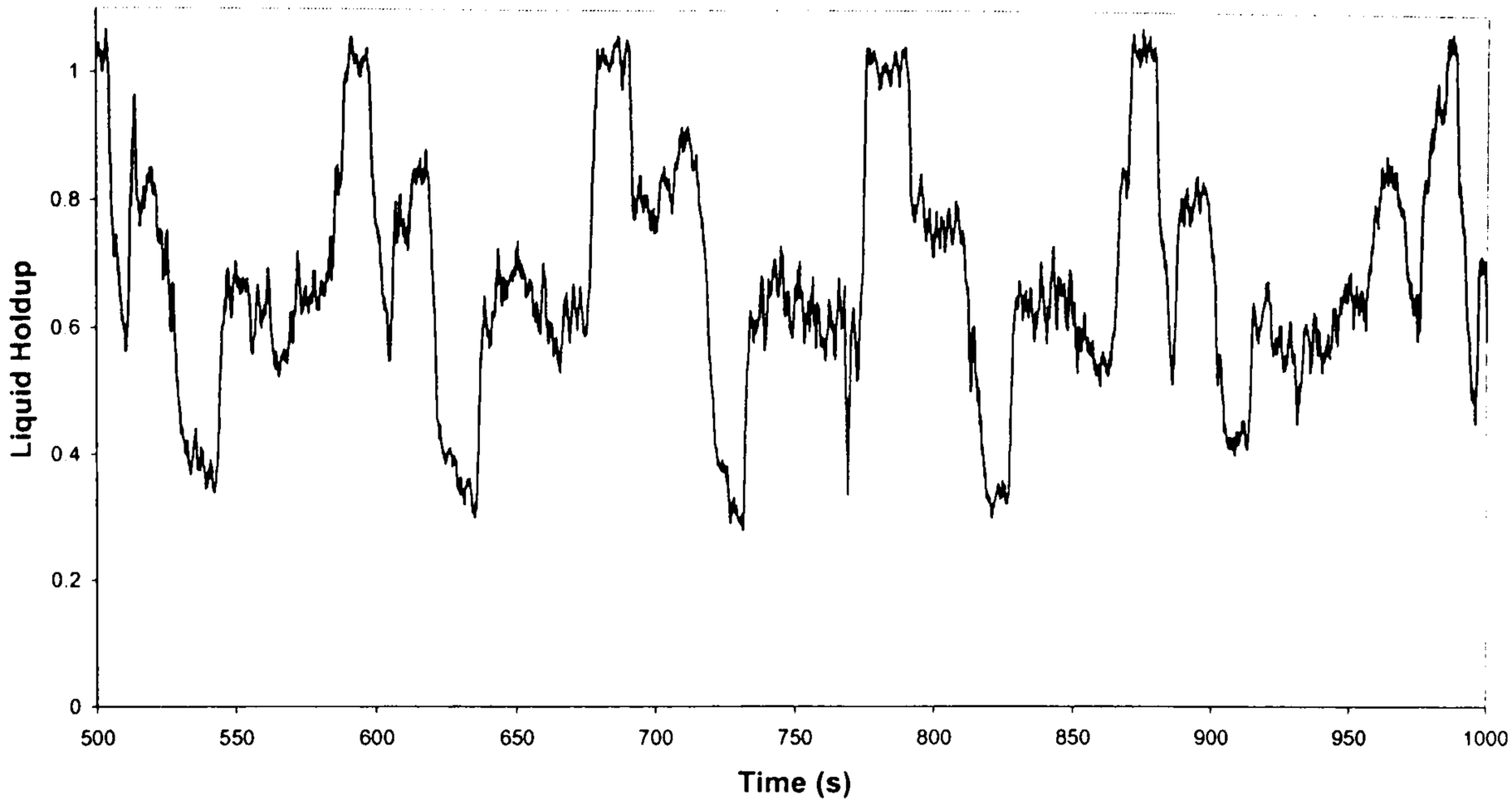

Figure 6.8 – Experimental Riser Base Liquid Holdup Profile for Case D, Severe Slugging 3

In terms of peak flow, the prediction is 87% of that in the experiments, even though there is a shorter severe slugging cycle time. There are two possible reasons for this behaviour – this first concerns the lift energy of the gas and the second relates to the bubble motion. With the gas continuously moving through the liquid mass in the riser, the potential lift energy of the gas is reliant on the quantity of gas in the pipeline prior to blowdown. Given that there is an increased gas flow through the slug in the simulation, there would be less gas accumulated in the pipeline to move the slug into the riser, the degree of gas expansion would be less, reducing the lift energy of the gas and hence the slug velocity would be reduced. In the second case, if there is an unrealistic modelling of the inter-phase slip, there would be an inaccurate prediction of the mixture velocity in the riser during blowdown, hence giving an inaccurate peak liquid flow value.

6.3.4 Detailed Results – Oscillation Flow

Again, the code has incorrectly predicted the flow regime in the pipeline/riser system – severe slugging 2 is predicted in place of the experimentally observed oscillation flow. Examining the pressure difference over each limb of the riser, Figure 6.9, it is evident that pressure cycling is predicted in each limb of the riser.

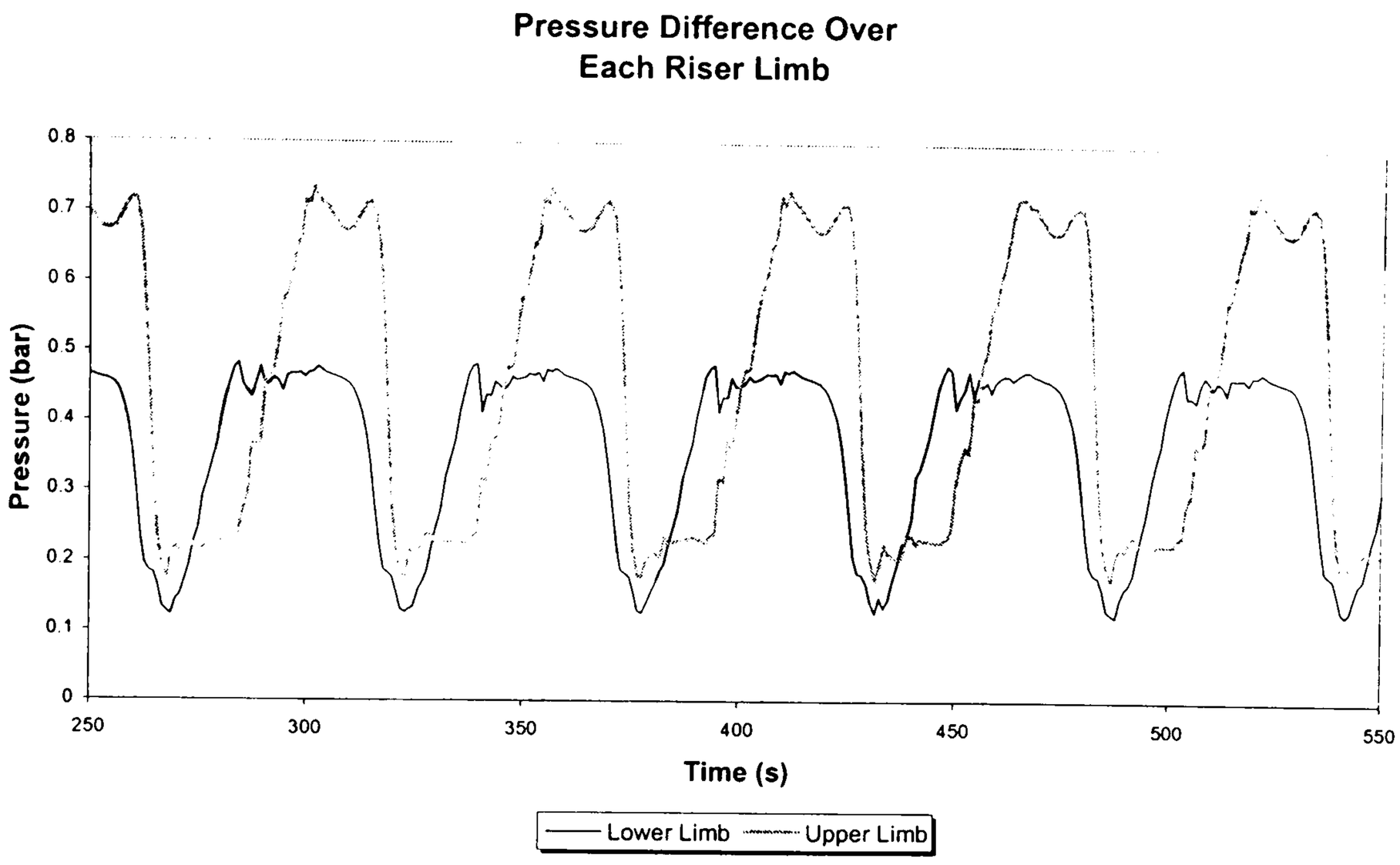

Figure 6.9 – Simulated Pressure Difference Profile Over Each Riser Limb for Case E, Oscillation Flow, Base Simulation

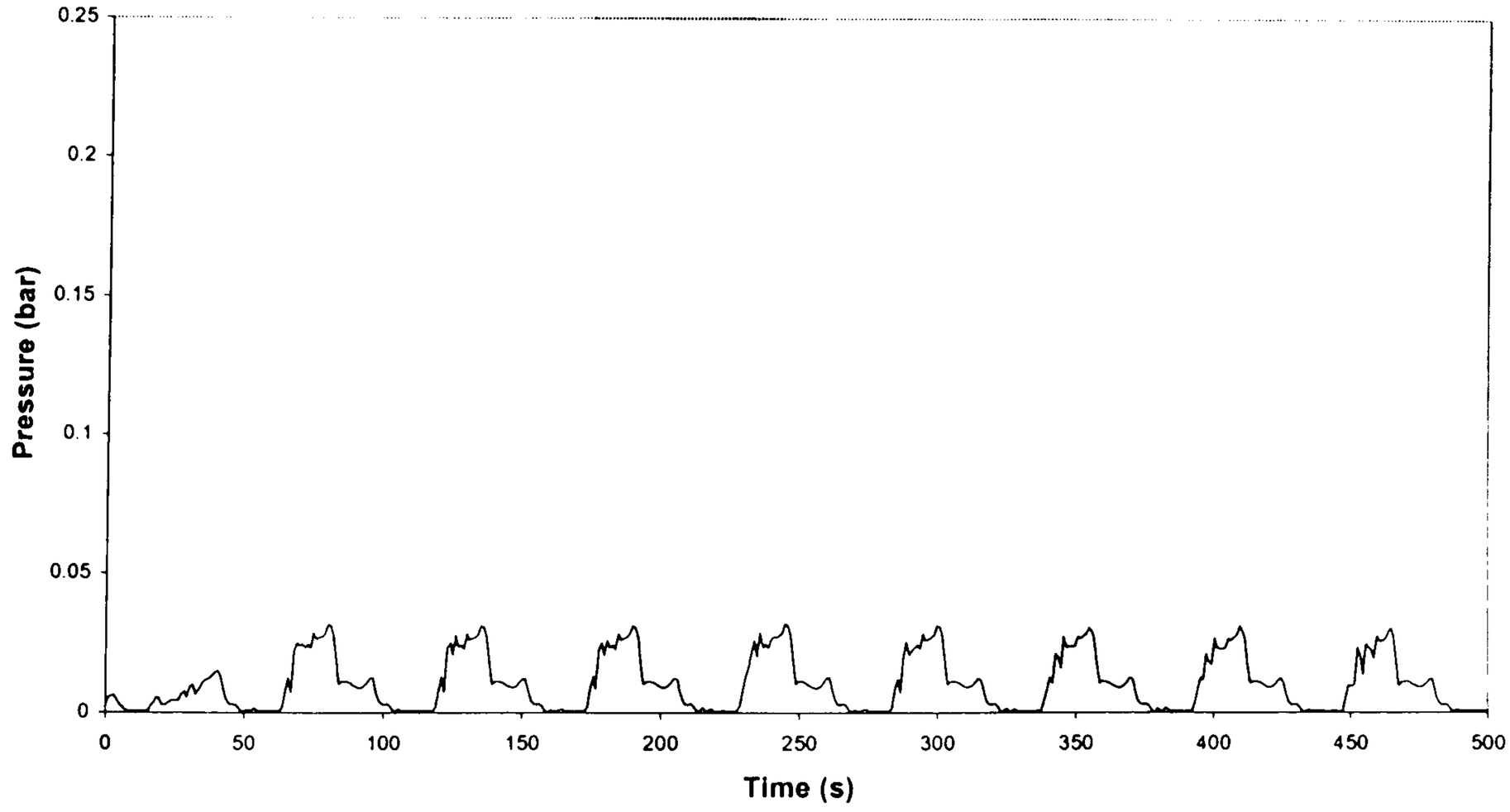

Figure 6.10 – Simulated Pressure Difference Profile Over Downcomer For Case E, Oscillation Flow, Base Simulation

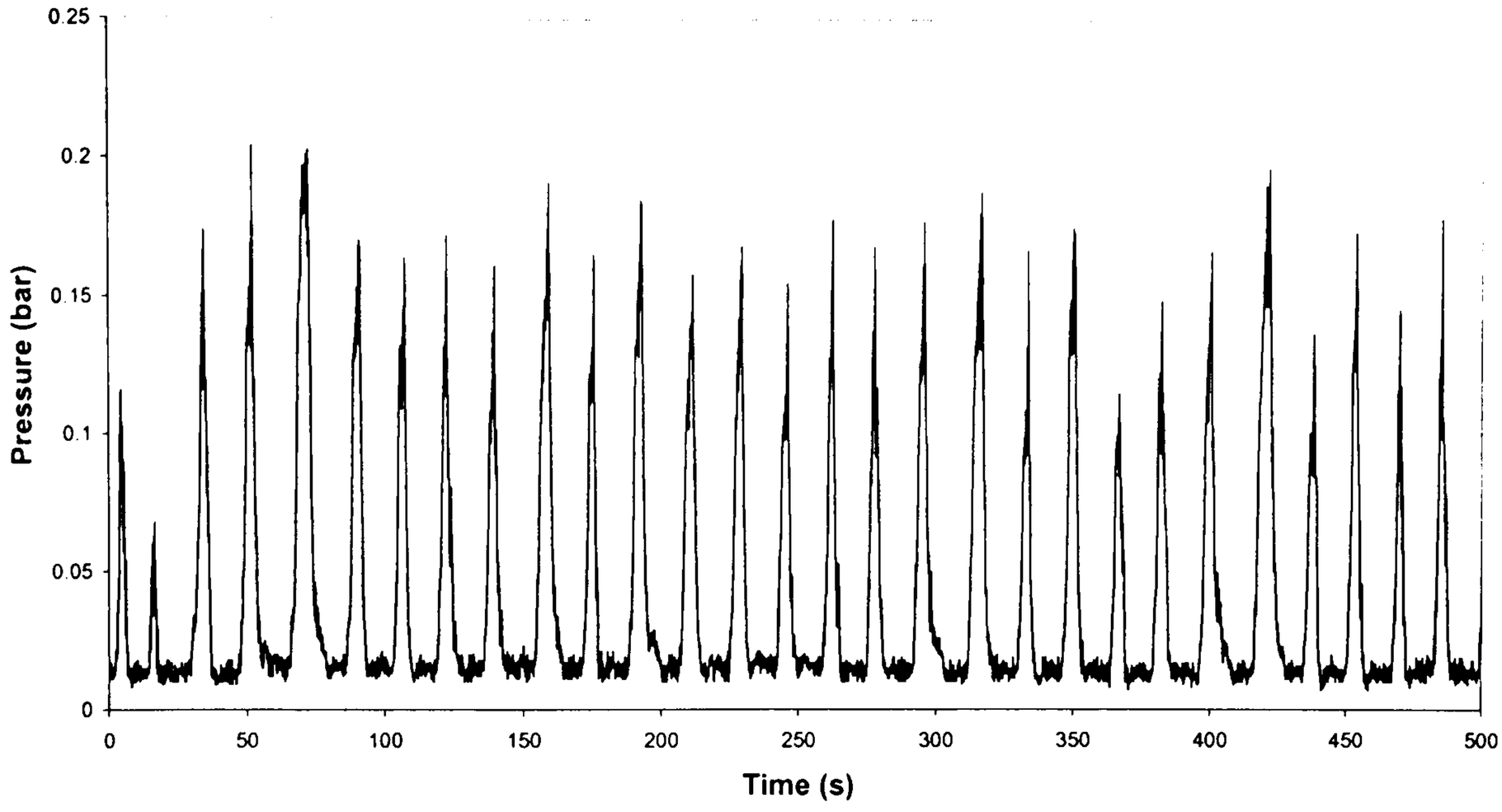

Figure 6.11 - Experimental Pressure Difference Profile Over Downcomer For Case E, Oscillation Flow

This means that the code predicts an unstable column of liquid in each upward limb of the riser. Experimentally it has been found that during oscillation flow the upper limb of the riser is stable, with no large-scale blow-out of the liquid column. This is caused by the interaction of the downcomer and the pressure cycling in the lower limb of the riser. The code predicts the lower limb cycling, however the downcomer behaviour is significantly different from the experimental case. Figure 6.10 shows the code-predicted downcomer behaviour, this shows an essentially empty downcomer, whose average liquid content is only 5%. During the experimentally observed oscillation flow, there is a definite accumulation of liquid from the lower limb in the downcomer, see Section 4.3. Comparing the predicted downcomer behaviour with the data from the experiments, Figure 6.11, it can be seen that this filling, present in the experiment, is not predicted by the code. This unrealistic prediction of the downcomer behaviour, it is suggested, is the reason that the code is not predicting oscillation flow.

6.3.5 Detailed Results – Slug Flow

As stated before, the code predicted bubbly flow in the riser rather than slug flow. A time profile of the liquid holdup local to the riser base shows a constant average liquid holdup, showing the code prediction of a steady-state behaviour in the system, Figure 6.12. Comparing this to the experimental result in Figure 6.13, the difference between the two is clear. The slugs are clearly identifiable in the experimental case.

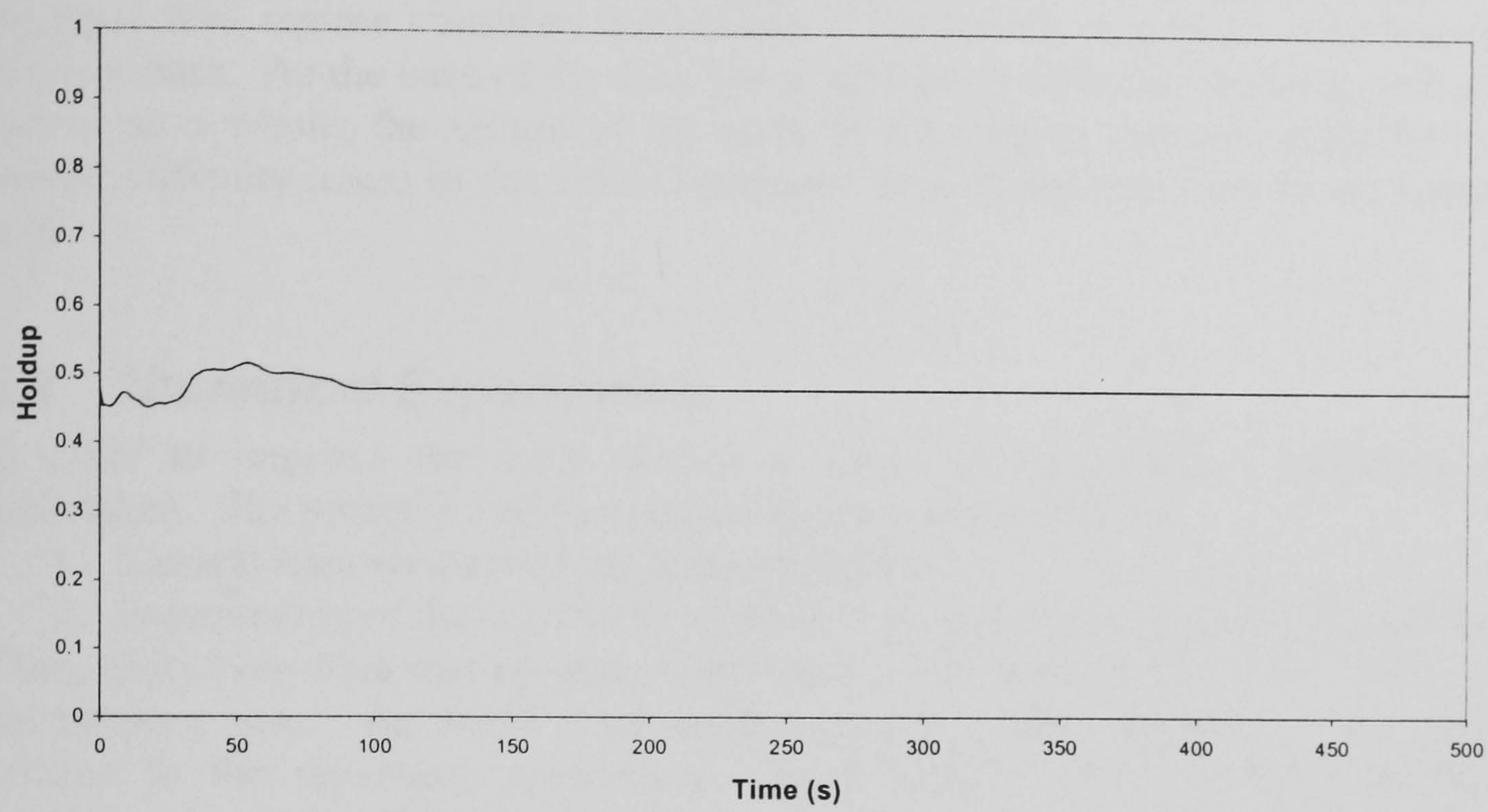

Figure 6.12 - Simulated Riser Base Liquid Holdup Profile for Case F, Slug Flow, Base Simulation

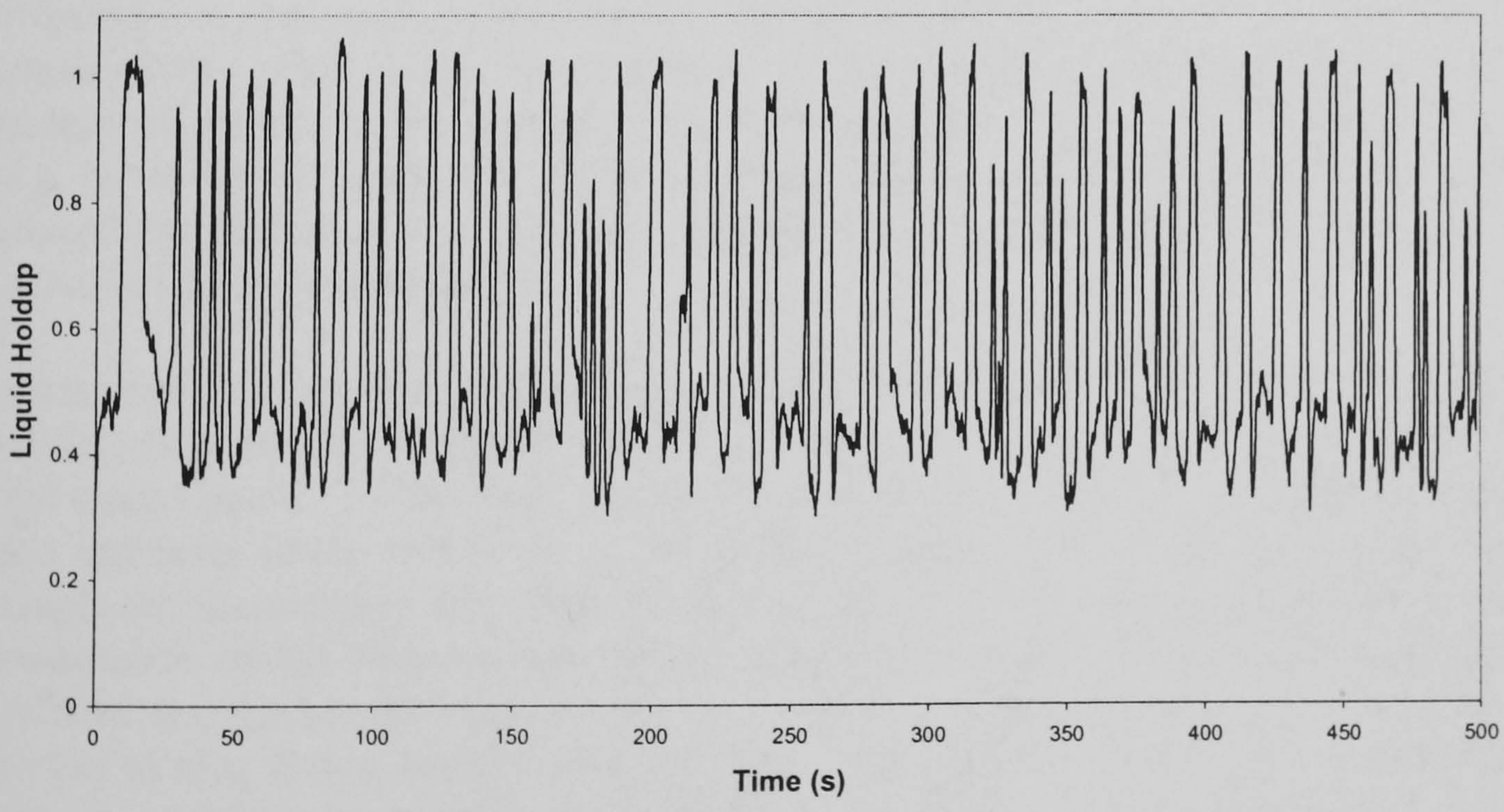

Figure 6.13 – Experimental Riser Base Liquid Holdup Profile for Case F, Slug Flow

Given that the slug flow cases observed experimentally are below the stratified-wavy flow transition line for the pipeline, some variation on stratified flow would be an expected output from the code. The prediction of a bubble flow regime indicates that the basic flow regime transition mechanism is not functioning in the region close to the riser base. As the base of the riser has a substantial effect on the behaviour of the system as a whole, the failure of the code in this region may be indicative of an overall difficulty posed by the fluids behaviour local to the riser base to the computer code.

6.4 Numerical Experiments

In order to improve the code results, a series of numerical experiments were undertaken. The objectives of these experiments were as follows:

1. General improvement of the code prediction
2. Examination of the sensitivity of the code results to computation parameters

These objectives were met by using a variation of the grid density and a variation of the timestep size. As stated previously there are issues specific to each code in relation to the modelling parameters, where permissible the general method of modifying the code will be presented.

6.4.1 Grid Density

As severe slugging is a phenomenon characterised by the propagation of sharp void fraction waves, numerical diffusion is an issue. This can arise particularly in two instances – firstly the formation of the slug body at the riser base and secondly in the blowdown/liquid sweep-out at the end of the cycle. As transient codes are designed primarily to efficiently solve long transients (AEAT 2000, Scandpower 2000), this diffusion is a particular problem when rapid transients occur. In order to examine the degree of this effect in the pipeline/riser system, the global density of the grid in the model was varied. In the numerical experiments, the grid density was increased twice by a factor of 'x2' and 'x4' of the original density – in essence, the cell size was reduced by a factor of two and four. The results of these simulations are summarised a series of tables in Appendix D.

In terms of flow regime, the increases in grid density have no material effect on the unstable flow results. The only case in which there is some effect of grid is the slug flow case, Case F. In this case, examination of the liquid holdup variation at the riser base indicates some variations in the liquid fraction at the riser base, Figure 6.14, though not identifiably slug flow when compared to the experimental case. Closer examination of the flow regime output from the code showed alternating periods of stratified and bubble flow at the riser base. This alternating behaviour may be said to be akin to slug flows, though the code does not recognise it as such. Hence, though there is some improvement in the code prediction of the riser base behaviour in Case E, changing of the overall grid density has no effect in improving the flow regime prediction.

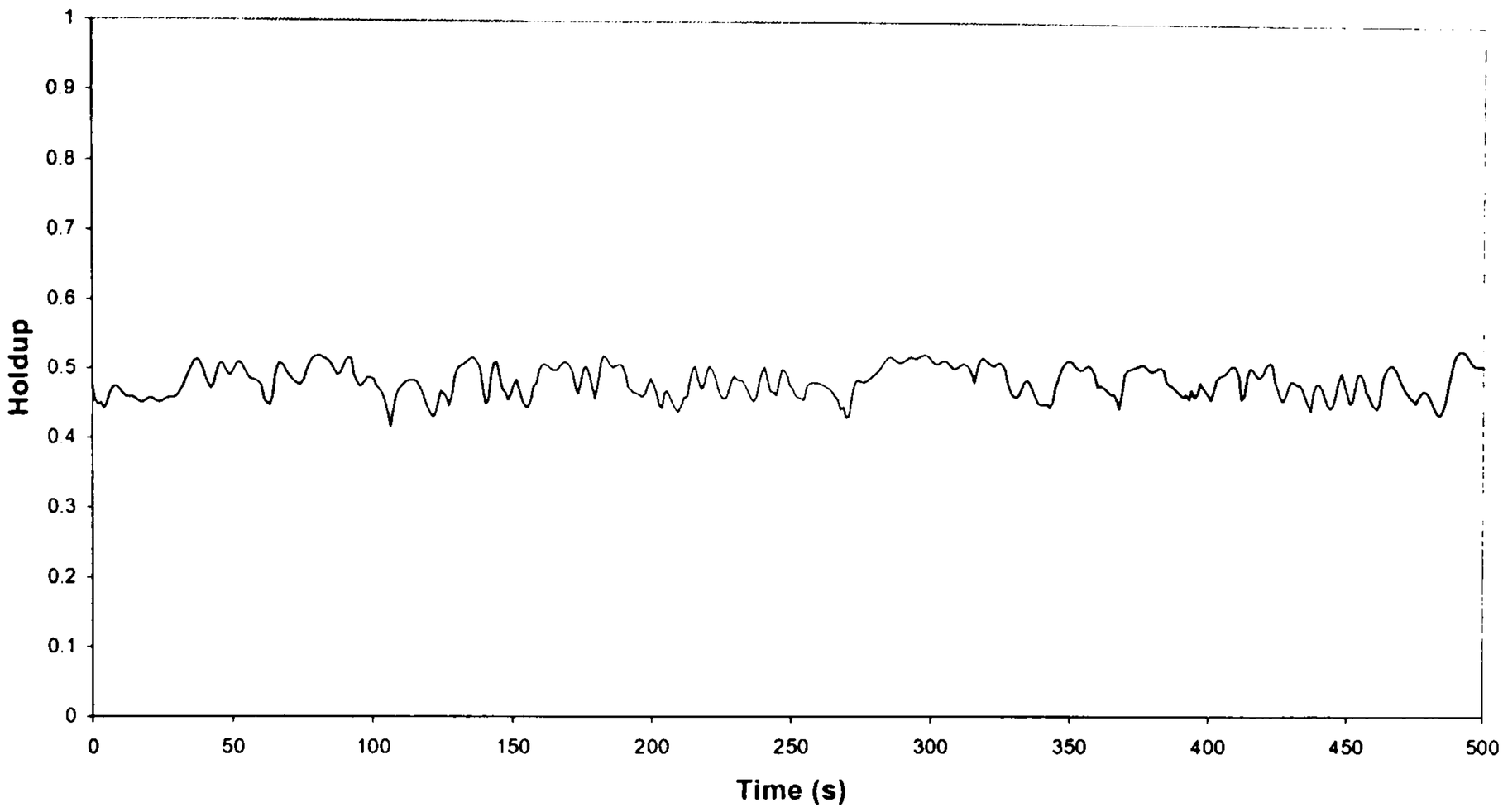

Figure 6.14 – Simulated Riser Base Liquid Holdup Profile for Case F, Slug Flow, 'x4' Grid Density Simulation

In terms of cycle time, the increase in grid density, in general, reduces the cycle times. The change in the cycle time is marginal though but on the whole there is a deterioration in the quality of code predictions. As an example, for Case A, the original simulation predicted a severe slugging 1 cycle time of 160.6 s, 82% of the experimental value. Doubling the grid density, the result is a cycle time of 157.7 s, 80.5% of the experimental value, a further reduction compared to the experimental value. The effect of the shorter cycle on the predicted fluid production characteristic is a marginal reduction in the predicted duration of the constant production period from 54.3 s (60% of the experimental value) to 53.8 s (59% of the experimental value). These changes have a proportional effect on the slug size and peak production rate – the slug size decreases from 83% of the experimental value to 81% of the experimental value and the peak production rate increases from 131% to 142% of the experimental value.

An additional increase in the grid density for the Case A simulation has mixed results. Some of the predicted characteristics decrease in a manner similar to before, that is by a marginal amount, within 5% of the simulation value, while others increase by a similar amount. Comparing these results to the previous simulation –the 'x2' grid density simulation, it is clear that for the most part, the simulated results are within ±5%, of each other. For example, the severe slugging cycle times are both 81% of the experimental value and the slug sizes are 81% and 82% of the experimental value. Given that the slugging characteristics are within the ±5% value of each other from simulation to simulation, it may be said that the simulation for Case A has converged in terms of the grid density and further increase in the density of the grid will have no

appreciable improvement in the result. However, there is exception to this - the peak liquid production rate. Here the simulation results are 142% and 150% of the experimental value for the 'x2' and 'x4' grid density cases. This shows sensitivity in the production rate value to changes in the grid density. Hence it may be asserted that the gas-liquid interface behaviour, which controls the propagation of the slug tail and hence the peak liquid production, is highly dependant on the grid structure for all simulation grids. This therefore shows that though the simulation of unstable flow has appeared to converge, there is a deficiency in the fine detail of the model that means that a complete, grid-independent solution is not achieved. More specifically, that the bubble flow through the curved riser is not predicted correctly.

Exploring the other simulations that were carried out with variations in grid density, it is evident that all unstable flow simulations have converged and the results have become generally independent of grid density. The only exception to this convergence is Case F, discussed above, where the flow regime changes from bubbly flow to a combination of bubbly/stratified flow. As in Case A, the quality of the code prediction degraded for the most part at the higher grid density, though the effect of the grid modification was marginal in the order of percent and hence negligible. Further details of the simulation results are presented in Appendix D.

6.4.2 Timestep Size

A set of numerical experiments for the timestep size during the simulation, similar to those described above, was carried out. However, the actual size of the timestep was not directly modified. In all transient multiphase codes, the timestep is selected automatically during the simulation, according to an internal code-specific logic. Some codes allow the specification of the maximum and minimum timestep size, while others allow only the maximum timestep size to be specified. In these experiments, the maximum timestep was manipulated from the initial size of 1 s by a factor of '$x^1/_{10}$', '$x^1/_{100}$' and 'x10'. As before, the results of these numerical experiments are summarised in Appendix D.

In terms of the flow regime, the decrease in timestep size has no effect for the majority of test cases; the flow regime remains the same as the basic simulations described in Section 6.3. The exception to this being Case D, the severe slugging 3 case, here the decrease in timestep size causes the simulation to predict unstable transitional flow – 'transition to oscillation'. This flow behaviour exhibits the high degree of gas penetration of severe slugging 3, with the low-magnitude pressure fluctuations of oscillation flow. The flow regime difference is characterised by an irregular slug flow behaviour at the riser base, giving unstable liquid columns in each upward limb of the riser. The slug formation at the riser base is characteristic of a relatively higher throughput of fluids at the riser base compared to the base simulation. This is confirmed by comparison of the outlet liquid peak flow rates between the two simulations. During unstable flow in the riser, the peak liquid production is dependent on the propagation of a slug tail through the riser, this tail is in actual fact a bubble front and hence effected by the mixture velocity through the riser base. Examining the base simulation, the peak flow experienced is 5.23 l/s, while in the '$x^1/_{10}$' timestep simulation the peak flow is 5.58 l/s, showing the

increased tail velocity. Hence, the propagation velocity of the slug tail in Case D, a bubble front, is dependent on the timestep size and to such a degree that the flow regime may be changed.

In terms of the change of the flow regime characteristics, as in the grid density experiment, the simulations do not converge. In the previous section it was shown the pressure cycling characteristics and slug sizes all lay within ±5% of one another. However the peak liquid production still exhibited a significant degree of variation with grid density. When manipulating the timestep size, there is a significant change in the flow regime characteristics between the base simulation and the '$x^1/_{10}$' timestep simulation. As the maximum timestep size is increased, there are changes in the pressure cycling characteristics for the severe slugging transition cases. In Case C, the liquid buildup shows significant variation, changing by 5% of the experimental value from base simulation to the '$x^1/_{10}$' simulation, while in Case D, the pressure cycling indicates a different flow regime. In terms of fluid production there are more significant deviations over the full range of test cases. The liquid slug size is only marginally affected by the change in timestep size, being within ±2% (in terms of the experimental value) of one another in the simulations. However the contributions of the individual stages of liquid production show a larger degree of variation. For Case B the variation in the size of the steady liquid production stage is from 67% of the experimental value in the '$x^1/_{100}$' simulation to 98% of the experimental value in the base simulation. In an opposite trend, the size of the peak production period varies from 112% of the experimental value to 91% of the experimental value for the '$x^1/_{100}$' simulation and base simulation respectively.

When comparing all results for the variation of timestep size, there is no indication that an increase in timestep size improves the simulation results. For the classical severe slugging cases, the pressure cycling and slug size are only marginally affected by the timestep size. For transitional flows, the code performance is degraded by the change in maximum timestep size, with the code predicting different flow regimes in two of three cases and in all three, the characteristics of the flows are substantially different from those observed experimentally.

6.5 Summary

In this chapter, a transient multiphase code has been tested against a series of six test cases covering the entire range of flow regimes in the pipeline/riser. The test series included two 'classical' severe slugging 1 cases, two transitional severe slugging test cases – one severe slugging 2 and one severe slugging 3 – one oscillation flow case and one slug flow case. A model of the pipeline/riser system was formulated with a constant inlet flow boundary and constant outlet pressure boundary for the two-phase air water system. A main set of simulations were performed to assess the general ability of the code to predict the unstable flow. Following this a series of numerical experiments were carried out, changing the density of the computation grid and restricting the maximum timestep size of the simulation. This was intended to examine how independent the results were from the computation parameters.

General Observations

Gathering together the results presented above for the base simulation results and the numerical experiments, the following general observations on the simulations are made:

1. The code is able to predict the occurrence of the 'classical' severe slugging 1 cases in the test series. The code has difficulty in predicting the transitional severe slugging flows, with respect to the bubble penetration at the riser base and the blowdown process. An over-prediction in the bubble penetration in the transitional severe slugging cases means severe slugging 3 is predicted in all cases. The prediction of a complete removal of liquid characterises severe slugging 2 rather than the experimentally observed oscillation flow. Finally, the code was unable to predict slug flow in the pipeline/riser. As the test case for this flow was below the stratified-wavy transition line, the flow regime transition mechanism in the code is supposed to be the reason for the code deficiency.
2. The detailed characteristics of the severe slugging are not predicted by the code, in particular the liquid production mechanism, the gas blowdown and the overall severe slugging cycle duration. The variation in production characteristics is attributable to the code prediction of the liquid behaviour and gas accumulation within the pipeline. The variation in the blowdown is ascribed to the difference in the code prediction of the slug tail movement through the curved riser. The effect of these differences is an overall reduction in the prediction of the severe slugging cycle time.
3. The variations in the cycle time, liquid production and gas blowdown stages has a knock-on effect on the instantaneous production rates from the riser outlet. Reduced cycle times are characteristic of shorter severe slugs. Reduced liquid production periods and shorter blowdown times are characteristic of higher flowrates during slug production and a higher peak liquid production rate.
4. Hence, though the code predicts the 'classical' severe slugging cycle, the detailed results show that the code does not give acceptable prediction of the characteristics of the observed 'classical' severe slugging.
5. In terms of transitional severe slugging, the predictions are less acceptable in terms of production transient size, with an over-prediction of gas holdup in the slug reducing the slug size to approximately 60% of the experimental value. The peak flow is also an issue – during severe slugging 2 the peak flow is over-predicted, while during severe slugging 3 it is under-predicted. This is consistent with an over-prediction of the gas flow through the riser. In the case of severe slugging 2, this causes an error in the slug tail velocity, whereas in severe slugging 3 this causes errors in the prediction of the gas blowdown.
6. Attempting to improve the simulation results using an increase in grid density were of limited success. An increase in the grid density by a factor of 'x2' and 'x4' has limited effect on the pressure cycling characteristics and the slug size but has a significant effect on the peak production rate, increasing the peak flow from 130% of the experimental value for the base simulation to 150% for the 'x4' simulation. The changes in the peak production velocity were again attributed to the bubble propagation through the curved riser. In terms of the slug flow case, Case F, the increase in grid density showed promising results,

predicting a period of bubbly flow followed by stratified flow – closely analogous to slug flow.

7. Similarly, it was attempted to improve the simulation results through manipulation of the maximum timestep size. This would exercise some control over the actual timestep size during calculations. The results of these simulations showed relatively less improvement in prediction results compared to the grid density variation tests. In the 'classical' severe slugging 1 cases, there was little improvement in the prediction of pressure cycling characteristics, the slug size and the peak liquid production rate. However there were substantial changes in the sizes of the constant production period and the production transient. These are associated with the liquid behaviour in the pipeline, the slug tail propagation in the riser and the accumulation of gas in the system as a whole. In the transitional severe slugging cases, the prediction degraded further as the maximum timestep was increased with shorter cycle times and slug sizes. Indeed, no severe slugging predicted for Case D. This was again attributable to the degree of gas penetration at the riser base and the aeration of the slug body.

Recommendations and Suggestions for Further Investigation

Based upon the general observations above, the following recommendations are made:

1. The behaviour and propagation of gas bubbles in the pipeline and particularly the curved riser must be investigated. Necessarily this will involve an examination how these flow regimes are predicted to occur and also how their propagation is modelled within the code. In particular, the effect of inclination on the bubble propagation must be examined as many models for such are based upon the results of horizontal or vertical flows. One challenge to this investigation is the understanding of the proprietary code models and the design of appropriate experiments to improve the predictions.
2. The gas accumulation and gas-liquid interface behaviour in the pipeline has been identified as a potential source of error in the simulations. Though the pvt behaviour of the system is a potential source of error, any variations in the inlet boundary flows may also cause errors in the simulation results. Hence it is recommended that simulations should be carried out with boundary conditions that any variations that are observed experimentally.
3. The outlet boundary condition for these simulations consisted of a simple constant pressure boundary at the riser outlet. In actual fact, the riser outlet was connected to a two-phase gas-liquid separator whose level was controlled by a PID controller. The interaction of the level control with the pressure cycling in the pipeline/riser would not necessarily be reflective of the constant pressure boundary assumed in the model described at the start of this chapter. Hence it is recommended that simulations using the separator models included in the codes are carried out to quantify the effect of this controller on the code performance.

Chapter 7 – Conclusions and Recommendations

This Chapter presents the findings of this work, combining the results from the three main results chapters – 4, 5 and 6. As such this chapter is divided into four main sections, the first three summarising the work undertaken and the results for each main research theme. The fourth section aims to draw this work to completion by presenting some recommendations and proposals for further work.

The work carried out in this thesis focused on the collection of new data on severe slugging and unstable flows within a riser, the comparison of these data with the existing models for the occurrence of severe slugging and commercial transient codes. Each of these main work tasks is described below.

7.1 Experimental Work

Based on the literature review, severe slugging in an S-Shaped riser was found to be a challenging flow regime in engineering terms, with a lack of data of the flow regime characteristics available. Previous works in this area had not provided information on the fluid production from the riser or the effect of pressure on the flow regime stability. Finally, though there had been some comparisons made with standard stability criteria before now, the quality of the data remained an issue.

7.1.1 Research Summary

In the present work, the following work was carried out:

1. A set of data on the general pressure cycling and riser base liquid holdup characteristics of severe slugging and unstable flows was collected in an S-shaped riser. This allowed the identification of all flow regimes occurring in the riser and the general mechanisms.
2. The probability density function (pdf) was used for the first time in the case of severe slugging to characterise the flow regime. The methodology was applied to pressure difference signals over the riser, rather than the liquid fraction measurements of previous workers. This method of analysis proved to be successful in identifying the flow regimes in the pipeline/riser system.
3. A mass balance was completed for the test separator allowing the inference of the liquid and gas mass production from the riser. Results showed the production profile during each flow regime and allowed the calculation of size of liquid slugs during unstable flows.
4. Experiments were carried out over three separator pressures – 2, 4 and 7 bar(a) to examine the effects of pressure on the flow regime and the occurrence of unstable flows.
5. The flow regime maps resulting from the experiments were compared to the existing stability criteria that are used for predicting the occurrence of severe slugging as a function of gas and liquid superficial velocity.

7.1.2 Conclusions

1. Unstable flows are split into three broad categories – 'classical' severe slugging1, transitional severe slugging and oscillation flows. Transitional severe slugging is further divided into two categories – severe slugging 2 and severe slugging 3. Severe slugging 1 is characterised by having both upward riser limbs filled with liquid and an identifiable period of slug production with no gas penetration at the riser base, followed by a pipeline gas blowdown to near-separator pressure. Transitional severe slugging exhibits an identifiable slug formation and blowdown period, without a slug production period. Severe slugging 2 displays no gas penetration at the riser base during the formation of the severe slug, whereas during severe slugging 3 there is continuous flow of gas through the riser base and the slug. Oscillation flow is characterised by an unstable column of liquid in the lower limb and a stable column of liquid in the upper limb.
2. In terms of liquid slug size, severe slugging 1 is the most problematic flow regime with the largest slugs, followed by severe slugging 2, 3 and oscillation flow in descending order. If however, the volume of the liquid production transient is of concern, transitional severe slugging is as problematic as 'classical' severe slugging – the production transients during severe slugging 2 can be greater than those experienced during 'classical' severe slugging, which are typically equal to the riser volume. Oscillation flow exhibits smaller transients than severe slugging, however the volume of the production surges is still significant, 40 % of the riser volume.
3. In terms of peak production rate 'classical' severe slugging and transitional severe slugging are as problematic as one another, with flow deviations in the order of 600-1200 % of the average production rate.
4. Increasing pressure was found to suppress 'classical' severe slugging 1 in terms of the maximum gas and liquid superficial velocities at which the flow regime occurs on a flow regime map. However, another form of severe slugging 1 was observed – denoted severe slugging 1*. This was characterised by continuous gas penetration at the riser base and a distinct period of slug production. Thus severe slugging is found on the flow regime map at 7 bar(a) separator pressure. In terms of the other pressure cycling flow regimes, the increase of separator pressure had a lesser effect than on severe slugging 1, with little change in the region of unstable flows as outlet pressure increases.
5. Comparison of the results of existing criteria for severe slugging to experimental results has shown how these models are unable to predict the entire pressure cycling region. As pressure increases, so too do the differences between the model predictions and the experimental results, with some models failing to predict the occurrence of any of the observed severe slugging at 7 bar(a). The only criterion able to predict the region of unstable flows was the stratified-wavy transition criterion, albeit with a significant degree of over-prediction.

7.2 Unstable Flow Criterion

Based on the literature review, experiments and comparisons described above, a new criterion for the occurrence of unstable flows was developed.

7.2.1 Research Summary

1. Based upon considerations of the liquid slug buildup, a condition for the formation of a large-scale instability was formulated. Though the analysis was carried out at a different stage of the severe slugging cycle, the similarity of this approach to other works was demonstrated.
2. Experiments conducted had indicated that not only is 'classical' severe slugging 1 a flow regime of concern, but that the other unstable flow regimes were of importance. Hence the criterion developed was required to predict the regions of severe slugging, transitional severe slugging and oscillation flow.
3. The criterion inequality in terms of pressure change in the pipeline and at the riser base was resolved using mass and pressure balances over the respective parts of the system. This gave the final form of the criterion in terms of pipeline conditions and gas flow at the riser base.
4. The gas flow at the riser base was resolved based upon considerations of the inclined bubble propagation at the riser base, while the pipeline conditions were resolved based upon considerations of the riser filling.
5. The criterion results were compared against data collected as part of this work and the Multiphase Pipelines and Equipment (MPE) project.

7.2.2 Conclusions

1. Results showed that the region of severe slugging 1 and pressure cycling are encompassed by the criterion, though there is some over-estimation of the region in terms of the maximum superficial gas velocity for unstable flows. However, the results were an order of magnitude improvement when compared to the other successful criterion – the Taitel and Dukler (1976) stratified-wavy flow regime transition criterion.
2. As the separator pressure increased, the criterion remained able to encompass the entire region of unstable flows. Again proving to be closer in agreement than other existing criteria for severe slugging.
3. The criterion also proved able to predict the severe slugging region for the MPE data. The region of oscillation flows was not completely predicted, though the criterion was again an improvement on those criteria used to date. However, there were uncertainties with regard to this data, particularly in respect to the accuracy of the flow regime identification, the quoted superficial gas and liquid velocities on the flow regime map and potential siphoning at the outlet.

7.3 Transient Code Modelling

A series of comparisons of the experimental results with a commercial transient code was carried out. The aim of this was to highlight the areas in which the code had difficulty in predicting the unstable flows and assess how best to improve the results of simulations.

7.3.1 Research Summary

1. A series of six test cases were selected, covering all flow regimes experienced in the S-shaped riser. The test cases were as follows – 2 off 'classical' severe slugging 1 cases, 1 off severe slugging 2, 1 off severe slugging 3, 1 off oscillation flow case and 1 off slug flow case.
2. A generic model of the pipeline/riser system was formulated and implemented in the code, giving a set of 'base' simulations. These were compared in detail to the experimental results.
3. A set of numerical experiments were attempted to improve the simulation results and to examine the effect of increased grid density and reduced timestep size. Two refinements in the original computational grid were used – x2 and x4. The timestep sizes were modified by the following increments – 10, $^1/_{10}$ and $^1/_{100}$.

7.3.2 Conclusions

1. The code is able to predict the occurrence of severe slugging 1, however there remain significant difficulties in the prediction of transitional severe slugging and oscillation conditions. An over-prediction of the bubble penetration at the riser base means that the code is predicting severe slugging 3 in all transitional severe slugging cases. Furthermore, over-prediction of the blowdown phenomenon means that oscillation flow is not predicted by the code. Finally, slug flow is not correctly predicted by the code, due to the presence of bubble flow at the riser base.
2. The detailed characteristics of the severe slugging process are not predicted by the code. Similarly to the above, this is attributable to inaccurate prediction of the riser base bubble penetration, pipeline liquid accumulation and the gas blowdown.
3. Increasing the grid density showed that, for the most part, the simulation had converged to a stable solution and that the variation in results was within ±2% of the original experimental result. The only exception to this is the peak predicted liquid production rate, which increases as grid density is increased.
4. When changing the timestep size, there was a similar convergence in the severe slugging 1 pressure cycling results as in the grid density cases. However, in these experiments, the rate of liquid production during the steady liquid production period of severe slugging 1 changed. In the transitional severe slugging cases and oscillation flow case, the quality of the prediction deteriorated with shorter cycle times and slug sizes as the timestep size reduced.

7.4 Recommendations and Suggestions for Further Work

This section is split into two parts, the first summarising the recommendations resulting from the research described here and the second detailing suggestions for future research. The recommendations are intended to broadly characterise the results in engineering terms for use when considering the implications of unstable flow in pipeline/riser systems.

7.4.1 Recommendations

1. When considering severe slugging in a pipeline/riser system, all forms of unstable flow should be investigated – 'classical' severe slugging 1, transitional severe slugging (2 and 3) and oscillation flows.
2. The characteristics of concern for these flow regimes are the pressure cycling and liquid production characteristics. In terms of liquid production, the slug size, the size of the production transient and the peak production rate are all of concern and considered in this work. Maximum and average backpressure are also of concern and have been examined in previous works.
3. As a rule of thumb, based upon and limited to this work in terms of generality, the size of the production transient during 'classical' severe slugging 1 can be expected to be approximately equal to the riser volume. Similarly the peak production rate during severe slugging can be expected to be two orders of magnitude greater than the average flow through the system. During severe slugging 2, the size of the production transient can be expected to be equal to or greater than that expected during severe slugging 1. Also, the peaks in liquid production during severe slugging 3 can be expected to be of a similar scale of deviation from the average to those experienced during severe slugging 1
4. The use of existing criteria for severe slugging is open to debate as they have been shown here to under-predict severe slugging. One qualification to this is the fact that if the criteria do predict severe slugging for a particular operating condition, it is most likely that severe slugging occurs.
5. When attempting to predict the occurrence of severe slugging using a transient multiphase code, the smallest practical grid cell size should be used.
6. The occurrence of 'classical' severe slugging is predicted by the code. However the slugging characteristics, particularly the slug size and peak production rate are not accurately predicted, with smaller slug sizes and larger peak production rates than found experimentally.
7. The exact occurrence and characteristics of transitional severe slugging and oscillation flows are not predicted accurately by the codes when a constant boundary condition is used.

7.4.2 Suggestions for Further Work

This section is split into three parts, each dealing with one of the research themes of this work.

Experimental

1. The fluids used in the experiments in this work are air and water. In reality the fluids in offshore production systems are oil and dissolved natural gas with varying amounts of produced water (brine). As such a system is difficult to reproduce in the current laboratory facility, it is suggested that experiments should firstly be conducted using air and oil as test fluids and secondly using a three-phase system of air, oil and water. This would confirm how dependent the characteristics of the severe slugging are on the fluid properties.

Furthermore, commercial codes have been developed for gas-oil systems, hence a more accurate judgement of their performance may be possible with two and three phase systems containing oil.

2. These experiments should also be carried out over a range of pressures to examine if the suppressing effect of increasing the separator pressure is similar for oil-containing systems and how gas/liquid density ratio effects the results.
3. The inaccurate prediction of pipeline gas and liquid behaviour has been identified as a potential source of error in the code predictions. Hence experiments in a small-scale pipeline/riser system are suggested to examine the liquid accumulation process in the pipeline. Detailed design of this experimental facility should allow replication of unstable flows similar to that experienced in this work and allow detailed experimental measurements to be made of the liquid fraction. Providing a large accumulation volume for the gas would enable an accumulation process similar to severe slugging in the pipeline/riser system examined in this work. Furthermore, the use of a clear pipe would allow visual examination of the processes particularly at the riser base as the gas/liquid interface moves into the riser.
4. Similar to the above, additional experimentation on bubble propagation through a curved pipe is suggested. This could be achieved by the use of additional instrumentation in the existing riser or a transparent rig for flow visualisation. These experiments would allow examination of the closure laws for the bubble motion used in the codes.

Unstable flow Criterion

1. Further development of the criterion should continue to examine the behaviour of the bubble, gas flow and liquid holdup at the base of the riser. The experiments in parts (3) and (4) above may provide additional information on how the current analysis could be modified.
2. Additional validation data is also required to confirm the prediction capability of the criterion, particularly in respect to different riser geometries, operating fluids and system pressure.
3. One suggestion by other workers has been the consideration of annular flow and bubble flow in the riser base as further areas of concern, particularly in the case of blowdown and 'slug release' as defined by Fuchs (1987). The additional analysis of the system for these flow regimes is also suggested.

Transient Code Comparisons

1. As stated previously the simulations carried out thus far have been carried out with constant boundary conditions. It is suggested that a series of future simulations be carried out, modelling any variation in boundary conditions that have been observed in the experiments. Furthermore, the simulations should also examine which combination of boundary condition variations is the most important and the magnitude of variation above which any effect is observed.
2. The experimental system is made up of a series of a fluid supply facility, a fluid processing facility, facilities process control and the pipeline/riser rig. Commercial transient codes now have the capability for the simulation of the combination of such units. Hence it is suggested that a model of the full

system is formulated that can be used examine rig effects on the observed severe slugging.

3. As stated previously, the pipeline behaviour is an area of concern for the prediction of severe slugging. Thus it is suggested that simulations be carried out where the pipeline grid structure is modified and the degree of pipeline liquid backup be examined.
4. Finally, the closure laws in the transient codes should be examined through interaction with the code developers, allowing suitable experiments to be formulated as described above.

References

AEA Technology, 1996, *PLAC Validation Case*, AEAT

AEA Technology, 2000, *ProFES Users Manual*, AEAT

Almeida A R and M de A Lima Gonçalves, 1999, *Venturi for Severe Slug Elimination*, Proceedings 9th International Conference on Multiphase Production, BHRg, pp 149-158

Barbuto F A A and E F Caetano, 1991, *On the Occurrence of Severe Slugging Phenomenon in Pargeo-1 Platform, Campos Basin, Offshore Brazil*, Proceedings 5th International Conference on Multiphase Production, BHRg, pp 491-503

Barratt N, T J Hill and M King, *Understanding and Development of a Slug Hysteresis Model for Hilly Terrain Pipelines*, Proceedings 1st North American Conference on Multiphase Production, BHRg

Beggs H D and J P Brill, 1973, *A Study of Two-Phase Flow in Inclined Pipes*, Journal of Petroleum Technology, May Issue, pp 607-617

Bendiksen K H, 1984, *An Experimental Investigation of the Motion of Long Bubbles in Inclined Tubes*, International Journal of Multiphase Flows, vol. 10, no. 4, pp 467-483

Bendiksen K H, D Malnes, R Moe and S Nuland, 1991, *The Dynamic Two-Fluid Model OLGA: Theory and Application*, SPE Production Engineering, May Issue, Society of Petroleum Engineers, pp 171-180

Black P S, L C Daniels, N C Hoyle and W P Jepson, 1990, *Studying Transient Multiphase Flow Using the Pipeline Analysis Code (PLAC)*, Journal of Energy Resources Technology, vol. 112, pp 25-29

Bøe A, 1981a, *Severe Slugging Characteristics, Part I, Flow Regime for Severe Slugging*, Presented at Special Topics in Two-Phase Flow, Trondheim, Norway

Bøe A, 1981b, *Severe Slugging Characteristics, Part II, Point Model Simulation Study*, Presented at Special Topics in Two-Phase Flow, Trondheim, Norway

Caltec, 1999, *Riser Test Facility Manual*, BHRg

Carew P S, N H Thomas and A B Johnson, 1995, *A Physically Based Correlation for the Effects of Power Law Rheology and Inclination on Slug Bubble Rise Velocity*, International Journal of Multiphase Flow, vol. 21, no. 6, pp 1091-1106

Corteville J, R Stehlé, D Ferré and C Pauchon, 1997, *An Experimental Study of Severe Slugging in Multiphase Production Lines*, Proceeding 8th International Conference on Multiphase Production, BHRg, pp 105-121

Cottrill A, 1999, *Thrust into the Limelight*, The Offshore Engineer, March Issue

Courbot, A, 1986, *Prevention of Severe Slugging in the Dunbar 16" Multiphase Pipeline*, OTC 8196, Offshore Technology Conference, pp 445-452

Das I, C Wordsworth and G McNulty, 1999a, *Living with Slugs on Floaters*, Presented at the Institute of Marine Engineers Deep and Ultradeep Water Offshore Technology Conference, March 25-26

Das I, C Wordsworth and G McNulty, 1999b, *Predicting, Detecting and Preventing Slugs in Flexible Riser Systems*, Proceedings 9th International Conference on Multiphase Production, BHRg

Das I, 2002, *Slug Loading in Flexible Risers*, PhD. Thesis In Preparation, Cranfield University

De Henau V and GD Raithby, 1995a, *A Transient Two-Fluid Model for the Simulation of Slug Flow in Pipelines – I Theory*, International Journal of Multiphase Flow, vol. 21, no. 3, pp 335-349

De Henau V and G D Raithby, 1995b, *A Transient Two-Fluid Model for the Simulation of Slug Flow in Pipelines – II Validation*, International Journal of Multiphase Flow, vol. 21, no. 3, pp 351-363

De Henau V and G D Raithby, 1995c, *A Study of Terrain-Induced Slugging in Two-Phase Flow Pipelines*, International Journal of Multiphase Flow, vol. 21, no. 3, pp 365-379

Fabre J, L L Peresson, R Odello and T Romanet, 1987, *Severe Slugging in Pipeline/Riser Systems*, SPE 16846, Presented at Society of Petroleum Engineers Annual Technical Conference, pp 113-129

Faille I and E Heintze, 1999, *A Rough Finite Volume Scheme for Modelling Two Phase Flow in a Pipeline*, Computers and Fluids, vol. 28, pp 213-241

Fairhurst P, 1999, Private Communication

Fernandez R C, R Semiat and A E Dukler, 1983, *Hydrodynamic Model for Gas-Liquid Slug Flow in Vertical Tubes*, American Institution of Chemical Engineers Journal, vol. 29, pp 981-989

Fuchs P, 1987, *The Pressure Limit for Terrain Slugging*, Proceedings 3rd International Conference on Multiphase Production, BHRg, pp 65-71

Goldzberg V and F McKee, 1985, *Model Predicts Liquid Accumulation, Severe Terrain-Induced Slugging for Two Phase Lines*, Oil and Gas Journal, August 19th, pp 105-109

Griffiths G W, D J Willis and W J Meiring, 1994a, *North West Shelf Gets Extensive Pipeline, Plant Management System, Trunkline Management – 1*, Oil and Gas Journal, January 3rd Issue, pp 42-45

Griffiths G W, D J Willis and W J Meiring, 1994b, *Shadow, Look-Ahead Models Keys to Pipeline-Transient Control, Trunkline Management – Conclusion*, Oil and Gas Journal, January 3rd Issue, pp 52-56

Hassanein T and P Fairhurst, 1998, *Challenges in the Mechanical and Hydraulic Aspects of Riser Design for Deepwater Developments*, Presented at Deepwater Technology Conference, Oslo

Henriot V, C Pauchon, P Duchet-Suchaux and F Leibovici, 1997, *TACITE: Contribution of Fluid Composition Tracking on Transient Multiphase Simulation*, OCT 8563, Offshore Technology Conference, pp 629-638

Hollenberg J F, S DeWolf and W J Meiring, 1995, *A Method to Suppress Severe Slugging in Flowline Riser Systems*, Proceeding 7th International Conference on Multiphase Flow, pp 89-103

Hill T J, 1987, *Multiphase Flow Field Trials on BP's Magnus Platform*, Journal of Energy Resources Technology, vol. 109, pp 142-147

Hill T J, 1989, *Riser-Base Gas Injection into the SE Forties Line*, Proceedings 4th International Conference on Multiphase Flow, BHRg, pp 133-147

Hill T J, and D G Wood, 1994, *Slug Flow: Occurrence, Consequences and Prediction*, SPE 27960, Presented at the University of Tulsa Centennial Petroleum Engineering Symposium, August 29-31

Hill T J, C P Fairhurst C J Nelson, H Becerra and R S Bailey, 1996, *Multiphase Production Through Hilly Terrain Pipelines in Cusiana Oilfield, Colombia*, SPE 36606, Presented at Society of Petroleum Engineers Annual Technical Conference and Exhibition, pp 319-334

Hill T J, 1997, *Gas-Liquid Challenges in Oil and Gas Production*, FEDSM97-3553, Presented at ASME Fluids Engineering Division Summer Meeting, June 22-26

Hunt A, 1998, *Where Are We Now, Where Are We Going? An Operator's Perspective*, Presented at the EPSRC London Meeting

IFP, 2000, *TACITE Users Manual*

Jansen, F E, O Shoham and Y Taitel, 1996, *The Elimination of Severe Slugging – Experimental and Modelling*, International Journal of Multiphase Flow, vol. 22 no. 6, pp 1055-1072

Kashou S, 1996, *Severe Slugging in an S-Shaped or Catenary Riser: OLGA Prediction and Experimental Verification*, Presented at Advances in Multiphase Technology

Knott, D, 1994, *Floating Production Systems Hit Stride in North Sea Fields*, Oil and Gas Journal, May 23

Larsen M, E Hustvedt, P Hedne, and T Straume, 1997, *PeTra: A Novel Computer Code for Simulation of Slug Flow*, SPE 38841, Presented at Society of Petroleum Engineers Annual Technical Conference and Exhibition, October 5-8

Larsen M and P Hedne, 2000, *Three Phase Slug Tracking with PeTra*, Proceedings 2nd North American Conference on Multiphase Production, BHRg, pp 170-192

Loh, W L and J Knopp, 1999, Private Communication

Lima P C R, 1999, *Modelling of Transient Gas-Liquid Flow and Pigging in Pipes*, PhD Thesis, Cranfield University

Linga H and D Østvang, 1985, *Tabulated Data from Transient Experiments with Naphtha*, Report No. 41, SINTEF

Linga H, 1987, *Terrain Slugging Phenomena, Some Experimental Results Obtained at the SINTEF Two-Phase Flow Laboratory*, Proceedings 3rd International Conference on Multiphase Production, BHRg, pp 37-53

Mackay D C, 1987, *Dynamic Simulation of the Effects of Slugging Flow on Process Plant – A Design Study*, Oil and Gas Journal, September 14, pp 67-72

Masella J M, Q H Tran, D Ferre and C Pauchon, 1997, *Transient Simulation of Two-Phase Flow in Pipes*, International Journal of Multiphase Flow, vol. 24, 739-755

Mazzoni A, M Villa, M Bonuccelli, G De Toma, D Mazzei and T Crescenzi, 1993, *Capability of the OLGA Computer Code to Simulate Measured Data from AGIP Oil Field*, Proceedings 6th International Conference on Multiphase Production, BHRg, pp 51-80

McGuinness M and D Cooke, 1993, *Partial Stabilisation at St. Joseph*, Proceedings 3rd International Offshore and Polar Engineering Conference, pp 235-241

McNulty J, 1995, *Assessing the Market for Multiphase Technology*, Proceedings 7th International Conference on Multiphase Flow, BHRg, pp 479-498

Milne-Thompson, 1960, *Theoretical Hydrodynamics*, The Mac-Millan Company, New York

Moe J, M N Lingelem, H Holm and O Oldervik, 1989, *Severe Slugging in Offshore Gas-Condensate Flowline-Riser Systems*, Proceedings 4th International Conference on Multiphase Production, BHRg, pp 527-560

Molyneux P, A Tait and J Kinvig, 2000, *Characterisation and Active Control of Slugging in a Vertical Riser*, Proceedings 2nd North American Conference on Multiphase Production, BHRg, pp 161-170

Montgomery J A, 1998, *Transient Simulations*, Internal Report, Cranfield University

Montgomery J A and H C Yeung, 2000a, *Flexible Risers Severe Slugging Phase II S-Shaped Riser Primary Experimental Results*, Report No. 00/JM/E1314N/219, Cranfield University.

Montgomery J A and H C Yeung, 2000b, *Flexible Risers Severe Slugging Phase II Report of Code Comparisons*, Report No. 00/HY/FO/E1314N/232, Cranfield University

Montgomery J A and H C Yeung, 2002, *The Stability of Fluid Production from a Flexible Riser*, To Be Published in Journal of Energy Resources Technology

Nicklin, D J, J O Wilkes and J F Davidson, 1962, *Two Phase Flow in Vertical Tubes, Transactions Institution of Chemical Engineers*, vol. 40, pp 497-514

Nydal O J, M Audibert and M Johansen, 2001, *Experiments and Modelling of Gas-Liquid Flow in and S-Shaped Riser*, Proceedings 10th International Conference on Multiphase Production, BHRg

Nydal O J and S Banjeree, 1996, *Dynamic Slug Tracking Simulation for Gas-Liquid Flow in Pipes*, Chemical Engineering Communications, vol. 141-142, pp 13-39

Pauchon C, H Dhulesia, D Lopez and J Fabre, 1993, *TACITE: A Comprehensive Mechanistic Model for Two-Phase Flow*, Proceedings 6th International Conference on Multiphase Production, BHRg, pp 29-50

Pauchon, C, H Dulseia, G B Cirlot and J Fabre, 1994, *TACITE: A Tool for Multiphase Pipeline and Well Simulation*, SPE 28545, Presented at Society of Petroleum Engineers Annual Technical Conference and Exhibition September 25-28, pp 311-326

Perry R H and D Green Eds., 1984, *Perry's Chemical Engineers Handbook*, 6th Ed. McGraw-Hill International

Philbin M T, 1991, *The Simulation of Transient Phenomena in Multiphase Production Systems*, Presented at IBC Multiphase Operations Offshore

Pots B F M, I G Bromilow and M J W F Konijn, 1985, *Severe Slug Flow in Offshore Flowline/Riser Systems*, SPE 70866, Presented at Society of Petroleum Engineers Middle East Oil Technical Conference and Exhibition, March 11-14, pp 347-356

Sarica C and O Shoham, 1991, *A Simplified Transient Model for Pipeline-Riser Systems*, Chemical Engineering Science, vol. 46, no. 9, pp 2167-2179

Scandpower, 1997, *OLGA Validation Case*

Scandpower, 2000, *OLGA 2000 Users Manual*

Scandpower, 2002, *OLGA 2000 Frequently Asked Questions*, Internet Reference, http://www.scandpower.com

Schmidt, Z, 1977, *Experimental Study of Two-Phase Slug Flow in a Pipeline Riser Pipe System*, PhD. Dissertation, University of Tulsa

Schmidt Z, J P Brill and D H Beggs, 1980, *Experimental Study of Severe Slugging in a Two-Phase Flow Pipeline-Riser Pipe System*, Society of Petroleum Engineers Journal, October, pp 407-414

Schmidt Z, J P Brill and D H Beggs, 1981, *Experimental Study of Normal Slug Flow in a Two-Phase Flow Pipeline-Riser Pipe System*, Journal of Energy Resources Technology, vol. 103, pp 67-75

Schmidt Z, D R Doty and K Dutta-Roy, 1985, *Severe Slugging in Offshore Pipeline Riser Pipe Systems*, Society of Petroleum Engineers Journal, February, pp 27-38

Schotbot K, 1986, *Methods for the Alleviation of Slug Flow Problems and Their Influence on Field Development Planning*, SPE 15891, Presented at the Society of Petroleum Engineers European Petroleum Conference, October 20-22

Straume T, M Nordsveen and K Bendiksen, 1992, *Numerical Simulation in Pipelines*, FED-144, ASME Fluid Engineering Division Multiphase Flow in Wells and Pipelines, pp 103-112

Taitel Y and A E Dukler, 1976, *A Model for Prediction Flow Regime Transitions in Horizontal and Near Horizontal Gas Liquid Flow*, American Institute of Chemical Engineers Journal, vol. 22, pp 47-55

Taitel Y, 1986, *Stability of Severe Slugging*, International Journal of Multiphase Flow, vol. 12, no. 2, pp 203-217

Taitel Y and D Barnea, 1990, *Two Phase Slug Flow*, Advances in Heat Transfer, Academic Press, pp 83-132

Taitel Y, S Vierkandt, O Shoham and J P Brill, 1990, *Severe Slugging in a Riser System, Experiment and Modelling*, International Journal of Multiphase Flow, vol. 16, no. 9, pp 57-68

Tin V and D Incoll, 1990, *Severe Slugging in Flexible Risers*, MPE Report 052, BHRg

Tin V, 1991, *Severe Slugging in Flexible Risers*, Proceeding 5th International Conference on Multiphase Production, BHRg, pp 507-525

Tin V and S Sarshar, 1993, *An Investigation of Severe Slugging Characteristics in Flexible Risers*, Proceedings 6th International Conference on Multiphase Production, BHRg, pp 205-227

Walpole R E and R H Myers, 1989, *Probability and Statistics for Engineers and Scientists*, 4th Ed., MacMillan Publishing

Wood, D G, 1991, *Mechanistic Modelling of Terrain-Induced Slugs in Gas/Condensate Lines*, Proceeding 5th International Conference on Multiphase Production, BHRg, pp 68-79

Yeung H, 1996, *Flexible Risers Severe Slugging, Progress Report Number 3*, Project 4 Managed Programme on Transient Multiphase Flows, Cranfield University

Yeung H, 1997, *Flexible Risers Severe Slugging, Phase I Final Report*, Managed Programme on Transient Multiphase Flows, Cranfield University

Yocum B T, 1973, *Offshore Riser Slug Flow Avoidance: Mathematical Models for Design and Optimisation*, SPE 4312, Presented at the Society of Petroleum Engineers London Meeting

Yuan H, C Sarcia, H Zhang and J P Brill, *Characterisation of Slug Dissipation in Downward Flow*, Proceedings 9th International Conference on Multiphase Production, BHRg, pp 119-131

Zheng G, J P Brill and Y Taitel, 1994, *Slug Flow Behaviour in a Hilly Terrain Pipeline*, Internation Journal of Multiphase flow, vol. 20, no. 1, pp 63-79

Zuber N and J A Findlay, 1960, *Average Volumetric Concentration in Two-Phase Flow Systems*, Journal of Heat Transfer, November, pp 453-468

Publications

Montgomery J A and H C Yeung, 2000, *The Stability of Fluid Production from a Flexible Riser*, ETCE/PROD-10072, Presented at ETCE 2000,

Montgomery J A and H C Yeung, 2002, *The Stability of Fluid Production from a Flexible Riser*, To Appear in Journal of Energy Resources Technology

Yeung H C and J A Montgomery, 2001, *Hydrodynamic Behaviour of a Flexible Riser – A Comparison of Experimental Data and Three Transient Code Predictions*, Proceedings 10th International Conference on Multiphase Production, BHRg

Appendix A

Matlab Script Files

Appendix A1 – Data Processing

There are two main files for processing data from the Cranfield University Three Phase Facility, these are dependent on the version number of the Data Acquisition System software. The first, dataproclg.m, is used for version 4, while the second, dataproclg2.m, is used for version 3.

The processing files are based upon the analysis presented in Chapter 3. The final result is a tab-delimited ASCII with a .RES suffix, containing the following information:

General Test Information

- Test Code
- Average Gas and Liquid Mass Flowrate During Test
- Average Gas and Liquid Velocity During Test
- Minimum and Maximum Riser Base Pressure
- Minimum and Maximum Separator Pressure
- Average and Minimum Liquid Holdup Local to the Riser Base

Time-Varying Data

- Riser Base Pressure
- Separator Pressure
- Pressure Difference Over Lower Limb
- Pressure Difference Over Downcomer
- Pressure Difference Over Upper Limb
- Riser Base Holdup
- Inlet Gas Mass Flow
- Inlet Gas Superficial Velocity
- Inlet Liquid Mass Flow
- Inlet Liquid Superficial Velocity
- Liquid Mass Production
- Outlet Liquid Mass Flow
- Outlet Liquid Superficial Velocity
- Outlet Gas Mass Flow
- Outlet Gas Superficial Velocity

Dataproclg.m

```
function dataproclg
%   dataprc a Matlab function to process the data from the flexible riser rig.
%   Output is a series of columns that can be used by a Matlab plotting routine.
%   This version of processing prog will give output from liquid and gas mass balance
%   Based upon analysis by Montgomery (2000).
%
%   First Created      7/4/2000       Version 3.0
%
fsname=input('Please enter filename for the processing file (inc. extension):      ');     % Standard initialisation
arrname=strtok(fsname,'.');
recfreq=input('Please enter the recording frequency: ');
ffile=fopen(fsname);
global results
for n=1:11                                                                               % Temp loop to get rid of header
   temp_header_line=fgetl(ffile);
end
temp_results=fscanf(ffile,'%g',[25 inf]);
fclose(ffile);
R=8314;
M_w=28.84;
A_p=2.1649e-03;
temp_results=temp_results';
res_size=size(temp_results);                                                             % Find size for relevant loops
results=zeros(res_size(1),16);                                                           % Output matrix definition
smooth_level=zeros(res_size(1),1);                                                       % Definition of the processing vectors
mass_gas_sep=zeros(res_size(1),1);
smooth_gas_mass_sep=zeros(res_size(1),1);
smooth_gas_flo_out=zeros(res_size(1),1);
gas_flo_out=zeros(res_size(1),1);
d_smooth_gas_flo_out=zeros(res_size(1),1);
d2_smooth_gas_flo_out_dt2=zeros(res_size(1),1);
mass_gas_out=zeros(res_size(1),1);
results(:,1)=temp_results(:,1);                                                          % Time column
results(:,2)=temp_results(:,5);                                                          % Riser base pressure
results(:,3)=temp_results(:,10);                                                         % Separator pressure
results(:,4)=temp_results(:,5)-temp_results(:,10);                                       % Riser pressure difference
results(:,5)=temp_results(:,5)-temp_results(:,6);                                        % Lower limb p. difference
results(:,6)=temp_results(:,7)-temp_results(:,6);                                        % Downcomer p. difference
results(:,7)=temp_results(:,7)-temp_results(:,10);                                       % Upper limb p. difference
gas_flo_out=temp_results(:,18);                                                          % Read in gas flow for smoothing
smooth_gas_flo_out=gas_flo_out;                                                          % Initialise the smooth vector
for n=1:res_size(1)-5
```

```
if n<=6     %       IF loop for the holdup results
   results(n,8)=temp_results(n,15)/1000;                                    % 1st 10 holdups same as raw data
   smooth_level(n)=0.5/100*temp_results(n,19);                              % Convert % height to m in the sep
else
   results(n,8)=0.1*(temp_results(n-1,15)+temp_results(n-2,15)+...
      temp_results(n-3,15)+temp_results(n-4,15)+temp_results(n-5,15)+...
      temp_results(n+1,15)+temp_results(n+2,15)+temp_results(n+3,15)+...
      temp_results(n+4,15)+temp_results(n+5,15))/1000;                      % 10 pt. moving average for holdup
   smooth_level(n)=0.1*(temp_results(n-1,19)+temp_results(n-2,19)+...
      temp_results(n-3,19)+temp_results(n-4,19)+temp_results(n-5,19)+...
      temp_results(n+1,19)+temp_results(n+2,19)+temp_results(n+3,19)+...
      temp_results(n+4,19)+temp_results(n+5,19))*0.5/100;                   % 10 pt. mov. ave. for sep. level
end
mass_gas_sep(n)=(0.19635*(0.5-smooth_level(n))+0.0248)*temp_results(n,10)*M_w/R/...
   (temp_results(n,14)+273.15)*100000;                                      % Note added volume in separator
if n<=6                                                                     % Loop to smooth the separator mass
   smooth_gas_mass_sep(n)=mass_gas_sep(n);
else
   smooth_gas_mass_sep(n)=0.1*(mass_gas_sep(n-1)+mass_gas_sep(n-2)+mass_gas_sep(n-3)+...
      mass_gas_sep(n-4)+mass_gas_sep(n-5)+mass_gas_sep(n+1)+mass_gas_sep(n+2)+...
      mass_gas_sep(n+3)+mass_gas_sep(n+4)+mass_gas_sep(n+5));
end
results(n,9)=((temp_results(n,16)/1000*temp_results(n,2)*M_w/R/...
   (temp_results(n,11)+273.15))+(temp_results(n,17)*M_w/1000*temp_results(n,3)/R/...
   (temp_results(n,12)+273.15)))*100000;                                    % Inlet Gas Mass Flow
   results(n,10)=results(n,9)*R*(temp_results(n,13)+273.15)/temp_results(n,4)/100000/...
      M_w/A_p;                                                              % Correct to the pipeline conditions
   %   Liquid Mass Balance Loop
   if n>=2
      results(n,13)=temp_results(n,23)*0.6+(1000*0.19635*(smooth_level(n)-...
         smooth_level(n-1))/(results(n,1)-results(n-1,1)));                 % Note mod. on measured flow
      if n>10                                                               % Pre-processing gas flow from sep.
         d_gas_flo_out_dt(n)=(gas_flo_out(n)-gas_flo_out(n-1))/(results(n,1)-results(n-1,1));
         d2_gas_flo_out_dt2(n)=(d_gas_flo_out_dt(n)-d_gas_flo_out_dt(n-1))/(results(n,1)-results(n-1,1));
         if norm(d_gas_flo_out_dt(n))>0                                     % Comparison
            if norm(d2_gas_flo_out_dt2(n))>20
               smooth_gas_flo_out(n)=1/10*(smooth_gas_flo_out(n+5)+smooth_gas_flo_out(n+4)+...
                  smooth_gas_flo_out(n+3)+smooth_gas_flo_out(n+2)+smooth_gas_flo_out(n+1)+...
                  smooth_gas_flo_out(n-5)+smooth_gas_flo_out(n-4)+smooth_gas_flo_out(n-3)+...
                  smooth_gas_flo_out(n-2)+smooth_gas_flo_out(n-1));         % Use smoothing on erroneous data
            end
         end
      end
   end
end
```

```
smooth_gas_flo_out=medfilt1(smooth_gas_flo_out,9);                              % Use median filter on remaining spikes
* Gas mass balance loop
for n=2:res_size(1)
   mass_gas_out(n)=smooth_gas_flo_out(n)/1000*temp_results(n,10)*M_w/R/...
      (temp_results(n,14)+273.15)*100000;                                       % Gas Mass Flow Out of Separator
   results(n,15)=(mass_gas_out(n)+(smooth_gas_mass_sep(n)-smooth_gas_mass_sep(n-1))/(results(n,1)-results(n-1,1)));
   results(n,16)=results(n,15)*R*(temp_results(n,14)+273.15)/temp_results(n,10)/100000/...
      M_w/A_p;
end
results(:,11)=temp_results(:,20)+temp_results(:,21);                            % Inlet Liquid Mass Flow
results(:,12)=(temp_results(:,20)+temp_results(:,21))/A_p/1000;                 % Inlet Liquid Velocity
results(:,14)=results(:,13)/A_p/1000;
%       Calculate the required variables - average velocities, average holdup, min holdup, etc., note all superficial
mg_ave=mean(results(:,9));
ml_ave=mean(results(:,11));
ug_ave=mean(results(:,10));
ul_ave=mean(results(:,12));
hl_ave=mean(results(:,8));
hl_min=min(results(:,8));
pbase_min=min(results(:,2));
pbase_max=max(results(:,2));
psep_min=min(results(:,3));
psep_max=max(results(:,3));
m_data=[mg_ave ml_ave];
u_data=[ug_ave ul_ave];
hl_data=[hl_ave/1000 hl_min/1000];
pbase_data=[pbase_min pbase_max];
psep_data=[psep_min psep_max];
%   Output section
outext='.res';
outputfname=strcat(arrname,outext);                                             % Prepare results file for output
ofile=fopen(outputfname,'w');
fprintf(ofile,'Test Case\t%s\n',arrname);
fprintf(ofile,'Gas Velocity (m/s)\t%6.4g\tLiquid Velocity (m/s)\t%6.4g\n',u_data);
fprintf(ofile,'Mass Flow Gas (kg/s)\t%6.4g\tMass Flow Liquid (kg/s)\t%6.4g\n',m_data);
fprintf(ofile,'Min Base Pressure (bara)\t%6.4g\nMax. Base Pressure (bara)\t%6.4g\n',pbase_data);
fprintf(ofile,'Min Sep Pressure (bara)\t%6.4g\nMax. Sep Pressure (bara)\t%6.4g\n',psep_data);
fprintf(ofile,'Ave. Riser Base Holdup\t%6.4g\nMin. Riser Base Holdup\t%6.4g\n',hl_data);
fprintf(ofile,'Time\tP Base\tP Sep\tdP Riser\tdP Lower\tdP Dcomer\tdP Upper\tHoldup\tInlet Gas Massflow\tInlet Gas Velocity\tInlet Liquid
Massflow\tInlet Liquid Velocity\tLiquid Mass Prodn\tOutlet Liquid Velocity\tGas Mass Prodn\tOutlet Gas Velocity\n');
fprintf(ofile,'(s)\t(bara)\t(bara)\t(bara\t(bara)\t(bara)\t(bara)\t\t(kg/s)\t(m/s)\t(kg/s)\t(m/s)\t(kg/s)\t(m/s)\t(kg/s)\t
(m/s)\n');
fprintf(ofile,'%8.6g\t%8.6g\t%8.6g\t%8.6g\t%8.6g\t%8.6g\t%8.6g\t%8.6g\t%8.6g\t%8.6g\t%8.6g\t%8.6g\t%8.6g\t%8.6g\t%8.6g\t
%8.6g\n',results');
fclose(ofile);
```

Dataproclg2.m

```
function dataproclg
%       dataprc a Matlab function to process the data from the flexible riser rig.
%       Output is a series of columns that can be used by a Matlab plotting routine.
%       This version of processing prog will give output from liquid and gas mass
%       balance
%
%       Based upon analysis by Montgomery (2000).
%
%       First Created  7/4/2000              Version 3.0
%       Last Modified  14/6/2000             Correct for new flow area and voltage for BP data
%
fsname=input('Please enter filename for the processing file (inc. extension):      ');     % Standard initialisation
arrname=strtok(fsname,'.');
recfreq=input('Please enter the recording frequency: ');
ffile=fopen(fsname);
global results
for n=1:11                                                                               % Temp loop to get rid of header
   temp_header_line=fgetl(ffile);
end
temp_results=fscanf(ffile,'%g',[25 inf]);
fclose(ffile);
R=8314;
M_w=28.84;
A_p=2.1649e-03;
temp_results=temp_results';
res_size=size(temp_results);                                                             % Find size for relevant loops
results=zeros(res_size(1),16);                                                           % Output matrix definition
smooth_level=zeros(res_size(1),1);                                                       % Definition of the processing vectors
mass_gas_sep=zeros(res_size(1),1);
smooth_gas_mass_sep=zeros(res_size(1),1);
smooth_gas_flo_out=zeros(res_size(1),1);
gas_flo_out=zeros(res_size(1),1);
d_smooth_gas_flo_out=zeros(res_size(1),1);
d2_smooth_gas_flo_out_dt2=zeros(res_size(1),1);
mass_gas_out=zeros(res_size(1),1);
results(:,1)=temp_results(:,1);                                                          % Time column
results(:,2)=temp_results(:,5);                                                          % Riser base pressure
results(:,3)=temp_results(:,10);                                                         % Separator pressure
results(:,4)=temp_results(:,5)-temp_results(:,10);                                       % Riser pressure difference
results(:,5)=temp_results(:,5)-temp_results(:,6);                                        % Lower limb p. difference
results(:,6)=temp_results(:,7)-temp_results(:,6);                                        % Downcomer p. difference
results(:,7)=temp_results(:,7)-temp_results(:,10);                                       % Upper limb p. difference
gas_flo_out=temp_results(:,18);                                                          % Read in the gas flow for calculation/smoothing
smooth_gas_flo_out=gas_flo_out;                                                          % Initialise the smooth vector prior to smoothing
```

```
for n=1:res_size(1)-5
   if n<=6
      results(n,8)=temp_results(n,15)/1000;                                    % IF loop for the holdup results
      smooth_level(n)=0.25*(temp_results(n,19)-1)*0.5;                         % 1st 10 holdups same as raw data
   else                                                                        % Convert Voltage to m in the sep
      results(n,8)=0.1*(temp_results(n-1,15)+temp_results(n-2,15)+...
         temp_results(n-3,15)+temp_results(n-4,15)+temp_results(n-5,15)+...
         temp_results(n+1,15)+temp_results(n+2,15)+temp_results(n+3,15)+...
         temp_results(n+4,15)+temp_results(n+5,15))/1000;                      % 10 pt. moving average for holdup
      smooth_level(n)=(0.1*(temp_results(n-1,19)+temp_results(n-2,19)+...
         temp_results(n-3,19)+temp_results(n-4,19)+temp_results(n-5,19)+...
         temp_results(n+1,19)+temp_results(n+2,19)+temp_results(n+3,19)+...
         temp_results(n+4,19)+temp_results(n+5,19))-1)*0.25*0.5;               % 10 pt. mov. ave. for sep. level
   end
   mass_gas_sep(n)=(0.19635*(0.5-smooth_level(n))+0.0248)*temp_results(n,10)*M_w/R/...
      (temp_results(n,14)+273.15)*100000;                                      % Note added volume in separator
   if n<=6                                                                     % Loop to smooth the separator mass
      smooth_gas_mass_sep(n)=mass_gas_sep(n);
   else
      smooth_gas_mass_sep(n)=0.1*(mass_gas_sep(n-1)+mass_gas_sep(n-2)+mass_gas_sep(n-3)+...
         mass_gas_sep(n-4)+mass_gas_sep(n-5)+mass_gas_sep(n+1)+mass_gas_sep(n+2)+...
         mass_gas_sep(n+3)+mass_gas_sep(n+4)+mass_gas_sep(n+5));
   end
   results(n,9)=((temp_results(n,16)/1000*temp_results(n,2)*M_w/R/...
      (temp_results(n,11)+273.15))+(temp_results(n,17)*M_w/1000*temp_results(n,3)/R/...
      (temp_results(n,12)+273.15)))*100000;  %       Inlet Gas Mass Flow
   results(n,10)=results(n,9)*R*(temp_results(n,13)+273.15)/temp_results(n,4)/100000/...
      M_w/A_p; %       Correct to the pipeline conditions
   if n>=2
results(n,13)=temp_results(n,23)*0.6+(1000*0.19635*(smooth_level(n)-...          % Liquid Mass Balance Loop
      smooth_level(n-1))/(results(n,1)-results(n-1,1)));                       % Note mod. on measured flow
      if n>10  %       Do Pre-processing of the gas volume flow from the riser
         d_gas_flo_out_dt(n)=(gas_flo_out(n)-gas_flo_out(n-1))/(results(n,1)-results(n-1,1));
         d2_gas_flo_out_dt2(n)=(d_gas_flo_out_dt(n)-d_gas_flo_out_dt(n-1))/(results(n,1)-results(n-1,1));
         if norm(d_gas_flo_out_dt(n))>0                                        % Comparison
            if norm(d2_gas_flo_out_dt2(n))>20
               smooth_gas_flo_out(n)=1/10*(smooth_gas_flo_out(n+5)+smooth_gas_flo_out(n+4)+...
                  smooth_gas_flo_out(n+3)+smooth_gas_flo_out(n+2)+smooth_gas_flo_out(n+1)+...
                  smooth_gas_flo_out(n-5)+smooth_gas_flo_out(n-4)+smooth_gas_flo_out(n-3)+...
                  smooth_gas_flo_out(n-2)+smooth_gas_flo_out(n-1));          % Use smoothing on erroneous data
            end
         end
      end
   end
end
```

```
smooth_gas_flo_out=medfilt1(smooth_gas_flo_out,9);                                  % Use median filter on remaining spikes
for n=2:res_size(1) %  Gas mass blance loop
   mass_gas_out(n)=smooth_gas_flo_out(n)/1000*temp_results(n,10)*M_w/R/...
      (temp_results(n,14)+273.15)*100000;                                           % Gas Mass Flow Out of Separator
   results(n,15)=(mass_gas_out(n)+(smooth_gas_mass_sep(n)-smooth_gas_mass_sep(n-1))/(results(n,1)-results(n-1,1)));
   results(n,16)=results(n,15)*R*(temp_results(n,14)+273.15)/temp_results(n,10)/100000/...
      M_w/A_p;
end
results(:,11)=temp_results(:,20)+temp_results(:,21);                                % Inlet Liquid Mass Flow
results(:,12)=(temp_results(:,20)+temp_results(:,21))/A_p/1000;                     % Inlet Liquid Velocity
results(:,14)=results(:,13)/A_p/1000;
%       Calculate the required variables - average velocities, average holdup, min holdup, etc., note all superficial
mg_ave=mean(results(:,9));
ml_ave=mean(results(:,11));
ug_ave=mean(results(:,10));
ul_ave=mean(results(:,12));
hl_ave=mean(results(:,8));
hl_min=min(results(:,8));
pbase_min=min(results(:,2));
pbase_max=max(results(:,2));
psep_min=min(results(:,3));
psep_max=max(results(:,3));
m_data=[mg_ave ml_ave];
u_data=[ug_ave ul_ave];
hl_data=[hl_ave/1000 hl_min/1000];
pbase_data=[pbase_min pbase_max];
psep_data=[psep_min psep_max];
%       Output section
outext='.res';
outputfname=strcat(arrname,outext);                                                 % Prepare results file for output
ofile=fopen(outputfname,'w');
fprintf(ofile,'Test Case\t%s\n',arrname);
fprintf(ofile,'Gas Velocity (m/s)\t%6.4g\tLiquid Velocity (m/s)\t%6.4g\n',u_data);
fprintf(ofile,'Mass Flow Gas (kg/s)\t%6.4g\tMass Flow Liquid (kg/s)\t%6.4g\n',m_data);
fprintf(ofile,'Min Base Pressure (bara)\t%6.4g\nMax. Base Pressure (bara)\t%6.4g\n',pbase_data);
fprintf(ofile,'Min Sep Pressure (bara)\t%6.4g\nMax. Sep Pressure (bara)\t%6.4g\n',psep_data);
fprintf(ofile,'Ave. Riser Base Holdup\t%6.4g\nMin. Riser Base Holdup\t%6.4g\n',hl_data);
fprintf(ofile,'Time\tP Base\tP Sep\tdP Riser\tdP Lower\tdP Dcomer\tdP Upper\tHoldup\tInlet Gas Massflow\tInlet Gas Velocity\tInlet Liquid
Massflow\tInlet Liquid Velocity\tLiquid Mass Prodn\tOutlet Liquid Velocity\tGas Mass Prodn\tOutlet Gas Velocity\n');
fprintf(ofile,'(s)\t(bara)\t(bara)\t(bara\t(bara)\t(bara)\t(bara)\t\t(kg/s)\t(m/s)\t(kg/s)\t(m/s)\t(kg/s)\t(m/s)\t(kg/s)\t(m/s)\n');
fprintf(ofile,'%8.6g\t%8.6g\t%8.6g\t%8.6g\t%8.6g\t%8.6g\t%8.6g\t%8.6g\t%8.6g\t%8.6g\t%8.6g\t%8.6g\t%8.6g\t%8.6g\t%8.6g\t%8.6g\t%8.6g\n',results');
fclose(ofile);
```

Appendix A2 – Probability Distribution Function

This script file calculates the probability density function (pdf) of an input signal, here the pressure difference over the riser. The pdf of the signal is defined by:

$$P(x_1 < X < x_2) = \int_{x_1}^{x_2} p(x)\, dx$$

Where $P(x_1 < X < x_2)$ is the probability that the value X lies between x_1 and x_2. In the above equation, the x value is the value of interest, in this case, the pressure difference over the riser. In order to calculate this value, the following process is used:

1. The data is read into an array, described as a band with x values over the range (x_0, x_N)
2. An appropriate number of 'bins' is set. Each bin corresponds to an interval over which the pdf is calculated.
3. Based upon the number of bins, the interval size, dx, is determined by

$$dx = \frac{\max(band)}{\|bins\|}$$

   and the limits of the bin are set as $(x_0, x_0 + dx)$.
4. All entries in the bin interval are read into an array, denoted 'elements'.
5. The number of entries in the 'elements' array is found:

$$n_{Bin} = card\{elements\}$$

   Where *card* is the cardinality of the array, or the number of elements of the array
6. The probability of an x value lying within the bin interval

$$p(x_0 < x < x_0 + dx) = \frac{n_{Bin}}{card\{band\}}$$

7. The bin limits are updated with lower and upper limits of $x_1 = x_0 + dx$ and $x_1 + dx$ respectively.
8. Steps 4 to 7 are repeated for the new bin interval.

This process is repeated until the entire band is covered and a distribution of probabilities over the entire range of x values is obtained, this is the probability density function. The sum of this probability distribution is unity.

Riser_pdf

```
function riser_pdf
%       riser_pdf a Matlab function to process the data from the flexible riser rig.
%       The purpose is to derive the probability density function and/or obtain a
%       power spectrum of the data from the riser flexible riser rig.
%
%       Based upon analysis by Montgomery (2000).
%
%       First Created  7/4/2001
%
fsname=input('Please enter filename for the processing file (inc. extension):      ');     % Standard initialisation
arrname=strtok(fsname,'.');
signal_no=input('Please enter the data signal for processing [4, 5, 7, 14 or 16]:  ');
detail=input('Please enter the detail level of analysis that you require [1-2]:    ');
ffile=fopen(fsname);
global results
for n=1:11                                                                          % Temp loop to get rid of header
   temp_header_line=fgetl(ffile);
end
temp_results=fscanf(ffile,'%g',[16 inf]);
fclose(ffile);
R=8314;
M_w=28.84;
A_p=2.1649e-03;
temp_results=temp_results';
res_size=size(temp_results);                                                        % Find size for relevant loops
results=zeros(res_size(1),4);                                                       % Output matrix definition
results(:,1)=temp_results(:,1);
results(:,2)=temp_results(:,signal_no);                                             % Initialisation
results(:,3)=temp_results(:,signal_no);
results(:,4)=temp_results(:,signal_no);
if detail==1                                                                        % Simply plots the results
   plot(results(:,1),results(:,2));
elseif detail==2
   band=input('Please enter the band for the processing of the data as a vector (in seconds):     ');
   density=200;                                                                     % Determine the number of bins
   upper_lim=max(results(:,2));
   if size(band)==0;
      position=[1 res_size(1)];
   else
      position=[band(1)*10+1 band(2)*10+1];                                         % Set the cell numbers for band
   end
   n_window=position(2)-position(1)+1;
```

```
   b_window=zeros(n_window,1);                                          % Initialise data array
   b_window=(results(position(1):position(2),2));
%   b_window=sort(b_window);
   limits=[0 upper_lim];
   dx=(limits(2)-limits(1))/density                                     % Set size of bin numerically
   res_array=zeros(density+1,2);
   x_l=0;                                                               % Set limits
   x_u=0;
   for i=1:density+1;
      x_u=x_l+dx;                                                       % Update upper limit
      k=0;
%      c=[x_l x_u];
%      disp(c)
%       Find number of entries lying in interval
      elements=find((b_window>x_l) & (b_window<x_u));                   % Find position of limit for bin arrays
      if size(elements)==0
         k=0;
      else
         a=size(elements);                                              % Find size of bin array
         k=a(1);                                                        % Find number of bin entries
      end
      res_array(i,1)=(x_u+x_l)/2;                                       % Set median value corresponding to bin
%      res_array(i,2)=k;
      count=k;
      p_x=count/n_window;                                               % Find probability
      res_array(i,2)=p_x;
      x_l=x_u;                                                          % Update lower limit
   end
%   plot(res_array(:,1),res_array(:,2));
end
outext='.rpd';
outputfname=strcat(arrname,outext);                                     % Prepare results file for output
ofile=fopen(outputfname,'w');
fprintf(ofile,'Test Case\t%s\n',arrname);
fprintf(ofile,'X\tp(X)\n');
fprintf(ofile,'%8.6g\t%8.6g\n',res_array');
fclose(ofile);
```

Appendix A3 – Integration

As described in Chapter 4, the slug size is determined from the integration of the liquid mass production from the riser. The integration is:

$$V_{SL} = \frac{M_{SL}}{\rho_L} = \frac{1}{\rho_L}\int_{t_1}^{t_2} G_{LO}(t)\,dt$$

Where G_{LO} is the outlet liquid mass flow from the riser or the liquid mass production rate. The integration method used for the calculation is and extended version of Simpson's Rule for non-overlapping intervals as described by Press *et al.* (1992):

$$\int_{x_1}^{x_n} f(x)\,dx = h\left[\frac{1}{3}f_1 + \frac{4}{3}f_2 + \frac{2}{3}f_3 + \frac{4}{3}f_4 + \ldots + \frac{2}{3}f_{N-2} + \frac{4}{3}f_{N-1} + \frac{1}{3}f_N\right]$$

This is comprehensively described in the references and is thus not repeated here. Comments provided in the script file describe the computations further.

Rinteg

```
Function rinteg
%
%       RINTEG programme to calculate the area beneath a curve from the Cranfield University
%       Three Phase Facility. The programme input is a pair of limits and a curve identifier for
%       the production graph required.
%
%       Written by:     Jonathan Montgomery
%       Orginated:      19/05/1999
%
%       Last Modified: 19/05/1999
%
%
fsname=input('Please enter filename for the processing file (inc. extension):      ');     % Standard initialisation
arrname=strtok(fsname,'.');
recfreq=input('Please enter the recording frequency: ');
ffile=fopen(fsname);
global results
for n=1:11                                                                                  % Temp loop to get rid of header
   temp_header_line=fgetl(ffile);
end
results=fscanf(ffile,'%g',[16 inf]);
fclose(ffile);
R=8314;
M_w=28.84;
A_p=2.1649e-03;
results=results';
cont=1;                                                                                     % Continuity counter
while cont==1
   time=input('Please input the range over which you wish to integrate:     ');           % Input of limits for integration
   nstart=(time(1)*10)+1;                                                                   % Find the start point of the integrand
   nend=(time(2)*10)+1;                                                                     % Find the end point of the intergrand
   h=1/recfreq;                                                                             % Determine the time interval
   nintervals=nend-nstart;                                                                  % Determine the number of intervals
   n=(nend-nstart)+1;
   if rem(nintervals,2)==0;
      else;
      disp('! Note: Uneven number of intervals, interval increased by a timestep !')       % Check for uneven intervals
      nend=nend+1;                                                                          % If so, increase limit by single timestep
   end;
   ninteravals=nend-nstart;
   n=(nend-nstart)+1;
   total=0;                                                                                 % Initialise the integral
```

```
%       Note as the mass production is in kg/s, the density and volume corrections cancel one another out
%       hence, 1 kg/s is 1 l/s, so direct integration of the mass flow gives the volume in l
   total=results(nstart,13)/3;                                                    % First step in integration
   for i=2:n-1;
      if   rem(i,2)==0;
         total=total+(4/3)*results(i+nstart,13);                                  % For even integral steps
      else;
         total=total+(2/3)*results(i+nstart,13);                                  % For uneven integral steps
      end;
   end;
   total=total+results(n,13)/3;                                                   % Final step in integration
   integ=h*total                                                                  % Complete integration using stepsize
   ave=total/nintervals                                                           % Find average flow
   peak=max(results(nstart:nend,13))                                              % Find peak flow
   clear total;                                                                   % Clear results for the next loop of script
   clear n;
   clear nintervals;
   clear nend;
   clear nstart;
   clear time;
   %disp('The total mass production over the range',time(1),'to',time(2),'is:',integ)
   cont=input('Finished? (1 = continue, 0 = end):    ');
end
```

Appendix A4 – Criterion

The script file for the criterion is included here for reference. It implements the calculations as discussed in Chapter 5.

Slug_Stability

```
function Slug_Stability
%       Slug_Stability a Matlab function to calculate the stability of severe slugging
%       in a riser.
%
%       Based upon analysis by Montgomery (2000).
%
%       First Created  9/3/2000              Version 3.0
%       Last Modified  10/3/2000      Added in graphical output inc. graph options
%       Last Modified  21/3/2000      Added in Annular flow calculation
%       Last Modified  22/3/2000      Added in Bubble flow calculation
%   Last Modified   17/2/2002   Modified calculation of drift parameters & changed output
%
global results %       Declaration of global in.put vector and output matrix
global hr L beta theta D A f Psep Tsep rho_L mu_L mu_G STP_rhoG M_w Z rho_G sigma
global bubbndry
%   Filename input section
name=input('Please enter Case Name (Inc. Extension): ');                    % Get output file
input_name=input('Please enter Input Filename (Inc. Extension):     ');     % Reading in data from pre-prepared files.
input_data=fopen(input_name,'r');                                           % Open input file
data=fscanf(input_data,'%g');                                               % Read input file (preset length)
fclose(input_data);
%   Initialisation, read values into the variable names
hr=data(1);                                                                 % Effective Riser Height
L=data(2);                                                                  % Pipeline length
beta=data(3);                                                               % Pipeline inclination
theta=data(4);                                                              % Inclination at the riser base
D=data(5);                                                                  % Pipe internal diameter
A=data(6);                                                                  % Pipeline area
f=data(7);                                                                  % Moody Friction factor
Psep=data(8);                                                               % Separator pressure
Tsep=data(9);                                                               % Separarator temperature
rho_L=data(10);                                                             % Liquid density
mu_L=data(11);                                                              % Liquid viscosity
mu_G=data(12);                                                              % Gas viscosity
STP_rhoG=data(13);                                                          % STP gas density
M_w=data(14);                                                               % Molecular wt. of gas
Z=data(15);                                                                 % Compressibility factor
sigma=data(16);                                                             % Surface tension
%   Note: extra empty element at the file end
%   Other data required (standard values)
g=9.81;
R=8314;
```

```
C0_H=1.05;                                                  % Standard value from Bendiksem (1984)
C0_V=1.2;                                                   % Standard value from Bendiksem (1984)
U_d_H=0.54*sqrt(g*D);
U_d_V=0.35*sqrt(g*D);
a=[0.099 0.7771 -0.2913 0.0525 -0.0036];                    % Coefficients for the holdup calculations
%       Preliminary calculations
%   Note: Below Fr Critical, hence check on
%   C0 and U_d not carried out
dPhy=rho_L*g*hr                                             % Hydrostatic head
P_b=Psep+dPhy;                                              % Calculate pipeline pressure
rho_G=P_b/Z/R/Tsep*M_w;                                     % Calculate Gas Density
C0=C0_H+(C0_V-C0_H)*sin(theta/180*pi)*sin(theta/180*pi);
U_d=U_d_H*cos(theta/180*pi)+U_d_V*sin(theta/180*pi);        % Calculate drift velocity
alpha_T=0.59+0.3031*((theta/90)^0.2308);                    % Taylor bubble film void fraction
output_file=fopen(name,'w');                                % Open the case file
% First calculation for the first map point
U_LS=0.01;
dp_dl=f/D*rho_L*U_LS*U_LS/2;                                % Pressure drop for the Taitel correlation
phi=rho_L*g*(sin(beta*pi/180))/dp_dl;
Chi=log10(phi);
alpha_P=a(1)+(a(2)*Chi)+(a(3)*Chi*Chi)+(a(4)*Chi*Chi*Chi)+...
   (a(5)*Chi*Chi*Chi*Chi);
ALPHA=[alpha_T alpha_P];                                    % Read fractions into vector for debugging
alpha_b=min(ALPHA);                                         % Select the minimum void fraction
CAlpha=C0*alpha_b;
U_GB=(CAlpha/(1-CAlpha))*U_LS+(alpha_b/(1-CAlpha))*U_d;     % Calculate base gas vel.
U_GI=(1-(g*(rho_L-rho_G)*sin(theta*pi/180)*alpha_P*L/P_b))*U_GB;  % Criterion
count=fprintf(output_file,'%g\t%g\n',[U_GI U_LS]);          % Output results to text file
%       Iteration for the other map points as above
for k=1:160
   loop=k-1;
   for l=1:10
      U_LS=0.01*k+0.001*(l);
      dp_dl=f/D*rho_L*U_LS*U_LS/2;
      phi=rho_L*g*(sin(beta*pi/180))/dp_dl;
      Chi=log10(phi);
      alpha_P=a(1)+(a(2)*Chi)+(a(3)*Chi*Chi)+(a(4)*Chi*Chi*Chi)+...
         (a(5)*Chi*Chi*Chi*Chi);
      ALPHA=[alpha_T alpha_P];
      alpha_b=min(ALPHA);
      CAlpha=C0*alpha_b;
      U_GB=(CAlpha/(1-CAlpha))*U_LS+(alpha_b/(1-CAlpha))*U_d;
      U_GI=(1-(g*(rho_L-rho_G)*sin(theta*pi/180)*alpha_P*L/P_b))*U_GB;
      count=fprintf(output_file,'%g\t%g\n',[U_GI U_LS]);
   end
```

```
end
fclose(output_file);                                                    % Close the file for writing, so as not to loose results
%       Segment for outputting to log-log plot, also new plot option
output_file=fopen(name,'r');                                            % Open for reading
results=fscanf(output_file,'%g %g',[2 inf]);                            % Read in and transpose to column vector
results=results';
fclose(output_file);
new_plot=input('New Plot? Y/N [N]:    ','s');                           % New plot option
if isempty(new_plot)
   new_plot='N';
end
if new_plot=='N';
   outplot(results);
elseif new_plot=='n';
   outplot(results);
else
   figure;
   outplot(results);
end
```

Appendix B

Frictional Loss Calculations

Relevance

Frictional losses are important in two main areas of this work – the use of pressure difference to estimate the liquid inventory in the pipeline/riser and the estimation of the friction factor for modelling/transient code simulations.

Pressure Difference Considerations

When examining the pressure difference over the riser, the pressure balance equation:

$$P_B = P_D + \rho_L g h' + \Delta P_{Loss} \qquad (B.1)$$

was modified to:

$$\Delta P_R = P_B - P_S = \rho_L g h' + \Delta P_{Loss} \approx \rho_L g h' \qquad (B.2)$$

by grouping the pressure terms at the inlet and outlet of the riser together and assuming the loss terms, particularly the frictional loss term, were negligible. This then related the effective height of liquid (and hence volume of liquid) in the riser to a measured pressure difference. This was repeated for each limb of the riser, allowing the quantity of liquid in the system to be estimated. This procedure was reliant on the assumption that losses were negligible. It is assumed in this analysis that friction losses will be the dominant loss terms and hence the discussion will focus on these losses alone.

Modelling/Transient Code Simulation Considerations

When calculating the pipeline liquid holdup according to the 1986 method of Taitel (see Appendix E), an estimation of the single-phase liquid pressure drop for the pipeline is required. This is estimated using the following formulation of the pressure drop equation[1]:

$$\Delta P_{FR} = \left(\frac{f' L}{D}\right)\frac{\rho_L U_L^2}{2} \qquad (B.3)$$

f', is the Moody friction factor such that:

$$f' = 4f \qquad (B.4)$$

Where f is the Fanning friction factor. It is this friction factor that must be estimated in order to complete the model calculations.

In order to close the model equations for a two or three-fluid model, a transient code requires an estimate of the wall shear stress. This is estimated through a range of correlations. As an input to the codes, users are required to enter one of two values –

[1] Note: This is the alternative formulation of the loss formula to the D'Arcy formula

an estimate of the Fanning friction factor for the pipe or an estimate of the roughness of the pipe wall.

Experiments

To resolve the issue of estimating appropriate values for f', f and the surface roughness, ε, a pair of single-phase liquid flow experiments were carried out:

- tmf2-2p-p2-v1-c5 – superficial liquid velocity 0.51 m/s
- tmf2-2p-p2-v1-c6 – superficial liquid velocity 0.63 m/s

These tests consisted of running liquid through the pipeline/riser system and measuring the steady-state pressure drop across a known section length. The riser was used in the tests as the height and length are known – 17.78 m and 9.982 m respectively. Furthermore, processing the data into the pressure difference over the riser, automatically extracts the desired pressure drop information.

So as to prevent trapped bubbles in the downcomer changing the effective hydrostatic head over the riser, see Chapter 5, the top of the riser bend was drained during a slow filling period prior to each test. Thus any trapped gas was bled from the system.

A sample graph from the first test is included below:

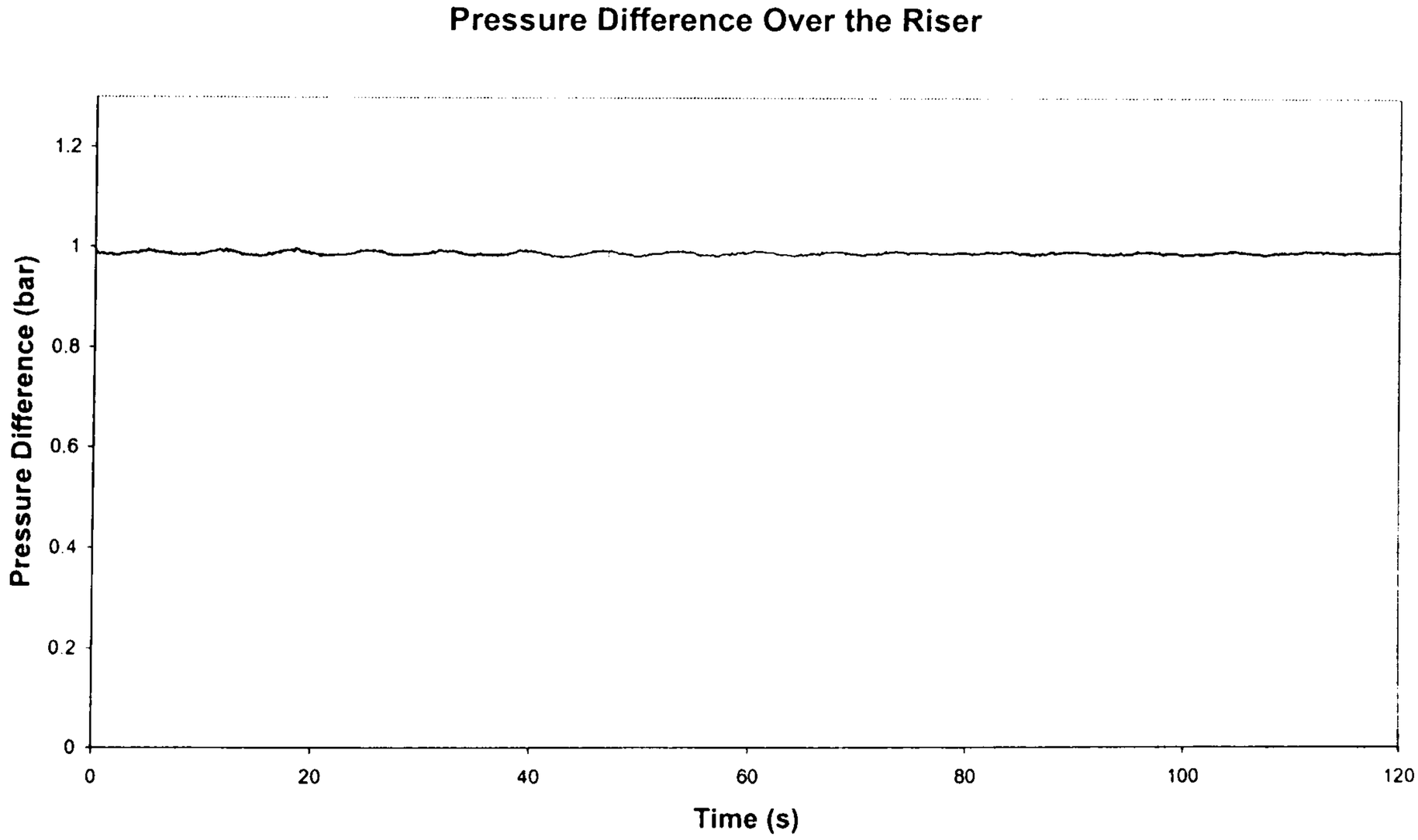

Figure B1 – Pressure Difference Over Riser

Summarising the raw test results:

Test Code	Superficial Liquid Velocity (m/s)	Pressure Difference (bar)
tmf2-2p-p2-v1-c5	0.51	0.988
tmf2-2p-p2-v1-c6	0.63	0.992

Table B1 – Raw Data from Single Phase Liquid Tests

Data Processing

The results are processed as follows:

1. The hydrostatic pressure difference over the riser is subtracted to give the frictional loss:

$$P_B - P_S = (\Delta P_R)_{MEAS} = \rho_L g h_R{}' + \Delta P_{FRs} \qquad (B.5)$$

As the riser is filled completely with liquid, the effective riser height is the actual riser height, h_R, and hence the hydrostatic head can be calculated. $(\Delta P_R)_{MEAS}$ is the measured pressure difference over the riser. This gives the friction losses as:

$$\Delta P_{Loss} = (\Delta P_R)_{MEAS} - \rho_L g h_R \qquad (B.6)$$

2. Using the formula provided by Bird, Stewart and Lightfoot (1960), the Fanning friction factor can be calculated from the measurements and the dimensions of the system:

$$f = \frac{1}{4}\left(\frac{D}{L}\right)\left(\frac{\Delta P_{FR}}{\frac{1}{2}\rho_L U_L^2}\right) \qquad (B.7)$$

3. Thus f* can be estimated from the equation presented above
4. Finally, an estimate of the pipe wall roughness is obtainable using the von Karman equation for Fanning friction factor for rough pipes:

$$\frac{1}{\sqrt{f}} = -4\log_{10}\left(\frac{\varepsilon}{3D}\right) \qquad (B.8)$$

Allowing an explicit solution to be obtained for ε.

Results

The results of the data processing are provided in Table B2 below:

Test Case	U_L^S (m/s)	ΔP_{FR} (Pa)	ΔP_{FR} (bar)	f	f'	ε (mm)	ε/D_P
c5	0.51	893	0.00893	0.00513	0.02052	0.062	0.0012
c6	0.63	1225	0.01225	0.00461	0.01844	0.041	0.00074
Average[2]				0.0049	0.0196	0.05	0.001

These values are used as input to the code and the criterion model. The values used in the calculations have been rounded to the nearest significant figure, rounding up. This reflects the fact that the obtained values are estimated and as such approximate where over-estimation of the frictional losses is more desirable then under-prediction.

Examining the values of the friction loss, the magnitude of the loss is negligible compared to the pressure difference in the riser and over each riser limb due to the liquid hydrostatic head, justifying the approach described in Chapter 5.

---

[2] This average is corrected to two significant decimals. This reflects the approximate nature of these estimations

Appendix C

Operating Procedures

Overview

The operation of the Cranfield University Three Phase Facility has been documented in works by Das (2001) and Wordsworth (1998). Below is attached a summary of the operating procedures.

Start-Up Checks

1. Ensure the test facility is isolated from other low-pressure facilities.
2. Ensure water outlet valve from Three-Phase Separator is closed.
3. Ensure all vents and drains in the facility are closed.
4. Ensure main vent valve on the Three-Phase Separator is opened.
5. Ensure oil return valves from the coalescers are closed.
6. Ensure water pump bypass valve is open.
7. Check water level in tank is above the minimum value of 4 m^3
8. Ensure gas flow control valve is closed.
9. Ensure buffer vessel drain valve is closed.
10. Ensure water pump control valve open.
11. Ensure water supply valves closed.
12. Ensure FL4 is turned on
13. Ensure water meters turned on
14. Turn on Data Acquisition System on.

Start-Up Procedure, P_S < 7 bar(a)

1. Remove pressure transducers P4 and P6, drain liquid, clean transducer and replace in riser.
2. Re-zero pressure transducer calibrations using DAS (see below)
3. Close main gas vent valve
4. Set the Three-Phase Separator pressure to the maximum setpoint value
5. Open the water recycle valves from the coalescers to the main water tank
6. Check compressor operation log, ensure the compressor is within service period
7. Check oil level and add oil if required
8. Drain condensate moisture traps
9. Prime cooling water pump
10. Start cooling water pump and open flow control value to the compressor

11. Check for a continuous coolant flow into the sump from the return line
12. Ensure the compressor operation switch is set to UNLOAD before starting
13. Turn on main isolator switch
14. Start compressor and wait until the motor has turned from STAR to DELTA configuration, recognisable by audible switching
15. Turn operating switch from UNLOAD to AUTOMATIC
16. Allow buffer vessel to reach set pressure, recognisable by an audible loading/unloading operation of the compressor.
17. Carry out compressor checks on compressor daily check list, see Wordsworth (1998) for details
18. Open gas isolation valve for the large gas flowmeter, FG3
19. Open gas regulating valve and start the flow of gas to the Three Phase Separator.
20. Allow pressure to increase to near the desired operating pressure. Adjust pressure control to begin actuation to regular the separator pressure.
21. Reduce the gas flow and ensure the separator pressure is maintained.
22. Ensure liquid pump bypass line valve is open.
23. Switch on main isolation valve for the water flow
24. Switch on main water pump
25. Open the required isolation valve for the liquid supply and adjust the liquid flow using the bypass valve
26. Allow gas and liquid flow to stabilise, paying particular attention to the flow as the liquid column build up in the riser.
27. Check main water level on the Separator and coalescers
28. Record data for desired time period

Shutdown Procedure

1. Turn off flowmeter for liquid flow from the top separator, FL4.
2. Open bypass valve on liquid feed pump
3. Turn off liquid feed pump and turn off isolation switch
4. Close the isolation valve for the liquid supply
5. Close the small gas flow metering isolation valve (if appropriate) and open large gas flow metering isolation valve
6. Open the gas flow control valve to remove liquid from the pipeline/riser system
7. Allow ten (10) minutes for initial removal of the bulk of liquid

8. Turn off compressor and the electrical isolation switch
9. Close cooling water control valve, switch off pump and isolator
10. Drain condensate moisture traps
11. Slowly open main gas control valve to relieve pressure in Three Phase Separator. Note: Due to high gas flow, the actual separator may be greater than the setpoint.
12. Close all outlet valves from the coalescers

Data Acquisition System Operating Procedure

Prior to Operation of Compressor

1. Turn on PC
2. Start LABView runtime
3. Press run on main screen.
4. Automatically, the programme will bring the users to a calibration screen. Enter the calibration process by clicking on the A/D Cals pushbutton
5. Check/confirm the calibration settings and set using the 'Confirm Changes?' pushbutton. Note also that the required flowmeters are set in the lookup table.
6. Select the Analogue Meters display and re-zero pressure transducers.

Post Compressor Operation

1. Allow system to reach regular pressure cycling
2. Record data to hard disc using the 'Save Data to File' screen

Shutdown Procedure

1. Return to Main Menu screen and select the large red button to shut down. Subsequent to this, the data is dumped into the system. Note: The data is only recorded at the end of the run. Hence this is a required step
2. Exit the LABView programme and shut down PC
3. Turn off power

Appendix D

Tables

Appendix D1 – Results Tables

This appendix presents summary tables for the experimental data in tabulated form. As stated in Chapter 3, the experiments were conducted in two campaigns, the first is denoted 'Series 1' while the second is denoted 'Series 2'. The separator pressure for the experiments is found from the second set of numbers – P2, P4 or P7. There is a volume variable V1, this is related to other experimental programmes and not relevant in this work. Finally, the test code denotes the sequence number of the experiment and is related to the original test matrix used when planning these experiments.

Series 1 P2 V1

Test Code	Flow Velocity		Flow Regime	Pressure Cycling					Liquid Production			
	Gas (m/s)	Liquid (m/s)		Cycle Time (s)	Buildup Time (s)	Production Time (s)	Bubble Pen. Time (s)	Blowdown Time (s)	Slug Size (kg)	Constant Size (kg)	Transient Size (kg)	Peak Prod. Rate (kg/s)
T1	0.0562	0.1205	SS1	543.5	197.1	317.8	13.6	15	138.63	106.41	27.24	4.7
T2	0.0623	0.7361	Osc(T)									
T3	0.1092	0.6572	Osc									
T4	0.2094	0.0583	SS2	232.1	199.4	7.7	10.1	14.9	29.23		29.23	6.37
T5	0.1511	0.1863	SS1	137.8	100.4	10	8	9.4	58.82	22.63	32.2	3.99
T6	0.3352	0.2015	SS3	222.4	153.4		5.6	18.8	89.5		89.5	8.1
T7	0.2622	0.3205	SS1	85.2	64.4	6.2	3.6	11	53.34	21.42	31.92	6.16
T8	0.2674	0.6829	Osc									
T9	0.3158	1.8152	Slug									
T10	0.3647	0.0528	SS3	147.4	124.9		7.1	15.4	16.77		16.77	3.62
T11	0.597	0.1337	Bubble									
T12	0.4916	0.2937	SS3	64.8	49		7.2	8.6	34.31		34.31	4.77
T13	0.9191	0.1046	Bubble									
T14	0.9058	0.2129	SS3	37.6	22.2		6.8	8.6	17.42		17.42	4.46
T15	0.9306	0.2779	SS3	39.4	25.2		5.5	8.7	21.89		21.89	4.94
T16	0.9347	0.7184	Slug									
T17	1.919	0.2292	Bubble									
T18	1.818	0.6594	Slug									
T19	1.844	1.8585	Slug									
T20	2.718	0.6084	Slug									
T21	0.2789	1.7436	Slug(T)									
T22	0.8262	0.2207	SS3	36.3	19		8.5	8.8	18.46		18.46	4.49
T23	1.78	0.2291	Bubble									

.

Series 1 P4V1

Test Code	Flow Velocity		Flow Regime	Pressure Cycling					Liquid Production			
	Gas (m/s)	Liquid (m/s)		Cycle Time (s)	Buildup Time (s)	Production Time (s)	Bubble Pen. Time (s)	Blowdown Time (s)	Slug Size (kg)	Constant Size (kg)	Transient Size (kg)	Peak Prod. Rate (kg/s)
T1	0.1531	0.1453	SS2	585.6	534.4		27.6	23.6	94.32		94.32	6.17
T2	0.0973	0.1488	SS2	312.4	278.1		16.4	17.9	120.72		120.72	9.27
T3	0.2045	0.1609	SS3	209.6	179.9		10.2	19.5	74.67		74.67	8.57
T4	0.3378	0.5206	Bubble									
T5	0.0493	0.1078	SS1	287.2	102.5		13.3	15.4	59.54	34.29	25.15	3.054
T6	0.0937	0.1230	SS1	221.5	105.5		11.3	16.4	52.23	26.2	26.03	3.52
T7	0.2211	0.1431	SS3	107	79.3		9.3	13.3	28.4		28.4	4.
T8	0.3698	0.1566	Bubble									
T9	0.6277	0.1714	Bubble									
T10	0.0996	0.3624	SS3	75.9			16.4	4.1	60.12		60.12	3.255
T11	0.2179	0.3821	Osc									
T12	0.2156	0.5985	Slug(T)									
T13	0.112	0.5621	Slug(T)									
T14	0.357	0.6038	Slug(T)									
T15	0.3664	0.3038	Osc									
T16	0.6343	0.1568	Bubble									
T17	0.6051	0.4651	Slug(T)									
T18	2.628	0.6329	Slug									
T19	1.382	0.4854	Slug									
T20	0.2162	1.0353	Bubble									
T21	0.0269	1.0895	Bubble									

Series 1 P7V1

Test Code	Flow Velocity		Flow Regime	Pressure Cycling					Liquid Production			
	Gas (m/s)	Liquid (m/s)		Cycle Time (s)	Buildup Time (s)	Production Time (s)	Bubble Pen. Time (s)	Blowdown Time (s)	Slug Size (kg)	Constant Size (kg)	Transient Size (kg)	Peak Prod. Rate (kg/s)
T1	0.0728	0.1375	Osc(T)									
T2	0.1828	0.1317	Bubble									
T3	0.3792	0.1831	Bubble									
T4	0.7414	0.1903	Bubble									
T5	1.823	0.1763	Bubble									
T6	0.088	0.2769	Osc(T)									
T7	0.1023	0.7353	Slug(T)									
T8	0.3648	0.7359	Slug(T)									
T9	0.3751	0.4937	Slug									
T10	0.0903	0.3647	Osc(T)									
T11	0.0521	0.4351	Osc(T)									
T12	0.0534	0.6197	Osc(T)									
T13	0.0458	0.2767	Osc(T)									
T14	0.044	0.1121	Bubble									

Series 2 P2V1

Test Code	Flow Velocity		Flow Regime	Pressure Cycling					Liquid Production			
	Gas (m/s)	Liquid (m/s)		Cycle Time (s)	Buildup Time (s)	Production Time (s)	Bubble Pen. Time (s)	Blowdown Time (s)	Slug Size (kg)	Constant Size (kg)	Transient Size (kg)	Peak Prod. Rate (kg/s)
T1	0.0985	0.2017	SS1	193.2	79.9	90.3	5.7	17.3	85.29	47.144	38.14	4.31
T2	0.082	0.4483	Osc(T)									
T3	0.0868	0.5599	Osc(T)									
T4	0.0846	0.6413	Osc(T)									
T5	0.0828	0.5478	Osc(T)									
T6	0.0775	0.7532	Slug(T)									
T7	0.075	0.9408	Bubble									
T8	0.161	0.1313	SS1	227.7	133.9	71.2	4.4	18.2	59.84	24.2	35.64	4.73
T9	0.127	0.3667	SS1	105	42.7	44.9	3.2	14.2	79.79	38.5	41.29	3.40
T10	0.2406	0.5152	SS2	46.2					49.84		49.84	3.99
T11	0.2475	0.4306	Osc	16.5								
T12	0.224	0.8724	Slug(T)									
T13	0.2649	0.2348	SS1	115	70.6	29.9	4.2	10.3	56.56	18.59	37.97	3.74
T14	0.3238	0.1246	SS2	233	210.7		3	17.3	34.82		34.82	3.74
T15	0.2944	0.2152	SS1	113.3	76.5	23.5	2.6	10.7	51.53	15.17	36.36	3.64
T16	0.3425	0.372	SS2	76.2	46.5		10.6	19.1	59.23		59.23	4.81
T17	0.3297	0.4988	SS2	39.7					41.76		41.76	4.49
T18	0.4001	0.6334	Slug(T)	19.5								
T19	0.3971	0.5314	Slug(T)	11.9								
T20	0.3894	0.6823	Slug	11.8								
T21	0.3704	0.7921	Slug									
T22	0.3997	1.071	Slug									
T23	0.5893	0.0238	Bubble									
T24	0.6716	0.1645	SS3	57.4	41.4			15.8	24.29		24.29	4.16512
T25	0.6966	0.3722	SS2	58.5	42.9		3.2	13.2			40.42	5.28

Series 2 P2V1 (ctd.)

Test Code	Flow Velocity		Flow Regime	Pressure Cycling					Liquid Production			
	Gas (m/s)	Liquid (m/s)		Cycle Time (s)	Buildup Time (s)	Production Time (s)	Bubble Pen. Time (s)	Blowdown Time (s)	Slug Size (kg)	Constant Size (kg)	Transient Size (kg)	Peak Prod. Rate (kg/s)
T26	0.6795	0.5449	SS3	42.5	23.6		2.1	16.8	47.22		47.22	4.88
T27	0.6528	0.7039	Slug									
T28	0.9289	0.5477	Slug									
T29	1.927	0.3597	Slug									
T30	0.9398	0.6016	Slug									
T31	1.027	0.1749	Slug									

Series 2 P4V1

Test Code	Flow Velocity		Flow Regime	Pressure Cycling					Liquid Production			
	Gas (m/s)	Liquid (m/s)		Cycle Time (s)	Buildup Time (s)	Production Time (s)	Bubble Pen. Time (s)	Blowdown Time (s)	Slug Size (kg)	Constant Size (kg)	Transient Size (kg)	Peak Prod. Rate (kg/s)
T1	0.0567	0.2305	SS1	159.3	56	72.8	18.5	12	73.88	38.79	35.09	2.3
T2	0.0996	0.384	SS1	77.	30.6	25.1	5.2	16.2	61.91	27.088	34.82	2.44
T3	0.0965	0.524	Osc	20.1								
T4	0.0924	0.527	Osc(T)	18.7								
T5	0.0875	0.767	Bubble									
T6	0.0847	0.925	Bubble									
T7	0.1957	0.889	Osc(T)									
T8	0.1803	0.506	Osc	18.8								
T9	0.1818	0.322	Osc	20.2								
T10	0.1869	0.198	SS2	87.9	70.4		5	17	32.38		32.38	2.87
T11	0.263	0.345	Osc	17.2								
T12	0.3749	0.351	Osc	14.3								
T13	0.3698	0.215	Slug(T)									
T14	0.3708	0.109	Bubble									
T15	0.3906	0.46	Slug(T)									
T16	0.3737	0.91	Slug									
T17	0.542	0.85	Slug									
T18	0.58	0.608	Slug									
T19	0.6031	0.331	SS3(T)	34.5								
T20	0.7238	0.335	SS3(T)	33.5								
T21	0.8979	0.336	Bubble									
T22	0.5042	0.133	Bubble									

Series 2 P7V1

Test Code	Flow Velocity		Flow Regime	Pressure Cycling					Liquid Production			
	Gas (m/s)	Liquid (m/s)		Cycle Time (s)	Buildup Time (s)	Production Time (s)	Bubble Pen. Time (s)	Blowdown Time (s)	Slug Size (kg)	Constant Size (kg)	Transient Size (kg)	Peak Prod. Rate (kg/s)
T1	0.0632	0.0538	SS1	310.7	125	153	10	21.9	52.62	28.05	24.57	1.67
T2	0.0794	0.233	Osc(T)									
T3	0.1003	0.35	SS2	157.4								
T4	0.191	0.307	SS1	166.9	78.6	72.6		5.7	83.01	49.56	33.45	2.31
T5	0.2967	0.332	Osc									
T6	0.4443	0.34	Bubble									
T7	0.344	0.752	Osc	13.4								
T8	0.1692	0.736	Bubble									
T9	0.0680	0.464	Osc(T)	13.2								
T10	0.065	0.535	Slug(T)									
T11	0.0930	0.736	Bubble	17.2								
T12	0.2002	0.5238	Osc	17								
T13	0.28	0.649	Bubble									
T14	0.2809	0.483	Slug(T)	12.4								
T15	0.2798	0.466	Osc	16.7								
T16	0.3217	0.329	SS2(T)									
T17	0.4233	0.496	Bubble									
T18	0.5331	0.468	Bubble									
T19	0.5306	0.304	Bubble									
T20	0.5455	0.218	Bubble									
T21	0.3559	0.2159	Bubble									
T22	0.2675	0.184	SS2(T)									
T23	0.1873	0.188	SS1	146.1	97	15		31.2	49.043	16.61	32.43	2.41
T24	0.0904	0.130	SS1	183.3	93.3	68.3	6	15.7	64.35	34.63	29.73	2.56
T25	0.0632	0.0539	SS1	259.4	107.1	118.3	9.6	34	69.12	42.22088	26.89838	1.97952
T26	0.0794	0.233	Osc(T)									

Appendix D2 – MPE Data

This Appendix contains data from the MPE project that is used in comparison with the criterion for the formation of large scale instabilities

Superficial Gas Velocity (m/s)	Superficial Liquid Velocity (m/s)	Flow Regime
0.0625	0.103	SS1
0.1175	0.11	SS1
0.075	0.14	SS1
0.06935	0.265	SS1
0.16075	0.107	SS1
0.15	0.23	SS1
0.1525	0.28	SS1
0.1525	0.41	SS1
0.2475	0.17	SS1
0.255	0.29	SS1
0.2675	0.42	SS1
0.42235	0.2486	SS1
0.4875	0.254	SS1
0.4029	0.6433	SS2
0.485	0.59	SS2
0.7475	0.67	SS2
0.069325	0.0622	SS3
0.1625	0.07	SS3
0.2675	0.03	SS3
0.265	0.07	SS3
0.2625	0.1	SS3
0.4325	0.09	SS3
0.42315	0.14844	SS3
0.4225	0.07	SS3
0.485	0.11	SS3
0.49	0.16	SS3
0.7575	0.27	SS3
0.07925	0.655	OSC(T)
0.1425	0.65	OSC(T)
0.2625	0.66	OSC(T)
0.08	0.45	SS1
0.73	0.39	SS1
0.42	0.42	SS1
0.4875	0.38	SS1
0.12	2.29	BUBBLE
0.2075	2.4	BUBBLE
0.3375	2.44	BUBBLE
0.4475	2.44	BUBBLE
0.68	2.44	BUBBLE
0.925	1.64	BUBBLE

MPE Data Ctd.

1.8325	1.61	BUBBLE
0.4375	0.08	SLUG
0.665	0.08	SLUG
0.685	0.1	SLUG
0.755	0.17	SLUG
0.935	0.07	SLUG
0.9575	0.16	SLUG
0.95	0.26	SLUG
0.95	0.41	SLUG
0.075	0.96	OSC
0.0725	1.62	OSC
0.1325	1.07	OSC
0.12	1.67	OSC
0.2375	1.08	OSC
0.225	1.57	OSC
0.3575	1.52	OSC
0.475	1.56	OSC
0.7325	1.63	OSC
0.9575	0.65	OSC
0.9525	1.05	OSC
0.4125	1.04	OSC(T)
0.4775	1.07	OSC(T)
0.7425	1.03	OSC(T)

D3 Simulation Results

This set of tables summarises the simulation results. Each test case is given a table, including the different simulation scenarios – grid variations and timestep variations.

Case A

	Experimental Data	Basic	Increase Grid x2	Increase Grid x4	Time x1/10	Time x1/100	Time x10
Flow Regime	SS1	SS1	SS1	SS1	SS1	SS1	SS1
Time Data							
Cycle Time	195.9	160.6	157.7	158.7	160.4	160.3	160.8
Liquid Buildup	88.0	94.1	93.4	93.2	92.7	92.8	94.1
Slug Production	91.2	54.3	53.8	54.7	53.6	51.8	54.7
Bubble Penetration	3.9	3.9	2.9	3.1	5.8	6.6	4.4
Gas Blowdown	12.8	8.3	7.6	7.6	8.4	9.1	7.7
Liquid Flow Data							
Size of Steady Production	47.14	36.19	37.38	36.88	34.25	33.92	36.52
Size of Production Transient	38.15	34.36	32.13	32.93	35.24	36.74	33.68
Slug Size	85.29	70.55	69.51	69.81	69.50	70.66	70.20
Rate of Constant Production	0.53	0.69	0.70	0.67	0.686306515	0.681782888	0.689670792
Peak Production Rate	4.305	5.743	6.13	6.47	5.695	5.69	5.73

Case B

	Experimental Data	Basic	Increase Grid x2	Increase Grid x4	Time x1/10	Time x1/100	Time x10
Flow Regime	SS1	SS1	SS1		SS1	SS1	SS1
Time Data							
Cycle Time	105.0	96.8	97.7		91.9	92.4	92.0
Liquid Buildup	46.1	48.3	48.8		49.0	48.9	49.6
Slug Production	43.3	37.1	38.1		27.6	26.0	28.7
Bubble Penetration	2.1	2.6	1.9		5.8	7.6	4.5
Gas Blowdown	13.5	8.8	8.8		9.5	9.9	9.2
Liquid Flow Data							
Size of Steady Production	38.50	37.87	40.11		26.98153193	25.93456845	29.10287333
Size of Production Transient	41.29	37.77	35.94		44.09848867	46.27148018	42.2021576
Slug Size	79.79	75.64	76.05		71.0800206	72.20604864	71.30503093
Rate of Constant Production	0.88	1.11	1.466918443		1.090684714	1.082646234	1.110520235
Peak Production	3.402	4.687	4.93		4.752733333	4.824636364	4.7748

Case C

	Experimental Data	Basic	Increase Grid x2	Increase Grid x4	Time x1/10	Time x1/100	Time x10
Flow Regime	SS2	SS3	SS3	SS3	SS3	SS3	SS3
Time Data							
Cycle Time	135.6	96.9	89.5	89.6	100.6	95.5	95.4
Liquid Buildup	114.0	88.0	80.7	80.3	92.2	80.9	86.4
Slug Production	0.0						
Bubble Penetration	2.3						
Gas Blowdown	19.3	8.9	8.8	9.3	8.3	14.6	9.0
Liquid Flow Data							
Size of Steady Production	0.00						
Size of Production Transient	38.81	25.94	24.68986269	24.7635726	26.61161593	25.96751793	25.83515867
Slug Size	38.81	25.94	24.68986269	24.7635726	26.61161593	25.96751793	25.83515867
Peak Production	3.737	6.373	6.16	7.052	6.591888889	6.432166667	6.254642857

Case D

	Experimental Data	Basic	Increase Grid x2	Increase Grid x4	Time x1/10	Time x1/100	Time x10
Flow Regime	SS3	SS3	SS3	SS3	SS3 -> Osc	SS3 -> Osc	SS3 -> Osc
Time Data							
Cycle Time	93.91	42.3	41.2	40.83333333			
Liquid Buildup	78.86	32.4	32.48333333	31.65			
Slug Production							
Bubble Penetration							
Gas Blowdown	15.05	9.9	8.716666667	9.183333333			
Liquid Flow Data							
Size of Steady Production							
Size of Production Transient							
Slug Size	24.30	15.1	14.2	14.6			
Peak Production	4.17	3.6	3.9	4.1			

Case E

	Experimental Data	Basic	Increase Grid x2	Increase Grid x4	Time x1/10	Time x1/100	Time x10
Flow Regime	Osc	SS2	SS2	SS2	SS2	SS2	SS2
Time Data							
Cycle Time	16.254	54.7	54.04	53.6	54.82222222	54.6625	54.6
Liquid Buildup							
Slug Production							
Bubble Penetration							
Gas Blowdown							
Liquid Flow Data							
Size of Steady Production	16.254	51.0351	50.90568	50.116	50.76976613	50.85301975	50.52835943
Size of Production Transient							
Slug Size							
Peak Production	2.459	5.951888889	6.4968	6.899	5.91925	6.022375	6.004285714

Case F

	Experimental Data	Basic	Increase Grid x2	Increase Grid x4	Time x1/10	Time x1/100	Time x1
Flow Regime	Slug	Bubble	Bubble	Bubble/Stratified	Bubble	Bubble	Bubble
Time Data							
Cycle Time	7.7						
Liquid Buildup							
Slug Production							
Bubble Penetration							
Gas Blowdown							
Liquid Flow Data							
Size of Steady Production							
Size of Production Transient							
Slug Size							
Peak Production							

Appendix E

Taitel Correlation for the Pipeline Liquid Fraction

Overview

This appendix details the calculations used to estimate the pipeline liquid holdup, ε_{LP}, based upon the superficial liquid velocity, U_L^S. This method is based upon the work of Taitel (1986) and the computation method developed by Yeung (1996).

The basis of this model is the calculation of a hypothetical single-phase liquid pressure drop in the pipeline. This is then equated with the hydrostatic pressure drop along the pipeline containing the stratified liquid film.

Model Basis

Assuming steady, fully developed stratified flow in a pipeline, where the gas density is low and the pressure drop due to the gas flow is negligible, the momentum balance becomes:

$$\tau_L S_L = \rho_L g A_L \sin\beta \qquad (E.1)$$

Where the symbols have their usual meaning. The wall shear stress is calculated from an appropriate correlation, for example:

$$\tau_L = f_L \frac{\rho_L U_L^2}{2} \qquad (E.2)$$

Where f_L is the Fanning friction factor for the liquid phase in the pipe. This can be calculated from the correlation:

$$f_L = C_L \left(\frac{4 A_L U_L}{S_L \nu_L} \right)^{-m} \qquad (E.3)$$

Where $C_L = 0.046$ and $m = 0.2$ for turbulent flow and $C_L = 16$ and $m = 1$ for laminar flow. A_L is the liquid flow area given by:

$$A_L = \frac{D^2}{4}\left[\pi - \cos^2\left(2\frac{h_L}{D} - 1\right) + \left(2\frac{h_L}{D} - 1\right)\sqrt{1 - \left(2\frac{h_L}{D} - 1\right)^2} \right] \qquad (E.4)$$

S_L, the liquid wetted perimeter along the pipe wall is given by:

$$S_L = D\left[\pi - \cos^{-1}\left(2\frac{h_L}{D} - 1\right) \right] \qquad (E.5)$$

Combining Equations (E.1) - (E.5), a trial and error solution for the height of liquid in the pipe, h_L, is obtainable and hence the liquid fraction can be found from the basic relation:

$$\varepsilon_L = 1 - \frac{A_L}{A} \qquad \text{(E.6)}$$

A general solution to this was presented graphically by Taitel (1986):

$$\varepsilon_L = \varepsilon_L[\phi] = \varepsilon_L\left[\frac{(\rho_L - \rho_G)g\sin\beta}{(dP/dx)_{LS}}\right] \qquad \text{(E.7)}$$

Where $(dP/dx)_{LS}$ is the axial pressure gradient in the pipeline if the liquid alone occupies the pipe cross section. Yeung (1996) provided a correlation for the Equation, (E.7) of the form:

$$\varepsilon_L = \varepsilon_L[\mathrm{X}] = \varepsilon_L[\log_{10}\phi] \qquad \text{(E.8)}$$

and

$$\varepsilon_L = a_1 + a_2\mathrm{X} + a_3\mathrm{X}^2 + a_4\mathrm{X}^3 + a_5\mathrm{X}^4 \qquad \text{(E.9)}$$

Where ϕ and X are correlation variables defined in the above equations, the a_i values are provided by Yeung (1996). Yeung (1996) calculates the single-phase liquid pressure gradient in the pipeline using the Moody friction factor, f':

$$\left(\frac{dP}{dx}\right)_{LS} = \left(\frac{f'}{D}\right)\frac{\rho_L U_L^2}{2} \qquad \text{(E.10)}$$

Referring to the results in Appendix B, the estimated Moody friction factor is 0.002, allowing ε_L as a function of $U_L{}^S$ to be calculated.

Appendix F

Generic Transient Code Model

Overview

This appendix gives a generic, plain text version of the model used in the transient code. It is intended that this version of the model can be modified for use with all three commercial codes – PLAC, OLGA and TACITE. The model is based upon Case A from the test series used in Chapter 6, details of which are available in Appendix D.

PVT Description

Fluid components: Nitrogen (N_2), Water (H_2O)
Fluid composition by Weight: Nitrogen 2%, Water 98%
PVT pressure range: 1 - 11 bar(a)
PVT temperature range: 5 - 55 °C

Pipeline Model

Pipe Material Characteristics
Pipe wall material: Carbon steel
Material density: 7850 kg/m^3
Material heat capacity: 500 J/kg K
Thermal Conductivity: 50 W/m K
Wall internal diameter: 52.5018 mm
Wall thickness: 10 mm
Pipe roughness: 0.1 mm

Geometry Model
Pipeline origin: x = -57.4 m, y = 2 m
Pipeline x-y co-ordinates:

x	y
-57.4	2
0	0
0.831	0.223
1.494	0.961
2.032	2.059
2.198	2.889
2.315	3.933
2.369	4.435
2.441	4.778
2.524	4.873
2.663	4.945
2.814	4.954
2.949	4.907
3.075	4.788
3.117	4.700
3.151	4.520
3.186	4.295
3.218	4.089
3.259	3.837
3.382	3.472
3.948	2.829
4.238	2.679
4.621	2.624
5.032	2.730

5.426	3.047
6.025	3.756
6.412	4.394
6.659	4.944
6.884	5.680
7.006	6.498
7.020	7.835
7.020	9.258
7.020	9.982
10.020	9.982

Boundary Conditions

Inlet Boundary
Source types: x1 pure liquid, x1 pure gas
Liquid source flow: 0.422 k/s
Gas source flow: 0.0007423 kg/s
Source temperature: 20.77 °C

Outlet Boundary
Pressure: 2.064 bar(a)
Temperature: 25 °C
Gas fraction at outlet source: 100%

Model Execution

Initial Conditions
Pipeline temperature: 25 °C

Runtime Options
Simulation time: 1500 s
Initial timestep size: 0.01 s
Maximum timestep size: 1 s
Minimum timestep size 0.001 s

Output Options
Output timestep: 1 s
Output variables: Pressure, liquid fraction, mass flow, superficial velocity
Output locations: x = 0 m, y = 0 m
x = 2.814 m, y = 4.954 m
x = 4.621 m, y = 2.624
x = 10.020 m, y = 9.982 m